DNA-Advanced Techniques wk4v5

Version 5 of 34 Mb, 245 pages

DNA

Deoxyribonucleic acid (**DNA**) is a nucleic acid that contains the genetic instructions used in the development and functioning of all known living organisms and some viruses. The main role of DNA molecules is the long-term storage of information. DNA is often compared to a set of blueprints or a recipe, or a code, since it contains the instructions needed to construct other components of cells, such as proteins and RNA molecules. The DNA segments that carry this genetic information are called genes, but other DNA sequences have structural purposes, or are involved in regulating the use of this genetic information.

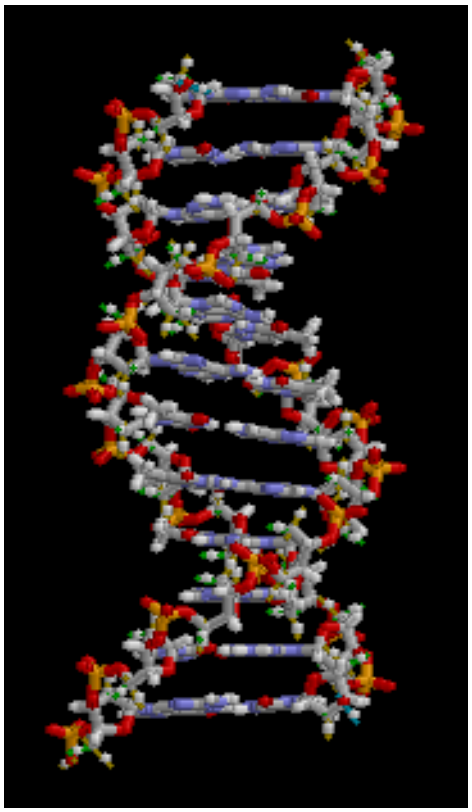

The structure of part of a DNA double helix

Chemically, DNA consists of two long polymers of simple units called nucleotides, with backbones made of sugars and phosphate groups joined by ester bonds. These two strands run in opposite directions to each other and are therefore anti-parallel. Attached to each sugar is one of four types of molecules called bases. It is the sequence of these four bases along the backbone that encodes information. This information is read using the genetic code, which specifies the sequence of the amino acids within proteins. The code is read by copying stretches of DNA into the related nucleic acid RNA, in a process called transcription.

Within cells, DNA is organized into X-shaped structures called chromosomes. These chromosomes are duplicated before cells divide, in a process called DNA replication. Eukaryotic organisms (animals, plants, fungi, and protists) store most of their DNA inside the cell nucleus and some of their DNA in the mitochondria (animals and plants) and chloroplasts (plants only)[1] . Prokaryotes (bacteria and archaea) however, store their DNA in the cell's cytoplasm. Within the chromosomes, chromatin proteins such as histones compact and organize DNA. These compact structures guide the interactions between DNA and other proteins, helping control which parts of the DNA are transcribed.

Properties

Strands of purified DNA precipitated from solutions of cell components are visible as viscous white substance.

DNA is a long polymer made from repeating units called nucleotides.[2] [3] [4] These nucleotides are adenine (A), guanine (G), cytosine (C) and thymine (T). In the related nucleic acid RNA, thymine is replaced by uracil (U). These nucleotides can be classified into two groups: purines (adenine and guanine) and pyrimidines (thymine and cytosine).

The DNA chain is 22 to 26 Ångströms wide (2.2 to 2.6 nanometres), and one nucleotide unit is 3.3 Å (0.33 nm) long.[5] Although each individual repeating unit is very small, DNA polymers can be very large molecules containing millions of nucleotides. For instance, the largest human chromosome, chromosome number 1, is approximately 220 million base pairs long.[6]

In living organisms, DNA does not usually exist as a single molecule, but instead as a pair of molecules that are held tightly together.[7] [8] These two long strands entwine like vines, in the shape of a double helix. The nucleotide repeats contain both the segment of the backbone of the molecule, which holds the chain together, and a base, which interacts with the other DNA strand in the helix. In general, a base linked to a sugar is called a nucleoside and a base linked to a sugar and one or more phosphate groups is called a nucleotide. If multiple nucleotides are linked together, as in DNA, this polymer is called a polynucleotide.[9]

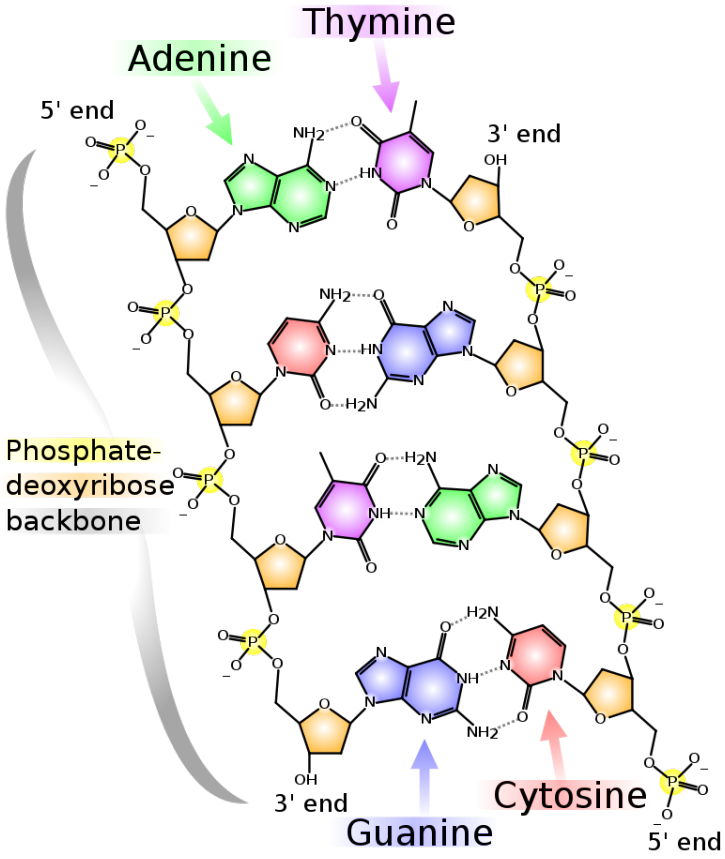

The chemical structure of DNA. Hydrogen bonds are shown as dotted lines.

The backbone of the DNA strand is made from alternating phosphate and sugar residues.[10] The sugar in DNA is 2-deoxyribose, which is a pentose (five-carbon) sugar. The sugars are joined together by phosphate groups that form phosphodiester bonds between

the third and fifth carbon atoms of adjacent sugar rings. These asymmetric bonds mean a strand of DNA has a direction. In a double helix the direction of the nucleotides in one strand is opposite to their direction in the other strand. This arrangement of DNA strands is called antiparallel. The asymmetric ends of DNA strands are referred to as the 5′ (*five prime*) and 3′ (*three prime*) ends, with the 5' end being that with a terminal phosphate group and the 3' end that with a terminal hydroxyl group. One of the major differences between DNA and RNA is the sugar, with 2-deoxyribose being replaced by the alternative pentose sugar ribose in RNA.[8]

The DNA double helix is stabilized by hydrogen bonds between the bases attached to the two strands. The four bases found in DNA are adenine (abbreviated A), cytosine (C), guanine (G) and thymine (T). These four bases are attached to the sugar/phosphate to form the complete nucleotide, as shown for adenosine monophosphate.

These bases are classified into two types; adenine and guanine are fused five- and six-membered heterocyclic compounds called purines, while cytosine and thymine are six-membered rings called pyrimidines.[8] A fifth pyrimidine base, called uracil (U), usually takes the place of thymine in RNA and differs from thymine by lacking a methyl group on its ring. Uracil is not usually found in DNA, occurring only as a breakdown product of cytosine.

Grooves

Twin helical strands form the DNA backbone. Another double helix may be found by tracing the spaces, or grooves, between the strands. These voids are adjacent to the base pairs and may provide a binding site. As the strands are not directly opposite each other, the grooves are unequally sized. One groove, the major groove, is 22 Å wide and the other, the minor groove, is 12 Å wide.[12] The narrowness of the minor groove means that the edges of the bases are more accessible in the major groove. As a result, proteins like transcription factors that can bind to specific sequences in double-stranded DNA usually make contacts to the sides of the bases exposed in the major groove.[13] This situation varies in unusual conformations of DNA within the cell *(see below)*, but the major and minor grooves are always named to reflect the differences in size that would be seen if the DNA is twisted back into the ordinary B form.

Structure of a section of DNA. The bases lie horizontally between the two spiraling strands.[11] Animated version at File:DNA orbit animated.gif - over 3 megabytes.

Base pairing

Each type of base on one strand forms a bond with just one type of base on the other strand. This is called complementary base pairing. Here, purines form hydrogen bonds to pyrimidines, with A bonding only to T, and C bonding only to G. This arrangement of two nucleotides binding together across the double helix is called a base pair. As hydrogen bonds are not covalent, they can be broken and rejoined relatively easily.

The two strands of DNA in a double helix can therefore be pulled apart like a zipper, either by a mechanical force or high temperature.[14] As a result of this complementarity, all the information in the double-stranded sequence of a DNA helix is duplicated on each strand, which is vital in DNA replication. Indeed, this reversible and specific interaction between complementary base pairs is critical for all the functions of DNA in living organisms.[3]

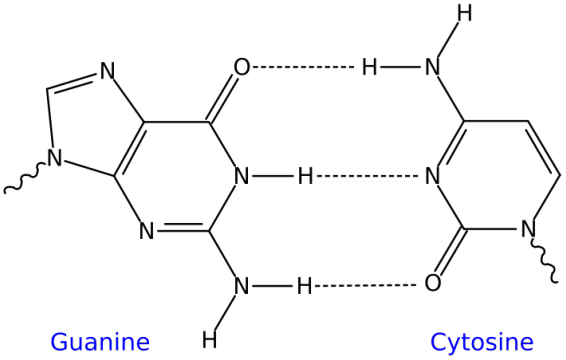

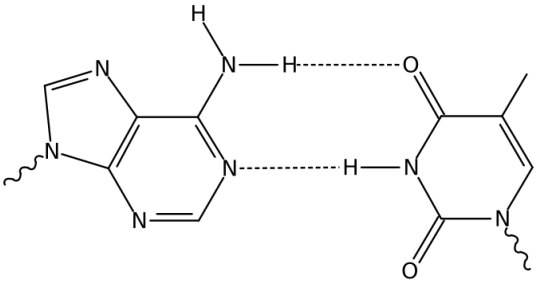

Top, a **GC** base pair with three hydrogen bonds. Bottom, an **AT** base pair with two hydrogen bonds. Non-covalent hydrogen bonds between the pairs are shown as dashed lines.

The two types of base pairs form different numbers of hydrogen bonds, AT forming two hydrogen bonds, and GC forming three hydrogen bonds (see figures, left). DNA with high GC-content is more stable than DNA with low GC-content, but contrary to popular belief, this is not due to the extra hydrogen bond of a GC basepair but rather the contribution of stacking interactions (hydrogen bonding merely provides specificity of the pairing, not stability).[15] As a result, it is both the percentage of GC base pairs and the overall length of a DNA double helix that determine the strength of the association between the two strands of DNA. Long DNA helices with a high GC content have stronger-interacting strands, while short helices with high AT content have weaker-interacting strands.[16] In biology, parts of the DNA double helix that need to separate easily, such as the TATAAT Pribnow box in some promoters, tend to have a high AT content, making the strands easier to pull apart.[17] In the laboratory, the strength of this interaction can be measured by finding the temperature required to break the hydrogen bonds, their melting temperature (also called T_m value). When all the base pairs in a DNA double helix melt, the strands separate and exist in solution as two entirely independent molecules. These single-stranded DNA molecules have no single common shape, but some conformations are more stable than others.[18]

Sense and antisense

A DNA sequence is called "sense" if its sequence is the same as that of a messenger RNA copy that is translated into protein.[19] The sequence on the opposite strand is called the "antisense" sequence. Both sense and antisense sequences can exist on different parts of the same strand of DNA (i.e. both strands contain both sense and antisense sequences). In both prokaryotes and eukaryotes, antisense RNA sequences are produced, but the functions of these RNAs are not entirely clear.[20] One proposal is that antisense RNAs are involved in regulating gene expression through RNA-RNA base pairing.[21]

A few DNA sequences in prokaryotes and eukaryotes, and more in plasmids and viruses, blur the distinction between sense and antisense strands by having overlapping genes.[22] In these cases, some DNA sequences do double duty, encoding one protein when read along one strand, and a second protein when read in the opposite direction along the other strand. In bacteria, this overlap may be involved in the regulation of gene transcription,[23] while in viruses, overlapping genes increase the amount of information that can be encoded within the small viral genome.[24]

Supercoiling

DNA can be twisted like a rope in a process called DNA supercoiling. With DNA in its "relaxed" state, a strand usually circles the axis of the double helix once every 10.4 base pairs, but if the DNA is twisted the strands become more tightly or more loosely wound.[25] If the DNA is twisted in the direction of the helix, this is positive supercoiling, and the bases are held more tightly together. If they are twisted in the opposite direction, this is negative supercoiling, and the bases come apart more easily. In nature, most DNA has slight negative supercoiling that is introduced by enzymes called topoisomerases.[26] These enzymes are also needed to relieve the twisting stresses introduced into DNA strands during processes such as transcription and DNA replication.[27]

Alternate DNA structures

DNA exists in many possible conformations that include A-DNA, B-DNA, and Z-DNA forms, although, only B-DNA and Z-DNA have been directly observed in functional organisms.[10] The conformation that DNA adopts depends on the hydration level, DNA sequence, the amount and direction of supercoiling, chemical modifications of the bases, the type and concentration of metal ions, as well as the presence of polyamines in solution.[28]

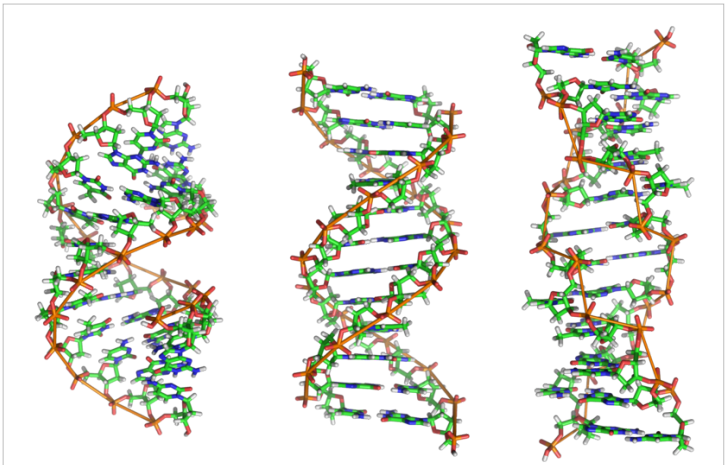

From left to right, the structures of A, B and Z DNA

The first published reports of A-DNA X-ray diffraction patterns— and also B-DNA used analyses based on Patterson transforms that provided only a limited amount of structural information for oriented fibers of DNA.[29] [30] An alternate analysis was then proposed by Wilkins *et al.*, in 1953, for the *in vivo* B-DNA X-ray diffraction/scattering patterns of highly

hydrated DNA fibers in terms of squares of Bessel functions.[31] In the same journal, Watson and Crick presented their molecular modeling analysis of the DNA X-ray diffraction patterns to suggest that the structure was a double-helix.[7]

Although the `B-DNA form' is most common under the conditions found in cells,[32] it is not a well-defined conformation but a family of related DNA conformations[33] that occur at the high hydration levels present in living cells. Their corresponding X-ray diffraction and scattering patterns are characteristic of molecular paracrystals with a significant degree of disorder.[34] [35]

Compared to B-DNA, the A-DNA form is a wider right-handed spiral, with a shallow, wide minor groove and a narrower, deeper major groove. The A form occurs under non-physiological conditions in partially dehydrated samples of DNA, while in the cell it may be produced in hybrid pairings of DNA and RNA strands, as well as in enzyme-DNA complexes.[36] [37] Segments of DNA where the bases have been chemically modified by methylation may undergo a larger change in conformation and adopt the Z form. Here, the strands turn about the helical axis in a left-handed spiral, the opposite of the more common B form.[38] These unusual structures can be recognized by specific Z-DNA binding proteins and may be involved in the regulation of transcription.[39]

Quadruplex structures

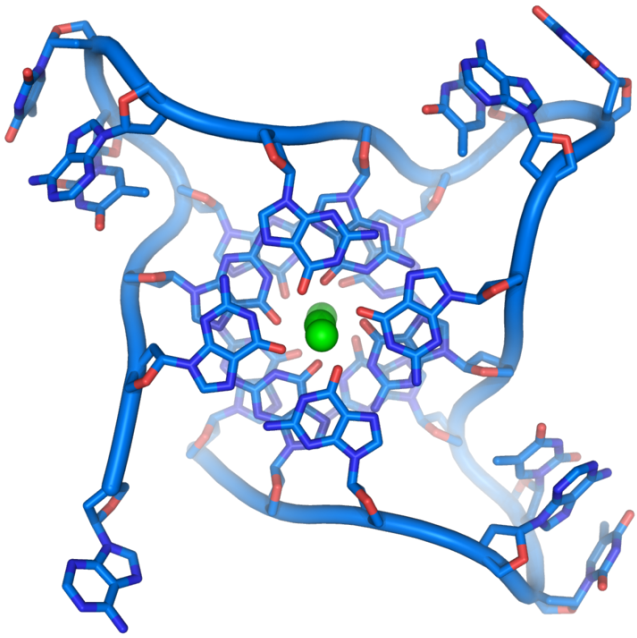

Structure of a DNA quadruplex formed by telomere repeats. The looped conformation of the DNA backbone is very different from the typical helical structure.[40]

At the ends of the linear chromosomes are specialized regions of DNA called telomeres. The main function of these regions is to allow the cell to replicate chromosome ends using the enzyme telomerase, as the enzymes that normally replicate DNA cannot copy the extreme 3′ ends of chromosomes.[41] These specialized chromosome caps also help protect the DNA ends, and stop the DNA repair systems in the cell from treating them as damage to be corrected.[42] In human cells, telomeres are usually lengths of single-stranded DNA containing several thousand repeats of a simple TTAGGG sequence.[43]

These guanine-rich sequences may stabilize chromosome ends by forming structures of stacked sets of four-base units, rather than the usual base pairs found in other DNA molecules. Here, four guanine bases form a flat plate and these flat four-base units then stack on top of each other, to form a stable *G-quadruplex* structure.[44] These structures are stabilized by hydrogen bonding between the edges of the bases and chelation of a metal ion in the centre of each four-base unit.[45]

Other structures can also be formed, with the central set of four bases coming from either a single strand folded around the bases, or several different parallel strands, each contributing one base to the central structure.

In addition to these stacked structures, telomeres also form large loop structures called telomere loops, or T-loops. Here, the single-stranded DNA curls around in a long circle stabilized by telomere-binding proteins.[46] At the very end of the T-loop, the single-stranded telomere DNA is held onto a region of double-stranded DNA by the telomere strand disrupting the double-helical DNA and base pairing to one of the two strands. This triple-stranded structure is called a displacement loop or D-loop.[44]

Branched DNA

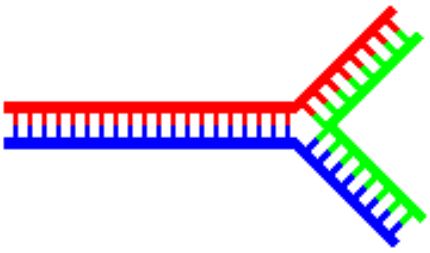

A DNA structure with a single branching point.

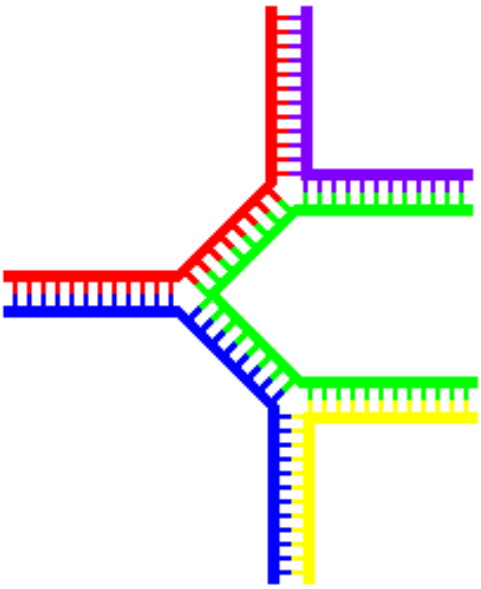

A DNA structure with multiple branches.

In DNA fraying occurs when non-complementary regions exist at the end of an otherwise complementary double-strand of DNA. However, branched DNA can occur if a third strand of DNA is introduced and contains adjoining regions able to hybridize with the frayed regions of the pre-existing double-strand. Although the simplest example of branched DNA involves only three strands of DNA, complexes involving additional strands and multiple branches are also possible.[47]

Chemical modifications

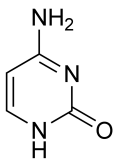	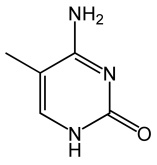	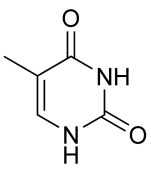
cytosine	5-methylcytosine	thymine

Structure of cytosine with and without the 5-methyl group. After deamination the 5-methylcytosine has the same structure as thymine

Base modifications

The expression of genes is influenced by how the DNA is packaged in chromosomes, in a structure called chromatin. Base modifications can be involved in packaging, with regions that have low or no gene expression usually containing high levels of methylation of cytosine bases. For example, cytosine methylation, produces 5-methylcytosine, which is important for X-chromosome inactivation.[48] The average level of methylation varies between organisms - the worm *Caenorhabditis elegans* lacks cytosine methylation, while vertebrates have higher levels, with up to 1% of their DNA containing 5-methylcytosine.[49] Despite the importance of 5-methylcytosine, it can deaminate to leave a thymine base, methylated cytosines are therefore particularly prone to mutations.[50] Other base modifications include adenine methylation in bacteria, the presence of 5-hydroxymethylcytosine in the brain,[51] and the glycosylation of uracil to produce the "J-base" in kinetoplastids.[52] [53]

Damage

DNA can be damaged by many different sorts of mutagens, which change the DNA sequence. Mutagens include oxidizing agents, alkylating agents and also high-energy electromagnetic radiation such as ultraviolet light and X-rays. The type of DNA damage produced depends on the type of mutagen. For example, UV light can damage DNA by producing thymine dimers, which are cross-links between pyrimidine bases.[55] On the other hand, oxidants such as free radicals or hydrogen peroxide produce multiple forms of damage, including base modifications, particularly of guanosine, and double-strand breaks.[56] A typical human cell contains about 150,000 bases that have suffered oxidative damage.[57] Of these oxidative lesions, the most dangerous are double-strand breaks, as these are difficult to repair and can produce point mutations, insertions and deletions from the DNA sequence, as well as chromosomal translocations.[58]

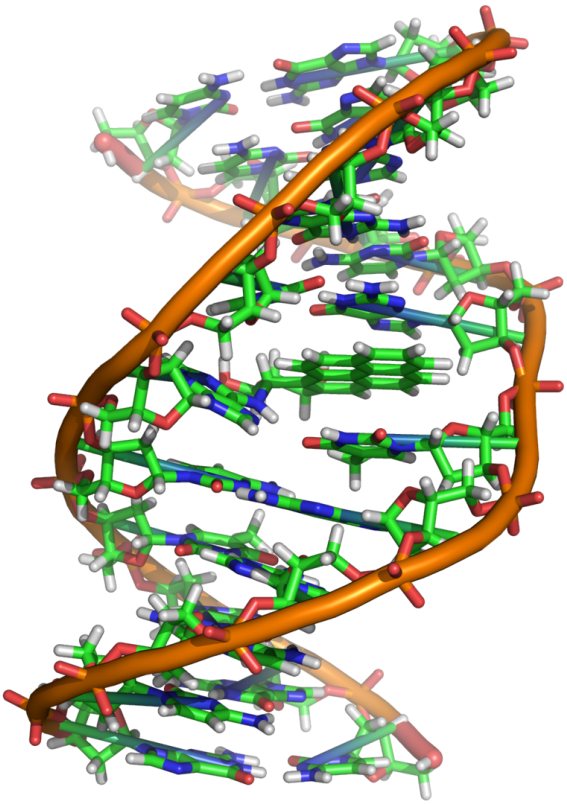

A covalent adduct between benzo[*a*]pyrene, the major mutagen in tobacco smoke, and DNA[54]

Many mutagens fit into the space between two adjacent base pairs, this is called *intercalating*. Most intercalators are aromatic and planar molecules, and include Ethidium bromide, daunomycin, and doxorubicin. In order for an intercalator to fit between base

pairs, the bases must separate, distorting the DNA strands by unwinding of the double helix. This inhibits both transcription and DNA replication, causing toxicity and mutations. As a result, DNA intercalators are often carcinogens, and Benzo[*a*]pyrene diol epoxide, acridines, aflatoxin and ethidium bromide are well-known examples.[59] [60] [61] Nevertheless, due to their ability to inhibit DNA transcription and replication, other similar toxins are also used in chemotherapy to inhibit rapidly growing cancer cells.[62]

Biological functions

DNA usually occurs as linear chromosomes in eukaryotes, and circular chromosomes in prokaryotes. The set of chromosomes in a cell makes up its genome; the human genome has approximately 3 billion base pairs of DNA arranged into 46 chromosomes.[63] The information carried by DNA is held in the sequence of pieces of DNA called genes. Transmission of genetic information in genes is achieved via complementary base pairing. For example, in transcription, when a cell uses the information in a gene, the DNA sequence is copied into a complementary RNA sequence through the attraction between the DNA and the correct RNA nucleotides. Usually, this RNA copy is then used to make a matching protein sequence in a process called translation which depends on the same interaction between RNA nucleotides. Alternatively, a cell may simply copy its genetic information in a process called DNA replication. The details of these functions are covered in other articles; here we focus on the interactions between DNA and other molecules that mediate the function of the genome.

Genes and genomes

Genomic DNA is located in the cell nucleus of eukaryotes, as well as small amounts in mitochondria and chloroplasts. In prokaryotes, the DNA is held within an irregularly shaped body in the cytoplasm called the nucleoid.[64] The genetic information in a genome is held within genes, and the complete set of this information in an organism is called its genotype. A gene is a unit of heredity and is a region of DNA that influences a particular characteristic in an organism. Genes contain an open reading frame that can be transcribed, as well as regulatory sequences such as promoters and enhancers, which control the transcription of the open reading frame.

In many species, only a small fraction of the total sequence of the genome encodes protein. For example, only about 1.5% of the human genome consists of protein-coding exons, with over 50% of human DNA consisting of non-coding repetitive sequences.[65] The reasons for the presence of so much non-coding DNA in eukaryotic genomes and the extraordinary differences in genome size, or *C-value*, among species represent a long-standing puzzle known as the "C-value enigma."[66] However, DNA sequences that do not code protein may still encode functional non-coding RNA molecules, which are involved in the regulation of gene expression.[67]

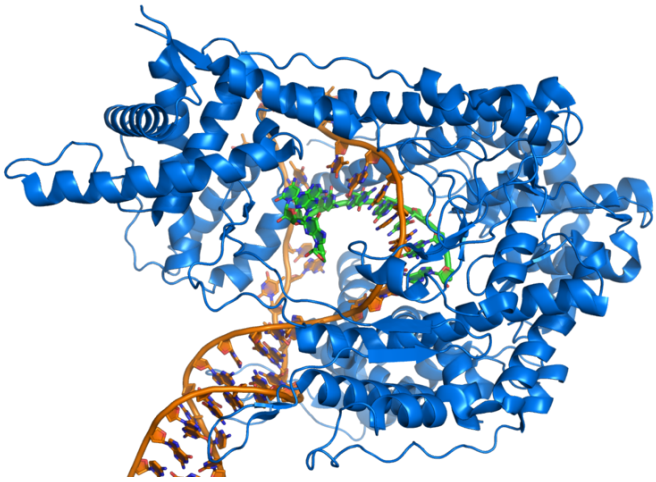

T7 RNA polymerase (blue) producing a mRNA (green) from a DNA template (orange).[68]

Some non-coding DNA sequences play structural roles in chromosomes. Telomeres and centromeres typically contain few genes, but are important for the function and stability of chromosomes.[42] [69] An abundant form of non-coding DNA in humans are pseudogenes, which are copies of genes that have been disabled by mutation.[70] These sequences are usually just molecular fossils, although they can occasionally serve as raw genetic material for the creation of new genes through the process of gene duplication and divergence.[71]

Transcription and translation

A gene is a sequence of DNA that contains genetic information and can influence the phenotype of an organism. Within a gene, the sequence of bases along a DNA strand defines a messenger RNA sequence, which then defines one or more protein sequences. The relationship between the nucleotide sequences of genes and the amino-acid sequences of proteins is determined by the rules of translation, known collectively as the genetic code. The genetic code consists of three-letter 'words' called *codons* formed from a sequence of three nucleotides (e.g. ACT, CAG, TTT).

In transcription, the codons of a gene are copied into messenger RNA by RNA polymerase. This RNA copy is then decoded by a ribosome that reads the RNA sequence by base-pairing the messenger RNA to transfer RNA, which carries amino acids. Since there are 4 bases in 3-letter combinations, there are 64 possible codons (4^3combinations). These encode the twenty standard amino acids, giving most amino acids more than one possible codon. There are also three 'stop' or 'nonsense' codons signifying the end of the coding region; these are the TAA, TGA and TAG codons.

Replication

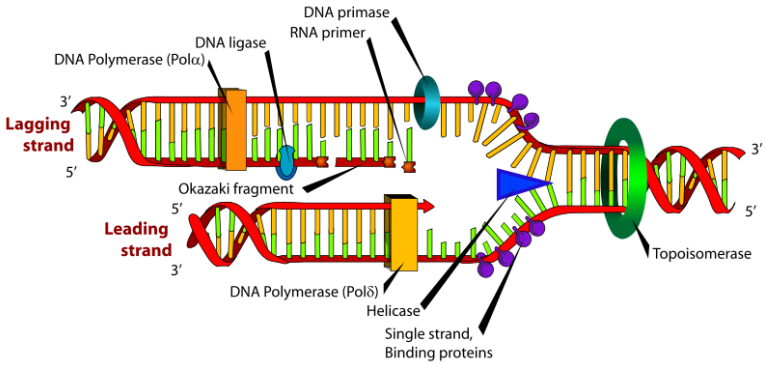

DNA replication. The double helix is unwound by a helicase and topoisomerase. Next, one DNA polymerase produces the leading strand copy. Another DNA polymerase binds to the lagging strand. This enzyme makes discontinuous segments (called Okazaki fragments) before DNA ligase joins them together.

Cell division is essential for an organism to grow, but when a cell divides it must replicate the DNA in its genome so that the two daughter cells have the same genetic information as their parent. The double-stranded structure of DNA provides a simple mechanism for DNA replication. Here, the two strands are separated and then each strand's complementary DNA sequence is recreated by an enzyme called DNA polymerase. This enzyme makes the complementary strand by finding the correct base through complementary base pairing, and bonding it onto the original strand. As DNA polymerases can only extend a DNA strand in a 5′ to 3′ direction, different mechanisms are used to copy the antiparallel strands of the double helix.[72] In this way, the base on the old strand dictates which base appears on the new strand, and the cell ends up with a perfect copy of its DNA.

Interactions with proteins

All the functions of DNA depend on interactions with proteins. These protein interactions can be non-specific, or the protein can bind specifically to a single DNA sequence. Enzymes can also bind to DNA and of these, the polymerases that copy the DNA base sequence in transcription and DNA replication are particularly important.

DNA-binding proteins

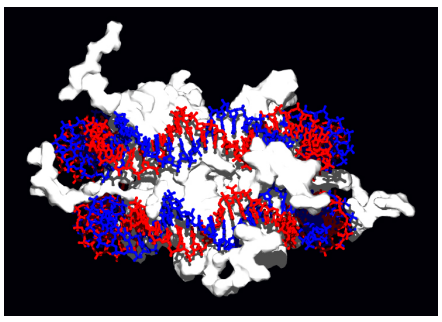

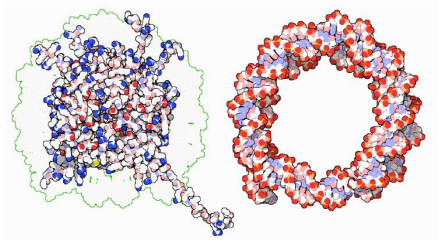

Interaction of DNA with histones (shown in white, top). These proteins' basic amino acids (below left, blue) bind to the acidic phosphate groups on DNA (below right, red).

Structural proteins that bind DNA are well-understood examples of non-specific DNA-protein interactions. Within chromosomes, DNA is held in complexes with structural proteins. These proteins organize the DNA into a compact structure called chromatin. In eukaryotes this structure involves DNA binding to a complex of small basic proteins called histones, while in prokaryotes multiple types of proteins are involved.[73] [74] The histones form a disk-shaped complex called a nucleosome, which contains two complete turns of double-stranded DNA wrapped around its surface. These non-specific interactions are formed through basic residues in the histones making ionic bonds to the acidic sugar-phosphate backbone of the DNA, and are therefore largely independent of the base sequence.[75] Chemical modifications of these basic amino acid residues include methylation, phosphorylation and acetylation.[76] These chemical changes alter the strength of the interaction between the DNA and the histones, making the DNA more or less accessible to transcription factors and changing the rate of transcription.[77] Other non-specific DNA-binding proteins in chromatin include the high-mobility group proteins, which bind to bent or distorted DNA.[78] These proteins are important in bending arrays of nucleosomes and arranging them into the larger structures that make up chromosomes.[79]

A distinct group of DNA-binding proteins are the DNA-binding proteins that specifically bind single-stranded DNA. In humans, replication protein A is the best-understood member of this family and is used in processes where the double helix is separated, including DNA replication, recombination and DNA repair.[80] These binding proteins seem to stabilize single-stranded DNA and protect it from forming stem-loops or being degraded by nucleases.

In contrast, other proteins have evolved to bind to particular DNA sequences. The most intensively studied of these are the various transcription factors, which are proteins that regulate transcription. Each transcription factor binds to one particular set of DNA sequences and activates or inhibits the transcription of genes that have these sequences close to their promoters. The transcription factors do this in two ways. Firstly, they can bind the RNA polymerase responsible for transcription, either directly or through other mediator proteins; this locates the polymerase at the promoter and allows it to begin transcription.[82] Alternatively, transcription factors can bind enzymes that modify the histones at the promoter; this will change the accessibility of the DNA template to the polymerase.[83]

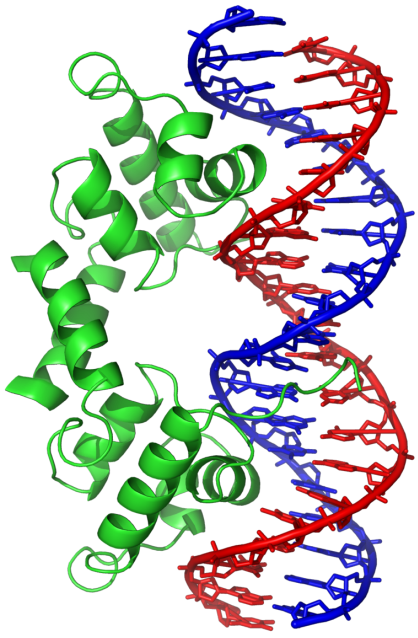

The lambda repressor helix-turn-helix transcription factor bound to its DNA target[81]

As these DNA targets can occur throughout an organism's genome, changes in the activity of one type of transcription factor can affect thousands of genes.[84] Consequently, these proteins are often the targets of the signal transduction processes that control responses to environmental changes or cellular differentiation and development. The specificity of these transcription

factors' interactions with DNA come from the proteins making multiple contacts to the edges of the DNA bases, allowing them to "read" the DNA sequence. Most of these base-interactions are made in the major groove, where the bases are most accessible.[85]

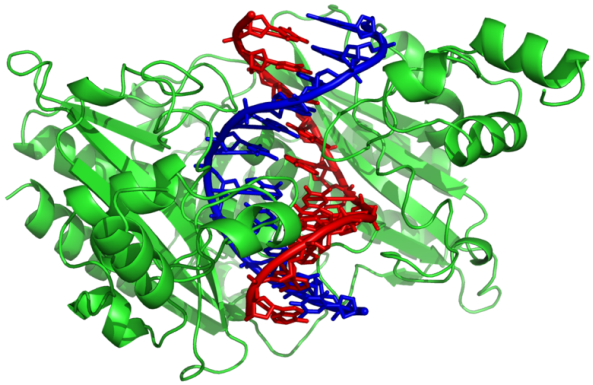

The restriction enzyme EcoRV (green) in a complex with its substrate DNA[86]

DNA-modifying enzymes

Nucleases and ligases

Nucleases are enzymes that cut DNA strands by catalyzing the hydrolysis of the phosphodiester bonds. Nucleases that hydrolyse nucleotides from the ends of DNA strands are called exonucleases, while endonucleases cut within strands. The most frequently used nucleases in molecular biology are the restriction endonucleases, which cut DNA at specific sequences. For instance, the EcoRV enzyme shown to the left recognizes the 6-base sequence 5′-GAT|ATC-3′ and makes a cut at the vertical line. In nature, these enzymes protect bacteria against phage infection by digesting the phage DNA when it enters the bacterial cell, acting as part of the restriction modification system.[87] In technology, these sequence-specific nucleases are used in molecular cloning and DNA fingerprinting.

Enzymes called DNA ligases can rejoin cut or broken DNA strands.[88] Ligases are particularly important in lagging strand DNA replication, as they join together the short segments of DNA produced at the replication fork into a complete copy of the DNA template. They are also used in DNA repair and genetic recombination.[88]

Topoisomerases and helicases

Topoisomerases are enzymes with both nuclease and ligase activity. These proteins change the amount of supercoiling in DNA. Some of these enzyme work by cutting the DNA helix and allowing one section to rotate, thereby reducing its level of supercoiling; the enzyme then seals the DNA break.[26] Other types of these enzymes are capable of cutting one DNA helix and then passing a second strand of DNA through this break, before rejoining the helix.[89] Topoisomerases are required for many processes involving DNA, such as DNA replication and transcription.[27]

Helicases are proteins that are a type of molecular motor. They use the chemical energy in nucleoside triphosphates, predominantly ATP, to break hydrogen bonds between bases and unwind the DNA double helix into single strands.[90] These enzymes are essential for most processes where enzymes need to access the DNA bases.

Polymerases

Polymerases are enzymes that synthesize polynucleotide chains from nucleoside triphosphates. The sequence of their products are copies of existing polynucleotide chains - which are called *templates*. These enzymes function by adding nucleotides onto the 3′ hydroxyl group of the previous nucleotide in a DNA strand. Consequently, all polymerases work in a 5′ to 3′ direction.[91] In the active site of these enzymes, the incoming nucleoside triphosphate base-pairs to the template: this allows polymerases to accurately synthesize the complementary strand of their template. Polymerases are classified according to the type of template that they use.

In DNA replication, a DNA-dependent DNA polymerase makes a copy of a DNA sequence. Accuracy is vital in this process, so many of these polymerases have a proofreading activity. Here, the polymerase recognizes the occasional mistakes in the synthesis reaction by the lack of base pairing between the mismatched nucleotides. If a mismatch is detected, a 3′ to 5′ exonuclease activity is activated and the incorrect base removed.[92] In most organisms DNA polymerases function in a large complex called the replisome that contains multiple accessory subunits, such as the DNA clamp or helicases.[93]

RNA-dependent DNA polymerases are a specialized class of polymerases that copy the sequence of an RNA strand into DNA. They include reverse transcriptase, which is a viral enzyme involved in the infection of cells by retroviruses, and telomerase, which is required for the replication of telomeres.[41] [94] Telomerase is an unusual polymerase because it contains its own RNA template as part of its structure.[42]

Transcription is carried out by a DNA-dependent RNA polymerase that copies the sequence of a DNA strand into RNA. To begin transcribing a gene, the RNA polymerase binds to a sequence of DNA called a promoter and separates the DNA strands. It then copies the gene sequence into a messenger RNA transcript until it reaches a region of DNA called the terminator, where it halts and detaches from the DNA. As with human DNA-dependent DNA polymerases, RNA polymerase II, the enzyme that transcribes most of the genes in the human genome, operates as part of a large protein complex with multiple regulatory and accessory subunits.[95]

Genetic recombination

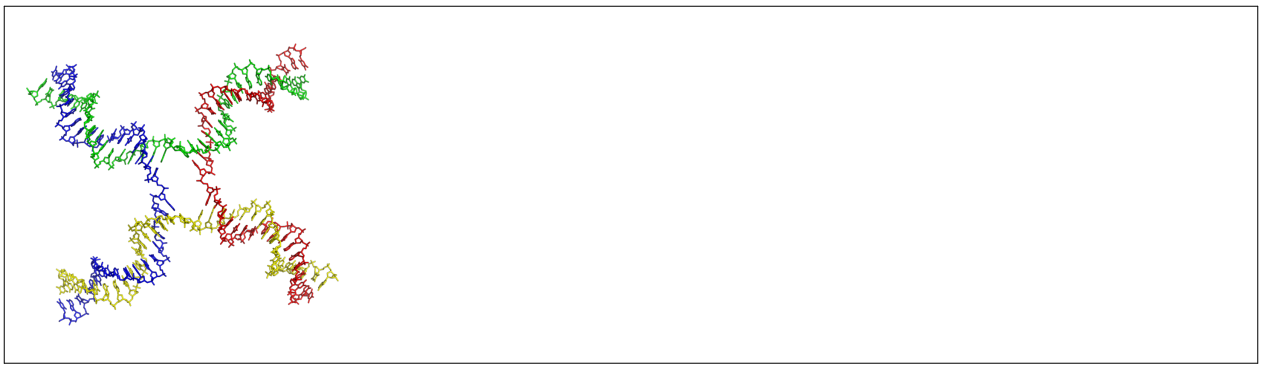

Structure of the Holliday junction intermediate in genetic recombination. The four separate DNA strands are coloured red, blue, green and yellow.[96]

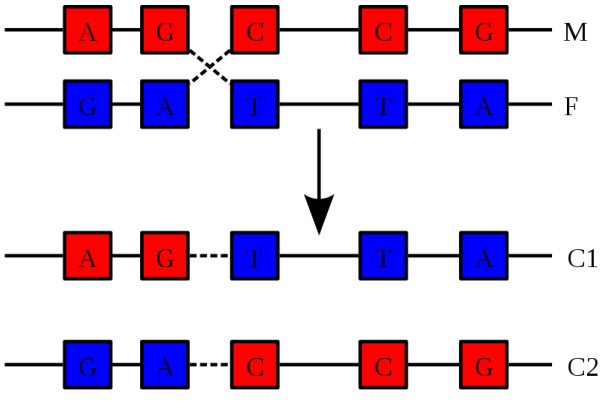

Recombination involves the breakage and rejoining of two chromosomes (M and F) to produce two re-arranged chromosomes (C1 and C2).

A DNA helix usually does not interact with other segments of DNA, and in human cells the different chromosomes even occupy separate areas in the nucleus called "chromosome territories".[97] This physical separation of different chromosomes is important for the ability of DNA to function as a stable repository for information, as one of the few times chromosomes interact is during chromosomal crossover when they recombine. Chromosomal crossover is when two DNA helices break, swap a section and then rejoin.

Recombination allows chromosomes to exchange genetic information and produces new combinations of genes, which increases the efficiency of natural selection and can be important in the rapid evolution of new proteins.[98] Genetic recombination can also be involved in DNA repair, particularly in the cell's response to double-strand breaks.[99]

The most common form of chromosomal crossover is homologous recombination, where the two chromosomes involved share very similar sequences. Non-homologous recombination can be damaging to cells, as it can produce chromosomal translocations and genetic abnormalities. The recombination reaction is catalyzed by enzymes known as *recombinases*, such as RAD51.[100] The first step in recombination is a double-stranded break either caused by an endonuclease or damage to the DNA.[101] A series of steps catalyzed in part by the recombinase then leads to joining of the two helices by at least one Holliday junction, in which a segment of a single strand in each helix is annealed to the complementary strand in the other helix. The Holliday junction is a tetrahedral junction structure that can be moved along the pair of chromosomes, swapping one strand for another. The recombination reaction is then halted by cleavage of the junction and re-ligation of the released DNA.[102]

Evolution

DNA contains the genetic information that allows all modern living things to function, grow and reproduce. However, it is unclear how long in the 4-billion-year history of life DNA has performed this function, as it has been proposed that the earliest forms of life may have used RNA as their genetic material.[91] [103] RNA may have acted as the central part of early cell metabolism as it can both transmit genetic information and carry out catalysis as part of ribozymes.[104] This ancient RNA world where nucleic acid would have been used for both catalysis and genetics may have influenced the evolution of the current genetic code based on four nucleotide bases. This would occur since the number of unique bases in such an organism is a trade-off between a small number of bases increasing replication accuracy and a large number of bases increasing the catalytic efficiency of ribozymes.[105]

Unfortunately, there is no direct evidence of ancient genetic systems, as recovery of DNA from most fossils is impossible. This is because DNA will survive in the environment for less than one million years and slowly degrades into short fragments in solution.[106] Claims for older DNA have been made, most notably a report of the isolation of a viable bacterium from a salt crystal 250-million years old,[107] but these claims are controversial.[108] [109]

Uses in technology

Genetic engineering

Methods have been developed to purify DNA from organisms, such as phenol-chloroform extraction and manipulate it in the laboratory, such as restriction digests and the polymerase chain reaction. Modern biology and biochemistry make intensive use of these techniques in recombinant DNA technology. Recombinant DNA is a man-made DNA sequence that has been assembled from other DNA sequences. They can be transformed into organisms in the form of plasmids or in the appropriate format, by using a viral vector.[110] The genetically modified organisms produced can be used to produce products such as recombinant proteins, used in medical research,[111] or be grown in agriculture.[112] [113]

Forensics

Forensic scientists can use DNA in blood, semen, skin, saliva or hair found at a crime scene to identify a matching DNA of an individual, such as a perpetrator. This process is called genetic fingerprinting, or more accurately, DNA profiling. In DNA profiling, the lengths of variable sections of repetitive DNA, such as short tandem repeats and minisatellites, are compared between people. This method is usually an extremely reliable technique for identifying a matching DNA.[114] However, identification can be complicated if the scene is contaminated with DNA from several people.[115] DNA profiling was developed in 1984 by British geneticist Sir Alec Jeffreys,[116] and first used in forensic science to convict Colin Pitchfork in the 1988 Enderby murders case.[117]

People convicted of certain types of crimes may be required to provide a sample of DNA for a database. This has helped investigators solve old cases where only a DNA sample was obtained from the scene. DNA profiling can also be used to identify victims of mass casualty incidents.[118] On the other hand, many convicted people have been released from prison on the basis of DNA techniques, which were not available when a crime had originally been committed.

Bioinformatics

Bioinformatics involves the manipulation, searching, and data mining of DNA sequence data. The development of techniques to store and search DNA sequences have led to widely applied advances in computer science, especially string searching algorithms, machine learning and database theory.[119] String searching or matching algorithms, which find an occurrence of a sequence of letters inside a larger sequence of letters, were developed to search for specific sequences of nucleotides.[120] In other applications such as text editors, even simple algorithms for this problem usually suffice, but DNA sequences cause these algorithms to exhibit near-worst-case behaviour due to their small number of distinct characters. The related problem of sequence alignment aims to identify homologous sequences and locate the specific mutations that make them distinct. These techniques, especially multiple sequence alignment, are used in studying phylogenetic relationships and protein function.[121] Data sets representing entire genomes' worth of DNA sequences, such as those produced by the Human Genome Project, are difficult to use without annotations, which label the locations of genes and regulatory elements on each chromosome. Regions of DNA sequence that have the characteristic patterns associated with protein- or RNA-coding genes can be identified by gene finding algorithms, which allow researchers to predict the presence of particular gene products in an organism even before they have been isolated experimentally.[122]

DNA nanotechnology

DNA nanotechnology uses the unique molecular recognition properties of DNA and other nucleic acids to create self-assembling branched DNA complexes with useful properties.[124] DNA is thus used as a structural material rather than as a carrier of biological information. This has led to the creation of two-dimensional periodic lattices (both tile-based as well as using the "DNA origami" method) as well as three-dimensional structures in the shapes of polyhedra.[125] Nanomechanical devices and algorithmic self-assembly have also been demonstrated,[126] and these DNA structures have been used to template the arrangement of other molecules such as gold nanoparticles and streptavidin proteins.[127]

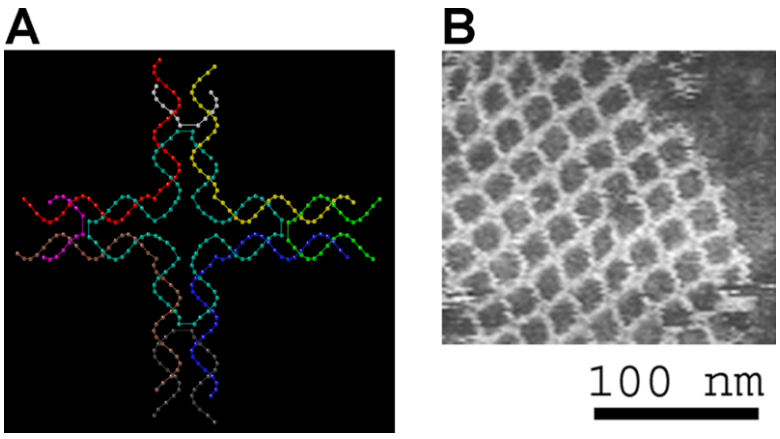

The DNA structure at left (schematic shown) will self-assemble into the structure visualized by atomic force microscopy at right. DNA nanotechnology is the field which seeks to design nanoscale structures using the molecular recognition properties of DNA molecules. Image from Strong, 2004.[123]

History and anthropology

Because DNA collects mutations over time, which are then inherited, it contains historical information and by comparing DNA sequences, geneticists can infer the evolutionary history of organisms, their phylogeny.[128] This field of phylogenetics is a powerful tool in evolutionary biology. If DNA sequences within a species are compared, population geneticists can learn the history of particular populations. This can be used in studies ranging from ecological genetics to anthropology; for example, DNA evidence is being used to try to identify the Ten Lost Tribes of Israel.[129] [130]

DNA has also been used to look at modern family relationships, such as establishing family relationships between the descendants of Sally Hemings and Thomas Jefferson. This usage is closely related to the use of DNA in criminal investigations detailed above. Indeed, some criminal investigations have been solved when DNA from crime scenes has matched relatives of the guilty individual.[131]

History of DNA research

DNA was first isolated by the Swiss physician Friedrich Miescher who, in 1869, discovered a microscopic substance in the pus of discarded surgical bandages. As it resided in the nuclei of cells, he called it "nuclein".[132] In 1919, Phoebus Levene identified the base, sugar and phosphate nucleotide unit.[133] Levene suggested that DNA consisted of a string of nucleotide units linked together through the phosphate groups. However, Levene thought the chain was short and the bases repeated in a fixed order. In 1937 William Astbury produced the first X-ray diffraction patterns that showed that DNA had a regular structure.[134]

In 1928, Frederick Griffith discovered that traits of the "smooth" form of the *Pneumococcus* could be transferred to the "rough" form of the same bacteria by mixing killed "smooth" bacteria with the live "rough" form.[135] This system provided the first clear suggestion that DNA carried genetic information—the Avery-MacLeod-McCarty experiment—when Oswald Avery, along with coworkers Colin MacLeod and Maclyn McCarty, identified DNA as the transforming principle in 1943.[136] DNA's role in heredity was confirmed in 1952, when Alfred Hershey and Martha Chase in the Hershey-Chase experiment showed that DNA is the genetic material of the T2 phage.[137]

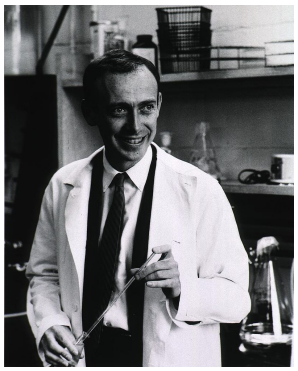

James D. Watson

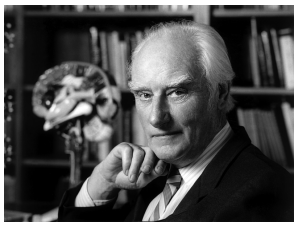

Francis Crick

Francis Crick

Rosalind Franklin

Raymond Gosling

Maurice F. Wilkins

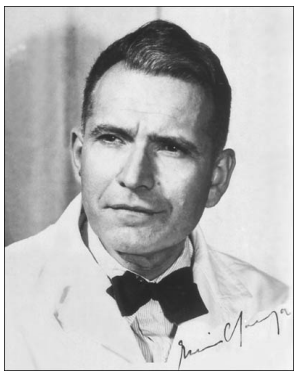

Erwin Chargaff

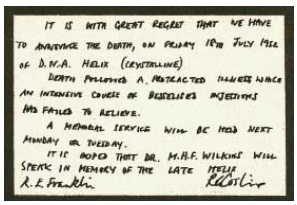

IT IS WITH GREAT REGRET THAT WE HAVE TO ANNOUNCE THE DEATH, ON FRIDAY 16TH JULY 1958 OF D.N.A. HELIX (CRYSTALLINE)
DEATH FOLLOWED A PROTRACTED ILLNESS WHICH AN INTENSIVE COURSE OF BIOLOGICAL INJECTIONS HAS FAILED TO RELIEVE.
A MEMORIAL SERVICE WILL BE HELD NEXT MONDAY OR TUESDAY.
IT IS HOPED THAT DR. M.H.F. WILKINS WILL SPEAK IN MEMORY OF THE LATE MISS R.E. Franklin

DNA Helix controversy

In 1953 James D. Watson and Francis Crick suggested what is now accepted as the first correct double-helix model of DNA structure in the journal *Nature*.[7] Their double-helix, molecular model of DNA was then based on a single X-ray diffraction image (labeled as "Photo 51")[138] taken by Rosalind Franklin and Raymond Gosling in May 1952, as well as the information that the DNA bases were paired—also obtained through private communications from Erwin Chargaff in the previous years. Chargaff's rules played a very important role in establishing double-helix configurations for B-DNA as well as A-DNA.

Experimental evidence supporting the Watson and Crick model were published in a series of five articles in the same issue of *Nature*.[139] Of these, Franklin and Gosling's paper was the first publication of their own X-ray diffraction data and original analysis method that partially supported the Watson and Crick model[30] [140] ; this issue also contained an article on DNA structure by Maurice Wilkins and two of his colleagues, whose analysis and *in vivo* B-DNA X-ray patterns also supported the presence *in vivo* of the double-helical DNA configurations as proposed by Crick and Watson for their double-helix molecular model of DNA in the previous two pages of *Nature*.[31] In 1962, after Franklin's death, Watson, Crick, and Wilkins jointly received the Nobel Prize in Physiology or Medicine.[141] Unfortunately, Nobel rules of the time allowed only living recipients, but a vigorous debate continues on who should receive credit for the discovery.[142]

In an influential presentation in 1957, Crick laid out the "Central Dogma" of molecular biology, which foretold the relationship between DNA, RNA, and proteins, and articulated the "adaptor hypothesis".[143] Final confirmation of the replication mechanism that was implied by the double-helical structure followed in 1958 through the Meselson-Stahl experiment.[144] Further work by Crick and coworkers showed that the genetic code was based on non-overlapping triplets of bases, called codons, allowing Har Gobind Khorana, Robert W. Holley and Marshall Warren Nirenberg to decipher the genetic code.[145] These findings represent the birth of molecular biology.

See also

- Molecular Structure of Nucleic Acids: A Structure for Deoxyribose Nucleic Acid
- Molecular models of DNA
- DNA microarray
- DNA sequencing
- Paracrystal model and theory
- X-ray scattering
- Crystallography
- X-ray crystallography
- Genetic disorder
- Junk DNA
- Nucleic acid analogues
- Nucleic acid methods
- Nucleic acid modeling
- Nucleic Acid Notations
- Phosphoramidite
- Plasmid
- Polymerase chain reaction
- *Proteopedia DNA* [146]
- Southern blot
- Triple-stranded DNA

Notes

[1] Russell, Peter (2001). *iGenetics*. New York: Benjamin Cummings. ISBN 0-805-34553-1.

[2] Saenger, Wolfram (1984). *Principles of Nucleic Acid Structure*. New York: Springer-Verlag. ISBN 0387907629.

[3] Alberts, Bruce; Alexander Johnson, Julian Lewis, Martin Raff, Keith Roberts, and Peter Walters (2002). *http://www.ncbi.nlm.nih.gov/books/bv.fcgi?call=bv.View..ShowTOC&rid=mboc4.TOC&depth=2|Molecular Biology of the Cell; Fourth Edition*. New York and London: Garland Science. ISBN 0-8153-3218-1. OCLC 145080076 48122761 57023651 69932405 (http://worldcat.org/oclc/145080076+48122761+57023651+69932405). http://www.ncbi.nlm.nih.gov/books/bv.fcgi?call=bv.View..ShowTOC&rid=mboc4.TOC&depth=2.

[4] Butler, John M. (2001). *Forensic DNA Typing*. Elsevier. ISBN 978-0-12-147951-0. OCLC 223032110 45406517 (http://worldcat.org/oclc/223032110+45406517). pp. 14–15.

[5] Mandelkern M, Elias J, Eden D, Crothers D (1981). "The dimensions of DNA in solution". *J Mol Biol* **152** (1): 153–61. doi: 10.1016/0022-2836(81)90099-1 (http://dx.doi.org/10.1016/0022-2836(81)90099-1). PMID 7338906.

[6] Gregory S, *et al.* (2006). "The DNA sequence and biological annotation of human chromosome 1". *Nature* **441** (7091): 315–21. doi: 10.1038/nature04727 (http://dx.doi.org/10.1038/nature04727). PMID 16710414.

[7] Watson J.D. and Crick F.H.C. (1953). "http://www.nature.com/nature/dna50/watsoncrick.pdf|A Structure for Deoxyribose Nucleic Acid" (PDF). *Nature* **171**: 737–738. doi: 10.1038/171737a0 (http://dx.doi.org/10.1038/171737a0). PMID 13054692. http://www.nature.com/nature/dna50/watsoncrick.pdf. Retrieved on 4 May 2009.

[8] Berg J., Tymoczko J. and Stryer L. (2002) *Biochemistry.* W. H. Freeman and Company ISBN 0-7167-4955-6

[9] Abbreviations and Symbols for Nucleic Acids, Polynucleotides and their Constituents (http://www.chem.qmul.ac.uk/iupac/misc/naabb.html) IUPAC-IUB Commission on Biochemical Nomenclature (CBN), Accessed 03 January 2006

[10] Ghosh A, Bansal M (2003). "A glossary of DNA structures from A to Z". *Acta Crystallogr D Biol Crystallogr* **59** (Pt 4): 620–6. doi: 10.1107/S0907444903003251 (http://dx.doi.org/10.1107/S0907444903003251). PMID 12657780.

[11] Created from PDB 1D65 (http://www.rcsb.org/pdb/cgi/explore.cgi?pdbId=1D65)

[12] Wing R, Drew H, Takano T, Broka C, Tanaka S, Itakura K, Dickerson R (1980). "Crystal structure analysis of a complete turn of B-DNA". *Nature* **287** (5784): 755–8. doi: 10.1038/287755a0 (http://dx.doi.org/10.1038/

287755a0). PMID 7432492.
[13] Pabo C, Sauer R (1984). "Protein-DNA recognition". *Annu Rev Biochem* **53**: 293–321. doi: 10.1146/annurev.bi.53.070184.001453 (http://dx.doi.org/10.1146/annurev.bi.53.070184.001453). PMID 6236744.
[14] Clausen-Schaumann H, Rief M, Tolksdorf C, Gaub H (2000). "http://www.pubmedcentral.nih.gov/articlerender.fcgi?tool=pmcentrez&artid=1300792|Mechanical stability of single DNA molecules". *Biophys J* **78** (4): 1997–2007. doi: 10.1016/S0006-3495(00)76747-6 (http://dx.doi.org/10.1016/S0006-3495(00)76747-6). PMID 10733978.
[15] Yakovchuk P, Protozanova E, Frank-Kamenetskii MD (2006). "http://nar.oxfordjournals.org/cgi/pmidlookup?view=long&pmid=16449200|Base-stacking and base-pairing contributions into thermal stability of the DNA double helix". *Nucleic Acids Res.* **34** (2): 564–74. doi: 10.1093/nar/gkj454 (http://dx.doi.org/10.1093/nar/gkj454). PMID 16449200. PMC: 1360284 (http://www.pubmedcentral.nih.gov/articlerender.fcgi?tool=pmcentrez&artid=1360284). http://nar.oxfordjournals.org/cgi/pmidlookup?view=long&pmid=16449200.
[16] Chalikian T, Völker J, Plum G, Breslauer K (1999). "http://www.pubmedcentral.nih.gov/articlerender.fcgi?tool=pmcentrez&artid=22151|A more unified picture for the thermodynamics of nucleic acid duplex melting: a characterization by calorimetric and volumetric techniques". *Proc Natl Acad Sci USA* **96** (14): 7853–8. doi: 10.1073/pnas.96.14.7853 (http://dx.doi.org/10.1073/pnas.96.14.7853). PMID 10393911.
[17] deHaseth P, Helmann J (1995). "Open complex formation by Escherichia coli RNA polymerase: the mechanism of polymerase-induced strand separation of double helical DNA". *Mol Microbiol* **16** (5): 817–24. doi: 10.1111/j.1365-2958.1995.tb02309.x (http://dx.doi.org/10.1111/j.1365-2958.1995.tb02309.x). PMID 7476180.
[18] Isaksson J, Acharya S, Barman J, Cheruku P, Chattopadhyaya J (2004). "Single-stranded adenine-rich DNA and RNA retain structural characteristics of their respective double-stranded conformations and show directional differences in stacking pattern". *Biochemistry* **43** (51): 15996–6010. doi: 10.1021/bi048221v (http://dx.doi.org/10.1021/bi048221v). PMID 15609994.
[19] Designation of the two strands of DNA (http://www.chem.qmul.ac.uk/iubmb/newsletter/misc/DNA.html) JCBN/NC-IUB Newsletter 1989, Accessed 07 May 2008
[20] Hüttenhofer A, Schattner P, Polacek N (2005). "Non-coding RNAs: hope or hype?". *Trends Genet* **21** (5): 289–97. doi: 10.1016/j.tig.2005.03.007 (http://dx.doi.org/10.1016/j.tig.2005.03.007). PMID 15851066.
[21] Munroe S (2004). "Diversity of antisense regulation in eukaryotes: multiple mechanisms, emerging patterns". *J Cell Biochem* **93** (4): 664–71. doi: 10.1002/jcb.20252 (http://dx.doi.org/10.1002/jcb.20252). PMID 15389973.
[22] Makalowska I, Lin C, Makalowski W (2005). "Overlapping genes in vertebrate genomes". *Comput Biol Chem* **29** (1): 1–12. doi: 10.1016/j.compbiolchem.2004.12.006 (http://dx.doi.org/10.1016/j.compbiolchem.2004.12.006). PMID 15680581.
[23] Johnson Z, Chisholm S (2004). "Properties of overlapping genes are conserved across microbial genomes". *Genome Res* **14** (11): 2268–72. doi: 10.1101/gr.2433104 (http://dx.doi.org/10.1101/gr.2433104). PMID 15520290.
[24] Lamb R, Horvath C (1991). "Diversity of coding strategies in influenza viruses". *Trends Genet* **7** (8): 261–6. PMID 1771674.
[25] Benham C, Mielke S (2005). "DNA mechanics". *Annu Rev Biomed Eng* **7**: 21–53. doi: 10.1146/annurev.bioeng.6.062403.132016 (http://dx.doi.org/10.1146/annurev.bioeng.6.062403.132016). PMID 16004565.
[26] Champoux J (2001). "DNA topoisomerases: structure, function, and mechanism". *Annu Rev Biochem* **70**: 369–413. doi: 10.1146/annurev.biochem.70.1.369 (http://dx.doi.org/10.1146/annurev.biochem.70.1.369). PMID 11395412.
[27] Wang J (2002). "Cellular roles of DNA topoisomerases: a molecular perspective". *Nat Rev Mol Cell Biol* **3** (6): 430–40. doi: 10.1038/nrm831 (http://dx.doi.org/10.1038/nrm831). PMID 12042765.
[28] Basu H, Feuerstein B, Zarling D, Shafer R, Marton L (1988). "Recognition of Z-RNA and Z-DNA determinants by polyamines in solution: experimental and theoretical studies". *J Biomol Struct Dyn* **6** (2): 299–309. PMID 2482766.
[29] Franklin RE, Gosling RG (6 March 1953). "http://hekto.med.unc.edu:8080/CARTER/carter_WWW/Bioch_134/PDF_files/Franklin_Gossling.pdf|The Structure of Sodium Thymonucleate Fibres I. The Influence of Water Content". *Acta Cryst* **6** (8-9): 673–7. doi: 10.1107/S0365110X53001939 (http://dx.doi.org/10.1107/S0365110X53001939). http://hekto.med.unc.edu:8080/CARTER/carter_WWW/Bioch_134/PDF_files/Franklin_Gossling.pdf.
Franklin RE, Gosling RG (September 1953). "The structure of sodium thymonucleate fibres. II. The cylindrically

symmetrical Patterson function". *Acta Cryst* **6** (8-9): 678–85. doi: 10.1107/S0365110X53001940 (http://dx.doi.org/10.1107/S0365110X53001940).

[30] Franklin, Rosalind and Gosling, Raymond (1953). "http://www.nature.com/nature/dna50/franklingosling.pdf|Molecular Configuration in Sodium Thymonucleate. Franklin R. and Gosling R.G" (PDF). *Nature* **171**: 740–1. doi: 10.1038/171740a0 (http://dx.doi.org/10.1038/171740a0). PMID 13054694. http://www.nature.com/nature/dna50/franklingosling.pdf.

[31] Wilkins M.H.F., A.R. Stokes A.R. & Wilson, H.R. (1953). "http://www.nature.com/nature/dna50/wilkins.pdf|Molecular Structure of Deoxypentose Nucleic Acids" (PDF). *Nature* **171**: 738–740. doi: 10.1038/171738a0 (http://dx.doi.org/10.1038/171738a0). PMID 13054693. http://www.nature.com/nature/dna50/wilkins.pdf.

[32] Leslie AG, Arnott S, Chandrasekaran R, Ratliff RL (1980). "Polymorphism of DNA double helices". *J. Mol. Biol.* **143** (1): 49–72. doi: 10.1016/0022-2836(80)90124-2 (http://dx.doi.org/10.1016/0022-2836(80)90124-2). PMID 7441761.

[33] Baianu, I.C. (1980). "Structural Order and Partial Disorder in Biological systems". *Bull. Math. Biol.* **42** (4): 137–141. http://cogprints.org/3822/

[34] Hosemann R., Bagchi R.N., *Direct analysis of diffraction by matter*, North-Holland Publs., Amsterdam – New York, 1962.

[35] Baianu, I.C. (1978). "X-ray scattering by partially disordered membrane systems.". *Acta Cryst.,* **A34** (5): 751–753. doi: 10.1107/S0567739478001540 (http://dx.doi.org/10.1107/S0567739478001540).

[36] Wahl M, Sundaralingam M (1997). "Crystal structures of A-DNA duplexes". *Biopolymers* **44** (1): 45–63. doi:10.1002/(SICI)1097-0282(1997)44:1 (inactive 2009-03-14) . PMID 9097733.

[37] Lu XJ, Shakked Z, Olson WK (2000). "A-form conformational motifs in ligand-bound DNA structures". *J. Mol. Biol.* **300** (4): 819–40. doi: 10.1006/jmbi.2000.3690 (http://dx.doi.org/10.1006/jmbi.2000.3690). PMID 10891271.

[38] Rothenburg S, Koch-Nolte F, Haag F (2001). "DNA methylation and Z-DNA formation as mediators of quantitative differences in the expression of alleles". *Immunol Rev* **184**: 286–98. doi: 10.1034/j.1600-065x.2001.1840125.x (http://dx.doi.org/10.1034/j.1600-065x.2001.1840125.x). PMID 12086319.

[39] Oh D, Kim Y, Rich A (2002). "http://www.pnas.org/cgi/pmidlookup?view=long&pmid=12486233|Z-DNA-binding proteins can act as potent effectors of gene expression in vivo". *Proc. Natl. Acad. Sci. U.S.A.* **99** (26): 16666–71. doi: 10.1073/pnas.262672699 (http://dx.doi.org/10.1073/pnas.262672699). PMID 12486233. PMC: 139201 (http://www.pubmedcentral.nih.gov/articlerender.fcgi?tool=pmcentrez&artid=139201). http://www.pnas.org/cgi/pmidlookup?view=long&pmid=12486233.

[40] Created from NDB UD0017 (http://ndbserver.rutgers.edu/atlas/xray/structures/U/ud0017/ud0017.html)

[41] Greider C, Blackburn E (1985). "Identification of a specific telomere terminal transferase activity in Tetrahymena extracts". *Cell* **43** (2 Pt 1): 405–13. doi: 10.1016/0092-8674(85)90170-9 (http://dx.doi.org/10.1016/0092-8674(85)90170-9). PMID 3907856.

[42] Nugent C, Lundblad V (1998). "http://www.genesdev.org/cgi/content/full/12/8/1073|The telomerase reverse transcriptase: components and regulation". *Genes Dev* **12** (8): 1073–85. doi: 10.1101/gad.12.8.1073 (http://dx.doi.org/10.1101/gad.12.8.1073). PMID 9553037. http://www.genesdev.org/cgi/content/full/12/8/1073.

[43] Wright W, Tesmer V, Huffman K, Levene S, Shay J (1997). "http://www.genesdev.org/cgi/content/full/11/21/2801|Normal human chromosomes have long G-rich telomeric overhangs at one end". *Genes Dev* **11** (21): 2801–9. doi: 10.1101/gad.11.21.2801 (http://dx.doi.org/10.1101/gad.11.21.2801). PMID 9353250. http://www.genesdev.org/cgi/content/full/11/21/2801.

[44] Burge S, Parkinson G, Hazel P, Todd A, Neidle S (2006). "http://nar.oxfordjournals.org/cgi/pmidlookup?view=long&pmid=17012276|Quadruplex DNA: sequence, topology and structure". *Nucleic Acids Res* **34** (19): 5402–15. doi: 10.1093/nar/gkl655 (http://dx.doi.org/10.1093/nar/gkl655). PMID 17012276. PMC: 1636468 (http://www.pubmedcentral.nih.gov/articlerender.fcgi?tool=pmcentrez&artid=1636468). http://nar.oxfordjournals.org/cgi/pmidlookup?view=long&pmid=17012276.

[45] Parkinson G, Lee M, Neidle S (2002). "Crystal structure of parallel quadruplexes from human telomeric DNA". *Nature* **417** (6891): 876–80. doi: 10.1038/nature755 (http://dx.doi.org/10.1038/nature755). PMID 12050675.

[46] Griffith J, Comeau L, Rosenfield S, Stansel R, Bianchi A, Moss H, de Lange T (1999). "Mammalian telomeres end in a large duplex loop". *Cell* **97** (4): 503–14. doi: 10.1016/S0092-8674(00)80760-6 (http://dx.doi.org/10.1016/S0092-8674(00)80760-6). PMID 10338214.

[47] Seeman NC (November 2005). "DNA enables nanoscale control of the structure of matter". *Q. Rev. Biophys.* **38** (4): 363–71. doi: 10.1017/S0033583505004087 (http://dx.doi.org/10.1017/S0033583505004087). PMID 16515737.
[48] Klose R, Bird A (2006). "Genomic DNA methylation: the mark and its mediators". *Trends Biochem Sci* **31** (2): 89–97. doi: 10.1016/j.tibs.2005.12.008 (http://dx.doi.org/10.1016/j.tibs.2005.12.008). PMID 16403636.
[49] Bird A (2002). "DNA methylation patterns and epigenetic memory". *Genes Dev* **16** (1): 6–21. doi: 10.1101/gad.947102 (http://dx.doi.org/10.1101/gad.947102). PMID 11782440.
[50] Walsh C, Xu G (2006). "Cytosine methylation and DNA repair". *Curr Top Microbiol Immunol* **301**: 283–315. doi: 10.1007/3-540-31390-7_11 (http://dx.doi.org/10.1007/3-540-31390-7_11). PMID 16570853.
[51] Kriaucionis S, Heintz N (May 2009). "The nuclear DNA base 5-hydroxymethylcytosine is present in Purkinje neurons and the brain". *Science* **324** (5929): 929–30. doi: 10.1126/science.1169786 (http://dx.doi.org/10.1126/science.1169786). PMID 19372393.
[52] Ratel D, Ravanat J, Berger F, Wion D (2006). "N6-methyladenine: the other methylated base of DNA". *Bioessays* **28** (3): 309–15. doi: 10.1002/bies.20342 (http://dx.doi.org/10.1002/bies.20342). PMID 16479578.
[53] Gommers-Ampt J, Van Leeuwen F, de Beer A, Vliegenthart J, Dizdaroglu M, Kowalak J, Crain P, Borst P (1993). "beta-D-glucosyl-hydroxymethyluracil: a novel modified base present in the DNA of the parasitic protozoan T. brucei". *Cell* **75** (6): 1129–36. doi: 10.1016/0092-8674(93)90322-H (http://dx.doi.org/10.1016/0092-8674(93)90322-H). PMID 8261512.
[54] Created from PDB 1JDG (http://www.rcsb.org/pdb/cgi/explore.cgi?pdbId=1JDG)
[55] Douki T, Reynaud-Angelin A, Cadet J, Sage E (2003). "Bipyrimidine photoproducts rather than oxidative lesions are the main type of DNA damage involved in the genotoxic effect of solar UVA radiation". *Biochemistry* **42** (30): 9221–6. doi: 10.1021/bi034593c (http://dx.doi.org/10.1021/bi034593c). PMID 12885257.,
[56] Cadet J, Delatour T, Douki T, Gasparutto D, Pouget J, Ravanat J, Sauvaigo S (1999). "Hydroxyl radicals and DNA base damage". *Mutat Res* **424** (1–2): 9–21. PMID 10064846.
[57] Beckman KB, Ames BN (August 1997). "http://www.jbc.org/cgi/pmidlookup?view=long&pmid=9289489|Oxidative decay of DNA". *J. Biol. Chem.* **272** (32): 19633–6. PMID 9289489. http://www.jbc.org/cgi/pmidlookup?view=long&pmid=9289489.
[58] Valerie K, Povirk L (2003). "Regulation and mechanisms of mammalian double-strand break repair". *Oncogene* **22** (37): 5792–812. doi: 10.1038/sj.onc.1206679 (http://dx.doi.org/10.1038/sj.onc.1206679). PMID 12947387.
[59] Ferguson L, Denny W (1991). "The genetic toxicology of acridines". *Mutat Res* **258** (2): 123–60. PMID 1881402.
[60] Jeffrey A (1985). "DNA modification by chemical carcinogens". *Pharmacol Ther* **28** (2): 237–72. doi: 10.1016/0163-7258(85)90013-0 (http://dx.doi.org/10.1016/0163-7258(85)90013-0). PMID 3936066.
[61] Stephens T, Bunde C, Fillmore B (2000). "Mechanism of action in thalidomide teratogenesis". *Biochem Pharmacol* **59** (12): 1489–99. doi: 10.1016/S0006-2952(99)00388-3 (http://dx.doi.org/10.1016/S0006-2952(99)00388-3). PMID 10799645.
[62] Braña M, Cacho M, Gradillas A, de Pascual-Teresa B, Ramos A (2001). "Intercalators as anticancer drugs". *Curr Pharm Des* **7** (17): 1745–80. doi: 10.2174/1381612013397113 (http://dx.doi.org/10.2174/1381612013397113). PMID 11562309.
[63] Venter J, *et al.* (2001). "The sequence of the human genome". *Science* **291** (5507): 1304–51. doi: 10.1126/science.1058040 (http://dx.doi.org/10.1126/science.1058040). PMID 11181995.
[64] Thanbichler M, Wang S, Shapiro L (2005). "The bacterial nucleoid: a highly organized and dynamic structure". *J Cell Biochem* **96** (3): 506–21. doi: 10.1002/jcb.20519 (http://dx.doi.org/10.1002/jcb.20519). PMID 15988757.
[65] Wolfsberg T, McEntyre J, Schuler G (2001). "Guide to the draft human genome". *Nature* **409** (6822): 824–6. doi: 10.1038/35057000 (http://dx.doi.org/10.1038/35057000). PMID 11236998.
[66] Gregory T (2005). "http://aob.oxfordjournals.org/cgi/content/full/95/1/133|The C-value enigma in plants and animals: a review of parallels and an appeal for partnership". *Ann Bot (Lond)* **95** (1): 133–46. doi: 10.1093/aob/mci009 (http://dx.doi.org/10.1093/aob/mci009). PMID 15596463. http://aob.oxfordjournals.org/cgi/content/full/95/1/133.
[67] The ENCODE Project Consortium (2007). "Identification and analysis of functional elements in 1% of the human genome by the ENCODE pilot project". *Nature* **447** (7146): 799–816. doi: 10.1038/nature05874 (http://dx.doi.org/10.1038/nature05874).
[68] Created from PDB 1MSW (http://www.rcsb.org/pdb/explore/explore.do?structureId=1MSW)
[69] Pidoux A, Allshire R (2005). "http://www.pubmedcentral.nih.gov/articlerender.fcgi?tool=pmcentrez&artid=1569473|The role of heterochromatin in centromere function". *Philos Trans R Soc Lond B Biol Sci* **360** (1455): 569–79. doi: 10.1098/rstb.2004.1611 (http://dx.doi.org/10.1098/rstb.2004.1611). PMID 15905142.

[70] Harrison P, Hegyi H, Balasubramanian S, Luscombe N, Bertone P, Echols N, Johnson T, Gerstein M (2002). "http://www.genome.org/cgi/content/full/12/2/272|Molecular fossils in the human genome: identification and analysis of the pseudogenes in chromosomes 21 and 22". *Genome Res* **12** (2): 272–80. doi: 10.1101/gr.207102 (http://dx.doi.org/10.1101/gr.207102). PMID 11827946. http://www.genome.org/cgi/content/full/12/2/272.

[71] Harrison P, Gerstein M (2002). "Studying genomes through the aeons: protein families, pseudogenes and proteome evolution". *J Mol Biol* **318** (5): 1155–74. doi: 10.1016/S0022-2836(02)00109-2 (http://dx.doi.org/10.1016/S0022-2836(02)00109-2). PMID 12083509.

[72] Albà M (2001). "http://genomebiology.com/1465-6906/2/REVIEWS3002|Replicative DNA polymerases". *Genome Biol* **2** (1): REVIEWS3002. doi: 10.1186/gb-2001-2-1-reviews3002 (http://dx.doi.org/10.1186/gb-2001-2-1-reviews3002). PMID 11178285. PMC: 150442 (http://www.pubmedcentral.nih.gov/articlerender.fcgi?tool=pmcentrez&artid=150442). http://genomebiology.com/1465-6906/2/REVIEWS3002.

[73] Sandman K, Pereira S, Reeve J (1998). "Diversity of prokaryotic chromosomal proteins and the origin of the nucleosome". *Cell Mol Life Sci* **54** (12): 1350–64. doi: 10.1007/s000180050259 (http://dx.doi.org/10.1007/s000180050259). PMID 9893710.

[74] Dame RT (2005). "The role of nucleoid-associated proteins in the organization and compaction of bacterial chromatin". *Mol. Microbiol.* **56** (4): 858–70. doi: 10.1111/j.1365-2958.2005.04598.x (http://dx.doi.org/10.1111/j.1365-2958.2005.04598.x). PMID 15853876.

[75] Luger K, Mäder A, Richmond R, Sargent D, Richmond T (1997). "Crystal structure of the nucleosome core particle at 2.8 A resolution". *Nature* **389** (6648): 251–60. doi: 10.1038/38444 (http://dx.doi.org/10.1038/38444). PMID 9305837.

[76] Jenuwein T, Allis C (2001). "Translating the histone code". *Science* **293** (5532): 1074–80. doi: 10.1126/science.1063127 (http://dx.doi.org/10.1126/science.1063127). PMID 11498575.

[77] Ito T. "Nucleosome assembly and remodelling". *Curr Top Microbiol Immunol* **274**: 1–22. PMID 12596902.

[78] Thomas J (2001). "HMG1 and 2: architectural DNA-binding proteins". *Biochem Soc Trans* **29** (Pt 4): 395–401. doi: 10.1042/BST0290395 (http://dx.doi.org/10.1042/BST0290395). PMID 11497996.

[79] Grosschedl R, Giese K, Pagel J (1994). "HMG domain proteins: architectural elements in the assembly of nucleoprotein structures". *Trends Genet* **10** (3): 94–100. doi: 10.1016/0168-9525(94)90232-1 (http://dx.doi.org/10.1016/0168-9525(94)90232-1). PMID 8178371.

[80] Iftode C, Daniely Y, Borowiec J (1999). "Replication protein A (RPA): the eukaryotic SSB". *Crit Rev Biochem Mol Biol* **34** (3): 141–80. doi: 10.1080/10409239991209255 (http://dx.doi.org/10.1080/10409239991209255). PMID 10473346.

[81] Created from PDB 1LMB (http://www.rcsb.org/pdb/explore/explore.do?structureId=1LMB)

[82] Myers L, Kornberg R (2000). "Mediator of transcriptional regulation". *Annu Rev Biochem* **69**: 729–49. doi: 10.1146/annurev.biochem.69.1.729 (http://dx.doi.org/10.1146/annurev.biochem.69.1.729). PMID 10966474.

[83] Spiegelman B, Heinrich R (2004). "Biological control through regulated transcriptional coactivators". *Cell* **119** (2): 157–67. doi: 10.1016/j.cell.2004.09.037 (http://dx.doi.org/10.1016/j.cell.2004.09.037). PMID 15479634.

[84] Li Z, Van Calcar S, Qu C, Cavenee W, Zhang M, Ren B (2003). "http://www.pnas.org/cgi/pmidlookup?view=long&pmid=12808131|A global transcriptional regulatory role for c-Myc in Burkitt's lymphoma cells". *Proc Natl Acad Sci USA* **100** (14): 8164–9. doi: 10.1073/pnas.1332764100 (http://dx.doi.org/10.1073/pnas.1332764100). PMID 12808131. PMC: 166200 (http://www.pubmedcentral.nih.gov/articlerender.fcgi?tool=pmcentrez&artid=166200). http://www.pnas.org/cgi/pmidlookup?view=long&pmid=12808131.

[85] Pabo C, Sauer R (1984). "Protein-DNA recognition". *Annu Rev Biochem* **53**: 293–321. doi: 10.1146/annurev.bi.53.070184.001453 (http://dx.doi.org/10.1146/annurev.bi.53.070184.001453). PMID 6236744.

[86] Created from PDB 1RVA (http://www.rcsb.org/pdb/explore/explore.do?structureId=1RVA)

[87] Bickle T, Krüger D (1993). "http://www.pubmedcentral.nih.gov/articlerender.fcgi?tool=pmcentrez&artid=372918|Biology of DNA restriction". *Microbiol Rev* **57** (2): 434–50. PMID 8336674.

[88] Doherty A, Suh S (2000). "http://nar.oxfordjournals.org/cgi/pmidlookup?view=long&pmid=11058099|Structural and mechanistic conservation in DNA ligases". *Nucleic Acids Res* **28** (21): 4051–8. doi: 10.1093/nar/28.21.4051 (http://dx.doi.org/10.1093/nar/28.21.4051). PMID 11058099. PMC: 113121 (http://www.pubmedcentral.nih.gov/articlerender.fcgi?tool=pmcentrez&artid=113121). http://nar.oxfordjournals.org/cgi/pmidlookup?view=long&pmid=11058099.

[89] Schoeffler A, Berger J (2005). "Recent advances in understanding structure-function relationships in the type II topoisomerase mechanism". *Biochem Soc Trans* **33** (Pt 6): 1465–70. doi: 10.1042/BST20051465 (http://dx.doi.org/10.1042/BST20051465). PMID 16246147.
[90] Tuteja N, Tuteja R (2004). "Unraveling DNA helicases. Motif, structure, mechanism and function". *Eur J Biochem* **271** (10): 1849–63. doi: 10.1111/j.1432-1033.2004.04094.x (http://dx.doi.org/10.1111/j.1432-1033.2004.04094.x). PMID 15128295.
[91] Joyce C, Steitz T (1995). "http://www.pubmedcentral.nih.gov/articlerender.fcgi?tool=pmcentrez&artid=177480|Polymerase structures and function: variations on a theme?". *J Bacteriol* **177** (22): 6321–9. PMID 7592405.
[92] Hubscher U, Maga G, Spadari S (2002). "Eukaryotic DNA polymerases". *Annu Rev Biochem* **71**: 133–63. doi: 10.1146/annurev.biochem.71.090501.150041 (http://dx.doi.org/10.1146/annurev.biochem.71.090501.150041). PMID 12045093.
[93] Johnson A, O'Donnell M (2005). "Cellular DNA replicases: components and dynamics at the replication fork". *Annu Rev Biochem* **74**: 283–315. doi: 10.1146/annurev.biochem.73.011303.073859 (http://dx.doi.org/10.1146/annurev.biochem.73.011303.073859). PMID 15952889.
[94] Tarrago-Litvak L, Andréola M, Nevinsky G, Sarih-Cottin L, Litvak S (01 May 1994). "http://www.fasebj.org/cgi/reprint/8/8/497|The reverse transcriptase of HIV-1: from enzymology to therapeutic intervention". *Faseb J* **8** (8): 497–503. PMID 7514143. http://www.fasebj.org/cgi/reprint/8/8/497.
[95] Martinez E (2002). "Multi-protein complexes in eukaryotic gene transcription". *Plant Mol Biol* **50** (6): 925–47. doi: 10.1023/A:1021258713850 (http://dx.doi.org/10.1023/A:1021258713850). PMID 12516863.
[96] Created from PDB 1M6G (http://www.rcsb.org/pdb/explore/explore.do?structureId=1M6G)
[97] Cremer T, Cremer C (2001). "Chromosome territories, nuclear architecture and gene regulation in mammalian cells". *Nat Rev Genet* **2** (4): 292–301. doi: 10.1038/35066075 (http://dx.doi.org/10.1038/35066075). PMID 11283701.
[98] Pál C, Papp B, Lercher M (2006). "An integrated view of protein evolution". *Nat Rev Genet* **7** (5): 337–48. doi: 10.1038/nrg1838 (http://dx.doi.org/10.1038/nrg1838). PMID 16619049.
[99] O'Driscoll M, Jeggo P (2006). "The role of double-strand break repair - insights from human genetics". *Nat Rev Genet* **7** (1): 45–54. doi: 10.1038/nrg1746 (http://dx.doi.org/10.1038/nrg1746). PMID 16369571.
[100] Vispé S, Defais M (1997). "Mammalian Rad51 protein: a RecA homologue with pleiotropic functions". *Biochimie* **79** (9-10): 587–92. doi: 10.1016/S0300-9084(97)82007-X (http://dx.doi.org/10.1016/S0300-9084(97)82007-X). PMID 9466696.
[101] Neale MJ, Keeney S (2006). "Clarifying the mechanics of DNA strand exchange in meiotic recombination". *Nature* **442** (7099): 153–8. doi: 10.1038/nature04885 (http://dx.doi.org/10.1038/nature04885). PMID 16838012.
[102] Dickman M, Ingleston S, Sedelnikova S, Rafferty J, Lloyd R, Grasby J, Hornby D (2002). "The RuvABC resolvasome". *Eur J Biochem* **269** (22): 5492–501. doi: 10.1046/j.1432-1033.2002.03250.x (http://dx.doi.org/10.1046/j.1432-1033.2002.03250.x). PMID 12423347.
[103] Orgel L (2004). "http://www.crbmb.com/cgi/reprint/39/2/99.pdf|Prebiotic chemistry and the origin of the RNA world" (PDF). *Crit Rev Biochem Mol Biol* **39** (2): 99–123. doi: 10.1080/10409230490460765 (http://dx.doi.org/10.1080/10409230490460765). PMID 15217990. http://www.crbmb.com/cgi/reprint/39/2/99.pdf.
[104] Davenport R (2001). "Ribozymes. Making copies in the RNA world". *Science* **292** (5520): 1278. doi: 10.1126/science.292.5520.1278a (http://dx.doi.org/10.1126/science.292.5520.1278a). PMID 11360970.
[105] Szathmáry E (1992). "http://www.pnas.org/cgi/reprint/89/7/2614.pdf|What is the optimum size for the genetic alphabet?" (PDF). *Proc Natl Acad Sci USA* **89** (7): 2614–8. doi: 10.1073/pnas.89.7.2614 (http://dx.doi.org/10.1073/pnas.89.7.2614). PMID 1372984. http://www.pnas.org/cgi/reprint/89/7/2614.pdf.
[106] Lindahl T (1993). "Instability and decay of the primary structure of DNA". *Nature* **362** (6422): 709–15. doi: 10.1038/362709a0 (http://dx.doi.org/10.1038/362709a0). PMID 8469282.
[107] Vreeland R, Rosenzweig W, Powers D (2000). "Isolation of a 250 million-year-old halotolerant bacterium from a primary salt crystal". *Nature* **407** (6806): 897–900. doi: 10.1038/35038060 (http://dx.doi.org/10.1038/35038060). PMID 11057666.
[108] Hebsgaard M, Phillips M, Willerslev E (2005). "Geologically ancient DNA: fact or artefact?". *Trends Microbiol* **13** (5): 212–20. doi: 10.1016/j.tim.2005.03.010 (http://dx.doi.org/10.1016/j.tim.2005.03.010). PMID 15866038.
[109] Nickle D, Learn G, Rain M, Mullins J, Mittler J (2002). "Curiously modern DNA for a "250 million-year-old" bacterium". *J Mol Evol* **54** (1): 134–7. doi: 10.1007/s00239-001-0025-x (http://dx.doi.org/10.1007/s00239-001-0025-x). PMID 11734907.
[110] Goff SP, Berg P (1976). "Construction of hybrid viruses containing SV40 and lambda phage DNA segments and their propagation in cultured monkey cells". *Cell* **9** (4 PT 2): 695–705. doi: 10.1016/0092-8674(76)90133-1

(http://dx.doi.org/10.1016/0092-8674(76)90133-1). PMID 189942.
[111] Houdebine L. "Transgenic animal models in biomedical research". *Methods Mol Biol* **360**: 163–202. PMID 17172731.
[112] Daniell H, Dhingra A (2002). "Multigene engineering: dawn of an exciting new era in biotechnology". *Curr Opin Biotechnol* **13** (2): 136–41. doi: 10.1016/S0958-1669(02)00297-5 (http://dx.doi.org/10.1016/S0958-1669(02)00297-5). PMID 11950565.
[113] Job D (2002). "Plant biotechnology in agriculture". *Biochimie* **84** (11): 1105–10. doi: 10.1016/S0300-9084(02)00013-5 (http://dx.doi.org/10.1016/S0300-9084(02)00013-5). PMID 12595138.
[114] Collins A, Morton N (1994). "http://www.pnas.org/cgi/reprint/91/13/6007.pdf|Likelihood ratios for DNA identification" (PDF). *Proc Natl Acad Sci USA* **91** (13): 6007–11. doi: 10.1073/pnas.91.13.6007 (http://dx.doi.org/10.1073/pnas.91.13.6007). PMID 8016106. http://www.pnas.org/cgi/reprint/91/13/6007.pdf.
[115] Weir B, Triggs C, Starling L, Stowell L, Walsh K, Buckleton J (1997). "Interpreting DNA mixtures". *J Forensic Sci* **42** (2): 213–22. PMID 9068179.
[116] Jeffreys A, Wilson V, Thein S (1985). "Individual-specific 'fingerprints' of human DNA". *Nature* **316** (6023): 76–9. doi: 10.1038/316076a0 (http://dx.doi.org/10.1038/316076a0). PMID 2989708.
[117] Colin Pitchfork — first murder conviction on DNA evidence also clears the prime suspect (http://www.forensic.gov.uk/forensic_t/inside/news/list_casefiles.php?case=1) Forensic Science Service Accessed 23 December 2006
[118] http://massfatality.dna.gov/Introduction/|"DNA Identification in Mass Fatality Incidents". National Institute of Justice. September 2006. http://massfatality.dna.gov/Introduction/.
[119] Baldi, Pierre; Brunak, Soren (2001), *Bioinformatics: The Machine Learning Approach*, MIT Press, ISBN 978-0-262-02506-5, OCLC 45951728 57562233 (http://worldcat.org/oclc/45951728+57562233).
[120] Gusfield, Dan. *Algorithms on Strings, Trees, and Sequences: Computer Science and Computational Biology*. Cambridge University Press, 15 January 1997. ISBN 978-0-521-58519-4.
[121] Sjölander K (2004). "http://bioinformatics.oxfordjournals.org/cgi/reprint/20/2/170|Phylogenomic inference of protein molecular function: advances and challenges". *Bioinformatics* **20** (2): 170–9. doi: 10.1093/bioinformatics/bth021 (http://dx.doi.org/10.1093/bioinformatics/bth021). PMID 14734307. http://bioinformatics.oxfordjournals.org/cgi/reprint/20/2/170.
[122] Mount DM (2004). *Bioinformatics: Sequence and Genome Analysis* (2 ed.). Cold Spring Harbor, NY: Cold Spring Harbor Laboratory Press. ISBN 0879697121. OCLC 55106399 (http://worldcat.org/oclc/55106399).
[123] http://dx.doi.org/10.1371/journal.pbio.0020073
[124] Rothemund PW (March 2006). "Folding DNA to create nanoscale shapes and patterns". *Nature* **440** (7082): 297–302. doi: 10.1038/nature04586 (http://dx.doi.org/10.1038/nature04586). PMID 16541064.
[125] Andersen ES, Dong M, Nielsen MM, *et al.* (May 2009). "Self-assembly of a nanoscale DNA box with a controllable lid". *Nature* **459** (7243): 73–6. doi: 10.1038/nature07971 (http://dx.doi.org/10.1038/nature07971). PMID 19424153.
[126] Ishitsuka Y, Ha T (May 2009). "DNA nanotechnology: a nanomachine goes live". *Nat Nanotechnol* **4** (5): 281–2. doi: 10.1038/nnano.2009.101 (http://dx.doi.org/10.1038/nnano.2009.101). PMID 19421208.
[127] Aldaye FA, Palmer AL, Sleiman HF (September 2008). "Assembling materials with DNA as the guide". *Science* **321** (5897): 1795–9. doi: 10.1126/science.1154533 (http://dx.doi.org/10.1126/science.1154533). PMID 18818351.
[128] Wray G (2002). "http://genomebiology.com/1465-6906/3/REVIEWS0001|Dating branches on the tree of life using DNA". *Genome Biol* **3** (1): REVIEWS0001. doi: 10.1046/j.1525-142X.1999.99010.x (http://dx.doi.org/10.1046/j.1525-142X.1999.99010.x). PMID 11806830. PMC: 150454 (http://www.pubmedcentral.nih.gov/articlerender.fcgi?tool=pmcentrez&artid=150454). http://genomebiology.com/1465-6906/3/REVIEWS0001.
[129] *Lost Tribes of Israel*, NOVA, PBS airdate: 22 February 2000. Transcript available from PBS.org, (http://www.pbs.org/wgbh/nova/transcripts/2706israel.html) (last accessed on 4 March 2006)
[130] Kleiman, Yaakov. "The Cohanim/DNA Connection: The fascinating story of how DNA studies confirm an ancient biblical tradition". (http://www.aish.com/societywork/sciencenature/the_cohanim_-_dna_connection.asp) *aish.com* (January 13, 2000). Accessed 4 March 2006.
[131] Bhattacharya, Shaoni. "Killer convicted thanks to relative's DNA". (http://www.newscientist.com/article.ns?id=dn4908) *newscientist.com* (20 April 2004). Accessed 22 December 06
[132] Dahm R (January 2008). "Discovering DNA: Friedrich Miescher and the early years of nucleic acid research". *Hum. Genet.* **122** (6): 565–81. doi: 10.1007/s00439-007-0433-0 (http://dx.doi.org/10.1007/s00439-007-0433-0). PMID 17901982.
[133] Levene P, (01 December 1919). "http://www.jbc.org/cgi/reprint/40/2/415|The structure of yeast nucleic acid". *J Biol Chem* **40** (2): 415–24. http://www.jbc.org/cgi/reprint/40/2/415.
[134] Astbury W, (1947). "Nucleic acid". *Symp. SOC. Exp. Bbl* **1** (66).

[135] Lorenz MG, Wackernagel W (01 September 1994). "http://mmbr.asm.org/cgi/pmidlookup?view=long&pmid=7968924|Bacterial gene transfer by natural genetic transformation in the environment". *Microbiol. Rev.* **58** (3): 563–602. PMID 7968924. PMC: 372978 (http://www.pubmedcentral.nih.gov/articlerender.fcgi?tool=pmcentrez&artid=372978). http://mmbr.asm.org/cgi/pmidlookup?view=long&pmid=7968924.
[136] Avery O, MacLeod C, McCarty M (1944). "http://www.jem.org/cgi/reprint/149/2/297|Studies on the chemical nature of the substance inducing transformation of pneumococcal types. Inductions of transformation by a desoxyribonucleic acid fraction isolated from pneumococcus type III". *J Exp Med* **79** (2): 137–158. doi: 10.1084/jem.79.2.137 (http://dx.doi.org/10.1084/jem.79.2.137). http://www.jem.org/cgi/reprint/149/2/297.
[137] Hershey A, Chase M (1952). "http://www.jgp.org/cgi/reprint/36/1/39.pdf|Independent functions of viral protein and nucleic acid in growth of bacteriophage" (PDF). *J Gen Physiol* **36** (1): 39–56. doi: 10.1085/jgp.36.1.39 (http://dx.doi.org/10.1085/jgp.36.1.39). PMID 12981234. http://www.jgp.org/cgi/reprint/36/1/39.pdf.
[138] The B-DNA X-ray pattern on the right of this linked image (http://osulibrary.oregonstate.edu/specialcollections/coll/pauling/dna/pictures/sci9.001.5.html) was obtained by Rosalind Franklin and Raymond Gosling in May 1952 at high hydration levels of DNA and it has been labeled as "Photo 51"
[139] Nature Archives Double Helix of DNA: 50 Years (http://www.nature.com/nature/dna50/archive.html)
[140] Original X-ray diffraction image (http://osulibrary.oregonstate.edu/specialcollections/coll/pauling/dna/pictures/franklin-typeBphoto.html)
[141] The Nobel Prize in Physiology or Medicine 1962 (http://nobelprize.org/nobel_prizes/medicine/laureates/1962/) Nobelprize .org Accessed 22 December 06
[142] Brenda Maddox (23 January 2003). "http://www.biomath.nyu.edu/index/course/hw_articles/nature4.pdf|The double helix and the 'wronged heroine'" (PDF). *Nature* **421**: 407–408. doi: 10.1038/nature01399 (http://dx.doi.org/10.1038/nature01399). PMID 12540909. http://www.biomath.nyu.edu/index/course/hw_articles/nature4.pdf.
[143] Crick, F.H.C. On degenerate templates and the adaptor hypothesis (PDF). (http://genome.wellcome.ac.uk/assets/wtx030893.pdf) genome.wellcome.ac.uk (Lecture, 1955). Accessed 22 December 2006
[144] Meselson M, Stahl F (1958). "The replication of DNA in *Escherichia coli*". *Proc Natl Acad Sci USA* **44** (7): 671–82. doi: 10.1073/pnas.44.7.671 (http://dx.doi.org/10.1073/pnas.44.7.671). PMID 16590258.
[145] The Nobel Prize in Physiology or Medicine 1968 (http://nobelprize.org/nobel_prizes/medicine/laureates/1968/) Nobelprize.org Accessed 22 December 06
[146] http://proteopedia.org/wiki/index.php/DNA

Further reading

- Calladine, Chris R.; Drew, Horace R.; Luisi, Ben F. and Travers, Andrew A. (2003). *Understanding DNA: the molecule & how it works*. Amsterdam: Elsevier Academic Press. ISBN 0-12-155089-3.
- Dennis, Carina; Julie Clayton (2003). *50 years of DNA*. Basingstoke: Palgrave Macmillan. ISBN 1-4039-1479-6.
- Judson, Horace Freeland (1996). *The eighth day of creation: makers of the revolution in biology*. Plainview, N.Y: CSHL Press. ISBN 0-87969-478-5.
- Olby, Robert C. (1994). *The path to the double helix: the discovery of DNA*. New York: Dover Publications. ISBN 0-486-68117-3., first published in October 1974 by MacMillan, with foreword by Francis Crick;the definitive DNA textbook,revised in 1994 with a 9 page postscript.
- Olby, Robert C. (2009). *Francis Crick: A Biography*. Plainview, N.Y: Cold Spring Harbor Laboratory Press. ISBN 0-87969-798-9.
- Ridley, Matt (2006). *Francis Crick: discoverer of the genetic code*. [Ashland, OH: Eminent Lives, Atlas Books. ISBN 0-06-082333-X.
- Berry, Andrew; Watson, James D. (2003). *DNA: the secret of life*. New York: Alfred A. Knopf. ISBN 0-375-41546-7.

- Stent, Gunther Siegmund; Watson, James D. (1980). *The double helix: a personal account of the discovery of the structure of DNA*. New York: Norton. ISBN 0-393-95075-1.
- Wilkins, Maurice (2003). *The third man of the double helix the autobiography of Maurice Wilkins*. Cambridge, Eng: University Press. ISBN 0-19-860665-6.

External links

- DNA (http://www.dmoz.org/Science/Biology/Biochemistry_and_Molecular_Biology/Biomolecules/Nucleic_Acids/DNA//) at the Open Directory Project
- DNA binding site prediction on protein (http://pipe.scs.fsu.edu/displar.html)
- DNA coiling to form chromosomes (http://biostudio.com/c_ education mac.htm)
- DNA from the Beginning (http://www.dnaftb.org/dnaftb/) Another DNA Learning Center site on DNA, genes, and heredity from Mendel to the human genome project.
- DNA Lab, demonstrates how to extract DNA from wheat using readily available equipment and supplies. (http://ca.youtube.com/watch?v=iyb7fwduuGM)
- DNA the Double Helix Game (http://nobelprize.org/educational_games/medicine/dna_double_helix/) From the official Nobel Prize web site
- DNA under electron microscope (http://www.fidelitysystems.com/Unlinked_DNA.html)
- Dolan DNA Learning Center (http://www.dnalc.org/)
- Double Helix: 50 years of DNA (http://www.nature.com/nature/dna50/archive.html), *Nature*
- Double Helix 1953–2003 (http://www.ncbe.reading.ac.uk/DNA50/) National Centre for Biotechnology Education
- Francis Crick and James Watson talking on the BBC in 1962, 1972, and 1974 (http://www.bbc.co.uk/bbcfour/audiointerviews/profilepages/crickwatson1.shtml)
- Genetic Education Modules for Teachers (http://www.genome.gov/10506718) — *DNA from the Beginning* Study Guide
- Guide to DNA cloning (http://www.blackwellpublishing.com/trun/artwork/Animations/cloningexp/cloningexp.html)
- Olby R (January 2003). "http://chem-faculty.ucsd.edu/joseph/CHEM13/DNA1.pdf|Quiet debut for the double helix". *Nature* **421** (6921): 402–5. doi: 10.1038/nature01397 (http://dx.doi.org/10.1038/nature01397). PMID 12540907. http://chem-faculty.ucsd.edu/joseph/CHEM13/DNA1.pdf.
- PDB Molecule of the Month *pdb23_1* (http://www.rcsb.org/pdb/static.do?p=education_discussion/molecule_of_the_month/pdb23_1.html)
- Rosalind Franklin's contributions to the study of DNA (http://mason.gmu.edu/~emoody/rfranklin.html)
- The Register of Francis Crick Personal Papers 1938 - 2007 (http://orpheus.ucsd.edu/speccoll/testing/html/mss0660a.html#abstract) at Mandeville Special Collections Library, Geisel Library, University of California, San Diego
- U.S. National DNA Day (http://www.genome.gov/10506367) — watch videos and participate in real-time chat with top scientists
- "http://www.nytimes.com/packages/pdf/science/dna-article.pdf|Clue to chemistry of heredity found". *The New York Times*. Saturday, June 13, 1953. http://www.nytimes.com/packages/pdf/science/dna-article.pdf. The first American newspaper coverage of the discovery of the DNA structure.
- (http://www.elmhurst.edu/~chm/vchembook/581nucleotides.html)

Molecular models of DNA

Molecular models of DNA structures are representations of the molecular geometry and topology of Deoxyribonucleic acid (DNA) molecules using one of several means, such as: closely packed spheres (CPK models) made of plastic, metal wires for 'skeletal models', graphic computations and animations by computers, artistic rendering, and so on, with the aim of simplifying and presenting the essential, physical and chemical, properties of DNA molecular structures either *in vivo* or *in vitro*. Computer molecular models also allow animations and molecular dynamics simulations that are very important for understanding how DNA functions *in vivo*. Thus, an old standing dynamic problem is how DNA "self-replication" takes place in living cells that should involve transient uncoiling of supercoiled DNA fibers. Although DNA consists of relatively rigid, very large elongated biopolymer molecules called "fibers" or chains (that are made of repeating nucleotide units of four basic types, attached to deoxyribose and phosphate groups), its molecular structure *in vivo* undergoes dynamic configuration changes that involve dynamically attached water molecules and ions. Supercoiling, packing with histones in chromosome structures, and other such supramolecular aspects also involve *in vivo* DNA topology which is even more complex than DNA molecular geometry, thus turning molecular modeling of DNA into an especially challenging problem for both molecular biologists and biotechnologists. Like other large molecules and biopolymers, DNA often exists in multiple stable geometries (that is, it exhibits conformational isomerism) and configurational, quantum states which are close to each other in energy on the potential energy surface of the DNA molecule. Such geometries can also be computed, at least in principle, by employing *ab initio* quantum chemistry methods that have high accuracy for small molecules. Such quantum geometries define an important class of *ab initio* molecular models of DNA whose exploration has barely started.

In an interesting twist of roles, the DNA molecule itself was proposed to be utilized for quantum computing. Both DNA nanostructures as well as DNA 'computing' biochips have been built (see biochip image at right).

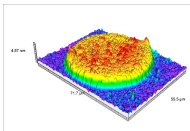

DNA computing biochip:3D

The more advanced, computer-based molecular models of DNA involve molecular dynamics simulations as well as quantum mechanical computations of vibro-rotations, delocalized molecular orbitals (MOs), electric dipole moments, hydrogen-bonding, and so on.

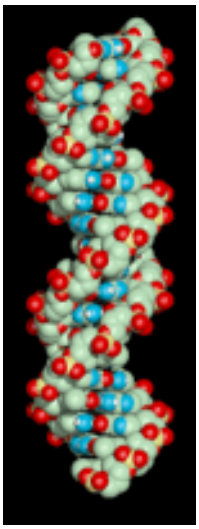

Spinning DNA generic model.

Importance

From the very early stages of structural studies of DNA by X-ray diffraction and biochemical means, molecular models such as the Watson-Crick double-helix model were successfully employed to solve the 'puzzle' of DNA structure, and also find how the latter relates to its key functions in living cells. The first high quality X-ray diffraction patterns of A-DNA were reported by Rosalind Franklin and Raymond Gosling in 1953[1] . The first calculations of the Fourier transform of an atomic helix were reported one year earlier by Cochran, Crick and Vand [2] , and were followed in 1953 by the computation of the Fourier transform of a coiled-coil by Crick[3] . The first reports of a double-helix molecular model of B-DNA structure were made by Watson and Crick in 1953[4] [5] . Last-but-not-least, Maurice F. Wilkins, A. Stokes and H.R. Wilson, reported the first X-ray patterns of *in vivo* B-DNA in partially oriented salmon sperm heads [6] . The development of the first correct double-helix molecular model of DNA by Crick and Watson may not have been possible without the biochemical evidence for the nucleotide base-pairing ([A---T]; [C---G]), or Chargaff's rules[7] [8] [9] [10] [11] [12] .

Examples of DNA molecular models

Animated molecular models allow one to visually explore the three-dimensional (3D) structure of DNA. The first DNA model is a space-filling, or CPK, model of the DNA double-helix whereas the third is an animated wire, or skeletal type, molecular model of DNA. The last two DNA molecular models in this series depict quadruplex DNA [13] that may be involved in certain cancers[14] [15] . The last figure on this panel is a molecular model of hydrogen bonds between water molecules in ice that are similar to those found in DNA.

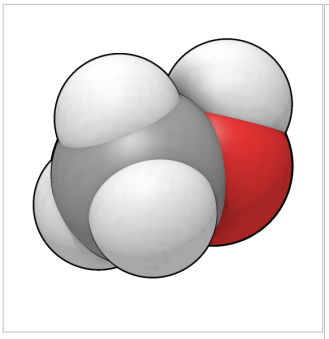

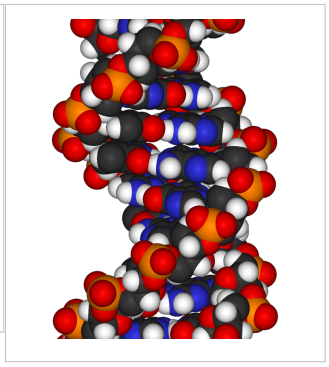

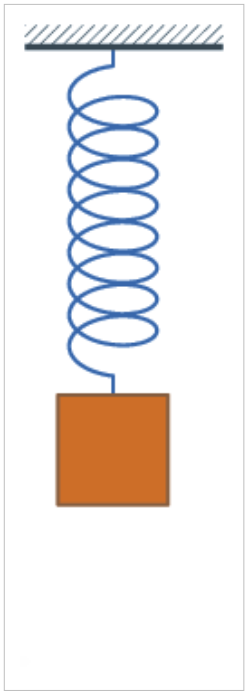

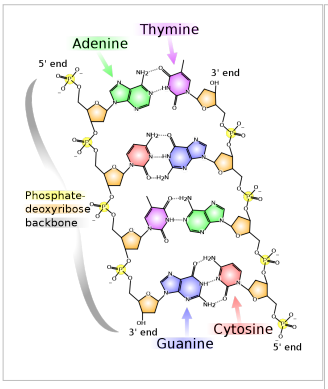
Thymine
Adenine
5' end
3' end
Phosphate-
deoxyribose
backbone
3' end
Guanine
Cytosine
5' end

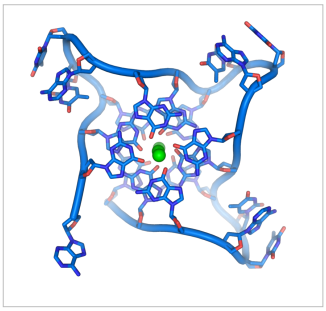

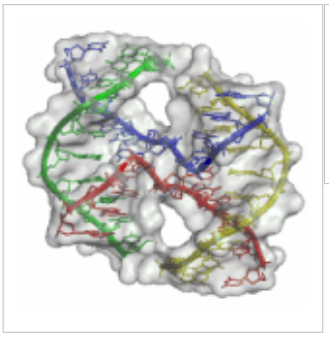

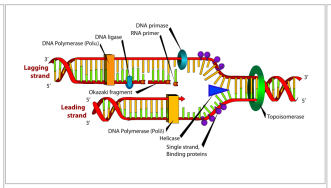
Lagging strand
Leading strand
Okazaki fragment
DNA Polymerase (Pol I)
DNA ligase
DNA primase
RNA primer
DNA Polymerase (Pol III)
Helicase
Single strand. Binding proteins
Topoisomerase

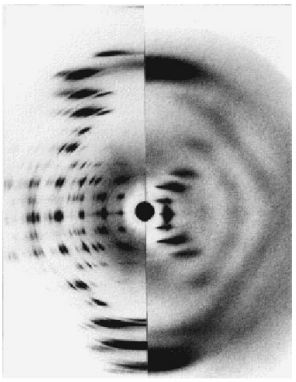

A-DNA B-DNA

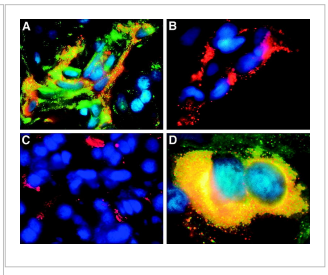
A
B
C
D

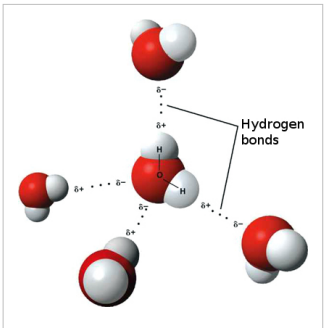

- Spacefilling model or CPK model - a molecule is represented by overlapping spheres representing the atoms.

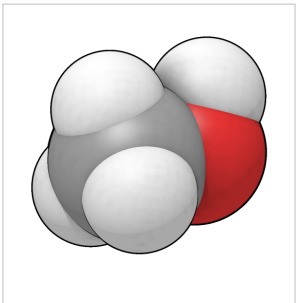

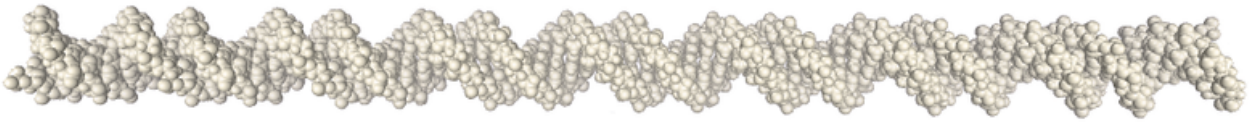

DNA Spacefilling molecular model

Images for DNA Structure Determination from X-Ray Patterns

The following images illustrate both the principles and the main steps involved in generating structural information from X-ray diffraction studies of oriented DNA fibers with the help of molecular models of DNA that are combined with crystallographic and mathematical analysis of the X-ray patterns. From left to right the gallery of images shows:

- *First row*:
- 1. Constructive X-ray interference, or diffraction, following Bragg's Law of X-ray "*reflection by the crystal planes*";
- 2. A comparison of A-DNA (crystalline) and highly hydrated B-DNA (paracrystalline) X-ray diffraction, and respectively, X-ray scattering patterns (courtesy of Dr. Herbert R. Wilson, FRS- see refs. list);
- 3. Purified DNA precipitated in a water jug;
- 4. The major steps involved in DNA structure determination by X-ray crystallography showing the important role played by molecular models of DNA structure in this iterative, structure--determination process;
  - *Second row*:

- 5. Photo of a modern X-ray diffractometer employed for recording X-ray patterns of DNA with major components: X-ray source, goniometer, sample holder, X-ray detector and/or plate holder;
- 6. Illustrated animation of an X-ray goniometer;
- 7. X-ray detector at the SLAC synchrotron facility;
- 8. Neutron scattering facility at ISIS in UK;
  - *Third and fourth rows*: *Molecular models of DNA structure at various scales*; figure #11 is an actual electron micrograph of a DNA fiber bundle, presumably of a single bacterial chromosome loop.

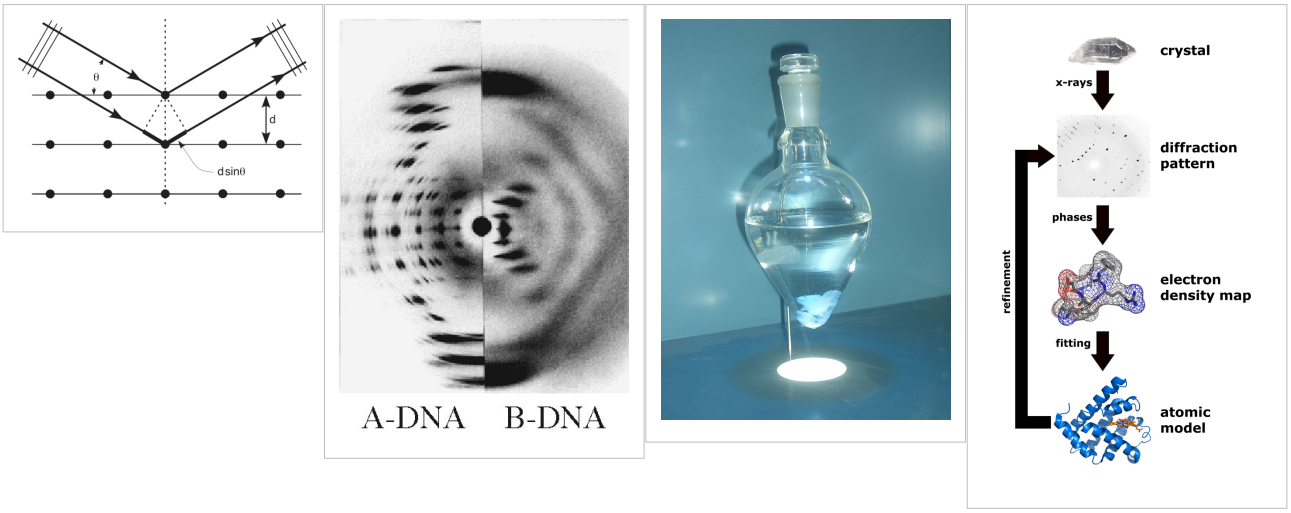

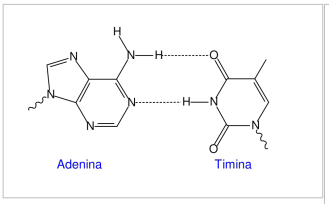

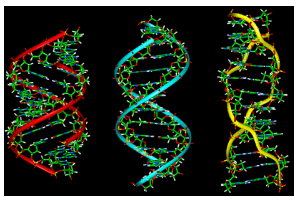

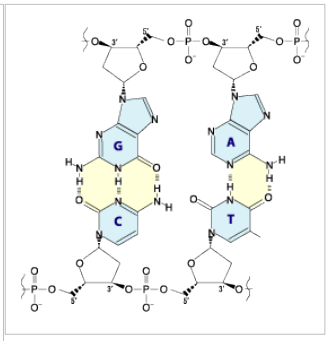

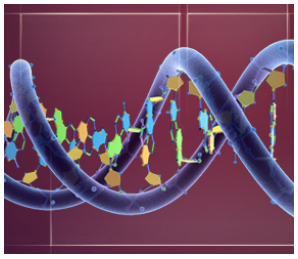

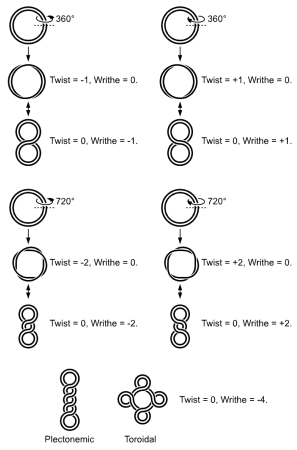

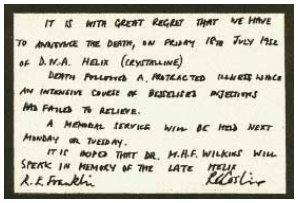

Paracrystalline lattice models of B-DNA structures

A paracrystalline lattice, or paracrystal, is a molecular or atomic lattice with significant amounts (e.g., larger than a few percent) of partial disordering of molecular arranegements. Limiting cases of the paracrystal model are nanostructures, such as glasses, liquids, etc., that may possess only local ordering and no global order. Liquid crystals also have paracrystalline rather than crystalline structures.

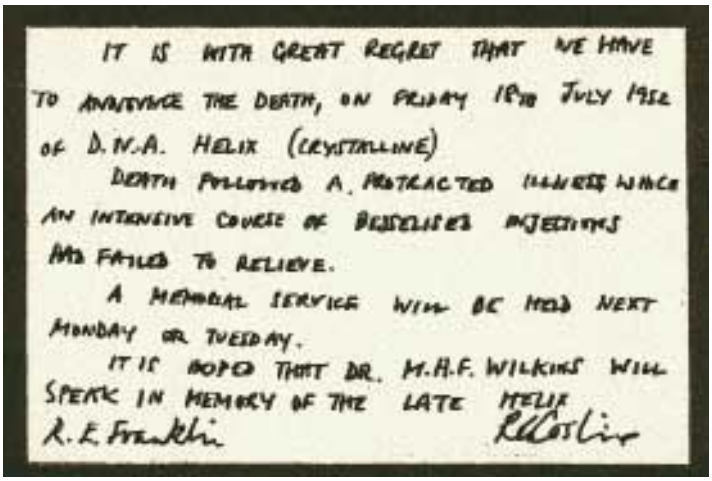

DNA Helix controversy in 1952

Highly hydrated B-DNA occurs naturally in living cells in such a paracrystalline state, which is a dynamic one in spite of the relatively rigid DNA double-helix stabilized by parallel hydrogen bonds between the nucleotide base-pairs in the two complementary, helical DNA chains (see figures). For simplicity most DNA molecular models ommit both water and ions dynamically bound to B-DNA, and are thus less useful for understanding the dynamic behaviors of B-DNA *in vivo*. The physical and mathematical analysis of X-ray[16] [17] and spectroscopic data for paracrystalline B-DNA is therefore much more complicated than that of crystalline, A-DNA X-ray diffraction patterns. The paracrystal model is also important for DNA technological applications such as DNA nanotechnology. Novel techniques that combine X-ray diffraction of DNA with X-ray microscopy in hydrated living cells are now also being developed (see, for example, "Application of X-ray microscopy in the analysis of living hydrated cells" [18]).

Genomic and Biotechnology Applications of DNA molecular modeling

The following gallery of images illustrates various uses of DNA molecular modeling in Genomics and Biotechnology research applications from DNA repair to PCR and DNA nanostructures; each slide contains its own explanation and/or details. The first slide presents an overview of DNA applications, including DNA molecular models, with emphasis on Genomics and Biotechnology.

Gallery: DNA Molecular modeling applications

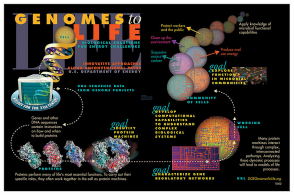

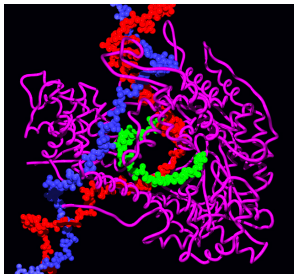
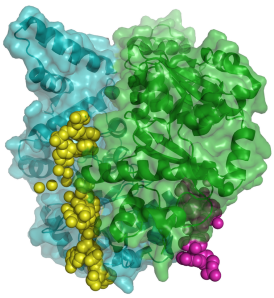

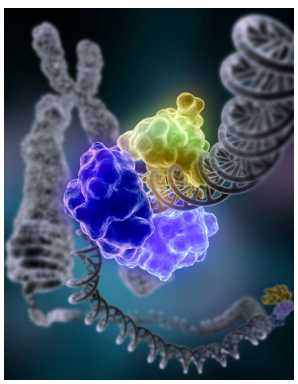
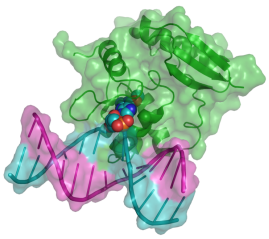
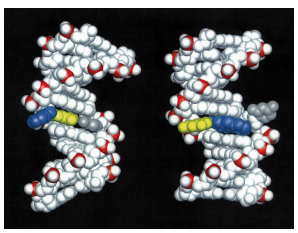
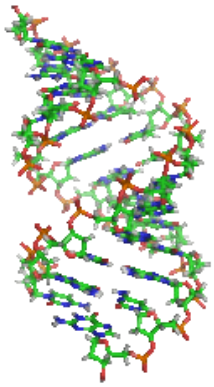

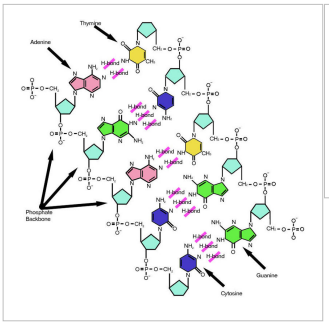
Thymine
Adenine
Phosphate Backbone
Guanine
Cytosine

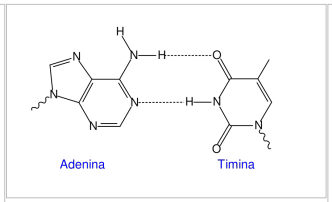
Adenina
Timina

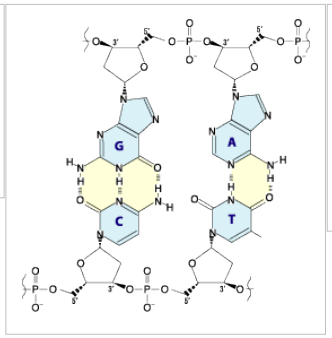
G
C
A
T

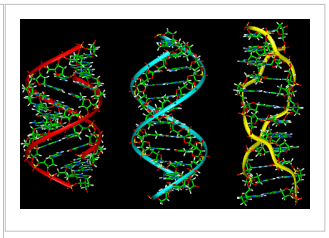

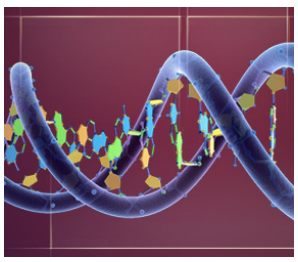

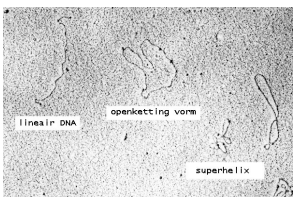
linear DNA
openkettling vorm
superhelix

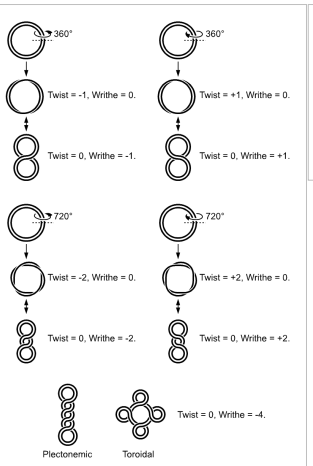
360°
Twist = -1, Writhe = 0.
Twist = 0, Writhe = -1.
360°
Twist = +1, Writhe = 0.
Twist = 0, Writhe = +1.
720°
Twist = -2, Writhe = 0.
Twist = 0, Writhe = -2.
720°
Twist = +2, Writhe = 0.
Twist = 0, Writhe = +2.
Twist = 0, Writhe = -4.
Plectonemic
Toroidal

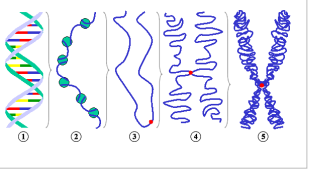
1
2
3
4
5

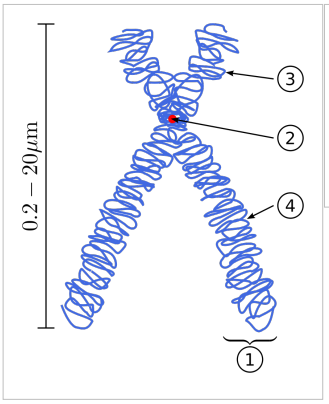
0.2 – 20μm
1
2
3
4

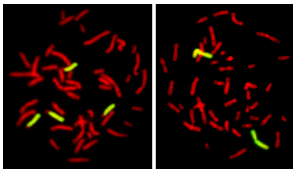

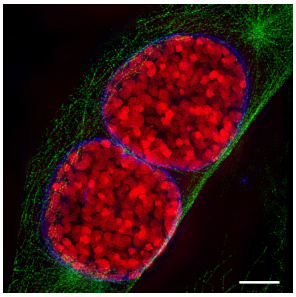

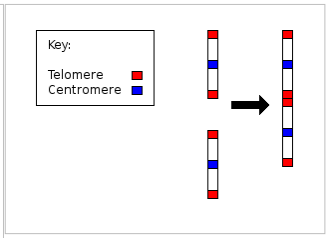
Key:
Telomere
Centromere

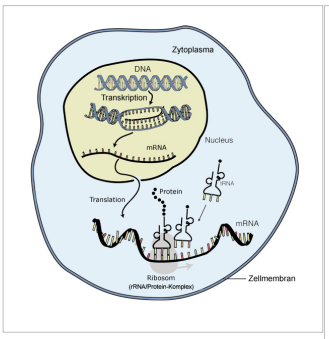
Zytoplasma
DNA
Transkription
Nucleus
mRNA
Translation
Protein
tRNA
mRNA
Ribosom
(rRNA/Protein-Komplex)
Zellmembran

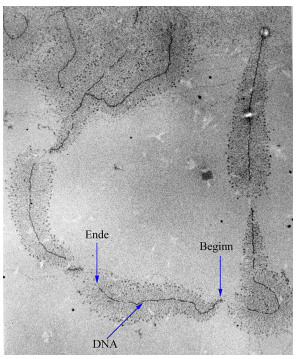
Ende
Beginn
DNA

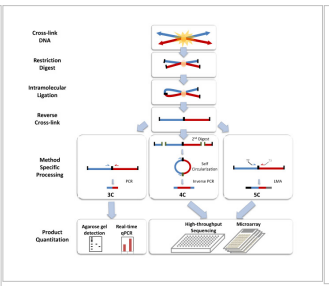
Cross-link DNA
Restriction Digest
Intramolecular Ligation
Reverse Cross-link
Method Specific Processing
3C
4C
5C
Product Quantitation
Agarose gel detection
Real-time qPCR
High-throughput Sequencing
Microarray

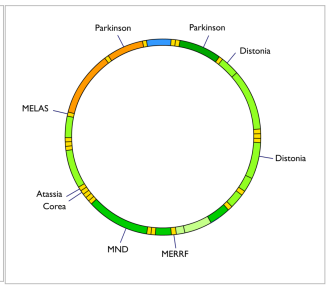
Parkinson
Parkinson
Distonia
MELAS
Distonia
Atassia
Corea
MND
MERRF

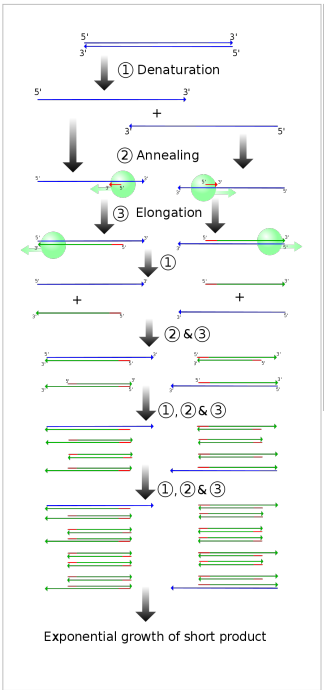

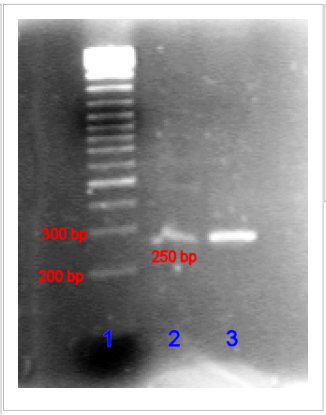

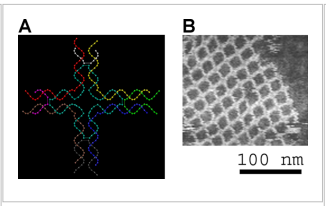

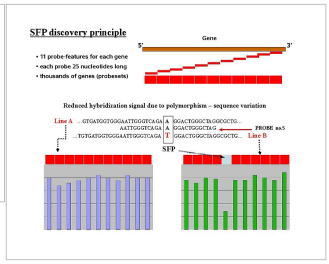

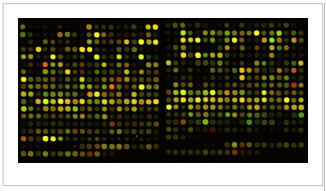

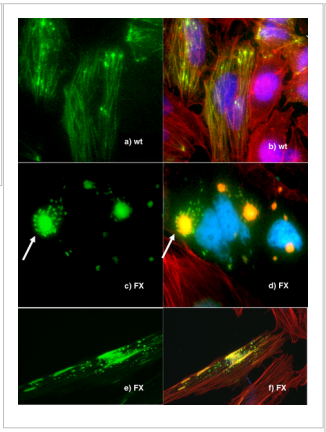

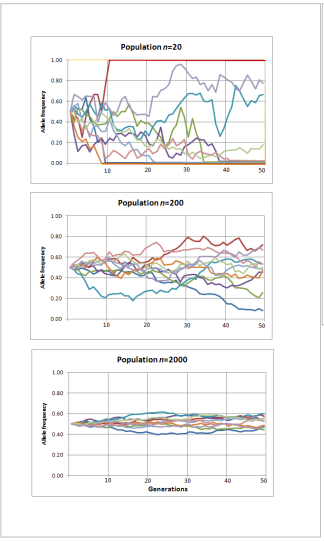

Databases for DNA molecular models and sequences

X-ray diffraction

- NDB ID: UD0017 Database [13]
- X-ray Atlas -database [19]
- PDB files of coordinates for nucleic acid structures from X-ray diffraction by NA (incl. DNA) crystals [20]
- Structure factors dowloadable files in CIF format [21]

Neutron scattering

- ISIS neutron source
- ISIS pulsed neutron source:A world centre for science with neutrons & muons at Harwell, near Oxford, UK. [22]

X-ray microscopy

- Application of X-ray microscopy in the analysis of living hydrated cells [18]

Electron microscopy

- DNA under electron microscope [23]

Atomic Force Microscopy (AFM)

Two-dimensional DNA junction arrays have been visualized by Atomic Force Microscopy (AFM)[24] . Other imaging resources for AFM/Scanning probe microscopy(SPM) can be freely accessed at:

- How SPM Works [25]
- SPM Image Gallery - AFM STM SEM MFM NSOM and more. [26]

Gallery of AFM Images

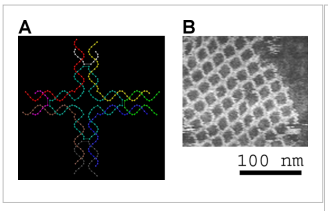

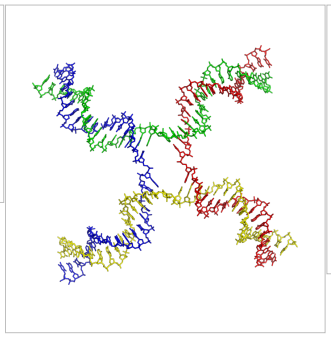

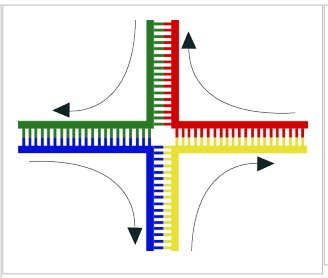

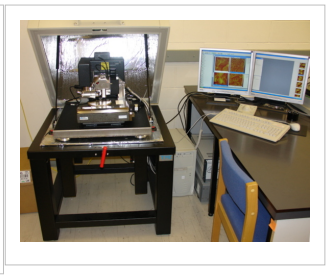

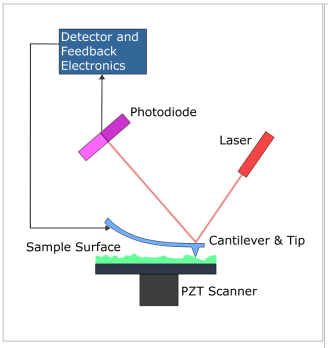

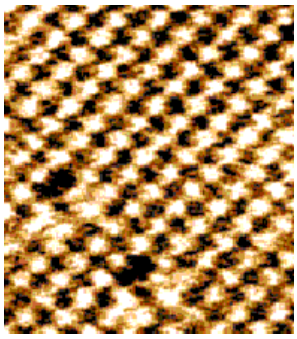

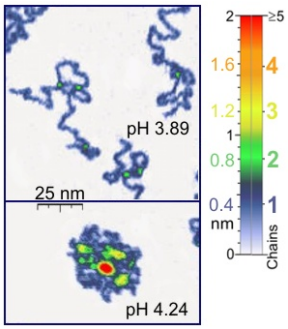

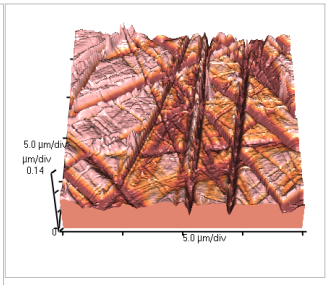

Mass spectrometry--Maldi informatics

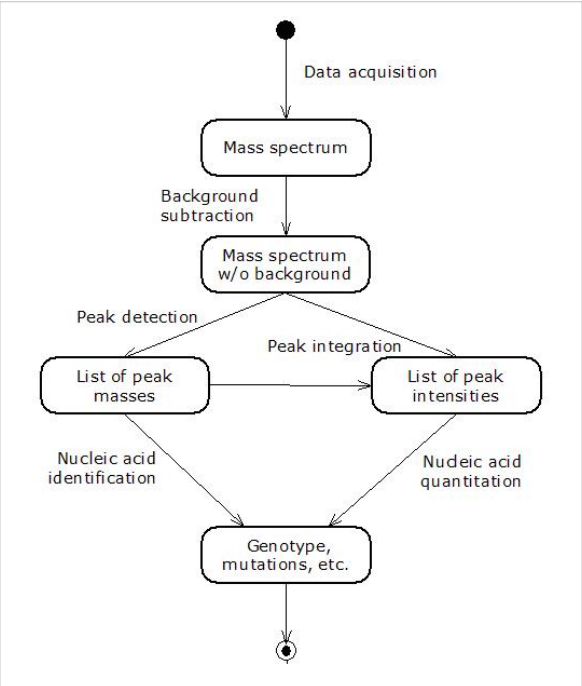

Spectroscopy

- Vibrational circular dichroism (VCD)
- FT-NMR[27] [28]
  - NMR Atlas--database [29]
  - mmcif downloadable coordinate files of nucleic acids in solution from 2D-FT NMR data [30]
  - NMR constraints files for NAs in PDB format [31]
- NMR microscopy[32]
- Microwave spectroscopy
- FT-IR
- FT-NIR[33] [34] [35]
- Spectral, Hyperspectral, and Chemical imaging)[36] [37] [38] [39] [40] [41] [42] .
- Raman spectroscopy/microscopy[43] and CARS[44] .
- Fluorescence correlation spectroscopy[45] [46] [47] [48] [49] [50] [51] [52] , Fluorescence cross-correlation spectroscopy and FRET[53] [54] [55] .
- Confocal microscopy[56]

Gallery: CARS (Raman spectroscopy), Fluorescence confocal microscopy, and Hyperspectral imaging

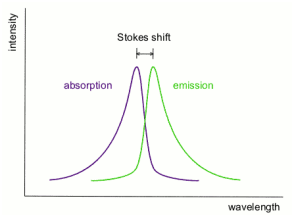

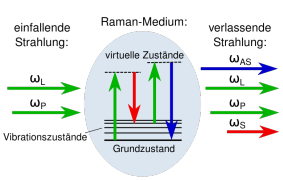

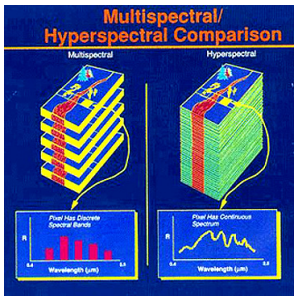

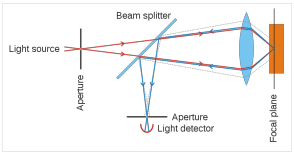

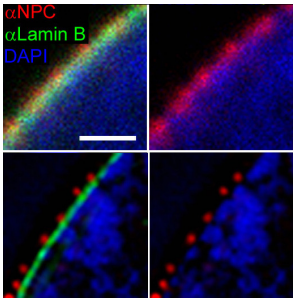

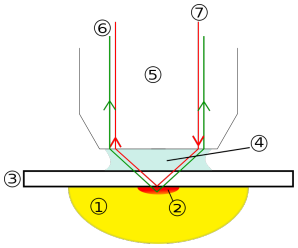

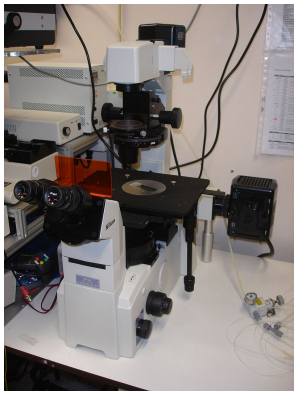

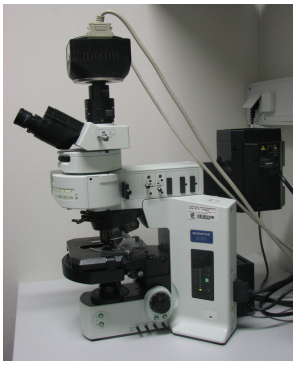

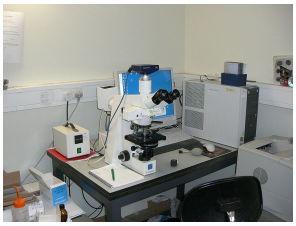

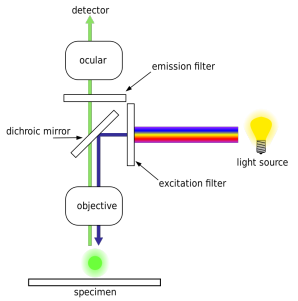

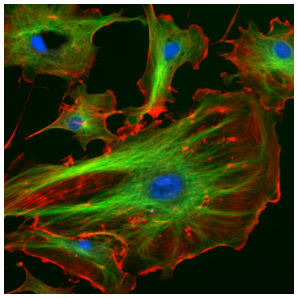

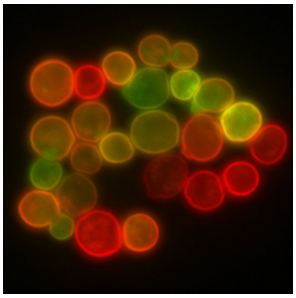

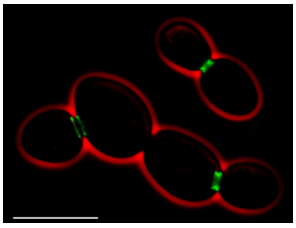

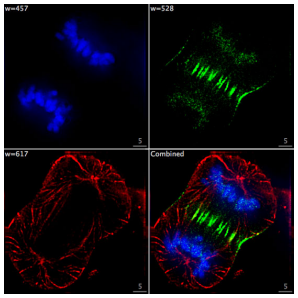

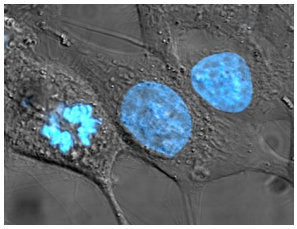

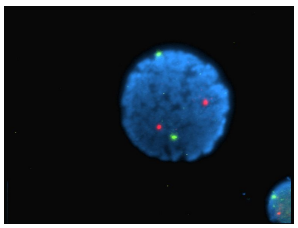

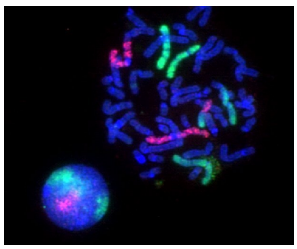

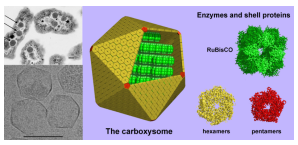

Genomic and structural databases

- CBS Genome Atlas Database [57] — contains examples of base skews.[58]
- The Z curve database of genomes — a 3-dimensional visualization and analysis tool of genomes [59][60] .
- DNA and other nucleic acids' molecular models: Coordinate files of nucleic acids molecular structure models in PDB and CIF formats [61]

Notes

[1] Franklin, R.E. and Gosling, R.G. recd.6 March 1953. Acta Cryst. (1953). 6, 673 The Structure of Sodium Thymonucleate Fibres I. The Influence of Water Content Acta Cryst. (1953). and 6, 678 The Structure of Sodium Thymonucleate Fibres II. The Cylindrically Symmetrical Patterson Function.

[2] Cochran, W., Crick, F.H.C. and Vand V. 1952. The Structure of Synthetic Polypeptides. 1. The Transform of Atoms on a Helix. Acta Cryst. 5(5):581-586.

[3] Crick, F.H.C. 1953a. The Fourier Transform of a Coiled-Coil., Acta Crystallographica 6(8-9):685-689.

[4] Watson, J.D; Crick F.H.C. 1953a. Molecular Structure of Nucleic Acids- A Structure for Deoxyribose Nucleic Acid., Nature 171(4356):737-738.

[5] Watson, J.D; Crick F.H.C. 1953b. The Structure of DNA., Cold Spring Harbor Symposia on Qunatitative Biology 18:123-131.

[6] Wilkins M.H.F., A.R. Stokes A.R. & Wilson, H.R. (1953). "http://www.nature.com/nature/dna50/wilkins.pdf|Molecular Structure of Deoxypentose Nucleic Acids" (PDF). *Nature* **171**: 738–740. doi: 10.1038/171738a0 (http://dx.doi.org/10.1038/171738a0). PMID 13054693. http://www.nature.com/nature/dna50/wilkins.pdf.

[7] Elson D, Chargaff E (1952). "On the deoxyribonucleic acid content of sea urchin gametes". *Experientia* **8** (4): 143-145.

[8] Chargaff E, Lipshitz R, Green C (1952). "Composition of the deoxypentose nucleic acids of four genera of sea-urchin". *J Biol Chem* **195** (1): 155-160. PMID 14938364.

[9] Chargaff E, Lipshitz R, Green C, Hodes ME (1951). "The composition of the deoxyribonucleic acid of salmon sperm". *J Biol Chem* **192** (1): 223-230. PMID 14917668.

[10] Chargaff E (1951). "Some recent studies on the composition and structure of nucleic acids". *J Cell Physiol Suppl* **38** (Suppl).

[11] Magasanik B, Vischer E, Doniger R, Elson D, Chargaff E (1950). "The separation and estimation of ribonucleotides in minute quantities". *J Biol Chem* **186** (1): 37-50. PMID 14778802.

[12] Chargaff E (1950). "Chemical specificity of nucleic acids and mechanism of their enzymatic degradation". *Experientia* **6** (6): 201-209.

[13] http://ndbserver.rutgers.edu/atlas/xray/structures/U/ud0017/ud0017.html

[14] http://www.phy.cam.ac.uk/research/bss/molbiophysics.php

[15] http://planetphysics.org/encyclopedia/TheoreticalBiophysics.html

[16] Hosemann R., Bagchi R.N., *Direct analysis of diffraction by matter*, North-Holland Publs., Amsterdam – New York, 1962.

[17] Baianu, I.C. (1978). "X-ray scattering by partially disordered membrane systems.". *Acta Cryst.,* **A34** (5): 751–753. doi: 10.1107/S0567739478001540 (http://dx.doi.org/10.1107/S0567739478001540).

[18] http://www.ncbi.nlm.nih.gov/entrez/query.fcgi?cmd=Retrieve&db=pubmed&dopt=Abstract&list_uids=12379938

[19] http://ndbserver.rutgers.edu/atlas/xray/index.html

[20] http://ndbserver.rutgers.edu/ftp/NDB/coordinates/na-biol/

[21] http://ndbserver.rutgers.edu/ftp/NDB/structure-factors/
[22] http://www.isis.rl.ac.uk/
[23] http://www.fidelitysystems.com/Unlinked_DNA.html
[24] Mao, Chengde; Sun, Weiqiong & Seeman, Nadrian C. (16 June 1999). "Designed Two-Dimensional DNA Holliday Junction Arrays Visualized by Atomic Force Microscopy". *Journal of the American Chemical Society* **121** (23): 5437–5443. doi: 10.1021/ja9900398 (http://dx.doi.org/10.1021/ja9900398). ISSN 0002-7863 (http://worldcat.org/issn/0002-7863).
[25] http://www.parkafm.com/New_html/resources/01general.php
[26] http://www.rhk-tech.com/results/showcase.php
[27] (http://www.jonathanpmiller.com/Karplus.html)- obtaining dihedral angles from ^{3}J coupling constants
[28] (http://www.spectroscopynow.com/FCKeditor/UserFiles/File/specNOW/HTML files/General_Karplus_Calculator.htm) Another Javascript-like NMR coupling constant to dihedral
[29] http://ndbserver.rutgers.edu/atlas/nmr/index.html
[30] http://ndbserver.rutgers.edu/ftp/NDB/coordinates/na-nmr-mmcif/
[31] http://ndbserver.rutgers.edu/ftp/NDB/nmr-restraints/
[32] Lee, S. C. et al., (2001). One Micrometer Resolution NMR Microscopy. *J. Magn. Res.*, **150**: 207-213.
[33] Near Infrared Microspectroscopy, Fluorescence Microspectroscopy,Infrared Chemical Imaging and High Resolution Nuclear Magnetic Resonance Analysis of Soybean Seeds, Somatic Embryos and Single Cells., Baianu, I.C. et al. 2004., In *Oil Extraction and Analysis.*, D. Luthria, Editor pp.241-273, AOCS Press., Champaign, IL.
[34] Single Cancer Cell Detection by Near Infrared Microspectroscopy, Infrared Chemical Imaging and Fluorescence Microspectroscopy.2004.I. C. Baianu, D. Costescu, N. E. Hofmann and S. S. Korban, q-bio/0407006 (July 2004) (http://arxiv.org/abs/q-bio/0407006)
[35] Raghavachari, R., Editor. 2001. *Near-Infrared Applications in Biotechnology*, Marcel-Dekker, New York, NY.
[36] http://www.imaging.net/chemical-imaging/Chemical imaging
[37] http://www.malvern.com/LabEng/products/sdi/bibliography/sdi_bibliography.htm E. N. Lewis, E. Lee and L. H. Kidder, Combining Imaging and Spectroscopy: Solving Problems with Near-Infrared Chemical Imaging. Microscopy Today, Volume 12, No. 6, 11/2004.
[38] D.S. Mantus and G. H. Morrison. 1991. Chemical imaging in biology and medicine using ion microscopy., *Microchimica Acta*, **104**, (1-6) January 1991, doi: 10.1007/BF01245536
[39] Near Infrared Microspectroscopy, Fluorescence Microspectroscopy,Infrared Chemical Imaging and High Resolution Nuclear Magnetic Resonance Analysis of Soybean Seeds, Somatic Embryos and Single Cells., Baianu, I.C. et al. 2004., In *Oil Extraction and Analysis.*, D. Luthria, Editor pp.241-273, AOCS Press., Champaign, IL.
[40] Single Cancer Cell Detection by Near Infrared Microspectroscopy, Infrared Chemical Imaging and Fluorescence Microspectroscopy.2004.I. C. Baianu, D. Costescu, N. E. Hofmann and S. S. Korban, q-bio/0407006 (July 2004) (http://arxiv.org/abs/q-bio/0407006)
[41] J. Dubois, G. Sando, E. N. Lewis, Near-Infrared Chemical Imaging, A Valuable Tool for the Pharmaceutical Industry, G.I.T. Laboratory Journal Europe, No.1-2, 2007.
[42] Applications of Novel Techniques to Health Foods, Medical and Agricultural Biotechnology.(June 2004).,I. C. Baianu, P. R. Lozano, V. I. Prisecaru and H. C. Lin q-bio/0406047 (http://arxiv.org/abs/q-bio/0406047)
[43] Chemical Imaging Without Dyeing (http://witec.de/en/download/Raman/ImagingMicroscopy04.pdf)
[44] C.L. Evans and X.S. Xie.2008. Coherent Anti-Stokes Raman Scattering Microscopy: Chemical Imaging for Biology and Medicine., doi:10.1146/annurev.anchem.1.031207.112754 *Annual Review of Analytical Chemistry*, **1**: 883-909.
[45] Eigen, M., Rigler, M. Sorting single molecules: application to diagnostics and evolutionary biotechnology,(1994) *Proc. Natl. Acad. Sci. USA*, 91,5740-5747.
[46] Rigler, M. Fluorescence correlations, single molecule detection and large number screening. Applications in biotechnology,(1995) J. Biotechnol., 41,177-186.
[47] Rigler R. and Widengren J. (1990). Ultrasensitive detection of single molecules by fluorescence correlation spectroscopy, *BioScience* (Ed. Klinge & Owman) p.180.
[48] Single Cancer Cell Detection by Near Infrared Microspectroscopy, Infrared Chemical Imaging and Fluorescence Microspectroscopy.2004.I. C. Baianu, D. Costescu, N. E. Hofmann, S. S. Korban and et al., q-bio/0407006 (July 2004) (http://arxiv.org/abs/q-bio/0407006)
[49] Oehlenschläger F., Schwille P. and Eigen M. (1996). Detection of HIV-1 RNA by nucleic acid sequence-based amplification combined with fluorescence correlation spectroscopy, *Proc. Natl. Acad. Sci. USA* **93**:1281.
[50] Bagatolli, L.A., and Gratton, E. (2000). Two-photon fluorescence microscopy of coexisting lipid domains in giant unilamellar vesicles of binary phospholipid mixtures. Biophys J., 78:290-305.

[51] Schwille, P., Haupts, U., Maiti, S., and Webb. W.(1999). Molecular dynamics in living cells observed by fluorescence correlation spectroscopy with one- and two-photon excitation. Biophysical Journal, 77(10):2251-2265.
[52] Near Infrared Microspectroscopy, Fluorescence Microspectroscopy,Infrared Chemical Imaging and High Resolution Nuclear Magnetic Resonance Analysis of Soybean Seeds, Somatic Embryos and Single Cells., Baianu, I.C. et al. 2004., In *Oil Extraction and Analysis.*, D. Luthria, Editor pp.241-273, AOCS Press., Champaign, IL.
[53] FRET description (http://dwb.unl.edu/Teacher/NSF/C08/C08Links/pps99.cryst.bbk.ac.uk/projects/gmocz/fret.htm)
[54] doi:10.1016/S0959-440X(00)00190-1 (http://dx.doi.org/10.1016/S0959-440X(00)00190-1)Recent advances in FRET: distance determination in protein–DNA complexes. *Current Opinion in Structural Biology* **2001**, *11(2)*, 201-207
[55] http://www.fretimaging.org/mcnamaraintro.html FRET imaging introduction
[56] Eigen, M., and Rigler, R. (1994). Sorting single molecules: Applications to diagnostics and evolutionary biotechnology, Proc. Natl. Acad. Sci. USA 91:5740.
[57] http://www.cbs.dtu.dk/services/GenomeAtlas/
[58] Hallin PF, David Ussery D (2004). "CBS Genome Atlas Database: A dynamic storage for bioinformatic results and DNA sequence data". *Bioinformatics* **20**: 3682-3686.
[59] http://tubic.tju.edu.cn/zcurve/
[60] Zhang CT, Zhang R, Ou HY (2003). "The Z curve database: a graphic representation of genome sequences". Bioinformatics 19 (5): 593-599. doi:10.1093/bioinformatics/btg041
[61] http://ndbserver.rutgers.edu/ftp/NDB/models/

References

- *Applications of Novel Techniques to Health Foods, Medical and Agricultural Biotechnology*.(June 2004) I. C. Baianu, P. R. Lozano, V. I. Prisecaru and H. C. Lin., q-bio/0406047.
- F. Bessel, *Untersuchung des Theils der planetarischen Störungen*, Berlin Abhandlungen (1824), article 14.
- Sir Lawrence Bragg, FRS. *The Crystalline State, A General survey.* London: G. Bells and Sons, Ltd., vols. 1 and 2., 1966., 2024 pages.
- Cantor, C. R. and Schimmel, P.R. *Biophysical Chemistry, Parts I and II.*, San Franscisco: W.H. Freeman and Co. 1980. 1,800 pages.
- Eigen, M., and Rigler, R. (1994). Sorting single molecules: Applications to diagnostics and evolutionary biotechnology, *Proc. Natl. Acad. Sci. USA* **91**:5740.
- Raghavachari, R., Editor. 2001. *Near-Infrared Applications in Biotechnology*, Marcel-Dekker, New York, NY.
- Rigler R. and Widengren J. (1990). Ultrasensitive detection of single molecules by fluorescence correlation spectroscopy, *BioScience* (Ed. Klinge & Owman) p.180.
- Single Cancer Cell Detection by Near Infrared Microspectroscopy, Infrared Chemical Imaging and Fluorescence Microspectroscopy.2004. I. C. Baianu, D. Costescu, N. E. Hofmann, S. S. Korban and et al., q-bio/0407006 (July 2004).
- Voet, D. and J.G. Voet. *Biochemistry*, 2nd Edn., New York, Toronto, Singapore: John Wiley & Sons, Inc., 1995, ISBN 0-471-58651-X., 1361 pages.
- Watson, G. N. *A Treatise on the Theory of Bessel Functions.*, (1995) Cambridge University Press. ISBN 0-521-48391-3.
- Watson, James D. and Francis H.C. Crick. A structure for Deoxyribose Nucleic Acid (http://www.nature.com/nature/dna50/watsoncrick.pdf) (PDF). *Nature* 171, 737–738, 25 April 1953.
- Watson, James D. *Molecular Biology of the Gene.* New York and Amsterdam: W.A. Benjamin, Inc. 1965., 494 pages.

- Wentworth, W.E. *Physical Chemistry. A short course.*, Malden (Mass.): Blackwell Science, Inc. 2000.
- Herbert R. Wilson, FRS. *Diffraction of X-rays by proteins, Nucleic Acids and Viruses.*, London: Edward Arnold (Publishers) Ltd. 1966.
- Kurt Wuthrich. *NMR of Proteins and Nucleic Acids.*, New York, Brisbane,Chicester, Toronto, Singapore: J. Wiley & Sons. 1986., 292 pages.
- Robinson, Bruche H.; Seeman, Nadrian C. (August 1987). "The Design of a Biochip: A Self-Assembling Molecular-Scale Memory Device". *Protein Engineering* **1** (4): 295–300. ISSN 0269-2139 (http://worldcat.org/issn/0269-2139). Link (http://peds.oxfordjournals.org/cgi/content/abstract/1/4/295)
- Rothemund, Paul W. K.; Ekani-Nkodo, Axel; Papadakis, Nick; Kumar, Ashish; Fygenson, Deborah Kuchnir & Winfree, Erik (22 December 2004). "Design and Characterization of Programmable DNA Nanotubes". *Journal of the American Chemical Society* **126** (50): 16344–16352. doi: 10.1021/ja044319l (http://dx.doi.org/10.1021/ja044319l). ISSN 0002-7863 (http://worldcat.org/issn/0002-7863).
- Keren, K.; Kinneret Keren, Rotem S. Berman, Evgeny Buchstab, Uri Sivan, Erez Braun (November 2003). "http://www.sciencemag.org/cgi/content/abstract/sci;302/5649/1380|DNA-Templated Carbon Nanotube Field-Effect Transistor". *Science* **302** (6549): 1380–1382. doi: 10.1126/science.1091022 (http://dx.doi.org/10.1126/science.1091022). ISSN 1095-9203 (http://worldcat.org/issn/1095-9203). http://www.sciencemag.org/cgi/content/abstract/sci;302/5649/1380.
- Zheng, Jiwen; Constantinou, Pamela E.; Micheel, Christine; Alivisatos, A. Paul; Kiehl, Richard A. & Seeman Nadrian C. (2006). "2D Nanoparticle Arrays Show the Organizational Power of Robust DNA Motifs". *Nano Letters* **6**: 1502–1504. doi: 10.1021/nl060994c (http://dx.doi.org/10.1021/nl060994c). ISSN 1530-6984 (http://worldcat.org/issn/1530-6984).
- Cohen, Justin D.; Sadowski, John P.; Dervan, Peter B. (2007). "Addressing Single Molecules on DNA Nanostructures". *Angewandte Chemie* **46** (42): 7956–7959. doi: 10.1002/anie.200702767 (http://dx.doi.org/10.1002/anie.200702767). ISSN 0570-0833 (http://worldcat.org/issn/0570-0833).
- Mao, Chengde; Sun, Weiqiong & Seeman, Nadrian C. (16 June 1999). "Designed Two-Dimensional DNA Holliday Junction Arrays Visualized by Atomic Force Microscopy". *Journal of the American Chemical Society* **121** (23): 5437–5443. doi: 10.1021/ja9900398 (http://dx.doi.org/10.1021/ja9900398). ISSN 0002-7863 (http://worldcat.org/issn/0002-7863).
- Constantinou, Pamela E.; Wang, Tong; Kopatsch, Jens; Israel, Lisa B.; Zhang, Xiaoping; Ding, Baoquan; Sherman, William B.; Wang, Xing; Zheng, Jianping; Sha, Ruojie & Seeman, Nadrian C. (2006). "Double cohesion in structural DNA nanotechnology". *Organic and Biomolecular Chemistry* **4**: 3414–3419. doi: 10.1039/b605212f (http://dx.doi.org/10.1039/b605212f).

See also

- DNA
- Molecular graphics
- DNA structure
- DNA Dynamics
- X-ray scattering
- Neutron scattering
- Crystallography
- Crystal lattices
- Paracrystalline lattices/Paracrystals
- 2D-FT NMRI and Spectroscopy
- NMR Spectroscopy
- Microwave spectroscopy
- Two-dimensional IR spectroscopy
- Spectral imaging
- Hyperspectral imaging
- Chemical imaging
- NMR microscopy
- VCD or Vibrational circular dichroism
- FRET and FCS- Fluorescence correlation spectroscopy
- Fluorescence cross-correlation spectroscopy (FCCS)
- Molecular structure
- Molecular geometry
- Molecular topology
- DNA topology
- Sirius visualization software
- Nanostructure
- DNA nanotechnology
- Imaging
- Atomic force microscopy
- X-ray microscopy
- Liquid crystal
- Glasses
- QMC@Home
- Sir Lawrence Bragg, FRS
- Sir John Randall
- James Watson
- Francis Crick
- Maurice Wilkins
- Herbert Wilson, FRS
- Alex Stokes

External links

- DNA the Double Helix Game (http://nobelprize.org/educational_games/medicine/dna_double_helix/) From the official Nobel Prize web site
- MDDNA: Structural Bioinformatics of DNA (http://humphry.chem.wesleyan.edu:8080/MDDNA/)
- Double Helix 1953–2003 (http://www.ncbe.reading.ac.uk/DNA50/) National Centre for Biotechnology Education
- DNA under electron microscope (http://www.fidelitysystems.com/Unlinked_DNA.html)
- Ascalaph DNA (http://www.agilemolecule.com/Ascalaph/Ascalaph_DNA.html) — Commercial software for DNA modeling
- DNAlive: a web interface to compute DNA physical properties (http://mmb.pcb.ub.es/DNAlive). Also allows cross-linking of the results with the UCSC Genome browser and DNA dynamics.
- DiProDB: Dinucleotide Property Database (http://diprodb.fli-leibniz.de). The database is designed to collect and analyse thermodynamic, structural and other dinucleotide properties.
- Further details of mathematical and molecular analysis of DNA structure based on X-ray data (http://planetphysics.org/encyclopedia/BesselFunctionsApplicationsToDiffractionByHelicalStructures.html)
- Bessel functions corresponding to Fourier transforms of atomic or molecular helices. (http://planetphysics.org/?op=getobj&from=objects&name=BesselFunctionsAndTheirApplicationsToDiffractionByHelicalStructures)
- Application of X-ray microscopy in analysis of living hydrated cells (http://www.ncbi.nlm.nih.gov/entrez/query.fcgi?cmd=Retrieve&db=pubmed&dopt=Abstract&list_uids=12379938)
- Characterization in nanotechnology some pdfs (http://nanocharacterization.sitesled.com/)
- overview of STM/AFM/SNOM principles with educative videos (http://www.ntmdt.ru/SPM-Techniques/Principles/)
- SPM Image Gallery - AFM STM SEM MFM NSOM and More (http://www.rhk-tech.com/results/showcase.php)
- How SPM Works (http://www.parkafm.com/New_html/resources/01general.php)
- U.S. National DNA Day (http://www.genome.gov/10506367) — watch videos and participate in real-time discussions with scientists.
- The Secret Life of DNA - DNA Music compositions (http://www.tjmitchell.com/stuart/dna.html)

DNA microarray

For terminology, see glossary below.

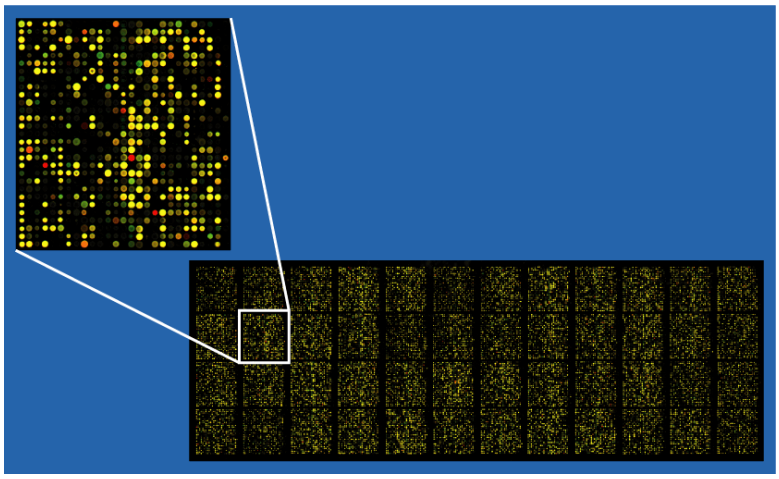

Example of an approximately 40,000 probe spotted oligo microarray with enlarged inset to show detail.

A **DNA microarray** is a multiplex technology used in molecular biology and in medicine. It consists of an arrayed series of thousands of microscopic spots of DNA oligonucleotides, called features, each containing picomoles of a specific DNA sequence. This can be a short section of a gene or other DNA element that are used as probes to hybridize a cDNA or cRNA sample (called target) under high-stringency conditions. Probe-target hybridization is usually detected and quantified by detection of fluorophore-, silver-, or chemiluminescence-labeled targets to determine relative abundance of nucleic acid sequences in the target.

In standard microarrays, the probes are attached to a solid surface by a covalent bond to a chemical matrix (via epoxy-silane, amino-silane, lysine, polyacrylamide or others). The solid surface can be glass or a silicon chip, in which case they are commonly known as *gene chip* or colloquially *Affy chip* when an Affymetrix chip is used. Other microarray platforms, such as Illumina, use microscopic beads, instead of the large solid support. DNA arrays are different from other types of microarray only in that they either measure DNA or use DNA as part of its detection system.

DNA microarrays can be used to measure changes in expression levels, to detect single nucleotide polymorphisms (SNPs) (*see uses and types section*), in genotyping or in resequencing mutant genomes. Microarrays also differ in fabrication, workings, accuracy, efficiency, and cost (*see fabrication section*). Additional factors for microarray experiments are the experimental design and the methods of analyzing the data (*see Bioinformatics section*).

History

Microarray technology evolved from Southern blotting, where fragmented DNA is attached to a substrate and then probed with a known gene or fragment. The use of a collection of distinct DNAs in arrays for expression profiling was first described in 1987, and the arrayed DNAs were used to identify genes whose expression is modulated by interferon.[1] These early gene arrays were made by spotting cDNAs onto filter paper with a pin-spotting device. The use of miniaturized microarrays for gene expression profiling was first reported in 1995, [2] and a complete eukaryotic genome (*Saccharomyces cerevisiae*) on a microarray was published in 1997. [3]

Uses and types

Arrays of DNA can be spatially arranged, as in the commonly known *gene chip* (also called *genome chip*, *DNA chip* or *gene array*), or can be specific DNA sequences labelled such that they can be independently identified in solution. The traditional solid-phase array is a collection of microscopic DNA spots attached to a solid surface, such as glass, plastic or silicon biochip. The affixed DNA segments are known as *probes* (although some sources use different terms such as *reporters*). Thousands of them can be placed in known locations on a single DNA microarray.

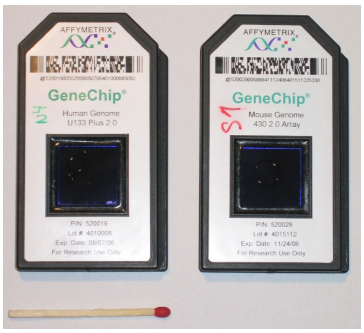

Two Affymetrix chips

DNA microarrays can be used to detect DNA (as in comparative genomic hybridization), or detect RNA (most commonly as cDNA after reverse transcription) that may or may not be translated into proteins. The process of measuring gene expression via cDNA is called expression analysis or expression profiling.

Since an array can contain tens of thousands of probes, a microarray experiment can accomplish that many genetic tests in parallel. Therefore arrays have dramatically accelerated many types of investigation.

Applications include:

Technology or Application	Synopsis
Gene expression profiling	In an mRNA or gene expression profiling experiment the expression levels of thousands of genes are simultaneously monitored to study the effects of certain treatments, diseases, and developmental stages on gene expression. For example, microarray-based gene expression profiling can be used to identify genes whose expression is changed in response to pathogens or other organisms by comparing gene expression in infected to that in uninfected cells or tissues. [4]
Comparative genomic hybridization	Assessing genome content in different cells or closely related organisms. [5] [6]
GeneID	Small microarrays to check IDs of organisms in food and feed (like GMO [7]), mycoplasms in cell culture, or pathogens for disease detection, mostly combining PCR and microarray technology.
Chromatin immunoprecipitation on Chip	DNA sequences bound to a particular protein can be isolated by immunoprecipitating that protein (ChIP), these fragments can be then hybridized to a microarray (such as a tiling array) allowing the determination of protein binding site occupancy throughout the genome. Example protein to immunoprecipitate are histone modifications (H3K27me3, H3K4me2, H3K9me3, etc), Polycomb-group protein (PRC2:Suz12, PRC1:YY1) and trithorax-group protein (Ash1) to study the epigenetic landscape or RNA Polymerase II to study the transcription landscape.
SNP detection	Identifying single nucleotide polymorphism among alleles within or between populations.[8] Several applications of microarrays make use of SNP detection, including Genotyping, forensic analysis, measuring predisposition to disease, identifying drug-candidates, evaluating germline mutations in individuals or somatic mutations in cancers, assessing loss of heterozygosity, or genetic linkage analysis.

Alternative splicing detection	An '*exon junction array* design uses probes specific to the expected or potential splice sites of predicted exons for a gene. It is of intermediate density, or coverage, to a typical gene expression array (with 1-3 probes per gene) and a genomic tiling array (with hundreds or thousands of probes per gene). It is used to assay the expression of alternative splice forms of a gene. Exon arrays have a different design, employing probes designed to detect each individual exon for known or predicted genes, and can be used for detecting different splicing isoforms.
Fusion genes microarray	A Fusion gene microarray can detect fusion transcripts, *e.g.* from cancer specimens. The principle behind this is building on the alternative splicing micorrays. The oligo design strategy enables combined measurements of chimeric transcript junctions with exon-wise measurements of individual fusion partners.
Tiling array	Genome tiling arrays consist of overlapping probes designed to densely represent a genomic region of interest, sometimes as large as an entire human chromosome. The purpose is to empirically detect expression of transcripts or alternatively splice forms which may not have been previously known or predicted.

Fabrication

Microarrays can be manufactured in different ways, depending on the number of probes under examination, costs, customization requirements, and the type of scientific question being asked. Arrays may have as few as 10 probes or up to 2.1 million (NimbleGen, Roche) micrometre-scale probes from commercial vendors.

Surface engineering

The first step of DNA microarray fabrication involves surface engineering of a substrate in order to obtain desirable surface properties for the application of interest. Optimal surface properties are those which produce high signal to noise ratios for the DNA targets of interest. Generally, this involves maximizing the probe surface density and activity while minimizing the non-specific binding of the targets of interest. Methods of surface engineering vary depending on the platform material, design, and application.

Spotted vs. oligonucleotide arrays

Microarrays can be fabricated using a variety of technologies, including printing with fine-pointed pins onto glass slides, photolithography using pre-made masks, photolithography using dynamic micromirror devices, ink-jet printing,[9] or electrochemistry on microelectrode arrays.

In *spotted microarrays*, the probes are oligonucleotides, cDNA or small fragments of PCR products that correspond to mRNAs. The probes are synthesized prior to deposition on the array surface and are then "spotted" onto glass. A common approach utilizes an array of fine pins or needles controlled by a robotic arm that is dipped into wells containing DNA probes and then depositing each probe at designated locations on the array surface. The resulting "grid" of probes represents the nucleic acid profiles of the prepared probes and is ready to receive complementary cDNA or cRNA "targets" derived from experimental or clinical samples. This technique is used by research scientists around the world to produce "in-house" printed microarrays from their own labs. These arrays may be easily customized for each experiment, because researchers can choose the probes and printing locations on

the arrays, synthesize the probes in their own lab (or collaborating facility), and spot the arrays. They can then generate their own labeled samples for hybridization, hybridize the samples to the array, and finally scan the arrays with their own equipment. This provides a relatively low-cost microarray that may be customized for each study, and avoids the costs of purchasing often more expensive commercial arrays that may represent vast numbers of genes that are not of interest to the investigator. Publications exist which indicate in-house spotted microarrays may not provide the same level of sensitivity compared to commercial oligonucleotide arrays,[10] possibly owing to the small batch sizes and reduced printing efficiencies when compared to industrial manufactures of oligo arrays.

In *oligonucleotide microarrays*, the probes are short sequences designed to match parts of the sequence of known or predicted open reading frames. Although oligonucleotide probes are often used in "spotted" microarrays, the term "oligonucleotide array" most often refers to a specific technique of manufacturing. Oligonucleotide arrays are produced by printing short oligonucleotide sequences designed to represent a single gene or family of gene splice-variants by synthesizing this sequence directly onto the array surface instead of depositing intact sequences. Sequences may be longer (60-mer probes such as the Agilent design) or shorter (25-mer probes produced by Affymetrix) depending on the desired purpose; longer probes are more specific to individual target genes, shorter probes may be spotted in higher density across the array and are cheaper to manufacture. One technique used to produce oligonucleotide arrays include photolithographic synthesis (Agilent and Affymetrix) on a silica substrate where light and light-sensitive masking agents are used to "build" a sequence one nucleotide at a time across the entire array.[11] Each applicable probe is selectively "unmasked" prior to bathing the array in a solution of a single nucleotide, then a masking reaction takes place and the next set of probes are unmasked in preparation for a different nucleotide exposure. After many repetitions, the sequences of every probe become fully constructed. More recently, Maskless Array Synthesis from NimbleGen Systems has combined flexibility with large numbers of probes.[12]

Two-channel vs. one-channel detection

Two-color microarrays or *two-channel microarrays* are typically hybridized with cDNA prepared from two samples to be compared (e.g. diseased tissue versus healthy tissue) and that are labeled with two different fluorophores.[13] Fluorescent dyes commonly used for cDNA labelling include Cy3, which has a fluorescence emission wavelength of 570 nm (corresponding to the green part of the light spectrum), and Cy5 with a fluorescence emission wavelength of 670 nm (corresponding to the red part of the light spectrum). The two Cy-labelled cDNA samples are mixed and hybridized to a single microarray that is then scanned in a microarray scanner to visualize fluorescence of the two fluorophores after excitation with a laser beam of a defined wavelength. Relative intensities of each fluorophore may then be used in ratio-based analysis to identify up-regulated and down-regulated genes.[14]

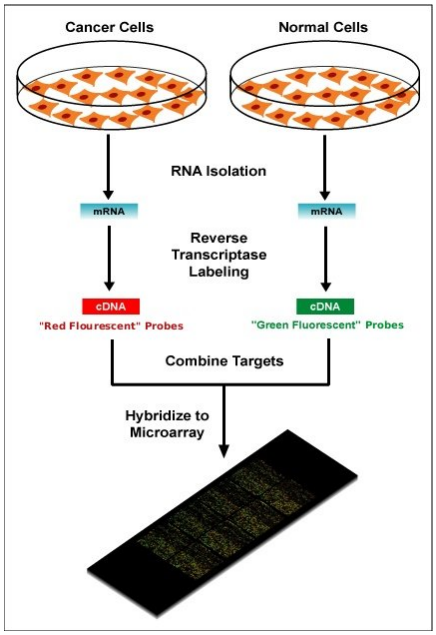

Diagram of typical dual-colour microarray experiment.

Oligonucleotide microarrays often contain control probes designed to hybridize with RNA spike-ins. The degree of hybridization between the spike-ins and the control probes is used to normalize the hybridization measurements for the target probes. Although absolute levels of gene expression may be determined in the two-color array, the relative differences in expression among different spots within a sample and between samples is the preferred method of data analysis for the two-color system. Examples of providers for such microarrays includes Agilent with their Dual-Mode platform, Eppendorf with their DualChip platform for colorimetric Silverquant labeling, and TeleChem International with Arrayit.

In *single-channel microarrays* or *one-color microarrays*, the arrays are designed to give estimations of the absolute levels of gene expression. Therefore the comparison of two conditions requires two separate single-dye hybridizations. As only a single dye is used, the data collected represent absolute values of gene expression. These may be compared to other genes within a sample or to reference "normalizing" probes used to calibrate data across the entire array and across multiple arrays. Three popular single-channel systems are the Affymetrix "Gene Chip", the Applied Microarrays "CodeLink" arrays, and the Eppendorf "DualChip & Silverquant". One strength of the single-dye system lies in the fact that an aberrant sample cannot affect the raw data derived from other samples, because each array chip is exposed to only one sample (as opposed to a two-color system in which a single low-quality sample may drastically impinge on overall data precision even if the other sample was of high quality). Another benefit is that data are more easily compared to arrays from different experiments; the absolute values of gene expression may be compared between studies conducted months or years apart. A drawback to the one-color system is that, when compared to the two-color system, twice as many microarrays are needed to compare samples within an experiment.

Microarrays and bioinformatics

The advent of inexpensive microarray experiments created several specific bioinformatics challenges:

- the multiple levels of replication in experimental design (Experimental design)
- the number of platforms and independent groups and data format (Standardization)
- the treatment of the data (Statistical analysis)
- accuracy and precision (Relation between probe and gene)
- the sheer volume of data and the ability to share it (Data warehousing)

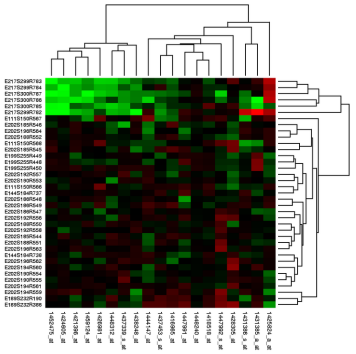

Gene expression values from microarray experiments can be represented as heat maps to visualize the result of data analysis.

Experimental design

Due to the biological complexity of gene expression, the considerations of experimental design that are discussed in the expression profiling article are of critical importance if statistically and biologically valid conclusions are to be drawn from the data.

There are three main elements to consider when designing a microarray experiment. First, replication of the biological samples is essential for drawing conclusions from the experiment. Second, technical replicates (two RNA samples obtained from each experimental unit) help to ensure precision and allow for testing differences within treatment groups. The technical replicates may be two independent RNA extractions or two aliquots of the same extraction. Third, spots of each cDNA clone or oligonucleotide are present as replicates (at least duplicates) on the microarray slide, to provide a measure of technical precision in each hybridization. It is critical that information about the sample preparation and handling is discussed, in order to help identify the independent units in the experiment and to avoid inflated estimates of statistical significance.[15]

Standardization

Microarray data is difficult to exchange due to the lack of standardization in platform fabrication, assay protocols, and analysis methods. This presents an interoperability problem in bioinformatics. Various grass-roots open-source projects are trying to ease the exchange and analysis of data produced with non-proprietary chips:

- For example, the "Minimum Information About a Microarray Experiment" (MIAME) checklist helps define the level of detail that should exist and is being adopted by many journals as a requirement for the submission of papers incorporating microarray results. But MIAME does not describe the format for the information, so while many formats can support the MIAME requirements, as of 2007 no format permits verification of complete semantic compliance.
- The "MicroArray Quality Control (MAQC) Project" is being conducted by the US Food and Drug Administration (FDA) to develop standards and quality control metrics which will eventually allow the use of MicroArray data in drug discovery, clinical practice and regulatory decision-making.[16]

- The MGED Society has developed standards for the representation of gene expression experiment results and relevant annotations.

Statistical analysis

The analysis of DNA microarrays poses a large number of statistical problems, including the normalization of the data. There are several normalization methods in the published literature some of which are platform specific; as in many other cases where authorities disagree, a sound conservative approach is to directly compare different normalization methods to determine the effects of these different methods on the results obtained. This can be done, for example, by investigating the performance of various methods on data from "spike-in" experiments.

Also, experimenters must account for multiple comparisons: even if the statistical P-value assigned to a gene indicates that it is extremely unlikely that differential expression of this gene was due to random rather than treatment effects, the very high number of genes on an array makes it likely that differential expression of some genes represent false positives or false negatives. Statistical methods tailored to microarray analyses have recently become available that assess statistical power based on the variation present in the data and the number of experimental replicates, and can help minimize type I and type II errors in the analyses.[17]

A basic difference between microarray data analysis and much traditional biomedical research is the dimensionality of the data. A large clinical study might collect 100 data items per patient for thousands of patients. A medium-size microarray study will obtain many thousands of numbers per sample for perhaps a hundred samples. Many analysis techniques treat each sample as a single point in a space with thousands of dimensions, then attempt by various techniques to reduce the dimensionality of the data to something humans can visualize.[18] An example for such a method is the Local Pooled Error (LPE) test, which pools standard deviations of genes with similar expression levels and thereby overcomes the problem of low replicate numbers.[19]

Relation between probe and gene

The relation between a probe and the mRNA that it is expected to detect is problematic. On the one hand, some mRNAs may cross-hybridize probes in the array that are supposed to detect another mRNA. On the other hand, probes that are designed to detect the mRNA of a particular gene may be relying on genomic EST information that is incorrectly associated with that gene.

Data warehousing

Microarray data was found to be more useful when compared to other similar datasets. The sheer volume (in bytes), specialized formats (such as MIAME), and curation efforts associated with the datasets require specialized databases to store the data.

See also

- Systems biology
- Microfluidics or lab-on-chip
- Cyanine dyes, such as Cy3 and Cy5, are commonly used fluorophores with microarrays
- Serial analysis of gene expression
- Significance analysis of microarrays
- Full Genome Sequencing

References

[1] Kulesh DA, Clive DR, Zarlenga DS, Greene JJ (1987). "Identification of interferon-modulated proliferation-related cDNA sequences". *Proc Natl Acad Sci USA* **84**: 8453–8457. doi: 10.1073/pnas.84.23.8453 (http://dx.doi.org/10.1073/pnas.84.23.8453). PMID 2446323.

[2] Schena M, Shalon D, Davis RW, Brown PO (1995). "Quantitative monitoring of gene expression patterns with a complementary DNA microarray". *Science* **270**: 467–470. doi: 10.1126/science.270.5235.467 (http://dx.doi.org/10.1126/science.270.5235.467). PMID 7569999.

[3] Lashkari DA, DeRisi JL, McCusker JH, Namath AF, Gentile C, Hwang SY, Brown PO, Davis RW (1997). "Yeast microarrays for genome wide parallel genetic and gene expression analysis". *Proc Natl Acad Sci USA* **94**: 13057–13062. doi: 10.1073/pnas.94.24.13057 (http://dx.doi.org/10.1073/pnas.94.24.13057). PMID 9371799.

[4] Adomas A, Heller G, Olson A, Osborne J, Karlsson M, Nahalkova J, Van Zyl L, Sederoff R, Stenlid J, Finlay R, Asiegbu FO (2008). "Comparative analysis of transcript abundance in Pinus sylvestris after challenge with a saprotrophic, pathogenic or mutualistic fungus". *Tree Physiol*. **28**: 885–897. PMID 18381269.

[5] Pollack JR, Perou CM, Alizadeh AA, Eisen MB, Pergamenschikov A, Williams CF, Jeffrey SS, Botstein D, Brown PO (1999). "Genome-wide analysis of DNA copy-number changes using cDNA microarrays". *Nat Genet* **23**: 41–46. doi: 10.1038/14385 (http://dx.doi.org/10.1038/14385). PMID 10471496.

[6] Moran G, Stokes C, Thewes S, Hube B, Coleman DC, Sullivan D (2004). "Comparative genomics using Candida albicans DNA microarrays reveals absence and divergence of virulence-associated genes in Candida dubliniensis". *Microbiology* **150**: 3363–3382. doi: 10.1099/mic.0.27221-0 (http://dx.doi.org/10.1099/mic.0.27221-0). PMID 15470115.

[7] http://bgmo.jrc.ec.europa.eu/home/docs.htm

[8] Hacia JG, Fan JB, Ryder O, Jin L, Edgemon K, Ghandour G, Mayer RA, Sun B, Hsie L, Robbins CM, Brody LC, Wang D, Lander ES, Lipshutz R, Fodor SP, Collins FS (1999). "Determination of ancestral alleles for human single-nucleotide polymorphisms using high-density oligonucleotide arrays". *Nat Genet* **22**: 164-167. doi: 10.1038/9674 (http://dx.doi.org/10.1038/9674). PMID 10369258.

[9] Lausted C et al. (2004). "http://genomebiology.com/2004/5/8/R58|POSaM: a fast, flexible, open-source, inkjet oligonucleotide synthesizer and microarrayer". *Genome Biology* **5**: R58. doi: 10.1186/gb-2004-5-8-r58 (http://dx.doi.org/10.1186/gb-2004-5-8-r58). PMID 15287980. http://genomebiology.com/2004/5/8/R58.

[10] Bammler T, Beyer RP, Bhattacharya S, Boorman GA, Boyles A, Bradford BU, Bumgarner RE, Bushel PR, Chaturvedi K, Choi D, Cunningham ML, Deng S, Dressman HK, Fannin RD, Farin FM, Freedman JH, Fry RC, Harper A, Humble MC, Hurban P, Kavanagh TJ, Kaufmann WK, Kerr KF, Jing L, Lapidus JA, Lasarev MR, Li J, Li YJ, Lobenhofer EK, Lu X, Malek RL, Milton S, Nagalla SR, O'malley JP, Palmer VS, Pattee P, Paules RS, Perou CM, Phillips K, Qin LX, Qiu Y, Quigley SD, Rodland M, Rusyn I, Samson LD, Schwartz DA, Shi Y, Shin JL, Sieber SO, Slifer S, Speer MC, Spencer PS, Sproles DI, Swenberg JA, Suk WA, Sullivan RC, Tian R, Tennant RW, Todd SA, Tucker CJ, Van Houten B, Weis BK, Xuan S, Zarbl H; Members of the Toxicogenomics Research Consortium. (2005). "Standardizing global gene expression analysis between laboratories and across platforms". *Nat Methods* **2**: 351–356. doi: 10.1038/nmeth0605-477a (http://dx.doi.org/10.1038/nmeth0605-477a). PMID 15846362.

[11] Pease AC, Solas D, Sullivan EJ, Cronin MT, Holmes CP, Fodor SP. (1994). "Light-generated oligonucleotide arrays for rapid DNA sequence analysis". *PNAS* **91**: 5022–5026. doi: 10.1073/pnas.91.11.5022 (http://dx.doi.

org/10.1073/pnas.91.11.5022). PMID 8197176.
[12] Nuwaysir EF, Huang W, Albert TJ, Singh J, Nuwaysir K, Pitas A, Richmond T, Gorski T, Berg JP, Ballin J, McCormick M, Norton J, Pollock T, Sumwalt T, Butcher L, Porter D, Molla M, Hall C, Blattner F, Sussman MR, Wallace RL, Cerrina F, Green RD. (2002). "Gene expression analysis using oligonucleotide arrays produced by maskless photolithography". *Genome Res* **12**: 1749–1755. doi: 10.1101/gr.362402 (http://dx.doi.org/10.1101/gr.362402). PMID 12421762.
[13] Shalon D, Smith SJ, Brown PO (1996). "A DNA microarray system for analyzing complex DNA samples using two-color fluorescent probe hybridization". *Genome Res* **6**: 639–645. doi: 10.1101/gr.6.7.639 (http://dx.doi.org/10.1101/gr.6.7.639). PMID 8796352.
[14] Tang T, François N, Glatigny A, Agier N, Mucchielli MH, Aggerbeck L, Delacroix H (2007). "Expression ratio evaluation in two-colour microarray experiments is significantly improved by correcting image misalignment". *Bioinformatics* **23**: 2686–2691. doi: 10.1093/bioinformatics/btm399 (http://dx.doi.org/10.1093/bioinformatics/btm399). PMID 17698492.
[15] Churchill GA (2002). "http://www.vmrf.org/research-websites/gcf/Forms/Churchill.pdf|Fundamentals of experimental design for cDNA microarrays" (– Scholar search (http://scholar.google.co.uk/scholar?hl=en&lr=&q=intitle:Fundamentals+of+experimental+design+for+cDNA+microarrays&as_publication=Nature+genetics+suppliment&as_ylo=2002&as_yhi=2002&btnG=Search)). *Nature genetics suppliment* **32**: 490. doi: 10.1038/ng1031 (http://dx.doi.org/10.1038/ng1031). http://www.vmrf.org/research-websites/gcf/Forms/Churchill.pdf.
[16] NCTR Center for Toxicoinformatics - MAQC Project (http://www.fda.gov/nctr/science/centers/toxicoinformatics/maqc/)
[17] Wei C, Li J, Bumgarner RE. (2004). "Sample size for detecting differentially expressed genes in microarray experiments". *BMC Genomics* **5**: 87. doi: 10.1186/1471-2164-5-87 (http://dx.doi.org/10.1186/1471-2164-5-87). PMID 15533245.
[18] Wouters L, Gõhlmann HW, Bijnens L, Kass SU, Molenberghs G, Lewi PJ (2003). "Graphical exploration of gene expression data: a comparative study of three multivariate methods". *Biometrics* **59**: 1131–1139. doi: 10.1111/j.0006-341X.2003.00130.x (http://dx.doi.org/10.1111/j.0006-341X.2003.00130.x).
[19] Jain N, Thatte J, Braciale T, Ley K, O'Connell M, Lee JK (2003). "Local-pooled-error test for identifying differentially expressed genes with a small number of replicated microarrays". *Bioinformatics* **19**: 1945–1951. doi: 10.1093/bioinformatics/btg264 (http://dx.doi.org/10.1093/bioinformatics/btg264).

Glossary

- An **Array** or **slide** is a collection of *features* spatially arranged in a two dimensional grid, arranged in columns and rows.
- **Block** or **subarray**: a group of spots, typically made in one print round; several subarrays/blocks form an array.
- **Case/control**: an experimental design paradigm especially suited to the two-colour array system, in which a condition chosen as control (such as healthy tissue or state) is compared to an altered condition (such as a diseased tissue or state).
- **Channel**: the fluorescence output recorded in the scanner for an individual fluorophore and can even be ultraviolet.
- **Dye flip** or **Dye swap** or **Fluor reversal**: reciprocal labelling of DNA targets with the two dyes to account for dye bias in experiments.
- **Scanner**: an instrument used to detect and quantify the intensity of fluorescence of spots on a microarray slide, by selectively exciting fluorophores with a laser and measuring the fluorescence with a filter (optics) photomultiplier system.
- **Spot** or **feature**: a small area on an array slide that contains picomoles of specific DNA samples.
- For other relevant terms see:

  Glossary of gene expression terms

  Protocol (natural sciences)

External links

- Many important links can be found at the Open Directory Project
  - Gene Expression (http://www.dmoz.org/Science/Biology/Biochemistry_and_Molecular_Biology/Gene_Expression/) at the Open Directory Project
  - Micro Scale Products and Services for Biochemistry and Molecular Biology (http://www.dmoz.org/Science/Biology/Biochemistry_and_Molecular_Biology/Products_and_Services/Micro_Scale/) at the Open Directory Project
  - Products and Services for Gene Expression (http://www.dmoz.org/Science/Biology/Biochemistry_and_Molecular_Biology/Gene_Expression/Products_and_Services/) at the Open Directory Project
- PLoS Biology Primer: Microarray Analysis (http://biology.plosjournals.org/perlserv/?request=get-document&doi=10.1371/journal.pbio.0000015)
- Rundown of microarray technology (http://www.genome.gov/page.cfm?pageID=10000533)
- ArrayMining.net (http://www.arraymining.net) - a free web-server for online microarray analysis
- CLASSIFI (http://pathcuric1.swmed.edu/pathdb/classifi.html) - Gene Ontology-based gene cluster classification resource
- Microarray - How does it work? (http://www.unsolvedmysteries.oregonstate.edu/microarray_07)
- Microarray data processing using Self-Organizing Maps tutorial: Part 1 (http://blog.peltarion.com/2007/04/10/the-self-organized-gene-part-1) Part 2 (http://blog.peltarion.com/2007/06/13/the-self-organized-gene-part-2)

DNA sequencing

The term **DNA sequencing** refers to methods for determining the order of the nucleotide bases, adenine, guanine, cytosine, and thymine, in a molecule of DNA. The first DNA sequences were obtained by academic researchers, using laborious methods based on 2-dimensional chromatography in the early 1970s. Following the development of dye-based sequencing methods with automated analysis, DNA sequencing has become easier and orders of magnitude faster. Knowledge of DNA sequences of genes and other parts of the genome of organisms has become indispensable for basic research studying biological processes, as well as in applied fields such as diagnostic or forensic research. The advent of DNA sequencing has significantly accelerated biological research and discovery. The rapid speed of sequencing attained with modern DNA sequencing technology has been instrumental in the sequencing of the human genome, in the Human Genome Project. Related projects, often by scientific collaboration across continents, have generated the complete DNA sequences of many animal, plant, and microbial genomes.

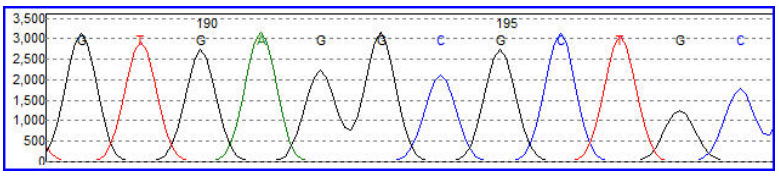

DNA Sequence Trace

RNA sequencing, which is technically easier to perform than DNA sequencing, was one of the earliest forms of nucleotide sequencing. The major landmark of RNA sequencing is the sequence of the first complete gene and the complete genome of Bacteriophage MS2, identified and published by Walter Fiers and his coworkers at the University of Ghent (Ghent, Belgium), between 1972[1] and 1976.[2]

Prior to the development of rapid DNA sequencing methods in the early 1970s by Frederick Sanger at the University of Cambridge, in England and Walter Gilbert and Allan Maxam at Harvard,[3] [4] a number of laborious methods were used. For instance, in 1973, Gilbert and Maxam reported the sequence of 24 basepairs using a method known as wandering-spot analysis. [5]

The chain-termination method developed by Sanger and coworkers in 1975 soon became the method of choice, owing to its relative ease and reliability.[6] [7]

Maxam-Gilbert sequencing

In 1976-1977, Allan Maxam and Walter Gilbert developed a DNA sequencing method based on chemical modification of DNA and subsequent cleavage at specific bases.[3] Although Maxam and Gilbert published their chemical sequencing method two years after the ground-breaking paper of Sanger and Coulson on plus-minus sequencing,[6] [8] Maxam-Gilbert sequencing rapidly became more popular, since purified DNA could be used directly, while the initial Sanger method required that each read start be cloned for production of single-stranded DNA. However, with the improvement of the chain-termination method (see below), Maxam-Gilbert sequencing has fallen out of favour due to its technical complexity prohibiting its use in standard molecular biology kits, extensive use of hazardous chemicals, and difficulties with scale-up.

The method requires radioactive labelling at one end and purification of the DNA fragment to be sequenced. Chemical treatment generates breaks at a small proportion of one or two of the four nucleotide bases in each of four reactions (G, A+G, C, C+T). Thus a series of labelled fragments is generated, from the radiolabelled end to the first 'cut' site in each molecule. The fragments in the four reactions are arranged side by side in gel electrophoresis for size separation. To visualize the fragments, the gel is exposed to X-ray film for autoradiography, yielding a series of dark bands each corresponding to a radiolabelled DNA fragment, from which the sequence may be inferred.

Also sometimes known as 'chemical sequencing', this method originated in the study of DNA-protein interactions (footprinting), nucleic acid structure and epigenetic modifications to DNA, and within these it still has important applications.

Chain-termination methods

Because the chain-terminator method (or Sanger method after its developer Frederick Sanger) is more efficient and uses fewer toxic chemicals and lower amounts of radioactivity than the method of Maxam and Gilbert, it rapidly became the method of choice. The key principle of the Sanger method was the use of dideoxynucleotide triphosphates (ddNTPs) as DNA chain terminators.

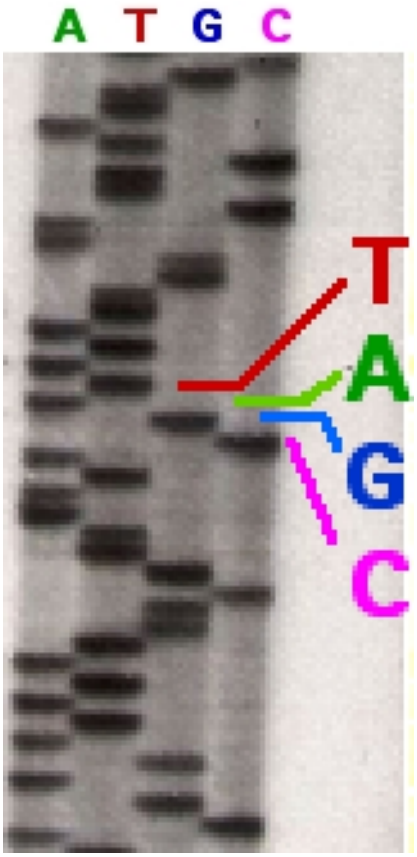

Part of a radioactively labelled sequencing gel

The classical chain-termination method requires a single-stranded DNA template, a DNA primer, a DNA polymerase, radioactively or fluorescently labeled nucleotides, and modified nucleotides that terminate DNA strand elongation. The DNA sample is divided into four separate sequencing reactions, containing all four of the standard deoxynucleotides (dATP, dGTP, dCTP and dTTP) and the DNA polymerase. To each reaction is added only one of the four dideoxynucleotides (ddATP, ddGTP, ddCTP, or ddTTP) which are the chain-terminating nucleotides, lacking a 3'-OH group required for the formation of a phosphodiester bond between two nucleotides, thus terminating DNA strand extension and resulting in various DNA fragments of varying length.

The newly synthesized and labeled DNA fragments are heat denatured, and separated by size (with a resolution of just one nucleotide) by gel electrophoresis on a denaturing polyacrylamide-urea gel with each of the four reactions run in one of four individual lanes (lanes A, T, G, C); the DNA bands are then visualized by autoradiography or UV light, and the DNA sequence can be directly read off the X-ray film or gel image. In the image on the right, X-ray film was exposed to the gel, and the dark bands correspond to DNA fragments of different lengths. A dark band in a lane indicates a DNA fragment that is the result of chain termination after incorporation of a dideoxynucleotide (ddATP, ddGTP, ddCTP, or ddTTP). The relative positions of the different bands among the four lanes are then used to read (from bottom to

top) the DNA sequence.

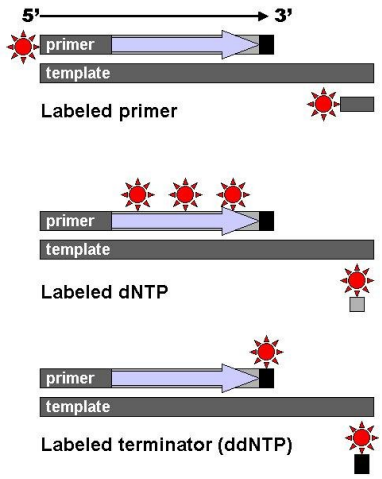

DNA fragments are labeled with a radioactive or fluorescent tag on the primer (1), in the new DNA strand with a labeled dNTP, or with a labeled ddNTP. (click to expand)

Technical variations of chain-termination sequencing include tagging with nucleotides containing radioactive phosphorus for radiolabelling, or using a primer labeled at the 5' end with a fluorescent dye. Dye-primer sequencing facilitates reading in an optical system for faster and more economical analysis and automation. The later development by Leroy Hood and coworkers [9] [10] of fluorescently labeled ddNTPs and primers set the stage for automated, high-throughput DNA sequencing.

Chain-termination methods have greatly simplified DNA sequencing. For example, chain-termination-based kits are commercially available that contain the reagents needed for sequencing, pre-aliquoted and ready to use. Limitations include non-specific binding of the primer to the DNA, affecting accurate read-out of the DNA sequence, and DNA secondary structures affecting the fidelity of the sequence.

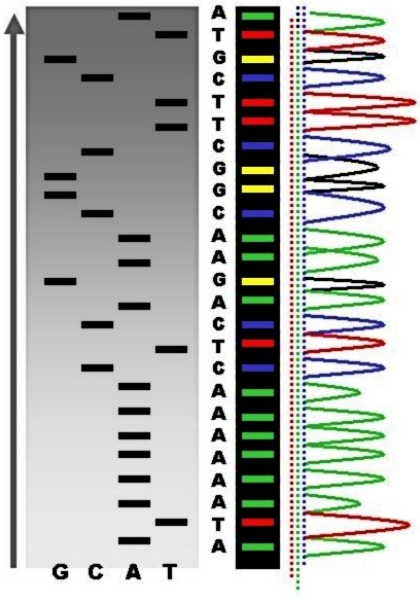

Sequence ladder by radioactive sequencing compared to fluorescent peaks (click to expand)

Dye-terminator sequencing

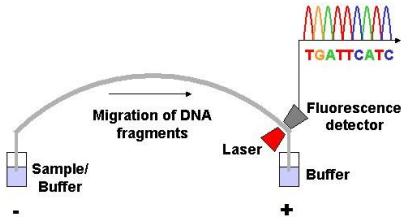

Capillary electrophoresis (click to expand)

Dye-terminator sequencing utilizes labelling of the chain terminator ddNTPs, which permits sequencing in a single reaction, rather than four reactions as in the labelled-primer method. In dye-terminator sequencing, each of the four dideoxynucleotide chain terminators is labelled with fluorescent dyes, each of which with different wavelengths of fluorescence and emission. Owing to its greater expediency and speed, dye-terminator sequencing is now the mainstay in automated sequencing. Its limitations include dye effects due to differences in the incorporation of the dye-labelled chain terminators into the DNA fragment, resulting in unequal peak heights and shapes in the electronic DNA sequence trace chromatogram after capillary electrophoresis (see figure to the right). This problem has been addressed with the use of modified DNA polymerase enzyme systems and dyes that minimize incorporation variability, as well as methods for eliminating "dye blobs". The dye-terminator sequencing method, along with automated high-throughput DNA sequence analyzers, is now being used for the vast majority of sequencing projects.

Challenges

Common challenges of DNA sequencing include poor quality in the first 15-40 bases of the sequence and deteriorating quality of sequencing traces after 700-900 bases. Base calling software typically gives an estimate of quality to aid in quality trimming.

In cases where DNA fragments are cloned before sequencing, the resulting sequence may contain parts of the cloning vector. In contrast, PCR-based cloning and emerging sequencing technologies based on pyrosequencing often avoid using cloning vectors.

Automation and sample preparation

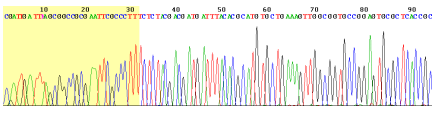

View of the start of an example dye-terminator read (click to expand)

Automated DNA-sequencing instruments (DNA sequencers) can sequence up to 384 DNA samples in a single batch (run) in up to 24 runs a day. DNA sequencers carry out capillary electrophoresis for size separation, detection and recording of dye fluorescence, and data output as fluorescent peak trace chromatograms. Sequencing reactions by thermocycling, cleanup and re-suspension in a buffer solution before loading onto the sequencer are performed separately. A number of commercial and non-commercial software packages can trim low-quality DNA traces automatically. These programs score the quality of each peak and remove low-quality base peaks (generally located at the ends of the sequence). The accuracy of such algorithms is below visual examination by a human operator, but sufficient for automated processing of large sequence data sets.

Large-scale sequencing strategies

Current methods can directly sequence only relatively short (300-1000 nucleotides long) DNA fragments in a single reaction.[11] The main obstacle to sequencing DNA fragments above this size limit is insufficient power of separation for resolving large DNA fragments that differ in length by only one nucleotide.

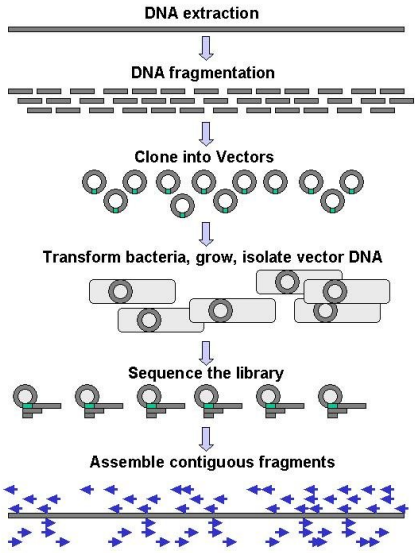

Genomic DNA is fragmented into random pieces and cloned as a bacterial library. DNA from individual bacterial clones is sequenced and the sequence is assembled by using overlapping DNA regions.(click to expand)

Large-scale sequencing aims at sequencing very long DNA pieces, such as whole chromosomes. Common approaches consist of cutting (with restriction enzymes) or shearing (with mechanical forces) large DNA fragments into shorter DNA fragments. The fragmented DNA is cloned into a DNA vector, and amplified in *Escherichia coli*. Short DNA fragments purified from individual bacterial colonies are individually sequenced and assembled electronically into one long, contiguous sequence. This method does not require any pre-existing information about the sequence of the DNA and is referred to as *de novo* sequencing. Gaps in the assembled sequence may be filled by primer walking. The different strategies have different tradeoffs in speed and accuracy; *shotgun methods* are often used for sequencing large genomes, but its assembly is complex and difficult, particularly with sequence repeats often causing gaps in genome assembly.

New sequencing methods

High-throughput sequencing

The high demand for low-cost sequencing has driven the development of high-throughput sequencing technologies that parallelize the sequencing process, producing thousands or millions of sequences at once.[12] [13] High-throughput sequencing technologies are intended to lower the cost of DNA sequencing beyond what is possible with standard dye-terminator methods.

In vitro clonal amplification

Molecular detection methods are not sensitive enough for single molecule sequencing, so most approaches use an *in vitro* cloning step to amplify individual DNA molecules. Emulsion PCR isolates individual DNA molecules along with primer-coated beads in aqueous droplets within an oil phase. Polymerase chain reaction (PCR) then coats each bead with clonal copies of the DNA molecule followed by immobilization for later sequencing. Emulsion PCR is used in the methods by Marguilis et al. (commercialized by 454 Life Sciences), Shendure and Porreca et al. (also known as "polony sequencing") and SOLiD sequencing, (developed by Agencourt, now Applied Biosystems).[14] [15] [16] Another method for *in vitro* clonal amplification is *bridge PCR*, where fragments are amplified upon primers attached to a

solid surface. The single-molecule method developed by Stephen Quake's laboratory (later commercialized by Helicos) skips this amplification step, directly fixing DNA molecules to a surface.[17]

Parallelized sequencing

DNA molecules are physically bound to a surface, and sequenced in parallel.*Sequencing by synthesis*, like dye-termination electrophoretic sequencing, uses a DNA polymerase to determine the base sequence. Reversible terminator methods (used by Illumina and Helicos) use reversible versions of dye-terminators, adding one nucleotide at a time, detect fluorescence at each position in real time, by repeated removal of the blocking group to allow polymerization of another nucleotide. Pyrosequencing (used by 454) also uses DNA polymerization, adding one nucleotide species at a time and detecting and quantifying the number of nucleotides added to a given location through the light emitted by the release of attached pyrophosphates.[14] [18]

Sequencing by ligation

This enzymatic sequencing method uses a DNA ligase to determine the target sequence.[15] [16] [19] Used in the polony method and in the SOLiD technology, it uses a pool of all possible oligonucleotides of a fixed length, labeled according to the sequenced position. Oligonucleotides are annealed and ligated; the preferential ligation by DNA ligase for matching sequences results in a signal informative of the nucleotide at that position.

Microfluidic Sanger Sequencing

In microfluidic Sanger sequencing the entire thermocycling amplification of DNA fragments as well as their separation by electrophoresis is done on a single chip (approximately 100 cm in diameter) thus reducing the reagent usage as well as cost. In some instances researchers have shown that they can increase the through-put of conventional sequencing through the use of microchips. Research will still need to be done in order to make this use of technology effective.

Other sequencing technologies

Sequencing by hybridization is a non-enzymatic method that uses a DNA microarray. A single pool of DNA whose sequence is to be determined is fluorescently labeled and hybridized to an array containing known sequences. Strong hybridization signals from a given spot on the array identifies its sequence in the DNA being sequenced.[20] Mass spectrometry may be used to determine mass differences between DNA fragments produced in chain-termination reactions.[21]

DNA sequencing methods currently under development include labeling the DNA polymerase,[22] reading the sequence as a DNA strand transits through nanopores,[23] [24] and microscopy-based techniques, such as AFM or electron microscopy that are used to identify the positions of individual nucleotides within long DNA fragments (>5,000 bp) by nucleotide labeling with heavier elements (e.g., halogens) for visual detection and recording.[25]

In October 2006, the X Prize Foundation established an initiative to promote the development of full genome sequencing technologies, called the Archon X Prize, intending to award $10 million to "the first Team that can build a device and use it to sequence 100 human genomes within 10 days or less, with an accuracy of no more than one error in every 100,000 bases sequenced, with sequences accurately covering at least 98% of the genome,

and at a recurring cost of no more than $10,000 (US) per genome."[26]

Major landmarks in DNA sequencing

- 1953 Discovery of the structure of the DNA double helix.
- 1972 Development of recombinant DNA technology, which permits isolation of defined fragments of DNA; prior to this, the only accessible samples for sequencing were from bacteriophage or virus DNA.
- 1975 The first complete DNA genome to be sequenced is that of bacteriophage φX174
- 1977 Allan Maxam and Walter Gilbert publish "DNA sequencing by chemical degradation".[3] Frederick Sanger, independently, publishes "DNA sequencing by enzymatic synthesis".
- 1980 Frederick Sanger and Walter Gilbert receive the Nobel Prize in Chemistry
- 1984 Medical Research Council scientists decipher the complete DNA sequence of the Epstein-Barr virus, 170 kb.
- 1986 Leroy E. Hood's laboratory at the California Institute of Technology and Smith announce the first semi-automated DNA sequencing machine.
- 1987 Applied Biosystems markets first automated sequencing machine, the model ABI 370.
- 1990 The U.S. National Institutes of Health (NIH) begins large-scale sequencing trials on *Mycoplasma capricolum*, *Escherichia coli*, *Caenorhabditis elegans*, and *Saccharomyces cerevisiae* (at 75 cents (US)/base).
- 1995 Richard Mathies *et al*. publish dye-based sequencing.[27]
- 1998 Phil Green and Brent Ewing of the University of Washington publish “`phred`” for sequencer data analysis [28] .

See also

- Sequencing
- Full Genome Sequencing
- Genome project
- Single Molecule Real Time Sequencing
- Applied Biosystems
- 454 Life Sciences
- Illumina (company)
- Pacific Biosciences
- Complete Genomics
- Joint Genome Institute
- DNA field-effect transistor
- DNA sequencing theory

References

[1] Min Jou W, Haegeman G, Ysebaert M, Fiers W (May 1972). "Nucleotide sequence of the gene coding for the bacteriophage MS2 coat protein". *Nature* **237** (5350): 82–8. doi: 10.1038/237082a0 (http://dx.doi.org/10.1038/237082a0). PMID 4555447.

[2] Fiers W, Contreras R, Duerinck F, *et al* (April 1976). "Complete nucleotide sequence of bacteriophage MS2 RNA: primary and secondary structure of the replicase gene". *Nature* **260** (5551): 500–7. doi: 10.1038/260500a0 (http://dx.doi.org/10.1038/260500a0). PMID 1264203.

[3] Maxam AM, Gilbert W (February 1977). "http://www.pubmedcentral.nih.gov/articlerender.fcgi?tool=pmcentrez&artid=392330|A new method for sequencing DNA". *Proc. Natl. Acad. Sci. U.S.A.* **74** (2): 560–4. doi: 10.1073/pnas.74.2.560 (http://dx.doi.org/10.1073/pnas.74.2.560). PMID 265521.

[4] Gilbert, W. DNA sequencing and gene structure (http://nobelprize.org/nobel_prizes/chemistry/laureates/1980/gilbert-lecture.pdf). Nobel lecture, 8 December 1980.

[5] Gilbert W, Maxam A (December 1973). "http://www.pubmedcentral.nih.gov/articlerender.fcgi?tool=pmcentrez&artid=427284|The nucleotide sequence of the lac operator". *Proc. Natl. Acad. Sci. U.S.A.* **70** (12): 3581–4. doi: 10.1073/pnas.70.12.3581 (http://dx.doi.org/10.1073/pnas.70.12.3581). PMID 4587255.

[6] Sanger F, Coulson AR (May 1975). "A rapid method for determining sequences in DNA by primed synthesis with DNA polymerase". *J. Mol. Biol.* **94** (3): 441–8. doi: 10.1016/0022-2836(75)90213-2 (http://dx.doi.org/10.1016/0022-2836(75)90213-2). PMID 1100841.

[7] Sanger F, Nicklen S, Coulson AR (December 1977). "http://www.pubmedcentral.nih.gov/articlerender.fcgi?tool=pmcentrez&artid=431765|DNA sequencing with chain-terminating inhibitors". *Proc. Natl. Acad. Sci. U.S.A.* **74** (12): 5463–7. doi: 10.1073/pnas.74.12.5463 (http://dx.doi.org/10.1073/pnas.74.12.5463). PMID 271968.

[8] Sanger F. Determination of nucleotide sequences in DNA (http://nobelprize.org/nobel_prizes/chemistry/laureates/1980/sanger-lecture.pdf). Nobel lecture, 8 December 1980.

[9] Smith LM, Sanders JZ, Kaiser RJ, *et al* (1986). "Fluorescence detection in automated DNA sequence analysis". *Nature* **321** (6071): 674–9. doi: 10.1038/321674a0 (http://dx.doi.org/10.1038/321674a0). PMID 3713851. "We have developed a method for the partial automation of DNA sequence analysis. Fluorescence detection of the DNA fragments is accomplished by means of a fluorophore covalently attached to the oligonucleotide primer used in enzymatic DNA sequence analysis. A different coloured fluorophore is used for each of the reactions specific for the bases A, C, G and T. The reaction mixtures are combined and co-electrophoresed down a single polyacrylamide gel tube, the separated fluorescent bands of DNA are detected near the bottom of the tube, and the sequence information is acquired directly by computer.".

[10] Smith LM, Fung S, Hunkapiller MW, Hunkapiller TJ, Hood LE (April 1985). "http://nar.oxfordjournals.org/cgi/pmidlookup?view=long&pmid=4000959|The synthesis of oligonucleotides containing an aliphatic amino group at the 5' terminus: synthesis of fluorescent DNA primers for use in DNA sequence analysis". *Nucleic Acids Res.* **13** (7): 2399–412. doi: 10.1093/nar/13.7.2399 (http://dx.doi.org/10.1093/nar/13.7.2399). PMID 4000959. PMC: 341163 (http://www.pubmedcentral.nih.gov/articlerender.fcgi?tool=pmcentrez&artid=341163). http://nar.oxfordjournals.org/cgi/pmidlookup?view=long&pmid=4000959.

[11] 3730xl DNA Analyzer (http://www.appliedbiosystems.com/catalog/myab/StoreCatalog/products/CategoryDetails.jsp?hierarchyID=102&category1st=a50&category2nd=a51&category3rd=111907)

[12] Hall N (May 2007). "Advanced sequencing technologies and their wider impact in microbiology". *J. Exp. Biol.* **210** (Pt 9): 1518–25. doi: 10.1242/jeb.001370 (http://dx.doi.org/10.1242/jeb.001370). PMID 17449817.

[13] Church GM (January 2006). "Genomes for all". *Sci. Am.* **294** (1): 46–54. PMID 16468433.

[14] Margulies M, Egholm M, Altman WE, *et al* (September 2005). "http://www.pubmedcentral.nih.gov/articlerender.fcgi?tool=pmcentrez&artid=1464427|Genome sequencing in microfabricated high-density picolitre reactors". *Nature* **437** (7057): 376–80. doi: 10.1038/nature03959 (http://dx.doi.org/10.1038/nature03959). PMID 16056220.

[15] Shendure J, Porreca GJ, Reppas NB, *et al* (September 2005). "Accurate multiplex polony sequencing of an evolved bacterial genome". *Science* **309** (5741): 1728–32. doi: 10.1126/science.1117389 (http://dx.doi.org/10.1126/science.1117389). PMID 16081699.

[16] Applied Biosystems' SOLiD technology (http://solid.appliedbiosystems.com/)

[17] Braslavsky I, Hebert B, Kartalov E, Quake SR (April 2003). "http://www.pubmedcentral.nih.gov/articlerender.fcgi?tool=pmcentrez&artid=153030|Sequence information can be obtained from single DNA molecules". *Proc. Natl. Acad. Sci. U.S.A.* **100** (7): 3960–4. doi: 10.1073/pnas.0230489100 (http://dx.doi.org/10.1073/pnas.0230489100). PMID 12651960.

[18] M. Ronaghi, S. Karamohamed, B. Pettersson, M. Uhlen, and P. Nyren (1996). "Real-time DNA sequencing using detection of pyrophosphate release". *Analytical Biochemistry* **242**: 84–9. doi: 10.1006/abio.1996.0432 (http://dx.doi.org/10.1006/abio.1996.0432).
[19] US5750341 (http://patft.uspto.gov/netacgi/nph-Parser?patentnumber=5750341) (1995-04-17) Macevicz SC, *DNA sequencing by parallel oligonucleotide extensions*.
[20] Hanna GJ, Johnson VA, Kuritzkes DR, *et al* (01 July 2000). "http://jcm.asm.org/cgi/pmidlookup?view=long&pmid=10878069|Comparison of sequencing by hybridization and cycle sequencing for genotyping of human immunodeficiency virus type 1 reverse transcriptase". *J. Clin. Microbiol.* **38** (7): 2715–21. PMID 10878069. PMC: 87006 (http://www.pubmedcentral.nih.gov/articlerender.fcgi?tool=pmcentrez&artid=87006). http://jcm.asm.org/cgi/pmidlookup?view=long&pmid=10878069.
[21] J.R. Edwards, H.Ruparel, and J. Ju (2005). "Mass-spectrometry DNA sequencing". *Mutation Research* **573** (1-2): 3–12.
[22] VisiGen Biotechnologies Inc. - Technology Overview (http://visigenbio.com/technology_overview.html)
[23] The Harvard Nanopore Group (http://mcb.harvard.edu/branton/index.htm)
[24] http://www.physorg.com/news157378086.html|"Nanopore Sequencing Could Slash DNA Analysis Costs". http://www.physorg.com/news157378086.html.
[25] US20060029957 (http://patft.uspto.gov/netacgi/nph-Parser?patentnumber=20060029957) (2005-07-14) ZS Genetics, *Systems and methods of analyzing nucleic acid polymers and related components*.
[26] "PRIZE Overview: Archon X PRIZE for Genomics" (http://genomics.xprize.org/genomics/archon-x-prize-for-genomics/prize-overview)
[27] Ju J, Ruan C, Fuller CW, Glazer AN, Mathies RA (May 1995). "http://www.pubmedcentral.nih.gov/articlerender.fcgi?tool=pmcentrez&artid=41941|Fluorescence energy transfer dye-labeled primers for DNA sequencing and analysis". *Proc. Natl. Acad. Sci. U.S.A.* **92** (10): 4347–51. doi: 10.1073/pnas.92.10.4347 (http://dx.doi.org/10.1073/pnas.92.10.4347). PMID 7753809.
[28] Ewing B, Green P (March 1998). "http://www.genome.org/cgi/pmidlookup?view=long&pmid=9521922|Base-calling of automated sequencer traces using phred. II. Error probabilities". *Genome Res.* **8** (3): 186–94. PMID 9521922. http://www.genome.org/cgi/pmidlookup?view=long&pmid=9521922.

External links

- Disruptive Gene Sequencing technology (http://en.wikipedia.org/wiki/Single_Molecule_Real_Time_Sequencing) - Single Molecule Real Time (SMRT) sequencing

Paracrystal model and theory

Paracrystalline materials are defined as having short and medium range ordering in their lattice (similar to the liquid crystal phases) but lacking long-range ordering at least in one direction.[1]

Ordering is the regularity in which atoms appear in a predictable lattice, as measured from one point. In a highly ordered, perfectly crystalline material, or single crystal, the location of every atom in the structure can be described exactly measuring out from a single origin. Conversely, in a disordered structure such as a liquid or amorphous solid, the location of the first and perhaps second nearest neighbors can be described from an origin (with some degree of uncertainty) and the ability to predict locations decreases rapidly from there out. The distance at which atom locations can be predicted is referred to as the correlation length ξ. A paracrystalline material exhibits correlation somewhere between the fully amorphous and fully crystalline.

The primary, most accessible source of crystallinity information is X-ray diffraction, although other techniques may be needed to observe the complex structure of paracrystalline materials, such as fluctuation electron microscopy [2] in combination with Density of states modeling[3] of electronic and vibrational states.

Paracrystalline Model

The paracrystalline model is a revision of the Continuous Random Network model first proposed by W. H. Zachariasen in 1932 [4] . The paracrystal model is defined as highly strained, microcrystalline grains surrounded by fully amorphous material [5] . This is a higher energy state then the continuous random network model. The important distinction between this model and the microcrystalline phases is the lack of defined grain boundaries and highly strained lattice parameters, which makes calculations of molecular and lattice dynamics difficult. A general theory of paracrystals has been formulated in a basic textbook[6] , and then further developed/refined by various authors.

Applications

The paracrystal model has been useful, for example, in describing the state of partially amorphous semiconductor materials after deposition. It has also been successfully applied to: synthetic polymers, liquid crystals, biopoloymers [7] ,[8] and biomembranes[9] .

See also

- X-ray scattering
- Amorphous solid
- Single Crystal
- Polycrystalline
- Crystallography
- DNA
- X-ray pattern of a B-DNA Paracrystal [10]

Notes

[1] Voyles, et al. Structure and physical properties of paracrystalline atomistic models of amorphous silicon. *J. Ap. Phys.*, **90**(2001) 4437, doi: 10.1063/1.1407319
[2] Biswas, P, et al. *J. Phys.:Condens. Matter*, **19** (2007) 455202, doi:10.1088/0953-8984/19/45/455202
[3] Nakhmanson, Voyles, Mousseau, Barkema, and Drabold. *Phys. Rev. B* **63**(2001) 235207. doi: 10.1103/PhysRevB.63.235207
[4] Zachariasen, W.H., *J. Am. Chem. Soc.,* **54**(1932) 3841.
[5] J.M. Cowley, Diffraction Studies on Non-Cryst. Substan. 13 (1981)
[6] Hosemann R., Bagchi R.N., Direct analysis of diffraction by matter, North-Holland Publs., Amsterdam – New York, 1962
[7] Bessel functions and diffraction by helical structures http://planetphysics.org/encyclopedia/BesselFunctionsAndTheirApplicationsToDiffractionByHelicalStructures.html
[8] X-Ray Diffraction Patterns of Double-Helical Deoxyribonucleic Acid (DNA) Crystals and Paracrystalline Fibers http://planetphysics.org/encyclopedia/BesselFunctionsApplicationsToDiffractionByHelicalStructures.html
[9] Baianu I.C., X-ray scattering by partially disordered membrane systems, *Acta Cryst*. **A**, **34** (1978), 751–753.
[10] http://commons.wikimedia.org/wiki/File:ABDNAxrgpj.jpg

X-ray scattering

1. REDIRECT X-ray scattering techniques

Crystallography

Crystallography is the experimental science of determining the arrangement of atoms in solids. In older usage, it is the scientific study of crystals. The word "crystallography" is derived from the Greek words *crystallon* = cold drop / frozen drop, with its meaning extending to all solids with some degree of transparency, and *graphein* = write.

Before the development of X-ray diffraction crystallography (see below), the study of crystals was based on the geometry of the crystals. This involves measuring the angles of crystal faces relative to theoretical reference axes (crystallographic axes), and establishing the symmetry of the crystal in question. The former is carried out using a goniometer. The position in 3D space of each crystal face is plotted on a stereographic net, e.g. Wulff net or Lambert net. In fact, the pole to each face is plotted on the net. Each point is labelled with its Miller index. The final plot allows the symmetry of the crystal to be established.

Crystallographic methods now depend on the analysis of the diffraction patterns that emerge from a sample that is targeted by a beam of some type. The beam is not always electromagnetic radiation, even though X-rays are the most common choice. For some purposes electrons or neutrons are used, which is possible due to the wave properties of the particles. Crystallographers often explicitly state the type of illumination used when referring to a method, as with the terms **X-ray diffraction, neutron diffraction** and **electron diffraction.**

These three types of radiation interact with the specimen in different ways. X-rays interact with the spatial distribution of the valence electrons, while electrons are charged particles and therefore feel the total charge distribution of both the atomic nuclei and the surrounding electrons. Neutrons are scattered by the atomic nuclei through the strong nuclear forces, but in addition, the magnetic moment of neutrons is non-zero. They are therefore also scattered by magnetic fields. When neutrons are scattered from

hydrogen-containing materials, they produce diffraction patterns with high noise levels. However, the material can sometimes be treated to substitute hydrogen for deuterium. Because of these different forms of interaction, the three types of radiation are suitable for different crystallographic studies.

Theory

An image of a small object is usually generated by using a lens to focus the illuminating radiation, as is done with the rays of the visible spectrum in light microscopy. However, the wavelength of visible light (about 4000 to 7000 Angstroms) is three orders of magnitude longer then the length of typical atomic bonds and atoms themselves (about 1 to 2 Angstroms). Therefore, obtaining information about the spatial arrangement of atoms requires the use of radiation with shorter wavelengths, such as X-rays. Employing shorter wavelengths implied abandoning microscopy and true imaging, however, because there exists no material from which a lens capable of focusing this type of radiation can be created. (That said, scientists have had some success focusing X-rays with microscopic Fresnel zone plates made from gold, and by critical-angle reflection inside long tapered capillaries[1]). Diffracted x-ray beams cannot be focused to produce images, so the sample structure must be reconstructed from the diffraction pattern. Sharp features in the diffraction pattern arise from periodic, repeating structure in the sample, which are often very strong due to coherent reflection of many photons from many regularly spaced instances of similar structure, while non-periodic components of the structure result in diffuse (and usually weak) diffraction features.

Because of their highly ordered and repetitive structure, crystals give diffraction patterns of sharp Bragg reflection spots, and are ideal for analyzing the structure of solids.

Notation

See Miller index for a full treatment of this topic.

- Coordinates in *square brackets* such as **[100]** denote a direction vector (in real space).
- Coordinates in *angle brackets* or *chevrons* such as **<100>** denote a *family* of directions which are related by symmetry operations. In the cubic crystal system for example, **<100>** would mean [100], [010], [001] or the negative of any of those directions.
- Miller indices in *parentheses* such as **(100)** denote a plane of the crystal structure, and regular repetitions of that plane with a particular spacing. In the cubic system, the normal to the (hkl) plane is the direction [hkl], but in lower-symmetry cases, the normal to (hkl) is not parallel to [hkl].
- Indices in *curly brackets* or *braces* such as **{100}** denote a family of planes and their normals which are equivalent in cubic materials due to symmetry operations, much the way angle brackets denote a family of directions. In non-cubic materials, <hkl> is not necessarily perpendicular to {hkl}.

Technique

Some materials studied using crystallography, proteins for example, do not occur naturally as crystals. Typically, such molecules are placed in solution and allowed to crystallize over days, weeks, or months through vapor diffusion. A drop of solution containing the molecule, buffer, and precipitants is sealed in a container with a reservoir containing a hygroscopic solution. Water in the drop diffuses to the reservoir, slowly increasing the concentration and allowing a crystal to form. If the concentration were to rise more quickly, the molecule would simply precipitate out of solution, resulting in disorderly granules rather than an orderly and hence usable crystal.

Once a crystal is obtained, data can be collected using a beam of radiation. Although many universities that engage in crystallographic research have their own X-ray producing equipment, synchrotrons are often used as X-ray sources, because of the purer and more complete patterns such sources can generate. Synchrotron sources also have a much higher intensity of X-ray beams, so data collection takes a fraction of the time normally necessary at weaker sources.

Producing an image from a diffraction pattern requires sophisticated mathematics and often an iterative process of **modelling and refinement.** In this process, the mathematically predicted diffraction patterns of an hypothesized or "model" structure are compared to the actual pattern generated by the crystalline sample. Ideally, researchers make several initial guesses, which through refinement all converge on the same answer. Models are refined until their predicted patterns match to as great a degree as can be achieved without radical revision of the model. This is a painstaking process, made much easier today by computers.

The mathematical methods for the analysis of diffraction data only apply to *patterns,* which in turn result only when waves diffract from orderly arrays. Hence crystallography applies for the most part only to crystals, or to molecules which can be coaxed to crystallize for the sake of measurement. In spite of this, a certain amount of molecular information can be deduced from the patterns that are generated by fibers and powders, which while not as perfect as a solid crystal, may exhibit a degree of order. This level of order can be sufficient to deduce the structure of simple molecules, or to determine the coarse features of more complicated molecules (the double-helical structure of DNA, for example, was deduced from an X-ray diffraction pattern that had been generated by a fibrous sample).

Crystallography in materials engineering

Crystallography is a tool that is often employed by materials scientists. In single crystals, the effects of the crystalline arrangement of atoms is often easy to see macroscopically, because the natural shapes of crystals reflect the atomic structure. In addition, physical properties are often controlled by crystalline defects. The understanding of crystal structures is an important prerequisite for understanding crystallographic defects. Mostly, materials do not occur in a single crystalline, but poly-crystalline form, such that the powder diffraction method plays a most important role in structural determination.

A number of other physical properties are linked to crystallography. For example, the minerals in clay form small, flat, platelike structures. Clay can be easily deformed because the platelike particles can slip along each other in the plane of the plates, yet remain strongly connected in the direction perpendicular to the plates. Such mechanisms can be

studied by crystallographic texture measurements.

In another example, iron transforms from a body-centered cubic (bcc) structure to a face-centered cubic (fcc) structure called austenite when it is heated. The fcc structure is a close-packed structure, and the bcc structure is not, which explains why the volume of the iron decreases when this transformation occurs.

Crystallography is useful in phase identification. When performing any process on a material, it may be desired to find out what compounds and what phases are present in the material. Each phase has a characteristic arrangement of atoms. Techniques like X-ray diffraction can be used to identify which patterns are present in the material, and thus which compounds are present (note: the determination of the "phases" within a material should not be confused with the more general problem of "phase determination," which refers to the phase of waves as they diffract from planes within a crystal, and which is a necessary step in the interpretation of complicated diffraction patterns).

Crystallography covers the enumeration of the symmetry patterns which can be formed by atoms in a crystal and for this reason has a relation to group theory and geometry. See symmetry group.

Biology

X-ray crystallography is the primary method for determining the molecular conformations of biological macromolecules, particularly protein and nucleic acids such as DNA and RNA. In fact, the double-helical structure of DNA was deduced from crystallographic data. The first crystal structure of a macromolecule was solved in 1958 (Kendrew, J.C. et al. (1958) A three-dimensional model of the myoglobin molecule obtained by X-ray analysis (*Nature* 181, 662–666). The Protein Data Bank (PDB) is a freely accessible repository for the structures of proteins and other biological macromolecules. Computer programs like RasMol or Pymol can be used to visualize biological molecular structures.

Electron crystallography has been used to determine some protein structures, most notably membrane proteins and viral capsids.

Scientists of note

- William Henry Bragg
- William Lawrence Bragg
- Auguste Bravais
- Francis Crick
- Pierre Curie
- Boris Delone
- Paul Peter Ewald
- Rosalind Franklin
- Georges Friedel
- René Just Haüy
- Carl Hermann
- Dorothy Crowfoot Hodgkin
- Robert Huber
- Max von Laue
- Kathleen Lonsdale

- Ernest-François Mallard
- Charles-Victor Mauguin
- William Hallowes Miller
- Max Perutz
- Hugo Rietveld
- Jean-Baptiste L. Romé de l'Isle
- Constance Tipper
- Don Craig Wiley
- Ada Yonath

See also

- Atomic packing factor
- Condensed Matter Physics
- Crystal engineering
- Crystal growth
- Crystal optics
- Crystal system
- Crystal
- Crystallite
- Crystallization processes
- Crystallographic database
- Crystallographic group
- Diffraction
- Dynamical theory of diffraction
- Electron crystallography
- Electron diffraction
- Euclidean plane isometry
- Fixed points of isometry groups in Euclidean space
- Group action
- Laser-heated pedestal growth
- Materials Science
- Metallurgy
- Mineralogy
- Neutron crystallography
- Neutron diffraction
- Neutron Diffraction at OPAL
- Permutation group
- Point group
- Powder diffraction
- Solid state chemistry
- Space group
- Symmetric group
- Symmetry group
- Symmetry
- X-ray crystallography
- X-ray diffraction

Further reading

- Burns, G.; Glazer, A.M. (1990). *Space Groups for Scientists and Engineers* (2nd ed.). Boston: Academic Press, Inc. ISBN 0-12-145761-3.
- Clegg, W (1998). *Crystal Structure Determination (Oxford Chemistry Primer)*. Oxford: Oxford University Press. ISBN 0-19-855-901-1.
- Drenth, J (1999). *Principles of Protein X-Ray Crystallography*. New York: Springer-Verlag. ISBN 0-387-98587-5.
- Giacovazzo, C; Monaco HL, Viterbo D, Scordari F, Gilli G, Zanotti G, and Catti M (1992). *Fundamentals of Crystallography*. Oxford: Oxford University Press. ISBN 0-19-855578-4.
- Glusker, JP; Lewis M, Rossi M (1994). *Crystal Structure Analysis for Chemists and Biologists*. New York: VCH Publishers. ISBN 0-471-18543-4.
- O'Keeffe, M.; Hyde, B.G. (1996). *Crystal Structures; I. Patterns and Symmetry*. Washington, DC: Mineralogical Society of America, *Monograph Series*. ISBN 0-939950-40-5.

Applied Computational Powder Diffraction Data Analysis

- Young, R.A., ed (1993). *The Rietveld Method*. Oxford: Oxford University Press & International Union of Crystallography. ISBN 0-19-855577-6.

External links

- Introduction to Crystallography and Mineral Crystal Systems [2]
- Crystallographic Teaching Pamphlets [3]
- Crystal Lattice Structures [4]
- Freely Available Crystallographic Software for Academia [5]
- NetSci Software Listing for Crystallography [6]
- SINCRIS Information Server for Crystallography [7]
- ORTEP a professional grade viewer for use on a PC which is based on the FORTRAN code which came from Oak Ridge [8]
- Vega Science Trust Interviews on Crystallography [9] Freeview video interviews with Max Pertuz, Rober Huber and Aaron Klug.
- Commission on Crystallographic Teaching, Pamphlets [10]
- Crystallography site of Steffen Weber with lots of Java Applets [11]
- IUCr Online Dictionary of Crystallography [12]
- American Crystallographic Association [13]
- Laue Measurement of Single-Crystal Turbine Blades [14]
- Ames Laboratory, US DOE Crystallography Research Resources [15]

References

[1] http://scripts.iucr.org/cgi-bin/paper?kv5037
[2] http://www.rockhounds.com/rockshop/xtal/index.html
[3] http://www.mineralogie.uni-wuerzburg.de/links/teach/crysteach.html
[4] http://cst-www.nrl.navy.mil/lattice/spcgrp/
[5] http://www.ccp14.ac.uk/
[6] http://www.netsci.org/Resources/Software/Struct/xray.html
[7] http://www.iucr.org/sincris-top/
[8] http://www.chem.gla.ac.uk/~louis/software/ortep3/download.html
[9] http://www.vega.org.uk
[10] http://www.iucr.org/iucr-top/comm/cteach/pamphlets.html
[11] http://www.jcrystal.com/steffenweber/
[12] http://reference.iucr.org/dictionary/Main_Page
[13] http://aca.hwi.buffalo.edu/
[14] http://www.geocities.com/psistar@sbcglobal.net/Laue.pdf
[15] http://www.mcbmm.ameslab.gov/index.html

X-ray crystallography

X-ray crystallography is a method of determining the arrangement of atoms within a crystal, in which a beam of X-rays strikes a crystal and scatters into many different directions. From the angles and intensities of these scattered beams, a crystallographer can produce a three-dimensional picture of the density of electrons within the crystal. From this electron density, the mean positions of the atoms in the crystal can be determined, as well as their chemical bonds, their disorder and various other information.

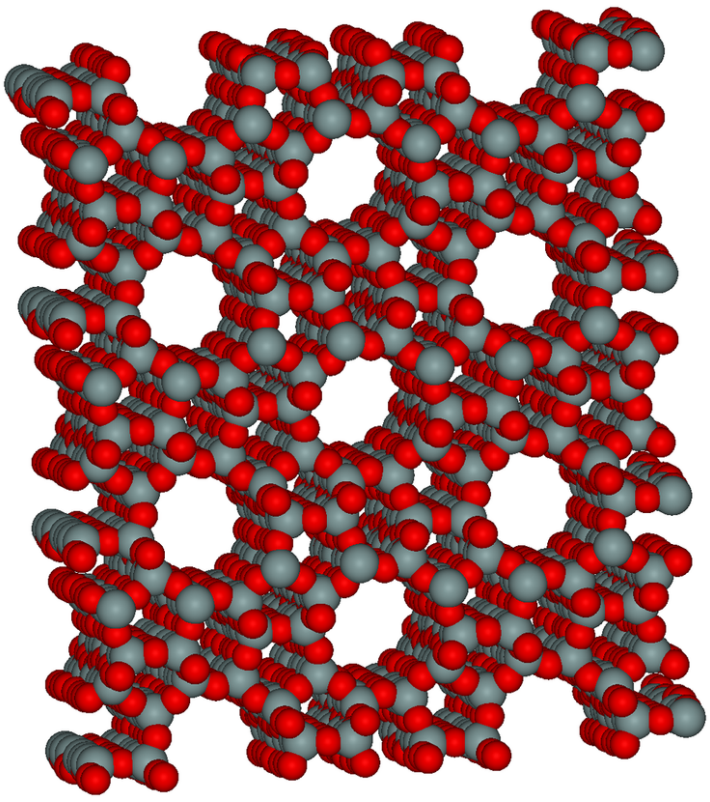

X-ray crystallography can locate every atom in a zeolite, an aluminosilicate with many important applications, such as water purification.

Since many materials can form crystals — such as salts, metals, minerals, semiconductors, as well as various inorganic, organic and biological molecules — X-ray crystallography has been fundamental in the development of many scientific fields. In its first decades of use, this method determined the size of atoms, the lengths and types of chemical bonds, and the atomic-scale differences among various materials, especially minerals and alloys. The method also revealed the structure and functioning of many biological molecules, including

vitamins, drugs, proteins and nucleic acids such as DNA. X-ray crystallography is still the chief method for characterizing the atomic structure of new materials and in discerning materials that appear similar by other experiments. X-ray crystal structures can also account for unusual electronic or elastic properties of a material, shed light on chemical interactions and processes, or serve as the basis for designing pharmaceuticals against diseases.

After a crystal has been obtained or grown in the laboratory, it is mounted on a goniometer and gradually rotated while being bombarded with X-rays, producing a diffraction pattern of regularly spaced spots known as *reflections*. The two-dimensional images taken at different rotations are converted into a three-dimensional model of the density of electrons within the crystal using the mathematical method of Fourier transforms, combined with chemical data known for the sample. Poor resolution (fuzziness) or even errors may result if the crystals are too small, or not uniform enough in their internal makeup.

X-ray crystallography is related to several other methods for determining atomic structures. Similar diffraction patterns can be produced by scattering electrons or neutrons, which are likewise interpreted as a Fourier transform. If single crystals of sufficient size cannot be obtained, various X-ray scattering methods can be applied to obtain less detailed information; such methods include fiber diffraction, powder diffraction and small-angle X-ray scattering (SAXS). In all these methods, the scattering is elastic; the scattered X-rays have the same wavelength as the incoming X-ray. By contrast, *inelastic* X-ray scattering methods are useful in studying excitations of the sample, rather than the distribution of its atoms.

History

Early scientific history of crystals and X-rays

Crystals have long been admired for their regularity and symmetry, but they were not investigated scientifically until the 17th century. Johannes Kepler hypothesized in his work *Strena seu de Nive Sexangula* (1611) that the hexagonal symmetry of snowflake crystals was due to a regular packing of spherical water particles.[1]

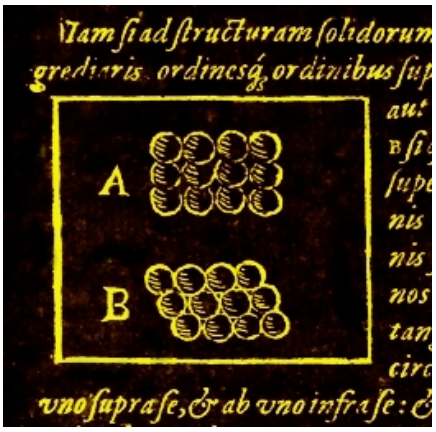

Drawing of square (Figure A, above) and hexagonal (Figure B, below) packing from Kepler's work, *Strena seu de Nive Sexangula*.

As shown by X-ray crystallography, the hexagonal symmetry of snowflakes results from the tetrahedral arrangement of hydrogen bonds about each water molecule. The water molecules are arranged simiarly to the silicon atoms in the tridymite polymorph of SiO_2. The resulting crystal structure has hexagonal symmetry when viewed along a principal axis.

Crystal symmetry was first investigated experimentally by Nicolas Steno (1669), who showed that the angles between the faces are the same in every exemplar of a particular type of crystal,[2] and by René Just Haüy (1784), who discovered that every face of a crystal can be described by simple stacking patterns of blocks of the same shape and size. Hence, William Hallowes Miller in 1839 was able to give each face a unique label of three small integers, the Miller indices which are still used today for identifying crystal faces. Haüy's study led to the correct idea that crystals are a regular three-dimensional array (a Bravais lattice) of atoms and molecules; a single unit cell is repeated indefinitely along three principal directions that are not necessarily perpendicular. In the 19th century, a complete catalog of the possible symmetries of a crystal was worked out by Johann Hessel,[3] Auguste Bravais,[4] Yevgraf Fyodorov,[5] , Arthur Schönflies[6] and (belatedly) William Barlow. On the basis of the available data and physical reasoning, Barlow proposed several crystal structures in the 1880s that were validated later by X-ray crystallography;[7] however, the available data were too few in the 1880s to accept his models as conclusive.

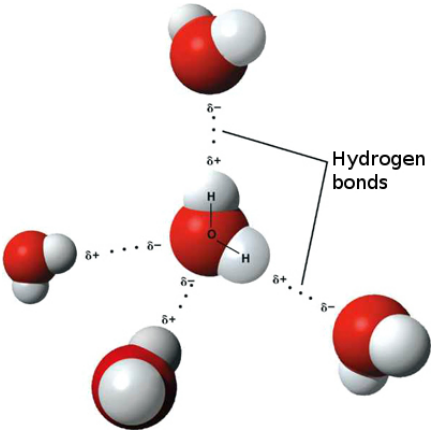

X-ray crystallography shows the arrangement of water molecules in ice, revealing the hydrogen bonds that hold the solid together. Few other methods can determine the structure of matter with such sub-atomic precision (*resolution*).

X-rays were discovered by Wilhelm Conrad Röntgen in 1895, just as the studies of crystal symmetry were being concluded. Physicists were initially uncertain of the nature of X-rays, although it was soon suspected (correctly) that they were waves of electromagnetic radiation, in other words, another form of light. At that time, the wave model of light — specifically, the Maxwell theory of electromagnetic radiation — was well accepted among scientists, and experiments by Charles Glover Barkla showed that X-rays exhibited phenomena associated with electromagnetic waves, including transverse polarization and spectral lines akin to those observed in the visible wavelengths. Single-slit experiments in the laboratory of Arnold Sommerfeld suggested the wavelength of X-rays was roughly 1 Angström, one ten millionth of a millimetre. However, X-rays are composed of photons, and thus are not only waves of electromagnetic radiation but also exhibit particle-like properties. The photon concept was introduced by Albert Einstein in 1905,[8] but it was not broadly accepted until 1922,[9] [10] when Arthur Compton confirmed it by the scattering of X-rays from electrons.[11] Therefore, these particle-like properties of X-rays, such as their ionization of gases, caused William Henry Bragg to argue in 1907 that X-rays were *not* electromagnetic radiation.[12] Nevertheless, Bragg's view was not broadly

accepted and the observation of X-ray diffraction in 1912[13] confirmed for most scientists that X-rays were a form of electromagnetic radiation.

X-ray analysis of crystals

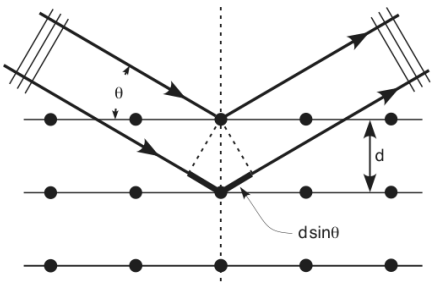

The incoming beam (coming from upper left) causes each scatterer to re-radiate a small portion of its energy as a spherical wave. If scatterers are arranged symmetrically with a separation *d*, these spherical waves will be in synch (add constructively) only in directions where their path-length difference 2*d* sin θ equals an integer multiple of the wavelength λ. In that case, part of the incoming beam is deflected by an angle 2θ, producing a *reflection* spot in the diffraction pattern.

Crystals are regular arrays of atoms, and X-rays can be considered waves of electromagnetic radiation. Atoms scatter X-ray waves, primarily through the atoms' electrons. Just as an ocean wave striking a lighthouse produces secondary circular waves emanating from the lighthouse, so an X-ray striking an electron produces secondary spherical waves emanating from the electron. This phenomenon is known as elastic scattering, and the electron (or lighthouse) is known as the *scatterer*. A regular array of scatterers produces a regular array of spherical waves. Although these waves cancel one another out in most directions through destructive interference, they add constructively in a few specific directions, determined by Bragg's law:

$$2d \sin\theta = n\lambda$$

where *d* is the spacing between diffracting planes, θ is the incident angle, *n* is any integer, and λ is the wavelength of the beam. These specific directions appear as spots on the diffraction pattern, often called *reflections*. Thus, X-ray diffraction results from an electromagnetic wave (the X-ray) impinging on a regular array of scatterers (the repeating arrangement of atoms within the crystal).

X-rays are used to produce the diffraction pattern because their wavelength λ is typically the same order of magnitude (1-100 Ångströms) as the spacing *d* between planes in the crystal. In principle, any wave impinging on a regular array of scatterers produces diffraction, as predicted first by Francesco Maria Grimaldi in 1665. To produce significant diffraction, the spacing between the scatterers and the wavelength of the impinging wave should be roughly similar in size. For illustration, the diffraction of sunlight through a bird's feather was first reported by James Gregory in the later 17th century. The first man-made diffraction gratings for visible light were constructed by David Rittenhouse in 1787, and Joseph von Fraunhofer in 1821. However, visible light has too long a wavelength (typically, 5500 Ångströms) to observe diffraction from crystals. However, prior to the first X-ray diffraction experiments, the spacings between lattice planes in a crystal were not known with certainty.

The idea that crystals could be used as a diffraction grating for X-rays arose in 1912 in a conversation between Paul Peter Ewald and Max von Laue in the English Garden in Munich. Ewald had proposed a resonator model of crystals for his thesis, but this model could not be validated using visible light, since the wavelength was much larger than the

spacing between the resonators. Von Laue realized that electromagnetic radiation of a shorter wavelength was needed to observe such small spacings, and suggested that X-rays might have a wavelength comparable to the unit-cell spacing in crystals. Von Laue worked with two technicians, Walter Friedrich and his assistant Paul Knipping, to shine a beam of X-rays through a copper sulphate crystal and record its diffraction on a photographic plate. After being developed, the plate showed a large number of well-defined spots arranged in a pattern of intersecting circles around the spot produced by the central beam.[13] [14] Von Laue developed a law that connects the scattering angles and the size and orientation of the unit-cell spacings in the crystal, for which he was awarded the Nobel Prize in Physics in 1914.[15]

As described in the mathematical derivation below, the X-ray scattering is determined by the density of electrons within the crystal. Since the energy of an X-ray is much greater than that of an atomic electron, the scattering may be modeled as Thomson scattering, the interaction of an electromagnetic ray with a free electron. This model is generally adopted to describe the polarization of the scattered radiation. The intensity of Thomson scattering declines as $1/m^2$ with the mass m of the charged particle that is scattering the radiation; hence, the atomic nuclei, which are thousands of times heavier than an electron, contribute negligibly to the scattered X-rays.

Development from 1912 to 1920

After Von Laue's pioneering research, the field developed rapidly, most notably by physicists William Lawrence Bragg and his father William Henry Bragg. In 1912-1913, the younger Bragg developed Bragg's law, which connects the observed scattering with reflections from evenly spaced planes within the crystal.[16] The earliest structures were generally simple and marked by one-dimensional symmetry. However, as computational and experimental methods improved over the next decades, it became feasible to deduce reliable atomic positions for more complicated two- and three-dimensional arrangements of atoms in the unit-cell.

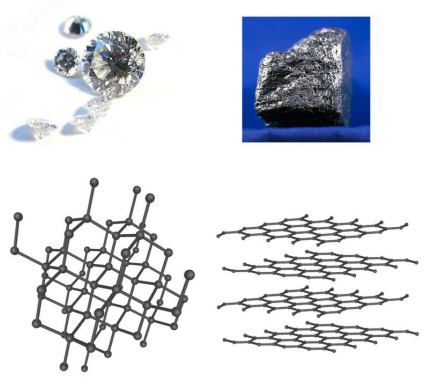

Although diamonds (top left) and graphite (top right) are identical in chemical composition — being both pure carbon — X-ray crystallography revealed the arrangement of their atoms (bottom), which accounts for their different properties. In diamond, the carbon atoms are arranged tetrahedrally and held together by single covalent bonds, making it strong in all directions. By contrast, graphite is composed of stacked sheets, in which the carbon atoms are bonded hexagonally by delocalized bonds of average order 4/3; there are no covalent bonds between sheets, making graphite easy to cleave into flakes.

The potential of X-ray crystallography for determining the structure of molecules and minerals — then only known vaguely from chemical and hydrodynamic experiments — was realized immediately. The earliest structures were simple inorganic crystals and minerals, but even these revealed fundamental laws of physics and chemistry. The first atomic-resolution structure to be solved (in 1914) was that of table salt.[17] (When an atomic structure is determined by X-ray crystallography, it is said to be "solved".) The distribution of electrons in the table-salt structure

showed that crystals are not necessarily comprised of covalently bonded molecules, and proved the existence of ionic compounds.[18] The structure of diamond was solved in the same year,[19] proving the tetrahedral arrangement of its chemical bonds and showing that the C-C single bond was 1.52 Ångströms. Other early structures included copper,[20] calcium fluoride (CaF_2, also known as *fluorite*), calcite ($CaCO_3$) and pyrite (FeS_2)[21] in 1914; spinel ($MgAl_2O_4$) in 1915;[22] the rutile and anatase forms of titanium dioxide (TiO_2) in 1916;[23] pyrochroite and, by extension, brucite [$Mn(OH)_2$ and $Mg(OH)_2$, respectively] in 1919;[24] and wurtzite (hexagonal ZnS) in 1920.[25]

The structure of graphite was solved in 1916[26] by the related method of powder diffraction,[27] which was developed by Peter Debye and Paul Scherrer and, independently, by Albert Hull in 1917.[28] The structure of graphite was determined from single-crystal diffraction in 1924 by two groups independently.[29] [30] Hull also used the powder method to determine the structures of various metals, such as iron[31] and magnesium.[32]

Contributions to chemistry and material science

X-ray crystallography has led to a better understanding of chemical bonds and non-covalent interactions. The initial studies revealed the typical radii of atoms, and confirmed many theoretical models of chemical bonding, such as the tetrahedral bonding of carbon in the diamond structure,[19] the octahedral bonding of metals observed in ammonium hexachloroplatinate (IV),[33] and the resonance observed in the planar carbonate group[21] and in aromatic molecules.[34] [35] Kathleen Lonsdale's 1928 structure of hexamethylbenzene[35] established the hexagonal symmetry of benzene and showed a clear difference in bond length between the aliphatic C-C bonds and aromatic C-C bonds; this finding led to the idea of resonance between chemical bonds, which had profound consequences for the development of chemistry.[36] Her conclusions were anticipated by William Henry Bragg, who published models of naphthalene and anthracene in 1921 based on other molecules, an early form of molecular replacement.[34]

Also in the 1920s, Victor Moritz Goldschmidt and later Linus Pauling developed rules for eliminating chemically unlikely structures and for determining the relative sizes of atoms. These rules led to the structure of brookite (1928) and an understanding of the relative stability of the rutile, brookite and anatase forms of titanium oxide.

The distance between two covalently bonded atoms is a sensitive measure of the bond strength and its bond order; thus, X-ray crystallographic studies have led to the discovery of even more exotic types of bonding in inorganic chemistry, such as metal-metal double bonds,[37] metal-metal quadruple bonds,[38] and three-center, two-electron bonds.[39] X-ray crystallography — or, strictly speaking, an inelastic Compton scattering experiment — has also provided evidence for the partially covalent character of hydrogen bonds.[40] In the field of organometallic chemistry, the X-ray structure of ferrocene initiated scientific studies of sandwich compounds,[41] while that of Zeise's salt stimulated research into "back bonding" and metal-pi complexes in general.[42] Finally, X-ray crystallography had a pioneering role in the development of supramolecular chemistry, particularly in clarifying the structures of the crown ethers and the principles of host-guest chemistry.

In material sciences, many complicated inorganic and organometallic systems have been analyzed using single-crystal methods, such as fullerenes, metalloporphyrins, and other complicated compounds. Single-crystal diffraction is also used in the pharmaceutical industry, due to recent problems with polymorphs. The major factors affecting the quality of

single-crystal structures are the crystal's size and regularity; recrystallization is a commonly used technique to improve these factors in small-molecule crystals. The Cambridge Structural Database contains over 400,000 structures; over 99% of these structures were determined by X-ray diffraction.

Mineralogy and metallurgy

Since the 1920s, X-ray diffraction has been the principal method for determining the arrangement of atoms in minerals and metals. The application of X-ray crystallography to mineralogy began with the structure of garnet, which was determined in 1924 by Menzer. A systematic X-ray crystallographic study of the silicates was undertaken in the 1920s. This study showed that, as the Si/O ratio is altered, the silicate crystals exhibit significant changes in their atomic arrangements. Machatschki extended these insights to minerals in which aluminium substitutes for the silicon atoms of the silicates. The first application of X-ray crystallography to metallurgy likewise occurred in the mid-1920s.[43] Most notably, Linus Pauling's structure of the alloy Mg_2Sn[44] led to his theory of the stability and structure of complex ionic crystals.[45]

Early organic and small biological molecules

The first structure of an organic compound, hexamethylenetetramine, was solved in 1923.[46] This was followed by several studies of long-chain fatty acids, which are an important component of biological membranes.[47] In the 1930s, the structures of much larger molecules with two-dimensional complexity began to be solved. A significant advance was the structure of phthalocyanine,[48] a large planar molecule that is closely related to porphyrin molecules important in biology, such as heme, corrin and chlorophyll.

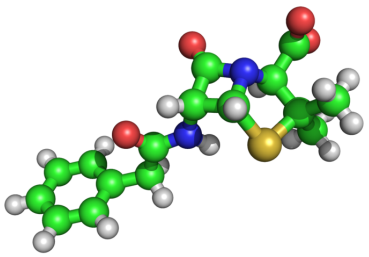

The three-dimensional structure of penicillin, for which Dorothy Crowfoot Hodgkin was awarded the Nobel Prize in Chemistry in 1964. The green, white, red, yellow and blue spheres represent atoms of carbon, hydrogen, oxygen, sulfur and nitrogen, respectively.

X-ray crystallography of biological molecules took off with Dorothy Crowfoot Hodgkin, who solved the structures of cholesterol (1937), vitamin B12 (1945) and penicillin (1954), for which she was awarded the Nobel Prize in Chemistry in 1964. In 1969, she succeeded in solving the structure of insulin, on which she worked for over thirty years.[49]

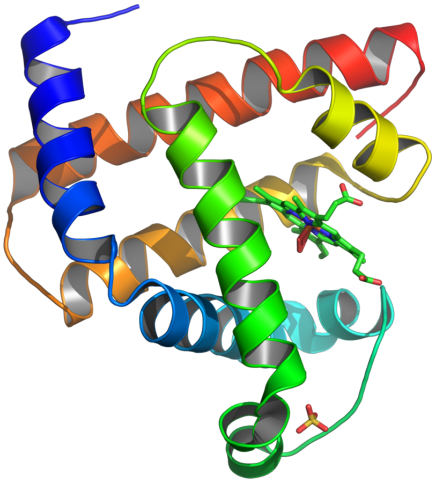

Ribbon diagram of the structure of myoglobin, showing colored alpha helices. Such proteins are long, linear molecules with thousands of atoms; yet the relative position of each atom has been determined with sub-atomic resolution by X-ray crystallography. Since it is difficult to visualize all the atoms at once, the ribbon shows the rough path of the protein polymer from its N-terminus (blue) to its C-terminus (red).

Protein crystallography

Crystal structures of proteins (which are irregular and hundreds of times larger than cholesterol) began to be solved in the late 1950s, beginning with the structure of sperm whale myoglobin by Max Perutz and Sir John Cowdery Kendrew, for which they were awarded the Nobel Prize in Chemistry in 1962.[50] Since that success, over 48970 X-ray crystal structures of proteins, nucleic acids and other biological molecules have been determined.[51] For comparison, the nearest competing method, nuclear magnetic resonance (NMR) spectroscopy has produced 7806 structures.[52] Moreover, crystallography can solve structures of arbitrarily large molecules, whereas solution-state NMR is restricted to relatively small molecules (less than 70 kDa). X-ray crystallography is now used routinely by scientists to determine how a pharmaceutical interacts with its protein target and what changes might be advisable to improve it.[53] However, intrinsic membrane proteins remain challenging to crystallize because they require detergents or other means to solubilize them in isolation, and such detergents often interfere with crystallization. Such membrane proteins are a large component of the genome and include many proteins of great physiological importance, such as ion channels and receptors.[54] [55]

Relationship to other scattering techniques

Elastic vs. inelastic scattering

X-ray crystallography is a form of elastic scattering; the outgoing X-rays have the same energy as the incoming X-rays, only with altered direction. Since the energy of a photon is inversely proportional to its wavelength, elastic scattering means that the outgoing photons have the same wavelength as the incoming photons. By contrast, *inelastic scattering* occurs when energy is transferred from the incoming X-ray to the crystal, e.g., by exciting an inner-shell electron to a higher energy level. Such inelastic scattering changes the wavelength of the outgoing beam, making it longer and less energetic. Inelastic scattering is useful for probing such excitations of matter, but are not as useful in determining the distribution of scatterers within the matter, which is the goal of X-ray crystallography.

X-rays range in wavelength from 10 to 0.01 nanometers; a typical wavelength used for crystallography is roughly 1 Å (0.1 nm), which is on the scale of covalent chemical bonds and the radius of a single atom. Longer-wavelength photons (such as ultraviolet radiation) would not have sufficient resolution to determine the atomic positions. At the other extreme, shorter-wavelength photons such as gamma rays are difficult to produce in large numbers, difficult to focus, and interact too strongly with matter, producing

particle-antiparticle pairs. Therefore, X-rays are the "sweetspot" for wavelength when determining atomic-resolution structures from the scattering of electromagnetic radiation.

Other types of X-ray scattering

X-ray diffraction involves the scattering of X-rays from a single crystal. Other forms of elastic X-ray scattering include powder diffraction, SAXS and several types of X-ray fiber diffraction, which was used by Rosalind Franklin in determining the double-helix structure of DNA. In general, X-ray diffraction produces isolated spots ("reflections"), while the other methods produce smooth, continuous scattering. In general, X-ray diffraction offers more structural information than these other techniques; however, it requires a sufficiently large and regular crystal, which is not always possible to obtain.

All of these scattering methods generally use *monochromatic* X-rays, which are restricted to a single wavelength with minor deviations. A broad spectrum of X-rays (that is, a blend of X-rays with different wavelengths) can also be used to carry out X-ray diffraction, a technique known as the Laue method. This is the method used in the original discovery of X-ray diffraction. Laue scattering provides much structural information with only a short exposure to the X-ray beam, and is therefore used in structural studies of very rapid events (time-resolved X-ray crystallography). However, it is not as well-suited as monochromatic scattering for determining the full atomic structure of a crystal. It is better suited to crystals with relatively simple atomic arrangements, such as minerals.

The Laue back reflection mode records X-rays scattered backwards also from a broad spectrum source. This is useful if the sample is too thick or bulky for X-rays to transmit through it. The diffracting planes in the crystal are determined by knowing that the normal to the diffracting plane bisects the angle between the incident beam and the diffracted beam. A Greninger chart can be used [56] to interpret the back reflection Laue photograph. The X-calibre RTXDB and MWL 110 are commercial systems for Laue back reflection pattern recording. This technique can be used in materials analysis or nondestructive testing.

Electron and neutron diffraction

Other particles, such as electrons and neutrons, may be used to produce a diffraction pattern. Although electron, neutron, and X-ray scattering use very different equipment, the resulting diffraction patterns are analyzed using the same coherent diffraction imaging techniques.

As derived below, the electron density within the crystal and the diffraction patterns are related by a simple mathematical method, the Fourier transform, which allows the density to be calculated relatively easily from the patterns. However, this works only if the scattering is *weak*, i.e., if the scattered beams are much less intense than the incoming beam. Weakly scattered beams pass through the remainder of the crystal without undergoing a second scattering event. Such re-scattered waves are called "secondary scattering" and hinder the calculation of the density of scatterers. Any sufficiently thick crystal will produce secondary scattering but since X-rays interact relatively weakly with the electrons, this is generally not a significant concern. By contrast, electron beams may produce strong secondary scattering even for very small crystals (e.g., 100 µm) used in X-ray crystallography. In such cases, extremely thin samples, roughly 100 nanometers or less, must be used to avoid secondary scattering; the primary scattered electron beams

leave the sample before they have a chance to undergo secondary scattering. Since this thickness corresponds roughly to the diameter of many viruses, a promising direction is the electron diffraction of isolated macromolecular assemblies, such as viral capsids and molecular machines, which may be carried out with a cryo-electron microscope.

Neutron diffraction is an excellent method for structure determination, although it has been difficult to obtain intense, monochromatic beams of neutrons in sufficient quantities. Traditionally, nuclear reactors have been used, although the new Spallation Neutron Source holds much promise in the near future. Being uncharged, neutrons scatter much more readily from the atomic nuclei rather than from the electrons. Therefore, neutron scattering is very useful for observing the positions of light atoms with few electrons, especially hydrogen, which is essentially invisible in the X-ray diffraction of larger molecules. Neutron scattering also has the remarkable property that the solvent can be made invisible by adjusting the ratio of normal water, H_2O, and heavy water, D_2O.

Methods

Overview of single-crystal X-ray diffraction

The oldest and most precise method of X-ray crystallography is *single-crystal X-ray diffraction*, in which a beam of X-rays strikes a single crystal, producing scattered beams. When they land on a piece of film or other detector, these beams make a *diffraction pattern* of spots; the strengths and angles of these beams are recorded as the crystal is gradually rotated.[57] Each spot is called a *reflection*, since it corresponds to the reflection of the X-rays from one set of evenly spaced planes within the crystal. For single crystals of sufficient purity and regularity, X-ray diffraction data can determine the mean chemical bond lengths and angles to within a few thousandths of an Ångström and to within a few tenths of a degree, respectively. The atoms in a crystal are also not static, but oscillate about their mean positions, usually by less than a few tenths of an Ångström. X-ray crystallography allows the size of these oscillations to be measured quantitatively.

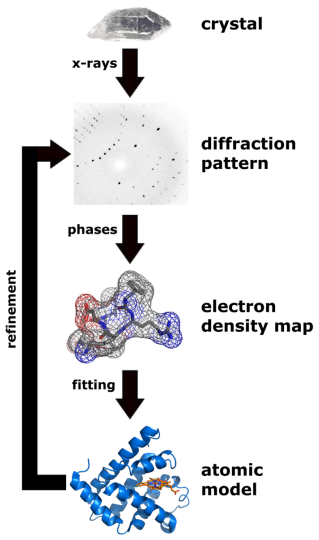

Workflow for solving the structure of a molecule by X-ray crystallography.

Procedure

The technique of single-crystal X-ray crystallography has three basic steps. The first — and often most difficult — step is to obtain an adequate crystal of the material under study. The crystal should be sufficiently large (typically larger than 100 micrometres in all dimensions), pure in composition and regular in structure, with no significant internal imperfections such as cracks or twinning. A small or irregular crystal will give fewer and less reliable data, from which it may be impossible to determine the atomic arrangement.

In the second step, the crystal is placed in an intense beam of X-rays, usually of a single wavelength (*monochromatic X-rays*), producing the regular pattern of reflections. As the

crystal is gradually rotated, previous reflections disappear and new ones appear; the intensity of every spot is recorded at every orientation of the crystal. Multiple data sets may have to be collected, with each set covering slightly more than half a full rotation of the crystal and typically containing tens of thousands of reflection intensities.

In the third step, these data are combined computationally with complementary chemical information to produce and refine a model of the arrangement of atoms within the crystal. The final, refined model of the atomic arrangement — now called a *crystal structure* — is usually stored in a public database.

Limitations

As the crystal's repeating unit, its unit cell, becomes larger and more complex, the atomic-level picture provided by X-ray crystallography becomes less well-resolved (more "fuzzy") for a given number of observed reflections. Two limiting cases of X-ray crystallography—"small-molecule" and "macromolecular" crystallography—are often discerned. *Small-molecule crystallography* typically involves crystals with fewer than 100 atoms in their asymmetric unit; such crystal structures are usually so well resolved that the atoms can be discerned as isolated "blobs" of electron density. By contrast, *macromolecular crystallography* often involves tens of thousands of atoms in the unit cell. Such crystal structures are generally less well-resolved (more "smeared out"); the atoms and chemical bonds appear as tubes of electron density, rather than as isolated atoms. In general, small molecules are also easier to crystallize than macromolecules; however, X-ray crystallography has proven possible even for viruses with hundreds of thousands of atoms.

Crystallization

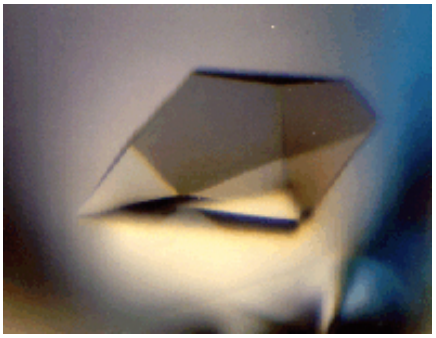

A protein crystal seen under a microscope. Crystals used in X-ray crystallography are generally smaller than a millimeter across.

Although crystallography can be used to characterize the disorder in an impure or irregular crystal, crystallography generally requires a pure crystal of high regularity to solve for the structure of a complicated arrangement of atoms. Pure, regular crystals can sometimes be obtained from natural or man-made materials, such as samples of metals, minerals or other macroscopic materials. The regularity of such crystals can sometimes be improved with annealing and other methods. However, in many cases, obtaining a diffraction-quality crystal is the chief barrier to solving its atomic-resolution structure.[58]

Small-molecule and macromolecular crystallography differ in the range of possible techniques used to produce diffraction-quality crystals. Small molecules generally have few degrees of conformational freedom, and may be crystallized by a wide range of methods, such as chemical vapor deposition and recrystallisation. By contrast, macromolecules generally have many degrees of freedom and their crystallization must be carried out to maintain a stable structure. For example, proteins and larger RNA molecules cannot be crystallized if their tertiary structure has been unfolded; therefore, the range of crystallization conditions is restricted to solution conditions in which such molecules remain folded.

Protein crystals are almost always grown in solution. The most common approach is to lower the solubility of its component molecules very gradually; however, if this is done too quickly, the molecules will precipitate from solution, forming a useless dust or amorphous gel on the bottom of the container. Crystal growth in solution is characterized by two steps: *nucleation* of a microscopic crystallite (possibly having only 100 molecules), followed by *growth* of that crystallite, ideally to a diffraction-quality crystal.[59] The solution conditions that favor the first step (nucleation) are not always the same conditions that favor the second step (its subsequent growth). The crystallographer's goal is to identify solution conditions that favor the development of a single, large crystal, since larger crystals offer improved resolution of the molecule. Consequently, the solution conditions should *disfavor* the first step (nucleation) but *favor* the second (growth), so that only one large crystal forms per droplet. If nucleation is favored too much, a shower of small crystallites will form in the droplet, rather than one large crystal; if favored too little, no crystal will form whatsoever.

It is extremely difficult to predict good conditions for nucleation or growth of well-ordered crystals.[60] In practice, favorable conditions are identified by *screening*; a very large batch of the molecules is prepared, and a wide variety of crystallization solutions are tested.[61] Hundreds, even thousands, of solution conditions are generally tried before finding one that succeeds in crystallizing the molecules. The various conditions can use one or more physical mechanisms to lower the solubility of the molecule; for example, some may change the pH, some contain salts of the Hofmeister series or chemicals that lower the dielectric constant of the solution, and still others contain large polymers such as polyethylene glycol that drive the molecule out of solution by entropic effects. It is also common to try several temperatures for encouraging crystallization, or to gradually lower the temperature so that the solution becomes supersaturated. These methods require large amounts of the target molecule, as they use high concentration of the molecule(s) to be crystallized. Due to the difficulty in obtaining such large quantities (milligrams) of crystallisation grade protein, dispensing robots have been developed that are capable of accurately dispensing crystallisation trial drops that are of the order on 100 nanoliters in volume. This means that roughly 10-fold less protein is used per-experiment when compared to crystallisation trials setup by hand (on the order on 1 microliter).[62]

Several factors are known to inhibit or mar crystallization. The growing crystals are generally held at a constant temperature and protected from shocks or vibrations that might disturb their crystallization. Impurities in the molecules or in the crystallization solutions are often inimical to crystallization. Conformational flexibility in the molecule also tends to make crystallization less likely, due to entropy. Ironically, molecules that tend to self-assemble into regular helices are often unwilling to assemble into crystals. Crystals can be marred by twinning, which can occur when a unit cell can pack equally favorably in multiple orientations; although recent advances in computational methods have begun to allow the structures of twinned crystals to be solved, it is still very difficult. Having failed to crystallize a target molecule, a crystallographer may try again with a slightly modified version of the molecule; even small changes in molecular properties can lead to large differences in crystallization behavior.

Data collection

Mounting the crystal

Once they are full-grown, the crystals are mounted so that they may be held in the X-ray beam and rotated. There are several methods of mounting. Although crystals were once loaded into glass capillaries with the crystallization solution (the mother liquor), a more modern approach is to scoop the crystal up in a tiny loop, made of nylon or plastic and attached to a solid rod, that is then flash-frozen with liquid nitrogen.[63] This freezing reduces the radiation damage of the X-rays, as well as the noise in the Bragg peaks due to thermal motion (the Debye-Waller effect). However, untreated crystals often crack if flash-frozen; therefore, they are generally pre-soaked in a cryoprotectant solution before freezing.[64] Unfortunately, this pre-soak may itself cause the crystal to crack, ruining it for crystallography. Generally, successful cryo-conditions are identified by trial and error.

The capillary or loop is mounted on a goniometer, which allows it to be positioned accurately within the X-ray beam and rotated. Since both the crystal and the beam are often very small, the crystal must be centered within the beam to within roughly 25 micrometres accuracy, which is aided by a camera focused on the crystal. The most common type of goniometer is the "kappa goniometer", which offers three angles of rotation: the ω angle, which rotates about an axis roughly perpendicular to the beam; the κ angle, about an axis at roughly 50° to the ω axis; and, finally, the φ angle about the loop/capillary axis. When the κ angle is zero, the ω and φ axes are aligned. The κ rotation allows for convenient mounting of the crystal, since the arm in which the crystal is mounted may be swung out towards the crystallographer. The oscillations carried out during data collection (mentioned below) involve the ω axis only. An older type of goniometer is the four-circle goniometer, and its relatives such as the six-circle goniometer.

X-ray sources

The mounted crystal is then irradiated with a beam of monochromatic X-rays. The brightest and most useful X-ray sources are synchrotrons; their much higher luminosity allows for better resolution. They also make it convenient to tune the wavelength of the radiation, which is useful for multi-wavelength anomalous dispersion (MAD) phasing, described below. Synchrotrons are generally national facilities, each with several dedicated beamlines where data is collected around the clock, seven days a week.

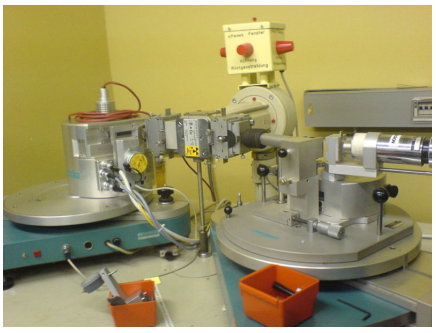

A diffractometer

Smaller, weaker X-ray sources are often used in laboratories to check the quality of crystals before bringing them to a synchrotron and sometimes to solve a crystal structure. In such systems, electrons are boiled off of a cathode and accelerated through a strong electric potential of roughly 50 kV; having reached a high speed, the electrons collide with a metal plate, emitting *bremsstrahlung* and some strong spectral lines corresponding to the excitation of inner-shell electrons of the metal. The most common metal used is copper, which can be kept cool easily, due to its high thermal conductivity, and which produces strong K_α and K_β lines. The K_β line is

sometimes suppressed with a thin layer (0.0005 in. thick) of nickel foil. The simplest and cheapest variety of sealed X-ray tube has a stationary anode (the Crookes tube) and produces *circa* 2 kW of X-ray radiation. The more expensive variety has a rotating-anode type source that produces *circa* 14 kW of X-ray radiation.

X-rays are generally filtered (by use of X-Ray Filters) to a single wavelength (made monochromatic) and collimated to a single direction before they are allowed to strike the crystal. The filtering not only simplifies the data analysis, but also removes radiation that degrades the crystal without contributing useful information. Collimation is done either with a collimator (basically, a long tube) or with a clever arrangement of gently curved mirrors. Mirror systems are preferred for small crystals (under 0.3 mm) or with large unit cells (over 150 Å).

Recording the reflections

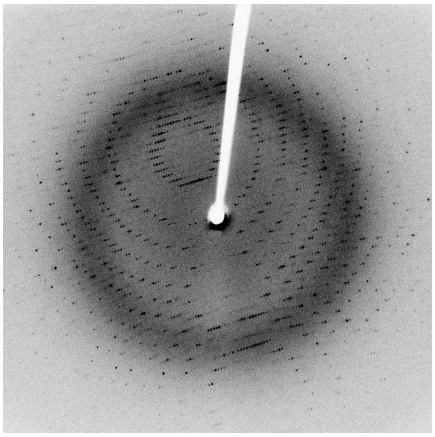

An X-ray diffraction pattern of a crystallized enzyme. The pattern of spots (called *reflections*) can be used to determine the structure of the enzyme.

When a crystal is mounted and exposed to an intense beam of X-rays, it scatters the X-rays into a pattern of spots or *reflections* that can be observed on a screen behind the crystal. A similar pattern may be seen by shining a laser pointer at a compact disc. The relative intensities of these spots provide the information to determine the arrangement of molecules within the crystal in atomic detail. The intensities of these reflections may be recorded with photographic film, an area detector or with a **charge-coupled device** (**CCD**) image sensor. The peaks at small angles correspond to low-resolution data, whereas those at high angles represent high-resolution data; thus, an upper limit on the eventual resolution of the structure can be determined from the first few images. Some measures of diffraction quality can be determined at this point, such as the mosaicity of the crystal and its overall disorder, as observed in the peak widths. Some pathologies of the crystal that would render it unfit for solving the structure can also be diagnosed quickly at this point.

One image of spots is insufficient to reconstruct the whole crystal; it represents only a small slice of the full Fourier transform. To collect all the necessary information, the crystal must be rotated step-by-step through 180°, with an image recorded at every step; actually, slightly more than 180° is required to cover reciprocal space, due to the curvature of the Ewald sphere. However, if the crystal has a higher symmetry, a smaller angle such as 90° or 45° may be recorded. The axis of the rotation should generally be changed at least once, to avoid developing a "blind spot" in reciprocal space close to the rotation axis. It is customary to rock the crystal slightly (by 0.5-2°) to catch a broader region of reciprocal space.

Multiple data sets may be necessary for certain phasing methods. For example, MAD phasing requires that the scattering be recorded at least three (and usually four, for redundancy) wavelengths of the incoming X-ray radiation. A single crystal may degrade too much during the collection of one data set, owing to radiation damage; in such cases, data sets on multiple crystals must be taken.[65]

Data analysis

Crystal symmetry, unit cell, and image scaling

Having recorded a series of diffraction patterns from the crystal, each corresponding to a different crystal orientation, the crystallographer must now convert these two-dimensional images into a three-dimensional model of the density of electrons throughout the crystal using the mathematical technique of Fourier transforms. (The relevance of this technique is explained below.) Roughly speaking, each spot corresponds to a different type of variation in the electron density; the crystallographer must determine *which* variation corresponds to *which* spot (*indexing*), the relative strengths of the spots in different images (*merging and scaling*) and how the variations should be combined to yield the total electron density (*phasing*).

In order to process the data, a crystallographer must first *index* the reflections within the multiple images recorded. This means identifying the dimensions of the unit cell and which image peak corresponds to which position in reciprocal space. A byproduct of indexing is to determine the symmetry of the crystal, i.e., its *space group*. Some space groups can be eliminated from the beginning, since they require symmetries known to be absent in the molecule itself. For example, reflection symmetries cannot be observed in chiral molecules; thus, only 65 space groups of 243 possible are allowed for protein molecules which are almost always chiral. Indexing is generally accomplished using an *autoindexing* routine.[66] Having assigned symmetry, the data is then *integrated*. This converts the hundreds of images containing the thousands of reflections into a single file, consisting of (at the very least) records of the Miller index of each reflection, and an intensity for each reflection (at this state the file often also includes error estimates and measures of partiality (what part of a given reflection was recorded on that image)).

A full data set may consist of hundreds of separate images taken at different orientations of the crystal. The first step is to merge and scale these various images, that is, to identify which peaks appear in two or more images (*merging*) and to scale the relative images so that they have a consistent intensity scale. Optimizing the intensity scale is critical because the relative intensity of the peaks is the key information from which the structure is determined. The repetitive technique of crystallographic data collection and the often high symmetry of crystalline materials cause the diffractometer to record many symmetry-equivalent reflections multiple times. This allows a merging or symmetry related R-factor to be calculated based upon how similar are the measured intensities of symmetry equivalent reflections, thus giving a score to assess the quality of the data.

Initial phasing

The data collected from a diffraction experiment is a reciprocal space representation of the crystal lattice. The position of each diffraction 'spot' is governed by the size and shape of the unit cell, and the inherent symmetry within the crystal. The intensity of each diffraction 'spot' is recorded, and this intensity is proportional to the square of the *structure factor* amplitude. The structure factor is a complex number containing information relating to both the amplitude and phase of a wave. In order to obtain an interpretable *electron density map*, both amplitude and phase must be known (an electron density map allows a crystallographer to build a starting model of the molecule). The phase cannot be directly recorded during a diffraction experiment: this is known as the phase problem. Initial phase estimates can be obtained in a variety of ways:

- ***Ab initio* phasing**, aka **direct methods** - This is usually the method of choice for small molecules (<1000 non-hydrogen atoms), and has been used successfully to solve the phase problems for small proteins. If the resolution of the data is better than 1.4 Å (140 pm), direct methods can be used to obtain phase information, by exploiting known phase relationships between certain groups of reflections.[67] [68]
- **Molecular replacement** - if a structure exists of a related structure, it can be used as a search model in molecular replacement to determine the orientation and position of the molecules within the unit cell. The phases obtained this way can be used to generate *electron density maps*.[69]
- **Anomalous X-ray scattering** (*MAD or SAD phasing*) - the X-ray wavelength may be scanned past an absorption edge of an atom, which changes the scattering in a known way. By recording full sets of reflections at three different wavelengths (far below, far above and in the middle of the absorption edge) one can solve for the substructure of the anomalously diffracting atoms and thence the structure of the whole molecule. The most popular method of incorporating anomalous scattering atoms into proteins is to express the protein in a methionine auxotroph (a host incapable of synthesising methionine) in a media rich in Seleno-methionine, which contains Selenium atoms. A MAD experiment can then be conducted around the absorption edge, which should then yield the position of any methionine residues within the protein, providing initial phases.[70]
- **Heavy atom methods** (ie MIR) - If electron-dense metal atoms can be introduced into the crystal, direct methods or Patterson-space methods can be used to determine their location and to obtain initial phases. Typically, a crystallographer can introduce such heavy atoms either by soaking the crystal in a heavy atom-containing solution, or by co-crystallization (growing the crystals in the presence of a heavy atom). As in MAD phasing, the changes in the scattering amplitudes can be interpreted to yield the phases. Although this is the original method by which protein crystal structures were solved, it has largely been superseded by MAD phasing with selenomethionine.[69]

While all four of the above methods are used to solve the phase problem for protein crystallography, small molecule crystallography generally yields data suitable for structure solution using direct methods (*ab initio* phasing).

Model building and phase refinement

Having obtained initial phases, an initial model can be built. This model can be used to refine the phases, leading to an improved model, and so on. Given a model of some atomic positions, these positions and their respective Debye-Waller factors (accounting for the thermal motion of the atom - aka **B**-factors) can be refined to fit the observed diffraction data, ideally yielding a better set of phases. A new model can then be fit to the new electron density map and a further round of refinement is carried out. This continues until the correlation between the diffraction data and the model is maximized. The agreement is measured by an *R*-factor defined as

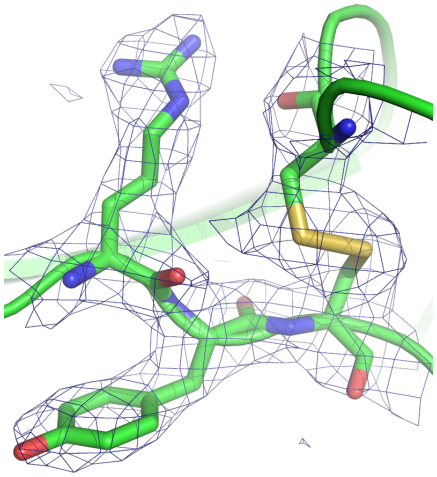

A protein crystal structure at 2.7 Å resolution. The mesh encloses the region in which the electron density exceeds a given threshold. The straight segments represent chemical bonds between the non-hydrogen atoms of an arginine (upper left), a tyrosine (lower left), a disulfide bond (upper right, in yellow), and some peptide groups (running left-right in the middle). The two curved green tubes represent spline fits to the polypeptide backbone.

$$R = \frac{\sum_{\text{all reflections}} |F_o - F_c|}{\sum_{\text{all reflections}} |F_o|}$$

A similar quality criterion is R_{free}, which is calculated from a subset (~10%) of reflections that were not included in the structure refinement. Both *R* factors depend on the resolution of the data. As a rule of thumb, R_{free} should be approximately the resolution in Ångströms divided by 10; thus, a data-set with 2 Å resolution should yield a final R_{free} of roughly 0.2. Chemical bonding features such as stereochemistry, hydrogen bonding and distribution of bond lengths and angles are complementary measures of the model quality. Phase bias is a serious problem in such iterative model building. *Omit maps* are a common technique used to check for this.

It may not be possible to observe every atom of the crystallized molecule - it must be remembered that the resulting electron density is an average of all the molecules within the crystal. In some cases, there is too much residual disorder in those atoms, and the resulting electron density for atoms existing in many conformations is smeared to such an extent that it is no longer detectable in the electron density map. Weakly scattering atoms such as hydrogen are routinely invisible. It is also possible for a single atom to appear multiple times in an electron density map, e.g., if a protein sidechain has multiple (<4) allowed conformations. In still other cases, the crystallographer may detect that the covalent structure deduced for the molecule was incorrect, or changed. For example, proteins may be cleaved or undergo post-translational modifications that were not detected prior to the crystallization.

Deposition of the structure

Once the model of a molecule's structure has been finalized, it is often deposited in a crystallographic database such as the Protein Data Bank (for protein structures) or the Cambridge Structural Database (for small molecules). Many structures obtained in private commercial ventures to crystallize medicinally relevant proteins, are not deposited in public crystallographic databases.

Diffraction theory

The main goal of X-ray crystallography is to determine the density of electrons $f(\mathbf{r})$ throughout the crystal, where $\mathbf{r}$ represents the three-dimensional position vector within the crystal. To do this, X-ray scattering is used to collect data about its Fourier transform $F(\mathbf{q})$, which is inverted mathematically to obtain the density defined in real space, using the formula

$$f(\mathbf{r}) = \int \frac{d\mathbf{q}}{(2\pi)^3} F(\mathbf{q}) e^{i\mathbf{q}\cdot\mathbf{r}}$$

where the integral is summed over all possible values of $\mathbf{q}$. The three-dimensional real vector $\mathbf{q}$ represents a point in reciprocal space, that is, to a particular oscillation in the electron density as one moves in the direction in which $\mathbf{q}$ points. The length of $\mathbf{q}$ corresponds to 2π divided by the wavelength of the oscillation. The corresponding formula for a Fourier transform will be used below

$$F(\mathbf{q}) = \int d\mathbf{r} f(\mathbf{r}) e^{-i\mathbf{q}\cdot\mathbf{r}}$$

where the integral is summed over all possible values of the position vector $\mathbf{r}$ within the crystal.

The Fourier transform $F(\mathbf{q})$ is generally a complex number, and therefore has a magnitude $|F(\mathbf{q})|$ and a phase $\varphi(\mathbf{q})$ related by the equation

$$F(\mathbf{q}) = |F(\mathbf{q})| e^{i\phi(\mathbf{q})}$$

The intensities of the reflections observed in X-ray diffraction give us the magnitudes $|F(\mathbf{q})|$ but not the phases $\varphi(\mathbf{q})$. To obtain the phases, full sets of reflections are collected with known alterations to the scattering, either by modulating the wavelength past a certain absorption edge or by adding strongly scattering (i.e., electron-dense) metal atoms such as mercury. Combining the magnitudes and phases yields the full Fourier transform $F(\mathbf{q})$, which may be inverted to obtain the electron density $f(\mathbf{r})$.

Crystals are often idealized as being *perfectly* periodic. In that ideal case, the atoms are positioned on a perfect lattice, the electron density is perfectly periodic, and the Fourier transform $F(\mathbf{q})$ is zero except when $\mathbf{q}$ belongs to the reciprocal lattice (the so-called *Bragg peaks*). In reality, however, crystals are not perfectly periodic; atoms vibrate about their mean position, and there may be disorder of various types, such as mosaicity, dislocations, various point defects, and heterogeneity in the conformation of crystallized molecules. Therefore, the Bragg peaks have a finite width and there may be significant *diffuse scattering*, a continuum of scattered X-rays that fall between the Bragg peaks.

Intuitive understanding by Bragg's law

An intuitive understanding of X-ray diffraction can be obtained from the Bragg model of diffraction. In this model, a given reflection is associated with a set of evenly spaced sheets running through the crystal, usually passing through the centers of the atoms of the crystal lattice. The orientation of a particular set of sheets is identified by its three Miller indices (*h*, *k*, *l*), and let their spacing be noted by *d*. William Lawrence Bragg proposed a model in which the incoming X-rays are scattered specularly (mirror-like) from each plane; from that assumption, X-rays scattered from adjacent planes will combine constructively (constructive interference) when the angle θ between the plane and the X-ray results in a path-length difference that is an integer multiple *n* of the X-ray wavelength λ.

$$2d \sin\theta = n\lambda$$

A reflection is said to be *indexed* when its Miller indices (or, more correctly, its reciprocal lattice vector components) have been identified from the known wavelength and the scattering angle 2θ. Such indexing gives the unit-cell parameters, the lengths and angles of the unit-cell, as well as its space group. Since Bragg's law does not interpret the relative intensities of the reflections, however, it is generally inadequate to solve for the arrangement of atoms within the unit-cell; for that, a Fourier transform method must be carried out.

Scattering as a Fourier transform

The incoming X-ray beam has a polarization and should be represented as a vector wave; however, for simplicity, let it be represented here as a scalar wave. We also ignore the complication of the time dependence of the wave and just focus on the wave's spatial dependence. Plane waves can be represented by a wave vector $\mathbf{k}_{\text{in}}$, and so the strength of the incoming wave at time *t=0* is given by

$$Ae^{i\mathbf{k}_{in}\cdot\mathbf{r}}$$

At position **r** within the sample, let there be a density of scatterers *f(***r***)*; these scatterers should produce a scattered spherical wave of amplitude proportional to the local amplitude of the incoming wave times the number of scatterers in a small volume *dV* about **r**

$$\text{amplitude of scattered wave} = Ae^{i\mathbf{k}\cdot\mathbf{r}}Sf(\mathbf{r})dV$$

where *S* is the proportionality constant.

Let's consider the fraction of scattered waves that leave with an outgoing wave-vector of $\mathbf{k}_{\text{out}}$ and strike the screen at $\mathbf{r}_{\text{screen}}$. Since no energy is lost (elastic, not inelastic scattering), the wavelengths are the same as are the magnitudes of the wave-vectors $|\mathbf{k}_{\text{in}}| = |\mathbf{k}_{\text{out}}|$. From the time that the photon is scattered at **r** until it is absorbed at $\mathbf{r}_{\text{screen}}$, the photon undergoes a change in phase

$$e^{i\mathbf{k}_{out}\cdot(\mathbf{r}_{\text{screen}}-\mathbf{r})}$$

The net radiation arriving at $\mathbf{r}_{\text{screen}}$ is the sum of all the scattered waves throughout the crystal

$$AS\int d\mathbf{r} f(\mathbf{r}) e^{i\mathbf{k}_{in}\cdot\mathbf{r}} e^{i\mathbf{k}_{out}\cdot(\mathbf{r}_{\text{screen}}-\mathbf{r})} = ASe^{i\mathbf{k}_{out}\cdot\mathbf{r}_{\text{screen}}}\int d\mathbf{r} f(\mathbf{r}) e^{i(\mathbf{k}_{in}-\mathbf{k}_{out})\cdot\mathbf{r}}$$

which may be written as a Fourier transform

$$ASe^{i\mathbf{k}_{out}\cdot\mathbf{r}_{\text{screen}}}\int d\mathbf{r} f(\mathbf{r}) e^{-i\mathbf{q}\cdot\mathbf{r}} = ASe^{i\mathbf{k}_{out}\cdot\mathbf{r}_{\text{screen}}}F(\mathbf{q})$$

where $\mathbf{q} = \mathbf{k}_{out} - \mathbf{k}_{in}$. The measured intensity of the reflection will be square of this amplitude

$$A^2 S^2 \left|F(\mathbf{q})\right|^2$$

Friedel and Bijvoet mates

For every reflection corresponding to a point $\mathbf{q}$ in the reciprocal space, there is another reflection of the same intensity at the opposite point $-\mathbf{q}$. This opposite reflection is known as the *Friedel mate* of the original reflection. This symmetry results from the mathematical fact that the density of electrons $f(\mathbf{r})$ at a position $\mathbf{r}$ is always a real number. As noted above, $f(\mathbf{r})$ is the inverse transform of its Fourier transform $F(\mathbf{q})$; however, such an inverse transform is a complex number in general. To ensure that $f(\mathbf{r})$ is real, the Fourier transform $F(\mathbf{q})$ must be such that the Friedel mates $F(-\mathbf{q})$ and $F(\mathbf{q})$ are complex conjugates of one another. Thus, $F(-\mathbf{q})$ has the same magnitude as $F(\mathbf{q})$— that is, $|F|(\mathbf{q}) = |F|(-\mathbf{q})$—but they have the opposite phase, i.e., $\varphi(\mathbf{q}) = -\varphi(\mathbf{q})$

$$F(-\mathbf{q}) = \left|F(-\mathbf{q})\right| e^{i\phi(-\mathbf{q})} = F^*(\mathbf{q}) = \left|F(\mathbf{q})\right| e^{-i\phi(\mathbf{q})}$$

The equality of their magnitudes ensures that the Friedel mates have the same intensity $|F|^2$. This symmetry allows one to measure the full Fourier transform from only half the reciprocal space, e.g., by rotating the crystal slightly more than a 180°, instead of a full turn. In crystals with significant symmetry, even more reflections may have the same intensity (Bijvoet mates); in such cases, even less of the reciprocal space may need to be measured, e.g., slightly more than 90°.

The Friedel-mate constraint can be derived from the definition of the inverse Fourier transform

$$f(\mathbf{r}) = \int \frac{d\mathbf{q}}{(2\pi)^3} F(\mathbf{q}) e^{i\mathbf{q}\cdot\mathbf{r}} = \int \frac{d\mathbf{q}}{(2\pi)^3} \left|F(\mathbf{q})\right| e^{i\phi(\mathbf{q})} e^{i\mathbf{q}\cdot\mathbf{r}}$$

Since Euler's formula states that $e^{ix} = \cos(x) + i\sin(x)$, the inverse Fourier transform can be separated into a sum of a purely real part and a purely imaginary part

$$f(\mathbf{r}) = \int \frac{d\mathbf{q}}{(2\pi)^3} \left|F(\mathbf{q})\right| e^{i(\phi+\mathbf{q}\cdot\mathbf{r})} = \int \frac{d\mathbf{q}}{(2\pi)^3} \left|F(\mathbf{q})\right| \cos\left(\phi + \mathbf{q}\cdot\mathbf{r}\right) + i \int \frac{d\mathbf{q}}{(2\pi)^3} \left|F(\mathbf{q})\right| \sin\left(\phi + \mathbf{q}\cdot\mathbf{r}\right) = I_c$$

The function $f(\mathbf{r})$ is real if and only if the second integral I_{sin} is zero for all values of $\mathbf{r}$. In turn, this is true if and only if the above constraint is satisfied

$$I_{\sin} = \int \frac{d\mathbf{q}}{(2\pi)^3} \left|F(\mathbf{q})\right| \sin\left(\phi + \mathbf{q}\cdot\mathbf{r}\right) = \int \frac{d\mathbf{q}}{(2\pi)^3} \left|F(-\mathbf{q})\right| \sin\left(-\phi - \mathbf{q}\cdot\mathbf{r}\right) = -I_{\sin}$$

since $I_{sin} = -I_{sin}$ implies that I_{sin}=0.

Ewald's sphere

Each X-ray diffraction image represents only a slice, a spherical slice of reciprocal space, as may be seen by the Ewald sphere construction. Both $\mathbf{k}_{out}$ and $\mathbf{k}_{in}$ have the same length, due to the elastic scattering, since the wavelength has not changed. Therefore, they may be represented as two radial vectors in a sphere in reciprocal space, which shows the values of $\mathbf{q}$ that are sampled in a given diffraction image. Since there is a slight spread in the incoming wavelengths of the incoming X-ray beam, the values of $|F(\mathbf{q})|$ can be measured only for $\mathbf{q}$ vectors located between the two spheres corresponding to those radii. Therefore, to obtain a full set of Fourier transform data, it is necessary to rotate the crystal through

slightly more than 180°, or sometimes less if sufficient symmetry is present. A full 360° rotation is not needed because of a symmetry intrinsic to the Fourier transforms of real functions (such as the electron density), but "slightly more" than 180° is needed to cover all of reciprocal space within a given resolution because of the curvature of the Ewald sphere (*add Figure to illustrate this*). In practice, the crystal is rocked by a small amount (0.25-1°) to incorporate reflections near the boundaries of the spherical Ewald shells.

Patterson function

A well-known result of Fourier transforms is the autocorrelation theorem, which states that the autocorrelation *c(***r***)* of a function *f(***r***)*

$$c(\mathbf{r}) = \int d\mathbf{x} f(\mathbf{x}) f(\mathbf{x}+\mathbf{r}) = \int \frac{d\mathbf{q}}{(2\pi)^3} C(\mathbf{q}) e^{i\mathbf{q}\cdot\mathbf{r}}$$

has a Fourier transform *C(***q***)*that is the squared magnitude of *F(***q***)*

$$C(\mathbf{q}) = |F(\mathbf{q})|^2$$

Therefore, the autocorrelation function *c(***r***)* of the electron density (also known as the *Patterson function*[71]) can be computed directly from the reflection intensities, without computing the phases. In principle, this could be used to determine the crystal structure directly; however, it is difficult to realize in practice. The autocorrelation function corresponds to the distribution of vectors between atoms in the crystal; thus, a crystal of *N* atoms in its unit cell may have *N(N-1)* peaks in its Patterson function. Given the inevitable errors in measuring the intensities, and the mathematical difficulties of reconstructing atomic positions from the interatomic vectors, this technique is rarely used to solve structures, except for the simplest crystals.

Advantages of a crystal

In principle, an atomic structure could be determined from applying X-ray scattering to non-crystalline samples, even to a single molecule. However, crystals offer a much stronger signal due to their periodicity.

A crystalline sample is by definition periodic; a crystal is composed of many unit cells repeated indefinitely in three independent directions. Such periodic systems have a Fourier transform that is concentrated at periodically repeating points in reciprocal space known as *Bragg peaks*; the Bragg peaks correspond to the reflection spots observed in the diffraction image. Since the amplitude at these reflections grows linearly with the number *N* of scatterers, the observed *intensity* of these spots should grow quadratically, like N^2. In other words, using a crystal concentrates the weak scattering of the individual unit cells into a much more powerful, coherent reflection that can be observed above the noise. This is an example of constructive interference.

In a non-crystalline sample, molecules within that sample would be in random orientations and therefore would have a continuous Fourier spectrum that spreads its amplitude more uniformly and with a much reduced intensity, as is observed in SAXS. More importantly, the orientational information is lost. In the crystal, the molecules adopt the same orientation within the crystal, whereas in a liquid, powder or amorphous state, the observed signal is averaged over the possible orientations of the molecules. Although theoretically possible with sufficiently low-noise data, it is generally difficult to obtain atomic-resolution structures of complicated, asymmetric molecules from such rotationally averaged

scattering data. An intermediate case is fiber diffraction in which the subunits are arranged periodically in at least one dimension.

See also

- Bragg diffraction
- Bravais lattice
- Crystallographic database
- Crystallographic point groups
- Difference density map
- Electron diffraction
- Neutron diffraction
- Powder diffraction
- Scherrer Equation
- Small angle X-ray scattering (SAXS)
- Structure determination
- Wide angle X-ray scattering (WAXS)
- Ptychography

References

[1] Kepler, J (1611). *http://www.thelatinlibrary.com/kepler/strena.html|Strena seu de Nive Sexangula*. Frankfurt: G. Tampach. http://www.thelatinlibrary.com/kepler/strena.html.

[2] Steno, N (1669). *De solido intra solidum naturaliter contento dissertationis prodromus*. Florentiae.

[3] Hessel, JFC (1831). *Kristallometrie oder Kristallonomie und Kristallographie*. Leipzig.

[4] Bravais, Auguste (1850). "Mémoire sur les systèmes formés par des points distribués regulièrement sur un plan ou dans l'espace". *J. L'Ecole Polytech.* **19**: 1–?.

[5] I. I. Shafranovskii and N. V. Belov (1962). "http://www.iucr.org/iucr-top/publ/50YearsOfXrayDiffraction/fedorov.pdf|E. S. Fedorov". *50 Years of X-Ray Diffraction, ed. Paul Ewald (Springer)*: 351–353. ISBN 90-277-9029-9. http://www.iucr.org/iucr-top/publ/50YearsOfXrayDiffraction/fedorov.pdf.

[6] Schönflies, A (1891). *Kristallsysteme und Kristallstruktur*. Leipzig.

[7] Barlow W (1883). "Probable nature of the internal symmetry of crystals". *Nature* **29**: 186–188. doi: 10.1038/029186a0 (http://dx.doi.org/10.1038/029186a0). See also Barlow W, *Nature*, **29**, 205, 383, 404 (1883-1884).

[8] Einstein, A (1905). "Über einen die Erzeugung und Verwandlung des Lichtes betreffenden heuristischen Gesichtspunkt (trans. A Heuristic Model of the Creation and Transformation of Light)". *Annalen der Physik* **17**: 132–148. **()**. An English translation is available from Wikisource.

[9] Einstein, A (1909). "Über die Entwicklung unserer Anschauungen über das Wesen und die Konstitution der Strahlung (trans. The Development of Our Views on the Composition and Essence of Radiation)". *Physikalische Zeitschrift* **10**: 817–825. **()**. An English translation is available from Wikisource.

[10] Pais, A. (1982). *Subtle is the Lord: The Science and the Life of Albert Einstein*. Oxford University Press.

[11] Compton, A (1923). " A Quantum Theory of the Scattering of X-rays by Light Elements (http://www.aip.org/history/gap/Compton/01_Compton.html)". *Physical Review* **21**: 483–502. doi: 10.1103/PhysRev.21.483 (http://dx.doi.org/10.1103/PhysRev.21.483).

[12] Bragg WH (1907). "The nature of Röntgen rays". *Transactions of the Royal Society of Science of Australia* **31**: 94–98.
Bragg WH (1908). "The nature of γ- and X-rays". *Nature* **77**: 270–271. doi: 10.1038/077270a0 (http://dx.doi.org/10.1038/077270a0). See also *Nature*, **78**, 271, 293–294, 665 (1908).
Bragg WH (1910). "The consequences of the corpuscular hypothesis of the γ- and X-rays, and the range of β-rays". *Philosophical Magazine* **20**: 385–416.
Bragg WH (1912). "On the direct or indirect nature of the ionization by X-rays". *Philosophical Magazine* **23**: 647–650.

[13] Friedrich W, Knipping P, von Laue M (1912). "Interferenz-Erscheinungen bei Röntgenstrahlen". *Sitzungsberichte der Mathematisch-Physikalischen Classe der Königlich-Bayerischen Akademie der*

Wissenschaften zu München **1912**: 303–322.
[14] von Laue, Max (1914). "http://nobelprize.org/nobel_prizes/physics/laureates/1914/laue-lecture.pdf|Concerning the detection of x-ray interferences" (PDF). *Nobel Lectures, Physics* **1901-1921**. http://nobelprize.org/nobel_prizes/physics/laureates/1914/laue-lecture.pdf. Retrieved on 2009-02-18.
[15] Dana ES, Ford WE (1932) *A Textbook of Mineralogy* fourth edition New York: John Wiley & Sons p 28
[16] Bragg WL (1912). "The Specular Reflexion of X-rays". *Nature* **90**: 410. doi: 10.1038/090410b0 (http://dx.doi.org/10.1038/090410b0).
Bragg WL (1913). "The Diffraction of Short Electromagnetic Waves by a Crystal". *Proceedings of the Cambridge Philosophical Society* **17**: 43–57.
Bragg WL (1914). "Die Reflexion der Röntgenstrahlen". *Jahrbuch der Radioaktivität und Elektronik* **11**: 350.
[17] Bragg, WL (1914). "The Structure of Some Crystals as Indicated by their Diffraction of X-rays". *Proceedings of the Royal Society (London)* **A89**: 248–277.
Bragg WL, James RW, Bosanquet CH (1921). "The Intensity of Reflexion of X-rays by Rock-Salt". *Philosophical Magazine* **41**: 309–337.
Bragg WL, James RW, Bosanquet CH (1921). "The Intensity of Reflexion of X-rays by Rock-Salt. Part II". *Philosophical Magazine* **42**: 1–17.
[18] Bragg WL, James RW, Bosanquet CH (1922). "The Distribution of Electrons around the Nucleus in the Sodium and Chlorine Atoms". *Philosophical Magazine* **44**: 433–449.
[19] Bragg WH, Bragg WL (1913). "The structure of the diamond". *Nature* **91**: 557. doi: 10.1038/091557a0 (http://dx.doi.org/10.1038/091557a0).
Bragg WH, Bragg WL (1913). "The structure of the diamond". *Proceedings of the Royal Society (London)* **A89**: 277–291. doi: 10.1098/rspa.1913.0084 (http://dx.doi.org/10.1098/rspa.1913.0084).
[20] Bragg WL (1914). "The Crystalline Structure of Copper". *Philosophical Magazine* **28**: 355–360.
[21] Bragg WL (1914). "The analysis of crystals by the X-ray spectrometer". *Proceedings of the Royal Society (London)* **A89**: 468–489.
[22] Bragg WH (1915). "The structure of the spinel group of crystals". *Philosophical Magazine* **30**: 305–315.
Nishikawa S (1915). "Structure of some crystals of spinel group". *Proc. Tokyo Math. Phys. Soc.* **8**: 199–209.
[23] Vegard L (1916). "Results of Crystal Analysis". *Philosophical Magazine* **32**: 65–96.
[24] Aminoff G (1919). "Crystal Structure of Pyrochroite". *Stockholm Geol. Fören. Förh.* **41**: 407–433.
Aminoff G (1921). "Über die Struktur des Magnesiumhydroxids". *Z. Kristallogr.* **56**: 505–509.
[25] Bragg WL (1920). "The crystalline structure of zinc oxide". *Philosophical Magazine* **39**: 647–651.
[26] Debije P, Scherrer P (1916). "Interferenz an regellos orientierten Teilchen im Röntgenlicht I". *Physikalische Zeitschrift* **17**: 277–283.
[27] Friedrich, W (1913). "Eine neue Interferenzerscheinung bei Röntgenstrahlen". *Physikalische Zeitschrift* **14**: 317–319.
[28] Hull, AW (1917). "A New Method of X-ray Crystal Analysis". *Physical Review* **10**: 661–696. doi: 10.1103/PhysRev.10.661 (http://dx.doi.org/10.1103/PhysRev.10.661).
[29] Bernal JD (1924). "The Structure of Graphite". *Proceedings of the Royal Society (London)* **A106**: 749–773.
[30] Hassel O, Mack H (1924). "Über die Kristallstruktur des Graphits". *Zeitschrift für Physik* **25**: 317–337. doi: 10.1007/BF01327534 (http://dx.doi.org/10.1007/BF01327534).
[31] Hull, AW (1917). "The Crystal Structure of Iron". *Physical Review* **9**: 84–87.
[32] Hull, AW (1917). "The Crystal Structure of Magnesium". *Proceedings of the National Academy of Science USA* **3**: 470–473. doi: 10.1073/pnas.3.7.470 (http://dx.doi.org/10.1073/pnas.3.7.470).
[33] Wyckoff RWG, Posnjak E (1921). "The Crystal Structure of Ammonium Chloroplatinate". *Journal of the American Chemical Society* **43**: 2292–2309. doi: 10.1021/ja01444a002 (http://dx.doi.org/10.1021/ja01444a002).
[34] Bragg WH (1921). "The structure of organic crystals". *Proceedings of the Royal Society (London)* **34**: 33–50.
Bragg WH (1922). "The crystalline structure of anthracene". *Proceedings of the Royal Society (London)* **35**: 167–169.
[35] Lonsdale, K (1928). "The structure of the benzene ring". *Nature* **122**: 810. doi: 10.1038/122810c0 (http://dx.doi.org/10.1038/122810c0).
[36] Pauling, L. *The Nature of the Chemical Bond* (3rd ed.). Ithaca, NY: Cornell University Press.
[37] Brosset, Cyrill (1935). "Unknown title". *Arkiv för Kemi, Mineralogi och Geologi* **12A**: No. 4.
Powell HM, Ewens RVG (1939). "The crystal structure of iron enneacarbonyl". *J. Chem. Soc.*: 286–292. doi: 10.1039/jr9390000286 (http://dx.doi.org/10.1039/jr9390000286).
Bertrand JA, Cotton FA, Dollase WA (1963). "The Metal-Metal Bonded, Polynuclear Complex Anion in $CsReCl_4$". *Journal of the American Chemical Society* **85**: 1349–1350. doi: 10.1021/ja00892a029 (http://dx.doi.org/10.1021/ja00892a029).
Robinson WT, Fergusson JE, Penfold BR (1963). "Configuration of Anion in $CsReCl_4$". *Proceedings of the*

Chemical Society of London: 116–?.

[38] Cotton FA, Curtis NF, Harris CB, Johnson BFG, Lippard SJ, Mague JT, Robinson WR, Wood JS (1964). "Mononuclear and Polynuclear Chemistry of Rhenium (III): Its Pronounced Homophilicity". *Science* **145**: 1305–1307. doi: 10.1126/science.145.3638.1305 (http://dx.doi.org/10.1126/science.145.3638.1305). PMID 17802015.
Cotton FA, Harris CB (1965). "The Crystal and Molecular Structure of Dipotassium Octachlorodirhenate(III) Dihydrate, $K_{2[Re2}Cl_8]2H_2O$". *Inorganic Chemistry* **4**: 330–333. doi: 10.1021/ic50025a015 (http://dx.doi.org/10.1021/ic50025a015).
Cotton, FA (1965). "Metal-Metal Bonding in $[Re_2X_8]^{2-}$ Ions and Other Metal Atom Clusters". *Inorganic Chemistry* **4**: 334–336. doi: 10.1021/ic50025a016 (http://dx.doi.org/10.1021/ic50025a016).

[39] Eberhardt WH, Crawford W, Jr., Lipscomb WN (1954). "The valence structure of the boron hydrides". *Journal of Chemical Physics* **22**: 989–1001. doi: 10.1063/1.1740320 (http://dx.doi.org/10.1063/1.1740320).

[40] Martin TW, Derewenda ZS (1999). "The name is Bond — H bond". *Nature Structural Biology* **6**: 403–406. doi: 10.1038/8195 (http://dx.doi.org/10.1038/8195).

[41] Dunitz JD, Orgel LE, Rich A (1956). "The crystal structure of ferrocene". *Acta Crystallographica* **9**: 373–375. doi: 10.1107/S0365110X56001091 (http://dx.doi.org/10.1107/S0365110X56001091).
Seiler P, Dunitz JD (1979). "A new interpretation of the disordered crystal structure of ferrocene". *Acta Crystallographica* **B35**: 1068–1074.

[42] Wunderlich JA, Mellor DP (1954). "A note on the crystal structure of Zeise's salt". *Acta Crystallographica* **7**: 130. doi: 10.1107/S0365110X5400028X (http://dx.doi.org/10.1107/S0365110X5400028X).
Jarvis JAJ, Kilbourn BT, Owston PG (1970). "A re-determination of the crystal and molecular structure of Zeise's salt, $KPtCl_3.C_2H_4.H_2O$. A correction". *Acta Crystallographica* **B26**: 876.
Jarvis JAJ, Kilbourn BT, Owston PG (1971). "A re-determination of the crystal and molecular structure of Zeise's salt, $KPtCl_3.C_2H_4.H_2O$". *Acta Crystallographica* **B27**: 366–372.
Love RA, Koetzle TF, Williams GJB, Andrews LC, Bau R (1975). "Neutron diffraction study of the structure of Zeise's salt, $KPtCl_3(C_2H_4).H_2O$". *Inorganic Chemistry* **14**: 2653–2657. doi: 10.1021/ic50153a012 (http://dx.doi.org/10.1021/ic50153a012).

[43] Westgren A, Phragmén G (1925). "X-ray Analysis of the Cu-Zn, Ag-Zn and Au-Zn Alloys". *Philosophical Magazine* **50**: 311–341.
Bradley AJ, Thewlis J (1926). "The structure of γ-Brass". *Proceedings of the Royal Society (London)* **112**: 678–692. doi: 10.1098/rspa.1926.0134 (http://dx.doi.org/10.1098/rspa.1926.0134).
Hume-Rothery W (1926). "Researches on the Nature, Properties and Conditions of Formation of Intermetallic Compounds (with special Reference to certain Compounds of Tin)". *Journal of the Institute of Metals* **35**: 295–361.
Bradley AJ, Gregory CH (1927). "The Structure of certain Ternary Alloys". *Nature* **120**: 678.
Westgren A (1932). "Zur Chemie der Legierungen". *Angewandte Chemie* **45**: 33–40. doi: 10.1002/ange.19320450202 (http://dx.doi.org/10.1002/ange.19320450202).
Bernal JD (1935). "The Electron Theory of Metals". *Annual Reports on the Progress of Chemistry* **32**: 181–184.

[44] Pauling, L (1923). "The Crystal Structure of Magnesium Stannide". *Journal of the American Chemical Society* **45**: 2777–2780. doi: 10.1021/ja01665a001 (http://dx.doi.org/10.1021/ja01665a001).

[45] Pauling, L (1929). "The Principles Determining the Structure of Complex Ionic Crystals". *Journal of the American Chemical Society* **51**: 1010–1026. doi: 10.1021/ja01379a006 (http://dx.doi.org/10.1021/ja01379a006).

[46] Dickinson RG, Raymond AL (1923). "The Crystal Structure of Hexamethylene-Tetramine". *Journal of the American Chemical Society* **45**: 22–29. doi: 10.1021/ja01654a003 (http://dx.doi.org/10.1021/ja01654a003).

[47] Müller A (1923). "The X-ray Investigation of Fatty Acids". *Journal of the Chemical Society (London)* **123**: 2043–2047.
Saville WB, Shearer G (1925). "An X-ray Investigation of Saturated Aliphatic Ketones". *Journal of the Chemical Society (London)* **127**: 591–598.
Bragg WH (1925). "The Investigation of thin Films by Means of X-rays". *Nature* **115**: 266–269. doi: 10.1038/115266a0 (http://dx.doi.org/10.1038/115266a0).
de Broglie M, Trillat JJ (1925). "Sur l'interprétation physique des spectres X d'acides gras". *Comptes rendus hebdomadaires des séances de l'Académie des sciences* **180**: 1485–1487.
Trillat JJ (1926). "Rayons X et Composeés organiques à longe chaine. Recherches spectrographiques sue leurs structures et leurs orientations". *Annales de physique* **6**: 5–101.
Caspari WA (1928). "Crystallography of the Aliphatic Dicarboxylic Acids". *Journal of the Chemical Society (London)* **?**: 3235–3241.
Müller A (1928). "X-ray Investigation of Long Chain Compounds (n. Hydrocarbons)". *Proceedings of the Royal Society (London)* **120**: 437–459. doi: 10.1098/rspa.1928.0158 (http://dx.doi.org/10.1098/rspa.1928.0158).

Piper SH (1929). "Some Examples of Information Obtainable from the long Spacings of Fatty Acids". *Transactions of the Faraday Society* **25**: 348–351. doi: 10.1039/tf9292500348 (http://dx.doi.org/10.1039/tf9292500348).
Müller A (1929). "The Connection between the Zig-Zag Structure of the Hydrocarbon Chain and the Alternation in the Properties of Odd and Even Numbered Chain Compounds". *Proceedings of the Royal Society (London)* **124**: 317–321. doi: 10.1098/rspa.1929.0117 (http://dx.doi.org/10.1098/rspa.1929.0117).

[48] Robertson, JM (1936). "An X-ray Study of the Phthalocyanines, Part II". *Journal of the Chemical Society*: 1195–1209.

[49] Crowfoot Hodgkin D (1935). "X-ray Single Crystal Photographs of Insulin". *Nature* **135**: 591–592. doi: 10.1038/135591a0 (http://dx.doi.org/10.1038/135591a0).

[50] Kendrew, J. C.; G. Bodo, H. M. Dintzis, R. G. Parrish, H. Wyckoff, D. C. Phillips (1958-03-08). "A Three-Dimensional Model of the Myoglobin Molecule Obtained by X-Ray Analysis". *Nature* **181** (4610): 662–666. doi: 10.1038/181662a0 (http://dx.doi.org/10.1038/181662a0).

[51] Table of entries in the PDB, arranged by experimental method. (http://www.rcsb.org/pdb/statistics/holdings.do)

[52] http://pdbbeta.rcsb.org/pdb/static.do?p=general_information/pdb_statistics/index.html|"PDB Statistics". RCSB Protein Data Bank. http://pdbbeta.rcsb.org/pdb/static.do?p=general_information/pdb_statistics/index.html. Retrieved on 2007-05-03.

[53] Scapin G (2006). "Structural biology and drug discovery". *Curr. Pharm. Des.* **12** (17): 2087–97. doi: 10.2174/138161206777585201 (http://dx.doi.org/10.2174/138161206777585201). PMID 16796557.

[54] Lundstrom K (2006). "Structural genomics for membrane proteins". *Cell. Mol. Life Sci.* **63** (22): 2597–607. doi: 10.1007/s00018-006-6252-y (http://dx.doi.org/10.1007/s00018-006-6252-y). PMID 17013556.

[55] Lundstrom K (2004). "Structural genomics on membrane proteins: mini review". *Comb. Chem. High Throughput Screen.* **7** (5): 431–9. PMID 15320710.

[56] AB Greninger Zeitschrift f. Kristallographie 91 (1935),pp. 424-432

[57] An analogous diffraction pattern may be observed by shining a laser pointer on a compact disc or DVD; the periodic spacing of the CD tracks corresponds to the periodic arrangement of atoms in a crystal.

[58] Geerlof A, Brown J, Coutard B, Egloff MP, Enguita FJ, Fogg MJ, Gilbert RJ, Groves MR, Haouz A, Nettleship JE, Nordlund P, Owens RJ, Ruff M, Sainsbury S, Svergun DI, Wilmanns M (2006). "The impact of protein characterization in structural proteomics". *Acta Crystallogr. D Biol. Crystallogr.* **62** (Pt 10): 1125–36. doi: 10.1107/S0907444906030307 (http://dx.doi.org/10.1107/S0907444906030307). PMID 17001090.

[59] Chernov AA (2003). "Protein crystals and their growth". *J. Struct. Biol.* **142** (1): 3–21. doi: 10.1016/S1047-8477(03)00034-0 (http://dx.doi.org/10.1016/S1047-8477(03)00034-0). PMID 12718915.

[60] Rupp B, Wang J (2004). "Predictive models for protein crystallization". *Methods* **34** (3): 390–407. doi: 10.1016/j.ymeth.2004.03.031 (http://dx.doi.org/10.1016/j.ymeth.2004.03.031). PMID 15325656.

[61] Chayen NE (2005). "Methods for separating nucleation and growth in protein crystallization". *Prog. Biophys. Mol. Biol.* **88** (3): 329–37. doi: 10.1016/j.pbiomolbio.2004.07.007 (http://dx.doi.org/10.1016/j.pbiomolbio.2004.07.007). PMID 15652248.

[62] Stock D, Perisic O, Lowe J (2005). "Robotic nanolitre protein crystallisation at the MRC Laboratory of Molecular Biology.". *Prog Biophys Mol Biol* **88** (3): 311–27. doi: 10.1016/j.pbiomolbio.2004.07.009 (http://dx.doi.org/10.1016/j.pbiomolbio.2004.07.009). PMID 15652247.

[63] Jeruzalmi D (2006). "First analysis of macromolecular crystals: biochemistry and x-ray diffraction". *Methods Mol. Biol.* **364**: 43–62. PMID 17172760.

[64] Helliwell JR (2005). "Protein crystal perfection and its application". *Acta Crystallogr. D Biol. Crystallogr.* **61** (Pt 6): 793–8. doi: 10.1107/S0907444905001368 (http://dx.doi.org/10.1107/S0907444905001368). PMID 15930642.

[65] Ravelli RB, Garman EF (2006). "Radiation damage in macromolecular cryocrystallography". *Curr. Opin. Struct. Biol.* **16** (5): 624–9. doi: 10.1016/j.sbi.2006.08.001 (http://dx.doi.org/10.1016/j.sbi.2006.08.001). PMID 16938450.

[66] Powell HR (1999). "The Rossmann Fourier autoindexing algorithm in MOSFLM.". *Acta Crystallogr. D Biol. Crystallogr.* **55** (Pt 10): 1690–95. doi: 10.1107/S0907444999009506 (http://dx.doi.org/10.1107/S0907444999009506). PMID 10531518.

[67] Hauptman H (1997). "Phasing methods for protein crystallography". *Curr. Opin. Struct. Biol.* **7** (5): 672–80. doi: 10.1016/S0959-440X(97)80077-2 (http://dx.doi.org/10.1016/S0959-440X(97)80077-2). PMID 9345626.

[68] Usón I, Sheldrick GM (1999). "Advances in direct methods for protein crystallography". *Curr. Opin. Struct. Biol.* **9** (5): 643–8. doi: 10.1016/S0959-440X(99)00020-2 (http://dx.doi.org/10.1016/S0959-440X(99)00020-2). PMID 10508770.

[69] Taylor G (2003). "The phase problem". *Acta Crystallogr. D Biol. Crystallogr.* **59** (Pt 11): 1881–90. doi: 10.1107/S0907444903017815 (http://dx.doi.org/10.1107/S0907444903017815). PMID 14573942.

[70] Ealick SE (2000). "Advances in multiple wavelength anomalous diffraction crystallography". *Current opinion in chemical biology* **4** (5): 495–9. doi: 10.1016/S1367-5931(00)00122-8 (http://dx.doi.org/10.1016/S1367-5931(00)00122-8). PMID 11006535.

[71] Patterson AL (1935). "A Direct Method for the Determination of the Components of Interatomic Distances in Crystals". *Zeitschrift für Kristallographie* **90**: 517–542.

Further reading

International Tables for Crystallography

- edited by Theo Hahn. Vol. A, Space-group symmetry. (2002). *International Tables for Crystallography. Volume A, Space-group Symmetry* (5th edition, ed. Theo Hahn ed.). Dordrecht: Kluwer Academic Publishers, for the International Union of Crystallography. ISBN 0-7923-6590-9.
- eds. Michael G. Rossmann and Eddy Arnold, ed (2001). *International Tables for Crystallography. Volume F, Crystallography of biological molecules*. Dordrecht: Kluwer Academic Publishers, for the International Union of Crystallography. ISBN 0-7923-6857-6.
- ed. by Theo Hahn. (1996). *International Tables for Crystallography. Brief Teaching Edition of Volume A, Space-group Symmetry* (4th revised and enlarged edition, ed. Theo Hahn ed.). Dordrecht: Kluwer Academic Publishers, for the International Union of Crystallography. ISBN 0-7923-4252-6.

Bound collections of articles

- edited by Charles W. Carter and Robert M. Sweet. (1997). *Macromolecular Crystallography, Part A (Methods in Enzymology, v. 276)* (edited by CW Carter, Jr. and RM Sweet ed.). San Diego: Academic Press. ISBN 0-12-182177-3.
- edited by Charles W. Carter Jr., Robert M. Sweet. (1997). *Macromolecular Crystallography, Part B (Methods in Enzymology, v. 277)* (edited by CW Carter, Jr. and RM Sweet ed.). San Diego: Academic Press. ISBN 0-12-182178-1.
- ed. by A. Ducruix ... (1999). *Crystallization of Nucleic Acids and Proteins: A Practical Approach* (2nd edition, edited by A. Ducruix and R. Giegé ed.). Oxford: Oxford University Press. ISBN 0-19-963678-8.

Textbooks

- Blow, D (2002). *Outline of Crystallography for Biologists*. Oxford: Oxford University Press. ISBN 0-19-851051-9.
- Burns, G.; Glazer, A.M. (1990). *Space Groups for Scientists and Engineers* (2nd ed.). Boston: Academic Press, Inc. ISBN 0-12-145761-3.
- Clegg, W (1998). *Crystal Structure Determination (Oxford Chemistry Primer)*. Oxford: Oxford University Press. ISBN 0-19-855901-1.
- Cullity, B.D. (1978). *Elements of X-Ray Diffraction* (2nd ed.). Reading, Massachusetts: Addison-Wesley Publishing Company. ISBN 0-534-55396-6.
- Drenth, J (1999). *Principles of Protein X-Ray Crystallography*. New York: Springer-Verlag. ISBN 0-387-98587-5.
- Giacovazzo, C; Monaco HL, Viterbo D, Scordari F, Gilli G, Zanotti G, and Catti M (1992). *Fundamentals of Crystallography*. Oxford: Oxford University Press. ISBN 0-19-855578-4.

- Glusker, JP; Lewis M, Rossi M (1994). *Crystal Structure Analysis for Chemists and Biologists*. New York: VCH Publishers. ISBN 0-471-18543-4.
- Massa, W (2004). *Crystal Structure Determination*. Berlin: Springer. ISBN 3-540-20644-2.
- McPherson, A (1999). *Crystallization of Biological Macromolecules*. Cold Spring Harbor, NY: Cold Spring Harbor Laboratory Press. ISBN 0-87969-617-6.
- McPherson, A (2003). *Introduction to Macromolecular Crystallography*. John Wiley & Sons. ISBN 0-471-25122-4.
- McRee, DE (1993). *Practical Protein Crystallography*. San Diego: Academic Press. ISBN 0-12-486050-8.
- O'Keeffe, M.; Hyde, B.G. (1996). *Crystal Structures; I. Patterns and Symmetry*. Washington, DC: Mineralogical Society of America, *Monograph Series*. ISBN 0-939950-40-5.
- Rhodes, G (2000). *Crystallography Made Crystal Clear*. San Diego: Academic Press. ISBN 0-12-587072-8., PDF copy of select chapters (http://www.chem.uwec.edu/Chem406_F06/Pages/lecture_notes/lect07/Crystallography_Rhodes.pdf)
- Zachariasen, WH (1945). *Theory of X-ray Diffraction in Crystals*. New York: Dover Publications. LCCN 67-26967 (http://lccn.loc.gov/67026967).

Applied Computational Data Analysis

- Young, R.A., ed (1993). *The Rietveld Method*. Oxford: Oxford University Press & International Union of Crystallography. ISBN 0-19-855577-6.

Historical

- Friedrich, W (1922). "Die Geschichte der Auffindung der Röntgenstrahlinterferenzen". *Die Naturwissenschaften* **10**: 363–366. doi: 10.1007/BF01565289 (http://dx.doi.org/10.1007/BF01565289).
- Lonsdale, K (1949). *Crystals and X-rays*. New York: D. van Nostrand.
- Bragg, William Lawrence, D. C. Phillips and H. Lipson (1992). *The Development of X-ray Analysis*. New York: Dover. ISBN 0-486-67316-2.
- Ewald PP, editor, and numerous crystallographers (1962). *Fifty Years of X-ray Diffraction*. Utrecht: published for the International Union of Crystallography by A. Oosthoek's Uitgeversmaatschappij N.V..
- Ewald, P. P., editor *50 Years of X-Ray Diffraction* (http://www.iucr.org/iucr-top/publ/50YearsOfXrayDiffraction/) (Reprinted in pdf format for the IUCr XVIII Congress, Glasgow, Scotland, Copyright © 1962, 1999 International Union of Crystallography).
- Bijvoet JM, Burgers WG, Hägg G, eds. (1969). *Early Papers on Diffraction of X-rays by Crystals (Volume I)*. Utrecht: published for the International Union of Crystallography by A. Oosthoek's Uitgeversmaatschappij N.V..
- Bijvoet JM, Burgers WG, Hägg G, eds. (1972). *Early Papers on Diffraction of X-rays by Crystals (Volume II)*. Utrecht: published for the International Union of Crystallography by A. Oosthoek's Uitgeversmaatschappij N.V..

External links

Tutorials

- Simple, non technical introduction (http://stein.bioch.dundee.ac.uk/~charlie/index.php?section=1)
- "Small Molecule Crystalization" (http://acaschool.iit.edu/lectures04/JLiangXtal.pdf) (PDF) at Illinois Institute of Technology website
- International Union of Crystallography (http://iucr.org)
- Crystallography 101 (http://www.ruppweb.org/Xray/101index.html)
- Interactive structure factor tutorial (http://www.ysbl.york.ac.uk/~cowtan/sfapplet/sfintro.html), demonstrating properties of the diffraction pattern of a 2D crystal.
- Picturebook of Fourier Transforms (http://www.ysbl.york.ac.uk/~cowtan/fourier/fourier.html), illustrating the relationship between crystal and diffraction pattern in 2D.
- Lecture notes on X-ray crystallography and structure determination (http://www.chem.uwec.edu/Chem406_F06/Pages/lectnotes.html#lecture7)

Primary databases

- Protein Data Bank (http://www.rcsb.org/pdb/home/home.do) (PDB)
- Nucleic Acid Databank (http://ndbserver.rutgers.edu/) (NDB)
- Cambridge Structural Database (http://www.ccdc.cam.ac.uk/products/csd/) (CSD)
- Inorganic Crystal Structure Database (http://www.fiz-karlsruhe.de/icsd.html) (ICSD)
- Biological Macromolecule Crystallization Database (http://xpdb.nist.gov:8060/BMCD4/) (BMCD)

Derivative databases

- PDBsum (http://www.ebi.ac.uk/thornton-srv/databases/pdbsum/)
- Proteopeida - the collaborative, 3D encyclopedia of proteins and other molecules (http://www.proteopedia.org)
- RNABase (http://www.rnabase.org/)
- HIC-Up database of PDB ligands (http://xray.bmc.uu.se/hicup/)
- Structural Classification of Proteins database
- CATH Protein Structure Classification
- List of transmembrane proteins with known 3D structure (http://blanco.biomol.uci.edu/Membrane_Proteins_xtal.html)
- Orientations of Proteins in Membranes database

Structural validation

- WHAT-IF structural validation suite (http://swift.cmbi.kun.nl/WIWWWI//)
- Biotech structural validation suite (http://biotech.ebi.ac.uk/) (formerly ProCheck)
- MolProbity structural validation suite (http://molprobity.biochem.duke.edu/)
- ProSA-web (https://prosa.services.came.sbg.ac.at/prosa.php)
- NQ-Flipper (https://flipper.services.came.sbg.ac.at/) (check for unfavorable rotamers of Asn and Gln residues)
- DALI server (http://www.ebi.ac.uk/dali/) (identifies proteins similar to a given protein)

DNA molecular modeling

X-ray diffraction

1. REDIRECT X-ray scattering techniques

X-ray microscopy

1. REDIRECT X-ray microscope

Electron microscopy

1. REDIRECT electron microscope

Vibrational circular dichroism

Vibrational circular dichroism (VCD) spectroscopy is basically circular dichroism spectroscopy in the infrared and near infrared ranges[1] . Because VCD is sensitive to the mutual orientation of distinct groups in a molecule, it provides three-dimensional structural information. Thus, it is a powerful technique as VCD spectra of enantiomers can be simulated using *ab initio* calculations, thereby allowing the identification of absolute configurations of small molecules in solution from VCD spectra. Among such quantum computations of VCD spectra resulting from the chiral properties of small organic molecules are those based on density functional theory (DFT) and gauge-invariant atomic orbitals (GIAO). As a simple example of the experimental results that were obtained by VCD are the spectral data obtained within the carbon-hydrogen (C-H) stretching region of 21 amino acids in heavy water solutions. Measurements of vibrational optical activity (VOA) have thus numerous applications, not only for small molecules, but also for large and complex biopolymers such as muscle proteins (myosin, for example) and DNA.

Vibrational modes

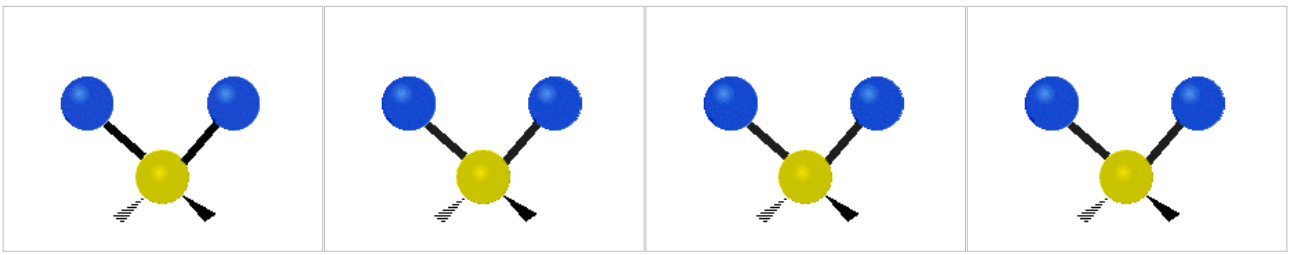

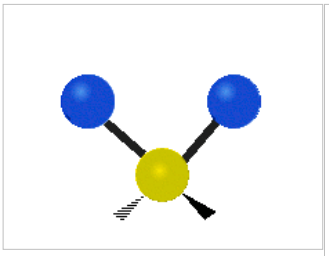

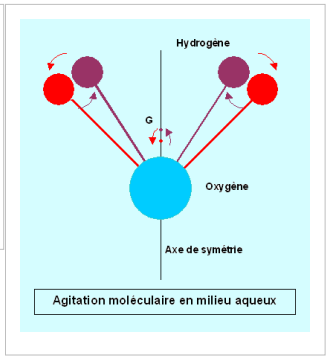

VCD of peptides and proteins

Extensive VCD studies have been reported for both polypeptides and several proteins in solution[2] [3] [4] ; several recent reviews were also compiled[5] [6] [7] [8] . An extensive but not comprehensive VCD publications list is also provided in the "References" section. The published reports over the last 22 years have established VCD as a powerful technique with improved results over those previously obtained by visible/UV circular dichroism (CD) or optical rotatory dispersion (ORD) for proteins and nucleic acids.

Amino acid and polypeptide structures

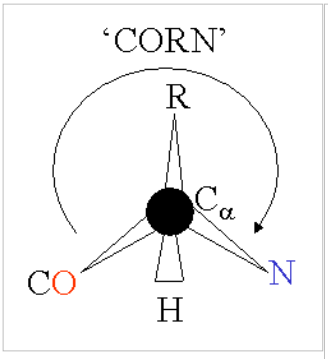

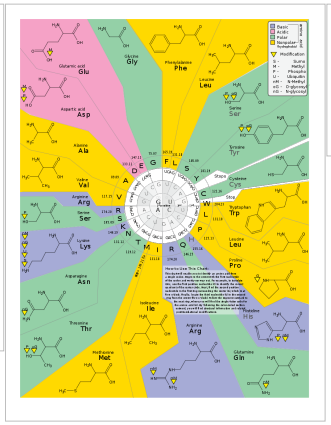

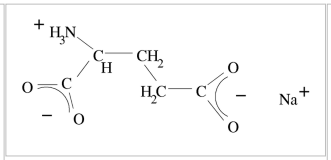

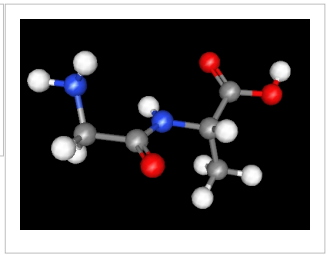

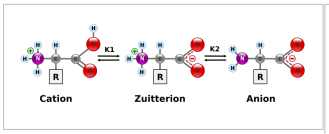

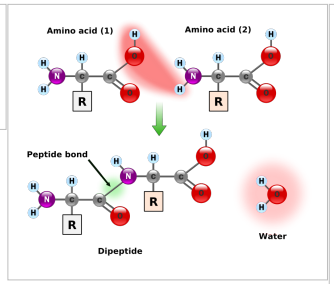

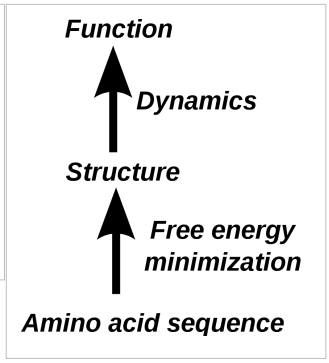

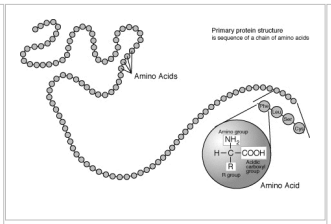
Primary protein structure
is sequence of a chain of amino acids
Amino Acids
Amino group
Acidic carbon group
Amino Acid

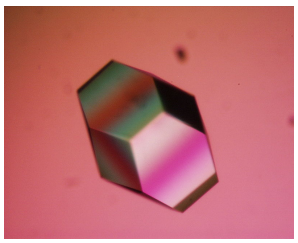

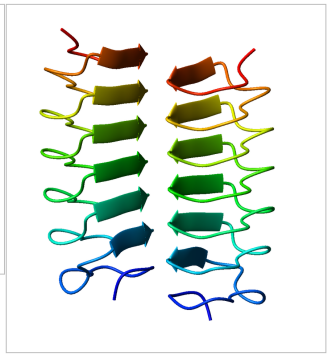

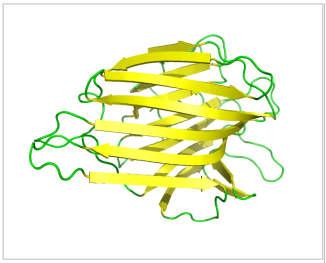

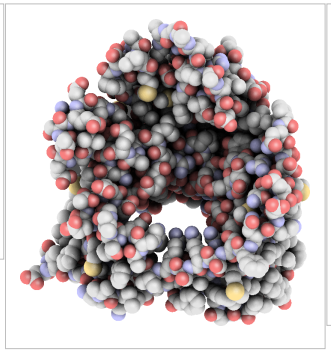

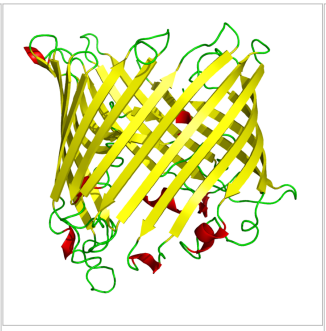

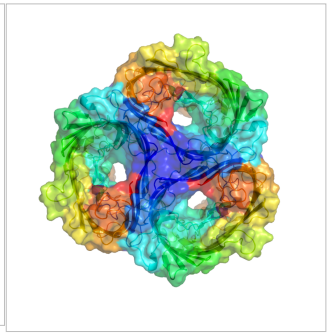

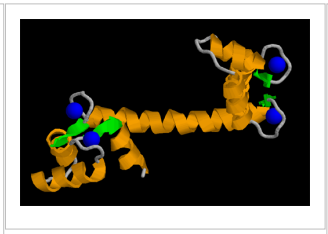

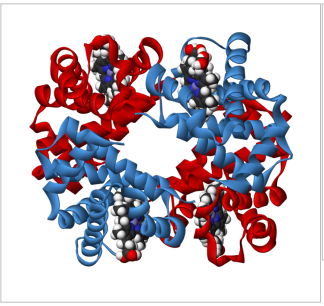

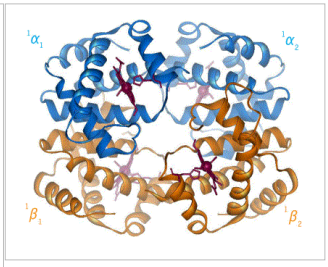
$^1\alpha_1$
$^1\alpha_2$
$^1\beta_1$
$^1\beta_2$

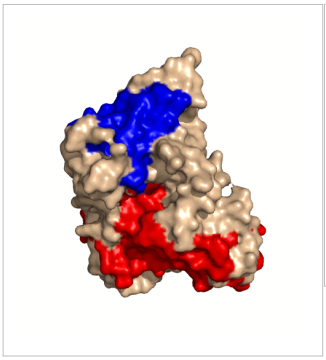

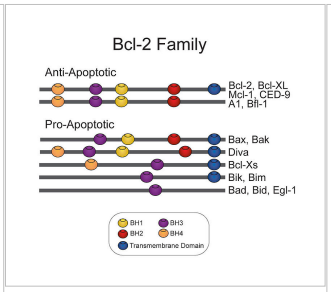
Bcl-2 Family
Anti-Apoptotic
Bcl-2, Bcl-XL
Mcl-1, CED-9
A1, Bfl-1
Pro-Apoptotic
Bax, Bak
Diva
Bcl-Xs
Bik, Bim
Bad, Bid, Egl-1
BH1
BH3
BH2
BH4
Transmembrane Domain

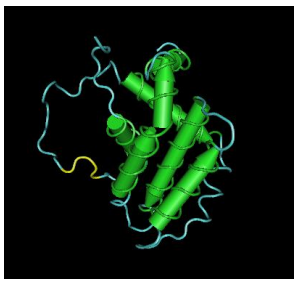

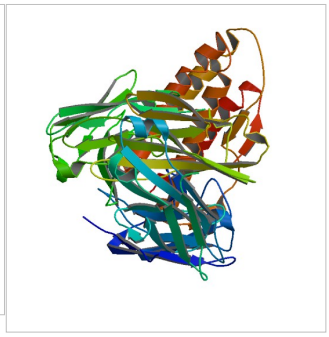

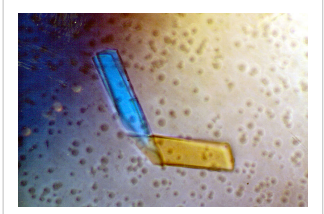

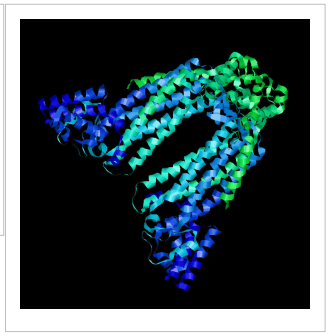

VCD of nucleic acids

VCD spectra of nucleotides, synthetic polynucleotides and several nucleic acids, including DNA, have been reported and assigned in terms of the type and number of helices present in A- , B-, and Z- DNA.

VCD Instrumentation

For biopolymers such as proteins and nucleic acids, the difference in absorbance between the levo- and dextro- configurations is five orders of magnitude smaller than the corresonding (unpolarized) absorbance. Therefore, VCD of biopolymers requires the use of very sensitive, specially built instrumentation as well as time-averaging over relatively long intervals of time even with such sensitive VCD spectrometers. Most CD instruments produce left- and right- circularly polarized light which is then either sine-wave or square-wave modulated, with subsequent phase-sensitive detection and lock-in amplification of the detected signal. In the case of FT-VCD, a photo-elastic modulator (PEM) is employed in conjunction with an FT-IR interferometer set-up. An example is that of a Bomem model MB-100 FT-IR interferometer equipped with additional polarizing optics/ accessories needed for recording VCD spectra. A parallel beam emerges through a side port of the interferometer which passes first through a wire grid linear polarizer and then through an octagonal-shaped ZnSe crystal PEM which modulates the polarized beam at a fixed, lower frequency such as 37.5 kHz. A mechanically stressed crystal such as ZnSe exhibits birefringence when stressed by an adjacent piezoelectric transducer. The linear polarizer is positioned close to, and at 45 degrees, with respect to the ZnSe crystal axis. The polarized radiation focused onto the detector is doubly modulated, both by the PEM and by the interferometer setup. A very low noise detector, such as MCT (HgCdTe), is also selected for the VCD signal phase-sensitive detection. Quasi-complete commercial FT-VCD instruments are also available from a few manufacturers but these are quite expensive and also have to be still considered as being at the prototype stage. To prevent detector saturation an appropriate, long wave pass filter is placed before the very low noise MCT detector, which allows only radiation below 1750 cm^{-1} to reach the MCT detector; the latter however measures radiation only down to 750 cm^{-1}. FT-VCD spectra accumulation of the selected sample solution is then carried out, digitized and stored by an in-line computer. Published reviews that compare various VCD methods are also available.[9] [10]

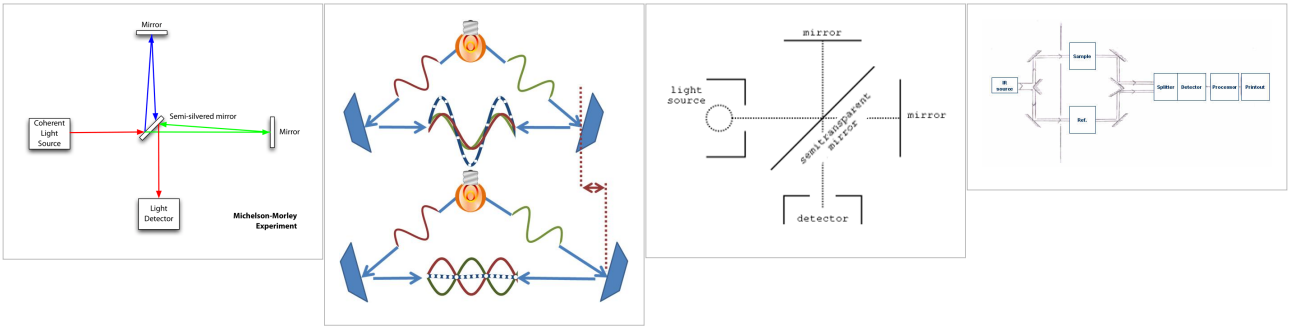


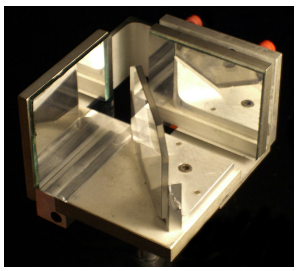
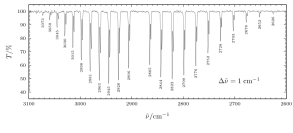
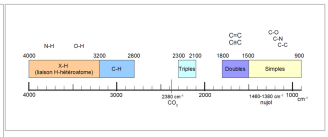
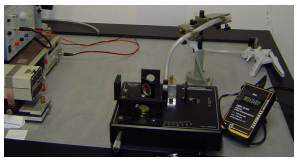
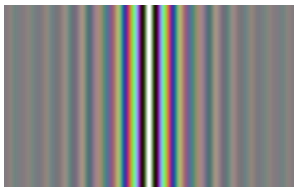
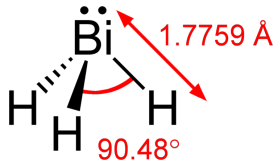

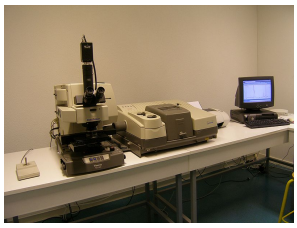

Magnetic VCD

VCD spectra have also been reported in the presence of an applied external magnetic field[11] . This method can enhance the VCD spectral resolution for small molecules[12] [13] [14] [15] [16] .

Raman optical activity (ROA)

ROA is a technique complementary to VCD especially useful in the 50—1600 cm^{-1} spectral region; it is considered as the technique of choice for determining optical activity for photon energies less then 600 cm^{-1}.

Notes

[1] http://planetphysics.org/?op=getobj;from=objects;id=410 Principles of IR and NIR Spectroscopy

[2] *"Vibrational Circular Dichroism of Polypeptides XII. Re-evaluation of the Fourier Transform Vibrational Circular Dichroism of Poly-gamma-Benzyl-L-Glutamate," P. Malon, R. Kobrinskaya, T. A. Keiderling, Biopolymers 27, 733-746 (1988).

[3] *"Vibrational Circular Dichroism of Biopolymers," T. A. Keiderling, S. C. Yasui, U. Narayanan, A. Annamalai, P. Malon, R. Kobrinskaya, L. Yang, in *Spectroscopy of Biological Molecules New Advances* ed. E. D. Schmid, F. W. Schneider, F. Siebert, p. 73-76 (1988).

[4] *"Vibrational Circular Dichroism of Polypeptides and Proteins," S. C. Yasui, T. A. Keiderling, *Mikrochimica Acta*, II, 325-327, (1988).

[5] *"Vibrational Circular Dichroism of Proteins Polysaccharides and Nucleic Acids" T. A. Keiderling, Chapter 8 in *Physical Chemistry of Food Processes, Vol. 2 Advanced Techniques, Structures and Applications.*, eds. I.C. Baianu, H. Pessen, T. Kumosinski, Van Norstrand--Reinhold, New York (1993), pp 307-337.

[6] "Spectroscopic characterization of Unfolded peptides and proteins studied with infrared absorption and vibrational circular dichroism spectra" T. A. Keiderling and Qi Xu, Advances in Protein Chemistry Volume 62, [Unfolded Proteins, Dedicated to John Edsall, Ed.: George Rose, Academic Press:New York] (2002), pp. 111-161.

[7] *"Protein and Peptide Secondary Structure and Conformational Determination with Vibrational Circular Dichroism " Timothy A. Keiderling, *Current Opinions in Chemical Biology* (Ed. Julie Leary and Mark Arnold) 6, 682-688 (2002).

[8] *Review: Conformational Studies of Peptides with Infrared Techniques. Timothy A. Keiderling and R. A. G. D. Silva, in Synthesis of Peptides and Peptidomimetics, Ed. M. Goodman and G. Herrman, Houben-Weyl, Vol 22Eb, Georg Thiem Verlag, New York (2002) pp. 715-738, (written and accepted in 2000).

[9] "Polarization Modulation Fourier Transform Infrared Spectroscopy with Digital SignalProcessing: Comparison of Vibrational Circular Dichroism Methods." Jovencio Hilario, DavidDrapcho, Raul Curbelo, Timothy A. Keiderling, Applied Spectroscopy 55, 1435-1447(2001)--
[10] "Vibrational circular dichroism of biopolymers. Summary of methods and applications.", Timothy A. Keiderling, Jan Kubelka, Jovencio Hilario, in *Vibrational spectroscopy of polymers and biological systems*, Ed. Mark Braiman, Vasilis Gregoriou, Taylor&Francis, Atlanta (CRC Press, Boca Raton, FL) (2006) pp. 253-324 (originally written in 2000, updated in 2003)
[11] "Observation of Magnetic Vibrational Circular Dichroism," T. A. Keiderling, Journal of Chemical Physics, 75, 3639-41 (1981).
[12] "Vibrational Spectral Assignment and Enhanced Resolution Using Magnetic Vibrational Circular Dichroism," T. R. Devine and T. A. Keiderling, *Spectrochimica Acta*, 43A, 627-629 (1987).
[13] "Magnetic Vibrational Circular Dichroism with an FTIR" P. V. Croatto, R. K. Yoo, T. A. Keiderling, SPIE Proceedings 1145 (7th International Conference on FTS, ed. D. G. Cameron) 152-153 (1989).
[14] "Direct Measurement of the Rotational g-Value in the Ground State of Acetylene by Magnetic Vibrational Circular Dichroism." C. N. Tam and T. A. Keiderling, Chemical Physics Letters, 243, 55-58 (1995).
[15] . "Ab initio calculation of the vibrational magnetic dipole moment" P. Bour, C. N. Tam, T. A. Keiderling, Journal of Physical Chemistry 99, 17810-17813 (1995)
[16] "Rotationally Resolved Magnetic Vibrational Circular Dichroism. Experimental Spectra and Theoretical Simulation for Diamagnetic Molecules." P. Bour, C. N. Tam, B. Wang, T. A. Keiderling, *Molecular Physics* 87, 299-318, (1996).

References

Peptides and proteins

- Huang R, Wu L, McElheny D, Bour P, Roy A, Keiderling TA. Cross-Strand Coupling and Site-Specific Unfolding Thermodynamics of a Trpzip beta-Hairpin Peptide Using (13)C Isotopic Labeling and IR Spectroscopy. *The journal of physical chemistry. B*. 2009 Apr;113(16):5661-74.
- "Vibrational Circular Dichroism of Poly alpha-Benzyl-L-Glutamate," R. D. Singh, and T. A. Keiderling, Biopolymers, 20, 237-40 (1981).
- "Vibrational Circular Dichroism of Polypeptides II. Solution Amide II and Deuteration Results," A. C. Sen and T. A. Keiderling, Biopolymers, 23, 1519-32 (1984).
- "Vibrational Circular Dichroism of Polypeptides III. Film Studies of Several alpha-Helical and ß-Sheet Polypeptides," A. C. Sen and T. A. Keiderling, Biopolymers, 23, 1533-46 (1984).
- "Vibrational Circular Dichroism of Polypeptides IV. Film Studies of L-Alanine Homo Oligopeptides," U. Narayanan, T. A. Keiderling, G. M. Bonora, and C. Toniolo, *Biopolymers* 24, 1257-63 (1985).
- "Vibrational Circular Dichroism of Polypeptides, T. A. Keiderling, S. C. Yasui, A. C. Sen, C. Toniolo, G. M. Bonora, in Peptides Structure and Function, Proceedings of the 9th American Peptide Symposium," ed. C. M. Deber, K. Kopple, V. Hruby; Pie rce Chemical: Rockford, IL; 167-172 (1985).
- "Vibrational Circular Dichroism of Polypeptides V. A Study of 310 Helical-Octapeptides" S. C. Yasui, T. A. Keiderling, G. M. Bonora, C. Toniolo, Biopolymers 25, 79-89 (1986).
- "Vibrational Circular Dichroism of Polypeptides VI. Polytyrosine alpha-helical and Random Coil Results," S. C. Yasui and T. A. Keiderling, Biopolymers 25, 5-15 (1986).
- "Vibrational Circular Dichroism of Polypeptides VII. Film and Solution Studies of alpha-forming Homo-Oligopeptides," U. Narayanan, T. A. Keiderling, G. M. Bonora, C. Toniolo, *Journal of the American Chemical Society*, 108, 2431-2437 (1986).
- "Vibrational Circular Dichroism of Polypeptides VIII. Poly Lysine Conformations as a Function of pH in Aqueous Solution," S. C. Yasui, T. A. Keiderling, Journal of the

American Chemical Society, 108, 5576-5581 (1986).
- "Vibrational Circular Dichroism of Polypeptides IX. A Study of Chain Length Dependence for 310-Helix Formation in Solution." S. C. Yasui, T. A. Keiderling, F. Formaggio, G. M. Bonora, C. Toniolo, Journal of the American Chemical Society 108, 4988-499 3 (1986).
- "Vibrational Circular Dichroism of Biopolymers." T. A. Keiderling, *Nature*, 322, 851-852 (1986).
- "Vibrational Circular Dichroism of Polypeptides X. A Study of alpha-Helical Oligopeptides in Solution." S. C. Yasui, T. A. Keiderling, R. Katachai, Biopolymers 26, 1407-1412 (1987).
- "Vibrational Circular Dichroism of Polypeptides XI. Conformation of Poly(L-Lysine(Z)-L-Lysine(Z)-L-1-Pyrenylalanine) and Poly(L-Lysine(Z)-L-Lysine(Z)-L-1-Napthylala-nine) in Solution" S. C. Yasui, T. A. Keiderling, and M. Sisido, *Macromolecules* 20, 2 403-2406 (1987).
- "Vibrational Circular Dichroism of Biopolymers" T. A. Keiderling, S. C. Yasui, A. C. Sen, U. Narayanan, A. Annamalai, P. Malon, R. Kobrinskaya, L. Yang, in "F.E.C.S. Second International Conference on Circular Dichroism, Conference Proceedings," ed. M. Kajtar, L. Eötvös Univ., Budapest, 1987, p. 155-161.
- "Vibrational Circular Dichroism of Poly-L-Proline and Other Helical Poly-peptides," R. Kobrinskaya, S. C. Yasui, T. A. Keiderling, in "Peptides: Chemistry and Biology, Proceedings of the 10th American Peptide Symposium," ed. G. R. Marshall, ESCOM, L eiden, 1988, p. 65-67.
- "Vibrational Circular Dichroism of Polypeptides with Aromatic Side Chains," S. C. Yasui, T. A. Keiderling, in "Peptides: Chemistry and Biology, Proceedings of the 10th American Peptide Symposium," ed. G. R. Marshall, ESCOM, Leiden, 1988, p. 90-92.
- "Vibrational Circular Dichroism of Polypeptides XII. Re-evaluation of the Fourier Transform Vibrational Circular Dichroism of Poly-gamma-Benzyl-L-Glutamate," P. Malon, R. Kobrinskaya, T. A. Keiderling, Biopolymers 27, 733-746 (1988).
- "Vibrational Circular Dichroism of Biopolymers," T. A. Keiderling, S. C. Yasui, U. Narayanan, A. Annamalai, P. Malon, R. Kobrinskaya, L. Yang, in *Spectroscopy of Biological Molecules New Advances* ed. E. D. Schmid, F. W. Schneider, F. Siebert, p. 73-76 (1988).
- "Vibrational Circular Dichroism of Polypeptides and Proteins," S. C. Yasui, T. A. Keiderling, *Mikrochimica Acta*, II, 325-327, (1988).
- "(1R,7R)-7-Methyl-6,9,-Diazatricyclo[6,3,0,01,6]Tridecanne-5,10-Dione, A Tricyclic Spirodilactam Containing Non-planar Amide Groups: Synthesis, NMR, Crystal Structure, Absolute Configuration, Electronic and Vibrational Circular Dichroism" P. Malon, C . L. Barness, M. Budesinsky, R. K. Dukor, D. van der Helm, T. A. Keiderling, Z. Koblicova, F. Pavlikova, M. Tichy, K. Blaha, Collections of Czechoslovak Chemical Communications 53, 2447-2472 (1988).
- "Vibrational Circular Dichroism of Poly Glutamic Acid" R. K. Dukor, T. A. Keiderling, in *Peptides 1988* (ed. G. Jung, E. Bayer) Walter de Gruyter, Berlin (1989) pp 519–521.
- "Biopolymer Conformational Studies with Vibrational Circular Dichroism" T. A. Keiderling, S. C. Yasui, P. Pancoska, R. K. Dukor, L. Yang, SPIE Proceeding 1057, ("Biomolecular Spectroscopy," ed. H. H. Mantsch, R. R. Birge) 7-14 (1989).
- "Vibrational Circular Dichroism. Comparison of Techniques and Practical Considerations" T. A. Keiderling, in "Practical Fourier Transform Infrared Spectroscopy. Industrial and Laboratory Chemical Analysis," ed. J. R. Ferraro, K. Krishnan (Academic Press, San Diego, 1990) p. 203-284.

- "Vibrational Circular Dichroism Study of Unblocked Proline Oligomers," R. K. Dukor, T. A. Keiderling, V. Gut, *International Journal of Peptide and Protein Research*, 38, 198-203 (1991).
- "Reassessment of the Random Coil Conformation. Vibrational CD Study of Proline Oligopeptides and Related Polypeptides" R. K. Dukor and T. A. Keiderling, Biopolymers 31 1747-1761 (1991).
- "Vibrational CD of the Amide II band in Some Model Polypeptides and Proteins" V. P. Gupta, T. A. Keiderling, Biopolymers 32 239-248 (1992).
- "Vibrational Circular Dichroism of Proteins Polysaccharides and Nucleic Acids" T. A. Keiderling, Chapter 8 in *Physical Chemistry of Food Processes, Vol. 2 Advanced Techniques, Structures and Applications.*, eds. I.C. Baianu, H. Pessen, T. Kumosinski, Van Norstrand—Reinhold, New York (1993), pp 307–337.
- "Structural Studies of Biological Macromolecules using Vibrational Circular Dichroism" T. A. Keiderling, P. Pancoska, Chapter 6 in Advances in Spectroscopy Vol. 21, *Biomolecular Spectroscopy Part B* eds. R. E. Hester, R. J. H. Clarke, John W iley Chichester (1993) pp 267–315.
- "Ab Initio Simulations of the Vibrational Circular Dichroism of Coupled Peptides" P. Bour and T. A. Keiderling, Journal of the American Chemical Society 115 9602-9607 (1993).
- "Ab initio Simulations of Coupled Peptide Vibrational Circular Dichroism" P. Bour, T. A. Keiderling in "Fifth International Conference on The Spectroscopy of Biological Molecules" Th. Theophanides, J. Anastassopoulou, N. Fotopoulos (Eds), Kluwen Aca demic Publ., Dortrecht, 1993, p. 29-30.
- "Vibrational Circular Dichroism Spectroscopy of Peptides and Proteins" T. A. Keiderling, in "Circular Dichroism Interpretations and Applications," K. Nakanishi, N. Berova, R. Woody, Eds., VCH Publishers, New York, (1994) pp 497–521.
- "Conformational Study of Sequential Lys-Leu Based Polymers and Oligomers using Vibrational and Electronic Circular Dichroism Spectra" V. Baumruk, D. Huo, R. K. Dukor, T. A. Keiderling, D. LeLeivre and A. Brack Biopolymers 34, 1115-1121 (1994).
- "Vibrational Optical Activity of Oligopeptides" T. B. Freedman, L. A. Nafie, T. A. Keiderling *Biopolymers* (Peptide Science) 37 (ed. C. Toniolo) 265-279 (1995).
- "Characterization of ß-bend ribbon spiral forming peptides using electronic and vibrational circular dichroism" G. Yoder, T. A. Keiderling, F. Formaggio, M. Crisma, C. Toniolo Biopolymers 35, 103-111 (1995).
- "Vibrational Circular Dichroism as a Tool for Determination of Peptide Secondary Structure" P. Bour, T. A. Keiderling, P. Malon, in "Peptides 1994 (Proceedings of the 23rd European Peptide Symposium,1994," (H.L.S. Maia, ed.), Escom, Le iden 1995, p.517-518.
- "Helical Screw Sense of homo-oligopeptides of C-alpha-methylated alpha-amino acids as Determined with Vibrational Circular Dichroism." G. Yoder, T. A. Keiderling, M. Crisma, F. Formaggio, C. Toniolo, J. Kamphuis, Tetrahedron Assymmetry 6, 687 -690 (1995).
- "Conformational Study of Linear Alternating and Mixed D- and L-Proline Oligomers Using Electronic and Vibrational CD and Fourier Transform IR." W. M&#228stle, R. K. Dukor, G. Yoder, T. A. Keiderling *Biopolymers* 36, 623-631 (1995).
- Review: "Vibrational Circular Dichroism Applications to Conformational Analysis of Biomolecules" T. A. Keiderling in *Circular Dichroism and the Conformational Analysis of Biomolecules* ed. G. D. Fasman, Plenum, New York (1996) p. 555-585.
- "Mutarotation studies of Poly L-Proline using FT-IR, Electronic and Vibrational Circular Dichroism" R. K. Dukor, T. A. Keiderling, Biospectroscopy 2, 83-100 (1996).

- "Vibrational Circular Dichroism Applications in Proteins and Peptides" T. A. Keiderling, Proceedings of the NATO ASI in Biomolecular Structure and Dynamics, Loutrakii Greece, May 1996, Ed. G. Vergoten (delayed second volume to 1998).
- "Transfer of Molecular Property Tensors in Cartesian Coordinates: A new algorithm for simulation of vibrational spectra" Petr Bour, Jana Sopkova, Lucie Bednarova, Petr Malon, T. A. Keiderling, *Journal of Computational Chemistry* 18, 6 46-659 (1997).
- "Vibrational Circular Dichroism Characterization of Alanine-Rich Peptides." Gorm Yoder and Timothy A. Keiderling, "Spectroscopy of Biological Molecules: Modern Trends," Ed. P. Carmona, R. Navarro, A. Hernanz, Kluwer Acad. Pub., Netherlands (1997) p p. 27-28.
- "Ionic strength effect on the thermal unfolding of alpha-spectrin peptides." D. Lusitani, N. Menhart, T.A. Keiderling and L. W. M. Fung. *Biochemistry* 37(1998)16546-16554.
- "In search of the earliest events of hCGb folding: structural studies of the 60-87 peptide fragment" S. Sherman, L. Kirnarsky, O. Prakash, H. M. Rogers, R.A.G.D. Silva, T.A. Keiderling, D. Smith, A.M. Hanly, F. Perini, and R.W. Ruddon, American Pep tide Symposium Proceedings, 1997.
- "Cold Denaturation Studies of (LKELPKEL)n Peptide Using Vibrational Circular Dichroism and FT-IR". R. A. G. D. Silva, Vladimir Baumruk, Petr Pancoska, T. A. Keiderling, Eric Lacassie, and Yves Trudelle, American Peptide Symposium Proceedings, 1997.
- "Simulations of oligopeptide vibrational CD. Effects of isotopic labeling." Petr Bour, Jan Kubelka,T. A. Keiderling Biopolymers 53, 380-395 (2000).
- "Site specific conformational determination in thermal unfolding studies of helical peptides using vibrational circular dichroism with isotopic substitution" R. A. G. D. Silva, Jan Kubelka, Petr Bour, Sean M. Decatur, Timothy A. Keiderling, *Proceedings of the National Academy of Sciences* (PNAS:USA) 97, 8318-8323 (2000).
- "Folding studies on the human chorionic gonadotropin b -subunit using optical spectroscopy of peptide fragments" R. A. G. D. Silva, S. A. Sherman, F. Perini, E. Bedows, T. A. Keiderling, Journal of the American Chemical Society, 122, 8623-8630 (2000).
- "Peptide and Protein Conformational Studies with Vibrational Circular Dichroism and Related Spectroscopies", Timothy A. Keiderling, (Revised and Expanded Chapter) In Circular Dichroism: Principles and Applications, 2nd Edition. (Eds. K. Nakanishi, N. Berova and R. A. Woody, John Wiley & Sons, New York (2000) p. 621-666.
- "Conformation studies with Optical Spectroscopy of peptides taken from hairpin sequences in the Human Chorionic Gonadotropin " R. A. G. D. Silva, S. A. Sherman, E. Bedows, T. A. Keiderling, Peptides for the New Millenium, Proceedings of the 16th American Peptide Symposium, (June, 1999 Minneapolis, MN) Ed.G. B. Fields, J. P. Tam, G. Barany, Kluwer Acad. Pub., Dordrecht,(2000) p. 325-326.
- "Analysis of Local Conformation within Helical Peptides via Isotope-Edited Vibrational Spectroscopy." S. M. Decatur, T. A. Keiderling, R. A. G. D.Silva, and P. Bour, Peptides for the New Millenium, Proceedings of the 16th American Peptide Symposium, (June, 1999 Minneapolis, MN) Ed. Ed.G. B. Fields, J. P. Tam, G. Barany, Kluwer Acad. Pub., Dordrecht, (2000) p. 414-416.
- "The anomalous infrared amide I intensity distribution in C-13 isotopically labeled peptide beta-sheets comes from extended, multiple stranded structures. An *Ab Initio* study." Jan Kubelka and T. A. Keiderling , *Journal of the American Chemical Society.* 123, 6142-6150 (2001).

- "Vibrational Circular Dichroism of Peptides and Proteins: Survey of Techniques, Qualitative and Quantitative Analyses, and Applications" Timothy A. Keiderling, Chapter in Infrared and Raman Spectroscopy of Biological Materials, Ed. Bing Yan and H.-U. Gremlich, Marcel Dekker, New York (2001) p.55-100.
- "Chirality in peptide vibrations. Ab initio computational studies of length, solvation, hydrogen bond, dipole coupling and isotope effects on vibrational CD. " Jan Kubelka, Petr Bour, R. A. Gangani D. Silva, Sean M. Decatur, Timothy A. Keiderling, ACS Symposium Series 810, ["Chirality: Physical Chemistry," (Ed. Janice Hicks) American Chemical Society, Washington, DC] (2002), pp. 50–64.
- "Spectroscopic Characterization of Selected b-Sheet Hairpin Models", J. Hilario, J. Kubelka, F. A. Syud, S. H. Gellman, and T. A. Keiderling. Biopolymers (Biospectroscopy) 67: 233-236 (2002)
- " Discrimination between peptide 3_{10}- and alpha-helices. Theoretical analysis of the impact of alpha-methyl substitution on experimental spectra " Jan Kubelka, R. A. Gangani D. Silva, and T. A. Keiderling, *Journal of the American Chemical Society*, 124, 5325-5332 (2002).
- "*Ab Initio* Quantum Mechanical Models of Peptide Helices and their Vibrational Spectra" Petr Bour, Jan Kubelka and T. A. Keiderling, Biopolymers 65, 45-59 (2002).
- "Discriminating 3_{10}- from alpha-helices. Vibrational and electronic CD and IR Absorption study of related Aib-contining oligopeptides" R. A. Gangani D. Silva, Sritana Yasui, Jan Kubelka, Fernando Formaggio, Marco Crisma, Claudio Toniolo, and Timothy A. Keiderling, Biopolymers 65, 229-243 (2002).
- "Spectroscopic characterization of Unfolded peptides and proteins studied with infrared absorption and vibrational circular dichroism spectra" T. A. Keiderling and Qi Xu, Advances in Protein Chemistry Volume 62, [Unfolded Proteins, Dedicated to John Edsall, Ed.: George Rose, Academic Press:New York] (2002), pp. 111–161.
- "Protein and Peptide Secondary Structure and Conformational Determination with Vibrational Circular Dichroism " Timothy A. Keiderling, *Current Opinions in Chemical Biology* (Ed. Julie Leary and Mark Arnold) 6, 682-688 (2002).
- Review: Conformational Studies of Peptides with Infrared Techniques. Timothy A. Keiderling and R. A. G. D. Silva, in Synthesis of Peptides and Peptidomimetics, Ed. M. Goodman and G. Herrman, Houben-Weyl, Vol 22Eb, Georg Thiem Verlag, New York (2002) pp. 715–738, (written and accepted in 2000).
- "Spectroscopic Studies of Structural Changes in Two beta-Sheet Forming Peptides Show an Ensemble of Structures That Unfold Non-Cooperatively" Serguei V. Kuznetsov, Jovencio Hilario, T. A. Keiderling, Anjum Ansari, *Biochemistry*, 42 :4321-4332, (2003).
- "Optical spectroscopic investigations of model beta-sheet hairpins in aqueous solution" Jovencio Hilario, Jan Kubelka, T. A. Keiderling, *Journal of the American Chemical Society* 125, 7562-7574 (2003).
- "Synthesis and conformational study of homopeptides based on (S)-Bin, a C2-symmetric binapthyl-derived Caa-disubstituted glycine with only axial chirality" J.-P. Mazaleyrat, K. Wright, A. Gaucher, M. Wakselman, S. Oancea, F. Formaggio, C. Toniolo, V. Setnicka, J. Kapitan, T. A. Keiderling, Tetrahedron Asymmetry, 14, 1879-1893 (2003).
- "Empirical modeling of the peptide amide I band IR intensity in water solution," Petr Bour, Timothy A. Keiderling, *Journal of Chemical Physics*, 119, 11253-11262 (2003)
- "The Nature of Vibrational Coupling in Helical Peptides: An Isotope Labeling Study" by R. Huang, J. Kubelka, W. Barber-Armstrong, R. A. G. D Silva, S. M. Decatur, and T. A.

Keiderling, *Journal of the American Chemical Society*, 126, 2346-2354 (2004).

- "The Complete Chirospectroscopic Signature of the Peptide 3_{10} Helix in Aqueous Solution" Claudio Toniolo, Fernando Formaggio, Sabrina Tognon, Quirinus B. Broxterman, Bernard Kaptein, Rong Huang, Vladimir Setnicka, Timothy A. Keiderling, Iain H. McColl, Lutz Hecht, Laurence D. Barron, Biopolymers 75, 32-45 (2004).
- "Induced axial chirality in the biphenyl core for the Ca-tetrasubstituted a-amino acid residue Bip and subsequent propagation of chirality in (Bip)n/Val oligopeptides" J.-P. Mazaleyrat, K. Wright, A. Gaucher, N. Toulemonde, M. Wakselman, S. Oancea, C. Peggion, F. Formaggio, V. Setnicka, T. A. Keiderling, C. Toniolo, *Journal of the American Chemical Society* 126; 12874-12879 (2004).
- *Ab initio* modeling of amide I coupling in anti-parallel b-sheets and the effect of the 13C isotopic labeling on vibrational spectra" Petr Bour, Timothy A. Keiderling, *Journal of Physical Chemistry B*, 109, 5348-5357 (2005)
- Solvent Effects on IR And VCD Spectra of Helical Peptides: Insights from Ab Initio Spectral Simulations with Explicit Water" Jan Kubelka and Timothy A. Keiderling, Journal of Physical Chemistry B 109, 8231-8243 (2005)
- IR Study of Cross-Strand Coupling in a beta-Hairpin Peptide Using Isotopic Labels., Vladimir Setnicka, Rong Huang, Catherine L. Thomas, Marcus A. Etienne, Jan Kubelka, Robert P. Hammer, Timothy A. Keiderling *Journal of the American Chemical Society* 127, 4992-4993 (2005).
- Vibrational spectral simulation for peptides of mixed secondary structure: Method comparisons with the trpzip model hairpin. Petr Bour and Timothy A. Keiderling, *Journal of Physical Chemistry B* 109, 232687-23697 (2005).
- Isotopically labeled peptides provide site-resolved structural data with infrared spectra. Probing the structural limit of optical spectroscopy, Timothy A. Keiderling, Rong Huang, Jan Kubelka, Petr Bour, Vladimir Setnicka, Robert P. Hammer, Marcus *A. Etienne, R. A. Gangani D. Silva, Sean M. Decatur Collections Symposium Series, 8, 42-49 (2005)—["Biologically Active Peptides" IXth Conference, Prague Czech Republic, April 20-22, 2005.

Nucleic acids and polynucleotides

- "Application of Vibrational Circular Dichroism to Synthetic Polypeptides and Polynucleic Acids" T. A. Keiderling, S. C. Yasui, R. K. Dukor, L. Yang, Polymer Preprints 30, 423-424 (1989).
- "Vibrational Circular Dichroism of Polyribonucleic Acids. A Comparative Study in Aqueous Solution." A. Annamalai and T. A. Keiderling, *Journal of the American Chemical Society*, 109, 3125-3132 (1987).
- "Conformational phase transitions (A-B and B-Z) of DNA and models using vibrational circular dichroism" L. Wang, L. Yang, T. A. Keiderling in *Spectroscopy of Biological Molecules.*, eds. R. E. Hester, R. B. Girling, Special Publication 94 Roya l Society of Chemistry, Cambridge (1991) p. 137-38.
- "Vibrational Circular Dichroism of Proteins Polysaccharides and Nucleic Acids" T. A. Keiderling, Chapter 8 in *Physical Chemistry of Food Processes, Vol. 2 Advanced Techniques, Structures and Applications* eds. I. C. Baianu, H. Pessen, T. Kumosinski, Van Norstrand—Reinhold, New York (1993) pp. 307–337.
- "Structural Studies of Biological Macromolecules using Vibrational Circular Dichroism" T. A. Keiderling, P. Pancoska, Chapter 6 in Advances in Spectroscopy Vol. 21,

"Biomolecular Spectroscopy Part B" ed. R. E. Hester, R. J. H. Clarke, John W iley Chichester (1993) pp 267–315.
- "Detection of Triple Helical Nucleic Acids with Vibrational Circular Dichroism," L. Wang, P. Pancoska, T. A. Keiderling in "Fifth International Conference on The Spectroscopy of Biological Molecules" Th. Theophanides, J. Anastassopoulou, N. Fotopoul os (Eds), Kluwen Academic Publ., Dortrecht, 1993, p. 81-82.
- "Helical Nature of Poly (dI-dC) • Poly (dI-dC). Vibrational Circular Dichroism Results" L. Wang and T. A. Keiderling Nucleic Acids Research 21 4127-4132 (1993).
- "Detection and Characterization of Triple Helical Pyrimidine-Purine-Pyrimidine Nucleic Acids with Vibrational Circular Dichroism" L. Wang, P. Pancoska, T. A. Keiderling, Biochemistry 33 8428-8435 (1994).
- "Vibrational Circular Dichroism of A-, B- and Z- form Nucleic Acids in the PO2- Stretching Region" L. Wang, L. Yang, T. A. Keiderling, Biophysical Journal 67, 2460-2467 (1994).
- "Studies of multiple stranded RNA and DNA with FTIR, vibrational and electronic circular dichroism," Zhihua Huang, Lijiang Wang and Timothy A. Keiderling, in Spectrosopy of Biological Molecules, Ed. J. C. Merlin, Kluwer Acad. Pub., Dordrecht, 1995, pp . 321-322.
- "Vibrational Circular Dichroism Applications to Conformational Analysis of Biomolecules" T. A. Keiderling in "Circular Dichroism and the Conformational Analysis of Biomolecules" ed G. D. Fasman, Plenum, New York (1996) pp. 555–598.
- "Vibrational Circular Dichroism Techniques and Application to Nucleic Acids" T. A. Keiderling, In "Biomolecular Structure and Dynamics", NATO ASI series, Series E: Applied Sciences- Vol.342, Eds: G. Vergoten and T. Theophanides, Kluwer Academ ic Publishers, Dordrecht, The Netherlands,pp. 299–317 (1997).

See also

- Circular dichroism
- Birefringence
- Optical rotatory dispersion
- IR spectroscopy
- Polarization
- Proteins
- Nucleic Acids
- DNA
- Molecular models of DNA
- DNA structure
- Protein structure
- Amino acids
- Density functional theory
- Quantum chemistry
- Raman optical activity (ROA)

FT-NMR

Nuclear magnetic resonance spectroscopy, most commonly known as **NMR spectroscopy**, is the name given to a technique which exploits the magnetic properties of certain nuclei. This phenomenon and its origins are detailed in a separate section on nuclear magnetic resonance. The most important applications for the organic chemist are proton NMR and carbon-13 NMR spectroscopy. In principle, NMR is applicable to any nucleus possessing spin.

A 900MHz NMR instrument with a 21.2 T magnet at HWB-NMR, Birmingham, UK, being loaded with a sample.

Many types of information can be obtained from an NMR spectrum. Much like using infrared spectroscopy to identify functional groups, analysis of a 1D NMR spectrum provides information on the number and type of chemical entities in a molecule. However, NMR provides much more information than IR.

The impact of NMR spectroscopy on the natural sciences has been substantial. It can, among other things, be used to study mixtures of analytes, to understand dynamic effects such as change in temperature and reaction mechanisms, and is an invaluable tool in understanding protein and nucleic acid structure and function. It can be applied to a wide variety of samples, both in the solution and the solid state.

Basic NMR techniques

When placed in a magnetic field, NMR active nuclei (such as ^{1}H or ^{13}C) absorb at a frequency characteristic of the isotope. The resonant frequency, energy of the absorption and the intensity of the signal are proportional to the strength of the magnetic field. For example, in a 21 tesla magnetic field, protons resonate at 900 MHz. It is common to refer to a 21 T magnet as a 900 MHz magnet, although different nuclei resonate at a different frequency at this field strength.

In the Earth's magnetic field the same nuclei resonate at audio frequencies. This effect is used in Earth's field NMR spectrometers and other instruments. Because these instruments are portable and inexpensive, they are often used for teaching and field work.

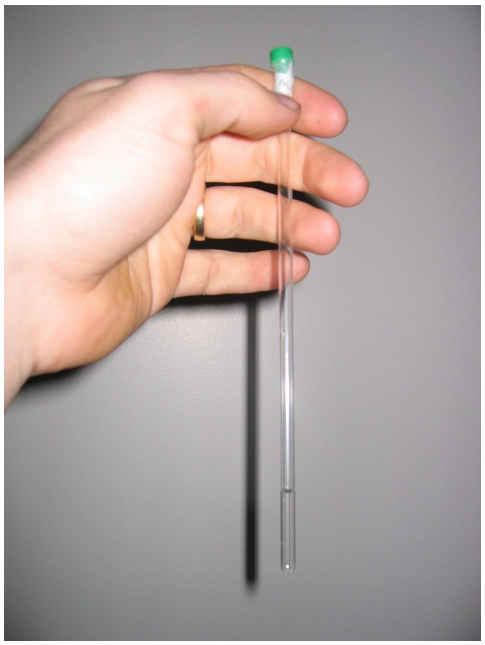

The NMR sample is prepared in a thin-walled glass tube - an NMR tube.

Chemical shift

Depending on the local chemical environment, different protons in a molecule resonate at slightly different frequencies. Since both this frequency shift and the fundamental resonant frequency are directly proportional to the strength of the magnetic field, the shift is converted into a *field-independent* dimensionless value known as the chemical shift. The chemical shift is reported as a relative measure from some reference resonance frequency. (For the nuclei ^{1}H, ^{13}C, and ^{29}Si, TMS (tetramethylsilane) is commonly used as a reference.) This difference between the frequency of the signal and the frequency of the reference is divided by frequency of the reference signal to give the chemical shift. The frequency shifts are extremely small in comparison to the fundamental NMR frequency. A typical frequency shift might be 100 Hz, compared to a fundamental NMR frequency of 100 MHz, so the chemical shift is generally expressed in parts per million (ppm).[1]

By understanding different chemical environments, the chemical shift can be used to obtain some structural information about the molecule in a sample. The conversion of the raw data to this information is called *assigning* the spectrum. For example, for the ^{1}H-NMR spectrum for ethanol (CH_3CH_2OH), one would expect three specific signals at three specific chemical shifts: one for the CH_3 group, one for the CH_2 group and one for the OH group. A typical CH_3 group has a shift around 1 ppm, a CH_2 attached to an OH has a shift of around 4 ppm and an OH has a shift around 2–3 ppm depending on the solvent used.

Because of molecular motion at room temperature, the three methyl protons *average* out during the course of the NMR experiment (which typically requires a few ms). These protons become degenerate and form a peak at the same chemical shift.

The shape and size of peaks are indicators of chemical structure too. In the example above—the proton spectrum of ethanol—the CH_3 peak would be three times as large as the OH. Similarly the CH_2 peak would be twice the size of the OH peak but only 2/3 the size of the CH_3 peak.

Modern analysis software allows analysis of the size of peaks to understand how many protons give rise to the peak. This is known as integration—a mathematical process which calculates the area under a graph (essentially what a spectrum is). The analyst must integrate the peak and not measure its height because the peaks also have *width*—and thus its size is dependent on its area not its height. However, it should be mentioned that the number of protons, or any other observed nucleus, is only proportional to the intensity, or the integral, of the NMR signal, in the very simplest one-dimensional NMR experiments. In more elaborate experiments, for instance, experiments typically used to obtain carbon-13 NMR spectra, the integral of the signals depends on the relaxation rate of the nucleus, and its scalar and dipolar coupling constants. Very often these factors are poorly understood - therefore, the integral of the NMR signal is very difficult to interpret in more complicated NMR experiments.

J-coupling

Multiplicity	Intensity Ratio
Singlet (s)	1
Doublet (d)	1:1
Triplet (t)	1:2:1
Quartet (q)	1:3:3:1
Quintet	1:4:6:4:1
Sextet	1:5:10:10:5:1
Septet	1:6:15:20:15:6:1

Some of the most useful information for structure determination in a one-dimensional NMR spectrum comes from **J-coupling** or **scalar coupling** (a special case of spin-spin coupling) between NMR active nuclei. This coupling arises from the interaction of different spin states through the chemical bonds of a molecule and results in the splitting of NMR signals. These splitting patterns can be complex or simple and, likewise, can be straightforwardly interpretable or deceptive. This coupling provides detailed insight into the connectivity of atoms in a molecule.

Coupling to n equivalent (spin ½) nuclei splits the signal into a n+1 **multiplet** with intensity ratios following Pascal's triangle as described on the right. Coupling to additional spins will lead to further splittings of each component of the multiplet e.g. coupling to two different spin ½ nuclei with significantly different coupling constants will lead to a *doublet of doublets* (abbreviation: dd). Note that coupling between nuclei that are chemically equivalent (that is, have the same chemical shift) has no effect of the NMR spectra and couplings between nuclei that are distant (usually more than 3 bonds apart for protons in flexible molecules) are usually too small to cause observable splittings. *Long-range* couplings over more than three bonds can often be observed in cyclic and aromatic compounds, leading to more complex splitting patterns.

For example, in the proton spectrum for ethanol described above, the CH_3 group is split into a *triplet* with an intensity ratio of 1:2:1 by the two neighboring CH_2 protons. Similarly, the CH_2 is split into a *quartet* with an intensity ratio of 1:3:3:1 by the three neighboring CH_3 protons. In principle, the two CH_2 protons would also be split again into a *doublet* to form a *doublet of quartets* by the hydroxyl proton, but intermolecular exchange of the

acidic hydroxyl proton often results in a loss of coupling information.

Coupling to any spin ½ nuclei such as phosphorus-31 or fluorine-19 works in this fashion (although the magnitudes of the coupling constants may be very different). But the splitting patterns differ from those described above for nuclei with spin greater than ½ because the spin quantum number has more than two possible values. For instance, coupling to deuterium (a spin 1 nucleus) splits the signal into a *1:1:1 triplet* because the spin 1 has three spin states. Similarly, a spin 3/2 nucleus splits a signal into a *1:1:1:1 quartet* and so on.

Coupling combined with the chemical shift (and the integration for protons) tells us not only about the chemical environment of the nuclei, but also the number of *neighboring* NMR active nuclei within the molecule. In more complex spectra with multiple peaks at similar chemical shifts or in spectra of nuclei other than hydrogen, coupling is often the only way to distinguish different nuclei.

Second-order (or strong) coupling

The above description assumes that the coupling constant is small in comparison with the difference in NMR frequencies between the inequivalent spins. If the shift separation decreases (or the coupling strength increases), the multiplet intensity patterns are first distorted, and then become more complex and less easily analyzed (especially if more than two spins are involved). Intensification of some peaks in a multiplet is achieved at the expense of the remainder, which sometimes almost disappear in the background noise, although the integrated area under the peaks remains constant. In most high-field NMR, however, the distortions are usually modest and the characteristic distortions (*roofing*) can in fact help to identify related peaks.

Second-order effects decrease as the frequency difference between multiplets increases, so that high-field (i.e. high-frequency) NMR spectra display less distortion than lower frequency spectra. Early spectra at 60 MHz were more prone to distortion than spectra from later machines typically operating at frequencies at 200 MHz or above.

Magnetic inequivalence

More subtle effects can occur if chemically equivalent spins (i.e. nuclei related by symmetry and so having the same NMR frequency) have different coupling relationships to external spins. Spins that are chemically equivalent but are not indistinguishable (based on their coupling relationships) are termed magnetically inequivalent. For example, the 4 H sites of 1,2-dichlorobenzene divide into two chemically equivalent pairs by symmetry, but an individual member of one of the pairs has different couplings to the spins making up the other pair. Magnetic inequivalence can lead to highly complex spectra which can only be analyzed by computational modeling. Such effects are more common in NMR spectra of aromatic and other non-flexible systems, while conformational averaging about C-C bonds in flexible molecules tends to equalize the couplings between protons on adjacent carbons, reducing problems with magnetic inequivalence.

Correlation spectroscopy

Correlation spectroscopy is one of several types of two-dimensional nuclear magnetic resonance (NMR) spectroscopy. This type of NMR experiment is best known by its acronym, COSY. Other types of two-dimensional NMR include J-spectroscopy, exchange spectroscopy (EXSY), Nuclear Overhauser effect spectroscopy (NOESY), total correlation spectroscopy (TOCSY) and heteronuclear correlation experiments, such as HSQC, HMQC, and HMBC. Two-dimensional NMR spectra provide more information about a molecule than one-dimensional NMR spectra and are especially useful in determining the structure of a molecule, particularly for molecules that are too complicated to work with using one-dimensional NMR. The first two-dimensional experiment, COSY, was proposed by Jean Jeener, a professor at Université Libre de Bruxelles, in 1971. This experiment was later implemented by Walter P. Aue, Enrico Bartholdi and Richard R. Ernst, who published their work in 1976.[2]

Solid-state nuclear magnetic resonance

A variety of physical circumstances does not allow molecules to be studied in solution, and at the same time not by other spectroscopic techniques to an atomic level, either. In solid-phase media, such as crystals, microcrystalline powders, gels, anisotropic solutions, etc., it is in particular the dipolar coupling and chemical shift anisotropy that become dominant to the behaviour of the nuclear spin systems. In conventional solution-state NMR spectroscopy, these additional interactions would lead to a significant broadening of spectral lines. A variety of techniques allows to establish high-resolution conditions, that can, at least for ^{13}C spectra, be comparable to solution-state NMR spectra.

Two important concepts for high-resolution solid-state NMR spectroscopy are the limitation of possible molecular orientation by sample orientation, and the reduction of anisotropic nuclear magnetic interactions by sample spinning. Of the latter approach, fast spinning around the magic angle is a very prominent method, when the system comprises spin 1/2 nuclei. A number of intermediate techniques, with samples of partial alignment or reduced mobility, is currently being used in NMR spectroscopy.

Applications in which solid-state NMR effects occur are often related to structure investigations on membrane proteins, protein fibrils or all kinds of polymers, and chemical analysis in inorganic chemistry, but also include "exotic" applications like the plant leaves and fuel cells.

NMR spectroscopy applied to proteins

Much of the recent innovation within NMR spectroscopy has been within the field of protein NMR, which has become a very important technique in structural biology. One common goal of these investigations is to obtain high resolution 3-dimensional structures of the protein, similar to what can be achieved by X-ray crystallography. In contrast to X-ray crystallography, NMR is primarily limited to relatively small proteins, usually smaller than 35 kDa, though technical advances allow ever larger structures to be solved. NMR spectroscopy is often the only way to obtain high resolution information on partially or wholly intrinsically unstructured proteins.

Proteins are orders of magnitude larger than the small organic molecules discussed earlier in this article, but the same NMR theory applies. Because of the increased number of each

element present in the molecule, the basic 1D spectra become crowded with overlapping signals to an extent where analysis is impossible. Therefore, multidimensional (2, 3 or 4D) experiments have been devised to deal with this problem. To facilitate these experiments, it is desirable to isotopically label the protein with ^{13}C and ^{15}N because the predominant naturally occurring isotope ^{12}C is not NMR-active, whereas the nuclear quadrupole moment of the predominant naturally occurring ^{14}N isotope prevents high resolution information to be obtained from this nitrogen isotope. The most important method used for structure determination of proteins utilizes NOE experiments to measure distances between pairs of atoms within the molecule. Subsequently, the obtained distances are used to generate a 3D structure of the molecule using a computer program.

See also

- In vivo magnetic resonance spectroscopy
- Low field NMR
- Magnetic Resonance Imaging
- Nuclear Magnetic Resonance
- NMR spectra database
- NMR tube - includes sample preparation
- Protein nuclear magnetic resonance spectroscopy

References

[1] James Keeler. http://www-keeler.ch.cam.ac.uk/lectures/Irvine/chapter2.pdf|"Chapter 2: NMR and energy levels" (reprinted at University of Cambridge). *Understanding NMR Spectroscopy*. University of California, Irvine. http://www-keeler.ch.cam.ac.uk/lectures/Irvine/chapter2.pdf. Retrieved on 2007-05-11.

[2] Martin, G.E; Zekter, A.S., *Two-Dimensional NMR Methods for Establishing Molecular Connectivity*; VCH Publishers, Inc: New York, 1988 (p.59)

External links

- Protein NMR- A Practical Guide (http://www.protein-nmr.org.uk) Practical guide to NMR, in particular protein NMR assignment
- James Keeler. http://www-keeler.ch.cam.ac.uk/lectures/Irvine/|"Understanding NMR Spectroscopy" (reprinted at University of Cambridge). University of California, Irvine. http://www-keeler.ch.cam.ac.uk/lectures/Irvine/. Retrieved on 2007-05-11.
- The Basics of NMR (http://www.cis.rit.edu/htbooks/nmr/) - A non-technical overview of NMR theory, equipment, and techniques by Dr. Joseph Hornak, Professor of Chemistry at RIT
- NMRWiki.ORG (http://nmrwiki.org) project, a Wiki dedicated to NMR, MRI, and EPR.
- NMR spectroscopy for organic chemistry (http://www.organicworldwide.net/nmr.html)
- The Spectral Game (http://spectralgame.com) NMR spectroscopy game.

Free NMR processing, analysis and simulation software

- WINDNMR-Pro (http://www.chem.wisc.edu/areas/reich/plt/windnmr.htm) - simulation software for interactive calculation of first and second-order spin-coupled multiplets and a variety of DNMR lineshapes.
- CARA (http://www.nmr.ch) - resonance assignment software developed at the Wüthrich group

- NMRShiftDB (http://www.nmrshiftdb.org) - open database and NMR prediction website
- Spinworks (http://www.umanitoba.ca/chemistry/nmr/spinworks/)

NMR microscopy

1. REDIRECTNuclear magnetic resonance

NIR

The three-letter acronym **NIR** may stand for

- Near Infrared, infrared radiation of a wave length near that of red
- Northern Ireland, a region of the United Kingdom
- Northern Ireland Railways
- National Identity Register
- National Internet Registry
- Nir, one of two cities with that name in Iran
- Nir, a Hebrew word meaning 'a plowed field'
- Nir, a common Hebrew name

Spectral

Spectral imaging is a branch of spectroscopy in which a complete spectrum or some spectral information (such as the Doppler shift or Zeeman splitting of a spectral line) is collected at every location in an image plane. Applications include astronomy, solar physics, analysis of plasmas in nuclear fusion experiments, planetology, and Earth remote sensing.

This is often referred to as hyperspectral imaging.

See also

- Dopplergraph

Hyperspectral

Hyperspectral imaging collects and processes information from across the electromagnetic spectrum. Unlike the human eye, which just sees visible light, hyperspectral imaging is more like the eyes of the mantis shrimp, which can see visible light as well as from the ultraviolet to infrared. Hyperspectral capabilities enable the mantis shrimp to recognize different types of coral, prey, or predators, all which may appear as the same color to the human eye.

Humans build sensors and processing systems to provide the same type of capability for application in agriculture, mineralogy, physics, and surveillance. Hyperspectral sensors look at objects using a vast portion of the electromagnetic spectrum. Certain objects leave unique 'fingerprints' across the electromagnetic spectrum. These 'fingerprints' are known as spectral signatures and enable identification of the materials that make up a scanned object. For example, having the spectral signature for oil helps mineralogists find new oil fields.

Acquisition and Analysis

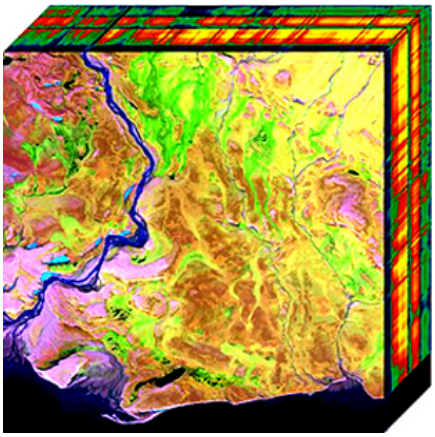

Example of a hyperspectral cube

Hyperspectral sensors collect information as a set of 'images'. Each image represents a range of the electromagnetic spectrum and is also known as a spectral band. These 'images' are then combined and form a three dimensional hyperspectral cube for processing and analysis.

Hyperspectral cubes are generated from airborne sensors like the NASA's *Airborne Visible/Infrared Imaging Spectrometer* (AVIRIS), or from satellites like NASA's Hyperion.[1] However, for many development and validation studies handheld sensors are used.[2]

The precision of these sensors is typically measured in spectral resolution, which is the width of each band of the spectrum that is captured. If the scanner picks up on a large number of fairly narrow frequency bands, it is possible to identify objects even if said objects are only captured in a handful of pixels. However, spatial resolution is a factor in addition to spectral resolution. If the pixels are too large, then multiple objects are captured in the same pixel and become difficult to identify. If the pixels are too small, then the energy captured by each sensor-cell is low, and the decreased signal-to-noise ratio reduces the reliability of measured features.

MicroMSI, Opticks and Envi are three remote sensing applications that support the processing and analysis of hyperspectral data. The acquisition and processing of hyperspectral images is also referred to as imaging spectroscopy.

Differences between Hyperspectral and Multispectral

Hyperspectral Imaging is part of a class of techniques commonly referred to as spectral imaging or spectral analysis. Hyperspectral Imaging is related to multispectral imaging. The distinction between hyperspectral and multispectral is usually defined as the number of spectral bands. Multispectral data contains from tens to hundreds of bands. Hyperspectral data contains hundreds to thousands of bands. However, hyperspectral imaging may be best defined by the manner in which the data is collected. Hyperspectral data is a set of contiguous bands (usually by one sensor). Multispectral is a set of optimally chosen spectral bands that are typically not contiguous and can be collected from multiple sensors.

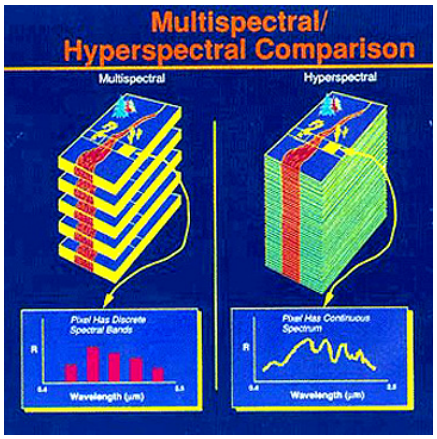

Hyperspectral and Multispectral Differences.

Applications

Hyperspectral remote sensing is used in a wide array of real-life applications. Although originally developed for mining and geology (The ability of hyperspectral imaging to identify various minerals makes it ideal for the mining and oil industries, where it can be used to look for ore and oil[2] [3] it has now spread into fields as wide-spread as ecology and surveillance, as well as historical manuscript research such as the imaging of the Archimedes Palimpsest. This technology is continually becoming more available to the public, and has been used in a wide variety of ways. Organizations such as NASA and the USGS have catalogues of various minerals and their spectral signatures, and have posted them online to make them readily available for researchers.

Agriculture

Although the costs of acquiring hyperspectral images is typically high, for specific crops and in specific climates hyperspectral remote sensing is used more and more for monitoring the development and health of crops. In Australia work is underway to use imaging spectrometers to detect grape variety, and develop an early warning system for disease outbreaks.[4] Furthermore work is underway to use hyperspectral data to detect the chemical composition of plants[5] which can be used to detect the nutrient and water status of wheat in irrigated systems[6]

Mineralogy

The original field of development for hyperspectral remote sensing, hyperspectral sensing of minerals is now well developed. Many minerals can be identified from images, and their relation to the presence of valuable minerals such as gold and diamonds is well understood. Currently the move is towards understanding the relation between oil and gas leakages from pipelines and natural wells; their effect on the vegetation and the spectral signatures. Recent work includes the PhD dissertations of Werff[7] and Noomen[8] .

Physics

Physicists use an electron microscopy technique that involves microanalysis using either Energy dispersive X-ray spectroscopy (EDS), Electron energy loss spectroscopy (EELS), Infrared Spectroscopy(IR), Raman Spectroscopy, or cathodoluminescence (CL) spectroscopy, in which the entire spectrum measured at each point is recorded. EELS hyperspectral imaging is performed in a scanning transmission electron microscope (STEM); EDS and CL mapping can be performed in STEM as well, or in a scanning electron microscope or electron probe microanalyzer (EPMA). Often, multiple techniques (EDS, EELS, CL) are used simultaneously.

In a "normal" mapping experiment, an image of the sample will be made that is simply the intensity of a particular emission mapped in an XY raster. For example, an EDS map could be made of a steel sample, in which iron x-ray intensity is used for the intensity grayscale of the image. Dark areas in the image would indicate not-iron-bearing impurities. This could potentially give misleading results; if the steel contained tungsten inclusions, for example, the high atomic number of tungsten could result in bremsstrahlung radiation that made the iron-free areas *appear* to be rich in iron.

By hyperspectral mapping, instead, the entire spectrum at each mapping point is acquired, and a quantitative analysis can be performed by computer post-processing of the data, and a quantitative map of iron content produced. This would show which areas contained no iron, despite the anomalous x-ray counts caused by bremsstrahlung. Because EELS core-loss edges are small signals on top of a large background, hyperspectral imaging allows large improvements to the quality of EELS chemical maps.

Similarly, in CL mapping, small shifts in the peak emission energy could be mapped, which would give information regarding slight chemical composition changes or changes in the stress state of a sample.

Surveillance

Hyperspectral surveillance is the implementation of hyperspectral scanning technology for surveillance purposes. Hyperspectral imaging is particularly useful in military surveillance because of measures that military entities now take to avoid airborne surveillance. Airborne surveillance has been in effect since soldiers used tethered balloons to spy on troops during the American Civil War, and since that time we have learned not only to hide from the naked eye, but to mask our heat signature to blend in to the surroundings and avoid infrared scanning, as well. The idea that drives hyperspectral surveillance is that hyperspectral scanning draws information from such a large portion of the light spectrum that any given object should have unique spectral signature in at least a few of the many bands that get scanned.[1]

Advantages and Disadvantages

The primary advantages to hyperspectral imaging is that, because an entire spectrum is acquired at each point, the operator needs no a priori knowledge of the sample, and post-processing allows all available information from the dataset to be mined.

The primary disadvantages are cost and complexity. Fast computers, sensitive detectors, and large data storage capacities are needed for analyzing hyperspectral data. Significant data storage capacity is necessary since hyperspectral cubes are large multi-dimensional datasets, potentially exceeding hundreds of megabytes. All of these factors greatly increase the cost of acquiring and processing hyperspectral data. Also, one of the hurdles that researchers have had to face is finding ways to program hyperspectral satellites to sort through data on their own and transmit only the most important images, as both transmission and storage of that much data could prove difficult and costly.[1] As a relatively new analytical technique, the full potential of hyperspectral imaging has not yet been realized.

See also

- Airborne Real-time Cueing Hyperspectral Enhanced Reconnaissance
- Full Spectral Imaging
- Multi-spectral image
- Chemical imaging
- Remote Sensing
- Sensor fusion

External Links

ITT Visual Information Solutions - ENVI Hyperspectral Image Processing Software [9]

References

[1] Schurmer, J.H., (Dec 2003) *Hyperspectral imaging from space* (http://www.afrlhorizons.com/Briefs/Dec03/VS0302.html), Air Force Research Laboratories Technology Horizons

[2] Ellis, J., (Jan 2001) *Searching for oil seeps and oil-impacted soil with hyperspectral imagery* (http://www.eomonline.com/Common/currentissues/Jan01/ellis.htm), Earth Observation Magazine.

[3] Smith, R.B. (July 14, 2006), *Introduction to hyperspectral imaging with TMIPS* (http://www.microimages.com/getstart/pdf/hyprspec.pdf), MicroImages Tutorial Web site

[4] Lacar, F.M., et al., *Use of hyperspectral imagery for mapping grape varieties in the Barossa Valley, South Australia* (http://hdl.handle.net/2440/39292), Geoscience and remote sensing symposium (IGARSS'01) - IEEE 2001 International, vol.6 2875-2877p. doi: 10.1109/IGARSS.2001.978191 (http://dx.doi.org/10.1109/IGARSS.2001.978191)

[5] Ferwerda, J.G. (2005), *Charting the quality of forage: measuring and mapping the variation of chemical components in foliage with hyperspectral remote sensing* (http://www.itc.nl/library/Papers_2005/phd/ferwerda.pdf), Wageningen University , ITC Dissertation 126, 166p. ISBN 90-8504-209-7

[6] Tilling, A.K., et al., (2006) *Remote sensing to detect nitrogen and water stress in wheat* (http://www.regional.org.au/au/asa/2006/plenary/technology/4584_tillingak.htm), The Australian Society of Agronomy

[7] Werff H. (2006), *Knowledge based remote sensing of complex objects: recognition of spectral and spatial patterns resulting from natural hydrocarbon seepages* (http://www.itc.nl/library/papers_2006/phd/vdwerff.pdf), Utrecht University, ITC Dissertation 131, 138p. ISBN 90-6164-238-8

[8] Noomen, M.F. (2007), *Hyperspectral reflectance of vegetation affected by underground hydrocarbon gas seepage* (http://www.itc.nl/library/papers_2007/phd/noomen.pdf), Enschede, ITC 151p. ISBN 978-90-8504-671-4.

[9] http://www.ittvis.com/ProductServices/ENVI.aspx

Chemical imaging

Chemical imaging is the simultaneous measurement of spectra (chemical information) and images or pictures (spatial information)[1] [2] The technique is most often applied to either solid or gel samples, and has applications in chemistry, biology[3] [4] [5] [6] [7] [8] , medicine[9] [10] , pharmacy[11] (see also for example: Chemical Imaging Without Dyeing [12]), food science, biotechnology[13] [14] , agriculture and industry (see for example:NIR Chemical Imaging in Pharmaceutical Industry [15] and Pharmaceutical Process Analytical Technology: [16]). NIR, IR and Raman chemical imaging is also referred to as hyperspectral, spectroscopic, spectral or multispectral imaging (also see microspectroscopy). However, other ultra-sensitive and selective, chemical imaging techniques are also in use that involve either UV-visible or fluorescence microspectroscopy. Chemical imaging techniques can be used to analyze samples of all sizes, from the single molecule[17] [18] to the cellular level in biology and medicine[19] [20] [21] , and to images of planetary systems in astronomy, but different instrumentation is employed for making observations on such widely different systems.

Chemical imaging instrumentation is composed of three components: a radiation source to illuminate the sample, a spectrally selective element, and usually a detector array (the camera) to collect the images. When many stacked spectral channels (wavelengths) are collected for different locations of the microspectrometer focus on a line or planar array in the focal plane, the data is called hyperspectral; fewer wavelength data sets are called multispectral. The data format is called a hypercube. The data set may be visualized as a three-dimensional block of data spanning two spatial dimensions (x and y), with a series of wavelengths (lambda) making up the third (spectral) axis. The hypercube can be visually and mathematically treated as a series of spectrally resolved images (each image plane corresponding to the image at one wavelength) or a series of spatially resolved spectra. The analyst may choose to view the spectrum measured at a particular spatial location; this is useful for chemical identification. Alternatively, selecting an image plane at a particular wavelength can highlight the spatial distribution of sample components, provided that their spectral signatures are different at the selected wavelength.

Many materials, both manufactured and naturally occurring, derive their functionality from the spatial distribution of sample components. For example, extended release pharmaceutical formulations can be achieved by using a coating that acts as a barrier layer. The release of active ingredient is controlled by the presence of this barrier, and imperfections in the coating, such as discontinuities, may result in altered performance. In the semi-conductor industry, irregularities or contaminants in silicon wafers or printed micro-circuits can lead to failure of these components. The functionality of biological systems is also dependent upon chemical gradients – a single cell, tissue, and even whole organs function because of the very specific arrangement of components. It has been shown that even small changes in chemical composition and distribution may be an early indicator of disease.

Any material that depends on chemical gradients for functionality may be amenable to study by an analytical technique that couples spatial and chemical characterization. To efficiently and effectively design and manufacture such materials, the ‘what’ and the ‘where’ must both be measured. The demand for this type of analysis is increasing as manufactured materials become more complex. Chemical imaging techniques not only

permit visualization of the spatially resolved chemical information that is critical to understanding modern manufactured products, but it is also a non-destructive technique so that samples are preserved for further testing.

History

Commercially available laboratory-based chemical imaging systems emerged in the early 1990s (ref. 1-5). In addition to economic factors, such as the need for sophisticated electronics and extremely high-end computers, a significant barrier to commercialization of infrared imaging was that the focal plane array (FPA) needed to read IR images were not readily available as commercial items. As high-speed electronics and sophisticated computers became more commonplace, and infrared cameras became readily commercially available, laboratory chemical imaging systems were introduced.

Initially used for novel research in specialized laboratories, chemical imaging became a more commonplace analytical technique used for general R&D, quality assurance (QA) and quality control (QC) in less than a decade. The rapid acceptance of the technology in a variety of industries (pharmaceutical, polymers, semiconductors, security, forensics and agriculture) rests in the wealth of information characterizing both chemical composition and morphology. The parallel nature of chemical imaging data makes it possible to analyze multiple samples simultaneously for applications that require high throughput analysis in addition to characterizing a single sample.

Principles

Chemical imaging shares the fundamentals of vibrational spectroscopic techniques, but provides additional information by way of the simultaneous acquisition of spatially resolved spectra. It combines the advantages of digital imaging with the attributes of spectroscopic measurements. Briefly, vibrational spectroscopy measures the interaction of light with matter. Photons that interact with a sample are either absorbed or scattered; photons of specific energy are absorbed, and the pattern of absorption provides information, or a fingerprint, on the molecules that are present in the sample.

On the other hand, in terms of the observation setup, chemical imaging can be carried out in one of the following modes: (optical) absorption, emission (fluorescence), (optical) transmission or scattering (Raman). A consensus currently exists that the fluorescence (emission) and Raman scattering modes are the most sensitive and powerful, but also the most expensive.

In a transmission measurement, the radiation goes through a sample and is measured by a detector placed on the far side of the sample. The energy transferred from the incoming radiation to the molecule(s) can be calculated as the difference between the quantity of photons that were emitted by the source and the quantity that is measured by the detector. In a diffuse reflectance measurement, the same energy difference measurement is made, but the source and detector are located on the same side of the sample, and the photons that are measured have re-emerged from the illuminated side of the sample rather than passed through it. The energy may be measured at one or multiple wavelengths; when a series of measurements are made, the response curve is called a spectrum.

A key element in acquiring spectra is that the radiation must somehow be energy selected – either before or after interacting with the sample. Wavelength selection can be

accomplished with a fixed filter, tunable filter, spectrograph, an interferometer, or other devices. For a fixed filter approach, it is not efficient to collect a significant number of wavelengths, and multispectral data are usually collected. Interferometer-based chemical imaging requires that entire spectral ranges be collected, and therefore results in hyperspectral data. Tunable filters have the flexibility to provide either multi- or hyperspectral data, depending on analytical requirements.

Spectra may be measured one point at a time using a single element detector (single-point mapping), as a line-image using a linear array detector (typically 16 to 28 pixels) (linear array mapping), or as a two-dimensional image using a Focal Plane Array (FPA)(typically 256 to 16,384 pixels) (FPA imaging). For single-point the sample is moved in the x and y directions point-by-point using a computer-controlled stage. With linear array mapping, the sample is moved line-by-line with a computer-controlled stage. FPA imaging data are collected with a two-dimensional FPA detector, hence capturing the full desired field-of-view at one time for each individual wavelength, without having to move the sample. FPA imaging, with its ability to collected tens of thousands of spectra simultaneously is orders of magnitude faster than linear arrays which are can typically collect 16 to 28 spectra simultaneously, which are in turn much faster than single-point mapping.

Terminology

Some words common in spectroscopy, optical microscopy and photography have been adapted or their scope modified for their use in chemical imaging. They include: resolution, field of view and magnification. There are two types of resolution in chemical imaging. The spectral resolution refers to the ability to resolve small energy differences; it applies to the spectral axis. The spatial resolution is the minimum distance between two objects that is required for them to be detected as distinct objects. The spatial resolution is influenced by the field of view, a physical measure of the size of the area probed by the analysis. In imaging, the field of view is a product of the magnification and the number of pixels in the detector array. The magnification is a ratio of the physical area of the detector array divided by the area of the sample field of view. Higher magnifications for the same detector image a smaller area of the sample.

Types of vibrational chemical imaging instruments

Chemical imaging has been implemented for mid-infrared, near-infrared spectroscopy and Raman spectroscopy. As with their bulk spectroscopy counterparts, each imaging technique has particular strengths and weaknesses, and are best suited to fulfill different needs.

Mid-infrared chemical imaging

Mid-infrared (MIR) spectroscopy probes fundamental molecular vibrations, which arise in the spectral range 2,500-25,000 nm. Commercial imaging implementations in the MIR region typically employ Fourier Transform Infrared (FT-IR) interferometers and the range is more commonly presented in wavenumber, 4,000 – 400 cm^{-1}. The MIR absorption bands tend to be relatively narrow and well-resolved; direct spectral interpretation is often possible by an experienced spectroscopist. MIR spectroscopy can distinguish subtle changes in chemistry and structure, and is often used for the identification of unknown materials. The absorptions in this spectral range are relatively strong; for this reason, sample presentation is important to limit the amount of material interacting with the

incoming radiation in the MIR region. Most data collected in this range is collected in transmission mode through thin sections (~10 micrometres) of material. Water is a very strong absorber of MIR radiation and wet samples often require advanced sampling procedures (such as attenuated total reflectance). Commercial instruments include point and line mapping, and imaging. All employ an FT-IR interferometer as wavelength selective element and light source.

For types of MIR microscope, see Microscopy#infrared microscopy.

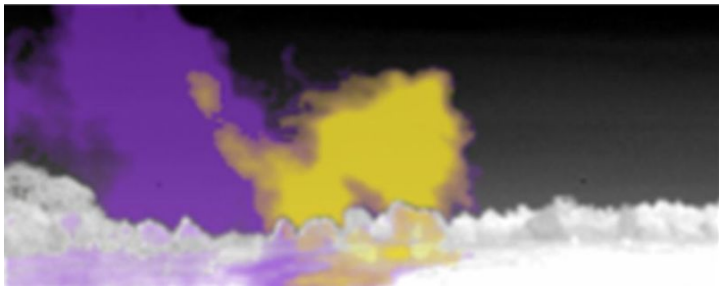

Remote chemical imaging of a simultaneous release of SF_6 and NH_3 at 1.5km using the FIRST imaging spectrometer[22]

Atmospheric windows in the infrared spectrum are also employed to perform chemical imaging remotely. In these spectral regions the atmospheric gases (mainly water and CO_2) present low absorption and allow infrared viewing over kilometer distances. Target molecules can then be viewed using the selective absorption/emission processes described above. An example of the chemical imaging of a simultaneous release of SF_6 and NH_3 is shown in the image.

Near-infrared chemical imaging

The analytical near infrared (NIR) region spans the range from approximately 700-2,500 nm. The absorption bands seen in this spectral range arise from overtones and combination bands of O-H, N-H, C-H and S-H stretching and bending vibrations. Absorption is one to two orders of magnitude smaller in the NIR compared to the MIR; this phenomenon eliminates the need for extensive sample preparation. Thick and thin samples can be analyzed without any sample preparation, it is possible to acquire NIR chemical images through some packaging materials, and the technique can be used to examine hydrated samples, within limits. Intact samples can be imaged in transmittance or diffuse reflectance.

The lineshapes for overtone and combination bands tend to be much broader and more overlapped than for the fundamental bands seen in the MIR. Often, multivariate methods are used to separate spectral signatures of sample components. NIR chemical imaging is particularly useful for performing rapid, reproducible and non-destructive analyses of known materials[23] [24] . NIR imaging instruments are typically based on one of two platforms: imaging using a tunable filter and broad band illumination, and line mapping employing an FT-IR interferometer as the wavelength filter and light source.

Raman chemical imaging

The Raman shift chemical imaging spectral range spans from approximately 50 to 4,000 cm^{-1}; the actual spectral range over which a particular Raman measurement is made is a function of the laser excitation frequency. The basic principle behind Raman spectroscopy differs from the MIR and NIR in that the x-axis of the Raman spectrum is measured as a function of energy shift (in cm^{-1}) relative to the frequency of the laser used as the source of radiation. Briefly, the Raman spectrum arises from inelastic scattering of incident photons, which requires a change in polarizability with vibration, as opposed to infrared absorption, which requires a change in dipole moment with vibration. The end result is spectral

information that is similar and in many cases complementary to the MIR. The Raman effect is weak - only about one in 10^7 photons incident to the sample undergoes Raman scattering. Both organic and inorganic materials possess a Raman spectrum; they generally produce sharp bands that are chemically specific. Fluorescence is a competing phenomenon and, depending on the sample, can overwhelm the Raman signal, for both bulk spectroscopy and imaging implementations.

Raman chemical imaging requires little or no sample preparation. However, physical sample sectioning may be used to expose the surface of interest, with care taken to obtain a surface that is as flat as possible. The conditions required for a particular measurement dictate the level of invasiveness of the technique, and samples that are sensitive to high power laser radiation may be damaged during analysis. It is relatively insensitive to the presence of water in the sample and is therefore useful for imaging samples that contain water such as biological material.

Fluorescence imaging (visible and NIR)

This emission microspectroscopy mode is the most sensitive in both visible and FT-NIR microspectroscopy, and has therefore numerous biomedical, biotechnological and agricultural applications. There are several powerful, highly specific and sensitive fluorescence techniques that are currently in use, or still being developed; among the former are FLIM, FRAP, FRET and FLIM-FRET; among the latter are NIR fluorescence and probe-sensitivity enhanced NIR fluorescence microspectroscopy and nanospectroscopy techniques (see "Further reading" section).

Sampling and samples

The value of imaging lies in the ability to resolve spatial heterogeneities in solid-state or gel/gel-like samples. Imaging a liquid or even a suspension has limited use as constant sample motion serves to average spatial information, unless ultra-fast recording techniques are employed as in fluorescence correlation microspectroscopy or FLIM obsevations where a single molecule may be monitored at extremely high (photon) detection speed. High-throughput experiments (such as imaging multi-well plates) of liquid samples can however provide valuable information. In this case, the parallel acquisition of thousands of spectra can be used to compare differences between samples, rather than the more common implementation of exploring spatial heterogeneity within a single sample.

Similarly, there is no benefit in imaging a truly homogeneous sample, as a single point spectrometer will generate the same spectral information. Of course the definition of homogeneity is dependent on the spatial resolution of the imaging system employed. For MIR imaging, where wavelengths span from 3-10 micrometres, objects on the order of 5 micrometres may theoretically be resolved. The sampled areas are limited by current experimental implementations because illumination is provided by the interferometer. Raman imaging may be able to resolve particles less than 1 micrometre in size, but the sample area that can be illuminated is severely limited. With Raman imaging, it is considered impractical to image large areas and, consequently, large samples. FT-NIR chemical/hyperspectral imaging usually resolves only larger objects (>10 micrometres), and is better suited for large samples because illumination sources are readily available. However, FT-NIR microspectroscopy was recently reported to be capable of about 1.2 micron (micrometer) resolution in biological samples[25] Furthermore, two-photon

excitation FCS experiments were reported to have attained 15 nanometer resolution on biomembrane thin films with a special coincidence photon-counting setup.

Detection limit

The concept of the detection limit for chemical imaging is quite different than for bulk spectroscopy, as it depends on the sample itself. Because a bulk spectrum represents an average of the materials present, the spectral signatures of trace components are simply overwhelmed by dilution. In imaging however, each pixel has a corresponding spectrum. If the physical size of the trace contaminant is on the order of the pixel size imaged on the sample, its spectral signature will likely be detectable. If however, the trace component is dispersed homogeneously (relative to pixel image size) throughout a sample, it will not be detectable. Therefore, detection limits of chemical imaging techniques are strongly influenced by particle size, the chemical and spatial heterogeneity of the sample, and the spatial resolution of the image.

Data analysis

Data analysis methods for chemical imaging data sets typically employ mathematical algorithms common to single point spectroscopy or to image analysis. The reasoning is that the spectrum acquired by each detector is equivalent to a single point spectrum; therefore pre-processing, chemometrics and pattern recognition techniques are utilized with the similar goal to separate chemical and physical effects and perform a qualitative or quantitative characterization of individual sample components. In the spatial dimension, each chemical image is equivalent to a digital image and standard image analysis and robust statistical analysis can be used for feature extraction.

See also

- Multispectral image
- Microspectroscopy
- Imaging spectroscopy

References

[1] http://www.imaging.net/chemical-imaging/Chemical imaging

[2] http://www.malvern.com/LabEng/products/sdi/bibliography/sdi_bibliography.htm E. N. Lewis, E. Lee and L. H. Kidder, Combining Imaging and Spectroscopy: Solving Problems with Near-Infrared Chemical Imaging. Microscopy Today, Volume 12, No. 6, 11/2004.

[3] C.L. Evans and X.S. Xie.2008. Coherent Anti-Stokes Raman Scattering Microscopy: Chemical Imaging for Biology and Medicine., doi:10.1146/annurev.anchem.1.031207.112754 *Annual Review of Analytical Chemistry*, **1**: 883-909.

[4] Diaspro, A., and Robello, M. (1999). Multi-photon Excitation Microscopy to Study Biosystems. European Microscopy and Analysis., 5:5-7.

[5] D.S. Mantus and G. H. Morrison. 1991. Chemical imaging in biology and medicine using ion microscopy., *Microchimica Acta*, **104**, (1-6) January 1991, doi: 10.1007/BF01245536

[6] Bagatolli, L.A., and Gratton, E. (2000). Two-photon fluorescence microscopy of coexisting lipid domains in giant unilamellar vesicles of binary phospholipid mixtures. Biophys J., 78:290-305.

[7] Schwille, P., Haupts, U., Maiti, S., and Webb. W.(1999). Molecular dynamics in living cells observed by fluorescence correlation spectroscopy with one- and two-photon excitation. Biophysical Journal, 77(10):2251-2265.

[8] 1.Lee, S. C. et al., (2001). One Micrometer Resolution NMR Microscopy. J. Magn. Res., 150: 207-213.

[9] Near Infrared Microspectroscopy, Fluorescence Microspectroscopy,Infrared Chemical Imaging and High Resolution Nuclear Magnetic Resonance Analysis of Soybean Seeds, Somatic Embryos and Single Cells., Baianu, I.C. et al. 2004., In *Oil Extraction and Analysis.*, D. Luthria, Editor pp.241-273, AOCS Press., Champaign, IL.
[10] Single Cancer Cell Detection by Near Infrared Microspectroscopy, Infrared Chemical Imaging and Fluorescence Microspectroscopy.2004.I. C. Baianu, D. Costescu, N. E. Hofmann and S. S. Korban, q-bio/0407006 (July 2004) (http://arxiv.org/abs/q-bio/0407006)
[11] J. Dubois, G. Sando, E. N. Lewis, Near-Infrared Chemical Imaging, A Valuable Tool for the Pharmaceutical Industry, G.I.T. Laboratory Journal Europe, No. 1-2, 2007.
[12] http://witec.de/en/download/Raman/ImagingMicroscopy04.pdf
[13] Raghavachari, R., Editor. 2001. *Near-Infrared Applications in Biotechnology*, Marcel-Dekker, New York, NY.
[14] Applications of Novel Techniques to Health Foods, Medical and Agricultural Biotechnology.(June 2004) I. C. Baianu, P. R. Lozano, V. I. Prisecaru and H. C. Lin q-bio/0406047 (http://arxiv.org/abs/q-bio/0406047)
[15] http://www.spectroscopyeurope.com/NIR_14_3.pdf
[16] http://www.fda.gov/cder/OPS/PAT.htm
[17] Eigen, M., and Rigler, R. (1994). Sorting single molecules: Applications to diagnostics and evolutionary biotechnology, Proc. Natl. Acad. Sci. USA 91:5740.
[18] Rigler R. and Widengren J. (1990). Ultrasensitive detection of single molecules by fluorescence correlation spectroscopy, *BioScience* (Ed. Klinge & Owman) p.180.
[19] Single Cancer Cell Detection by Near Infrared Microspectroscopy, Infrared Chemical Imaging and Fluorescence Microspectroscopy.2004.I. C. Baianu, D. Costescu, N. E. Hofmann, S. S. Korban and et al., q-bio/0407006 (July 2004) (http://arxiv.org/abs/q-bio/0407006)
[20] Oehlenschläger F., Schwille P. and Eigen M. (1996). Detection of HIV-1 RNA by nucleic acid sequence-based amplification combined with fluorescence correlation spectroscopy, *Proc. Natl. Acad. Sci. USA* **93**:1281.
[21] Near Infrared Microspectroscopy, Fluorescence Microspectroscopy,Infrared Chemical Imaging and High Resolution Nuclear Magnetic Resonance Analysis of Soybean Seeds, Somatic Embryos and Single Cells., Baianu, I.C. et al. 2004., In *Oil Extraction and Analysis.*, D. Luthria, Editor pp.241-273, AOCS Press., Champaign, IL.
[22] M. Chamberland, V. Farley, A. Vallières, L. Belhumeur, A. Villemaire, J. Giroux et J. Legault, High-Performance Field-Portable Imaging Radiometric Spectrometer Technology For Hyperspectral imaging Applications, Proc. SPIE 5994, 59940N, September 2005.
[23] Novel Techniques for Microspectroscopy and Chemical Imaging Analysis of Soybean Seeds and Embryos.(2002). Baianu, I.C., Costescu, D.M., and You, T. *Soy2002 Conference*, Urbana, Illinois.
[24] Near Infrared Microspectroscopy, Chemical Imaging and NMR Analysis of Oil in Developing and Mutagenized Soybean Embryos in Culture. (2003). Baianu, I.C., Costescu, D.M., Hofmann, N., and Korban, S.S. *AOCS Meeting, Analytical Division*.
[25] Near Infrared Microspectroscopy, Fluorescence Microspectroscopy,Infrared Chemical Imaging and High Resolution Nuclear Magnetic Resonance Analysis of Soybean Seeds, Somatic Embryos and Single Cells., Baianu, I.C. et al. 2004., In *Oil Extraction and Analysis.*, D. Luthria, Editor pp.241-273, AOCS Press., Champaign, IL.

Further reading

1. E. N. Lewis, P. J. Treado, I. W. Levin, Near-Infrared and Raman Spectroscopic Imaging, American Laboratory, 06/1994:16 (1994)
2. E. N. Lewis, P. J. Treado, R. C. Reeder, G. M. Story, A. E. Dowrey, C. Marcott, I. W. Levin, FTIR spectroscopic imaging using an infrared focal-plane array detector, Analytical Chemistry, 67:3377 (1995)
3. P. Colarusso, L. H. Kidder, I. W. Levin, J. C. Fraser, E. N. Lewis Infrared Spectroscopic Imaging: from Planetary to Cellular Systems, Applied Spectroscopy, 52 (3):106A (1998)
4. P. J. Treado I. W. Levin, E. N. Lewis, Near-Infrared Spectroscopic Imaging Microscopy of Biological Materials Using an Infrared Focal-Plane Array and an Acousto-Optic Tunable Filter (AOTF), Applied Spectroscopy, 48:5 (1994)
5. Hammond, S.V., Clarke, F. C., Near-infrared microspectroscopy. In: Handbook of Vibrational Spectroscopy, Vol. 2, J.M. Chalmers and P.R. Griffiths Eds. John Wiley and Sons, West Sussex, UK, 2002, p.1405-1418

6. L.H. Kidder, A.S. Haka, E.N. Lewis, Instrumentation for FT-IR Imaging. In: Handbook of Vibrational Spectroscopy, Vol. 2, J.M. Chalmers and P.R. Griffiths Eds. John Wiley and Sons, West Sussex, UK, 2002, pp.1386-1404
7. J. Zhang; A. O'Connor; J. F. Turner II, Cosine Histogram Analysis for Spectral Image Data Classification,Applied Spectroscopy, Volume 58, Number 11, November 2004, pp. 1318-1324(7)
8. J. F. Turner II; J. Zhang; A. O'Connor, A Spectral Identity Mapper for Chemical Image Analysis, Applied Spectroscopy, Volume 58, Number 11, November 2004, pp. 1308-1317(10)
9. H. R. MORRIS, J. F. TURNER II, B. MUNRO, R. A. RYNTZ, P. J. TREADO, Chemical imaging of thermoplastic olefin (TPO) surface architecture, Langmuir, 1999, vol. 15, no8, pp. 2961-2972
10. J. F. Turner II, Chemical imaging and spectroscopy using tunable filters: Instrumentation, methodology, and multivariate analysis, Thesis (PhD). UNIVERSITY OF PITTSBURGH, Source DAI-B 59/09, p. 4782, Mar 1999, 286 pages.
11. P. Schwille.(2001). in *Fluorescence Correlation Spectroscopy. Theory and applications.* R. Rigler & E.S. Elson, eds., p. 360. Springer Verlag: Berlin.
12. Schwille P., Oehlenschläger F. and Walter N. (1996). Analysis of RNA-DNA hybridization kinetics by fluorescence correlation spectroscopy, *Biochemistry* **35**:10182.
13. FLIM | Fluorescence Lifetime Imaging Microscopy: Fluorescence, fluorophore chemical imaging, confocal emission microspectroscopy, FRET, cross-correlation fluorescence microspectroscopy (http://www.nikoninstruments.com/infocenter.php?n=FLIM).
14. FLIM Applications: (http://www.nikoninstruments.com/infocenter.php?n=FLIM) "FLIM is able to discriminate between fluorescence emanating from different fluorophores and autoflorescing molecules in a specimen, even if their emission spectra are similar. It is, therefore, ideal for identifying fluorophores in multi-label studies. FLIM can also be used to measure intracellular ion concentrations without extensive calibration procedures (for example, Calcium Green) and to obtain information about the local environment of a fluorophore based on changes in its lifetime." FLIM is also often used in microspectroscopic/chemical imaging, or microscopic, studies to monitor spatial and temporal protein-protein interactions, properties of membranes and interactions with nucleic acids in living cells.
15. Gadella TW Jr., *FRET and FLIM techniques*, 33. Imprint: Elsevier, ISBN 978-0-08-054958-3. (2008) 560 pages
16. Langel FD, et al., Multiple protein domains mediate interaction between Bcl10 and Malt1, *J. Biol. Chem.*, (2008) 283(47):32419-31
17. Clayton AH. , The polarized AB plot for the frequency-domain analysis and representation of fluorophore rotation and resonance energy homotransfer. J *Microscopy*. (2008) 232(2):306-12
18. Clayton AH, et al., Predominance of activated EGFR higher-order oligomers on the cell surface. *Growth Factors* (2008) 20:1
19. Plowman et al., Electrostatic Interactions Positively Regulate K-Ras Nanocluster Formation and Function. *Molecular and Cellular Biology* (2008) 4377–4385
20. Belanis L, et al., Galectin-1 Is a Novel Structural Component and a Major Regulator of H-Ras Nanoclusters. *Molecular Biology of the Cell* (2008) 19:1404–1414
21. Van Manen HJ, Refractive index sensing of green fluorescent proteins in living cells using fluorescence lifetime imaging microscopy. Biophys J. (2008) 94(8):L67-9

22. Van der Krogt GNM, et al., A Comparison of Donor-Acceptor Pairs for Genetically Encoded FRET Sensors: Application to the Epac cAMP Sensor as an Example, PLoS ONE, (2008) 3(4):e1916
23. Dai X, et al., Fluorescence intensity and lifetime imaging of free and micellar-encapsulated doxorubicin in living cells. *Nanomedicine*. (2008) **4**(1):49-56.

External links

- NIR Chemical Imaging in Pharmaceutical Industry (http://www.spectroscopyeurope.com/NIR_14_3.pdf)
- Pharmaceutical Process Analytical Technology: (http://www.fda.gov/cder/OPS/PAT.htm)
- NIR Chemical Imaging for Counterfeit Pharmaceutical Product Analysis (http://www.spectroscopymag.com/spectroscopy/Near-IR+Spectroscopy/NIR-Chemical-Imaging-for-Counterfeit-Pharmaceutica/ArticleStandard/Article/detail/406629)
- Chemical Imaging: Potential New Crime Busting Tool (http://www.sciencedaily.com/releases/2007/08/070802103435.htm)
- Chemical Imaging Without Dyeing (http://witec.de/en/download/Raman/ImagingMicroscopy04.pdf) - Chemical Imaging Without Dyeing

Raman

Raman may refer to

- Chandrasekhara Venkata Raman, Indian physicist and Nobel laureate, discoverer of Raman scattering. See also Raman spectroscopy
- Raman Sundrum, theoretical physicist famous for the Randall-Sundrum model
- Raman (crater), lunar crater named after C.V. Raman
- Amphoe Raman, district in Yala Province, southern Thailand
- Raman, Punjab, India
- Raman, Rawalpindi, a village in Pakistani Punjab
- Raman spectroscopy, a spectroscopic technique used in condensed matter physics and chemistry
- Woorkeri Raman, Indian cricketer
- Ramen, a Japanese dish

Fluorescence correlation spectroscopy

Fluorescence correlation spectroscopy (**FCS**) is a common technique used by physicists, chemists, and biologists to experimentally characterize the dynamics of fluorescent species (e.g. single fluorescent dye molecules in nanostructured materials, autofluorescent proteins in living cells, etc.). Although the name indicates a specific link to fluorescence, the method is used today also for exploring other forms of luminescence (like reflections, luminescence from gold-beads or quantum dots or phosphorescent species). The "spectroscopy" in the name is not readily found as in common usage a spectrum is generally understood to be a frequency spectrum. The autocorrelation is a genuine form of spectrum, however: It is the time-spectrum generated from the power spectrum (via inverse fourier transform).

Commonly, FCS is employed in the context of optical microscopy, in particular confocal or two photon microscopy. In these techniques light is focused on a sample and the measured fluorescence intensity fluctuations (due to diffusion, physical or chemical reactions, aggregation, etc.) are analyzed using the temporal autocorrelation. Because the measured property is essentially related to the magnitude and/or the amount of fluctuations, there is an optimum measurement regime at the level when individual species enter or exit the observation volume (or turn on and off in the volume). When too many entities are measured at the same time the overall fluctuations are small in comparison to the total signal and may not be resolvable - in the other direction, if the individual fluctuation-events are too sparse in time, one measurement may take prohibitively too long. FCS is in a way the fluorescent counterpart to dynamic light scattering, which uses coherent light scattering, instead of (incoherent) fluorescence.

When an appropriate model is known, FCS can be used to obtain quantitative information such as

- diffusion coefficients
- hydrodynamic radii
- average concentrations
- kinetic chemical reaction rates
- singlet-triplet dynamics

Because fluorescent markers come in a variety of colors and can be specifically bound to a particular molecule (e.g. proteins, polymers, metal-complexes, etc.), it is possible to study the behavior of individual molecules (in rapid succession in composite solutions). With the development of sensitive detectors such as avalanche photodiodes the detection of the fluorescence signal coming from individual molecules in highly dilute samples has become practical. With this emerged the possibility to conduct FCS experiments in a wide variety of specimens, ranging from materials science to biology. The advent of engineered cells with genetically tagged proteins (like green fluorescent protein) has made FCS a common tool for studying molecular dynamics in living cells.

History

Signal-correlation techniques have first been experimentally applied to fluorescence in 1972 by Magde, Elson, and Webb[1] , who are therefore commonly credited as the "inventors" of FCS. The technique was further developed in a group of papers by these and other authors soon after, establishing the theoretical foundations and types of applications.[2] [3] [4] See Thompson (1991)[5] for a review of that period.

Beginning in 1993[6] , a number of improvements in the measurement techniques--notably using confocal microscopy, and then two photon microscopy--to better define the measurement volume and reject background greatly improved the signal-to-noise and allowed single molecule sensitivity.[7] [8] Since then, there has been a renewed interest in FCS, and as of August 2007 there has been over 3,000 papers using FCS found in Web of Science. See Krichevsky and Bonnet[9] for a recent review. In addition, there has been a flurry of activity extending FCS in various ways, for instance to laser scanning and spinning disk confocal microscopy (from a stationary, single point measurement), in using cross-correlation (FCCS) between two fluorescent channels instead of autocorrelation, and in using Förster Resonance Energy Transfer (FRET) instead of fluorescence.

Typical FCS setup

The typical FCS setup consists of a laser line (wavelengths ranging typically from 405 - 633 nm (cw), and from 690 - 1100 nm (pulsed)), which is reflected into a microscope objective by a dichroic mirror. The laser beam is focused in the sample, which contains fluorescent particles (molecules) in such high dilution, that only few are within the focal spot (usually 1 - 100 molecules in one fL). When the particles cross the focal volume, they fluoresce. This light is collected by the same objective and, because it is red-shifted with respect to the excitation light it passes the dichroic reaching a detector, typically a photomultiplier tube or avalanche photodiode detector. The resulting electronic signal can be stored either directly as an intensity versus time trace to be analyzed at a later point, or, computed to generate the autocorrelation directly (which requires special acquisition cards). The FCS curve by itself only represents a time-spectrum. Conclusions on physical phenomena have to be extracted from there with appropriate models. The parameters of interest are found after fitting the autocorrelation curve to modeled functional forms. [10] The setup is shown in Figure 1.

The Measurement Volume

The measurement volume is a convolution of illumination (excitation) and detection geometries, which result from the optical elements involved. The resulting volume is described mathematically by the point spread function (or PSF), it is essentially the image of a point source. The PSF is often described as an ellipsoid (with unsharp boundaries) of few hundred nanometers in focus diameter, and almost one micrometre along the optical axis. The shape varies significantly (and has a large impact on the resulting FCS curves) depending on the quality of the optical elements (it is crucial to avoid astigmatism and to check the real shape of the PSF on the instrument). In the case of confocal microscopy, and for small pinholes (around one Airy unit), the PSF is well approximated by Gaussians:

$$PSF(r,z) = I_0 e^{-2r^2/\omega_{xy}^2} e^{-2z^2/\omega_z^2}$$

where I_0 is the peak intensity, r and z are radial and axial position, and ω_{xy} and ω_z are the radial and axial radii, and $\omega_z > \omega_{xy}$. This Gaussian form is assumed in deriving the functional form of the autocorrelation.

Typically ω_{xy} is 200-300 nm, and ω_z is **2-6** times larger.[11] One common way of calibrating the measurement volume parameters is to perform FCS on a species with known diffusion coefficient and concentration (see below). Diffusion coefficients for common fluorophores in water are given in a later section.

The Gaussian approximation works to varying degrees depending on the optical details, and corrections can sometimes be applied to offset the errors in approximation.[12]

Autocorrelation Function

The (temporal) autocorrelation function is the correlation of a time series with itself shifted by time τ, as a function of τ:

$$G(\tau) = \frac{\langle \delta I(t) \delta I(t+\tau) \rangle}{\langle I(t) \rangle^2} = \frac{\langle I(t) I(t+\tau) \rangle}{\langle I(t) \rangle^2} - 1$$

where $\delta I(t) = I(t) - \langle I(t) \rangle$ is the deviation from the mean intensity. The normalization (denominator) here is the most commonly used for FCS, because then the correlation at $\tau = 0$, *G*(0), is related to the average number of particles in the measurement volume.

Interpreting the Autocorrelation Function

To extract quantities of interest, the autocorrelation data can be fitted, typically using a nonlinear least squares algorithm. The fit's functional form depends on the type of dynamics (and the optical geometry in question).

Normal Diffusion

The fluorescent particles used in FCS are small and thus experience thermal motions in solution. The simplest FCS experiment is thus normal 3D diffusion, for which the autocorrelation is:

$$G(\tau) = G(0) \frac{1}{(1 + (\tau/\tau_D))(1 + a^{-2}(\tau/\tau_D))^{1/2}} + G(\infty)$$

where $a = \omega_z/\omega_{xy}$ is the ratio of axial to radial e^{-2} radii of the measurement volume, and τ_D is the characteristic residence time. This form was derived assuming a Gaussian measurement volume. Typically, the fit would have three free parameters--G(0), $G(\infty)$, and τ_D--from which the diffusion coefficient and fluorophore concentration can be obtained.

With the normalization used in the previous section, G(0) gives the mean number of diffusers in the volume <N>, or equivalently--with knowledge of the observation volume size--the mean concentration:

$$G(0) = \frac{1}{< N >} = \frac{1}{V_{eff} < C >},$$

where the effective volume is found from integrating the Gaussian form of the measurement volume and is given by:

$$V_{eff} = \pi^{3/2} \omega_{xy}^2 \omega_z.$$

τ_D gives the diffusion coefficient: $D = \omega_{xy}^2 / 4\tau_D$.

Anomalous diffusion

If the diffusing particles are hindered by obstacles or pushed by a force (molecular motors, flow, etc.) the dynamics is often not sufficiently well-described by the normal diffusion model, where the mean squared displacement (MSD) grows linearly with time. Instead the diffusion may be better described as anomalous diffusion, where the temporal dependenc of the MSD is non-linear as in the power-law:

$$MSD = 6D_a t^{\alpha}$$

where D_a is an anomalous diffusion coefficient. "Anomalous diffusion" commonly refers only to this very generic model, and not the many other possibilities that might be described as anomalous. Also, a power law is, in a strict sense, the expected form only for a narrow range of rigorously defined systems, for instance when the distribution of obstacles is fractal. Nonetheless a power law can be a useful approximation for a wider range of systems.

The FCS autocorrelation function for anomalous diffusion is:

$$G(\tau) = G(0)\frac{1}{(1+(\tau/\tau_D)^{\alpha})(1+a^{-2}(\tau/\tau_D)^{\alpha})^{1/2}} + G(\infty),$$

where the anomalous exponent α is the same as above, and becomes a free parameter in the fitting.

Using FCS, the anomalous exponent has been shown to be an indication of the degree of molecular crowding (it is less than one and smaller for greater degrees of crowding)[13] .

Polydisperse diffusion

If there are diffusing particles with different sizes (diffusion coefficients), it is common to fit to a function that is the sum of single component forms:

$$G(\tau) = G(0)\sum_i \frac{\alpha_i}{(1+(\tau/\tau_{D,i}))(1+a^{-2}(\tau/\tau_{D,i}))^{1/2}} + G(\infty)$$

where the sum is over the number different sizes of particle, indexed by i, and α_i gives the weighting, which is related to the quantum yield and concentration of each type. This introduces new parameters, which makes the fitting more difficult as a higher dimensional space must be searched. Nonlinear least square fitting typically becomes unstable with even a small number of $\tau_{D,i}$ s. A more robust fitting scheme, especially useful for polydisperse samples, is the Maximum Entropy Method[14] .

Diffusion with flow

With diffusion together with a uniform flow with velocity v in the lateral direction, the autocorrelation is[15] :

$$G(\tau) = G(0)\frac{1}{(1+(\tau/\tau_D))(1+a^{-2}(\tau/\tau_D))^{1/2}} \times \exp[-(\tau/\tau_v)^2 \times \frac{1}{1+\tau/\tau_D}] + G(\infty)$$

where $\tau_v = \omega_{xy}/v$ is the average residence time if there is only a flow (no diffusion).

Chemical relaxation

A wide range of possible FCS experiments involve chemical reactions that continually fluctuate from equilibrium because of thermal motions (and then "relax"). In contrast to diffusion, which is also a relaxation process, the fluctuations cause changes between states of different energies. One very simple system showing chemical relaxation would be a stationary binding site in the measurement volume, where particles only produce signal when bound (e.g. by FRET, or if the diffusion time is much faster than the sampling interval). In this case the autocorrelation is:

$$G(\tau) = G(0)\exp(-\tau/\tau_B) + G(\infty)$$

where

$$\tau_B = (k_{on} + k_{off})^{-1}$$

is the relaxation time and depends on the reaction kinetics (on and off rates), and:

$$G(0) = \frac{1}{\langle N \rangle}\frac{k_{on}}{k_{off}} = \frac{1}{\langle N \rangle}K$$

is related to the equilibrium constant K.

Most systems with chemical relaxation also show measureable diffusion as well, and the autocorrelation function will depend on the details of the system. If the diffusion and chemical reaction are decoupled, the combined autocorrelation is the product of the chemical and diffusive autocorrelations.

Triplet State Correction

The autocorrelations above assume that the fluctuations are not due to changes in the fluorescent properties of the particles. However, for the majority of (bio)organic fluorophores--e.g. green fluorescent protein, rhodamine, Cy3 and Alexa Fluor dyes--some fraction of illuminated particles are excited to a triplet state (or other non-radiative decaying states) and then do not emit photons for a characteristic relaxation time τ_F. Typically τ_F is on the order of microseconds, which is usually smaller than the dynamics of interest (e.g. τ_D) but large enough to be measured. A multiplicative term is added to the autocorrelation account for the triplet state. For normal diffusion:

$$G(\tau) = G(0)\frac{1 - F + Fe^{-\tau/\tau_F}}{1 - F}\frac{1}{(1 + (\tau/\tau_{D,i}))(1 + a^{-2}(\tau/\tau_{D,i}))^{1/2}} + G(\infty)$$

where F is the fraction of particles that have entered the triplet state and τ_F is the corresponding triplet state relaxation time. If the dynamics of interest are much slower than the triplet state relaxation, the short time component of the autocorrelation can simply be truncated and the triplet term is unnecessary.

Common fluorescent probes

The fluorescent species used in FCS is typically a biomolecule of interest that has been tagged with a fluorophore (using immunohistochemistry for instance), or is a naked fluorophore that is used to probe some environment of interest (e.g. the cytoskeleton of a cell). The following table gives diffusion coefficients of some common fluorophores in water at room temperature, and their excitation wavelengths.

Fluorescent dye	D (x10^{-10} m^2 s^{-1})	Excitation wavelength (nm)	Reference

Rhodamine 6G	2.8, 3.0, 4.14 ± 0.05 @ 25.00 °C	514	[16], [17], [18]
Rhodamine 110	2.7	488	[19]
Tetramethyl rhodamine	2.6	543	
Cy3	2.8	543	
Cy5	2.5, 3.7 ± 0.15 @ 25.00 °C	633	[20], [21]
carboxyfluorescein	3.2	488	
Alexa-488	1.96	488	[22]
Atto655-maleimide	4.07 ± 0.1 @ 25.00 °C	663	[23]
Atto655-carboxylicacid	4.26 ± 0.08 @ 25.00 °C	663	[24]
2□, 7□-difluorofluorescein (Oregon Green488)	4.11 ± 0.06 @ 25.00 °C	498	[25]

Variations of FCS

FCS almost always refers to the single point, single channel, temporal autocorrelation measurement, although the term "fluorescence correlation spectroscopy" out of its historical scientific context implies no such restriction. FCS has been extended in a number of variations by different researchers, with each extension generating another name (usually an acronym).

Fluorescence Cross-Correlation Spectroscopy (FCCS)

FCS is sometimes used to study molecular interactions using differences in diffusion times (e.g. the product of an association reaction will be larger and thus have larger diffusion times than the reactants individually); however, FCS is relatively insensitive to molecular mass as can be seen from the following equation relating molecular mass to the diffusion time of globular particles (e.g. proteins):

$$\tau_D = \frac{3\pi\omega_{xy}^2\eta}{2kT}(M)^{1/3}$$

where η is the viscosity of the sample and M is the molecular mass of the fluorescent species. In practice, the diffusion times need to be sufficiently different--a factor of at least **1.6**--which means the molecular masses must differ by a factor of **4**.[26] Dual color fluorescence cross-correlation spectroscopy (FCCS) measures interactions by cross-correlating two or more fluorescent channels (one channel for each reactant), which distinguishes interactions more sensitively than FCS, particularly when the mass change in the reaction is small.

Two- and three- photon FCS excitation

Several advantages in both spatial resolution and minimizing photodamage/photobleaching in organic and/or biological samples are obtained by two-photon or three-photon excitation FCS[27] [28] [29] [30] [31] .

FRET-FCS

Another FCS based approach to studying molecular interactions uses fluorescence resonance energy transfer (FRET) instead of fluorescence, and is called FRET-FCS.[32] With FRET, there are two types of probes, as with FCCS; however, there is only one channel and light is only detected when the two probes are very close--close enough to ensure an interaction. The FRET signal is weaker than with fluorescence, but has the advantage that there is only signal during a reaction (aside from autofluorescence).

Image Correlation Spectroscopy (ICS)

When the motion is slow (in biology, for example, diffusion in a membrane), getting adequate statistics from a single-point FCS experiment may take a prohibitively long time. More data can be obtained by performing the experiment in multiple spatial points in parallel, using a laser scanning confocal microscope. This approach has been called Image Correlation Spectroscopy (ICS)[33] . The measurements can then be averaged together.

Another variation of ICS performs a spatial autocorrelation on images, which gives information about the concentration of particles[34] . The correlation is then averaged in time.

A natural extension of the temporal and spatial correlation versions is spatio-temporal ICS (STICS) [35] . In STICS there is no explicit averaging in space or time (only the averaging inherent in correlation). In systems with non-isotropic motion (e.g. directed flow, asymmetric diffusion), STICS can extract the directional information. A variation that is closely related to STICS (by the Fourier transform) is k-space Image Correlation Spectroscopy (kICS).[36]

There are cross-correlation versions of ICS as well.[33]

Scanning FCS variations

Some variations of FCS are only applicable to serial scanning laser microscopes. Image Correlation Spectroscopy and its variations all were implemented on a scanning confocal or scanning two photon microscope, but transfer to other microscopes, like a spinning disk confocal microscope. Raster ICS (RICS)[37] , and position sensitive FCS (PSFCS)[38] incorporate the time delay between parts of the image scan into the analysis. Also, low dimensional scans (e.g. a circular ring)[39] --only possible on a scanning system--can access time scales between single point and full image measurements. Scanning path has also been made to adaptively follow particles.[40]

Spinning disk FCS, and spatial mapping

Any of the image correlation spectroscopy methods can also be performed on a spinning disk confocal microscope, which in practice can obtain faster imaging speeds compared to a laser scanning confocal microscope. This approach has recently been applied to diffusion in a spatially varying complex environment, producing a pixel resolution map of diffusion coefficient.[41] . The spatial mapping of diffusion with FCS has subsequently been extended to TIRF system.[42] Spatial mapping of dynamics using correlation techniques had been applied before, but only at sparse points[43] or at coarse resolution[35] .

Total internal reflection FCS

Total internal reflection fluorescence (TIRF) is a microscopy approach that is only sensitive to a thin layer near the surface of a coverslip, which greatly minimizes background fluorscence. FCS has been extended to that type of microscope, and is called TIR-FCS[44] . Because the fluorescence intensity in TIRF falls off exponentially with distance from the coverslip (instead of as a Gaussian with a confocal), the autocorrelation function is different.

Other fluorescent dynamical approaches

There are two main non-correlation alternatives to FCS that are widely used to study the dynamics of fluorescent species.

Fluorescence recovery after photobleaching (FRAP)

In FRAP, a region is briefly exposed to intense light, irrecoverably photobleaching fluorophores, and the fluorescence recovery due to diffusion of nearby (non-bleached) fluorophores is imaged. A primary advantage of FRAP over FCS is the ease of interpreting qualitative experiments common in cell biology. Differences between cell lines, or regions of a cell, or before and after application of drug, can often be characterized by simple inspection of movies. FCS experiments require a level of processing and are more sensitive to potentially confounding influences like: rotational diffusion, vibrations, photobleaching, dependence on illumination and fluorescence color, inadequate statistics, etc. It is much easier to change the measurement volume in FRAP, which allows greater control. In practice, the volumes are typically larger than in FCS. While FRAP experiments are typically more qualitative, some researchers are studying FRAP quantitatively and including binding dynamics.[45] A disadvantage of FRAP in cell biology is the free radical perturbation of the cell caused by the photobleaching. It is also less versatile, as it cannot measure concentration or rotational diffusion, or co-localization. FRAP requires a significantly higher concentration of fluorophores than FCS.

Particle tracking

In particle tracking, the trajectories of a set of particles are measured, typically by applying particle tracking algorithms to movies.[46] Particle tracking has the advantage that all the dynamical information is maintained in the measurement, unlike FCS where correlation averages the dynamics to a single smooth curve. The advantage is apparent in systems showing complex diffusion, where directly computing the mean squared displacement allows straightforward comparison to normal or power law diffusion. To apply particle tracking, the particles have to be distinguishable and thus at lower concentration than

required of FCS. Also, particle tracking is more sensitive to noise, which can sometimes affect the results unpredictably.

References

[1] Magde, D., Elson, E. L., Webb, W. W. Thermodynamic fluctuations in a reacting system: Measurement by fluorescence correlation spectroscopy,(1972) *Phys Rev Lett*, **29**,705-708.

[2] Ehrenberg, M., Rigler, R. Rotational brownian motion and fluorescence intensity fluctuations,(1974) *Chem Phys*, **4**,390-401.

[3] Elson, E. L., Magde, D. Fluorescence correlation spectroscopy I. Conceptual basis and theory,(1974) *Biopolymers*, **13**,1-27.

[4] Magde, D., Elson, E. L., Webb, W. W. Fluorescence correlation spectroscopy II. An experimental realization,(1974) *Biopolymers*, **13**,29-61.

[5] Thompson N L 1991 Topics in Fluorescence Spectroscopy Techniques vol 1, ed J R Lakowicz (New York: Plenum) pp 337–78

[6] Rigler, R, Ü. Mets1, J. Widengren and P. Kask. Fluorescence correlation spectroscopy with high count rate and low background: analysis of translational diffusion. European Biophysics Journal (1993) 22(3), 159.

[7] Eigen, M., Rigler, M. Sorting single molecules: application to diagnostics and evolutionary biotechnology,(1994) *Proc. Natl. Acad. Sci. USA*, **91**,5740-5747.

[8] Rigler, M. Fluorescence correlations, single molecule detection and large number screening. Applications in biotechnology,(1995) *J. Biotechnol.*, **41**,177-186.

[9] O. Krichevsky, G. Bonnet, "Fluorescence correlation spectroscopy: the technique and its applications," Rep. Prog. Phys. 65, 251-297 (2002).

[10] Medina, M. A., Schwille, P. Fluorescence correlation spectroscopy for the detection and study of single molecules in biology, (2002)*BioEssays*, **24**,758-764.

[11] Mayboroda, O. A., van Remoortere, A., Tanke H. J., Hokke, C. H., Deelder, A. M., A new approach for fluorescence correlation spectroscopy (FCS) based immunoassays, (2003), *J. Biotechnol.*, **107**, 185-192.

[12] Hess, S.T., and W.W. Webb. 2002. Focal volume optics and experimental artifacts in confocal fluorescence correlation spectroscopy. Biophys. J. 83:2300-2317.

[13] Banks, D. S., and C. Fradin. 2005. Anomalous diffusion of proteins due to molecular crowding. Biophys. J. 89:2960–2971.

[14] Sengupta, P., K. Garai, J. Balaji, N. Periasamy, and S. Maiti. 2003. Measuring Size Distribution in Highly Heterogeneous Systems with Fluorescence Correlation Spectroscopy. Biophys. J. 84(3):1977-1984.

[15] Kohler, R.H., P. Schwille, W.W. Webb, and M.R. Hanson. 2000. Active protein transport through plastid tubules: velocity quantified by fluorescence correlation spectroscopy. J Cell Sci 113(22):3921-3930

[16] Magde, D., Elson, E. L., Webb, W. W. Fluorescence correlation spectroscopy II. An experimental realization,(1974) *Biopolymers*, **13**,29-61.

[17] Berland, K. M. Detection of specific DNA sequences using dual-color two-photon fluorescence correlation spectroscopy. (2004),*J. Biotechnol* ,**108(2)**, 127-136.

[18] Müller, C.B., Loman, A., Pacheco, V., Koberling, F., Willbold, D., Richtering, W., Enderlein, J. Precise measurement of diffusion by multi-color dual-focus fluorescence correlation spectroscopy (2008), *EPL*, **83**, 46001.

[19] Pristinski, D., Kozlovskaya, V., Sukhishvili, S. A. Fluorescence correlation spectroscopy studies of diffusion of a weak polyelectrolyte in aqueous solutions. (2005), *J. Chem. Phys.*, **122**, 014907.

[20] Widengren, J., Schwille, P., Characterization of photoinduced isomerization and back-isomerization of the cyanine dye Cy5 by fluorescence correlation spectroscopy. (2000), *J. Phys. Chem. A*, **104**, 6416-6428.

[21] Loman, A., Dertinger, T., Koberling, F., Enderlein, J. Comparison of optical saturation effects in conventional and dual-focus fluorescence correlation spectroscopy (2008), *Chem. Phys. Lett.*, **459**, 18–21.

[22] Pristinski, D., Kozlovskaya, V., Sukhishvili, S. A. Fluorescence correlation spectroscopy studies of diffusion of a weak polyelectrolyte in aqueous solutions. (2005), *J. Chem. Phys.*, **122**, 014907.

[23] Müller, C.B., Loman, A., Pacheco, V., Koberling, F., Willbold, D., Richtering, W., Enderlein, J. Precise measurement of diffusion by multi-color dual-focus fluorescence correlation spectroscopy (2008), *EPL*, **83**, 46001.

[24] Müller, C.B., Loman, A., Pacheco, V., Koberling, F., Willbold, D., Richtering, W., Enderlein, J. Precise measurement of diffusion by multi-color dual-focus fluorescence correlation spectroscopy (2008), *EPL*, **83**, 46001.

[25] Müller, C.B., Loman, A., Pacheco, V., Koberling, F., Willbold, D., Richtering, W., Enderlein, J. Precise measurement of diffusion by multi-color dual-focus fluorescence correlation spectroscopy (2008), *EPL*, **83**, 46001.

[26] Meseth, U., Wohland, T., Rigler, R., Vogel, H. Resolution of fluorescence correlation measurements. (1999) *Biophys. J.*, **76**, 1619-1631.
[27] Diaspro, A., and Robello, M. (1999). Multi-photon Excitation Microscopy to Study Biosystems. European Microscopy and Analysis., 5:5-7.
[28] Bagatolli, L.A., and Gratton, E. (2000). Two-photon fluorescence microscopy of coexisting lipid domains in giant unilamellar vesicles of binary phospholipid mixtures. Biophys J., 78:290-305.
[29] Schwille, P., Haupts, U., Maiti, S., and Webb. W.(1999). Molecular dynamics in living cells observed by fluorescence correlation spectroscopy with one- and two- photon excitation. *Biophysical Journal*, **77**(10):2251-2265.
[30] Near Infrared Microspectroscopy, Fluorescence Microspectroscopy,Infrared Chemical Imaging and High Resolution Nuclear Magnetic Resonance Analysis of Soybean Seeds, Somatic Embryos and Single Cells., Baianu, I.C. et al. 2004., In *Oil Extraction and Analysis.*, D. Luthria, Editor pp.241-273, AOCS Press., Champaign, IL.
[31] Single Cancer Cell Detection by Near Infrared Microspectroscopy, Infrared Chemical Imaging and Fluorescence Microspectroscopy.2004.I. C. Baianu, D. Costescu, N. E. Hofmann and S. S. Korban, q-bio/0407006 (July 2004) (http://arxiv.org/abs/q-bio/0407006)
[32] K. Remaut, B. Lucas, K. Braeckmans, N.N. Sanders, S.C. De Smedt and J. Demeester, FRET-FCS as a tool to evaluate the stability of oligonucleotide drugs after intracellular delivery, J Control Rel 103 (2005) (1), pp. 259–271.
[33] Wiseman, P. W., J. A. Squier, M. H. Ellisman, and K. R. Wilson. 2000. Two-photon video rate image correlation spectroscopy (ICS) and image cross-correlation spectroscopy (ICCS). J. Microsc. 200:14–25.
[34] Petersen, N. O., P. L. Ho¨ddelius, P. W. Wiseman, O. Seger, and K. E. Magnusson. 1993. Quantitation of membrane receptor distributions by image correlation spectroscopy: concept and application. Biophys. J. 65:1135–1146.
[35] Hebert, B., S. Constantino, and P. W. Wiseman. 2005. Spatio-temporal image correlation spectroscopy (STICS): theory, verification and application to protein velocity mapping in living CHO cells. Biophys. J. 88:3601–3614.
[36] Kolin, D.L., D. Ronis, and P.W. Wiseman. 2006. k-Space Image Correlation Spectroscopy: A Method for Accurate Transport Measurements Independent of Fluorophore Photophysics. Biophys. J. 91(8):3061-3075.
[37] Digman, M.A., P. Sengupta, P.W. Wiseman, C.M. Brown, A.R. Horwitz, and E. Gratton. 2005. Fluctuation Correlation Spectroscopy with a Laser-Scanning Microscope: Exploiting the Hidden Time Structure. Biophys. J. 88(5):L33-36.
[38] Skinner, J.P., Y. Chen, and J.D. Mueller. 2005. Position-Sensitive Scanning Fluorescence Correlation Spectroscopy. Biophys. J.:biophysj.105.060749.
[39] Ruan, Q., M.A. Cheng, M. Levi, E. Gratton, and W.W. Mantulin. 2004. Spatial-temporal studies of membrane dynamics: scanning fluorescence correlation spectroscopy (SFCS). Biophys. J. 87:1260–1267.
[40] A. Berglund and H. Mabuchi, "Tracking-FCS: Fluorescence correlation spectroscopy of individual particles," Opt. Express 13, 8069-8082 (2005).
[41] Sisan, D.R., R. Arevalo, C. Graves, R. McAllister, and J.S. Urbach. 2006. Spatially resolved fluorescence correlation spectroscopy using a spinning disk confocal microscope. Biophysical Journal 91(11):4241-4252.
[42] Kannan, B., L. Guo, T. Sudhaharan, S. Ahmed, I. Maruyama, and T. Wohland. 2007. Spatially resolved total internal reflection fluorescence correlation microscopy using an electron multiplying charge-coupled device camera. Analytical Chemistry 79(12):4463-4470
[43] Wachsmuth, M., W. Waldeck, and J. Langowski. 2000. Anomalous diffusion of fluorescent probes inside living cell nuclei investigated by spatially-resolved fluorescence correlation spectroscopy. J. Mol. Biol. 298(4):677-689.
[44] Lieto, A.M., and N.L. Thompson. 2004. Total Internal Reflection with Fluorescence Correlation Spectroscopy: Nonfluorescent Competitors. Biophys. J. 87(2):1268-1278.
[45] Sprague, B.L., and J.G. McNally. 2005. FRAP analysis of binding: proper and fitting. Trends in Cell Biology 15(2):84-91.
[46] http://www.physics.emory.edu/~weeks/idl/

See also

- Confocal microscopy
- Fluorescence cross-correlation spectroscopy
- FRET
- Dynamic light scattering
- Diffusion coefficient

External links

- Single-molecule spectroscopic methods (http://dx.doi.org/10.1016/j.sbi.2004.09.004)
- FCS Classroom (http://www.fcsxpert.com/classroom)

Molecular models of DNA

Molecular models of DNA structures are representations of the molecular geometry and topology of Deoxyribonucleic acid (DNA) molecules using one of several means, such as: closely packed spheres (CPK models) made of plastic, metal wires for 'skeletal models', graphic computations and animations by computers, artistic rendering, and so on, with the aim of simplifying and presenting the essential, physical and chemical, properties of DNA molecular structures either *in vivo* or *in vitro*. Computer molecular models also allow animations and molecular dynamics simulations that are very important for understanding how DNA functions *in vivo*. Thus, an old standing dynamic problem is how DNA "self-replication" takes place in living cells that should involve transient uncoiling of supercoiled DNA fibers. Although DNA consists of relatively rigid, very large elongated biopolymer molecules called "fibers" or chains (that are made of repeating nucleotide units of four basic types, attached to deoxyribose and phosphate groups), its molecular structure *in vivo* undergoes dynamic configuration changes that involve dynamically attached water molecules and ions. Supercoiling, packing with histones in chromosome structures, and other such supramolecular aspects also involve *in vivo* DNA topology which is even more complex than DNA molecular geometry, thus turning molecular modeling of DNA into an especially challenging problem for both molecular biologists and biotechnologists. Like other large molecules and biopolymers, DNA often exists in multiple stable geometries (that is, it exhibits conformational isomerism) and configurational, quantum states which are close to each other in energy on the potential energy surface of the DNA molecule. Such geometries can also be computed, at least in principle, by employing *ab initio* quantum chemistry methods that have high accuracy for small molecules. Such quantum geometries define an important class of *ab initio* molecular models of DNA whose exploration has barely started.

In an interesting twist of roles, the DNA molecule itself was proposed to be utilized for quantum computing. Both DNA nanostructures as well as DNA 'computing' biochips have been built (see biochip image at right).

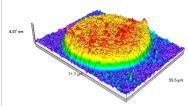

DNA computing biochip:3D

The more advanced, computer-based molecular models of DNA involve molecular dynamics simulations as well as quantum mechanical computations of vibro-rotations, delocalized molecular orbitals (MOs), electric dipole moments, hydrogen-bonding, and so on.

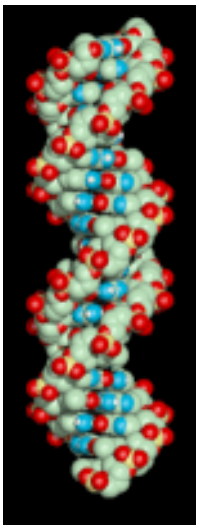

Spinning DNA generic model.

Importance

From the very early stages of structural studies of DNA by X-ray diffraction and biochemical means, molecular models such as the Watson-Crick double-helix model were successfully employed to solve the 'puzzle' of DNA structure, and also find how the latter relates to its key functions in living cells. The first high quality X-ray diffraction patterns of A-DNA were reported by Rosalind Franklin and Raymond Gosling in 1953[1] . The first calculations of the Fourier transform of an atomic helix were reported one year earlier by Cochran, Crick and Vand [2] , and were followed in 1953 by the computation of the Fourier transform of a coiled-coil by Crick[3] . The first reports of a double-helix molecular model of B-DNA structure were made by Watson and Crick in 1953[4] [5] . Last-but-not-least, Maurice F. Wilkins, A. Stokes and H.R. Wilson, reported the first X-ray patterns of *in vivo* B-DNA in partially oriented salmon sperm heads [6] . The development of the first correct double-helix molecular model of DNA by Crick and Watson may not have been possible without the biochemical evidence for the nucleotide base-pairing ([A---T]; [C---G]), or Chargaff's rules[7] [8] [9] [10] [11] [12] .

Examples of DNA molecular models

Animated molecular models allow one to visually explore the three-dimensional (3D) structure of DNA. The first DNA model is a space-filling, or CPK, model of the DNA double-helix whereas the third is an animated wire, or skeletal type, molecular model of DNA. The last two DNA molecular models in this series depict quadruplex DNA [13] that may be involved in certain cancers[13] [14] . The last figure on this panel is a molecular model of hydrogen bonds between water molecules in ice that are similar to those found in DNA.

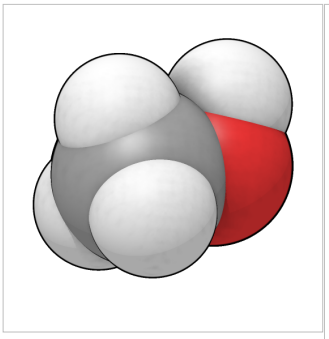

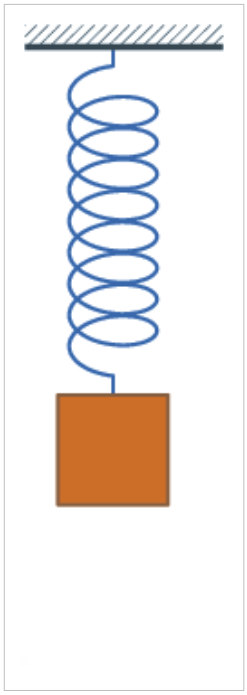

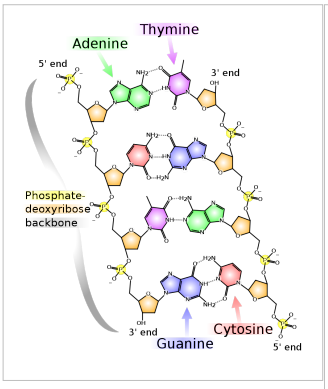
Thymine
Adenine
5' end
3' end
Phosphate-
deoxyribose
backbone
3' end
Guanine
Cytosine
5' end

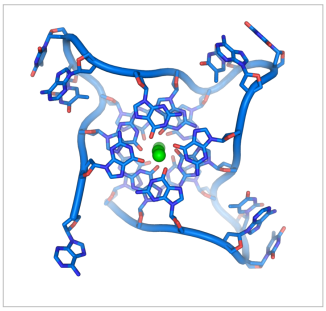

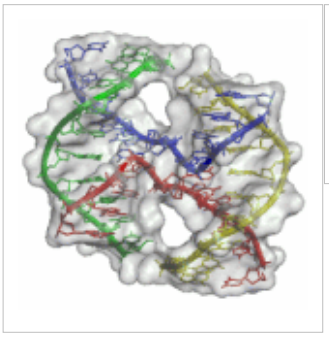

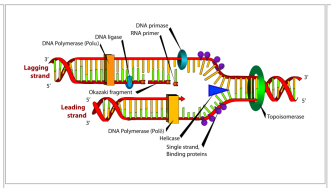
Lagging strand
Leading strand
DNA Polymerase (Pol I)
DNA ligase
DNA primase
RNA primer
Okazaki fragment
DNA Polymerase (Pol III)
Helicase
Single strand. Binding proteins
Topoisomerase

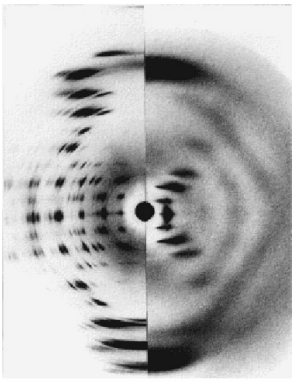

A-DNA B-DNA

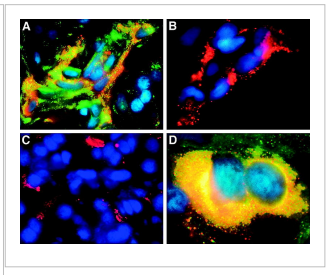
A
B
C
D

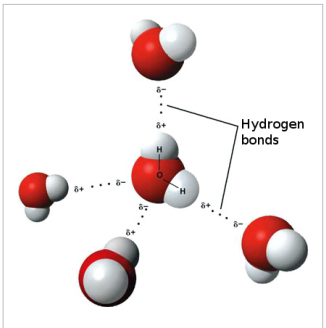

- Spacefilling model or CPK model - a molecule is represented by overlapping spheres representing the atoms.

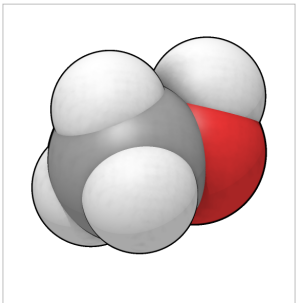

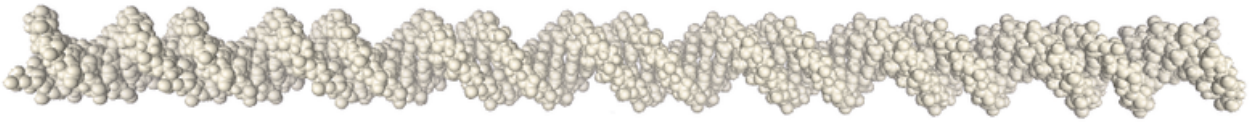

DNA Spacefilling molecular model

Images for DNA Structure Determination from X-Ray Patterns

The following images illustrate both the principles and the main steps involved in generating structural information from X-ray diffraction studies of oriented DNA fibers with the help of molecular models of DNA that are combined with crystallographic and mathematical analysis of the X-ray patterns. From left to right the gallery of images shows:

- *First row*:
- 1. Constructive X-ray interference, or diffraction, following Bragg's Law of X-ray "*reflection by the crystal planes*";
- 2. A comparison of A-DNA (crystalline) and highly hydrated B-DNA (paracrystalline) X-ray diffraction, and respectively, X-ray scattering patterns (courtesy of Dr. Herbert R. Wilson, FRS- see refs. list);
- 3. Purified DNA precipitated in a water jug;
- 4. The major steps involved in DNA structure determination by X-ray crystallography showing the important role played by molecular models of DNA structure in this iterative, structure--determination process;
- *Second row*:

- 5. Photo of a modern X-ray diffractometer employed for recording X-ray patterns of DNA with major components: X-ray source, goniometer, sample holder, X-ray detector and/or plate holder;
- 6. Illustrated animation of an X-ray goniometer;
- 7. X-ray detector at the SLAC synchrotron facility;
- 8. Neutron scattering facility at ISIS in UK;
  - *Third and fourth rows*: *Molecular models of DNA structure at various scales*; figure #11 is an actual electron micrograph of a DNA fiber bundle, presumably of a single bacterial chromosome loop.

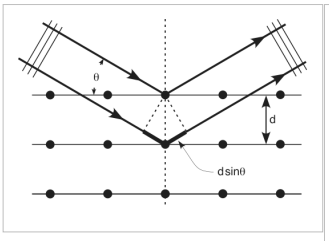

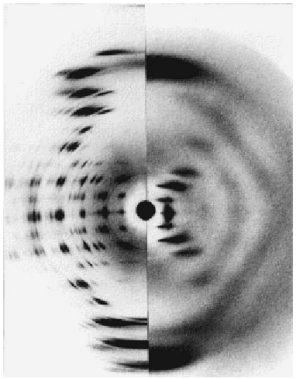

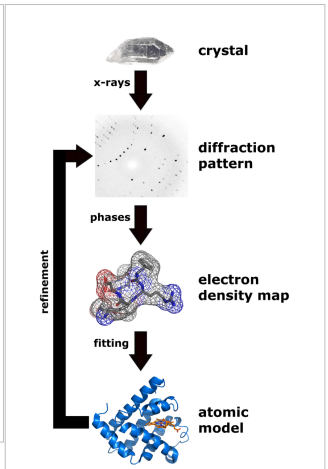

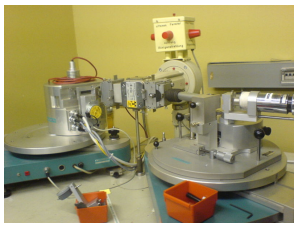

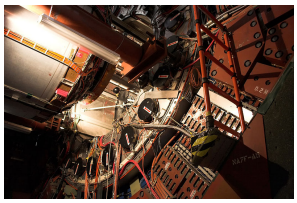

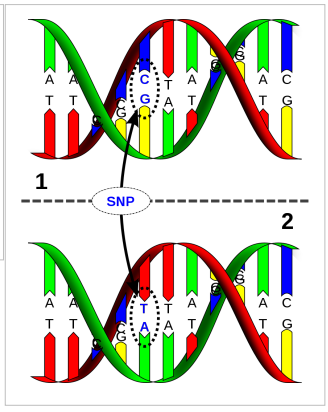

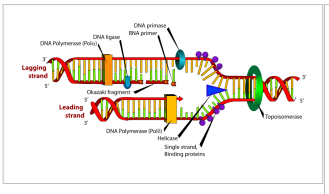

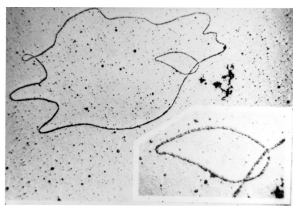

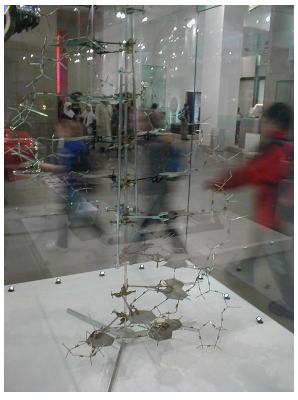

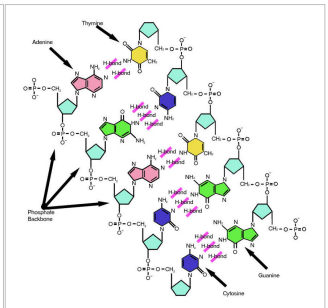

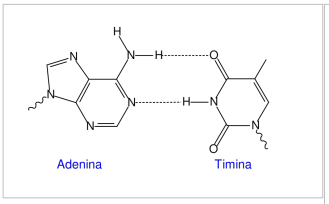

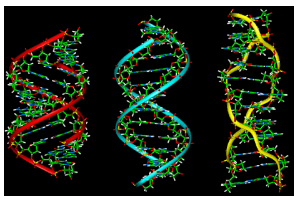

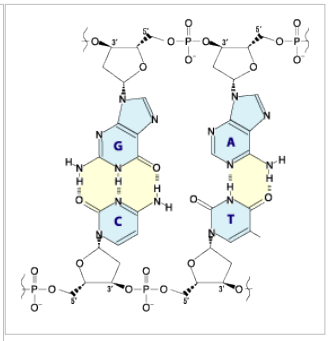

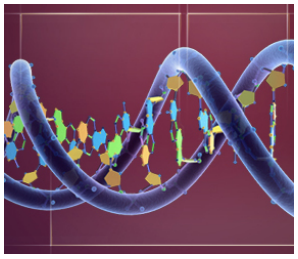

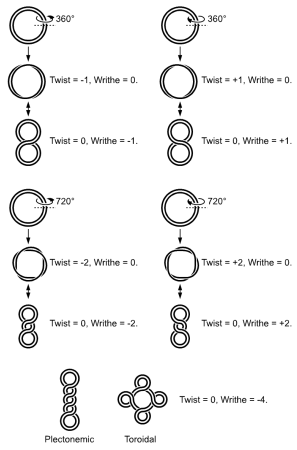

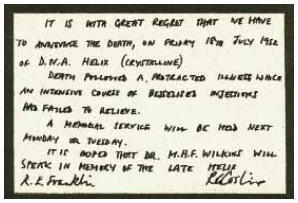

Paracrystalline lattice models of B-DNA structures

A paracrystalline lattice, or paracrystal, is a molecular or atomic lattice with significant amounts (e.g., larger than a few percent) of partial disordering of molecular arranegements. Limiting cases of the paracrystal model are nanostructures, such as glasses, liquids, etc., that may possess only local ordering and no global order. Liquid crystals also have paracrystalline rather than crystalline structures.

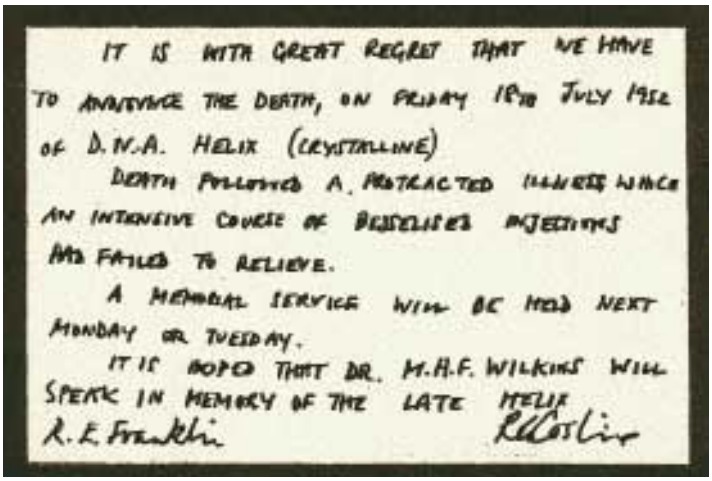

DNA Helix controversy in 1952

Highly hydrated B-DNA occurs naturally in living cells in such a paracrystalline state, which is a dynamic one in spite of the relatively rigid DNA double-helix stabilized by parallel hydrogen bonds between the nucleotide base-pairs in the two complementary, helical DNA chains (see figures). For simplicity most DNA molecular models ommit both water and ions dynamically bound to B-DNA, and are thus less useful for understanding the dynamic behaviors of B-DNA *in vivo*. The physical and mathematical analysis of X-ray[15] [16] and spectroscopic data for paracrystalline B-DNA is therefore much more complicated than that of crystalline, A-DNA X-ray diffraction patterns. The paracrystal model is also important for DNA technological applications such as DNA nanotechnology. Novel techniques that combine X-ray diffraction of DNA with X-ray microscopy in hydrated living cells are now also being developed (see, for example, "Application of X-ray microscopy in the analysis of living hydrated cells" [18]).

Genomic and Biotechnology Applications of DNA molecular modeling

The following gallery of images illustrates various uses of DNA molecular modeling in Genomics and Biotechnology research applications from DNA repair to PCR and DNA nanostructures; each slide contains its own explanation and/or details. The first slide presents an overview of DNA applications, including DNA molecular models, with emphasis on Genomics and Biotechnology.

Gallery: DNA Molecular modeling applications

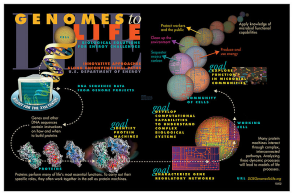

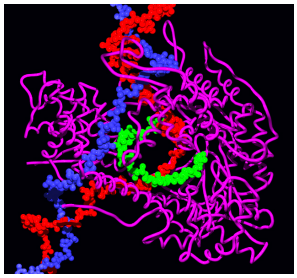
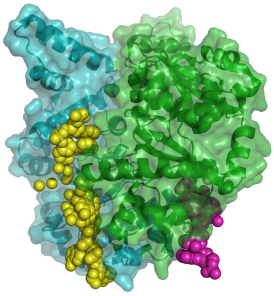

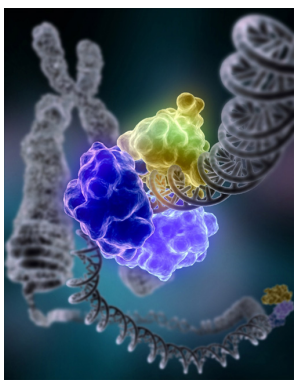
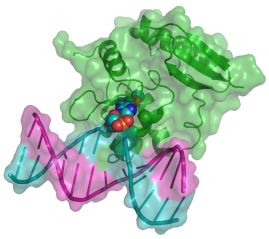
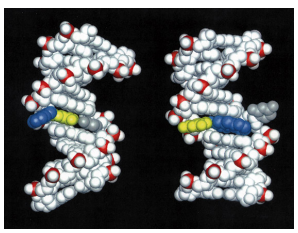
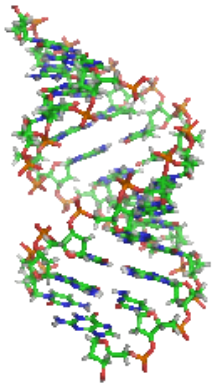

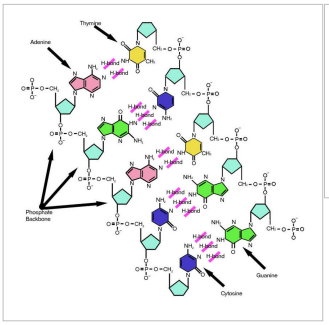
Thymine
Adenine
Phosphate Backbone
Guanine
Cytosine

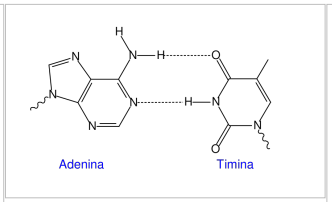
Adenina
Timina

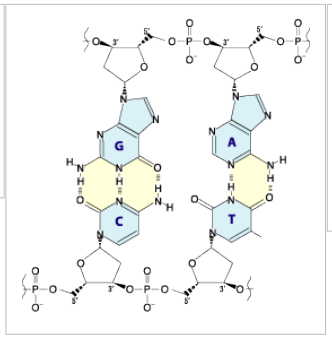
G
C
A
T

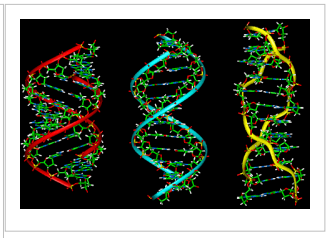

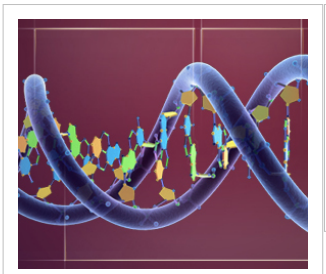

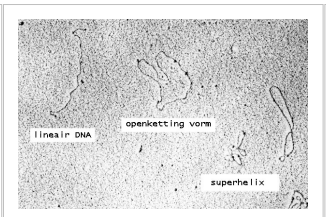
linear DNA
openkettling vorm
superhelix

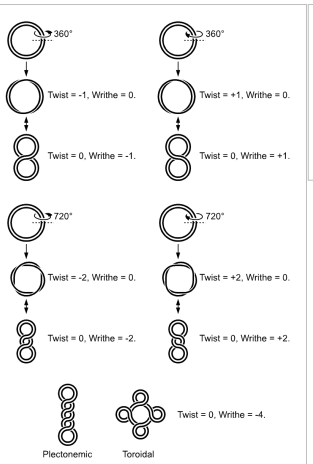
360°
Twist = -1, Writhe = 0.
Twist = 0, Writhe = -1.
360°
Twist = +1, Writhe = 0.
Twist = 0, Writhe = +1.
720°
Twist = -2, Writhe = 0.
Twist = 0, Writhe = -2.
720°
Twist = +2, Writhe = 0.
Twist = 0, Writhe = +2.
Twist = 0, Writhe = -4.
Plectonemic
Toroidal

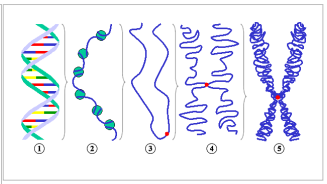
1
2
3
4
5

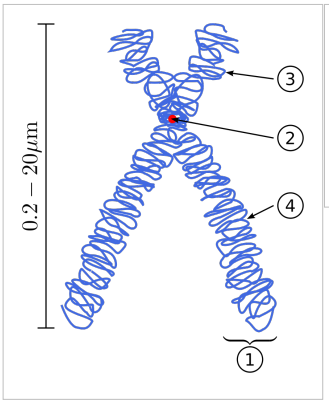
0.2 – 20µm
3
2
4
1

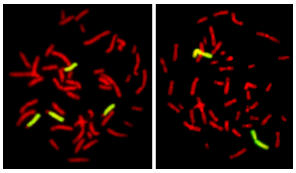

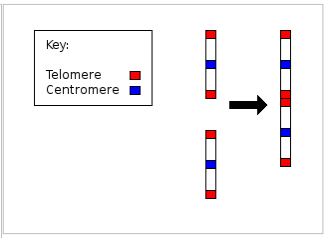
Key:
Telomere
Centromere

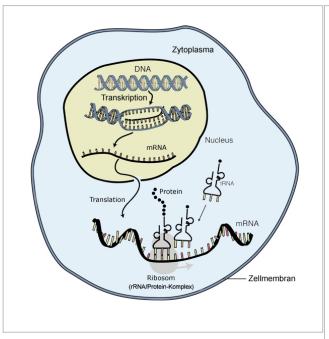
Zytoplasma
DNA
Transkription
Nucleus
mRNA
Translation
Protein
tRNA
mRNA
Ribosom
(rRNA/Protein-Komplex)
Zellmembran

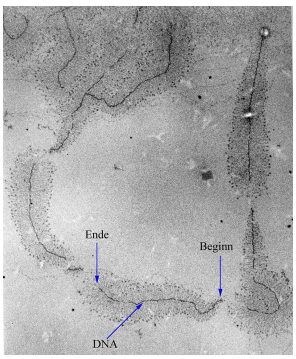
Ende
Beginn
DNA

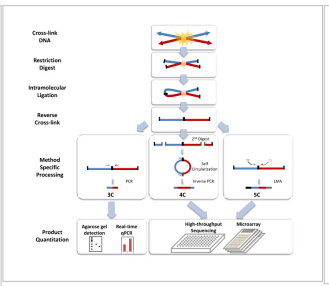
Cross-link DNA
Restriction Digest
Intramolecular Ligation
Reverse Cross-link
Method Specific Processing
3C
4C
5C
Product Quantitation

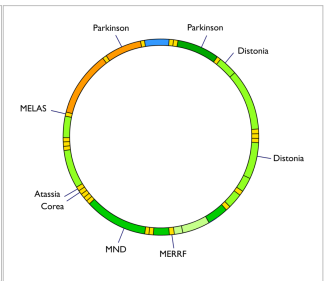
Parkinson
Parkinson
Distonia
MELAS
Distonia
Atassia
Corea
MND
MERRF

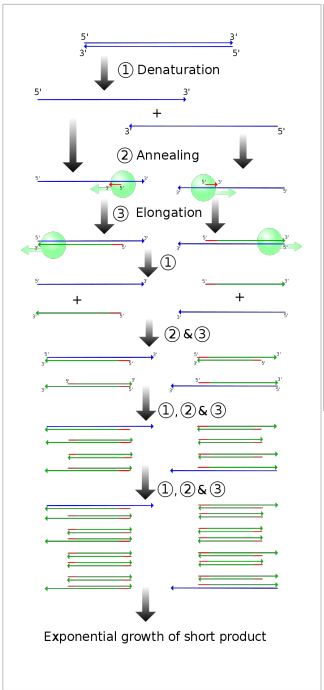

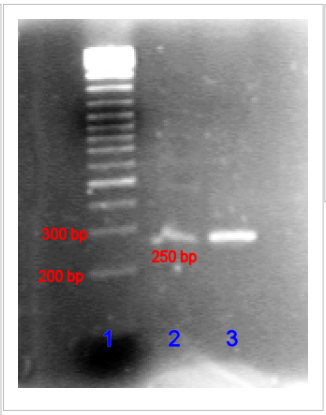

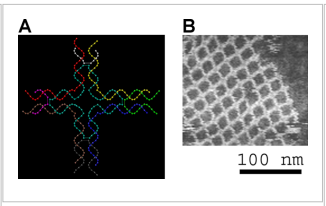

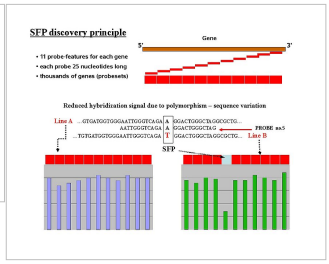

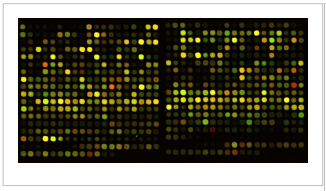

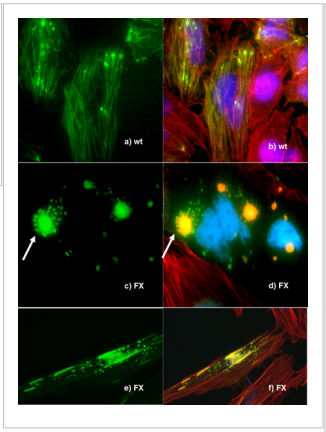

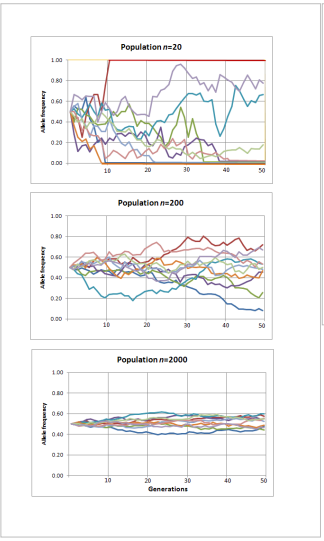

Databases for DNA molecular models and sequences

X-ray diffraction

- NDB ID: UD0017 Database [13]
- X-ray Atlas -database [19]
- PDB files of coordinates for nucleic acid structures from X-ray diffraction by NA (incl. DNA) crystals [20]
- Structure factors dowloadable files in CIF format [21]

Neutron scattering

- ISIS neutron source
- ISIS pulsed neutron source:A world centre for science with neutrons & muons at Harwell, near Oxford, UK. [22]

X-ray microscopy

- Application of X-ray microscopy in the analysis of living hydrated cells [18]

Electron microscopy

- DNA under electron microscope [23]

Atomic Force Microscopy (AFM)

Two-dimensional DNA junction arrays have been visualized by Atomic Force Microscopy (AFM)[17] . Other imaging resources for AFM/Scanning probe microscopy(SPM) can be freely accessed at:

- How SPM Works [25]
- SPM Image Gallery - AFM STM SEM MFM NSOM and more. [26]

Gallery of AFM Images

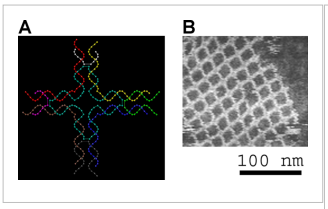

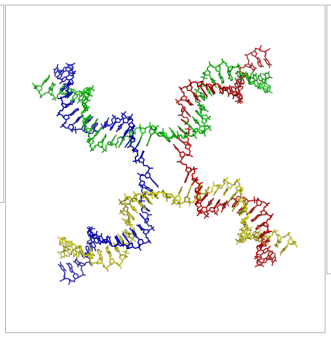

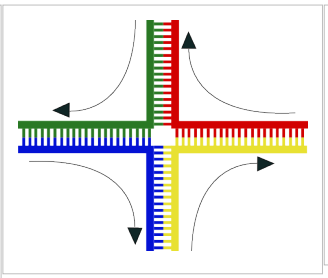

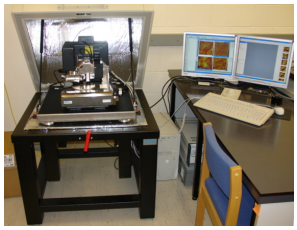

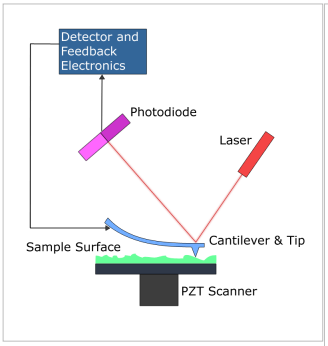

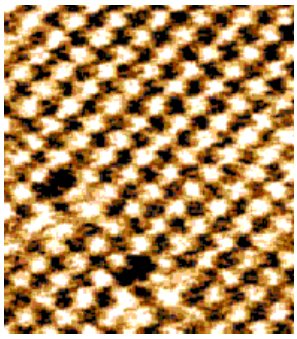

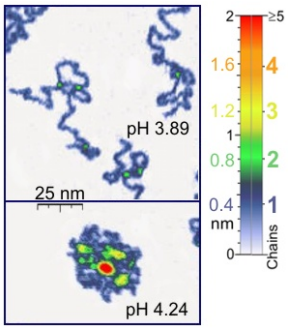

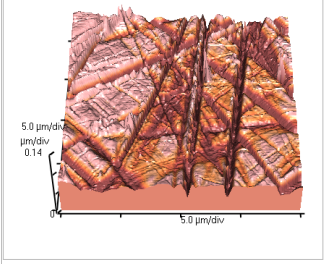

Mass spectrometry--Maldi informatics

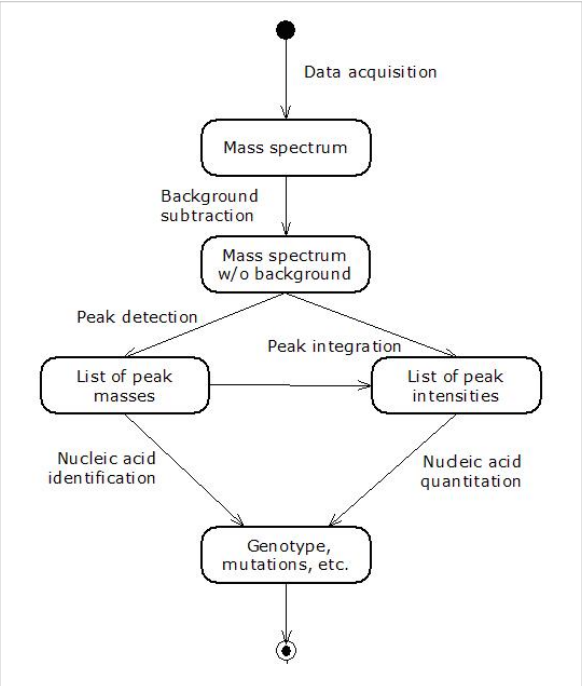

Spectroscopy

- Vibrational circular dichroism (VCD)
- FT-NMR[18] [19]
  - NMR Atlas--database [29]
  - mmcif downloadable coordinate files of nucleic acids in solution from 2D-FT NMR data [30]
  - NMR constraints files for NAs in PDB format [31]
- NMR microscopy[20]
- Microwave spectroscopy
- FT-IR
- FT-NIR[21] [22] [23]
- Spectral, Hyperspectral, and Chemical imaging)[24] [25] [26] [27] [28] [29] [30] .
- Raman spectroscopy/microscopy[31] and CARS[32] .
- Fluorescence correlation spectroscopy[33] [34] [35] [36] [37] [38] [39] [40] , Fluorescence cross-correlation spectroscopy and FRET[41] [42] [43] .
- Confocal microscopy[44]

Gallery: CARS (Raman spectroscopy), Fluorescence confocal microscopy, and Hyperspectral imaging

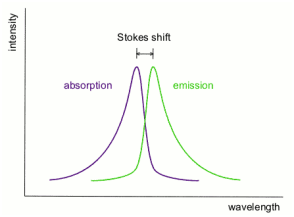

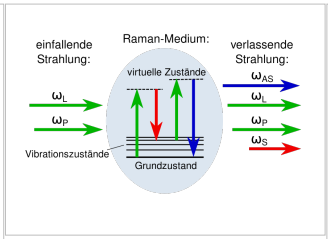

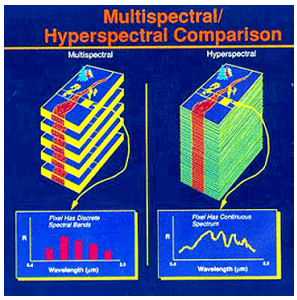

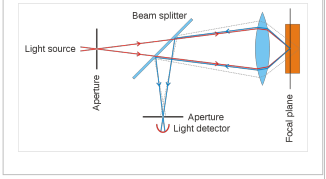

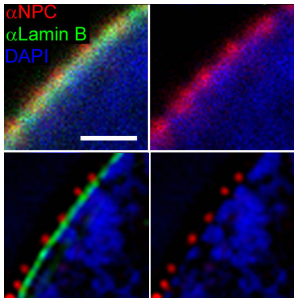

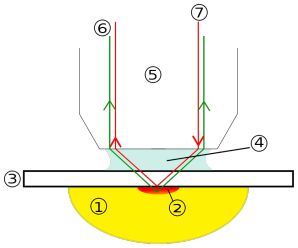

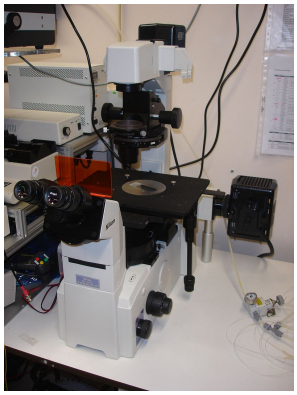

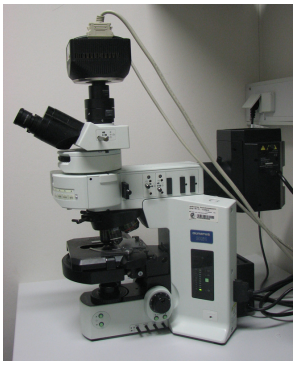

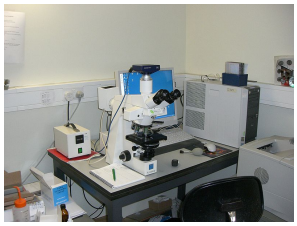

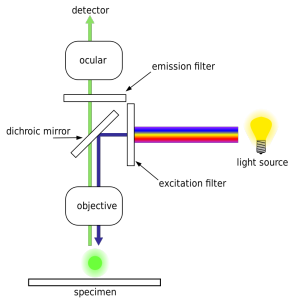

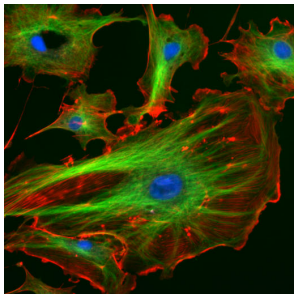

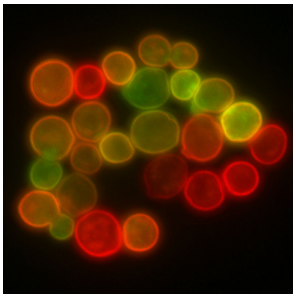

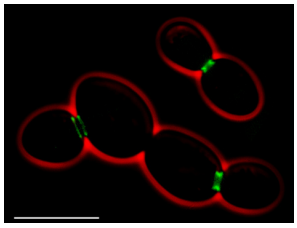

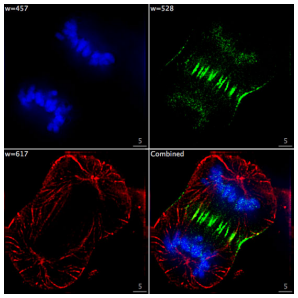

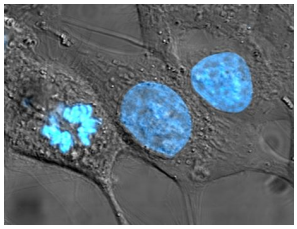

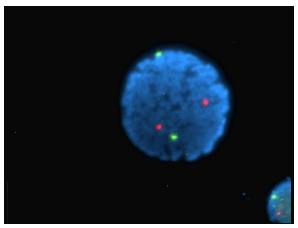

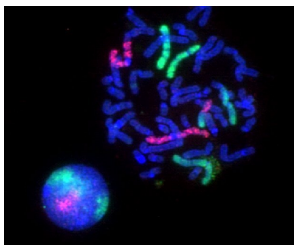

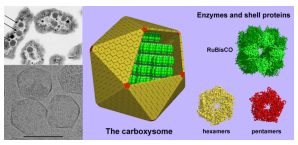

Genomic and structural databases

- CBS Genome Atlas Database [57] — contains examples of base skews.[45]
- The Z curve database of genomes — a 3-dimensional visualization and analysis tool of genomes [59][46] .
- DNA and other nucleic acids' molecular models: Coordinate files of nucleic acids molecular structure models in PDB and CIF formats [61]

Notes

[1] Franklin, R.E. and Gosling, R.G. recd.6 March 1953. Acta Cryst. (1953). 6, 673 The Structure of Sodium Thymonucleate Fibres I. The Influence of Water Content Acta Cryst. (1953). and 6, 678 The Structure of Sodium Thymonucleate Fibres II. The Cylindrically Symmetrical Patterson Function.

[2] Cochran, W., Crick, F.H.C. and Vand V. 1952. The Structure of Synthetic Polypeptides. 1. The Transform of Atoms on a Helix. Acta Cryst. 5(5):581-586.

[3] Crick, F.H.C. 1953a. The Fourier Transform of a Coiled-Coil., Acta Crystallographica 6(8-9):685-689.

[4] Watson, J.D; Crick F.H.C. 1953a. Molecular Structure of Nucleic Acids- A Structure for Deoxyribose Nucleic Acid., Nature 171(4356):737-738.

[5] Watson, J.D; Crick F.H.C. 1953b. The Structure of DNA., Cold Spring Harbor Symposia on Qunatitative Biology 18:123-131.

[6] Wilkins M.H.F., A.R. Stokes A.R. & Wilson, H.R. (1953). "http://www.nature.com/nature/dna50/wilkins.pdf|Molecular Structure of Deoxypentose Nucleic Acids" (PDF). *Nature* **171**: 738–740. doi: 10.1038/171738a0 (http://dx.doi.org/10.1038/171738a0). PMID 13054693. http://www.nature.com/nature/dna50/wilkins.pdf.

[7] Elson D, Chargaff E (1952). "On the deoxyribonucleic acid content of sea urchin gametes". *Experientia* **8** (4): 143-145.

[8] Chargaff E, Lipshitz R, Green C (1952). "Composition of the deoxypentose nucleic acids of four genera of sea-urchin". *J Biol Chem* **195** (1): 155-160. PMID 14938364.

[9] Chargaff E, Lipshitz R, Green C, Hodes ME (1951). "The composition of the deoxyribonucleic acid of salmon sperm". *J Biol Chem* **192** (1): 223-230. PMID 14917668.

[10] Chargaff E (1951). "Some recent studies on the composition and structure of nucleic acids". *J Cell Physiol Suppl* **38** (Suppl).

[11] Magasanik B, Vischer E, Doniger R, Elson D, Chargaff E (1950). "The separation and estimation of ribonucleotides in minute quantities". *J Biol Chem* **186** (1): 37-50. PMID 14778802.

[12] Chargaff E (1950). "Chemical specificity of nucleic acids and mechanism of their enzymatic degradation". *Experientia* **6** (6): 201-209.

[13] http://www.phy.cam.ac.uk/research/bss/molbiophysics.php

[14] http://planetphysics.org/encyclopedia/TheoreticalBiophysics.html

[15] Hosemann R., Bagchi R.N., *Direct analysis of diffraction by matter*, North-Holland Publs., Amsterdam – New York, 1962.

[16] Baianu, I.C. (1978). "X-ray scattering by partially disordered membrane systems.". *Acta Cryst.,* **A34** (5): 751–753. doi: 10.1107/S0567739478001540 (http://dx.doi.org/10.1107/S0567739478001540).

[17] Mao, Chengde; Sun, Weiqiong & Seeman, Nadrian C. (16 June 1999). "Designed Two-Dimensional DNA Holliday Junction Arrays Visualized by Atomic Force Microscopy". *Journal of the American Chemical Society* **121** (23): 5437–5443. doi: 10.1021/ja9900398 (http://dx.doi.org/10.1021/ja9900398). ISSN 0002-7863 (http://worldcat.org/issn/0002-7863).

[18] (http://www.jonathanpmiller.com/Karplus.html)- obtaining dihedral angles from ^{3}J coupling constants

[19] (http://www.spectroscopynow.com/FCKeditor/UserFiles/File/specNOW/HTML files/General_Karplus_Calculator.htm) Another Javascript-like NMR coupling constant to dihedral
[20] Lee, S. C. et al., (2001). One Micrometer Resolution NMR Microscopy. *J. Magn. Res.*, **150**: 207-213.
[21] Near Infrared Microspectroscopy, Fluorescence Microspectroscopy,Infrared Chemical Imaging and High Resolution Nuclear Magnetic Resonance Analysis of Soybean Seeds, Somatic Embryos and Single Cells., Baianu, I.C. et al. 2004., In *Oil Extraction and Analysis.*, D. Luthria, Editor pp.241-273, AOCS Press., Champaign, IL.
[22] Single Cancer Cell Detection by Near Infrared Microspectroscopy, Infrared Chemical Imaging and Fluorescence Microspectroscopy.2004.I. C. Baianu, D. Costescu, N. E. Hofmann and S. S. Korban, q-bio/0407006 (July 2004) (http://arxiv.org/abs/q-bio/0407006)
[23] Raghavachari, R., Editor. 2001. *Near-Infrared Applications in Biotechnology*, Marcel-Dekker, New York, NY.
[24] http://www.imaging.net/chemical-imaging/Chemical imaging
[25] http://www.malvern.com/LabEng/products/sdi/bibliography/sdi_bibliography.htm E. N. Lewis, E. Lee and L. H. Kidder, Combining Imaging and Spectroscopy: Solving Problems with Near-Infrared Chemical Imaging. Microscopy Today, Volume 12, No. 6, 11/2004.
[26] D.S. Mantus and G. H. Morrison. 1991. Chemical imaging in biology and medicine using ion microscopy., *Microchimica Acta*, **104**, (1-6) January 1991, doi: 10.1007/BF01245536
[27] Near Infrared Microspectroscopy, Fluorescence Microspectroscopy,Infrared Chemical Imaging and High Resolution Nuclear Magnetic Resonance Analysis of Soybean Seeds, Somatic Embryos and Single Cells., Baianu, I.C. et al. 2004., In *Oil Extraction and Analysis.*, D. Luthria, Editor pp.241-273, AOCS Press., Champaign, IL.
[28] Single Cancer Cell Detection by Near Infrared Microspectroscopy, Infrared Chemical Imaging and Fluorescence Microspectroscopy.2004.I. C. Baianu, D. Costescu, N. E. Hofmann and S. S. Korban, q-bio/0407006 (July 2004) (http://arxiv.org/abs/q-bio/0407006)
[29] J. Dubois, G. Sando, E. N. Lewis, Near-Infrared Chemical Imaging, A Valuable Tool for the Pharmaceutical Industry, G.I.T. Laboratory Journal Europe, No.1-2, 2007.
[30] Applications of Novel Techniques to Health Foods, Medical and Agricultural Biotechnology.(June 2004).,I. C. Baianu, P. R. Lozano, V. I. Prisecaru and H. C. Lin q-bio/0406047 (http://arxiv.org/abs/q-bio/0406047)
[31] Chemical Imaging Without Dyeing (http://witec.de/en/download/Raman/ImagingMicroscopy04.pdf)
[32] C.L. Evans and X.S. Xie.2008. Coherent Anti-Stokes Raman Scattering Microscopy: Chemical Imaging for Biology and Medicine., doi:10.1146/annurev.anchem.1.031207.112754 *Annual Review of Analytical Chemistry*, **1**: 883-909.
[33] Eigen, M., Rigler, M. Sorting single molecules: application to diagnostics and evolutionary biotechnology,(1994) *Proc. Natl. Acad. Sci. USA*, 91,5740-5747.
[34] Rigler, M. Fluorescence correlations, single molecule detection and large number screening. Applications in biotechnology,(1995) J. Biotechnol., 41,177-186.
[35] Rigler R. and Widengren J. (1990). Ultrasensitive detection of single molecules by fluorescence correlation spectroscopy, *BioScience* (Ed. Klinge & Owman) p.180.
[36] Single Cancer Cell Detection by Near Infrared Microspectroscopy, Infrared Chemical Imaging and Fluorescence Microspectroscopy.2004.I. C. Baianu, D. Costescu, N. E. Hofmann, S. S. Korban and et al., q-bio/0407006 (July 2004) (http://arxiv.org/abs/q-bio/0407006)
[37] Oehlenschläger F., Schwille P. and Eigen M. (1996). Detection of HIV-1 RNA by nucleic acid sequence-based amplification combined with fluorescence correlation spectroscopy, *Proc. Natl. Acad. Sci. USA* **93**:1281.
[38] Bagatolli, L.A., and Gratton, E. (2000). Two-photon fluorescence microscopy of coexisting lipid domains in giant unilamellar vesicles of binary phospholipid mixtures. Biophys J., 78:290-305.
[39] Schwille, P., Haupts, U., Maiti, S., and Webb. W.(1999). Molecular dynamics in living cells observed by fluorescence correlation spectroscopy with one- and two-photon excitation. Biophysical Journal, 77(10):2251-2265.
[40] Near Infrared Microspectroscopy, Fluorescence Microspectroscopy,Infrared Chemical Imaging and High Resolution Nuclear Magnetic Resonance Analysis of Soybean Seeds, Somatic Embryos and Single Cells., Baianu, I.C. et al. 2004., In *Oil Extraction and Analysis.*, D. Luthria, Editor pp.241-273, AOCS Press., Champaign, IL.
[41] FRET description (http://dwb.unl.edu/Teacher/NSF/C08/C08Links/pps99.cryst.bbk.ac.uk/projects/gmocz/fret.htm)
[42] doi:10.1016/S0959-440X(00)00190-1 (http://dx.doi.org/10.1016/S0959-440X(00)00190-1)Recent advances in FRET: distance determination in protein–DNA complexes. *Current Opinion in Structural Biology* **2001**, *11(2)*, 201-207
[43] http://www.fretimaging.org/mcnamaraintro.html FRET imaging introduction

[44] Eigen, M., and Rigler, R. (1994). Sorting single molecules: Applications to diagnostics and evolutionary biotechnology, Proc. Natl. Acad. Sci. USA 91:5740.
[45] Hallin PF, David Ussery D (2004). "CBS Genome Atlas Database: A dynamic storage for bioinformatic results and DNA sequence data". *Bioinformatics* **20**: 3682-3686.
[46] Zhang CT, Zhang R, Ou HY (2003). "The Z curve database: a graphic representation of genome sequences". Bioinformatics 19 (5): 593-599. doi:10.1093/bioinformatics/btg041

References

- *Applications of Novel Techniques to Health Foods, Medical and Agricultural Biotechnology*.(June 2004) I. C. Baianu, P. R. Lozano, V. I. Prisecaru and H. C. Lin., q-bio/0406047.
- F. Bessel, *Untersuchung des Theils der planetarischen Störungen*, Berlin Abhandlungen (1824), article 14.
- Sir Lawrence Bragg, FRS. *The Crystalline State, A General survey.* London: G. Bells and Sons, Ltd., vols. 1 and 2., 1966., 2024 pages.
- Cantor, C. R. and Schimmel, P.R. *Biophysical Chemistry, Parts I and II.*, San Franscisco: W.H. Freeman and Co. 1980. 1,800 pages.
- Eigen, M., and Rigler, R. (1994). Sorting single molecules: Applications to diagnostics and evolutionary biotechnology, *Proc. Natl. Acad. Sci. USA* **91**:5740.
- Raghavachari, R., Editor. 2001. *Near-Infrared Applications in Biotechnology*, Marcel-Dekker, New York, NY.
- Rigler R. and Widengren J. (1990). Ultrasensitive detection of single molecules by fluorescence correlation spectroscopy, *BioScience* (Ed. Klinge & Owman) p.180.
- Single Cancer Cell Detection by Near Infrared Microspectroscopy, Infrared Chemical Imaging and Fluorescence Microspectroscopy.2004. I. C. Baianu, D. Costescu, N. E. Hofmann, S. S. Korban and et al., q-bio/0407006 (July 2004).
- Voet, D. and J.G. Voet. *Biochemistry*, 2nd Edn., New York, Toronto, Singapore: John Wiley & Sons, Inc., 1995, ISBN 0-471-58651-X., 1361 pages.
- Watson, G. N. *A Treatise on the Theory of Bessel Functions.*, (1995) Cambridge University Press. ISBN 0-521-48391-3.
- Watson, James D. and Francis H.C. Crick. A structure for Deoxyribose Nucleic Acid (http://www.nature.com/nature/dna50/watsoncrick.pdf) (PDF). *Nature* 171, 737–738, 25 April 1953.
- Watson, James D. *Molecular Biology of the Gene.* New York and Amsterdam: W.A. Benjamin, Inc. 1965., 494 pages.
- Wentworth, W.E. *Physical Chemistry. A short course.*, Malden (Mass.): Blackwell Science, Inc. 2000.
- Herbert R. Wilson, FRS. *Diffraction of X-rays by proteins, Nucleic Acids and Viruses.*, London: Edward Arnold (Publishers) Ltd. 1966.
- Kurt Wuthrich. *NMR of Proteins and Nucleic Acids.*, New York, Brisbane,Chicester, Toronto, Singapore: J. Wiley & Sons. 1986., 292 pages.
- Robinson, Bruche H.; Seeman, Nadrian C. (August 1987). "The Design of a Biochip: A Self-Assembling Molecular-Scale Memory Device". *Protein Engineering* **1** (4): 295–300. ISSN 0269-2139 (http://worldcat.org/issn/0269-2139). Link (http://peds.oxfordjournals.org/cgi/content/abstract/1/4/295)
- Rothemund, Paul W. K.; Ekani-Nkodo, Axel; Papadakis, Nick; Kumar, Ashish; Fygenson, Deborah Kuchnir & Winfree, Erik (22 December 2004). "Design and Characterization of Programmable DNA Nanotubes". *Journal of the American Chemical Society* **126** (50):

16344–16352. doi: 10.1021/ja044319l (http://dx.doi.org/10.1021/ja044319l). ISSN 0002-7863 (http://worldcat.org/issn/0002-7863).
- Keren, K.; Kinneret Keren, Rotem S. Berman, Evgeny Buchstab, Uri Sivan, Erez Braun (November 2003). "http://www.sciencemag.org/cgi/content/abstract/sci;302/5649/1380|DNA-Templated Carbon Nanotube Field-Effect Transistor". *Science* **302** (6549): 1380–1382. doi: 10.1126/science.1091022 (http://dx.doi.org/10.1126/science.1091022). ISSN 1095-9203 (http://worldcat.org/issn/1095-9203). http://www.sciencemag.org/cgi/content/abstract/sci;302/5649/1380.
- Zheng, Jiwen; Constantinou, Pamela E.; Micheel, Christine; Alivisatos, A. Paul; Kiehl, Richard A. & Seeman Nadrian C. (2006). "2D Nanoparticle Arrays Show the Organizational Power of Robust DNA Motifs". *Nano Letters* **6**: 1502–1504. doi: 10.1021/nl060994c (http://dx.doi.org/10.1021/nl060994c). ISSN 1530-6984 (http://worldcat.org/issn/1530-6984).
- Cohen, Justin D.; Sadowski, John P.; Dervan, Peter B. (2007). "Addressing Single Molecules on DNA Nanostructures". *Angewandte Chemie* **46** (42): 7956–7959. doi: 10.1002/anie.200702767 (http://dx.doi.org/10.1002/anie.200702767). ISSN 0570-0833 (http://worldcat.org/issn/0570-0833).
- Mao, Chengde; Sun, Weiqiong & Seeman, Nadrian C. (16 June 1999). "Designed Two-Dimensional DNA Holliday Junction Arrays Visualized by Atomic Force Microscopy". *Journal of the American Chemical Society* **121** (23): 5437–5443. doi: 10.1021/ja9900398 (http://dx.doi.org/10.1021/ja9900398). ISSN 0002-7863 (http://worldcat.org/issn/0002-7863).
- Constantinou, Pamela E.; Wang, Tong; Kopatsch, Jens; Israel, Lisa B.; Zhang, Xiaoping; Ding, Baoquan; Sherman, William B.; Wang, Xing; Zheng, Jianping; Sha, Ruojie & Seeman, Nadrian C. (2006). "Double cohesion in structural DNA nanotechnology". *Organic and Biomolecular Chemistry* **4**: 3414–3419. doi: 10.1039/b605212f (http://dx.doi.org/10.1039/b605212f).

See also

- DNA
- Molecular graphics
- DNA structure
- DNA Dynamics
- X-ray scattering
- Neutron scattering
- Crystallography
- Crystal lattices
- Paracrystalline lattices/Paracrystals
- 2D-FT NMRI and Spectroscopy
- NMR Spectroscopy
- Microwave spectroscopy
- Two-dimensional IR spectroscopy
- Spectral imaging
- Hyperspectral imaging
- Chemical imaging
- NMR microscopy

- VCD or Vibrational circular dichroism
- FRET and FCS- Fluorescence correlation spectroscopy
- Fluorescence cross-correlation spectroscopy (FCCS)
- Molecular structure
- Molecular geometry
- Molecular topology
- DNA topology
- Sirius visualization software
- Nanostructure
- DNA nanotechnology
- Imaging
- Atomic force microscopy
- X-ray microscopy
- Liquid crystal
- Glasses
- QMC@Home
- Sir Lawrence Bragg, FRS
- Sir John Randall
- James Watson
- Francis Crick
- Maurice Wilkins
- Herbert Wilson, FRS
- Alex Stokes

External links

- DNA the Double Helix Game (http://nobelprize.org/educational_games/medicine/dna_double_helix/) From the official Nobel Prize web site
- MDDNA: Structural Bioinformatics of DNA (http://humphry.chem.wesleyan.edu:8080/MDDNA/)
- Double Helix 1953–2003 (http://www.ncbe.reading.ac.uk/DNA50/) National Centre for Biotechnology Education
- DNA under electron microscope (http://www.fidelitysystems.com/Unlinked_DNA.html)
- Ascalaph DNA (http://www.agilemolecule.com/Ascalaph/Ascalaph_DNA.html) — Commercial software for DNA modeling
- DNAlive: a web interface to compute DNA physical properties (http://mmb.pcb.ub.es/DNAlive). Also allows cross-linking of the results with the UCSC Genome browser and DNA dynamics.
- DiProDB: Dinucleotide Property Database (http://diprodb.fli-leibniz.de). The database is designed to collect and analyse thermodynamic, structural and other dinucleotide properties.
- Further details of mathematical and molecular analysis of DNA structure based on X-ray data (http://planetphysics.org/encyclopedia/BesselFunctionsApplicationsToDiffractionByHelicalStructures.html)
- Bessel functions corresponding to Fourier transforms of atomic or molecular helices. (http://planetphysics.org/?op=getobj&from=objects&name=BesselFunctionsAndTheirApplicationsToDiffractionByHelicalStructures)

- Application of X-ray microscopy in analysis of living hydrated cells (http://www.ncbi.nlm.nih.gov/entrez/query.fcgi?cmd=Retrieve&db=pubmed&dopt=Abstract&list_uids=12379938)
- Characterization in nanotechnology some pdfs (http://nanocharacterization.sitesled.com/)
- overview of STM/AFM/SNOM principles with educative videos (http://www.ntmdt.ru/SPM-Techniques/Principles/)
- SPM Image Gallery - AFM STM SEM MFM NSOM and More (http://www.rhk-tech.com/results/showcase.php)
- How SPM Works (http://www.parkafm.com/New_html/resources/01general.php)
- U.S. National DNA Day (http://www.genome.gov/10506367) — watch videos and participate in real-time discussions with scientists.
- The Secret Life of DNA - DNA Music compositions (http://www.tjmitchell.com/stuart/dna.html)

Molecular graphics

Molecular graphics (**MG**) is the discipline and philosophy of studying molecules and their properties through graphical representation.[1] IUPAC limits the definition to representations on a "graphical display device".[2] Ever since Dalton's atoms and Kekule's benzene, there has been a rich history of hand-drawn atoms and molecules, and these representations have had an important influence on modern molecular graphics. This article concentrates on the use of computers to create molecular graphics. Note, however, that many molecular graphics programs and systems have close coupling between the graphics and editing commands or calculations such as in molecular modelling.

Relation to molecular models

There has been a long tradition of creating molecular models from physical materials. Perhaps the best known is Crick and Watson's model of DNA built from rods and planar sheets, but the most widely used approach is to represent all atoms and bonds explicitly using the "ball and stick" approach. This can demonstrate a wide range of properties, such as shape, relative size, and flexibility. Many chemistry courses expect that students will have access to ball and stick models. One goal of mainstream molecular graphics has been to represent the "ball and stick" model as realistically as possible and to couple this with calculations of molecular properties.

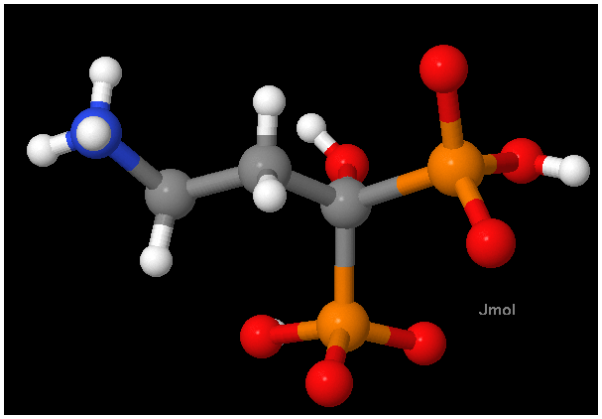

Fig. 1. Key: Hydrogen = white, carbon = grey, nitrogen = blue, oxygen = red, and phosphorus = orange.

Figure 1 shows a small molecule ($NH_3CH_2CH_2C(OH)(PO_3H)(PO_3H)$-), as drawn by the Jmol program. It is important to realise that the colours are purely a convention. Molecules can

never be visible under any light microscope and atoms are not coloured, do not have hard surfaces and do not reflect light. Bonds are not rod-shaped. If physical molecular models had not existed, it is unlikely that molecular graphics would currently use this metaphor.

Comparison of physical models with molecular graphics

Physical models and computer models have partially complementary strengths and weaknesses. Physical models can be used by those without access to a computer and now can be made cheaply out of plastic materials. Their tactile and visual aspects cannot be easily reproduced by computers (although haptic devices have occasionally been built). On a computer screen, the flexibility of molecules is also difficult to appreciate; illustrating the pseudorotation of cyclohexane is a good example of the value of mechanical models.

However, it is difficult to build large physical molecules, and all-atom physical models of even simple proteins could take weeks or months to build. Moreover, physical models are not robust and they decay over time. Molecular graphics is particularly valuable for representing global and local properties of molecules, such as electrostatic potential. Graphics can also be animated to represent molecular processes and chemical reactions, a feat that is not easy to reproduce physically.

History

Initially the rendering was on early CRT screens or through plotters drawing on paper. Molecular structures have always been an attractive choice for developing new computer graphics tools, since the input data are easy to create and the results are usually highly appealing. The first example of MG was a display of a protein molecule (Project MAC, 1966) by Cyrus Levinthal and Robert Langridge. Among the milestones in high-performance MG was the work of Nelson Max in "realistic" rendering of macromolecules using reflecting spheres.

By about 1980 many laboratories both in academia and industry had recognized the power of the computer to analyse and predict the properties of molecules, especially in materials science and the pharmaceutical industry. The discipline was often called "molecular graphics" and in 1982 a group of academics and industrialists in the UK set up the Molecular Graphics Society (MGS). Initially much of the technology concentrated either on high-performance 3D graphics, including interactive rotation or 3D rendering of atoms as spheres (sometimes with radiosity). During the 1980s a number of programs for calculating molecular properties (such as molecular dynamics and quantum mechanics) became available and the term "molecular graphics" often included these. As a result the MGS has now changed its name to the Molecular Graphics and Modelling Society (MGMS).

The requirements of macromolecular crystallography also drove MG because the traditional techniques of physical model-building could not scale. Alwyn Jones' FRODO program (and later "O") were developed to overlay the molecular electron density determined from X-ray crystallography and the hypothetical molecular structure.

Art, science and technology in molecular graphics

Both computer technology and graphic arts have contributed to molecular graphics. The development of structural biology in the 1950s led to a requirement to display molecules with thousands of atoms. The existing computer technology was limited in power, and in any case a naive depiction of all atoms left viewers overwhelmed. Most systems therefore used conventions where information was implicit or stylistic. Two vectors meeting at a point implied an atom or (in macromolecules) a complete residue (10-20 atoms).

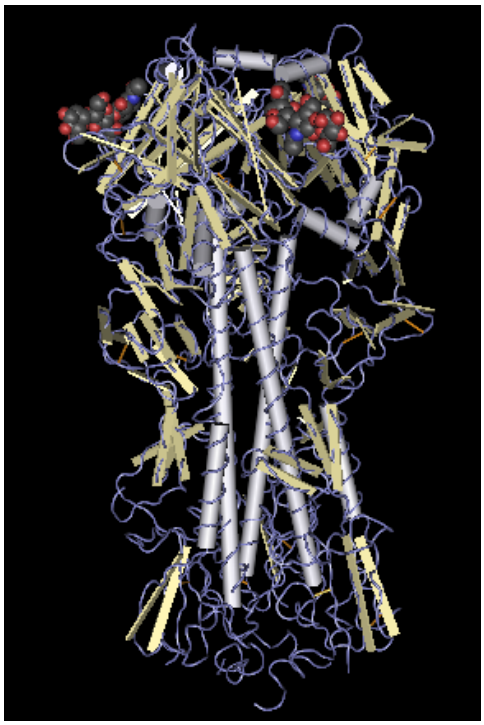

Fig. 2. Image of hemagglutinin with alpha helices depicted as cylinders and the rest of the chain as silver coils. The individual protein atoms (several thousand) have been hidden. All of the non-hydrogen atoms in the two ligands (presumably sialic acid) have been shown near the top of the diagram. Key: Carbon = grey, oxygen = red, nitrogen = blue.

The macromolecular approach was popularized by Dickerson and Geis' presentation of proteins and the graphic work of Jane Richardson through high-quality hand-drawn diagrams such as the "ribbon" representation. In this they strove to capture the intrinsic 'meaning' of the molecule. This search for the "messages in the molecule" has always accompanied the increasing power of computer graphics processing. Typically the depiction would concentrate on specific areas of the molecule (such as the active site) and this might have different colours or more detail in the number of explicit atoms or the type of depiction (e.g., spheres for atoms).

In some cases the limitations of technology have led to serendipitous methods for rendering. Most early graphics devices used vector graphics, which meant that rendering spheres and surfaces was impossible. Michael Connolly's program "MS" calculated points on the surface-accessible surface of a molecule, and the points were rendered as dots with good visibility using the new vector graphics technology, such as the Evans and Sutherland PS300 series. Thin sections ("slabs") through the structural display showed very clearly the complementarity of the surfaces for molecules binding to active sites, and the "Connolly surface" became a universal metaphor.

The relationship between the art and science of molecular graphics is shown in the exhibitions [3] sponsored by the Molecular Graphics Society. Some exhibits are created with molecular graphics programs alone, while others are collages, or involve physical materials. An example from Mike Hann (1994), inspired by Magritte's painting *Ceci n'est pas une pipe*, uses an image of a salmeterol molecule.

"*Ceci n'est pas une molecule*," writes Mike Hann, "serves to remind us that all of the graphics images presented here are not molecules, not even pictures of molecules, but pictures of icons which we believe represent some aspects of the molecule's properties."

Space-filling models

Fig. 4 is a "space-filling" representation of formic acid, where atoms are drawn to suggest the amount of space they occupy. This is necessarily an icon: in the quantum mechanical representation of molecules, there are only (positively charged) nuclei and a "cloud" of negative electrons. The electron cloud defines an approximate size for the molecule, though there can be no single precise definition of size. For many years the size of atoms has been approximated by mechanical models (CPK), where the atoms have been represented by plastic spheres whose radius (van der Waals radius) describes a sphere within which "most" of the electron density can be found. These spheres could be clicked together to show the steric aspects of the molecule rather than the positions of the nuclei. Fig. 4 shows the intricacy required to make sure that all spheres intersect correctly, and also demonstrates a reflective model.

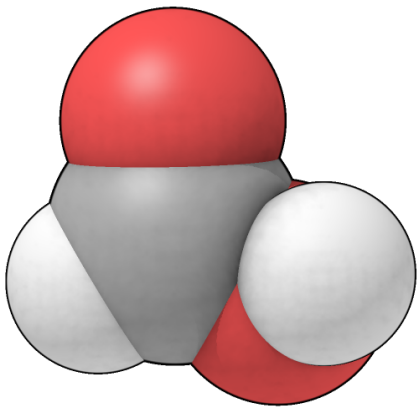

Fig. 4. Space-filling model of formic acid. Key: Hydrogen = white, carbon = black, oxygen = red.

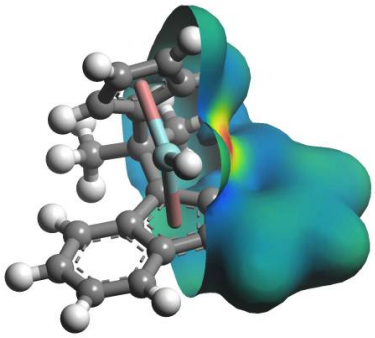

Fig. 5. A molecule (zirconocene) where part (left) is rendered as ball-and-stick and part (right) as an isosurface.

Since the atomic radii (e.g. in Fig. 4) are only slightly less than the distance between bonded atoms, the iconic spheres intersect, and in the CPK models, this was achieved by planar truncations along the bonding directions, the section being circular. When raster graphics became affordable, one of the common approaches was to replicate CPK models *in silico*. It is relatively straightforward to calculate the circles of intersection, but more complex to represent a model with hidden surface removal. A useful side product is that a conventional value for the molecular volume can be calculated.

The use of spheres is often for convenience, being limited both by graphics libraries and the additional effort required to compute complete electronic density or other space-filling quantities. It is now relatively common to see images of isosurfaces that have been coloured to show quantities such as electrostatic potential. The commonest isosurfaces are the Connolly surface, or the volume within which a given proportion of the electron density lies. The isosurface in Fig. 5 appears to show the electrostatic potential, with blue colours being negative and red/yellow (near the metal) positive. (There is no absolute convention of colouring, and red/positive, blue/negative are often confusingly reversed!) Opaque isosurfaces do not allow the atoms to be seen and identified and it is not easy to deduce them. Because of this, isosurfaces are often drawn with a degree of transparency.

Technology

Molecular graphics has always pushed the limits of display technology, and has seen a number of cycles of integration and separation of compute-host and display. Early systems like Project MAC were bespoke and unique, but in the 1970s the MMS-X and similar systems used (relatively) low-cost terminals, such as the Tektronix 4014 series, often over dial-up lines to multi-user hosts. The devices could only display static pictures but, were able to evangelize MG. In the late 1970s, it was possible for departments (such as crystallography) to afford their own hosts (e.g., PDP-11) and to attach a display (such as Evans & Sutherland's MPS) directly to the bus. The display list was kept on the host, and interactivity was good since updates were rapidly reflected in the display—at the cost of reducing most machines to a single-user system.

In the early 1980s, Evans & Sutherland (E&S) decoupled their PS300 display, which contained its own display information transformable through a dataflow architecture. Complex graphical objects could be downloaded over a serial line (e.g. 9600 baud) and then manipulated without impact on the host. The architecture was excellent for high performance display but very inconvenient for domain-specific calculations, such as electron-density fitting and energy calculations. Many crystallographers and modellers spent arduous months trying to fit such activities into this architecture.

The benefits for MG were considerable, but by the later 1980s, UNIX workstations such as Sun-3 with raster graphics (initially at a resolution of 256 by 256) had started to appear. Computer-assisted drug design in particular required raster graphics for the display of computed properties such as atomic charge and electrostatic potential. Although E&S had a high-end range of raster graphics (primarily aimed at the aerospace industry) they failed to respond to the low-end market challenge where single users, rather than engineering departments, bought workstations. As a result the market for MG displays passed to Silicon Graphics, coupled with the development of minisupercomputers (e.g., CONVEX and Alliant) which were affordable for well-supported MG laboratories. Silicon Graphics provided a graphics language, IrisGL, which was easier to use and more productive than the PS300 architecture. Commercial companies (e.g., Biosym, Polygen/MSI) ported their code to Silicon Graphics, and by the early 1990s, this was the "industry standard".

Stereoscopic displays were developed based on liquid crystal polarized spectacles, and while this had been very expensive on the PS300, it now became a commodity item. A common alternative was to add a polarizable screen to the front of the display and to provide viewers with extremely cheap spectacles with orthogonal polarization for separate eyes. With projectors such as Barco, it was possible to project stereoscopic display onto special silvered screens and supply an audience of hundreds with spectacles. In this way molecular graphics became universally known within large sectors of chemical and biochemical science, especially in the pharmaceutical industry. Because the backgrounds of many displays were black by default, it was common for modelling sessions and lectures to be held with almost all lighting turned off.

In the last decade almost all of this technology has become commoditized. IrisGL evolved to OpenGL so that molecular graphics can be run on any machine. In 1992, Roger Sayle released his RasMol program into the public domain. RasMol contained a very high-performance molecular renderer that ran on Unix/X Window, and Sayle later ported this to the Windows and Macintosh platforms. The Richardsons developed kinemages and the Mage software, which was also multi-platform. By specifying the chemical MIME type,

molecular models could be served over the Internet, so that for the first time MG could be distributed at zero cost regardless of platform. In 1995, Birkbeck College's crystallography department used this to run "Principles of Protein Structure", the first multimedia course on the Internet, which reached 100 to 200 scientists.

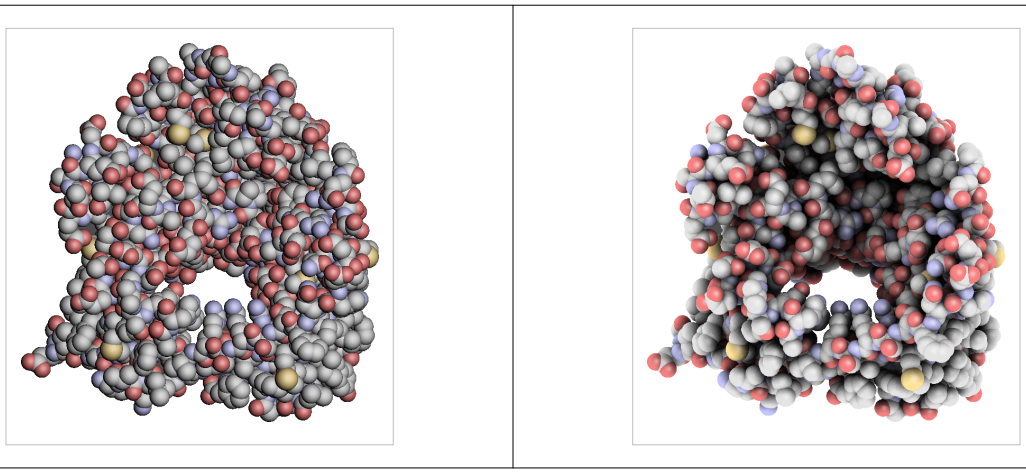

Fig. 6. A molecule of Porin (protein) shown without ambient occlusion (left) and with (right). Advanced rendering effects can improve the comprehension of the 3D shape of a molecule.

MG continues to see innovation that balances technology and art, and currently zero-cost or open source programs such as PyMOL and Jmol have very wide use and acceptance.

Recently the wide spread diffusion of advanced graphics hardware, has improved the rendering capabilities of the visualization tools. The capabilities of current shading languages allow the inclusion of advanced graphic effects (like ambient occlusion, cast shadows and non-photorealistic rendering techniques) in the interactive visualization of molecules. These graphic effects, beside being eye candy, can improve the comprehension of the three dimensional shapes of the molecules. An example of the effects that can be achieved exploiting recent graphics hardware can be seen in the simple open source visualization system QuteMol.

Algorithms

Reference frames

Drawing molecules requires a transformation between molecular coordinates (usually, but not always, in Angstrom units) and the screen. Because many molecules are chiral it is essential that the handedness of the system (almost always right-handed) is preserved. In molecular graphics the origin (0, 0) is usually at the lower left, while in many computer systems the origin is at top left. If the z-coordinate is out of the screen (towards the viewer) the molecule will be referred to right-handed axes, while the screen display will be left-handed.

Molecular transformations normally require:

- scaling of the display (but not the molecule).
- translations of the molecule and objects on the screen.
- rotations about points and lines.

Conformational changes (e.g. rotations about bonds) require rotation of one part of the molecule relative to another. The programmer must decide whether a transformation on the

screen reflects a change of view or a change in the molecule or its reference frame.

Simple

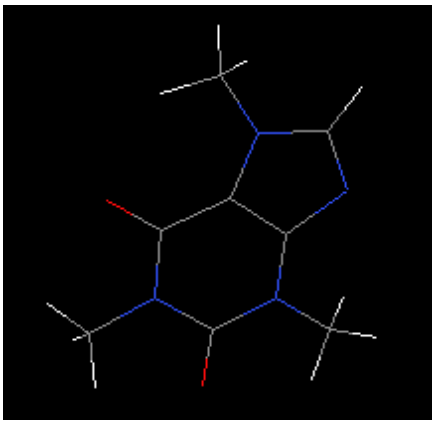

Fig. 7. Stick model of caffeine drawn in Jmol.

In early displays only vectors could be drawn e.g. (Fig. 7) which are easy to draw because no rendering or hidden surface removal is required.

On vector machines the lines would be smooth but on raster devices Bresenham's algorithm is used (note the "jaggies" on some of the bonds, which can be largely removed with antialiasing software.)

Atoms can be drawn as circles, but these should be sorted so that those with the largest z-coordinates (nearest the screen) are drawn last. Although imperfect, this often gives a reasonably attractive display. Other simple tricks which do not include hidden surface algorithms are:

- colouring each end of a bond with the same colour as the atom to which it is attached (Fig. 7).
- drawing less than the whole length of the bond (e.g. 10%-90%) to simulate the bond sticking out of a circle.
- adding a small offset white circle within the circle for an atom to simulate reflection.

Typical pseudocode for creating Fig. 7 (to fit the molecule exactly to the screen):

```
// assume:
// atoms with x, y, z coordinates (Angstrom) and elementSymbol
// bonds with pointers/references to atoms at ends
// table of colours for elementTypes
// find limits of molecule in molecule coordinates as xMin, yMin, xMax,
 yMax
scale = min(xScreenMax/(xMax-xMin), yScreenMax/(yMax-yMin))
xOffset = -xMin * scale; yOffset = -yMin * scale
for (bond in $bonds) {
  atom0 = bond.getAtom(0)
  atom1 = bond.getAtom(1)
  x0 = xOffset+atom0.getX()*scale; y0 = yOffset+atom0.getY()*scale //
(1)
  x1 = xOffset+atom1.getX()*scale; y1 = yOffset+atom1.getY()*scale //
(2)
  x1 = atom1.getX();  y1 = atom1.getY()
  xMid = (x0 + x1) /2;  yMid = (y0 + y1) /2;
  colour0 = ColourTable.getColour(atom0.getSymbol())
  drawLine (colour0, x0, y0, xMid, yMid)
  colour1 = ColourTable.getColour(atom1.getSymbol())
  drawLine (colour1, x1, y1, xMid, yMid)
}
```

Note that this assumes the origin is in the bottom left corner of the screen, with Y up the screen. Many graphics systems have the origin at the top left, with Y down the screen. In this case the lines (1) and (2) should have the y coordinate generation as:

```
y0 = yScreenMax -(yOffset+atom0.getY()*scale) // (1)
y1 = yScreenMax -(yOffset+atom1.getY()*scale) // (2)
```

Changes of this sort change the handedness of the axes so it is easy to reverse the chirality of the displayed molecule unless care is taken.

Advanced

For greater realism and better comprehension of the 3D structure of a molecule many computer graphics algorithms can be used. For many years molecular graphics has stressed the capabilities of graphics hardware and has required hardware-specific approaches. With the increasing power of machines on the desktop, portability is more important and programs such as Jmol have advanced algorithms that do not rely on hardware. On the other hand recent graphics hardware is able to interactively render very complex molecule shapes with a quality that would not be possible with standard software techniques.

Chronology

This table provides an incomplete chronology of molecular graphics advances.

Developer(s)	Approximate date	Technology	Comments
Crystallographers	< 1960	Hand-drawn	Crystal structures, with hidden atom and bond removal. Often clinographic projections.
Cyrus Levinthal, Bob Langridge	1960s	CRT	First protein display on screen (Project MAC).
Johnson, Motherwell	ca 1970	Pen plotter	ORTEP, PLUTO. Very widely deployed for publishing crystal structures.
Langridge, White, Marshall	Late 1970s	Departmental systems (PDP-11, Tektronix displays or DEC-VT11, e.g. MMS-X)	Mixture of commodity computing with early displays.
T. Alwyn Jones	1978	FRODO	Crystallographic structure solution.
Davies, Hubbard	Mid-1980s	CHEM-X, HYDRA	Laboratory systems with multicolor, raster and vector devices (Sigmex, PS300).
Biosym, Tripos, Polygen	Mid-1980s	PS300 and lower cost dumb terminals (VT200, SIGMEX)	Commercial integrated modelling and display packages.
Silicon Graphics, Sun	Late 1980s	IRIS GL (UNIX) workstations	Commodity-priced single-user workstations with stereoscopic display.
EMBL - WHAT IF [4]	1989, 2000	Machine independent	Nearly free, multifunctional, still fully supported, many free servers [5] based on it

Sayle, Richardson	1992, 1993	RasMol, Kinemage	Platform-independent MG.
MDL (van Vliet, Maffett, Adler, Holt)	1995-1998	Chime	proprietary C++ ; free browser plugin for Mac (OS9) and PCs
ChemAxon	1998-	MarvinSketch [6] & MarvinView [7]. MarvinSpace [8] (2005)	proprietary Java applet or stand-alone application.
Community efforts	2000-	Jmol, PyMol, Protein Workshop (www.pdb.org)	Open-source Java applet or stand-alone application.
San Diego Supercomputer Center	2006-	Sirius	Free for academic/non-profit institutions
NOCH	2002-	NOC [9]	Powerful and open source code molecular structure explorer
Weizmann Institute of Science - Community efforts	2008-	Proteopedia	Collaborative, 3D wiki encyclopedia of proteins & other molecules

References

[1] Dickerson, R.E.; Geis, I. (1969). *The structure and action of proteins*. Menlo Park, CA: W.A. Benjamin.
[2] International Union of Pure and Applied Chemistry (1997). " molecular graphics (http://goldbook.iupac.org/MT06970.html)". *Compendium of Chemical Terminology* Internet edition.
[3] http://www.scripps.edu/mb/goodsell/mgs_art/
[4] http://swift.cmbi.ru.nl/whatif/
[5] http://swift.cmbi.ru.nl/
[6] http://www.chemaxon.com/product/msketch.html
[7] http://www.chemaxon.com/product/mview.html
[8] http://www.chemaxon.com/product/mspace.html
[9] http://noch.sourceforge.net

See also

- Molecular Design software
- Molecular model
- Molecular modelling
- Molecular geometry
- Software for molecular mechanics modeling

External links

- The PyMOL Molecular Graphics System (http://pymol.sf.net) -- open source
  - PyMOLWiki (http://pymolwiki.org) -- community supported wiki for PyMOL
- History of Visualization of Biological Macromolecules (http://www.umass.edu/microbio/rasmol/history.htm) by Eric Martz and Eric Francoeur.
- Brief History of Molecular Mechanics/Graphics (http://stanley.chem.lsu.edu/webpub/7770-Lecture-1-intro.pdf) in LSU CHEM7770 lecture notes.
- Historical slides (http://luminary.stanford.edu/langridge/slides.htm) from Robert (Bob) Langridge. These show the influence of Crick and Watson on molecular graphics (including Levinthal's) and the development of early display technology, finishing with displays which were common in the mid-1980s on machines such as Evans and

Sutherland's PS300 series.

- Interview with Langridge. (http://luminary.stanford.edu/langridge/langridge.html) The display looking down the axis of B-DNA has been likened to a rose window.
- Nelson Max's home page (http://accad.osu.edu/~waynec/history/tree/max.html) with links to 1982 classics.
- Jmol home page (http://jmol.sourceforge.net/) contains an applet with an automatic display of many features of molecular graphics including metaphors, scripting, annotation and animation.
- Richardson Lab (http://kinemage.biochem.duke.edu/) includes Kinemage and molecular graphics images.
- History of RasMol. (http://www.openrasmol.org/history.html)
- Molecule of the Month (http://www.rcsb.org/pdb/static.do?p=education_discussion/molecule_of_the_month/index.html) at RCSB/PDB.
- xeo (http://sourceforge.net/projects/xeo) xeo is a free (GPL) open project management for nanostructures using Java
- Exhibitions of Molecular Graphics Art (http://www.scripps.edu/mb/goodsell/mgs_art/), 1994, 1998.
- NOCH home page (http://noch.sourceforge.net) A powerful, efficient and open source molecular graphics tool.
- eMovie (http://www.weizmann.ac.il/ISPC/eMovie.html): a tool for creation of molecular animations with PyMOL.
- Proteopedia (http://www.proteopedia.org): The collaborative, 3D encyclopedia of proteins and other molecules.
- Ascalaph Graphics (http://www.agilemolecule.com/Ascalaph/Ascalaph_Graphics.html): a molecular viewer with some geometry editing capabilities.
- Molecular Graphics and Modelling Society. (http://www.mgms.org/)
- *Journal of Molecular Graphics and Modelling* (http://www.sciencedirect.com/science?_ob=JournalURL&_cdi=5260&_auth=y&_acct=C000053194&_version=1&_urlVersion=0&_userid=1495569&md5=1e86bcce088e98890cea52f6eda84b64) (formally *Journal of Molecular Graphics*). This journal is not open access.

DNA structure

DNA structure shows a variety of forms, both double-stranded and single-stranded. The mechanical properties of DNA, which are directly related to its structure, are a significant problem for cells. Every process which binds or reads DNA is able to use or modify the mechanical properties of DNA for purposes of recognition, packaging and modification. The extreme length (a chromosome may contain a 10 cm long DNA strand), relative rigidity and helical structure of DNA has led to the evolution of histones and of enzymes such as topoisomerases and helicases to manage a cell's DNA. The properties of DNA are closely related to its molecular structure and sequence, particularly the weakness of the hydrogen bonds and electronic interactions that hold strands of DNA together compared to the strength of the bonds within each strand.

Experimental techniques which can directly measure the mechanical properties of DNA are relatively new, and high-resolution visualization in solution is often difficult. Nevertheless, scientists have uncovered large amount of data on the mechanical properties of this polymer, and the implications of DNA's mechanical properties on cellular processes is a topic of active current research.

It is important to note the DNA found in many cells can be macroscopic in length - a few centimetres long for each human chromosome. Consequently, cells must compact or "package" DNA to carry it within them. In eukaryotes this is carried by spool-like proteins known as histones, around which DNA winds. It is the further compaction of this DNA-protein complex which produces the well known mitotic eukaryotic chromosomes.

Structure determination

DNA structures can be determined using either nuclear magnetic resonance spectroscopy or X-ray crystallography. The first published reports of A-DNA X-ray diffraction patterns--and also B-DNA—employed analyses based on Patterson transforms that provided only a limited amount of structural information for oriented fibers of DNA isolated from calf thymus.[1] [2] An alternate analysis was then proposed by Wilkins et al. in 1953 for B-DNA X-ray diffraction/scattering patterns of hydrated, bacterial oriented DNA fibers and trout sperm heads in terms of squares of Bessel functions.[3] Although the `B-DNA form' is most common under the conditions found in cells,[4] it is not a well-defined conformation but a family or fuzzy set of DNA-conformations that occur at the high hydration levels present in a wide variety of living cells.[5] Their corresponding X-ray diffraction & scattering patterns are characteristic of molecular paracrystals with a significant degree of disorder (>20%)[6] [7] , and concomitantly the structure is not tractable using only the standard analysis.

On the other hand, the standard analysis, involving only Fourier transforms of Bessel functions[8] and DNA molecular models, is still routinely employed for the analysis of A-DNA and Z-DNA X-ray diffraction patterns.[9]

Base pair geometry

The geometry of a base, or base pair step can be characterized by 6 coordinates: Shift, Slide, Rise, Tilt, Roll, and Twist. These values precisely define the location and orientation in space of every base or base pair in a DNA molecule relative to its predecessor along the axis of the helix. Together, they characterize the helical structure of the molecule. In regions of DNA where the "normal" structure is disrupted the change in these values can be used to describe such disruption.

For each base pair, considered relative to its predecessor[10] [11] [12] :

Shear

Stretch

Stagger

Buckle

Propeller twist

Rotation of one base with respect to the other in the same base pair.

Opening

Shift

displacement along an axis in the base-pair plane perpendicular to the first, directed from the minor to the major groove.

Slide

displacement along an axis in the plane of the base pair directed from one strand to the other.

Rise

displacement along the helix axis.

Tilt

rotation around this axis.

Roll

rotation around this axis.

Twist

rotation around the helix axis.

x-displacement

y-displacement

inclination

tip

pitch

the number of base pairs per complete turn of the helix

Rise and twist determine the handedness and pitch of the helix. The other coordinates, by contrast, can be zero. Slide and shift are typically small in B-DNA, but are substantial in A- and Z-DNA. Roll and tilt make successive base pairs less parallel, and are typically small. A diagram [13] of these coordinates can be found in 3DNA [14] website.

Note that "tilt" has often been used differently in the scientific literature, referring to the deviation of the first, inter-strand base-pair axis from perpendicularity to the helix axis. This

corresponds to slide between a succession of base pairs, and in helix-based coordinates is properly termed "inclination".

DNA helix geometries

Three DNA conformations are believed to be found in nature, A-DNA, B-DNA, and Z-DNA. The "B" form described by James D. Watson and Francis Crick is believed to predominate in cells[15] . It is 23.7 Å wide and extends 34 Å per 10 bp of sequence. The double helix makes one complete turn about its axis every 10.4-10.5 base pairs in solution. This frequency of twist (known as the helical *pitch*) depends largely on stacking forces that each base exerts on its neighbours in the chain.

Other conformations are possible; A-DNA, B-DNA, C-DNA, D-DNA[16] , E-DNA[17] , L-DNA(enantiomeric form of D-DNA)[16] , P-DNA[18] , S-DNA, Z-DNA, etc. have been described so far.[19] In fact, only the letters F, Q, U, V, and Y are now available to describe any new DNA structure that may appear in the future.[20] [21] However, most of these forms have been created synthetically and have not been observed in naturally occurring biological systems. Also note the triple-stranded DNA possibility.

A- and Z-DNA

A-DNA and Z-DNA differ significantly in their geometry and dimensions to B-DNA, although still form helical structures. The A form appears likely to occur only in dehydrated samples of DNA, such as those used in crystallographic experiments, and possibly in hybrid pairings of DNA and RNA strands. Segments of DNA that cells have methylated for regulatory purposes may adopt the Z geometry, in which the strands turn about the helical axis the opposite way to A-DNA and B-DNA. There is also evidence of protein-DNA complexes forming Z-DNA structures.

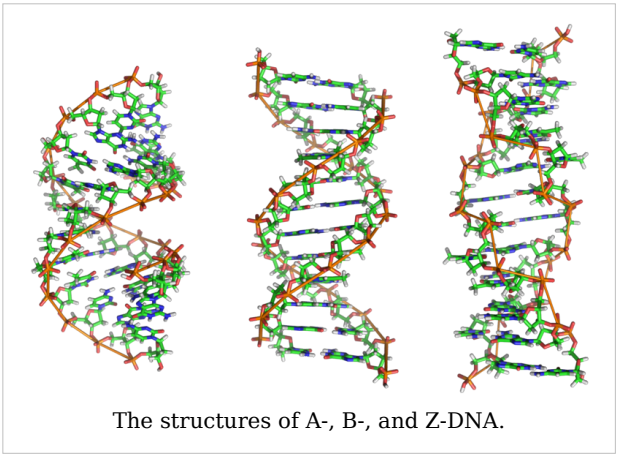

The structures of A-, B-, and Z-DNA.

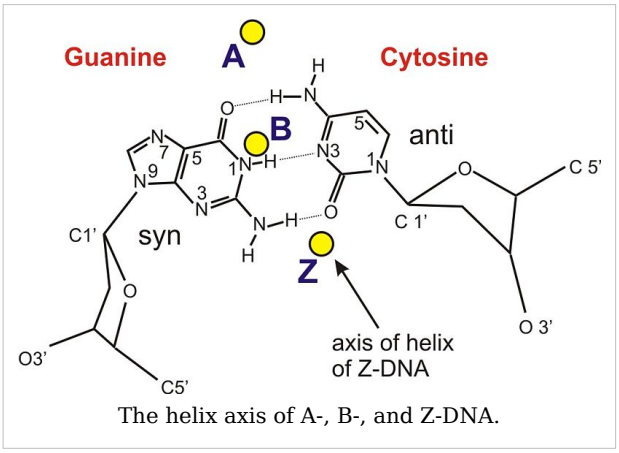

The helix axis of A-, B-, and Z-DNA.

Geometry attribute	A-DNA	B-DNA	Z-DNA
Helix sense	right-handed	right-handed	left-handed
Repeating unit	1 bp	1 bp	2 bp
Rotation/bp	33.6°	35.9°	60°/2bp
Mean bp/turn	10.7	10.0	12
Inclination of bp to axis	+19°	-1.2°	-9°
Rise/bp along axis	2.3 Å	3.32 Å	3.8 Å

Pitch/turn of helix	24.6 Å	33.2 Å	45.6 Å
Mean propeller twist	+18°	+16°	0°
Glycosyl angle	anti	anti	**C**: anti, **G**: syn
Sugar pucker	C3'-endo	C2'-endo	**C**: C2'-endo, **G**: C2'-exo
Diameter	25.5 Å	23.7 Å	18.4 Å

Supercoiled DNA

The B form of the DNA helix twists 360° per 10.4-10.5 bp in the absence of torsional strain. But many molecular biological processes can induce torsional strain. A DNA segment with excess or insufficient helical twisting is referred to, respectively, as positively or negatively "supercoiled". DNA *in vivo* is typically negatively supercoiled, which facilitates the unwinding (melting) of the double-helix required for RNA transcription.

Non-helical forms

Other non-double helical forms of DNA have been described, for example side-by-side (SBS) and triple helical configurations. Single stranded DNA may exist *in statu nascendi* or as thermally induced despiralized DNA.

DNA bending

DNA is a relatively rigid polymer, typically modelled as a worm-like chain. It has three significant degrees of freedom; bending, twisting and compression, each of which cause particular limitations on what is possible with DNA within a cell. Twisting/torsional stiffness is important for the circularisation of DNA and the orientation of DNA bound proteins relative to each other and bending/axial stiffness is important for DNA wrapping and circularisation and protein interactions. Compression/extension is relatively unimportant in the absence of high tension.

Persistence length/Axial stiffness

Example sequences and their persistence lengths (B DNA)

Sequence	Persistence Length /base pairs
Random	154±10
$(\mathbf{CA})_{\text{repeat}}$	133±10
$(\mathbf{CAG})_{\text{repeat}}$	124±10
$(\mathbf{TATA})_{\text{repeat}}$	137±10

DNA in solution does not take a rigid structure but is continually changing conformation due to thermal vibration and collisions with water molecules, which makes classical measures of rigidity impossible. Hence, the bending stiffness of DNA is measured by the persistence length, defined as:

> "The length of DNA over which the time-averaged orientation of the polymer becomes uncorrelated by a factor of *e*."

This value may be directly measured using an atomic force microscope to directly image DNA molecules of various lengths. In aqueous solution the average persistence length is 46-50 nm or 140-150 base pairs (the diameter of DNA is 2 nm), although can vary significantly. This makes DNA a moderately stiff molecule.

The persistence length of a section of DNA is somewhat dependent on its sequence, and this can cause significant variation. The variation is largely due to base stacking energies and the residues which extend into the minor and major grooves.

Models for DNA bending

Stacking stability of base steps (B DNA)

Step	Stacking ΔG /kcal mol^{-1}
T A	-0.19
T G or **C A**	-0.55
C G	-0.91
A G or **C T**	-1.06
A A or **T T**	-1.11
A T	-1.34
G A or **T C**	-1.43
C C or **G G**	-1.44
A C or **G T**	-1.81
G C	-2.17

The entropic flexibility of DNA is remarkably consistent with standard polymer physics models such as the *Kratky-Porod* worm-like chain model. Consistent with the worm-like chain model is the observation that bending DNA is also described by Hooke's law at very small (sub-piconewton) forces. However for DNA segments less than the persistence length, the bending force is approximately constant and behaviour deviates from the worm-like chain predictions.

This effect results in unusual ease in circularising small DNA molecules and a higher probability of finding highly bent sections of DNA.

Bending preference

DNA molecules often have a preferred direction to bend, ie. anisotropic bending. This is, again, due to the properties of the bases which make up the DNA sequence - a random sequence will have no preferred bend direction, i.e. isotropic bending.

Preferred DNA bend direction is determined by the stability of stacking each base on top of the next. If unstable base stacking steps are always found on one side of the DNA helix then the DNA will preferentially bend away from that direction. As bend angle increases then steric hindrances and ability to roll the residues relative to each other also play a role, especially in the minor groove. **A** and **T** residues will be preferentially be found in the minor

grooves on the inside of bends. This effect is particularly seen in DNA-protein binding where tight DNA bending is induced, such as in nucleosome particles. See base step distortions above.

DNA molecules with exceptional bending preference can become intrinsically bent. This was first observed in trypanosomatid kinetoplast DNA. Typical sequences which cause this contain stretches of 4-6 **T** and **A** residues separated by **G** and **C** rich sections which keep the A and T residues in phase with the minor groove on one side of the molecule. For example:

```
 |                 |                   |                   |
                  |                 |
G A T T C C C A A A A A T G T C A A A A A A T A G G C A A A A A A T G C
 C A A A A A A T C C C A A A C
```

The intrinsically bent structure is induced by the 'propeller twist' of base pairs relative to each other allowing unusual bifurcated Hydrogen-bonds between base steps. At higher temperatures this structure, and so the intrinsic bend, is lost.

All DNA which bends anisotropically has, on average, a longer persistence length and greater axial stiffness. This increased rigidity is required to prevent random bending which would make the molecule act isotropically.

DNA circularisation

DNA circularisation depends on both the axial (bending) stiffness and torsional (rotational) stiffness of the molecule. For a DNA molecule to successfully circularise it must be long enough to easily bend into the full circle and must have the correct number of bases so the ends are in the correct rotation to allow bonding to occur. The optimum length for circularisation of DNA is around 400 base pairs (136 nm), with an integral number of turns of the DNA helix, i.e. multiples of 10.4 base pairs. Having a non integral number of turns presents a significant energy barrier for circularisation, for example a 10.4 x 30 = 312 base pair molecule will circularise hundreds of times faster than 10.4 x 30.5 ≈ 317 base pair molecule.

DNA stretching

Longer stretches of DNA are entropically elastic under tension. When DNA is in solution, it undergoes continuous structural variations due to the energy available in the solvent. This is due to the thermal vibration of the molecule combined with continual collisions with water molecules. For entropic reasons, more compact relaxed states are thermally accessible than stretched out states, and so DNA molecules are almost universally found in a tangled relaxed layouts. For this reason, a single molecule of DNA will stretch under a force, straightening it out. Using optical tweezers, the entropic stretching behavior of DNA has been studied and analyzed from a polymer physics perspective, and it has been found that DNA behaves largely like the *Kratky-Porod* worm-like chain model under physiologically accessible energy scales.

Under sufficient tension and positive torque, DNA is thought to undergo a phase transition with the bases splaying outwards and the phosphates moving to the middle. This proposed structure for overstretched DNA has been called "P-form DNA," in honor of Linus Pauling who originally presented it as a possible structure of DNA[18]

The mechanical properties DNA under compression have not been characterized due to experimental difficulties in preventing the polymer from bending under the compressive force.

DNA melting

Melting stability of base steps (B DNA)

Step	Melting ΔG /Kcal mol^{-1}
T A	-0.12
T G or **C A**	-0.78
C G	-1.44
A G or **C T**	-1.29
A A or **T T**	-1.04
A T	-1.27
G A or **T C**	-1.66
C C or **G G**	-1.97
A C or **G T**	-2.04
G C	-2.70

DNA melting is the process by which the interactions between the strands of the double helix are broken, separating the two strands of DNA. These bonds are weak, easily separated by gentle heating, enzymes, or physical force. DNA melting preferentially occurs at certain points in the DNA.[22] **T** and **A** rich sequences are more easily melted than **C** and **G** rich regions. Particular base steps are also susceptible to DNA melting, particularly **T A** and **T G** base steps.[23] These mechanical features are reflected by the use of sequences such as **TATAA** at the start of many genes to assist RNA polymerase in melting the DNA for transcription.

Strand separation by gentle heating, as used in PCR, is simple providing the molecules have fewer than about 10,000 base pairs (10 kilobase pairs, or 10 kbp). The intertwining of the DNA strands makes long segments difficult to separate. The cell avoids this problem by allowing its DNA-melting enzymes (helicases) to work concurrently with topoisomerases, which can chemically cleave the phosphate backbone of one of the strands so that it can swivel around the other. Helicases unwind the strands to facilitate the advance of sequence-reading enzymes such as DNA polymerase.

DNA topology

Within the cell most DNA is topologically restricted. DNA is typically found in closed loops (such as plasmids in prokaryotes) which are topologically closed, or as very long molecules whose diffusion coefficients produce effectively topologically closed domains. Linear sections of DNA are also commonly bound to proteins or physical structures (such as membranes) to form closed topological loops.

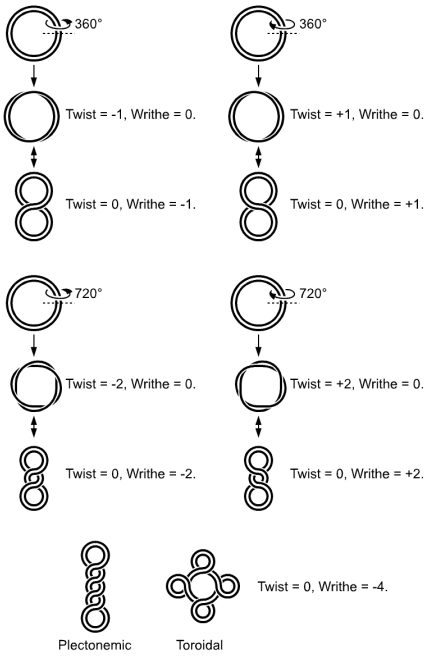

Supercoiled structure of circular DNA molecules with low writhe. Note that the helical nature of the DNA duplex is omitted for clarity.

Francis Crick was one of the first to propose the importance of linking numbers when considering DNA supercoils. In a paper published in 1976, Crick outlined the problem as follows:

> In considering supercoils formed by closed double-stranded molecules of DNA certain mathematical concepts, such as the linking number and the twist, are needed. The meaning of these for a closed ribbon is explained and also that of the writhing number of a closed curve. Some simple examples are given, some of which may be relevant to the structure of chromatin.[24]

Analysis of DNA topology uses three values:

L = linking number - the number of times one DNA strand wraps around the other. It is an integer for a closed loop and constant for a closed topological domain.

T = twist - total number of turns in the double stranded DNA helix. This will normally try to be equal to the number turns a DNA molecule will make while free in solution, ie. number of bases/10.4.

W = writhe - number of turns of the double stranded DNA helix around the superhelical axis

$$L = T + W \text{ and } \Delta L = \Delta T + \Delta W$$

Any change of T in a closed topological domain must be balanced by a change in W, and vice versa. This results in higher order structure of DNA. A circular DNA molecule with a writhe of 0 will be circular. If the twist of this molecule is subsequently increased or decreased by supercoiling then the writhe will be appropriately altered, making the molecule undergo plectonemic or toroidal superhelical coiling.

When the ends of a piece of double stranded helical DNA are joined so that it forms a circle the strands are topologically knotted. This means the single strands cannot be separated any process that does not involve breaking a strand (such as heating). The task of un-knotting topologically linked strands of DNA falls to enzymes known as topoisomerases. These enzymes are dedicated to un-knotting circular DNA by cleaving one or both strands so that another double or single stranded segment can pass through. This un-knotting is required for the replication of circular DNA and various types of recombination in linear DNA which have similar topological constraints.

The linking number paradox

For many years, the origin of residual supercoiling in eukaryotic genomes remained unclear. This topological puzzle was referred to by some as the "linking number paradox".[25] However, when experimentally determined structures of the nucleosome displayed an overtwisted left-handed wrap of DNA around the histone octamer[26] [27] , this "paradox" was solved.

See also

- DNA nanotechnology
- Molecular models of DNA

References

[1] Franklin, R.E. and Gosling, R.G. received 6 March 1953. *Acta Cryst.* (1953). **6**, 673: The Structure of Sodium Thymonucleate Fibres I. The Influence of Water Content.; also *Acta Cryst.* **6**, 678: The Structure of Sodium Thymonucleate Fibres II. The Cylindrically Symmetrical Patterson Function.

[2] Franklin, Rosalind (1953). "http://www.nature.com/nature/dna50/franklingosling.pdf|Molecular Configuration in Sodium Thymonucleate. Franklin R. and Gosling R.G" (PDF). *Nature* **171**: 740–741. doi: 10.1038/171740a0 (http://dx.doi.org/10.1038/171740a0). PMID 13054694. http://www.nature.com/nature/dna50/franklingosling.pdf.

[3] Wilkins M.H.F., A.R. Stokes A.R. & Wilson, H.R. (1953). "http://www.nature.com/nature/dna50/wilkins.pdf|Molecular Structure of Deoxypentose Nucleic Acids" (PDF). *Nature* **171**: 738–740. doi: 10.1038/171738a0 (http://dx.doi.org/10.1038/171738a0). PMID 13054693. http://www.nature.com/nature/dna50/wilkins.pdf.

[4] Leslie AG, Arnott S, Chandrasekaran R, Ratliff RL (1980). "Polymorphism of DNA double helices". *J. Mol. Biol.* **143** (1): 49–72. doi: 10.1016/0022-2836(80)90124-2 (http://dx.doi.org/10.1016/0022-2836(80)90124-2). PMID 7441761.

[5] Baianu, I.C. (1980). "Structural Order and Partial Disorder in Biological systems". *Bull. Math. Biol.* **42** (4): 464–468. doi: 10.1016/0022-2836(80)90124-2 (http://dx.doi.org/10.1016/0022-2836(80)90124-2).

[6] Hosemann R., Bagchi R.N., *Direct analysis of diffraction by matter*, North-Holland Publs., Amsterdam – New York, 1962

[7] Baianu I.C., X-ray scattering by partially disordered membrane systems, *Acta Cryst. A*, **34** (1978), 751–753.

[8] Bessel functions and diffraction by helical structures (http://planetphysics.org/encyclopedia/BesselFunctionsAndTheirApplicationsToDiffractionByHelicalStructures.html)

[9] X-Ray Diffraction Patterns of Double-Helical Deoxyribonucleic Acid (DNA) Crystals (http://planetphysics.org/encyclopedia/BesselFunctionsApplicationsToDiffractionByHelicalStructures.html)

[10] Dickerson RE (1989). "Definitions and nomenclature of nucleic acid structure components". *Nucleic Acids Res* **17** (5): 1797–1803. doi: 10.1093/nar/17.5.1797 (http://dx.doi.org/10.1093/nar/17.5.1797). PMID 2928107.

[11] Lu XJ, Olson WK (1999). "Resolving the discrepancies among nucleic acid conformational analyses". *J Mol Biol* **285** (4): 1563–1575. doi: 10.1006/jmbi.1998.2390 (http://dx.doi.org/10.1006/jmbi.1998.2390). PMID 9917397.

[12] Olson WK, Bansal M, Burley SK, Dickerson RE, Gerstein M, Harvey SC, Heinemann U, Lu XJ, Neidle S, Shakked Z, Sklenar H, Suzuki M, Tung CS, Westhof E, Wolberger C, Berman HM (2001). "A standard reference frame for the description of nucleic acid base-pair geometry". *J Mol Biol* **313** (1): 229–237. doi: 10.1006/jmbi.2001.4987 (http://dx.doi.org/10.1006/jmbi.2001.4987). PMID 11601858.

[13] http://rutchem.rutgers.edu/~xiangjun/3DNA/images/bp_step_hel.gif

[14] http://rutchem.rutgers.edu/~xiangjun/3DNA/examples.html

[15] Richmond, et al. (2003). "The structure of DNA in the nucleosome core". *Nature* **423**: 145–150. doi: 10.1038/nature01595 (http://dx.doi.org/10.1038/nature01595). PMID 12736678.

[16] Hayashi G, Hagihara M, Nakatani K (2005). "Application of L-DNA as a molecular tag". *Nucleic Acids Symp Ser (Oxf)* **49**: 261-262. PMID 17150733.

[17] Vargason JM, Eichman BF, Ho PS (2000). "The extended and eccentric E-DNA structure induced by cytosine methylation or bromination". *Nature Structural Biology* **7**: 758–761. doi: 10.1038/78985 (http://dx.doi.org/10.1038/78985).

[18] Allemand, et al. (1998). "Stretched and overwound DNA forms a Pauling-like structure with exposed bases". *PNAS* **24**: 14152–14157. doi: 10.1073/pnas.95.24.14152 (http://dx.doi.org/10.1073/pnas.95.24.14152). PMID 9826669.
[19] List of 55 fiber structures (http://rutchem.rutgers.edu/~xiangjun/3DNA/misc/fiber_model.txt)
[20] Bansal M (2003). "DNA structure: Revisiting the Watson-Crick double helix". *Current Science* **85** (11): 1556-1563.
[21] Ghosh A, Bansal M (2003). "A glossary of DNA structures from A to Z". *Acta Cryst* **D59**: 620-626. doi: 10.1107/S0907444903003251 (http://dx.doi.org/10.1107/S0907444903003251).
[22] Breslauer KJ, Frank R, Blöcker H, Marky LA (1986). "Predicting DNA duplex stability from the base sequence". *PNAS* **83** (11): 3746-3750. PMID 3459152.
[23] Richard Owczarzy (2008-08-28). http://www.owczarzy.net/tm.htm|"DNA melting temperature - How to calculate it?". *High-throughput DNA biophysics*. owczarzy.net. http://www.owczarzy.net/tm.htm. Retrieved on 2008-10-02.
[24] Crick FH (1976). "Linking numbers and nucleosomes". *Proc Natl Acad Sci USA* **73** (8): 2639–43. doi: 10.1073/pnas.73.8.2639 (http://dx.doi.org/10.1073/pnas.73.8.2639). PMID 1066673.
[25] Prunell A (1998). "A topological approach to nucleosome structure and dynamics: the linking number paradox and other issues". *Biophys J* **74** (5): 2531–2544. PMID 9591679.
[26] Luger K, Mader AW, Richmond RK, Sargent DF, Richmond TJ (1997). "Crystal structure of the nucleosome core particle at 2.8 A resolution". *Nature* **389** (6648): 251-260. doi: 10.1038/38444 (http://dx.doi.org/10.1038/38444). PMID 9305837.
[27] Davey CA, Sargent DF, Luger K, Maeder AW, Richmond TJ (2002). "Solvent mediated interactions in the structure of the nucleosome core particle at 1.9 Å resolution". *Journal of Molecular Biology* **319** (5): 1097-1113. doi: 10.1016/S0022-2836(02)00386-8 (http://dx.doi.org/10.1016/S0022-2836(02)00386-8). PMID 12079350.

External links

- MDDNA: Structural Bioinformatics of DNA (http://humphry.chem.wesleyan.edu:8080/MDDNA/)
- Ascalaph DNA (http://www.agilemolecule.com/Ascalaph/Ascalaph_DNA.html) — Commercial software for DNA modeling
- DNAlive: a web interface to compute DNA physical properties (http://mmb.pcb.ub.es/DNAlive). Also allows cross-linking of the results with the UCSC Genome browser and DNA dynamics.
- DiProDB: Dinucleotide Property Database (http://diprodb.fli-leibniz.de). The database is designed to collect and analyse thermodynamic, structural and other dinucleotide properties.

Neutron scattering

Neutron scattering encompasses all scientific techniques whereby the deflection of neutron radiation is used as a scientific probe. Neutrons readily interact with atomic nuclei and magnetic fields from unpaired electrons, making a useful probe of both structure and magnetic order. Neutron Scattering falls into two basic categories - elastic and inelastic. Elastic scattering is when a neutron interacts with a nucleus or electronic magnetic field but does not leave it in an excited state, meaning the emitted neutron has the same energy as the injected neutron. Scattering processes that involve an energetic excitation or relaxation by the neutron are inelastic: the injected neutron's energy is used or increased to create an excitation or by absorbing the excess energy from a relaxation, and consequently the emitted neutron's energy is reduced or increased respectively.

For several good reasons, moderated neutrons provide an ideal tool for the study of almost all forms of condensed matter. Firstly, they are readily produced at a nuclear research reactor or a spallation source. Normally in such processes neutrons are however produced with much higher energies than are needed. Therefore moderators are generally used which slow the neutrons down and therefore produce wavelengths that are comparable to the atomic spacing in solids and liquids, and kinetic energies that are comparable to those of dynamic processes in materials. Moderators can be made from Aluminium and filled with liquid hydrogen (for very long wavelength neutrons) or liquid methane (for shorter wavelength neutrons). Fluxes of 10^7/s - 10^8/s are not atypical in most neutron sources from any given moderator.

The neutrons cause pronounced interference and energy transfer effects in scattering experiments. Unlike an x-ray photon with a similar wavelength, which interacts with the electron cloud surrounding the nucleus, neutrons interact with the nucleus itself. Because the neutron is an electrically neutral particle, it is deeply penetrating, and is therefore more able to probe the bulk material. Consequently, it enables the use of a wide range of sample environments that are difficult to use with synchrotron x-ray sources. It also has the advantage that the cross sections for interaction do not increase with atomic number as they do with radiation from a synchrotron x-ray source. Thus neutrons can be used to analyse materials with low atomic numbers like proteins and surfactants. This can be done at synchrotron sources but very high intensities are needed which may cause the structures to change. Moreover, the nucleus provides a very short range, isotropic potential varying randomly from isotope to isotope, making it possible to tune the nuclear scattering contrast to suit the experiment:

The neutron has an additional advantage over the x-ray photon in the study of condensed matter. It readily interacts with internal magnetic fields in the sample. In fact, the strength of the magnetic scattering signal is often very similar to that of the nuclear scattering signal in many materials, which allows the simultaneous exploration of both nuclear and magnetic structure. Because the neutron scattering amplitude can be measured in absolute units, both the structural and magnetic properties as measured by neutrons can be compared quantitatively with the results of other characterisation techniques.

See also

- Neutron diffraction
- Small angle neutron scattering
- Neutron Reflectometry
- Inelastic neutron scattering
  - neutron triple-axis spectrometry
  - neutron time-of-flight scattering
  - neutron backscattering
  - neutron spin echo
  - neutron resonance spin echo
- Neutron scattering facilities

External links

- Neutron Scattering - A primer [1] (LANL-hosted black and white version [2]) - An introductory article written by Roger Pynn (Los Alamos National Laboratory)

References

[1] http://knocknick.files.wordpress.com/2008/04/neutrons-a-primer-by-rogen-pynn.pdf
[2] http://library.lanl.gov/cgi-bin/getfile?00326651.pdf

Paracrystalline lattices/Paracrystals

Paracrystalline materials are defined as having short and medium range ordering in their lattice (similar to the liquid crystal phases) but lacking long-range ordering at least in one direction.[1]

Ordering is the regularity in which atoms appear in a predictable lattice, as measured from one point. In a highly ordered, perfectly crystalline material, or single crystal, the location of every atom in the structure can be described exactly measuring out from a single origin. Conversely, in a disordered structure such as a liquid or amorphous solid, the location of the first and perhaps second nearest neighbors can be described from an origin (with some degree of uncertainty) and the ability to predict locations decreases rapidly from there out. The distance at which atom locations can be predicted is referred to as the correlation length ξ. A paracrystalline material exhibits correlation somewhere between the fully amorphous and fully crystalline.

The primary, most accessible source of crystallinity information is X-ray diffraction, although other techniques may be needed to observe the complex structure of paracrystalline materials, such as fluctuation electron microscopy [2] in combination with Density of states modeling[3] of electronic and vibrational states.

Paracrystalline Model

The paracrystalline model is a revision of the Continuous Random Network model first proposed by W. H. Zachariasen in 1932 [4] . The paracrystal model is defined as highly strained, microcrystalline grains surrounded by fully amorphous material [5] . This is a higher energy state then the continuous random network model. The important distinction between this model and the microcrystalline phases is the lack of defined grain boundaries and highly strained lattice parameters, which makes calculations of molecular and lattice dynamics difficult. A general theory of paracrystals has been formulated in a basic textbook[6] , and then further developed/refined by various authors.

Applications

The paracrystal model has been useful, for example, in describing the state of partially amorphous semiconductor materials after deposition. It has also been successfully applied to: synthetic polymers, liquid crystals, biopoloymers [7] ,[8] and biomembranes[9] .

See also

- X-ray scattering
- Amorphous solid
- Single Crystal
- Polycrystalline
- Crystallography
- DNA
- X-ray pattern of a B-DNA Paracrystal [10]

Notes

[1] Voyles, et al. Structure and physical properties of paracrystalline atomistic models of amorphous silicon. *J. Ap. Phys.*, **90**(2001) 4437, doi: 10.1063/1.1407319
[2] Biswas, P, et al. *J. Phys.:Condens. Matter*, **19** (2007) 455202, doi:10.1088/0953-8984/19/45/455202
[3] Nakhmanson, Voyles, Mousseau, Barkema, and Drabold. *Phys. Rev. B* **63**(2001) 235207. doi: 10.1103/PhysRevB.63.235207
[4] Zachariasen, W.H., *J. Am. Chem. Soc.,* **54**(1932) 3841.
[5] J.M. Cowley, Diffraction Studies on Non-Cryst. Substan. 13 (1981)
[6] Hosemann R., Bagchi R.N., Direct analysis of diffraction by matter, North-Holland Publs., Amsterdam – New York, 1962
[7] Bessel functions and diffraction by helical structures http://planetphysics.org/encyclopedia/BesselFunctionsAndTheirApplicationsToDiffractionByHelicalStructures.html
[8] X-Ray Diffraction Patterns of Double-Helical Deoxyribonucleic Acid (DNA) Crystals and Paracrystalline Fibers http://planetphysics.org/encyclopedia/BesselFunctionsApplicationsToDiffractionByHelicalStructures.html
[9] Baianu I.C., X-ray scattering by partially disordered membrane systems, *Acta Cryst*. **A**, **34** (1978), 751–753.

2D-FT NMRI and Spectroscopy

2D-FT Nuclear magnetic resonance imaging (**2D-FT NMRI**), or **Two-dimensional Fourier transform** nuclear magnetic resonance imaging (**NMRI**), is primarily a non—invasive imaging technique most commonly used in biomedical research and medical radiology/nuclear medicine/MRI to visualize structures and functions of the living systems and single cells. For example it can provides fairly detailed images of a human body in any selected cross-sectional plane, such as longitudinal, transversal, sagital, etc. The basic NMR phenomenon or physical principle[1] is essentially the same in N(MRI), nuclear magnetic resonance/FT (NMR) spectroscopy, topical NMR, or even in Electron Spin Resonance /EPR; however, the details are significantly different at present for EPR, as only in the early days of NMR the static magnetic field was scanned for obtaining spectra, as it is still the case in many EPR or ESR spectrometers. NMRI, on the other hand, often utilizes a linear magnetic field gradient to obtain an image that combines the visualization of molecular structure and dynamics. It is this dynamic aspect of NMRI, as well as its highest sensitivity for the ^{1}H nucleus that distinguishes it very dramatically from X-ray CAT scanning that 'misses' hydrogens because of their very low X-ray scattering factor.

Thus, NMRI provides much greater contrast especially for the different soft tissues of the body than computed tomography (CT) as its most sensitive option observes the nuclear spin distribution and dynamics of highly mobile molecules that contain the naturally abundant, stable hydrogen isotope ^{1}H as in plasma water molecules, blood, disolved metabolites and fats. This approach makes it most useful in cardiovascular, oncological (cancer), neurological (brain), musculoskeletal, and cartilage imaging. Unlike CT, it uses no ionizing radiation, and also unlike nuclear imaging it does not employ any radioactive isotopes. Some of the first MRI images reported were published in 1973[2] and the first study performed on a human took place on July 3, 1977.[3] Earlier papers were also published by Sir Peter Mansfield[4] in UK (Nobel Laureate in 2003), and R. Damadian in the USA[5] , (together with an approved patent for 'fonar', or magnetic imaging). The detailed physical theory of NMRI was published by Peter Mansfield in 1973[6] . Unpublished 'high-resolution' (50 micron resolution) images of other living systems, such as hydrated wheat grains, were also obtained and communicated in UK in 1977-1979, and were subsequently confirmed by articles published in *Nature* by Peter Callaghan.

NMR Principle

Advanced 4.7 T clinical diagnostics and biomedical research NMR Imaging instrument.

Certain nuclei such as ^{1}H nuclei, or `fermions' have spin-1/2, because there are two spin states, referred to as "up" and "down" states. The nuclear magnetic resonance absorption phenomenon occurs when samples containing such nuclear spins are placed in a static magnetic field and a very short radiofrequency pulse is applied with a center, or carrier, frequency matching that of the transition between the up and down states of the spin-1/2 ^{1}H nuclei that were polarized by the static magnetic field. [7] Very low field schemes have also been recently reported.[8]

Chemical Shifts

NMR is a very useful family of techniques for chemical and biochemical research because of the chemical shift; this effect consists in a frequency shift of the nuclear magnetic resonance for specific chemical groups or atoms as a result of the partial shielding of the corresponding nuclei from the applied, static external magnetic field by the electron orbitals (or molecular orbitals) surrounding such nuclei present in the chemical groups. Thus, the higher the electron density surrounding a specific nucleus the larger the chemical shift will be. The resulting magnetic field at the nucleus is thus lower than the applied external magnetic field and the resonance frequencies observed as a result of such shielding are lower than the value that would be observed in the absence of any electronic orbital shielding. Furthermore, in order to obtain a chemical shift value independent of the strength of the applied magnetic field and allow for the direct comparison of spectra obtained at different magnetic field values, the chemical shift is defined by the ratio of the strength of the local magnetic field value at the observed (electron orbital-shielded) nucleus by the external magnetic field strength, $\mathbf{H}_{loc}/\mathbf{H}_{0}$. The first NMR observations of the chemical shift, with the correct physical chemistry interpretation, were reported for ^{19}F containing compounds in the early 1950s by Herbert S. Gutowsky and Charles P. Slichter from the University of Illinois at Urbana (USA).

A related effect in metals is called the Knight shift, which is due only to the conduction electrons. Such conduction electrons present in metals induce an "additional" local field at the nuclear site, due to the spin re-orientation of the conduction electrons in the presence of the applied (constant), external magnetic field. This is only broadly `similar' to the chemical shift in either solutions or diamagnetic solids.

NMR Imaging Principles

A number of methods have been devised for combining magnetic field gradients and radiofrequency pulsed excitation to obtain an image. Two major maethods involve either 2D -FT or 3D-FT[9] reconstruction from projections, somewhat similar to Computed Tomography, with the exception of the image interpretation that in the former case must include dynamic and relaxation/contrast enhancement information as well. Other schemes involve building the NMR image either point-by-point or line-by-line. Some schemes use instead gradients in the rf field rather than in the static magnetic field. The majority of NMR images routinely obtained are either by the Two-Dimensional Fourier Transform (2D-FT) technique [10] (with slice selection), or by the Three-Dimensional Fourier Transform (3D—FT) techniques that are however much more time consuming at present. 2D-FT NMRI is sometime called in common parlance a "spin-warp". An NMR image corresponds to a spectrum consisting of a number of `spatial frequencies' at different locations in the sample investigated, or in a patient.[11] A two–dimensional Fourier transformation of such a "real" image may be considered as a representation of such "real waves" by a matrix of spatial frequencies known as the k–space. We shall see next in some mathematical detail how the 2D-FT computation works to obtain 2D-FT NMR images.

Two-dimensional Fourier transform imaging and spectroscopy

A two-dimensional Fourier transform (2D-FT) is computed numerically or carried out in two stages, both involving `standard', one-dimensional Fourier transforms. However, the second stage Fourier transform is not the inverse Fourier transform (which would result in the original function that was transformed at the first stage), but a Fourier transform in a second variable—which is `shifted' in value—relative to that involved in the result of the first Fourier transform. Such 2D-FT analysis is a very powerful method for both NMRI and two-dimensional nuclear magnetic resonance spectroscopy (2D-FT NMRS)[12] that allows the three-dimensional reconstruction of polymer and biopolymer structures at atomic resolution.[13] for molecular weights (Mw) of dissolved biopolymers in aqueous solutions (for example) up to about 50,000 Mw. For larger biopolymers or polymers, more complex methods have been developed to obtain limited structural resolution needed for partial 3D-reconstructions of higher molecular structures, e.g. for up 900,000 Mw or even oriented microcrystals in aqueous suspensions or single crystals; such methods have also been reported for *in vivo* 2D-FT NMR spectroscopic studies of algae, bacteria, yeast and certain mammalian cells, including human ones. The 2D-FT method is also widely utilized in optical spectroscopy, such as *2D-FT NIR hyperspectral imaging* (2D-FT NIR-HS), or in MRI imaging for research and clinical, diagnostic applications in Medicine. In the latter case, 2D-FT NIR-HS has recently allowed the identification of single, malignant cancer cells surrounded by healthy human breast tissue at about 1 micron resolution, well-beyond the resolution obtainable by 2D-FT NMRI for such systems in the limited time available for such diagnostic investigations (and also in magnetic fields up to the FDA approved magnetic field strength $\mathbf{H}_0$ of 4.7 T, as shown in the top image of the state-of-the-art NMRI instrument). A more precise mathematical definition of the `double' (2D) Fourier transform involved in both 2D NMRI and 2D-FT NMRS is specified next, and a precise example follows this generally accepted definition.

2D-FT Definition

A *2D-FT, or two-dimensional Fourier transform*, is a standard Fourier transformation of a function of two variables, $\mathbf{f}(x_1, x_2)$, carried first in the first variable x_1, followed by the Fourier transform in the second variable x_2 of the resulting function $\mathbf{F}(s_1,x_2)$. Note that in the case of both 2D-FT NMRI and 2D-FT NMRS the two independent variables in this definition are in the time domain, whereas the results of the two successive Fourier transforms have, of course, frequencies as the independent variable in the NMRS, and ultimately spatial coordinates for both 2D NMRI and 2D-FT NMRS following computer structural recontructions based on special algorithms that are different from FT or 2D-FT. Moreover, such structural algorithms are different for 2D NMRI and 2D-FT NMRS: in the former case they involve macroscopic, or anatomical structure detrmination, whereas in the latter case of 2D-FT NMRS the atomic structure reconstruction algorithms are based on the quantum theory of a microphysical (quantum) process such as nuclear Overhauser enhancement NOE, or specific magnetic dipole-dipole interactions[14] between neighbor nuclei.

Example 1

A 2D Fourier transformation and phase correction is applied to a set of 2D NMR (FID) signals: $\mathbf{s}(t_1,t_2)$ yielding a real 2D-FT NMR `spectrum' (collection of 1D FT-NMR spectra) represented by a matrix **S** whose elements are

$$\mathbf{S}\ (\nu_1, \nu_2) = \mathbf{Re} \int \int cos(\nu_1 t_1) exp^{(-i\nu_2 t_2)} s(t_1, t_2) dt_1 dt_2$$

where : $\nu_1$and : $\nu_2$denote the discrete indirect double-quantum and single-quantum(detection) axes, respectively, in the 2D NMR experiments. Next, the *covariance matrix* is calculated in the frequency domain according to the following equation

$$\mathbf{C}\quad (\nu_2', \nu_2) = S^T S = \sum_{\nu^1} [S(\nu_1, \nu_2') S(\nu_1, \nu_2)],$$ with : ν_2, ν_2'taking all possible single-quantum frequency values and with the summation carried out over all discrete, double quantum frequencies : ν_1.

Example 2

Atomic Structure from 2D-FT STEM Images [15] of electron distributions in a high-temperature cuprate superconductor `paracrystal' reveal both the domains (or `location') and the local symmetry of the 'pseudo-gap' in the electron-pair correlation band responsible for the high—temperature superconductivity effect (obtained at Cornell University). So far there have been three Nobel prizes awarded for 2D-FT NMR/MRI during 1992-2003, and an additional, earlier Nobel prize for 2D-FT of X-ray data (`CAT scans'); recently the advanced possibilities of 2D-FT techniques in Chemistry, Physiology and Medicine [16] received very significant recognition.[17]

Brief explanation of NMRI diagnostic uses in Pathology

As an example, a diseased tissue such as a malign tumor, can be detected by 2D-FT NMRI because the hydrogen nuclei of molecules in different tissues return to their equilibrium spin state at different relaxation rates, and also because of the manner in which a malign tumor spreads and grows rapidly along the blood vessels adjacent to the tumor, also inducing further vascularization to occur. By changing the pulse delays in the RF pulse

sequence employed, and/or the RF pulse sequence itself, one may obtain a `relaxation—based contrast', or contrast enhancement between different types of body tissue, such as normal vs. diseased tissue cells for example. Excluded from such diagnostic observations by NMRI are all patients with ferromagnetic metal implants, (e.g., cochlear implants), and all cardiac pacemaker patients who cannot undergo any NMRI scan because of the very intense magnetic and RF fields employed in NMRI which would strongly interfere with the correct functioning of such pacemakers. It is, however, conceivable that future developments may also include along with the NMRI diagnostic treatments with special techniques involving applied magnetic fields and very high frequency RF. Already, surgery with special tools is being experimented on in the presence of NMR imaging of subjects.Thus, NMRI is used to image almost every part of the body, and is especially useful for diagnosis in neurological conditions, disorders of the muscles and joints, for evaluating tumors, such as in lung or skin cancers, abnormalities in the heart (especially in children with hereditary disorders), blood vessels, CAD, atherosclerosis and cardiac infarcts [18] (courtesy of Dr. Robert R. Edelman)

See also

- Nuclear magnetic resonance (NMR)
- Edward Mills Purcell
- Felix Bloch
- Medical imaging
- Paul C. Lauterbur
- Magnetic resonance microscopy
- Peter Mansfield
- Computed tomography (CT)
- Solid-state NMR
- Knight shift
- John Hasbrouck Van Vleck
- Chemical shift
- Herbert S. Gutowsky
- John S. Waugh
- Charles Pence Slichter
- Protein nuclear magnetic resonance spectroscopy
- Kurt Wüthrich
- Nuclear Overhauser effect
- Fourier transform spectroscopy(FTS)
- Jean Jeneer
- Richard R. Ernst
- FT-NIRS (NIR)
- Magnetic resonance elastography
- Relaxation
- Earth's field NMR (EFNMR)
- Robinson oscillator

Footnotes

[1] Antoine Abragam. 1968. *Principles of Nuclear Magnetic Resonance.*, 895 pp., Cambridge University Press: Cambridge, UK.
[2] Lauterbur, P.C., Nobel Laureate in 2003 (1973). "Image Formation by Induced Local Interactions: Examples of Employing Nuclear Magnetic Resonance". *Nature* **242**: 190–1. doi: 10.1038/242190a0 (http://dx.doi.org/10.1038/242190a0).
[3] Howstuffworks "How MRI Works" (http://www.howstuffworks.com/mri.htm/printable)
[4] Peter Mansfield. 2003. Nobel Laureate in Physiology and Medicine for (2D and 3D) MRI (http://www.parteqinnovations.com/pdf-doc/fandr-Gaz1006.pdf)
[5] Damadian, R. V. "Tumor Detection by Nuclear Magnetic Resonance," Science, 171 (March 19, 1971): 1151-1153 (http://www.sciencemag.org/cgi/content/abstract/171/3976/1151)
[6] NMR 'diffraction' in solids? P. Mansfield et al. 1973 J. Phys. C: Solid State Phys. 6 L422-L426 doi: 10.1088/0022-3719 (http://www.iop.org/EJ/article/0022-3719/6/22/007/jcv6i22pL422.pdf)
[7] Antoine Abragam. 1968. *Principles of Nuclear Magnetic Resonance.*, 895 pp., Cambridge University Press: Cambridge, UK.
[8] Raftery D (August 2006). "http://www.pubmedcentral.nih.gov/articlerender.fcgi?tool=pmcentrez&artid=1568902|MRI without the magnet". *Proc Natl Acad Sci USA.* **103** (34): 12657–8. doi: 10.1073/pnas.0605625103 (http://dx.doi.org/10.1073/pnas.0605625103). PMID 16912110.
[9] Wu Y, Chesler DA, Glimcher MJ, *et al.* (February 1999). "http://www.pnas.org/cgi/pmidlookup?view=long&pmid=9990066|Multinuclear solid-state three-dimensional MRI of bone and synthetic calcium phosphates". *Proc. Natl. Acad. Sci. U.S.A.* **96** (4): 1574–8. doi: 10.1073/pnas.96.4.1574 (http://dx.doi.org/10.1073/pnas.96.4.1574). PMID 9990066. PMC: 15521 (http://www.pubmedcentral.nih.gov/articlerender.fcgi?tool=pmcentrez&artid=15521). http://www.pnas.org/cgi/pmidlookup?view=long&pmid=9990066.
[10] http://www.math.cuhk.edu.hk/course/mat2071a/lec1_08.ppt
[11] *Haacke, E Mark; Brown, Robert F; Thompson, Michael; Venkatesan, Ramesh (1999). *Magnetic resonance imaging: physical principles and sequence design*. New York: J. Wiley & Sons. ISBN 0-471-35128-8.
[12] Richard R. Ernst. 1992. Nuclear Magnetic Resonance Fourier Transform (2D-FT) Spectroscopy. Nobel Lecture (http://nobelprize.org/nobel_prizes/chemistry/laureates/1991/ernst-lecture.pdf), on December 9, 1992.
[13] http://en.wikipedia.org/wiki/Nuclear_magnetic_resonance#Nuclear_spin_and_magnets Kurt Wüthrich in 1982-1986 : 2D-FT NMR of solutions
[14] Charles P. Slichter.1996. *Principles of Magnetic Resonance.* Springer: Berlin and New York, Third Edition., 651pp. ISBN 0-387-50157-6.
[15] http://www.physorg.com/news129395045.html
[16] http://nobelprize.org/nobel_prizes/chemistry/laureates/1991/ernst-lecture.pdf
[17] Protein structure determination in solution by NMR spectroscopy (http://www.ncbi.nlm.nih.gov/entrez/query.fcgi?cmd=Retrieve&db=pubmed&dopt=Abstract&list_uids=2266107&query_hl=33&itool=pubmed_docsum) Kurt Wüthrich. J Biol Chem. 1990 December 25;265(36):22059-62.
[18] http://www.mr-tip.com/serv1.php?type=img&img=Cardiac%20Infarct%20Short%20Axis%20Cine%204

References

- Antoine Abragam. 1968. *Principles of Nuclear Magnetic Resonance.*, 895 pp., Cambridge University Press: Cambridge, UK.
- Charles P. Slichter.1996. *Principles of Magnetic Resonance.* Springer: Berlin and New York, Third Edition., 651pp. ISBN 0-387-50157-6.
- Kurt Wüthrich. 1986, *NMR of Proteins and Nucleic Acids.*, J. Wiley and Sons: New York, Chichester, Brisbane, Toronto, Singapore. (Nobel Laureate in 2002 for 2D-FT NMR Studies of Structure and Function of Biological Macromolecules (http://nobelprize.org/nobel_prizes/chemistry/laureates/2002/wutrich-lecture.pdf)
- Protein structure determination in solution by NMR spectroscopy (http://www.ncbi.nlm.nih.gov/entrez/query.fcgi?cmd=Retrieve&db=pubmed&dopt=Abstract&list_uids=2266107&query_hl=33&itool=pubmed_docsum) Kurt Wüthrich. J Biol Chem.

1990 December 25;265(36):22059-62

- 2D-FT NMRI Instrument image: A JPG color image of a 2D-FT NMRI `monster' Instrument (http://upload.wikimedia.org/wikipedia/en/b/bf/HWB-NMRv900.jpg).
- Richard R. Ernst. 1992. Nuclear Magnetic Resonance Fourier Transform (2D-FT) Spectroscopy. Nobel Lecture (http://nobelprize.org/nobel_prizes/chemistry/laureates/1991/ernst-lecture.pdf), on December 9, 1992.
- Peter Mansfield. 2003. Nobel Laureate in Physiology and Medicine for (2D and 3D) MRI (http://www.parteqinnovations.com/pdf-doc/fandr-Gaz1006.pdf)
- D. Benett. 2007. PhD Thesis. Worcester Polytechnic Institute. PDF of 2D-FT Imaging Applications to NMRI in Medical Research. (http://www.wpi.edu/Pubs/ETD/Available/etd-081707-080430/unrestricted/dbennett.pdf) Worcester Polytechnic Institute. (Includes many 2D-FT NMR images of human brains.)
- Paul Lauterbur. 2003. Nobel Laureate in Physiology and Medicine for (2D and 3D) MRI. (http://nobelprize.org/nobel_prizes/medicine/laureates/2003/)
- Jean Jeener. 1971. Two-dimensional Fourier Transform NMR, presented at an Ampere International Summer School, Basko Polje, unpublished. A verbatim quote follows from Richard R. Ernst's Nobel Laureate Lecture delivered on December 2, 1992, "A new approach to measure two-dimensional (2D) spectra." has been proposed by Jean Jeener at an Ampere Summer School in Basko Polje, Yugoslavia, 1971 (Jean Jeneer,1971)). He suggested a 2D Fourier transform experiment consisting of two $\pi/2$ pulses with a variable time t_1 between the pulses and the time variable t_2 measuring the time elapsed after the second pulse as shown in Fig. 6 that expands the principles of Fig. 1. Measuring the response $s(t_1,t_2)$ of the two-pulse sequence and Fourier-transformation with respect to both time variables produces a two-dimensional spectrum $S(O_1,O_2)$ of the desired form. This two-pulse experiment by Jean Jeener is the forefather of a whole class of $2D$ experiments that can also easily be expanded to multidimensional spectroscopy.
- Dudley, Robert, L (1993). "High-Field NMR Instrumentation". *Ch. 10 in Physical Chemistry of Food Processes* (New York: Van Nostrand-Reinhold) **2**: 421-30. ISBN 0-442-00582-2.
- Baianu, I.C.; Kumosinski, Thomas (August 1993). "NMR Principles and Applications to Structure and Hydration,". *Ch.9 in Physical Chemistry of Food Processes* (New York: Van Nostrand-Reinhold) **2**: 338-420. ISBN 0-442-00582-2.
- Haacke, E Mark; Brown, Robert F; Thompson, Michael; Venkatesan, Ramesh (1999). *Magnetic resonance imaging: physical principles and sequence design*. New York: J. Wiley & Sons. ISBN 0-471-35128-8.
- Raftery D (August 2006). "http://www.pubmedcentral.nih.gov/articlerender.fcgi?tool=pmcentrez&artid=1568902|MRI without the magnet". *Proc Natl Acad Sci USA.* **103** (34): 12657–8. doi: 10.1073/pnas.0605625103 (http://dx.doi.org/10.1073/pnas.0605625103). PMID 16912110.
- Wu Y, Chesler DA, Glimcher MJ, *et al.* (February 1999). "http://www.pnas.org/cgi/pmidlookup?view=long&pmid=9990066|Multinuclear solid-state three-dimensional MRI of bone and synthetic calcium phosphates". *Proc. Natl. Acad. Sci. U.S.A.* **96** (4): 1574–8. doi: 10.1073/pnas.96.4.1574 (http://dx.doi.org/10.

1073/pnas.96.4.1574). PMID 9990066. PMC: 15521 (http://www.pubmedcentral.nih.gov/articlerender.fcgi?tool=pmcentrez&artid=15521). http://www.pnas.org/cgi/pmidlookup?view=long&pmid=9990066.

External links

- Cardiac Infarct or "heart attack" Imaged in Real Time by 2D-FT NMRI (http://www.mr-tip.com/exam_gifs/cardiac_infarct_short_axis_cine_6.gif)
- Interactive Flash Animation on MRI (http://www.e-mri.org) - *Online Magnetic Resonance Imaging physics and technique course*
- Herbert S. Gutowsky
- Jiri Jonas and Charles P. Slichter: NMR Memoires at NAS about Herbert Sander Gutowsky; NAS = National Academy of Sciences, USA, (http://books.nap.edu/html/biomems/hgutowsky.pdf)
- 3D Animation Movie about MRI Exam (http://www.patiencys.com/MRI/)
- International Society for Magnetic Resonance in Medicine (http://www.ismrm.org)
- Danger of objects flying into the scanner (http://www.simplyphysics.com/flying_objects.html)

Related Wikipedia websites

- Medical imaging
- Computed tomography
- Magnetic resonance microscopy
- Fourier transform spectroscopy
- FT-NIRS
- Chemical imaging
- Magnetic resonance elastography
- Nuclear magnetic resonance (NMR)
- Chemical shift
- Relaxation
- Robinson oscillator
- Earth's field NMR (EFNMR)
- Rabi cycle

FRET and FCS-Fluorescence correlation spectroscopy

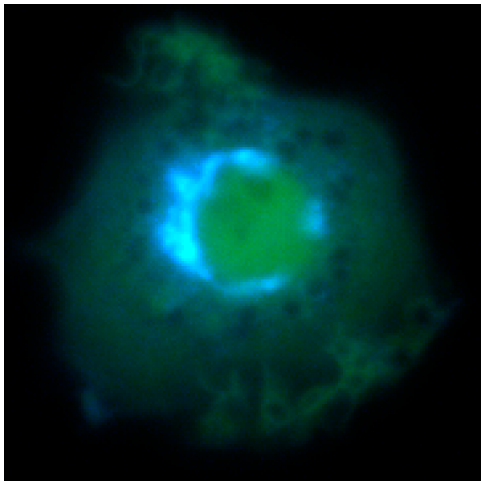

Fluorescently-labeled guanosine 5'-triphosphate hydrolase ARF reveals the protein's localization in the Golgi apparatus of a living macrophage. FRET studies revealed ARF activation in the Golgi and in the formation of phagosomes.[1]

Förster resonance energy transfer (abbreviated **FRET**), also known as **fluorescence resonance energy transfer**, **resonance energy transfer** (**RET**) or **electronic energy transfer** (**EET**), is a mechanism describing energy transfer between two chromophores.

A donor chromophore, intially in its electronic excited state, may transfer energy to an acceptor chromophore (in close proximity, typically <10 nm) through nonradiative dipole-dipole coupling. This mechanism is termed "Förster resonance energy transfer" and is named after the German scientist Theodor Förster.[2] When both chromophores are fluorescent, the term "fluorescence resonance energy transfer" is often used instead, although the energy is not actually transferred by fluorescence.[3],[4] In order to avoid an erroneous interpretation of the phenomenon that (even when occurring between two fluorescent chromophores) is always a nonradiative transfer of energy, the name "Förster resonance energy transfer" is preferred to "fluorescence resonance energy transfer" - although the latter enjoys common usage in scientific literature. FRET is analogous to Near Field Communication, in that the radius of interaction is much smaller than the wavelength of light emitted. In the near field region, the excited chromophore emits a virtual photon that is instantly absorbed by a receiving chromophore. These virtual photons are undetectable, since their existence violates the conservation of energy and momentum, and hence FRET is known as a radiationless mechanism. From quantum electrodynamical calculations, it is determined that radiationless (FRET) and radiative energy transfer are the short- and long-range asymptotes of a single unified mechanism.[5],[6]

Theoretical basis

The FRET efficiency (E) is the quantum yield of the energy transfer transition, *i.e.* the fraction of energy transfer event occurring per donor excitation event:

$$E = \frac{k_{ET}}{k_f + k_{ET} + \sum k_i}$$

where k_{ET} is the rate of energy transfer, k_f the radiative decay rate and the k_i are the rate constants of any other de-excitation pathway.
The FRET efficiency depends on many parameters that can be grouped as follows:

- The distance between the donor and the acceptor

- The spectral overlap of the donor emission spectrum and the acceptor absorption spectrum.
- The relative orientation of the donor emission dipole moment and the acceptor absorption dipole moment.

E depends on the donor-to-acceptor separation distance r with an inverse 6th power law due to the dipole-dipole coupling mechanism:

$$E = \frac{1}{1 + (r/R_0)^6}$$

with R_0 being the Förster distance of this pair of donor and acceptor i.e. the distance at which the energy transfer efficiency is 50%. The Förster distance depends on the overlap integral of the donor emission spectrum with the acceptor absorption spectrum and their mutual molecular orientation as expressed by the following equation:

$${R_0}^6 = \frac{9\,Q_0\,(\ln 10)\kappa^2\,J}{128\,\pi^5\,n^4\,N_A}$$

where Q_0 is the fluorescence quantum yield of the donor in the absence of the acceptor, κ^2 is the dipole orientation factor, n is the refractive index of the medium, N_A is Avogadro's number, and J is the spectral overlap integral calculated as

$$J = \int f_{\mathrm{D}}(\lambda)\,\epsilon_{\mathrm{A}}(\lambda)\,\lambda^4\,d\lambda$$

where f_{D} is the normalized donor emission spectrum, and ϵ_{A} is the acceptor molar extinction coefficient. κ^2 =2/3 is often assumed. This value is obtained when both dyes are freely rotating and can be considered to be isotropically oriented during the excited state lifetime. If either dye is fixed or not free to rotate, then κ^2 =2/3 will not be a valid assumption. In most cases, however, even modest reorientation of the dyes results in enough orientational averaging that κ^2 = 2/3 does not result in a large error in the estimated energy transfer distance due to the sixth power dependence of R_0 on κ^2. Even when κ^2 is quite different from 2/3 the error can be associated with a shift in R_0 and thus determinations of changes in relative distance for a particular system are still valid. Fluorescent proteins do not reorient on a timescale that is faster than their fluorescence lifetime. In this case $0 \le \kappa^2 \le 4$.

The FRET efficiency relates to the quantum yield and the fluorescence lifetime of the donor molecule as follows:

$$E = 1 - \tau'_{\mathrm{D}}/\tau_{\mathrm{D}}$$

where τ'_{D} and τ_{D} are the donor fluorescence lifetimes in the presence and absence of an acceptor, respectively, or as

$$E = 1 - F'_{\mathrm{D}}/F_{\mathrm{D}}$$

where F'_{D} and F_{D} are the donor fluorescence intensities with and without an acceptor, respectively.

Methods

In fluorescence microscopy, fluorescence confocal laser scanning microscopy, as well as in molecular biology, FRET is a useful tool to quantify molecular dynamics in biophysics and biochemistry, such as protein-protein interactions, protein-DNA interactions, and protein conformational changes. For monitoring the complex formation between two molecules, one of them is labeled with a donor and the other with an acceptor, and these fluorophore-labeled molecules are mixed. When they are dissociated, the donor emission is detected upon the donor excitation. On the other hand, when the donor and acceptor are in proximity (1-10 nm) due to the interaction of the two molecules, the acceptor emission is predominantly observed because of the intermolecular FRET from the donor to the acceptor. For monitoring protein conformational changes, the target protein is labeled with a donor and an acceptor at two loci. When a twist or bend of the protein brings the change in the distance or relative orientation of the donor and acceptor, FRET change is observed. If a molecular interaction or a protein conformational change is dependent on ligand binding, this FRET technique is applicable to fluorescent indicators for the ligand detection.

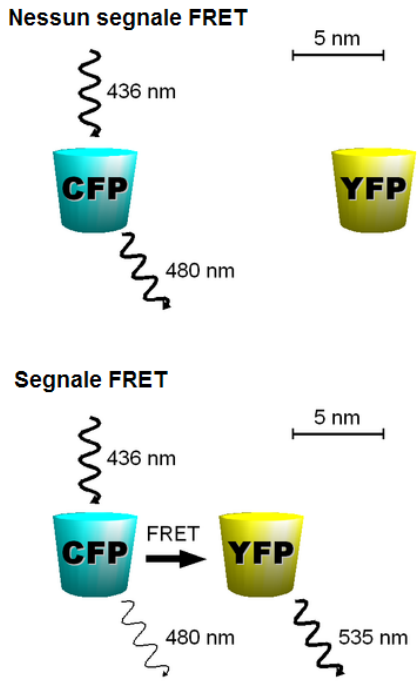

Example of FRET between CFP and YFP (Wavelength vs. Absorption): a fusion protein containing CFP and YFP excited at 440nm wavelength. The fluorescent emission peak of CFP overlaps the excitation peak of YFP. Because the two proteins are adjacent to each other, the energy transfer is significant–a large proportion of the energy from CFP is transferred to YFP and creates a much larger YFP emission peak.

FRET studies are scalable: the extent of energy transfer is often quantified from the milliliter scale of cuvette-based experiments to the femtoliter scale of microscopy-based experiments. This quantification can be based directly (sensitized emission method) on detecting two emission channels under two different excitation conditions (primarily donor and primarily acceptor). However, for robustness reasons, FRET quantification is most often based on measuring changes in fluorescence intensity or fluorescence lifetime upon changing the experimental conditions (e.g. a microscope image of donor emission is taken with the acceptor being present. The acceptor is then bleached, such that it is incapable of accepting energy transfer and another donor emission image is acquired. A pixel-based quantification using the second equation in the theory section above is then possible.) An alternative way of temporarily deactivating the acceptor is based on its fluorescence saturation. Exploiting polarisation characteristics of light, a FRET quantification is also possible with only a single camera exposure.

CFP-YFP pairs

The most popular FRET pair for biological use is a cyan fluorescent protein (**CFP**)-yellow fluorescent protein (**YFP**) pair. Both are color variants of green fluorescent protein (GFP). While labeling with organic fluorescent dyes requires troublesome processes of purification, chemical modification, and intracellular injection of a host protein, GFP variants can be easily attached to a host protein by genetic engineering. By virtue of GFP variants, the use of FRET techniques for biological research is becoming more and more popular.

BRET

A limitation of FRET is the requirement for external illumination to initiate the fluorescence transfer, which can lead to background noise in the results from direct excitation of the acceptor or to photobleaching. To avoid this drawback, Bioluminescence Resonance Energy Transfer (or **BRET**) has been developed. This technique uses a bioluminescent luciferase (typically the luciferase from *Renilla reniformis*) rather than CFP to produce an initial photon emission compatible with YFP.

FRET and BRET are also the common tools in the study of biochemical reaction kinetics and molecular motors.

Photobleaching FRET

FRET efficiencies can also be inferred from the photobleaching rates of the donor in the presence and absence of an acceptor. This method can be performed on most fluorescence microscopes; one simply shines the excitation light (of a frequency that will excite the donor but not the acceptor significantly) on specimens with and without the acceptor fluorophore and monitors the donor fluorescence (typically separated from acceptor fluorescence using a bandpass filter) over time. The timescale is that of photobleaching, which is seconds to minutes, with fluorescence in each curve being given by

$$(\text{background}) + (\text{constant}) * e^{-(\text{time})/\tau_{\text{pb}}}$$

where $\tau_{\text{pb}}$is the photobleaching decay time constant and depends on whether the acceptor is present or not. Since photobleaching consists in the permanent inactivation of excited fluorophores, resonance energy transfer from an excited donor to an acceptor fluorophore prevents the photobleaching of that donor fluorophore, and thus high FRET efficiency leads to a longer photobleaching decay time constant:

$$E = 1 - \tau_{\text{pb}}/\tau'_{\text{pb}}$$

where $\tau'_{\text{pb}}$and $\tau_{\text{pb}}$are the photobleaching decay time constants of the donor in the presence and in the absence of the acceptor, respectively. (Notice that the fraction is the reciprocal of that used for lifetime measurements).

This technique was introduced by Jovin in 1989.[7] Its use of an entire curve of points to extract the time constants can give it accuracy advantages over the other methods. Also, the fact that time measurements are over seconds rather than nanoseconds makes it easier than fluorescence lifetime measurements, and because photobleaching decay rates do not generally depend on donor concentration (unless acceptor saturation is an issue), the careful control of concentrations needed for intensity measurements is not needed. It is, however, important to keep the illumination the same for the with- and without-acceptor measurements, as photobleaching increases markedly with more intense incident light.

Other methods

A different, but related, mechanism is Dexter Electron Transfer.

An alternative method to detecting protein-protein proximity is BiFC where two halves of a YFP are fused to a protein (Hu, Kerppola et al. 2002). When these two halves meet they form a fluorophore after about 60 s - 1 hr.

Applications

FRET has been applied in an experimental method for the detection of phosgene. In it, phosgene or rather triphosgene as a safe substitute serves as a linker between an acceptor and a donor coumarine (forming urea groups).[8] The presence of phosgene is detected at $5x10^{-5}$M with a typical FRET emission at 464 nm.

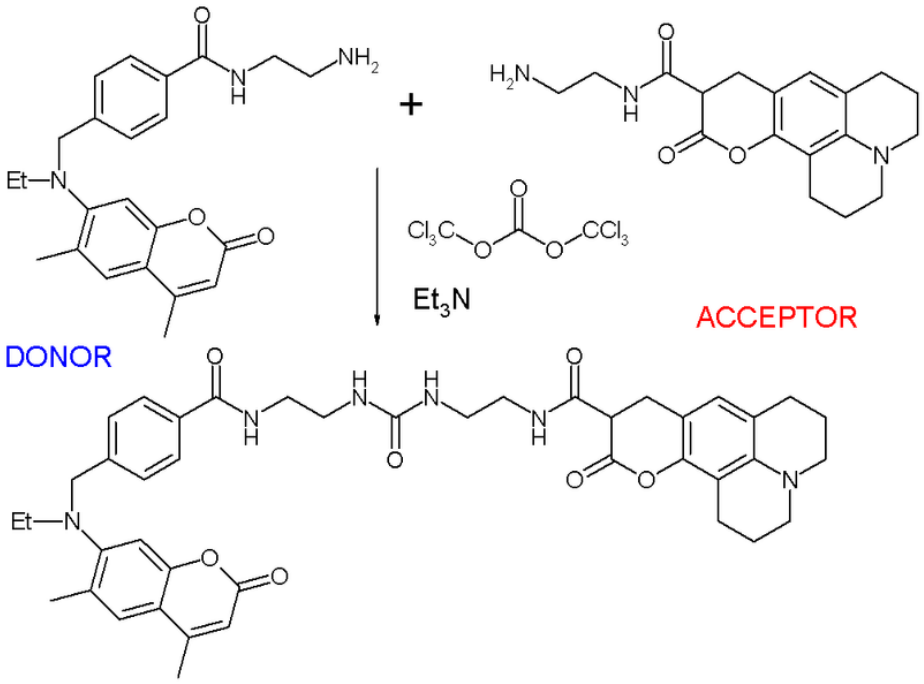

MISTAKE: The chromophore on the right must be also coumarine (double bond is missing)

FRET is also used to study lipid rafts in cell membranes.[9]

External links

- Browser-based calculator to find the critical distance and FRET efficiency with known spectral overlap [10]
- FCS[11] [12] [13] [14] [15] .

References

[1] *Inconspicuous Consumption: Uncovering the Molecular Pathways behind Phagocytosis.* Inman M, PLoS Biology Vol. 4/6/**2006**, e190. doi: 10.1371/journal.pbio.0040190 (http://dx.doi.org/10.1371/journal.pbio.0040190)

[2] Förster T., Zwischenmolekulare Energiewanderung und Fluoreszenz, *Ann. Physik* **1948**, *437*, 55. doi: 10.1002/andp.19484370105 (http://dx.doi.org/10.1002/andp.19484370105)

[3] Joseph R. Lakowicz, "Principles of Fluorescence Spectroscopy", Plenum Publishing Corporation, 2nd edition (July 1, 1999)

[4] FRET microscopy tutorial from Olympus (http://www.olympusfluoview.com/applications/fretintro.html)

[5] D. L. Andrews, "A unified theory of radiative and radiationless molecular energy transfer", *Chem. Phys.* **1989**, 135, 195-201. doi: 10.1016/0301-0104(89)87019-3 (http://dx.doi.org/10.1016/0301-0104(89)87019-3)
[6] D. L. Andrews and D. S. Bradshaw, "Virtual photons, dipole fields and energy transfer: A quantum electrodynamical approach", *Eur. J. Phys.* **2004**, 25, 845-858. doi: 10.1088/0143-0807/25/6/017 (http://dx.doi.org/10.1088/0143-0807/25/6/017)
[7] Jovin, T.M. and Arndt-Jovin, D.J. FRET microscopy: Digital imaging of fluorescence resonance energy transfer. Application in cell biology. In Cell Structure and Function by Microspectrofluometry, E. Kohen, J. G. Hirschberg and J. S. Ploem. London: Academic Press, 1989. pp. 99-117.
[8] *A FRET approach to phosgene detection* Hexiang Zhang and Dmitry M. Rudkevich Chem. Commun., **2007**, 1238 - 1239, doi: 10.1039/b614725a (http://dx.doi.org/10.1039/b614725a)
[9] Silvius, J.R. and Nabi, I.R. Fluorescence-quenching and resonance energy transfer studies of lipid microdomains in model and biological membranes. (Review) *Molec. Membr. Bio.* **2006**, *23*, 5-16. doi: 10.1080/09687860500473002 (http://dx.doi.org/10.1080/09687860500473002)
[10] http://www.calctool.org/CALC/chem/photochemistry/fret
[11] Diaspro, A., and Robello, M. (1999). Multi-photon Excitation Microscopy to Study Biosystems. European Microscopy and Analysis., 5:5-7.
[12] Bagatolli, L.A., and Gratton, E. (2000). Two-photon fluorescence microscopy of coexisting lipid domains in giant unilamellar vesicles of binary phospholipid mixtures. Biophys J., 78:290-305.
[13] Schwille, P., Haupts, U., Maiti, S., and Webb. W.(1999). Molecular dynamics in living cells observed by fluorescence correlation spectroscopy with one- and two- photon excitation. *Biophysical Journal*, **77**(10):2251-2265.
[14] Near Infrared Microspectroscopy, Fluorescence Microspectroscopy,Infrared Chemical Imaging and High Resolution Nuclear Magnetic Resonance Analysis of Soybean Seeds, Somatic Embryos and Single Cells., Baianu, I.C. et al. 2004., In *Oil Extraction and Analysis.*, D. Luthria, Editor pp.241-273, AOCS Press., Champaign, IL.
[15] Single Cancer Cell Detection by Near Infrared Microspectroscopy, Infrared Chemical Imaging and Fluorescence Microspectroscopy.2004.I. C. Baianu, D. Costescu, N. E. Hofmann and S. S. Korban, q-bio/0407006 (July 2004) (http://arxiv.org/abs/q-bio/0407006)

DNA Dynamics

DNA Molecular dynamics modeling involves simulations of DNA molecular geometry and topology changes with time as a result of both intra- and inter- molecular interactions of DNA. Whereas molecular models of Deoxyribonucleic acid (DNA) molecules such as closely packed spheres (CPK models) made of plastic or metal wires for 'skeletal models' are useful representations of static DNA structures, their usefulness is very limited for representing complex DNA dynamics. Computer molecular modeling allows both animations and molecular dynamics simulations that are very important for understanding how DNA functions *in vivo*.

An old standing dynamic problem is how DNA "self-replication" takes place in living cells that should involve transient uncoiling of supercoiled DNA fibers. Although DNA consists of relatively rigid, very large elongated biopolymer molecules called "fibers" or chains its molecular structure *in vivo* undergoes dynamic configuration changes that involve dynamically attached water molecules, ions or proteins/enzymes. Supercoiling, packing with histones in chromosome structures, and other such supramolecular aspects also involve *in vivo* DNA topology which is even more complex than DNA molecular geometry, thus turning molecular modeling of DNA dynamics into a series of challenging problems for biophysical chemists, molecular biologists and biotechnologists. Thus, DNA exists in multiple stable geometries (called conformational isomerism) and has a rather large number of configurational, quantum states which are close to each other in energy on the potential energy surface of the DNA molecule.

Such varying molecular geometries can also be computed, at least in principle, by employing *ab initio* quantum chemistry methods that can attain high accuracy for small molecules, although claims that acceptable accuracy can be also achieved for polynuclelotides, as well as DNA conformations, were recently made on the basis of VCD spectral data. Such quantum geometries define an important class of *ab initio* molecular models of DNA whose exploration has barely started especially in connection with results obtained by VCD in solutions. More detailed comparisons with such *ab initio* quantum computations are in principle obtainable through 2D-FT NMR spectroscopy and relaxation studies of polynucleotide solutions or specifically labeled DNA, as for example with deuterium labels.

Importance of DNA molecular structure and dynamics modeling for Genomics and beyond

From the very early stages of structural studies of DNA by X-ray diffraction and biochemical means, molecular models such as the Watson-Crick double-helix model were successfully employed to solve the 'puzzle' of DNA structure, and also find how the latter relates to its key functions in living cells. The first high quality X-ray diffraction patterns of A-DNA were reported by Rosalind Franklin and Raymond Gosling in 1953[1] . The first reports of a double-helix molecular model of B-DNA structure were made by Watson and Crick in 1953[2] [3] . Then Maurice F. Wilkins, A. Stokes and H.R. Wilson, reported the first X-ray patterns of *in vivo* B-DNA in partially oriented salmon sperm heads [4] . The development of the first correct double-helix molecular model of DNA by Crick and Watson may not have been possible without the biochemical evidence for the nucleotide base-pairing ([A---T]; [C---G]), or Chargaff's rules[5] [6] [7] [8] [9] [10] . Although such initial studies of DNA structures with the help of molecular models were essentially static, their consequences for explaining the *in vivo* functions of DNA were significant in the areas of protein biosynthesis and the quasi-universality of the genetic code. Epigenetic transformation studies of DNA *in vivo* were however much slower to develop in spite of their importance for embryology, morphogenesis and cancer research. Such chemical dynamics and biochemical reactions of DNA are much more complex than the molecular dynamics of DNA physical interactions with water, ions and proteins/enzymes in living cells.

Animated DNA molecular models and hydrogen-bonding

Animated molecular models allow one to visually explore the three-dimensional (3D) structure of DNA. The first DNA model is a space-filling, or CPK, model of the DNA double-helix whereas the third is an animated wire, or skeletal type, molecular model of DNA. The last two DNA molecular models in this series depict quadruplex DNA [13] that may be involved in certain cancers[11] [12] . The first CPK model in the second row is a molecular model of hydrogen bonds between water molecules in ice that are broadly similar to those found in DNA; the hydrogen bonding dynamics and proton exchange is however very different by many orders of magnitude between the two systems of fully hydrated DNA and water molecules in ice. Thus, the DNA dynamics is complex, involving nanosecond and several tens of picosecond time scales, whereas that of liquid ice is on the picosecond time scale, and that of proton exchange in ice is on the millisecond time scale; the proton exchange rates in DNA and attached proteins may vary from picosecond to nanosecond, minutes or years, depending on the exact locations of the exchanged protons in the large

biopolymers. The simple harmonic oscillator 'vibration' in the third, animated image of the next gallery is only an oversimplified dynamic representation of the longitudinal vibrations of the DNA intertwined helices which were found to be anharmonic rather than harmonic as often assumed in quantum dynamic simulations of DNA.

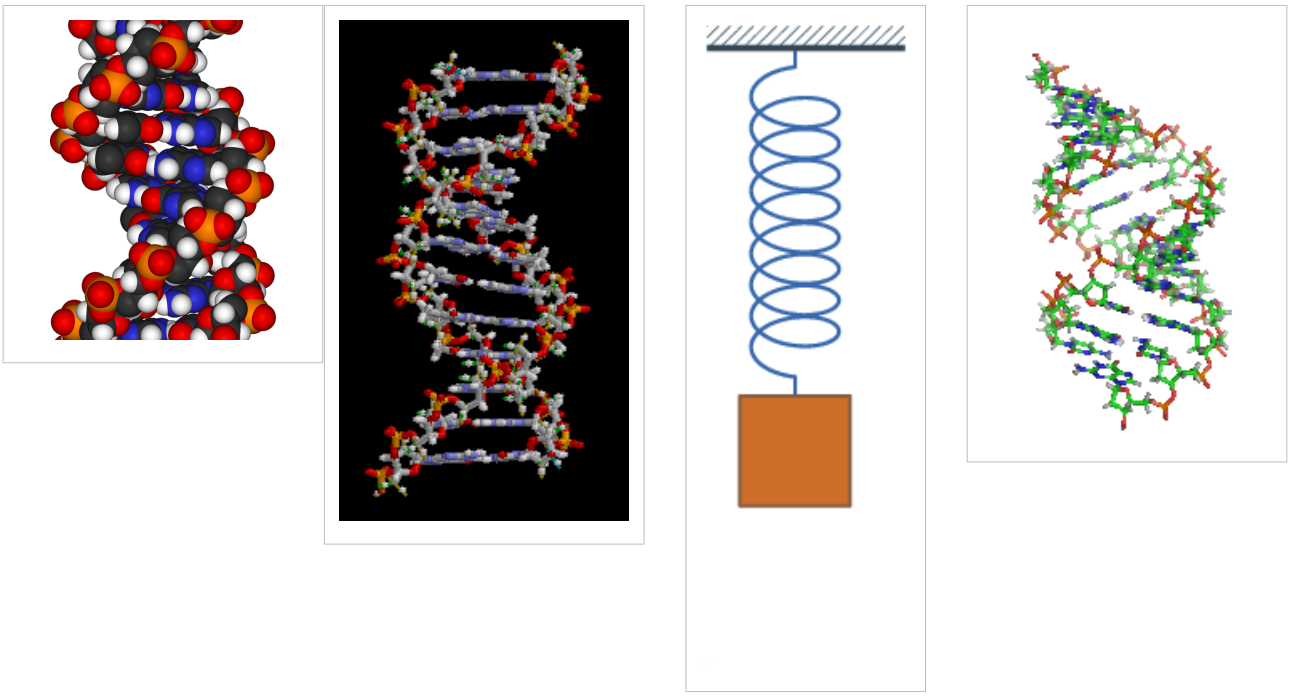

Human Genomics and Biotechnology Applications of DNA Molecular Modeling

The following two galleries of images illustrate various uses of DNA molecular modeling in Genomics and Biotechnology research applications from DNA repair to PCR and DNA nanostructures; each slide contains its own explanation and/or details. The first slide presents an overview of DNA applications, including DNA molecular models, with emphasis on Genomics and Biotechnology.

Applications of DNA molecular dynamics computations

- *First row* images present a DNA biochip and DNA nanostructures designed for DNA computing and other dynamic applications of DNA nanotechnology; last image in this row is of DNA arrays that display a representation of the Sierpinski gasket on their surfaces.
- *Second row*: the first two images show computer molecular models of RNA polymerase, followed by that of an E. coli, bacterial DNA primase template suggesting very complex dynamics at the interfaces between the enzymes and the DNA template; the fourth image illustrates in a computed molecular model the mutagenic, chemical interaction of a potent carcinogen molecule with DNA, and the last image shows the different interactions of specific fluorescence labels with DNA in human and orangoutan chromosomes.

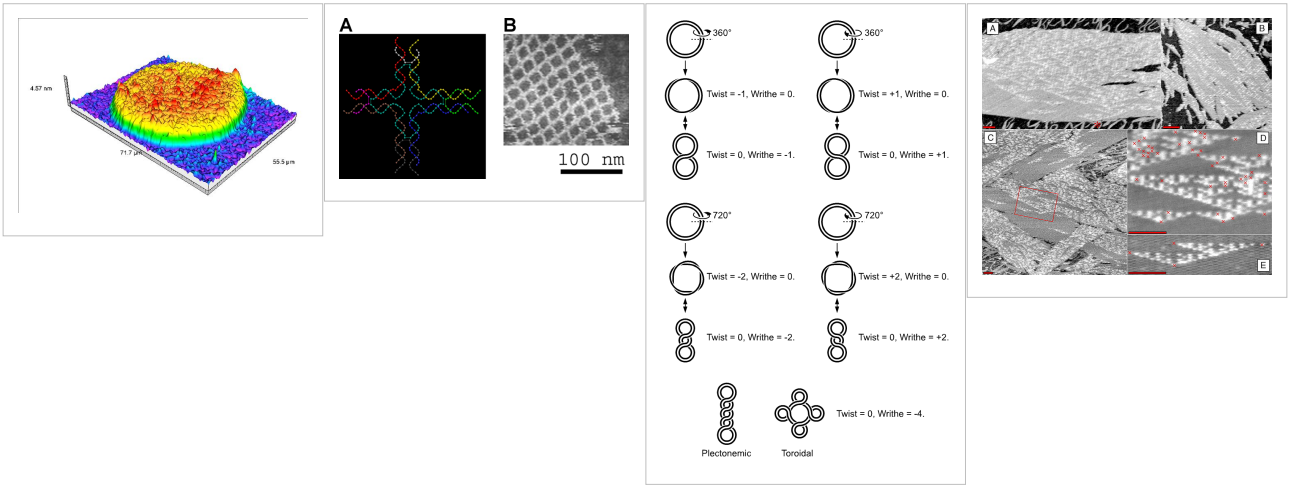

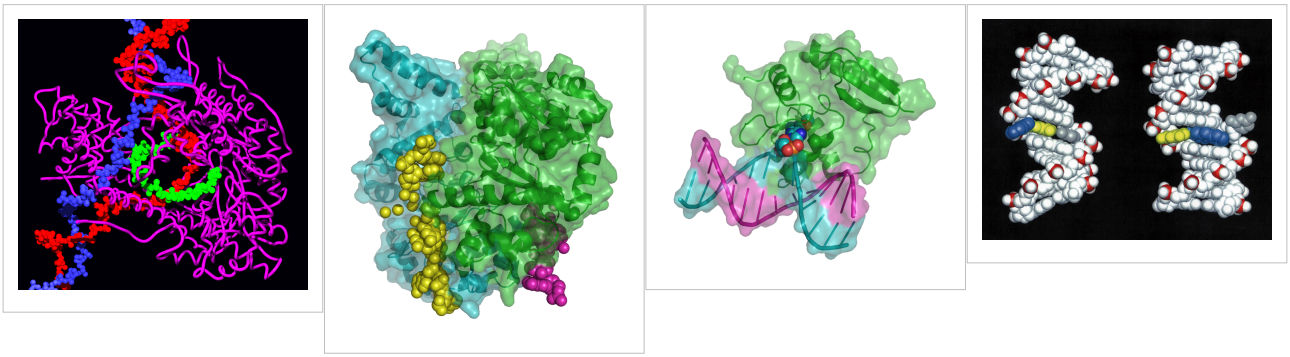

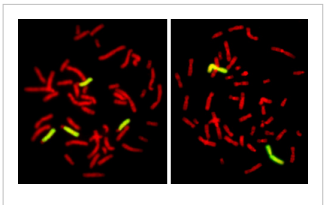

Image Gallery: *DNA Applications and Technologies at various scales in Biotechnology and Genomics research*

The first figure is an actual electron micrograph of a DNA fiber bundle, presumably of a single plasmid, bacterial DNA loop.

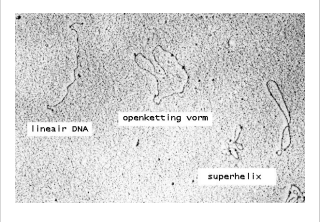

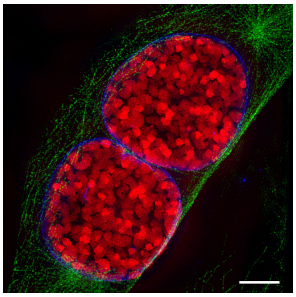

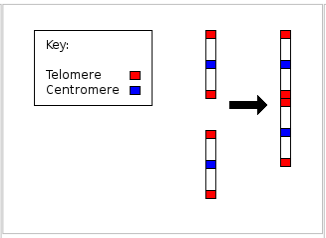

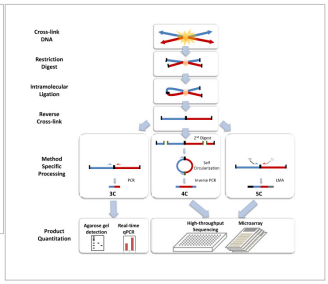

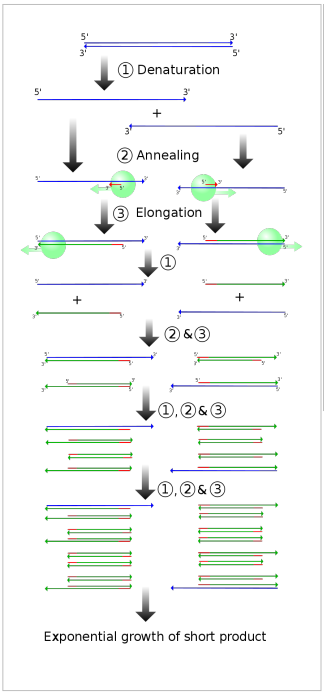

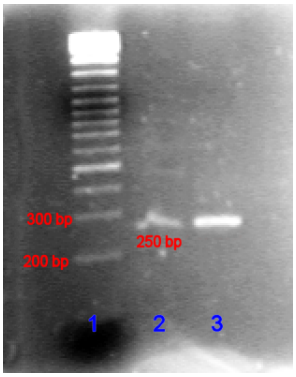

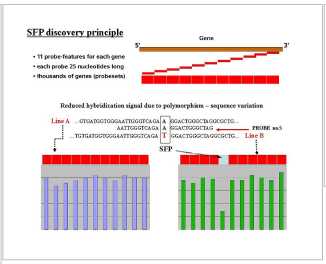

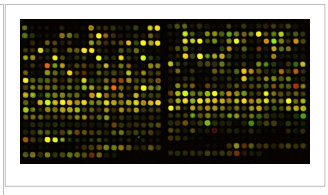

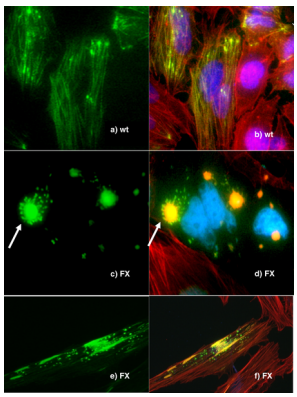

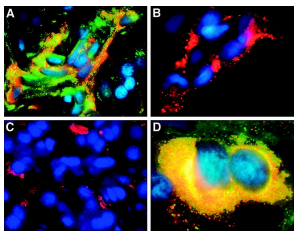

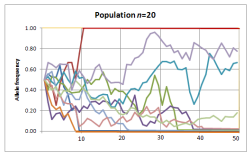

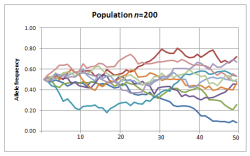

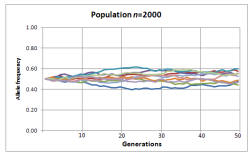

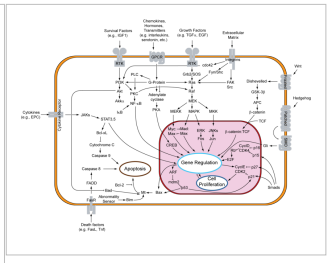

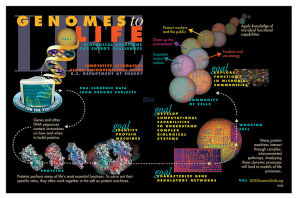

Databases for Genomics, DNA Dynamics and Sequencing

Genomic and structural databases

- CBS Genome Atlas Database [57] — contains examples of base skews.[13]
- The Z curve database of genomes — a 3-dimensional visualization and analysis tool of genomes [59][14] .
- DNA and other nucleic acids' molecular models: Coordinate files of nucleic acids molecular structure models in PDB and CIF formats [61]

Mass spectrometry--Maldi informatics

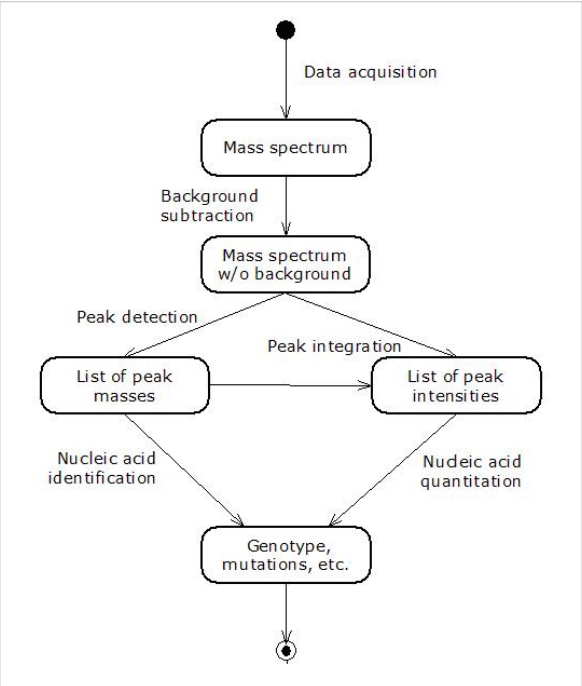

DNA Dynamics Data from Spectroscopy

- FT-NMR[15] [16]
  - NMR Atlas--database [29]
  - mmcif downloadable coordinate files of nucleic acids in solution from 2D-FT NMR data [30]
  - NMR constraints files for NAs in PDB format [31]
- NMR microscopy[17]
- Vibrational circular dichroism (VCD)
- Microwave spectroscopy
- FT-IR
- FT-NIR[18] [19] [20]
- Spectral, Hyperspectral, and Chemical imaging)[21] [22] [23] [24] [25] [26] [27] .
- Raman spectroscopy/microscopy[28] and CARS[29] .
- Fluorescence correlation spectroscopy[30] [31] [32] [33] [34] [35] [36] [37] , Fluorescence cross-correlation spectroscopy and FRET[38] [39] [40] .
- Confocal microscopy[41]

Gallery: CARS (Raman spectroscopy), Fluorescence confocal microscopy, and Hyperspectral imaging

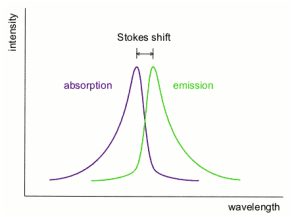

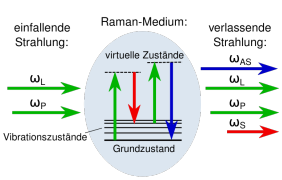

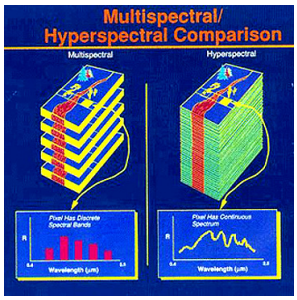

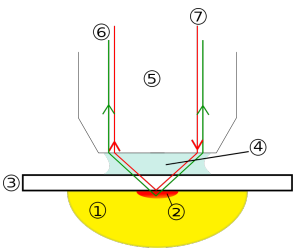

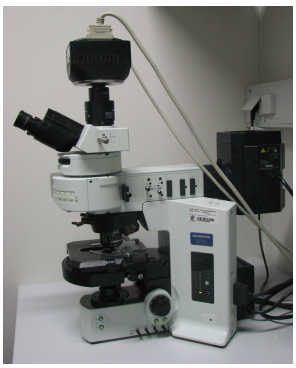

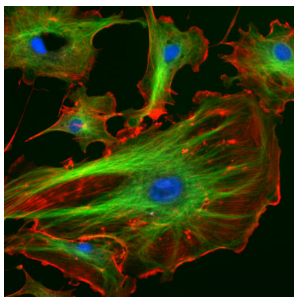

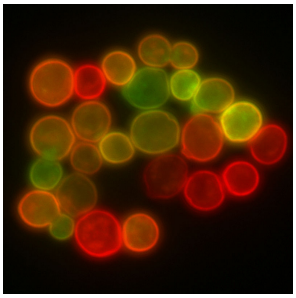

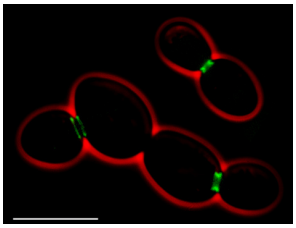

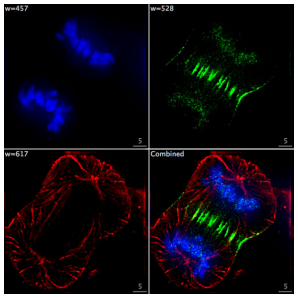

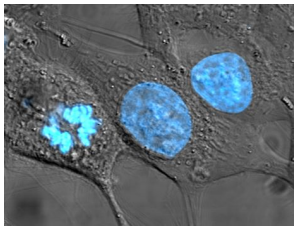

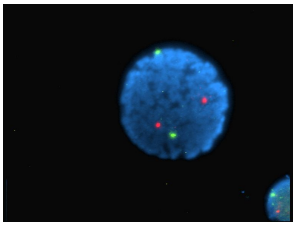

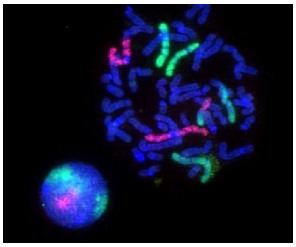

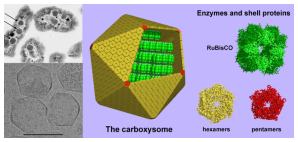

X-ray microscopy

- Application of X-ray microscopy in the analysis of living hydrated cells [18]

Atomic Force Microscopy (AFM)

Two-dimensional DNA junction arrays have been visualized by Atomic Force Microscopy (AFM)[42] . Other imaging resources for AFM/Scanning probe microscopy(SPM) can be freely accessed at:

- How SPM Works [25]
- SPM Image Gallery - AFM STM SEM MFM NSOM and more. [26]

Gallery of AFM Images of DNA Nanostructures

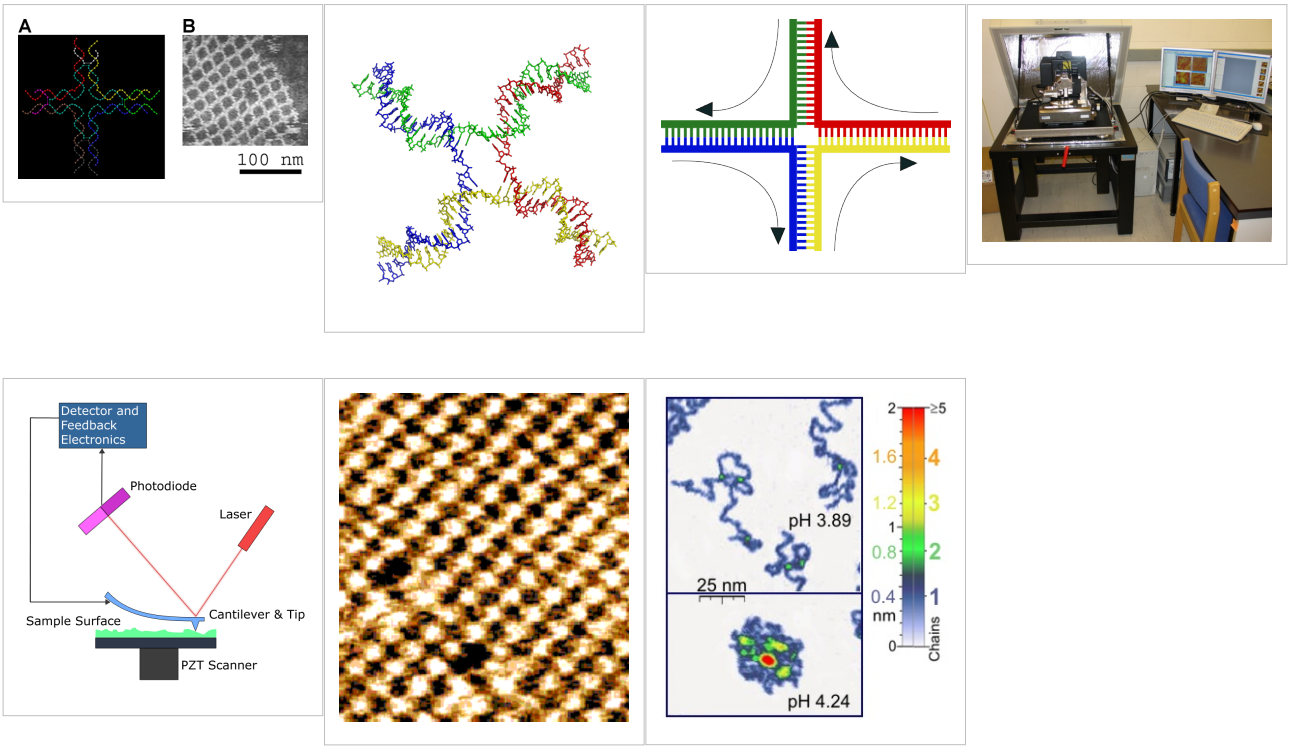

Notes

[1] Franklin, R.E. and Gosling, R.G. recd.6 March 1953. Acta Cryst. (1953). 6, 673 The Structure of Sodium Thymonucleate Fibres I. The Influence of Water Content Acta Cryst. (1953). and 6, 678 The Structure of Sodium Thymonucleate Fibres II. The Cylindrically Symmetrical Patterson Function.

[2] Watson, J.D; Crick F.H.C. 1953a. Molecular Structure of Nucleic Acids- A Structure for Deoxyribose Nucleic Acid., Nature 171(4356):737-738.

[3] Watson, J.D; Crick F.H.C. 1953b. The Structure of DNA., Cold Spring Harbor Symposia on Quantitative Biology 18:123-131.

[4] Wilkins M.H.F., A.R. Stokes A.R. & Wilson, H.R. (1953). "http://www.nature.com/nature/dna50/wilkins.pdf|Molecular Structure of Deoxypentose Nucleic Acids" (PDF). *Nature* **171**: 738–740. doi: 10.1038/171738a0 (http://dx.doi.org/10.1038/171738a0). PMID 13054693. http://www.nature.com/nature/dna50/wilkins.pdf.

[5] Elson D, Chargaff E (1952). "On the deoxyribonucleic acid content of sea urchin gametes". *Experientia* **8** (4): 143-145.

[6] Chargaff E, Lipshitz R, Green C (1952). "Composition of the deoxypentose nucleic acids of four genera of sea-urchin". *J Biol Chem* **195** (1): 155-160. PMID 14938364.

[7] Chargaff E, Lipshitz R, Green C, Hodes ME (1951). "The composition of the deoxyribonucleic acid of salmon sperm". *J Biol Chem* **192** (1): 223-230. PMID 14917668.

[8] Chargaff E (1951). "Some recent studies on the composition and structure of nucleic acids". *J Cell Physiol Suppl* **38** (Suppl).
[9] Magasanik B, Vischer E, Doniger R, Elson D, Chargaff E (1950). "The separation and estimation of ribonucleotides in minute quantities". *J Biol Chem* **186** (1): 37-50. PMID 14778802.
[10] Chargaff E (1950). "Chemical specificity of nucleic acids and mechanism of their enzymatic degradation". *Experientia* **6** (6): 201-209.
[11] http://www.phy.cam.ac.uk/research/bss/molbiophysics.php
[12] http://planetphysics.org/encyclopedia/TheoreticalBiophysics.html
[13] Hallin PF, David Ussery D (2004). "CBS Genome Atlas Database: A dynamic storage for bioinformatic results and DNA sequence data". *Bioinformatics* **20**: 3682-3686.
[14] Zhang CT, Zhang R, Ou HY (2003). "The Z curve database: a graphic representation of genome sequences". Bioinformatics 19 (5): 593-599. doi:10.1093/bioinformatics/btg041
[15] (http://www.jonathanpmiller.com/Karplus.html)- obtaining dihedral angles from ^{3}J coupling constants
[16] (http://www.spectroscopynow.com/FCKeditor/UserFiles/File/specNOW/HTML files/General_Karplus_Calculator.htm) Another Javascript-like NMR coupling constant to dihedral
[17] Lee, S. C. et al., (2001). One Micrometer Resolution NMR Microscopy. *J. Magn. Res.*, **150**: 207-213.
[18] Near Infrared Microspectroscopy, Fluorescence Microspectroscopy,Infrared Chemical Imaging and High Resolution Nuclear Magnetic Resonance Analysis of Soybean Seeds, Somatic Embryos and Single Cells., Baianu, I.C. et al. 2004., In *Oil Extraction and Analysis.*, D. Luthria, Editor pp.241-273, AOCS Press., Champaign, IL.
[19] Single Cancer Cell Detection by Near Infrared Microspectroscopy, Infrared Chemical Imaging and Fluorescence Microspectroscopy.2004.I. C. Baianu, D. Costescu, N. E. Hofmann and S. S. Korban, q-bio/0407006 (July 2004) (http://arxiv.org/abs/q-bio/0407006)
[20] Raghavachari, R., Editor. 2001. *Near-Infrared Applications in Biotechnology*, Marcel-Dekker, New York, NY.
[21] http://www.imaging.net/chemical-imaging/Chemical imaging
[22] http://www.malvern.com/LabEng/products/sdi/bibliography/sdi_bibliography.htm E. N. Lewis, E. Lee and L. H. Kidder, Combining Imaging and Spectroscopy: Solving Problems with Near-Infrared Chemical Imaging. Microscopy Today, Volume 12, No. 6, 11/2004.
[23] D.S. Mantus and G. H. Morrison. 1991. Chemical imaging in biology and medicine using ion microscopy., *Microchimica Acta*, **104**, (1-6) January 1991, doi: 10.1007/BF01245536
[24] Near Infrared Microspectroscopy, Fluorescence Microspectroscopy,Infrared Chemical Imaging and High Resolution Nuclear Magnetic Resonance Analysis of Soybean Seeds, Somatic Embryos and Single Cells., Baianu, I.C. et al. 2004., In *Oil Extraction and Analysis.*, D. Luthria, Editor pp.241-273, AOCS Press., Champaign, IL.
[25] Single Cancer Cell Detection by Near Infrared Microspectroscopy, Infrared Chemical Imaging and Fluorescence Microspectroscopy.2004.I. C. Baianu, D. Costescu, N. E. Hofmann and S. S. Korban, q-bio/0407006 (July 2004) (http://arxiv.org/abs/q-bio/0407006)
[26] J. Dubois, G. Sando, E. N. Lewis, Near-Infrared Chemical Imaging, A Valuable Tool for the Pharmaceutical Industry, G.I.T. Laboratory Journal Europe, No.1-2, 2007.
[27] Applications of Novel Techniques to Health Foods, Medical and Agricultural Biotechnology.(June 2004).,I. C. Baianu, P. R. Lozano, V. I. Prisecaru and H. C. Lin q-bio/0406047 (http://arxiv.org/abs/q-bio/0406047)
[28] Chemical Imaging Without Dyeing (http://witec.de/en/download/Raman/ImagingMicroscopy04.pdf)
[29] C.L. Evans and X.S. Xie.2008. Coherent Anti-Stokes Raman Scattering Microscopy: Chemical Imaging for Biology and Medicine., doi:10.1146/annurev.anchem.1.031207.112754 *Annual Review of Analytical Chemistry*, **1**: 883-909.
[30] Eigen, M., Rigler, M. Sorting single molecules: application to diagnostics and evolutionary biotechnology,(1994) *Proc. Natl. Acad. Sci. USA*, 91,5740-5747.
[31] Rigler, M. Fluorescence correlations, single molecule detection and large number screening. Applications in biotechnology,(1995) J. Biotechnol., 41,177-186.
[32] Rigler R. and Widengren J. (1990). Ultrasensitive detection of single molecules by fluorescence correlation spectroscopy, *BioScience* (Ed. Klinge & Owman) p.180.
[33] Single Cancer Cell Detection by Near Infrared Microspectroscopy, Infrared Chemical Imaging and Fluorescence Microspectroscopy.2004.I. C. Baianu, D. Costescu, N. E. Hofmann, S. S. Korban and et al., q-bio/0407006 (July 2004) (http://arxiv.org/abs/q-bio/0407006)
[34] Oehlenschläger F., Schwille P. and Eigen M. (1996). Detection of HIV-1 RNA by nucleic acid sequence-based amplification combined with fluorescence correlation spectroscopy, *Proc. Natl. Acad. Sci. USA* **93**:1281.
[35] Bagatolli, L.A., and Gratton, E. (2000). Two-photon fluorescence microscopy of coexisting lipid domains in giant unilamellar vesicles of binary phospholipid mixtures. Biophys J., 78:290-305.

[36] Schwille, P., Haupts, U., Maiti, S., and Webb. W.(1999). Molecular dynamics in living cells observed by fluorescence correlation spectroscopy with one- and two-photon excitation. Biophysical Journal, 77(10):2251-2265.
[37] Near Infrared Microspectroscopy, Fluorescence Microspectroscopy,Infrared Chemical Imaging and High Resolution Nuclear Magnetic Resonance Analysis of Soybean Seeds, Somatic Embryos and Single Cells., Baianu, I.C. et al. 2004., In *Oil Extraction and Analysis.*, D. Luthria, Editor pp.241-273, AOCS Press., Champaign, IL.
[38] FRET description (http://dwb.unl.edu/Teacher/NSF/C08/C08Links/pps99.cryst.bbk.ac.uk/projects/gmocz/fret.htm)
[39] doi:10.1016/S0959-440X(00)00190-1 (http://dx.doi.org/10.1016/S0959-440X(00)00190-1)Recent advances in FRET: distance determination in protein–DNA complexes. *Current Opinion in Structural Biology* **2001**, *11(2)*, 201-207
[40] http://www.fretimaging.org/mcnamaraintro.html FRET imaging introduction
[41] Eigen, M., and Rigler, R. (1994). Sorting single molecules: Applications to diagnostics and evolutionary biotechnology, Proc. Natl. Acad. Sci. USA 91:5740.
[42] Mao, Chengde; Sun, Weiqiong & Seeman, Nadrian C. (16 June 1999). "Designed Two-Dimensional DNA Holliday Junction Arrays Visualized by Atomic Force Microscopy". *Journal of the American Chemical Society* **121** (23): 5437–5443. doi: 10.1021/ja9900398 (http://dx.doi.org/10.1021/ja9900398). ISSN 0002-7863 (http://worldcat.org/issn/0002-7863).

References

- Sir Lawrence Bragg, FRS. *The Crystalline State, A General survey.* London: G. Bells and Sons, Ltd., vols. 1 and 2., 1966., 2024 pages.
- F. Bessel, *Untersuchung des Theils der planetarischen Störungen*, Berlin Abhandlungen (1824), article 14.
- Cantor, C. R. and Schimmel, P.R. *Biophysical Chemistry, Parts I and II.*, San Franscisco: W.H. Freeman and Co. 1980. 1,800 pages.
- Eigen, M., and Rigler, R. (1994). Sorting single molecules: Applications to diagnostics and evolutionary biotechnology, *Proc. Natl. Acad. Sci. USA* **91**:5740.
- Raghavachari, R., Editor. 2001. *Near-Infrared Applications in Biotechnology*, Marcel-Dekker, New York, NY.
- Rigler R. and Widengren J. (1990). Ultrasensitive detection of single molecules by fluorescence correlation spectroscopy, *BioScience* (Ed. Klinge & Owman) p.180.
- *Applications of Novel Techniques to Health Foods, Medical and Agricultural Biotechnology*.(June 2004) I. C. Baianu, P. R. Lozano, V. I. Prisecaru and H. C. Lin., q-bio/0406047.
- Single Cancer Cell Detection by Near Infrared Microspectroscopy, Infrared Chemical Imaging and Fluorescence Microspectroscopy.2004. I. C. Baianu, D. Costescu, N. E. Hofmann, S. S. Korban and et al., q-bio/0407006 (July 2004).
- Voet, D. and J.G. Voet. *Biochemistry*, 2nd Edn., New York, Toronto, Singapore: John Wiley & Sons, Inc., 1995, ISBN 0-471-58651-X., 1361 pages.
- Watson, G. N. *A Treatise on the Theory of Bessel Functions.*, (1995) Cambridge University Press. ISBN 0-521-48391-3.
- Watson, James D. and Francis H.C. Crick. A structure for Deoxyribose Nucleic Acid (http://www.nature.com/nature/dna50/watsoncrick.pdf) (PDF). *Nature* 171, 737–738, 25 April 1953.
- Watson, James D. *Molecular Biology of the Gene.* New York and Amsterdam: W.A. Benjamin, Inc. 1965., 494 pages.
- Wentworth, W.E. *Physical Chemistry. A short course.*, Malden (Mass.): Blackwell Science, Inc. 2000.

- Herbert R. Wilson, FRS. *Diffraction of X-rays by proteins, Nucleic Acids and Viruses.*, London: Edward Arnold (Publishers) Ltd. 1966.
- Kurt Wuthrich. *NMR of Proteins and Nucleic Acids.*, New York, Brisbane,Chicester, Toronto, Singapore: J. Wiley & Sons. 1986., 292 pages.
- Robinson, Bruche H.; Seeman, Nadrian C. (August 1987). "The Design of a Biochip: A Self-Assembling Molecular-Scale Memory Device". *Protein Engineering* **1** (4): 295–300. ISSN 0269-2139 (http://worldcat.org/issn/0269-2139). Link (http://peds.oxfordjournals.org/cgi/content/abstract/1/4/295)
- Rothemund, Paul W. K.; Ekani-Nkodo, Axel; Papadakis, Nick; Kumar, Ashish; Fygenson, Deborah Kuchnir & Winfree, Erik (22 December 2004). "Design and Characterization of Programmable DNA Nanotubes". *Journal of the American Chemical Society* **126** (50): 16344–16352. doi: 10.1021/ja044319l (http://dx.doi.org/10.1021/ja044319l). ISSN 0002-7863 (http://worldcat.org/issn/0002-7863).
- Keren, K.; Kinneret Keren, Rotem S. Berman, Evgeny Buchstab, Uri Sivan, Erez Braun (November 2003). "http://www.sciencemag.org/cgi/content/abstract/sci;302/5649/1380|DNA-Templated Carbon Nanotube Field-Effect Transistor". *Science* **302** (6549): 1380–1382. doi: 10.1126/science.1091022 (http://dx.doi.org/10.1126/science.1091022). ISSN 1095-9203 (http://worldcat.org/issn/1095-9203). http://www.sciencemag.org/cgi/content/abstract/sci;302/5649/1380.
- Zheng, Jiwen; Constantinou, Pamela E.; Micheel, Christine; Alivisatos, A. Paul; Kiehl, Richard A. & Seeman Nadrian C. (2006). "2D Nanoparticle Arrays Show the Organizational Power of Robust DNA Motifs". *Nano Letters* **6**: 1502–1504. doi: 10.1021/nl060994c (http://dx.doi.org/10.1021/nl060994c). ISSN 1530-6984 (http://worldcat.org/issn/1530-6984).
- Cohen, Justin D.; Sadowski, John P.; Dervan, Peter B. (2007). "Addressing Single Molecules on DNA Nanostructures". *Angewandte Chemie* **46** (42): 7956–7959. doi: 10.1002/anie.200702767 (http://dx.doi.org/10.1002/anie.200702767). ISSN 0570-0833 (http://worldcat.org/issn/0570-0833).
- Mao, Chengde; Sun, Weiqiong & Seeman, Nadrian C. (16 June 1999). "Designed Two-Dimensional DNA Holliday Junction Arrays Visualized by Atomic Force Microscopy". *Journal of the American Chemical Society* **121** (23): 5437–5443. doi: 10.1021/ja9900398 (http://dx.doi.org/10.1021/ja9900398). ISSN 0002-7863 (http://worldcat.org/issn/0002-7863).
- Constantinou, Pamela E.; Wang, Tong; Kopatsch, Jens; Israel, Lisa B.; Zhang, Xiaoping; Ding, Baoquan; Sherman, William B.; Wang, Xing; Zheng, Jianping; Sha, Ruojie & Seeman, Nadrian C. (2006). "Double cohesion in structural DNA nanotechnology". *Organic and Biomolecular Chemistry* **4**: 3414–3419. doi: 10.1039/b605212f (http://dx.doi.org/10.1039/b605212f).

See also

- DNA
- Molecular modeling of DNA
- Genomics
- Signal transduction
- Transcriptomics
- Interactomics
- Biotechnology
- Molecular graphics
- Quantum computing
- MAYA-II
- DNA computing
- DNA structure
- Molecular structure
- Molecular dynamics
- Molecular topology
- DNA topology
- DNA, the Genome and Interactome
- Molecular structure
- Molecular geometry fluctuations
- Molecular interactions
- Molecular topology
- Hydrogen bonding
- Hydrophobic interactions
- DNA dynamics and conformations
- DNA Conformational isomerism
- 2D-FT NMRI and Spectroscopy
- Paracrystalline lattices/Paracrystals
- NMR Spectroscopy
- VCD or Vibrational circular dichroism
- Microwave spectroscopy
- Two-dimensional IR spectroscopy
- FRET and FCS- Fluorescence correlation spectroscopy
- Fluorescence cross-correlation spectroscopy (FCCS)
- Spectral imaging
- Hyperspectral imaging
- Chemical imaging
- NMR microscopy
- X-ray scattering
- Neutron scattering
- Crystallography
- Crystal lattices
- Molecular geometry
- Nanostructure
- DNA nanotechnology
- Imaging
- Sirius visualization software

- Atomic force microscopy
- X-ray microscopy
- Liquid crystals
- Glasses
- QMC@Home
- Sir Lawrence Bragg, FRS
- Sir John Randall
- Francis Crick
- Manfred Eigen
- Felix Bloch
- Paul Lauterbur
- Maurice Wilkins
- Herbert Wilson, FRS
- Alex Stokes

External links

- DNAlive: a web interface to compute DNA physical properties (http://mmb.pcb.ub.es/DNAlive). Also allows cross-linking of the results with the UCSC Genome browser and DNA dynamics.
- Application of X-ray microscopy in analysis of living hydrated cells (http://www.ncbi.nlm.nih.gov/entrez/query.fcgi?cmd=Retrieve&db=pubmed&dopt=Abstract&list_uids=12379938)
- DiProDB: Dinucleotide Property Database (http://diprodb.fli-leibniz.de). The database is designed to collect and analyse thermodynamic, structural and other dinucleotide properties.
- DNA the Double Helix Game (http://nobelprize.org/educational_games/medicine/dna_double_helix/) From the official Nobel Prize web site
- MDDNA: Structural Bioinformatics of DNA (http://humphry.chem.wesleyan.edu:8080/MDDNA/)
- Double Helix 1953–2003 (http://www.ncbe.reading.ac.uk/DNA50/) National Centre for Biotechnology Education
- DNA under electron microscope (http://www.fidelitysystems.com/Unlinked_DNA.html)
- Further details of mathematical and molecular analysis of DNA structure based on X-ray data (http://planetphysics.org/encyclopedia/BesselFunctionsApplicationsToDiffractionByHelicalStructures.html)
- Bessel functions corresponding to Fourier transforms of atomic or molecular helices. (http://planetphysics.org/?op=getobj&from=objects&name=BesselFunctionsAndTheirApplicationsToDiffractionByHelicalStructures)
- Characterization in nanotechnology some pdfs (http://nanocharacterization.sitesled.com/)
- An overview of STM/AFM/SNOM principles with educative videos (http://www.ntmdt.ru/SPM-Techniques/Principles/)
- SPM Image Gallery - AFM STM SEM MFM NSOM and More (http://www.rhk-tech.com/results/showcase.php)
- How SPM Works (http://www.parkafm.com/New_html/resources/01general.php)

- U.S. National DNA Day (http://www.genome.gov/10506367) — watch videos and participate in real-time discussions with scientists.
- The Secret Life of DNA - DNA Music compositions (http://www.tjmitchell.com/stuart/dna.html)
- Ascalaph DNA (http://www.agilemolecule.com/Ascalaph/Ascalaph_DNA.html) — Commercial software for DNA modeling

DNA nanotechnology

Part of a series of articles on **Molecular self-assembly**
Self-assembled monolayer Supramolecular assembly DNA nanotechnology
See also Nanotechnology

DNA nanotechnology is a subfield of nanotechnology which seeks to use the unique molecular recognition properties of DNA and other nucleic acids to create novel, controllable structures out of DNA. The DNA is thus used as a structural material rather than as a carrier of genetic information, making it an example of bionanotechnology. This has possible applications in molecular self-assembly and in DNA computing.

Introduction: DNA crossover molecules

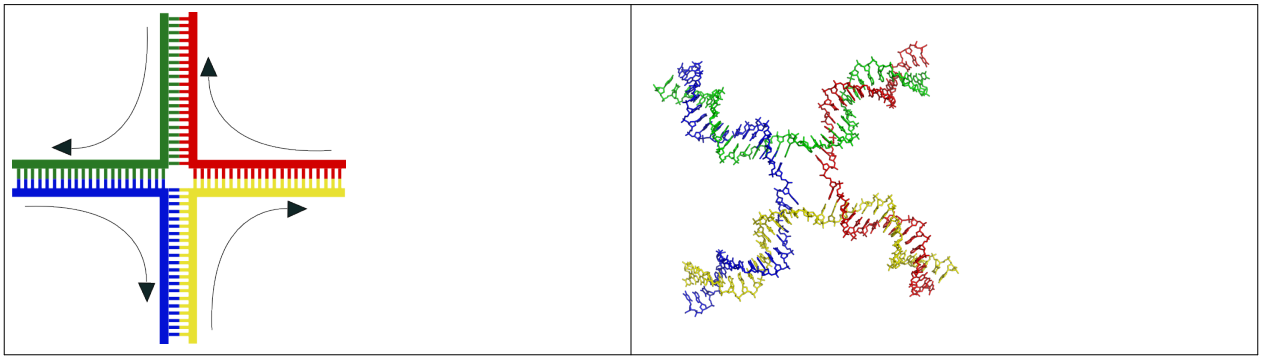

Structure of the 4-arm junction.
Left: A schematic. **Right**: A more realistic model.[1]
Each of the four separate DNA single strands are shown in different colors.

DNA nanotechnology makes use of branched DNA structures to create DNA complexes with useful properties. DNA is normally a linear molecule, in that its axis is unbranched. However, DNA molecules containing junctions can also be made. For example, a four-arm junction can be made using four individual DNA strands which are complementary to each other in the correct pattern. Due to Watson-Crick base pairing, only portions of the strands which are complementary to each other will attach to each other to form duplex DNA. This four-arm junction is an immobile form of a Holliday junction.

Junctions can be used in more complex molecules. The most important of these is the "double-crossover" or DX motif. Here, two DNA duplexes lie next to each other, and share two junction points where strands cross from one duplex into the other. This molecule has the advantage that the junction points are now constrained to a single orientation as opposed to being flexible as in the four-arm junction. This makes the DX motif suitible as a structural building block for larger DNA complexes.[3]

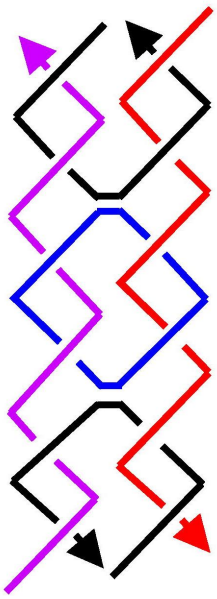

A double-crossover (DX) molecule. This molecule consists of five DNA single strands which form two double-helical domains, on the left and the right in this image. There are two crossover points where the strands cross from one domain into the other. Image from Mao, 2004. [2]

Tile-based arrays

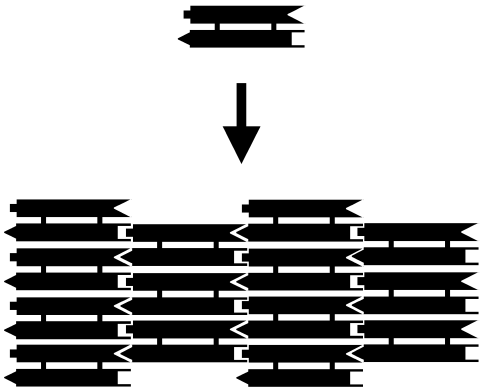

Assembly of a DX array. Each bar represents a double-helical domain of DNA, with the shapes representing comlimentary sticky ends. The DX molecule at top will combine into the two-dimensional DNA array shown at bottom. Image from Mao, 2004. [2]

DX arrays

DX, Double Crossover, molecules can be equipped with sticky ends in order to combine them into a two-dimenstional periodic lattice. Each DX molecule has four termini, one at each end of the two double-helical domains, and these can be equipped with sticky ends that program them to combine into a specific pattern. More than one type of DX can be used which can be made to arrange in rows or any other tessellated pattern. They thus form extended flat sheets which are essentially two-dimensional crystals of DNA.[4]

DNA nanotubes

In addition to flat sheets, DX arrays have been made to form hollow tubes of 4-20 nm diameter. These DNA nanotubes are somewhat similar in size and shape to carbon nanotubes, but the carbon nanotubes are stronger and better conductors, whereas the DNA nanotubes are more easily modified and connected to other structures.[5]

Other tile arrays

Two-dimensional arrays have been made out of other motifs as well, including the Holliday junction rhombus array as well as various DX-based arrays in the shapes of triangles and hexagons.[6] Another motif, the six-helix bundle, has the ability to form three-dimensional DNA arrays as well.[7]

DNA origami

As an alternative to the tile-based approach, two-dimensional DNA structures can be made from a single, long DNA strand of arbitrary sequence which is folded into the desired shape by using shorter, "staple" strands. This allows the creation of two-dimensional shapes at the nanoscale using DNA. Demonstrated designs have included the smiley face and a coarse map of North America. DNA origami was the cover story of *Nature* on March 15, 2006.[8]

DNA polyhedra

A number of three-dimensional DNA molecules have been made which have the connectivity of a polyhedron such as an octahedron or cube. In other words, the DNA duplexes trace the edges of a polyhedron with a DNA junction at each vertex. The earliest demonstrations of DNA polyhedra involved multiple ligations and solid-phase synthesis steps to create catenated polyhedra. More recently, there have been demonstrations of a DNA truncated octahedron made from a long single strand designed to fold into the correct conformation, as well as a tetrahedron which can be produced from four DNA strands in a single step.[9]

DNA nanomechanical devices

DNA complexes have been made which change their conformation upon some stimulus. These are intended to have applications in nanorobotics. One of the first such devices, called "molecular tweezers," changes from an open to a closed state based upon the presence of control strands.

DNA machines have also been made which show a twisting motion. One of these makes use of the transition between the B-DNA and Z-DNA forms to respond to a change in buffer conditions. Another relies on the presence of control strands to switch from a paranemic-crossover (PX) conformation to a double-junction (JX2) conformation.[10]

Stem Loop Controllers

A design called a *stem loop*, consisting of a single strand of DNA which has a loop at an end, are a dynamic structure that opens and closes when a piece of DNA bonds to the loop part. This effect has been exploited to create several logic gates. [11] [12] These logic gates have been used to create the computers MAYA I and MAYA II which can play tick-tac-toe to some extent.[13]

Applications

Algorithmic self-assembly

DNA nanotechnology has been applied to the related field of DNA computing. A DX array has been demonstrated whose assembly encodes an XOR operation, which allows the DNA array to implement a cellular automaton which generates a fractal called the Sierpinski gasket. This shows that computation can be incorporated into the assembly of DNA arrays, increasing its scope beyond simple periodic arrays.

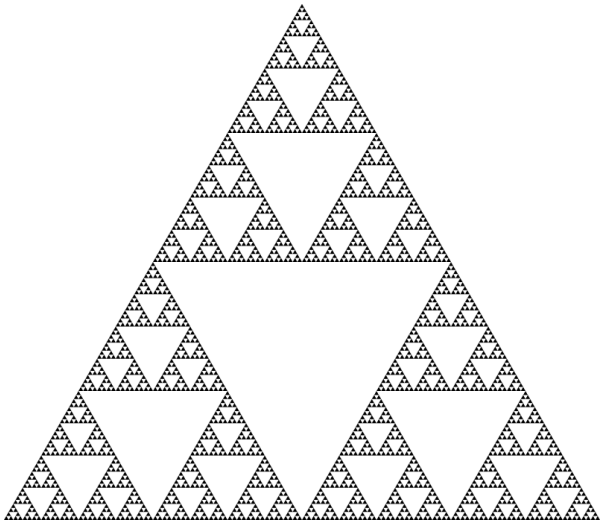

The Sierpinski gasket.

Note that DNA computing overlaps with, but is distinct from, DNA nanotechnology. The latter uses the specificity of Watson-Crick basepairing to make novel structures out of DNA. These structures can be used for DNA computing, but they do not have to be. Additionally, DNA computing can be done without using the types of molecules made possible by DNA Nanotechnology.[15]

Nanoarchitecture

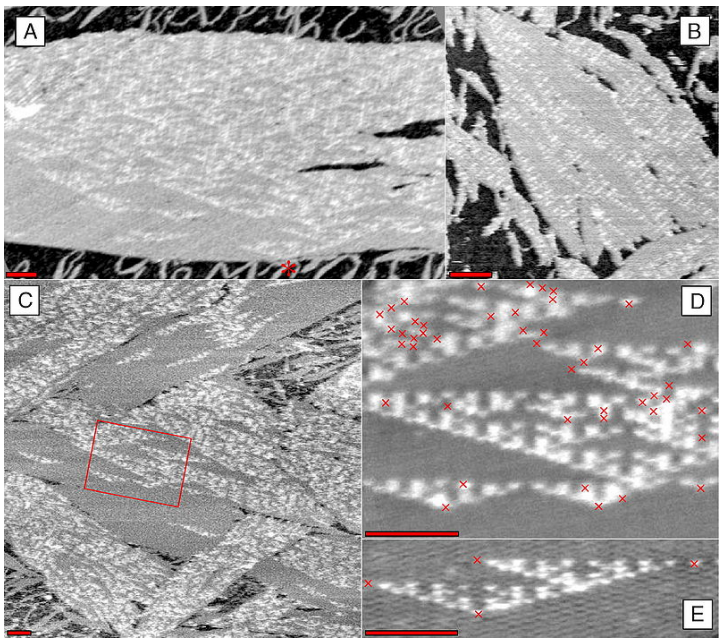

DNA arrays that display a representation of the Sierpinski gasket on their surfaces. Click the image for further details. Image from Rothemund *et al.*, 2004. [14]

The idea of using DNA arrays to template the assembly of other functional molecules has been around for a while, but only recently has progress been made in reducing these kinds of schemes to practice. In 2006, researchers covalently attached gold nanoparticles to a DX-based tile and showed that self-assembly of the DNA structures also assembled the nanoparticles hosted on them. A non-covalent hosting scheme was shown in 2007, using Dervan polyamides on a DX array to arrange streptavidin proteins on specific kinds of tiles on the DNA array.[16] Previously in 2006 LaBean demonstrated the letters "D" "N" and "A" created on a 4x4 DX array using streptavidin. [17]

DNA has also been used to assemble a single walled carbon nanotube Field-effect transistor.[18]

See also

- Mechanical properties of DNA

External links

- Chengde Mao page at Purdue University [19]
- John Reif lab at Duke University [20]
- Nadrian Seeman lab at NYU [21]
- William M. Shih lab at Harvard Medical School [22]
- Andrew Turberfield lab at Oxford University [23]
- Erik Winfree lab at Caltech [24]
- Hao Yan lab at Arizona State University [25]
- Bernard Yurke formerly at Bell Labs [26] now at Boise State University [27]
- Thom LaBean at Duke University [28]
- Software for 3D DNA design, modeling and/or simulation:
  - Ascalaph Designer [29]
  - caDNAno [30]
  - GIDEON [31]
  - NanoEngineer-1 [32]
- International Society for Nanoscale Science, Computation and Engineering [33]

References

Note: Click on the doi to access the text of the referenced article.

[1] Created from PDB 1M6G (http://www.rcsb.org/pdb/explore/explore.do?structureId=1M6G)
[2] http://dx.doi.org/10.1371/journal.pbio.0020431

- Seeman, Nadrian C. (1 November 1999). "DNA Engineering and its Application to Nanotechnology". *Trends in Biotechnology* **17** (11): 437–443. doi: 10.1016/S0167-7799(99)01360-8 (http://dx.doi.org/10.1016/S0167-7799(99)01360-8). ISSN 0167-7799 (http://worldcat.org/issn/0167-7799).
- Seeman, Nadrian C. (January 2001). "DNA Nicks and Nodes and Nanotechnology". *Nano Letters* **1** (1): 22–26. doi: 10.1021/nl000182v (http://dx.doi.org/10.1021/nl000182v). ISSN 1530-6984 (http://worldcat.org/issn/1530-6984).
- Mao, Chengde (December 2004). "The Emergence of Complexity: Lessons from DNA". *PLoS Biology* **2** (12): 2036–2038. doi: 10.1371/journal.pbio.0020431 (http://dx.doi.org/10.1371/journal.pbio.0020431). ISSN 1544-9173 (http://worldcat.org/issn/1544-9173).
- Kumara, Mudalige T. (July 2008). "Assembly pathway analysis of DNA nanostructures and the construction of parallel motifs". *Nano Letters* **8** (7): 1971–1977. doi: 10.1021/nl800907y (http://dx.doi.org/10.1021/nl800907y). ISSN .
- Winfree, Erik; Liu, Furong; Wenzler, Lisa A. & Seeman, Nadrian C. (6 August 1998). "Design and self-assembly of two-dimensional DNA crystals". *Nature* **394**: 529–544. doi: 10.1038/28998 (http://dx.doi.org/10.1038/28998). ISSN 0028-0836 (http://worldcat.org/issn/0028-0836).
- Liu, Furong; Sha, Ruojie & Seeman, Nadrian C. (10 February 1999). "Modifying the Surface Features of Two-Dimensional DNA Crystals". *Journal of the American Chemical Society* **121** (5): 917–922. doi: 10.1021/ja982824a (http://dx.doi.org/10.1021/ja982824a). ISSN 0002-7863 (http://worldcat.org/issn/0002-7863).
- Rothemund, Paul W. K.; Ekani-Nkodo, Axel; Papadakis, Nick; Kumar, Ashish; Fygenson, Deborah Kuchnir & Winfree, Erik (22 December 2004). "Design and Characterization of Programmable DNA Nanotubes". *Journal of the American Chemical Society* **126** (50): 16344–16352. doi: 10.1021/ja044319l (http://dx.doi.org/10.1021/ja044319l). ISSN 0002-7863 (http://worldcat.org/issn/0002-7863).
- Mao, Chengde; Sun, Weiqiong & Seeman, Nadrian C. (16 June 1999). "Designed Two-Dimensional DNA Holliday Junction Arrays Visualized by Atomic Force Microscopy". *Journal of the American Chemical Society* **121** (23): 5437–5443. doi: 10.1021/ja9900398 (http://dx.doi.org/10.1021/ja9900398). ISSN 0002-7863 (http://worldcat.org/issn/0002-7863).
- Constantinou, Pamela E.; Wang, Tong; Kopatsch, Jens; Israel, Lisa B.; Zhang, Xiaoping; Ding, Baoquan; Sherman, William B.; Wang, Xing; Zheng, Jianping; Sha, Ruojie & Seeman, Nadrian C. (2006). "Double cohesion in structural DNA nanotechnology". *Organic and Biomolecular Chemistry* **4**: 3414–3419. doi: 10.1039/b605212f (http://dx.doi.org/10.1039/b605212f).
- Mathieu, Frederick; Liao, Shiping; Kopatsch, Jens; Wang, Tong; Mao, Chengde & Seeman, Nadrian C. (April 2005). "Six-Helix Bundles Designed from DNA". *Nano Letters* **5** (4): 661–665. doi: 10.1021/nl050084f (http://dx.doi.org/10.1021/nl050084f). ISSN 1530-6984 (http://worldcat.org/issn/1530-6984).
- Rothemund, Paul W. K. (2006). "Folding DNA to create nanoscale shapes and patterns". *Nature* **440**: 297–302. doi: 10.1038/nature04586 (http://dx.doi.org/10.1038/nature04586). ISSN 0028-0836 (http://worldcat.org/issn/0028-0836).
- Zhang, Yuwen; Seeman, Nadrian C. (1994). "Construction of a DNA-truncated octahedron". *Journal of the American Chemical Society* **116** (5): 1661–1669. doi: 10.1021/ja00084a006 (http://dx.doi.org/10.1021/ja00084a006). ISSN 0002-7863 (http://worldcat.org/issn/0002-7863).
- Shih, William M.; Quispe, Joel D.; Joyce, Gerald F. (12 February 2004). "A 1.7-kilobase single-stranded DNA that folds into a nanoscale octahedron". *Nature* **427**: 618–621. doi: 10.1038/nature02307 (http://dx.doi.org/10.1038/nature02307). ISSN 0028-0836 (http://worldcat.org/issn/0028-0836).
- Goodman, R.P.; Schaap, I.A.T.; Tardin, C.F.; Erben, C.M.; Berry, R.M.; Schmidt, C.F.; Turberfield, A.J. (9 December 2005). "Rapid chiral assembly of rigid DNA building blocks for molecular nanofabrication". *Science* **310** (5754): 1661–1665. doi: 10.1126/science.1120367 (http://dx.doi.org/10.1126/science.1120367). ISSN 0036-8075 (http://worldcat.org/issn/0036-8075).
- Yurke, Bernard; Turberfield, Andrew J.; Mills, Allen P., Jr; Simmel, Friedrich C. & Neumann, Jennifer L. (10 August 2000). "A DNA-fuelled molecular machine made of DNA". *Nature* **406**: 605–609. doi: 10.1038/35020524 (http://dx.doi.org/10.1038/35020524). ISSN 0028-0836 (http://worldcat.org/issn/

0028-0836).

- Mao, Chengde; Sun, Weiqiong; Shen, Zhiyong & Seeman, Nadrian C. (14 January 1999). "A DNA Nanomechanical Device Based on the B-Z Transition". *Nature* **397**: 144–146. doi: 10.1038/16437 (http://dx.doi.org/10.1038/16437). ISSN .
- Yan, Hao; Zhang, Xiaoping; Shen, Zhiyong & Seeman, Nadrian C. (3 January 2002). "A robust DNA mechanical device controlled by hybridization topology". *Nature* **415**: 62–65. doi: 10.1038/415062a (http://dx.doi.org/10.1038/415062a). ISSN .

[11] DNA Logic Gates (https://digamma.cs.unm.edu/wiki/bin/view/McogPublicWeb/MolecularLogicGates)
[12] (http://www.duke.edu/~jme17/Joshua_E._Mendoza-Elias/Research_Ideas.html)
[13] MAYA II (https://digamma.cs.unm.edu/wiki/bin/view/McogPublicWeb/MolecularAutomataMAYAII)
[14] http://dx.doi.org/10.1371/journal.pbio.0020424

- Rothemund, Paul W. K.; Papadakis, Nick & Winfree, Erik (December 2004). "Algorithmic Self-Assembly of DNA Sierpinski Triangles". *PLoS Biology* **2** (12): 2041–2053. doi: 10.1371/journal.pbio.0020424 (http://dx.doi.org/10.1371/journal.pbio.0020424). ISSN 1544-9173 (http://worldcat.org/issn/1544-9173).
- Robinson, Bruche H.; Seeman, Nadrian C. (August 1987). "The Design of a Biochip: A Self-Assembling Molecular-Scale Memory Device". *Protein Engineering* **1** (4): 295–300. ISSN 0269-2139 (http://worldcat.org/issn/0269-2139). Link (http://peds.oxfordjournals.org/cgi/content/abstract/1/4/295)
- Zheng, Jiwen; Constantinou, Pamela E.; Micheel, Christine; Alivisatos, A. Paul; Kiehl, Richard A. & Seeman Nadrian C. (2006). "2D Nanoparticle Arrays Show the Organizational Power of Robust DNA Motifs". *Nano Letters* **6**: 1502–1504. doi: 10.1021/nl060994c (http://dx.doi.org/10.1021/nl060994c). ISSN 1530-6984 (http://worldcat.org/issn/1530-6984).
- Cohen, Justin D.; Sadowski, John P.; Dervan, Peter B. (2007). "Addressing Single Molecules on DNA Nanostructures". *Angewandte Chemie* **46** (42): 7956–7959. doi: 10.1002/anie.200702767 (http://dx.doi.org/10.1002/anie.200702767). ISSN 0570-0833 (http://worldcat.org/issn/0570-0833).

[17] Park, Sung Ha; Sung Ha Park, Constantin Pistol, Sang Jung Ahn, John H. Reif, Alvin R. Lebeck, Chris Dwyer, Thomas H. LaBean (October 2006). "http://www3.interscience.wiley.com/journal/113390879/abstract|Finite-Size, Fully Addressable DNA Tile Lattices Formed by Hierarchical Assembly Procedures". *Angewandte Chemie* **118** (40): 749–753. doi: 10.1002/ange.200690141 (http://dx.doi.org/10.1002/ange.200690141). ISSN 1521-3757 (http://worldcat.org/issn/1521-3757). http://www3.interscience.wiley.com/journal/113390879/abstract.
[18] Keren, K.; Kinneret Keren, Rotem S. Berman, Evgeny Buchstab, Uri Sivan, Erez Braun (November 2003). "http://www.sciencemag.org/cgi/content/abstract/sci;302/5649/1380|DNA-Templated Carbon Nanotube Field-Effect Transistor". *Science* **302** (6549): 1380–1382. doi: 10.1126/science.1091022 (http://dx.doi.org/10.1126/science.1091022). ISSN 1095-9203 (http://worldcat.org/issn/1095-9203). http://www.sciencemag.org/cgi/content/abstract/sci;302/5649/1380.
[19] http://www.chem.purdue.edu/people/faculty/faculty.asp?itemID=46
[20] http://www.cs.duke.edu/~reif/BMC/Reif.BMCproject.html
[21] http://seemanlab4.chem.nyu.edu/
[22] http://research2.dfci.harvard.edu/shih/SHIH_LAB/Home.html
[23] http://www.physics.ox.ac.uk/cm/people/turberfield.htm
[24] http://dna.caltech.edu/
[25] http://chemistry.asu.edu/faculty/hao_yan.asp
[26] http://www.bell-labs.com/org/physicalsciences/profiles/yurke.html
[27] http://coen.boisestate.edu/departments/faculty.asp?ID=134
[28] http://www.cs.duke.edu/~thl/
[29] http://www.agilemolecule.com/Ascalaph/Ascalaph_Designer.html
[30] http://cadnano.org
[31] http://www.subirac.com
[32] http://www.nanoengineer-1.net
[33] http://www.isnsce.org/

Imaging

Imaging is the representation or reproduction of an object's outward form; especially a visual representation (i.e., the formation of an image).

Imaging methodologies and technologies

- Chemical imaging, the simultaneous measurement of spectra and pictures
- Creation of a disk image, a file which contains the exact content of a non-volatile computer data storage medium. See also disk cloning
- Digital imaging, creating digital images, generally by scanning, or through digital photography
- Document imaging, replicating documents commonly used in business
- Geophysical imaging
- Medical imaging, creating images of the human body or parts of it, to diagnose or examine disease
  - Magnetic resonance imaging
- Molecular imaging
- Optical imaging
- Personal imaging, real-time sharing of personal experience through images
- Radar imaging, or imaging radar, for obtaining an image of an object, not just its location and speed
- Reprography, reproduction of graphics through electrical and mechanical means
  - Cinematography
  - Photography, the process of creating still images
  - Xerography, the method of photocopying
- Speckle imaging, a method of shift-and-add for astronomical imaging
- Stereo imaging, an aspect of sound recording and reproduction concerning spatial locations of the performers
- Thermography, infrared imaging

Proper names

- Imaging for Windows, a software product for scanning paper documents

See also

- Image processing
- Imaging technology
- Imaging science, which includes many fields of science
- Remote sensing, imaging the Earth or a planet from space or aircraft

Atomic force microscope

The **atomic force microscope** (AFM) or scanning force microscope (SFM) is a very high-resolution type of scanning probe microscopy, with demonstrated resolution of fractions of a nanometer, more than 1000 times better than the optical diffraction limit. The precursor to the AFM, the scanning tunneling microscope, was developed by Gerd Binnig and Heinrich Rohrer in the early 1980s, a development that earned them the Nobel Prize for Physics in 1986. Binnig, Quate and Gerber invented the first AFM in 1986. The AFM is one of the foremost tools for imaging, measuring and manipulating matter at the nanoscale. The information is gathered by "feeling" the surface with a mechanical probe. Piezoelectric elements that facilitate tiny but accurate and precise movements on (electronic) command enable the very precise scanning.

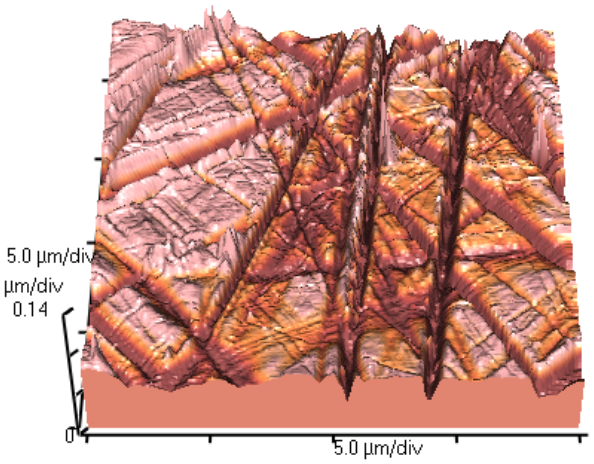

Topographic scan of a glass surface

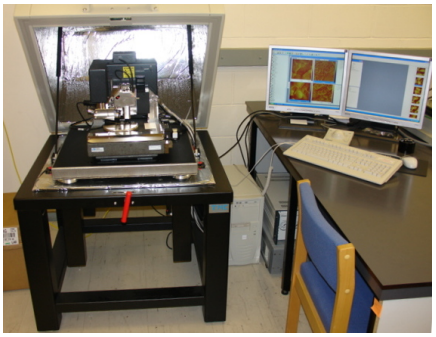

Microscope AFM

Basic principle

Part of a series of articles on

Nanotechnology

History
Implications
Applications
Regulation
Organizations
Popular culture
List of topics

Nanomaterials

Fullerene
Carbon Nanotubes
Nanoparticles

Nanomedicine

Nanotoxicology
Nanosensor

Molecular self-assembly

Self-assembled monolayer
Supramolecular assembly
DNA nanotechnology

Nanoelectronics

Molecular electronics
Nanolithography

Scanning probe microscopy

Atomic force microscope
Scanning tunneling microscope

Molecular nanotechnology

Molecular assembler
Nanorobotics
Mechanosynthesis

Nanotechnology Portal

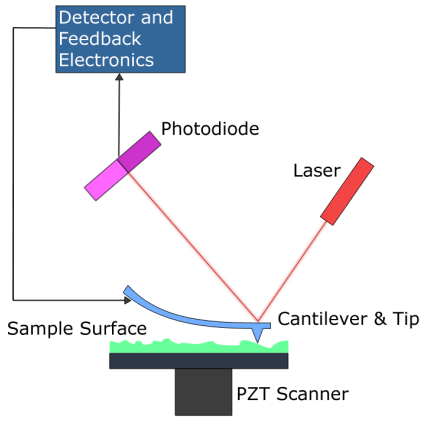

Block Diagram of Atomic Force Microscope

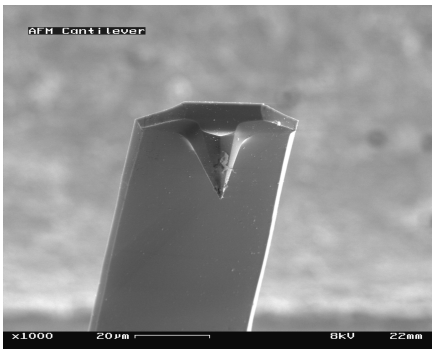

AFM cantilever (after use) in the Scanning Electron Microscope, magnification 1,000 x (image width ~ 100 micrometers)

The AFM consists of a microscale cantilever with a sharp tip (probe) at its end that is used to scan the specimen surface. The cantilever is typically silicon or silicon nitride with a tip radius of curvature on the order of nanometers. When the tip is brought into proximity of a sample surface, forces between the tip and the sample lead to a deflection of the cantilever according to Hooke's law. Depending on the situation, forces that are measured in AFM include mechanical contact force, Van der Waals forces, capillary forces, chemical bonding, electrostatic forces, magnetic forces (see Magnetic force microscope (MFM)), Casimir forces, solvation forces etc. As well as force, additional quantities may simultaneously be measured through the use of specialised types of probe (see Scanning thermal microscopy, photothermal microspectroscopy, etc.). Typically, the deflection is measured using a laser spot reflected from the top surface of the cantilever into an array of photodiodes. Other methods that are used include optical interferometry, capacitive sensing or piezoresistive AFM cantilevers. These cantilevers are fabricated with piezoresistive elements that act as a strain gauge. Using a Wheatstone bridge, strain in the AFM cantilever due to deflection can be measured, but this method is not as sensitive as laser deflection or interferometry.

If the tip was scanned at a constant height, a risk would exist that the tip collides with the surface, causing damage. Hence, in most cases a feedback mechanism is employed to adjust the tip-to-sample distance to maintain a constant force between the tip and the

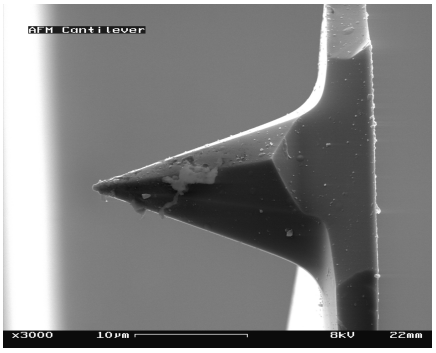

AFM cantilever (after use) in the Scanning Electron Microscope, magnification 3,000 x (image width ~ 30 micrometers)

sample. Traditionally, the sample is mounted on a piezoelectric tube, that can move the sample in the *z* direction for maintaining a constant force, and the *x* and *y* directions for scanning the sample. Alternatively a 'tripod' configuration of three piezo crystals may be employed, with each responsible for scanning in the x,y and z directions. This eliminates some of the distortion effects seen with a tube scanner. In newer designs, the tip is mounted on a vertical piezo scanner while the sample is being scanned in X and Y using another piezo block. The resulting map of the area $s = f(x,y)$ represents the topography of the sample.

The AFM can be operated in a number of modes, depending on the application. In general, possible imaging modes are divided into static (also called Contact) modes and a variety of dynamic (or non-contact) modes where the cantilever is vibrated.

Imaging modes

The primary modes of operation are static (contact) mode and dynamic mode. In the static mode operation, the static tip deflection is used as a feedback signal. Because the measurement of a static signal is prone to noise and drift, low stiffness cantilevers are used to boost the deflection signal. However, close to the surface of the sample, attractive forces can be quite strong, causing the tip to 'snap-in' to the surface. Thus static mode AFM is almost always done in contact where the overall force is repulsive. Consequently, this technique is typically called 'contact mode'. In contact mode, the force between the tip and the surface is kept constant during scanning by maintaining a constant deflection.

In the dynamic mode, the cantilever is externally oscillated at or close to its fundamental resonance frequency or a harmonic. The oscillation amplitude, phase and resonance frequency are modified by tip-sample interaction forces; these changes in oscillation with respect to the external reference oscillation provide information about the sample's characteristics. Schemes for dynamic mode operation include frequency modulation and the more common amplitude modulation. In frequency modulation, changes in the oscillation frequency provide information about tip-sample interactions. Frequency can be measured with very high sensitivity and thus the frequency modulation mode allows for the use of very stiff cantilevers. Stiff cantilevers provide stability very close to the surface and, as a result, this technique was the first AFM technique to provide true atomic resolution in ultra-high vacuum conditions (Giessibl).

In amplitude modulation, changes in the oscillation amplitude or phase provide the feedback signal for imaging. In amplitude modulation, changes in the phase of oscillation can be used to discriminate between different types of materials on the surface. Amplitude modulation can be operated either in the non-contact or in the intermittent contact regime. In ambient conditions, most samples develop a liquid meniscus layer. Because of this, keeping the probe tip close enough to the sample for short-range forces to become detectable while preventing the tip from sticking to the surface presents a major hurdle for the non-contact dynamic mode in ambient conditions. Dynamic contact mode (also called

intermittent contact or tapping mode) was developed to bypass this problem (Zhong et al.). In dynamic contact mode, the cantilever is oscillated such that the separation distance between the cantilever tip and the sample surface is modulated.

Amplitude modulation has also been used in the non-contact regime to image with atomic resolution by using very stiff cantilevers and small amplitudes in an ultra-high vacuum environment.

Tapping Mode

In *tapping mode* the cantilever is driven to oscillate up and down at near its resonance frequency by a small piezoelectric element mounted in the AFM tip holder. The amplitude of this oscillation is greater than 10 nm, typically 100 to 200 nm. Due to the interaction of forces acting on the cantilever when the tip comes close to the surface, Van der Waals force or dipole-dipole interaction, electrostatic forces, etc cause the amplitude of this oscillation to decrease as the tip gets closer to the sample. An electronic servo uses the piezoelectric actuator to control the height of the cantilever above the sample. The servo adjusts the height to maintain a set cantilever oscillation amplitude as the cantilever is scanned over the sample. A *Tapping AFM* image is therefore produced by imaging the force of the oscillating contacts of the tip with the sample surface. This is an improvement on conventional contact AFM, in which the cantilever just drags across the surface at constant force and can result in surface damage. Tapping mode is gentle enough even for the visualization of supported lipid bilayers or adsorbed single polymer molecules (for instance, 0.4 nm thick chains of synthetic polyelectrolytes) under liquid medium. At the application of proper scanning parameters, the conformation of single molecules remains unchanged for hours (Roiter and Minko, 2005).

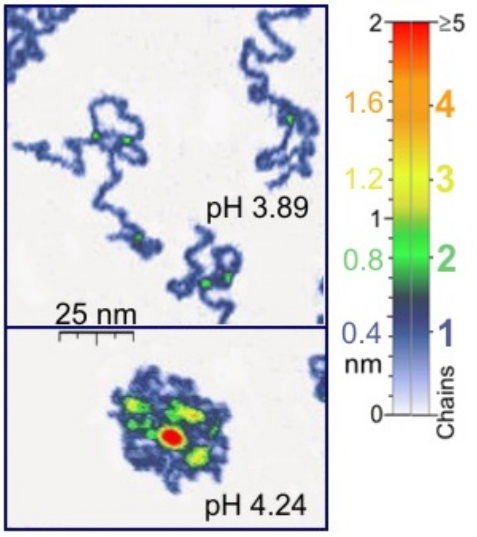

Single polymer chains (0.4 nm thick) recorded in a tapping mode under aqueous media with different pH. Green locations of the two-chains-superposition correspond to 0.8 nm thickness (Roiter and Minko, 2005).

Non-Contact Mode

Here the tip of the cantilever does not contact the sample surface. The cantilever is instead oscillated at a frequency slightly above its resonance frequency where the amplitude of oscillation is typically a few nanometers (<10nm). The van der Waals forces, which are strongest from 1nm to 10nm above the surface, or any other long range force which extends above the surface acts to decrease the resonance frequency of the cantilever. This decrease in resonance frequency combined with the feedback loop system maintains a constant oscillation amplitude or frequency by adjusting the average tip-to-sample distance. Measuring the tip-to-sample distance at each (x,y) data point allows the scanning software to construct a topographic image of the sample surface.

Non-contact mode AFM does not suffer from tip or sample degradation effects that are sometimes observed after taking numerous scans with contact AFM. This makes

non-contact AFM preferable to contact AFM for measuring soft samples. In the case of rigid samples, contact and non-contact images may look the same. However, if a few monolayers of adsorbed fluid are lying on the surface of a rigid sample, the images may look quite different. An AFM operating in contact mode will penetrate the liquid layer to image the underlying surface, whereas in non-contact mode an AFM will oscillates above the adsorbed fluid layer to image both the liquid and surface.

AFM -Beam Deflection Detection

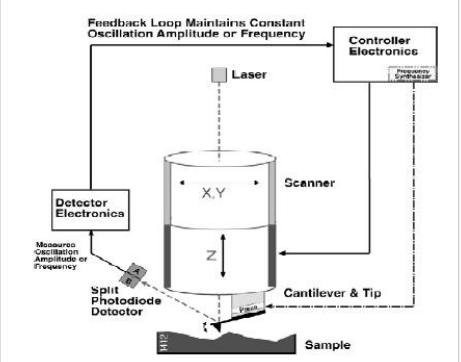

AFM - Non-Contact Mode

Laser light from a solid state diode is reflected off the back of the cantilever and collected by a position sensitive detector (PSD) consisting of two closely spaced photodiodes whose output signal is collected by a differential amplifier. Angular displacement of cantilever results in one photodiode collecting more light than the other photodiode, producing an output signal (the difference between the photodiode signals normalized by their sum) which is proportional to the deflection of the cantilever. It detects cantilever deflections <1Å (thermal noise limited). A long beam path (several cm) amplifies changes in beam angle.

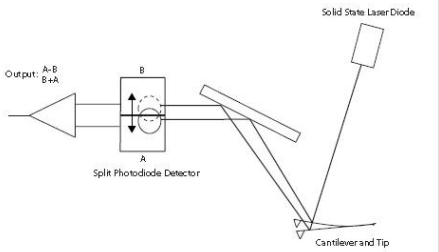

AFM Beam Deflection Detection

Force spectroscopy

Another major application of AFM (besides imaging) is force spectroscopy, the measurement of force-distance curves. For this method, the AFM tip is extended towards and retracted from the surface as the static deflection of the cantilever is monitored as a function of piezoelectric displacement. These measurements have been used to measure nanoscale contacts, atomic bonding, Van der Waals forces, and Casimir forces, dissolution forces in liquids and single molecule stretching and rupture forces (Hinterdorfer & Dufrêne). Forces of the order of a few pico-Newton can now be routinely measured with a vertical distance resolution of better than 0.1 nanometer.

Problems with the technique include no direct measurement of the tip-sample separation and the common need for low stiffness cantilevers which tend to 'snap' to the surface. The snap-in can be reduced by measuring in liquids or by using stiffer cantilevers, but in the latter case a more sensitive deflection sensor is needed. By applying a small dither to the tip, the stiffness (force gradient) of the bond can be measured as well (Hoffmann et al.).

Identification of individual surface atoms

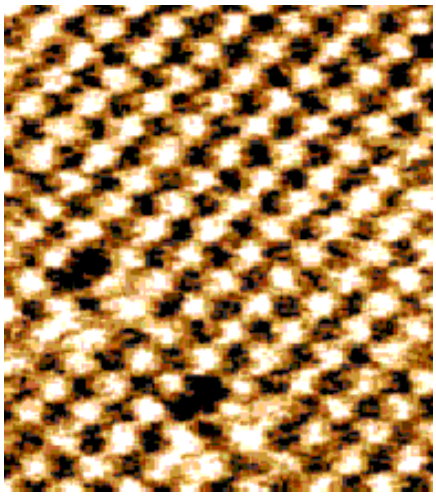

The atoms of a Sodium Chloride crystal viewed with an Atomic Force Microscope

The AFM can be used to image and manipulate atoms and structures on a variety of surfaces. The atom at the apex of the tip "senses" individual atoms on the underlying surface when it forms incipient chemical bonds with each atom. Because these chemical interactions subtly alter the tip's vibration frequency, they can be detected and mapped.

Physicist Oscar Custance (Osaka University, Graduate School of Engineering, Osaka, Japan) and his team used this principle to distinguish between atoms of silicon, tin and lead on an alloy surface (*Nature* 2007, 446, 64).

The trick is to first measure these forces precisely for each type of atom expected in the sample. The team found that the tip interacted most strongly with silicon atoms, and interacted 23% and 41% less strongly with tin and lead atoms, respectively. Thus, each different type of atom can be identified in the matrix as the tip is moved across the surface.

Such a technique has been used now in biology and extended recently to cell biology. Forces corresponding to (i) the unbinding of receptor ligand couples (ii) unfolding of proteins (iii) cell adhesion at single cell scale have been gathered.

Advantages and disadvantages

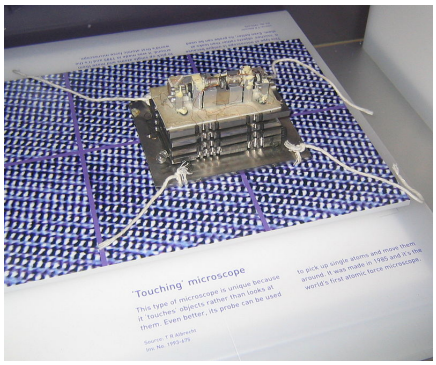

The first Atomic Force Microscope

The AFM has several advantages over the scanning electron microscope (SEM). Unlike the electron microscope which provides a two-dimensional projection or a two-dimensional image of a sample, the AFM provides a true three-dimensional surface profile. Additionally, samples viewed by AFM do not require any special treatments (such as metal/carbon coatings) that would irreversibly change or damage the sample. While an electron microscope needs an expensive vacuum environment for proper operation, most AFM modes can work perfectly well in ambient air or even a liquid environment. This makes it possible to study biological macromolecules and even living organisms. In principle, AFM can provide higher resolution than SEM. It has been shown to give true atomic resolution in ultra-high vacuum (UHV) and, more recently, in liquid environments. High resolution AFM is comparable in resolution to Scanning Tunneling Microscopy and Transmission Electron Microscopy.

A disadvantage of AFM compared with the scanning electron microscope (SEM) is the image size. The SEM can image an area on the order of millimetres by millimetres with a depth of field on the order of millimetres. The AFM can only image a maximum height on the order of micrometres and a maximum scanning area of around 150 by 150 micrometres.

Another inconvenience is that an incorrect choice of tip for the required resolution can lead to image artifacts. Traditionally the AFM could not scan images as fast as an SEM, requiring several minutes for a typical scan, while a SEM is capable of scanning at near real-time (although at relatively low quality) after the chamber is evacuated. The relatively slow rate of scanning during AFM imaging often leads to thermal drift in the image (Lapshin, 2004, 2007), making the AFM microscope less suited for measuring accurate distances between artifacts on the image. However, several fast-acting designs were suggested to increase microscope scanning productivity (Lapshin and Obyedkov, 1993) including what is being termed videoAFM (reasonable quality images are being obtained with videoAFM at video rate - faster than the average SEM). To eliminate image distortions induced by thermodrift, several methods were also proposed (Lapshin, 2004, 2007).

AFM images can also be affected by hysteresis of the piezoelectric material (Lapshin, 1995) and cross-talk between the (x,y,z) axes that may require software enhancement and filtering. Such filtering could "flatten" out real topographical features. However, newer AFM use real-time correction software (for example, feature-oriented scanning, Lapshin, 2004, 2007) or closed-loop scanners which practically eliminate these problems. Some AFM also use separated orthogonal scanners (as opposed to a single tube) which also serve to eliminate cross-talk problems.

Due to the nature of AFM probes, they cannot normally measure steep walls or overhangs. Specially made cantilevers can be modulated sideways as well as up and down (as with dynamic contact and non-contact modes) to measure sidewalls, at the cost of more expensive cantilevers and additional artifacts.

Piezoelectric Scanners

AFM scanners are made from piezoelectric material, which expands and contracts proportionally to an applied voltage. Whether they elongate or contract depends upon the polarity of the voltage applied. The scanner is constructed by combining independently operated piezo electrodes for X, Y, & Z into a single tube, forming a scanner which can manipulate samples and probes with extreme precision in 3 dimensions.

Scanners are characterized by their sensitivity which is the ratio of piezo movement to piezo voltage, i.e. by how much the piezo material extends or contracts per applied volt. Because of differences in material or size, the sensitivity varies from scanner to scanner.

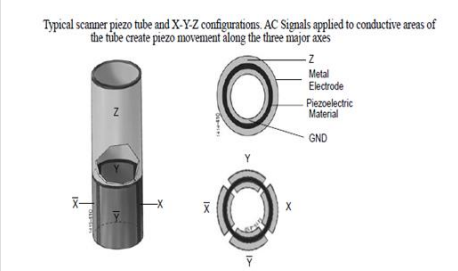

Piezoelectric Scanner

Sensitivity varies non-linearly with respect to scan size. Piezo scanners exhibit more sensitivity at the end than at the beginning of a scan. This causes the forward and reverse scans to behave differently and display hysteresis between the two scan directions. This can be corrected by applying a non-linear voltage to the piezo electrodes to cause linear scanner movement and calibrating the scanner accordingly.

The sensitivity of piezoelectric materials decreases exponentially with time. This causes most of the change in sensitivity to occur in the initial stages of the scanner's life. Piezoelectric scanners are run for approximately 48 hours before they are shipped from the factory so that they are past the point where we can expect large changes in sensitivity. As the scanner ages, the sensitivity will change less with time and the scanner would seldom

require recalibration.

See also

- Interfacial force microscope
- Friction force microscope
- Scanning tunneling microscope
- Scanning probe microscopy
- Scanning voltage microscopy

References

- A. D L. Humphris, M. J. Miles, J. K. Hobbs, A mechanical microscope: High-speed atomic force microscopy [1], Applied Physics Letters 86, 034106 (2005).
- D. Sarid, Scanning Force Microscopy, Oxford Series in Optical and Imaging Sciences, Oxford University Press, New York (1991)
- R. Dagani, Individual Surface Atoms Identified, Chemical & Engineering News, 5 March 2007, page 13. Published by American Chemical Society
- Q. Zhong, D. Inniss, K. Kjoller, V. B. Elings, Surf. Sci. Lett. 290, L688 (1993).
- V. J. Morris, A. R. Kirby, A. P. Gunning, Atomic Force Microscopy for Biologists. (Book) (December 1999) Imperial College Press.
- J. W. Cross *SPM - Scanning Probe Microscopy Website* [2]
- P. Hinterdorfer, Y. F. Dufrêne, Nature Methods, 3, 5 (2006)
- F. Giessibl, Advances in Atomic Force Microscopy, Reviews of Modern Physics 75 (3), 949-983 (2003).
- R. H. Eibl, V.T. Moy, Atomic force microscopy measurements of protein-ligand interactions on living cells. Methods Mol Biol. 305:439-50 (2005)
- P. M. Hoffmann, A. Oral, R. A. Grimble, H. Ö. Özer, S. Jeffery, J. B. Pethica, Proc. Royal Soc. A 457, 1161 (2001).
- R. V. Lapshin, O. V. Obyedkov, Fast-acting piezoactuator and digital feedback loop for scanning tunneling microscopes [3], Review of Scientific Instruments, vol. 64, no. 10, pp. 2883-2887, 1993.
- R. V. Lapshin, Analytical model for the approximation of hysteresis loop and its application to the scanning tunneling microscope [4], Review of Scientific Instruments, vol. 66, no. 9, pp. 4718-4730, 1995.
- R. V. Lapshin, Feature-oriented scanning methodology for probe microscopy and nanotechnology [5], Nanotechnology, vol. 15, iss. 9, pp. 1135-1151, 2004.
- R. V. Lapshin, Automatic drift elimination in probe microscope images based on techniques of counter-scanning and topography feature recognition [6], Measurement Science and Technology, vol. 18, iss. 3, pp. 907-927, 2007.
- P. West, Introduction to Atomic Force Microscopy: Theory, Practice and Applications --- www.AFMUniversity.org
- R. W. Carpick and M. Salmeron, Scratching the surface: Fundamental investigations of tribology with atomic force microscopy [7], Chemical Reviews, vol. 97, iss. 4, pp. 1163-1194 (2007).
- Y. Roiter and S. Minko, AFM Single Molecule Experiments at the Solid-Liquid Interface: In Situ Conformation of Adsorbed Flexible Polyelectrolyte Chains [8], Journal of the American Chemical Society, vol. 127, iss. 45, pp. 15688-15689 (2005).

References

[1] http://www.infinitesima.com/downloads/APL_paper.pdf
[2] http://www.mobot.org/jwcross/spm/
[3] http://www.nanoworld.org/homepages/lapshin/publications.htm#fast1993
[4] http://www.nanoworld.org/homepages/lapshin/publications.htm#analytical1995
[5] http://www.nanoworld.org/homepages/lapshin/publications.htm#feature2004
[6] http://www.nanoworld.org/homepages/lapshin/publications.htm#automatic2007
[7] http://dx.doi.org/10.1021/cr960068q
[8] http://dx.doi.org/10.1021/ja0558239

Electron microscope

An **electron microscope** is a type of microscope that uses a particle beam of electrons to illuminate a specimen and create a highly-magnified image. Electron microscopes have much greater resolving power than light microscopes that use electromagnetic radiation and can obtain much higher magnifications of up to 2 million times, while the best light microscopes are limited to magnifications of 2000 times. Both electron and light microscopes have resolution limitations, imposed by the wavelength of the radiation they use. The greater resolution and magnification of the electron microscope is because the wavelength of an electron, its de Broglie wavelength, is much smaller than that of a photon of visible light.

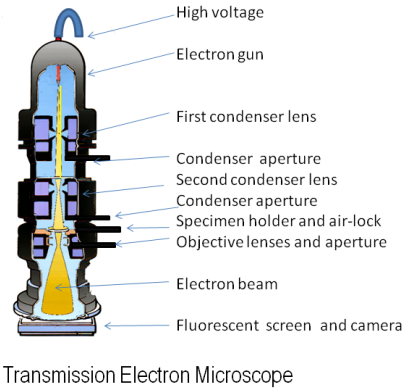

Diagram of a transmission electron microscope

The electron microscope uses electrostatic and electromagnetic lenses in forming the image by controlling the electron beam to focus it at a specific plane relative to the specimen in a manner similar to how a light microscope uses glass lenses to focus light on or through a specimen to form an image.

History

Electron microscope constructed by Ernst Ruska in 1933

The first electron microscope prototype was built in 1931 by the German engineers Ernst Ruska and Max Knoll.[1] Although this initial instrument was capable of magnifying objects by only four hundred times, it demonstrated the principles of an electron microscope. Two years later, Ruska constructed an electron microscope that exceeded the resolution possible with an optical microscope.[1]

Reinhold Rudenberg, the scientific director of Siemens, had patented the electron microscope in 1931, stimulated by family illness to make the poliomyelitis virus particle visible. In 1937 Siemens began funding Ruska and Bodo von Borries to develop an electron microscope. Siemens also employed Ruska's brother Helmut to work on applications, particularly with biological specimens.[2] [3]

In the same decade Manfred von Ardenne pioneered the scanning electron microscope and his universal electron microscope.[4]

Siemens produced the first commercial Transmision Electron Microscope (TEM) in 1939, but the first practical electron microscope had been built at the University of Toronto in 1938, by Eli Franklin Burton and students Cecil Hall, James Hillier, and Albert Prebus.[5]

Although modern electron microscopes can magnify objects up to two million times, they are still based upon Ruska's prototype. The electron microscope is an essential item of equipment in many laboratories. Researchers use them to examine biological materials (such as microorganisms and cells), a variety of large molecules, medical biopsy samples, metals and crystalline structures and the characteristics of various surfaces. The electron microscope is also used extensively for inspection, quality assurance and failure analysis applications in industry, including, in particular, semiconductor device fabrication.

Types

Transmission Electron Microscope (TEM)

The original form of electron microscope, the transmission electron microscope (TEM) uses a high voltage electron beam to create an image. The electrons are emitted by an electron gun, commonly fitted with a tungsten filament cathode as the electron source. The electron beam is accelerated by an anode typically at +100keV (40 to 400 keV) with respect to the cathode, focused by electrostatic and electromagnetic lenses, and transmitted through the specimen that is in part transparent to electrons and in part scatters them out of the beam. When it emerges from the specimen, the electron beam carries information about the structure of the specimen that is magnified by the objective lens system of the microscope. The spatial variation in this information (the "image") is viewed by projecting the magnified electron image onto a fluorescent viewing screen coated with a phosphor or scintillator

material such as zinc sulfide. The image can be photographically recorded by exposing a photographic film or plate directly to the electron beam, or a high-resolution phosphor may be coupled by means of a lens optical system or a fibre optic light-guide to the sensor of a CCD (charge-coupled device) camera. The image detected by the CCD may be displayed on a monitor or computer.

Resolution of the TEM is limited primarily by spherical aberration, but a new generation of aberration correctors have been able to partially overcome spherical aberration to increase resolution. Software correction of spherical aberration for the High Resolution TEM (HRTEM) has allowed the production of images with sufficient resolution to show carbon atoms in diamond separated by only 0.89 ångström (89 picometers) and atoms in silicon at 0.78 ångström (78 picometers)[6] [7] at magnifications of 50 million times.[8] The ability to determine the positions of atoms within materials has made the HRTEM an important tool for nano-technologies research and development.[9]

Scanning Electron Microscope (SEM)

An image of an ant from a scanning electron microscope

Unlike the TEM, where electrons of the high voltage beam carry the image of the specimen, the electron beam of the Scanning Electron Microscope (SEM)[10] does not at any time carry a complete image of the specimen. The SEM produces images by probing the specimen with a focused electron beam that is scanned across a rectangular area of the specimen (raster scanning). At each point on the specimen the incident electron beam loses some energy, and that lost energy is converted into other forms, such as heat, emission of low-energy secondary electrons, light emission (cathodoluminescence) or x-ray emission. The display of the SEM maps the varying intensity of any of these signals into the image in a position corresponding to the position of the beam on the specimen when the signal was generated. In the SEM image of an ant shown at right, the image was constructed from signals produced by a secondary electron detector, the normal or conventional imaging mode in most SEMs.

Generally, the image resolution of an SEM is about an order of magnitude poorer than that of a TEM. However, because the SEM image relies on surface processes rather than transmission it is able to image bulk samples up to several centimetres in size (depending on instrument design) and has a much greater depth of view, and so can produce images that are a good representation of the 3D structure of the sample.

Reflection Electron Microscope (REM)

In the **Reflection Electron Microscope** (REM) as in the TEM, an electron beam is incident on a surface, but instead of using the transmission (TEM) or secondary electrons (SEM), the reflected beam of elastically scattered electrons is detected. This technique is typically coupled with Reflection High Energy Electron Diffraction (RHEED) and *Reflection high-energy loss spectrum (RHELS)*. Another variation is Spin-Polarized Low-Energy Electron Microscopy (SPLEEM), which is used for looking at the microstructure of magnetic domains.[11]

Scanning Transmission Electron Microscope (STEM)

The STEM rasters a focused incident probe across a specimen that (as with the TEM) has been thinned to facilitate detection of electrons scattered *through* the specimen. The high resolution of the TEM is thus possible in STEM. The focusing action (and aberrations) occur before the electrons hit the specimen in the STEM, but afterward in the TEM. The STEM's use of SEM-like beam rastering simplifies annular dark-field imaging, and other analytical techniques, but also means that image data is acquired in serial rather than in parallel fashion.

Sample preparation

Materials to be viewed under an electron microscope may require processing to produce a suitable sample. The technique required varies depending on the specimen and the analysis required:

An insect coated in gold for viewing with a scanning electron microscope.

- Chemical Fixation for biological specimens aims to stabilize the specimen's mobile macromolecular structure by chemical crosslinking of proteins with aldehydes such as formaldehyde and glutaraldehyde, and lipids with osmium tetroxide.
- *Cryofixation* – freezing a specimen so rapidly, to liquid nitrogen or even liquid helium temperatures, that the water forms vitreous (non-crystalline) ice. This preserves the specimen in a snapshot of its solution state. An entire field called cryo-electron microscopy has branched from this technique. With the development of cryo-electron microscopy of vitreous sections (CEMOVIS), it is now possible to observe samples from virtually any biological specimen close to its native state.
- *Dehydration* – freeze drying, or replacement of water with organic solvents such as ethanol or acetone, followed by critical point drying or infiltration with embedding resins.
- *Embedding, biological specimens* – after dehydration, tissue for observation in the transmission electron microscope is embedded so it can be sectioned ready for viewing. To do this the tissue is passed through a 'transition solvent' such as epoxy propane and then infiltrated with a resin such as Araldite epoxy resin; tissues may also be embedded directly in water-miscible acrylic resin. After the resin has been polymerised (hardened) the sample is thin sectioned (ultrathin sections) and stained - it is then ready for viewing.
- *Embedding, materials* - after embedding in resin, the specimen is usually ground and polished to a mirror-like finish using ultra-fine abrasives. The polishing process must be performed carefully to minimize scratches and other polishing artifacts that reduce image quality.
- *Sectioning* – produces thin slices of specimen, semitransparent to electrons. These can be cut on an ultramicrotome with a diamond knife to produce ultrathin slices about 60-90nm thick. Disposable glass knives are also used because they can be made in the lab and are much cheaper.
- *Staining* – uses heavy metals such as lead, uranium or tungsten to scatter imaging electrons and thus give contrast between different structures, since many (especially

biological) materials are nearly "transparent" to electrons (weak phase objects). In biology, specimens are can be stained "en bloc" before embedding and also later after sectioning. Typically thin sections are stained for several minutes with an aqueous or acoholic solution of uranyl acetate followed by aqueous lead citrate.

- *Freeze-fracture or freeze-etch* – a preparation method particularly useful for examining lipid membranes and their incorporated proteins in "face on" view. The fresh tissue or cell suspension is frozen rapidly (cryofixed), then fractured by simply breaking or by using a microtome while maintained at liquid nitrogen temperature. The cold fractured surface (sometimes "etched" by increasing the temperature to about -100°C for several minutes to let some ice sublime) is then shadowed with evaporated platinum or gold at an average angle of 45° in a high vacuum evaporator. A second coat of carbon, evaporated perpendicular to the average surface plane is often performed to improve stability of the replica coating. The specimen is returned to room temperature and pressure, then the extremely fragile "pre-shadowed" metal replica of the fracture surface is released from the underlying biological material by careful chemical digestion with acids, hypochlorite solution or SDS detergent. The still-floating replica is thoroughly washed from residual chemicals, carefully fished up on EM grids, dried then viewed in the TEM.
- *Ion Beam Milling* – thins samples until they are transparent to electrons by firing ions (typically argon) at the surface from an angle and sputtering material from the surface. A subclass of this is Focused ion beam milling, where gallium ions are used to produce an electron transparent membrane in a specific region of the sample, for example through a device within a microprocessor. Ion beam milling may also be used for cross-section polishing prior to SEM analysis of materials that are difficult to prepare using mechanical polishing.
- *Conductive Coating* – An ultrathin coating of electrically-conducting material, deposited either by high vacuum evaporation or by low vacuum sputter coating of the sample. This is done to prevent the accumulation of static electric fields at the specimen due to the electron irradiation required during imaging. Such coatings include gold, gold/palladium, platinum, tungsten, graphite etc. and are especially important for the study of specimens with the scanning electron microscope. Another reason for coating, even when there is more than enough conductivity, is to improve contrast, a situation more common with the operation of a FESEM (field emission SEM). When an osmium coater is used, a layer far thinner than would be possible with any of the previously mentioned sputtered coatings is possible.[12]

Disadvantages

Electron microscopes are expensive to build and maintain, but the capital and running costs of confocal light microscope systems now overlaps with those of basic electron microscopes. They are dynamic rather than static in their operation, requiring extremely stable high-voltage supplies, extremely stable currents to each electromagnetic coil/lens, continuously-pumped high- or ultra-high-vacuum systems, and a cooling water supply circulation through the lenses and pumps. As they are very sensitive to vibration and external magnetic fields, microscopes designed to achieve high resolutions must be housed in stable buildings (sometimes underground) with special services such as magnetic field cancelling systems. Some desktop low voltage electron microscopes have TEM capabilities at very low voltages (around 5 kV) without stringent voltage supply, lens coil current, cooling water or vibration isolation requirements and as such are much less expensive to buy and far easier to install and maintain, but do not have the same ultra-high (atomic scale) resolution capabilities as the larger instruments.

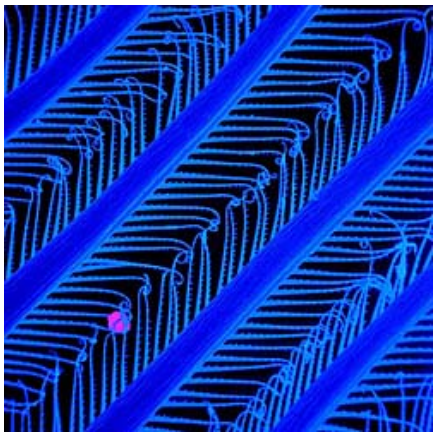

Pseudocolored SEM image of the feeding basket of Antarctic krill. Real electron microscope images do not carry any color information; they are greyscale. The first degree filter setae carry in v-form two rows of second degree setae, pointing towards the inside of the feeding basket. The purple ball is one micrometer in diameter. To display the total area of this structure one would have to tile this image 7500 times.

The samples largely have to be viewed in vacuum, as the molecules that make up air would scatter the electrons. One exception is the environmental scanning electron microscope, which allows hydrated samples to be viewed in a low-pressure (up to 20 Torr/2.7 kPa), wet environment.

Scanning electron microscopes usually image conductive or semi-conductive materials best. Non-conductive materials can be imaged by an environmental scanning electron microscope. A common preparation technique is to coat the sample with a several-nanometer layer of conductive material, such as gold, from a sputtering machine; however, this process has the potential to disturb delicate samples.

Small, stable specimens such as carbon nanotubes, diatom frustules and small mineral crystals (asbestos fibres, for example) require no special treatment before being examined in the electron microscope. Samples of hydrated materials, including almost all biological specimens have to be prepared in various ways to stabilize them, reduce their thickness (ultrathin sectioning) and increase their electron optical contrast (staining). These processes may result in *artifacts*, but these can usually be identified by comparing the results obtained by using radically different specimen preparation methods. It is generally believed by scientists working in the field that as results from various preparation techniques have been compared and that there is no reason that they should all produce similar artifacts, it is reasonable to believe that electron microscopy features correspond with those of living cells. In addition, higher-resolution work has been directly compared to results from X-ray crystallography, providing independent confirmation of the validity of this technique. Since the 1980s, analysis of cryofixed, vitrified specimens has also become increasingly used by scientists, further confirming the validity of this technique.[13] [14] [15]

Applications

Semiconductor and data storage

- Circuit edit
- Defect analysis
- Failure analysis

Biology and life sciences

- Diagnostic electron microscopy
- Cryobiology
- Protein localization
- Electron tomography
- Cellular tomography
- Cryo-electron microscopy
- Toxicology
- Biological production and viral load monitoring
- Particle analysis
- Pharmaceutical QC
- Structural biology
- 3D tissue imaging
- Virology
- Vitrification

Research

- Electron beam induced depostion
- Materials qualification
- Materials and sample preparation
- Nanoprototyping
- Nanometrology
- Device testing and characterization

Industry

- High-resolution imaging
- 2D & 3D micro-characterization
- Macro sample to nanometer metrology
- Particle detection and characterization
- Direct beam-writing fabrication
- Dynamic materials experiments
- Sample preparation
- Forensics
- Mining (mineral liberation analysis)
- Chemical/Petrochemical

See also

- Category:Electron microscope images
- Field emission microscope
- Scanning tunneling microscope

References

[1] Ernst Ruska Nobel Prize autobiography (http://nobelprize.org/nobel_prizes/physics/laureates/1986/ruska-autobio.html)

[2] Ernst Ruska (1986). http://nobelprize.org/nobel_prizes/physics/laureates/1986/ruska-autobio.html|"Ernst Ruska Autobiography". Nobel Foundation. http://nobelprize.org/nobel_prizes/physics/laureates/1986/ruska-autobio.html. Retrieved on 2007-02-06.

[3] DH Kruger, P Schneck and HR Gelderblom (May 13, 2000). "Helmut Ruska and the visualisation of viruses". *The Lancet* **355** (9216): 1713–1717. doi: 10.1016/S0140-6736(00)02250-9 (http://dx.doi.org/10.1016/S0140-6736(00)02250-9).

[4] M von Ardenne and D Beischer (1940). "Untersuchung von metalloxud-rauchen mit dem universal-elektronenmikroskop" (in German). *Zeitschrift Electrochemie* **46**: 270–277.

[5] MIT biography of Hillier (http://web.mit.edu/Invent/iow/hillier.html)

[6] OÅM: World-Record Resolution at 0.78 Å (http://www.lbl.gov/Publications/Currents/Archive/May-18-2001.html#_Hlk514817949), (May 18, 2001) Berkeley Lab Currents.

[7] P. D. Nellist, M. F. Chisholm, N. Dellby, O. L. Krivanek, M. F. Murfitt, Z. S. Szilagyi, A. R. Lupini, A. Borisevich, W. H. Sides, Jr., S. J. Pennycook (September 17, 2004). "http://www.sciencemag.org/cgi/content/abstract/305/5691/1741|Direct Sub-Angstrom Imaging of a Crystal Lattice". *Science* **305** (5691): 1741. doi: 10.1126/science.1100965 (http://dx.doi.org/10.1126/science.1100965). PMID 15375260. http://www.sciencemag.org/cgi/content/abstract/305/5691/1741.

[8] The Scale of Things (http://www.sc.doe.gov/bes/scale_of_things.html), DOE Office of Basic Energy Sciences (BES).

[9] Michael A. O'Keefe, Lawrence F. Allard. *http://www.osti.gov/bridge/servlets/purl/821768-E3YVgN/native/821768.pdf|Sub-Ångstrom Electron Microscopy for Sub-Ångstrom Nano-Metrology*. http://www.osti.gov/bridge/servlets/purl/821768-E3YVgN/native/821768.pdf.

[10] SCANNING ELECTRON MICROSCOPY 1928 - 1965 (http://www-g.eng.cam.ac.uk/125/achievements/mcmullan/mcm.htm)
[11] NCEM National Center for Electron Microscopy: SPLEEM (http://ncem.lbl.gov/frames/spleem.html)
[12] http://www.2spi.com/catalog/osmi-coat.html
[13] Adrian, Marc; Dubochet, Jacques; Lepault, Jean; McDowall, Alasdair W. (1984). "Cryo-electron microscopy of viruses". *Nature* **308** (5954): 32–36. doi: 10.1038/308032a0 (http://dx.doi.org/10.1038/308032a0).
[14] Sabanay, I.; Arad, T.; Weiner, S.; Geiger, B. (01 Sep 1991). "http://jcs.biologists.org/cgi/content/abstract/100/1/227|Study of vitrified, unstained frozen tissue sections by cryoimmunoelectron microscopy". *Journal of Cell Science* **100** (1): 227–236. PMID 1795028. http://jcs.biologists.org/cgi/content/abstract/100/1/227.
[15] Kasas, S.; Dumas, G.; Dietler, G.; Catsicas, S.; Adrian, M. (2003). "Vitrification of cryoelectron microscopy specimens revealed by high-speed photographic imaging". *Journal of Microscopy* **211** (1): 48–53. doi: 10.1046/j.1365-2818.2003.01193.x (http://dx.doi.org/10.1046/j.1365-2818.2003.01193.x).

External links

- Cell Centered Database - Electron microscopy data (http://ccdb.ucsd.edu/sand/main?typeid=4&event=showMPByType&start=1)

General

- Nanohedron.com | Nano image gallery (http://www.nanohedron.com/) beautiful images generated with electron microscopes.
- electron microscopy (http://www.microscopy.ethz.ch) Website of the ETH Zurich: Very good graphics and images, which illustrate various procedures.
- Environmental Scanning Electron Microscope (ESEM) (http://www.danilatos.com)
- X-ray element analysis in electron microscope (http://www.microanalyst.net/index_e.phtml) – Information portal with X-ray microanalysis and EDX contents

History

- John H.L. Watson: Very early Electron Microscopy in the Department of Physics, the University of Toronto – A personal recollection (http://www.physics.utoronto.ca/overview/history/microsco)
- Rubin Borasky Electron Microscopy Collection, 1930-1988 (http://americanhistory.si.edu/archives/d8452.htm) Archives Center, National Museum of American History, Smithsonian Institution.

Other

- The Royal Microscopical Society, Electron Microscopy Section (UK) (http://www.rms.org.uk/em.shtml)
- Albert Lleal microphotography. Scanning Electron Microphotography Coloured SEM (http://www.albertlleal.com/microphotography.html)

X-ray microscope

An **X-ray microscope** uses electromagnetic radiation in the soft X-ray band to produce images of very small objects.

Unlike visible light, X-rays do not reflect or refract easily, and they are invisible to the human eye. Therefore the basic process of an X-ray microscope is to expose film or use a charge-coupled device (CCD) detector to detect X-rays that pass through the specimen. It is a contrast imaging technology using the difference in absorption of soft x-ray in the water window region (wavelength region: 2.3 - 4.4 nm, photon energy region: 0.28 - 0.53 keV) by the carbon atom (main element composing the living cell) and the oxygen atom (main element for water).

Early X-ray microscopes by Paul Kirkpatrick and Albert Baez used grazing-incidence reflective optics to focus the X-rays, which grazed X-rays off parabolic curved mirrors at a very high angle of incidence. An alternative method of focusing X-rays is to use a tiny fresnel zone plate of concentric gold or nickel rings on a silicon dioxide substrate. Sir Lawrence Bragg produced some of the first usable X-ray images with his apparatus in the late 1940's.

In the 1950's Newberry produced a shadow X-ray microscope which placed the specimen between the source and a target plate, this became the basis for the first commercial X-ray microscopes from the General Electric Company.

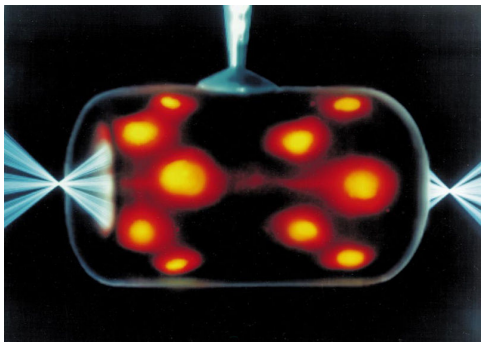

Indirect drive laser inertial confinement fusion uses a "hohlraum" which is irradiated with laser beam cones from either side on it its inner surface to bathe a fusion microcapsule inside with smooth high intensity X-rays. The highest energy X-rays which penetrate the hohlraum can be visualized using an X-ray microscope such as here, where X-radiation is represented in orange/red.

The Advanced Light Source (ALS)[1] in Berkeley CA is home to XM-1 (http://www.cxro.lbl.gov/BL612/), a full field soft X-ray microscope operated by the Center for X-ray Optics [2] and dedicated to various applications in modern nanoscience, such as nanomagnetic materials, environmental and materials sciences and biology. XM-1 uses an X-ray lens to focus X-rays on a CCD, in a manner similar to an optical microscope. XM-1 still holds the world record in spatial resolution with Fresnel zone plates down to 15nm and is able to combine high spatial resolution with a sub-100ps time resolution to study e.g. ultrafast spin dynamics.

The ALS is also home to the world's first soft x-ray microscope designed for biological and biomedical research. This new instrument, XM-2 was designed and built by scientists from the National Center for X-ray Tomography (http:/ / ncxt. lbl. gov). XM-2 is capable of producing 3-Dimensional tomograms of cells.

Sources of soft X-rays suitable for microscopy, such as synchrotron radiation sources, have fairly low brightness of the required wavelengths, so an alternative method of image formation is scanning transmission soft X-ray microscopy. Here the X-rays are focused to a point and the sample is mechanically scanned through the produced focal spot. At each point the transmitted X-rays are recorded with a detector such as a proportional counter or an avalanche photodiode. This type of Scanning Transmission X-ray Microscope (STXM)

was first developed by researchers at Stony Brook University and was employed at the National Synchrotron Light Source at Brookhaven National Laboratory.

The resolution of X-ray microscopy lies between that of the optical microscope and the electron microscope. It has an advantage over conventional electron microscopy in that it can view biological samples in their natural state. Electron microscopy is widely used to obtain images with nanometer level resolution but the relatively thick living cell cannot be observed as the sample has to be chemically fixed, dehydrated, embedded in resin, then sliced ultra thin. However, it should be mentioned that cryo-electron microscopy allows the observation of biological specimens in their hydrated natural state. Until now, resolutions of 30 nanometer are possible using the Fresnel zone plate lens which forms the image using the soft x-rays emitted from a synchrotron. Recently, more researchers have begun to use the soft x-rays emitted from laser-produced plasma rather than synchrotron radiation.

Additionally, X-rays cause fluorescence in most materials, and these emissions can be analyzed to determine the chemical elements of an imaged object. Another use is to generate diffraction patterns, a process used in X-ray crystallography. By analyzing the internal reflections of a diffraction pattern (usually with a computer program), the three-dimensional structure of a crystal can be determined down to the placement of individual atoms within its molecules. X-ray microscopes are sometimes used for these analyses because the samples are too small to be analyzed in any other way.

See also

- Synchrotron X-ray tomographic microscopy

External links

- Application of X-ray microscopy in analysis of living hydrated cells [18]
- Hard X-ray microbeam experiments with a sputtered-sliced Fresnel zone plate and its applications [3]
- Scientific applications of soft x-ray microscopy [4]
- Microarrays products [5]

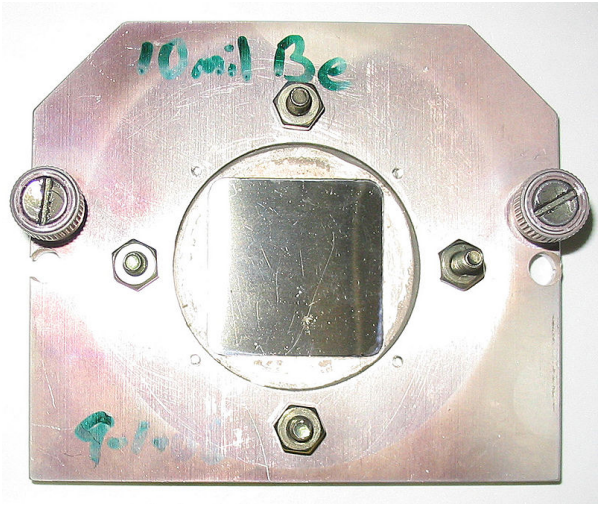

A square beryllium foil mounted in a steel case to be used as a window between a vacuum chamber and an X-ray microscope. Beryllium, due to its low Z number is highly transparent to X-rays.

References

[1] http://www-als.lbl.gov
[2] http://www.cxro.lbl.gov
[3] http://www.ncbi.nlm.nih.gov/entrez/query.fcgi?cmd=Retrieve&db=pubmed&dopt=Abstract&list_uids=11972376
[4] http://www.cxro.lbl.gov/BL612/index.php?content=research.html
[5] http://www.ibio.co.il/Products.aspx?level=2&prodID=17

Article Sources and Contributors

DNA *Source*: http://en.wikipedia.org/windex.php?oldid=296241303 *Contributors*: (, (jarbarf), -Majestic-, 168.., 168..., 169, 17Drew, 3dscience, 4u1e, 62.253.64.xxx, 7434be, 84user, A D 13, A bit iffy, A-giau, Aaaxlp, Aatomic1, Academic Challenger, Acer, Adam Bishop, Adambiswanger1, Adamstevenson, Adashiel, Adenosine, Adrian.benko, Ahoerstemeier, Aitias, Aj123456, Alai, Alan Au, Aldaron, Aldie, Alegoo92, Alexandremas, Alkivar, Alphachimp, Alzhaid, Amboo85, Anarchy on DNA, Ancheta Wis, AndonicO, Andre Engels, Andrew wilson, Andreww, Andrij Kursetsky, Andycjp, Anita1988, Anomalocaris, Antandrus, Ante Aikio, Anthere, Anthony, Anthony Appleyard, Antilived, Antony-22, Aquaplus, Aquilla34, ArazZeynili, Arcadian, Ardyn, ArielGold, Armored Ear, Artichoker, Asbestos, Astrowob, Atlant, Aude, Autonova, Avala, AxelBoldt, AySz88, AzaToth, BD2412, BMF81, Banus, BaronLarf, Bbatsell, Bci2, Bcorr, Ben Webber, Ben-Zin, BenBildstein, Benjah-bmm27, Bensaccount, Bernie Sanders' DNA, Bevo, Bhadani, Bhar100101, BiH, Bijee, BikA06, Bill Nelson's DNA, Billmcgn189, Biolinker, Biriwilg, Bjwebb, Blastwizard, Blondtraillite, Bmtbomb, Bobblewik, Bobo192, Bongwarrior, Borisblue, Bornhj, Brian0918, Brighterorange, Briland, Brim, Brockett, Bryan, Bryan Derksen, CWY2190, Cacycle, Caerwine, Cainer91, Cal 1234, Calaschysm, Can't sleep, clown will eat me, Canadaduane, Carbon-16, Carcharoth, Carlo.milanesi, Carlwev, Casliber, Cathalgarvey, CatherineMunro, CattleGirl, Causa sui, Cburnett, Cerberus lord, Chanora, Chanting Fox, Chaojoker, Charm, Chill Pill Bill, Chino, Chodges, Chris 73, Chris84, Chuck Grassley's DNA, Chuck02, Clivedelmonte, ClockworkSoul, CloudNine, Collins.mc, Colorajo, CommonsDelinker, Conversion script, Cool3, Coolawesome, Coredesat, Cornacchia123, Cosmotron, Cradlelover123, Crazycomputers, Crowstar, Crusadeonilliteracy, CryptoDerk, Crzrussian, Cubskrazy29, CupOBeans, Curps, Cyan, Cyclonenim, Cyrius, D6, DIREKTOR, DJAX, DJRafe, DNA EDIT WAR, DNA is shyt, DVD R W, Daniel Olsen, Daniel987600, Danielkueh, Danny, Danny B-), Danski14, Darklilac, Darth Panda, Davegrupp, David D., David Eppstein, Davidbspalding, Daycd, Db099221, Dbabbitt, Dcoetzee, DeAceShooter, DeadEyeArrow, Delldot, Delta G, Deltabeignet, DevastatorIIC, Diberri, Dicklyon, Digger3000, Digitalme, Dina, Djm1279, Dlohcierekim's sock, Dmn, Docjames, Doctor Faust, Docu, Dogposter, DonSiano, Donarreiskoffer, Dr d12, Dr.Kerr, Drini, Dudewheresmywallet, Dullhunk, Duncan.france, Dungodung, Dysmorodrepanis, E. Wayne, ERcheck, ESkog, Echo park00, Echuck215, Eddycrai, Editing DNA, Edwy, Efbfweborg, Egil, ElTyrant, Elb2000, Eleassar777, EliasAlucard, ElinorD, Ellmist, Eloquence, Emoticon, Epingchris, Erik Zachte, Escape Artist Swyer, Esurnir, Etanol, Ettrig, EurekaLott, Everyking, Evil Monkey, Ewawer, Execvator, FOTEMEH, Fabhcún, Factual, Fagstein, Fastfission, Fconaway, Fcrick, Fernando S. Aldado, Ffirehorse, Figma, Figure, Firefoxman, Firetrap9254, Fishingpal99, Flavaflav1005, Florentino floro, Fnielsen, Forluvoft, Freakofnurture, FreplySpang, Friendly Neighbour, Frostyservant, Fruge, Fvasconcellos, G3pro, GAThrawn22, GHe, GODhack, Gaara san, Galoubet, Gary King, Gatortpk, Gazibara, GeeJo, Gene Nygaard, GeoMor, Giftlite, Gilisa, Gilliam, Gimmetrow, Gjuggler, Glen Hunt's DNA, Glenn, Gmaxwell, GoETHe, Goatasaur, Gogo Dodo, Golnazfotohabadi, GordonWatts, Gracenotes, Graeme Bartlett, GraemeL, Grafikm fr, Graft, Graham87, GrahamColm, Grandegrandegrande, GregorB, Grover cleveland, Gurko, Gustav von Humpelschmumpel, Gutza, Gwsrinme, Hadal, Hagerman, Hairchrm, Hairwheel, Hannes Röst, Harianto, Heathhunnicutt, Hephaestos, Heron, Heyheyhack, Hockey21dude, Horatio, Hu, Hughdbrown, Hurricanehink, Hut 8.5, Hvn0413, I Seek To Help & Repair!, I hate DNA, Iapetus, Icairns, Ilia Kr., Impamiizgraa, InShaneee, Inge-Lyubov, Isilanes, Isis07, Itub, Ixfd64, Izehar, JHMM13, JWSchmidt, JWSurf, Jacek Kendysz, Jackrm, JamesMLane, JamesMt1984, Janejellyroll, Jaxl, Jeka911, Jer ome, JeremyA, Jerzy, Jetsetpainter, Jh51681, Jiddisch, Jimriz, Jimwong, Jlh29, Jls043, Jmcc150, Jo9100, JoanneB, Joconnol, Johanvs, JohnArmagh, Johntex, Johnuniq, Jojit fb, JonMoulton, Jonrunles, Jorvik, JoshuaZ, Josq, Jossi, Jstech, Julian Diamond, Jumbo Snails, Junes, Jwrosenzweig, Kahlfin, Kapow, Karrmann, Kazkaskazkasako, Kbh3rd, Keegan, Keepweek, Keilana, Kelly Martin, Kemyou, Kendrick7, KerryO77, Kevin Breitenstein, Kevmitch, Kghose, Kholdstare99, Kierano, KimvdLinde, King of Hearts, KingTT, Kingturtle, Kitch, Knaggs, Knowledge Seeker, KnowledgeOfSelf, Koavf, KrakatoaKatie, Kums, Kungfuadam, Kuru, Kwamikagami, Kwekubo, KyNephi, LA2, La goutte de pluie, Lascorz, Latka, Lavateraguy, Lee Daniel Crocker, Lemchesvej, Lerdsuwa, Leuko, Lexor, Lhenslee, Lia Todua, LightFlare, Lightmouse, Lightspeedchick, Ligulem, Lincher, Lion Wilson, Lir, Llongland, Llull, Lockesdonkey, Logical2u, Loginbuddy, Looxix, Loren36, Loris, Luigi30, Luk, Lumos3, Luna Santin, Luuva, MER-C, MKoltnow, MONGO, Mac, Madeleine Price Ball, Madhero88, Magadan, Magnus Manske, Majorly, Malcolm rowe, Malo, Mandyj61596, Mantissa128, Marcus.aerlous, Marj Tiefert, MarvPaule, Master dingley, Mattbr, Mattbrundage, Mattjblythe, Mav, Max Baucus' DNA, Max Naylor, McDogm, Medessec, Medos2, Melaen, Melchoir, Mentalmaniac07, Mgiganteus1, Mgtoohey, Mhking, Michael Devore, MichaelHa, Michaelas10, Michigan user, MidgleyDJ, Midnightblueowl, Midoriko, Mika293, Mike Rosoft, Mikker, Mikko Paananen, Mintman16, MisfitToys, Misza13, Mithent, Mjpieters, Mleefs7, Moink, Moorice, Mortene, Mr Bungle, Mr Meow Meow, Mr Stephen, MrErku, Mstislavl, Mstroeck, Mulad, Munita Prasad, Muro de Aguas, Mwanner, Mxn, Nakon, Narayanese, Natalie Erin, Natarajanganesan, Nate1028, NatureA16, Nauseam, Nbauman, Neckro, Netkinetic, Netoholic, Neutrality, NewEnglandYankee, Nighthawk380, NighthawkJ, Nihiltres, Nirajrm, Nishkid64, Nitecrawler, Nitramrekcap, No Guru, NoIdeaNick, NochnoiDozor, Nohat, Northfox, NorwegianBlue, Nthornberry, Nunh-huh, OBloodyHell, OOODDD, Obli, Oblivious, Ocolon, Ojl, Omicronpersei8, Onco p53, Opabinia regalis, Opelio, Orrin Hatch's DNA, Orthologist, Ortolan88, Ouishoebean, Outriggr, OwenX, P99am, PDH, PFHLai, PaePae, Pakaran, Pascal666, Patrick0Moran, Patrick2480, Patstuart, Paul venter, Paulinho28, Pcb21, Pde, Peak, Pedro, Persian Poet Gal, Peter Isotalo, Peter K., Peter Winnberg, Pgan002, Philip Trueman, PhilipO, Phoenix Hacker, Pierceno, PierreAbbat, Pigman, Pigmietheclub, Pilotguy, Pkirlin, Poor Yorick, Portugue6927, Potatoswatter, Preston47, Priscilla 95925, Pristontale111, Pro crast in a tor, Prodego, Psora, PsyMar, Psymier, Pumpkingrower05, Pyrospirit, Quebec99, Quickbeam, Qutezuce, Qxz, R'n'B, R. S. Shaw, RDBrown, RSido, Ragesoss, Rajwiki123, RandomP, Randomblue, Raul654, Raven in Orbit, Ravidreams, Rdb, Rdsmith4, Red Director, Reddi, Rednblu, Redneckjimmy, Redquark, Retired username, Rettetast, RexNL, Rich Farmbrough, RichG, Richard Durbin's DNA, Ricky81682, Rjwilmsi, Roadnottaken, Robdurbar, RobertG, Rocastelo, RoddyYoung, Rory096, Rotem Dan, Roy Brumback, RoyBoy, RoyLaurie, Royalguard11, RunOrDie, Russ47025, RxS, RyanGerbil10, Ryulong, S77914767, SCEhardt, STAN SWANSON, SWAdair, Sabbre, Safwan40, Sakkura, SallyForth123, Sam Burne James, Samsara, Samuel, Samuel Blanning, SandyGeorgia, Sango123, Sangwine, Savidan, Sceptre, Schutz, Sciencechick, Scienceman123, Scincesociety, Sciurinæ, Scope creep, Scotterican, Sean William, SeanMack, Seans Potato Business, SebastianHawes, Seldon1, Sentausa, Serephine, Shadowlynk, Shanes, ShaunL, Shekharsuman, Shizhao, Shmee47, Shoy, Silsor, SimonD, Sintaku, Sir.Loin, Sjjupadhyay, Sjollema, Sloth monkey, Slrubenstein, Sly G, SmilesALot, Smithbrenon, Snowmanradio, Snowolf, Snurks, Solipsist, Someone else, Sonett72, Sopoforic, Spaully, Spectrogram, Splette, Spondoolicks, Spongebobsqpants, SpuriousQ, Squidonius, Squirepants101, Statsone, Steel, Steinsky, Stemonitis, Stephenb, SteveHopson, Stevertigo, Stevietheman, Stewartadcock, Stuart7m, Stuhacking, SupaStarGirl, Supspirit, Susvolans, Sverdrup, Swid, Switchercat, T'Shael, Taco325i, Takometer, TakuyaMurata, Tariqabjotu, Tarret, Taulant23, Tavilis, Tazmaniacs, Ted Longstaffe, Tellyaddict, TenOfAllTrades, Terraguy, Test100000, TestPilot, The Rambling Man, The WikiWhippet, TheAlphaWolf, TheChrisD, TheGrza, TheKMan, TheRanger, Thorwald, ThreeDaysGraceFan101, Thue, Tiddly Tom, Tide rolls, TigerShark, TimVickers, Timewatcher, Timir2, Timl2k4, Timrollpickering, Timwi, Tobogganoggin, Toby Bartels, TobyWilson1992, Tom Allen, Tom Harkin's DNA, Tomgally, Toninu, Tony1, Tonyrenploki, Trd300gt, Trent Lott's DNA, Triwbe, Troels Arvin, Tstrobaugh, Tufflaw, Turnstep, Twilight Realm, Ty146Ty146, UBeR, Unint, Unukorno, Usergreatpower, Utcursch, Uthbrian, Vaernnond, Vandelizer, Vanished user, Vary, Virtualphtn, Visium, Vividonset, VladimirKorablin, Vsmith, Vyasa, WAS 4.250, WAvegetarian, WHeimbigner, WJBscribe, Wafulz, WarthogDemon, Wavelength, WelshMatt, West Brom 4ever, Where, Whosasking, Whoutz, Why My Fleece?, Wik, Wiki alf, Wiki emma johnson, Wikiborg, Wikipedia Administration, William Pietri, WillowW, Wimt, Wknight94, Wmahan, Wnt, Wobble, WolfmanSF, Wouterstomp, Wwwwolf, Xy7, YOUR DNA, Yahel Guhan, Yamamoto Ichiro, Yamla, YanWong, Yansa, Yaser al-Nabriss, Yasha, Yomama9753, Younusporteous, Yurik, ZScout370, Zahid Abdassabur, Zahiri, Zazou, Zell Miller's DNA, Zephyris, Zoicon5, Zouavman Le Zouave, Zsinj, Zven, 1329 anonymous edits

Molecular models of DNA *Source*: http://en.wikipedia.org/windex.php?oldid=296455180 *Contributors*: Bci2, Chris the speller, CommonsDelinker, Oscarthecat, Until It Sleeps

DNA microarray *Source*: http://en.wikipedia.org/windex.php?oldid=294655982 *Contributors*: 168..., 3 Löwi, Aciel, AdamRetchless, Adenosine, Afluegel, AlastairM3754, Albinpaulxavier, Amar kamath, Amarilla858, Amosfolarin, Andrew73, Andrewericoleman, Angr, Apers0n, Arcadian, Aremith, Artgen, Aurelduv, AxelBoldt, Barticus88, Bender235, Bensaccount, Big Bird, Bioinformin, Blacksun, Brian Crawford, Broadbeer, Brooke618, Calmargulis, Carlsbad, Cathleenmrocco, Ceyockey, Chemist234, Ciar, Cmungall, Cobalt137cc, Crissmyass, DGG, Dacharle, Davidweisss, Denix13, Dicklyon, Discospinster, DoctorDNA, Dr. William Jacobs, Drdaveng, Duncharris, Environmatt, Fawcett5, Figma, GV wiki, GeeJo, Geno-Supremo, Giftlite, GiollaUidir, Glane23, Glashedy, GoldenTorc, Gurmukh.s, Gustavocarra, HankMansion, Hephaestos, Hgfernan, Hraefen, Hu12, Hydkat, Iidnormal, Ilovemicroarrays, Ipodamos, Jack-A-Roe, Jackhynes, Jafield, Jahiegel, Jeff Marks, Jethero, Jfdwolff, Jgreene1305, Jgruszynski, JonHarder, Jonathan Hall, Jondel, JosephBarillari, Jotomicron, Jubal, Kantokano, Khalid hassani, KirbyRandolf, Klamber, Kurykh, La goutte de pluie, Lantonov, Larssono, Lassefolkersen, Lea Cleary, Lexor, Lfrench, Lightmouse, Lindsay658, Lisa230579, Lord.lucan, Luwo, Malljaja, MatthewBChambers, Mattpope, Michael Hardy, Miguel Andrade, Movado73, Mxn, Natarajanganesan, NicolasStransky, Nieselt, NoQuarter, Nrhoads, Nuptsey, Olympos, Paphrag, Parijata, Parkinson, Patrick Maitland, Peipei, PeterCanthropus, Pgan002, Pixelface, Postglock, Pvosta, Qinatan, Quartertone, Radagast83, RainbowOfLight, Raul654, Rebut, Rich Farmbrough, Rlockner, Ruud no1, Sandrauesugi, Schutz, Scott.spillman, Sentausa, Shabd sound, Shamrocktuesday, Slustbader, Speedyboy, Spongebobsqpants, Squidonius, Srlasky, SteveChervitzTrutane, Tameeria, Terrace4, TestPilot, Thdog42, The Sunshine Man, TheiNhibition, Thingg, Thomas.Hentrich, Thripsi, Thumperward, Toddmartinsky, Tombadog, Toniosky, Tstokes, Tstrobaugh, Tuskaloosa, Twisp, Typochimp, Tysi, Unint, Vegetarianrage, Venullian, Vladimír Pilný, Vrr, WAS 4.250, WMod-NS, Webridge, West Brom 4ever, Whosasking, Willia, Wk muriithi, Wleizero, Wli625,

Woohookitty, WriterHound, Yaki-gaijin, Zven, 330 anonymous edits

DNA sequencing *Source*: http://en.wikipedia.org/windex.php?oldid=294391714 *Contributors*: 25or6to4, 5piggies, Abanima, Abduallah mohammed, Abdull, Abizar, Agricola44, Akita86, Akjosh, Akriasas, AxelBoldt, BaChev, Bhar100101, Bjorn9800991, Brice one, Charles Gaudette, Cinnamon colbert, Clicketyclack, ConfuciusOrnis, Crana, Cremepuff222, Cspenser, CultureDrone, DWeissman, Dai mingjie, David Schaich, DerHexer, Discospinster, Dkropf, Dnacash, DoctorDNA, Dupz, DutchDevil, Dysmorodrepanis, ERcheck, ESanchez013, Eimeim, Ejwong, Eric-Wester, Eyu100, Fedra, Frankatca, Furby100, Fuxx, George Church, God Emperor, Graminophile, Hoe4sho, Jacopo Werther, Johnuniq, Jvbishop, Keaka411, Ketil, Kku, Kymacpherson, Lantonov, Lenoxus, Lmsutton1, Loris, Luckas Blade, MBCF, Madeleine Price Ball, Magnus Manske, Malljaja, MarcoTolo, Mikael Häggström, Naturespace, Neffk, NewEnglandYankee, Nono64, Novangelis, Noveltyghost, Ohnoitsjamie, Omegatron, Oxymoron83, PDH, Peripitus, Pharos, Pixelface, Pvosta, RDBrown, RJaguar3, RRphys, Red89011, Rees11, Res2216firestar, Rjwilmsi, Robert K S, Robin klein, Robinatron, Rosyaraur, RoyBoy, SJP, Sandahl, Schnarr, Schtina, Seans Potato Business, Sentausa, Shrimp wong, Shyamal, Sintaku, SomethingCatchy, Spellmaster, SteveChervitzTrutane, Su-no-G, Tammyz06, TestPilot, Trevyn, Tsmith423, Twas Now, Victor D, Vinylmeister, Xenon54, Yurivict, Zaimon, 189 anonymous edits

Paracrystal model and theory *Source*: http://en.wikipedia.org/windex.php?oldid=291869326 *Contributors*: Bci2, CharlotteWebb, Furmanj, Giftlite, Sting au, Venny85, Warut, 1 anonymous edits

X-ray scattering *Source*: http://en.wikipedia.org/windex.php?oldid=186202604 *Contributors*: -

Crystallography *Source*: http://en.wikipedia.org/windex.php?oldid=294865893 *Contributors*: 168..., Addere, Ahoerstemeier, Alansohn, Alphachimp, Baldhur, Berland, BlindEagle42, Bluemask, C quest000, Cadmium, Cchoongcc, Cdnc, Christopherlin, Ck lostsword, Commander Nemet, Constructive editor, Conversion script, Coolguy92591, Crystal whacker, Cstras, Cutler, Daarznieks, Drue, Duncan.france, Gcm, Geologyguy, Giftlite, Gilliam, Glenn, Gombang, Gyrofrog, Headbomb, Heron, Hugh2414, Hugo-cs, Invitatious, J.delanoy, Jimfbleak, Jitse Niesen, Jittat, JohnOwens, KSmrq, Kafuffle, Kalpanaiitm, Karol Langner, Kcordina, Kdliss, Kokoriko, Krauss, Kurykh, Leonard G., Linas, Ling.Nut, Luna Santin, M stone, Mahlerite, Malcolm Farmer, Menchi, Mentifisto, Mhaitham.shammaa, Michael Hardy, MikeW25, Mikenorton, Mirokado, Mkosmul, Moonshiner, Mxpule, Olof, Oneforlogic, Oysteinp, Patrick, PhilKnight, Phys, Piano non troppo, Pion, Polyparadigm, Profjohn, PsiStar, Puchiko, Quantockgoblin, Quickbeam, Reciproc08, Rob Hooft, Robinh, Romaioi, SchfiftyThree, Seanwal111111, Siim, Simesa, Substatique, Suisui, TantalumTelluride, TenOfAllTrades, Terrace4, Triops, Uber-Nerd, Van helsing, Vsmith, Walkerma, Walkiped, Wik, Zundark, Zzuuzz, 109 anonymous edits

X-ray crystallography *Source*: http://en.wikipedia.org/windex.php?oldid=296516892 *Contributors*: 168..., 2over0, 84user, ABiochemist, Adenosine, Almostfly, Awadewit, BarretBonden, Bassophile, Ben.c.roberts, Bfiene, Biophys, BlastOButter42, Bobblehead, BokicaK, C. Foultz, C.Fred, Cacycle, Cadmium, Capecodeph, Carcharoth, CardinalDan, Castor canadensis, Cdang, Chem-awb, ChemGrrl, ChemicalBit, Christopherlin, Chrumps, Cometstyles, Conversion script, Cryptophile, Crystal whacker, D4g0thur, Dark link, Dewhastme, EdJohnston, Eequor, ElBenevolente, Enochlau, Evil Monkey, Foobar, Fourchannel, Gcm, Gene Nygaard, Geni, Genisock2, Gertlex, Glen, Graeme Bartlett, Graham87, Gurch, Headbomb, Ian Pitchford, Icek, Ike9898, IowaStateUniversity, Irene Ringworm, Itub, JLaTondre, JMatthews, Jaapkroe, Jcwf, Jdrewitt, Jeff Dahl, Jevinsweval, Jjron, Jmath666, Joachim Wuttke, John, Jonathan Drain, Kaluza, Karelj, Karol Langner, Kazkaskazkasako, Kdliss, Keenan Pepper, Kevin Cowtan, Kjaergaard, Kznf, Leonard G., Lightmouse, Lintze, Lipuju, Liveste, LostLucidity, M stone, Maneesh, MarcoTolo, Marj Tiefert, MartinSchneebeli, Mashford, Maxim, Melamed katz, Memenen, Michael Devore, Michael Hardy, Mikeyrocksya, Moink, Mr Stephen, Msebast, N p holmes, Naudefj, NerdyNSK, Nihiltres, O RLY?, Oeffner, Opabinia regalis, Oysteinp, Paolo.dL, Paul Henning, Phe, Philip Trueman, Pilatus, Pjacobi, Polyparadigm, Prashanthns, Protonk, Quantockgoblin, Quickbeam, Quixeh, RJHall, Ravi22, Reciproc08, Riana, Rifleman 82, Rmhermen, Romaioi, S Levchenkov, STHayden, Sasakthi, Seans Potato Business, ShadE04, Shenme, Silly rabbit, SimonP, Sintaku, Splette, Srleffler, Ssteinz13, Starnestommy, Stewartadcock, TBChem, Tasfhkl, Tassedethe, Tempodivalse, The Special Six, Thincat, TimVickers, Tpikonen, Tralala, TreeSmiler, V8rik, Voorlandt, Vossman, Vsmith, WahreJakob, Wavelength, WaysToEscape, Webridge, Wheedhee, WillowW, Wimvandorst, Xcomradex, Yardgnome, Yyy, 225 anonymous edits

X-ray diffraction *Source*: http://en.wikipedia.org/windex.php?oldid=113378071 *Contributors*: -

X-ray microscopy *Source*: http://en.wikipedia.org/windex.php?oldid=16987920 *Contributors*: -

Electron microscopy *Source*: http://en.wikipedia.org/windex.php?oldid=15996062 *Contributors*: -

Vibrational circular dichroism *Source*: http://en.wikipedia.org/windex.php?oldid=295070744 *Contributors*: Aktsu, Auntof6, Bci2, Buurma, Jndurand, Slaweks

FT-NMR *Source*: http://en.wikipedia.org/windex.php?oldid=280684865 *Contributors*: Aihre, Andy M. Wang, AxelBoldt, Bci2, Beetstra, Benandjonice, Biophysik, Borisovav, Bruker, CaneryMBurns, Ceyockey, ChemistHans, Cryptophile, DMacks, Djdaedalus, Flogiston, Freestyle-69, G-W, GeeJo, Gehtnix, Gene Nygaard, Ghiles, Graeme Bartlett, Hammer1980, Headbomb, Jclerman, Jenpen, Jingxin, Jrizor8504, Julesd, Kafziel, Kaiserkarl13, Keraman, Kjaergaard, Kkmurray, La goutte de pluie, Lee-Jon, LinguisticDemographer, Linmhall, Mac Davis, Markjoseph125, Mboverload, Measure4Measure, Mike.lifeguard, Neparis, OMCV, Oxymoron83, Pekaje, Quantockgoblin, RG2, Ribol, Rifleman 82, Runningonbrains, Salsb, Santiago Dominguez, Shalom Yechiel, Shrew, Sikkema, Smokefoot, Spellmaster, Srnec, Stepa, Takometer, TenOfAllTrades, Tkircher, Troodon, V8rik, Walkerma, WhatamIdoing, Xenonice, Zosma, 55 anonymous edits

NMR microscopy *Source*: http://en.wikipedia.org/windex.php?oldid=17600642 *Contributors*: -

NIR *Source*: http://en.wikipedia.org/windex.php?oldid=273506815 *Contributors*: AndreaM519, Barticus88, BoomerAB, D6, Dachannien, Deglr6328, Doktorbuk, Fennessy, Hauserns, Ice Cold Beer, Jamesbrownontheroad, JavierMC, Jeff3000, Knowme23, Kusunose, Modest Genius, Mrz94, Numbo3, Patman, Pebb, Pwilson@apnic.net, Richardcavell, SHARU(ja), Sam Hocevar, Sanders muc, Transfinite, Wafulz, 24 anonymous edits

Spectral *Source*: http://en.wikipedia.org/windex.php?oldid=218583547 *Contributors*: BenFrantzDale, Bobo192, Cm the p, Krash, PAR, RJHall, Zowie, 2 anonymous edits

Hyperspectral *Source*: http://en.wikipedia.org/windex.php?oldid=291759304 *Contributors*: Adoniscik, Andrew c, Bci2, Cm the p, Dhaluza, Gcrisford, Geologicharka, Hankwang, Jprikkel, Lantonov, Moin95, Victorsong, 15 anonymous edits

Chemical imaging *Source*: http://en.wikipedia.org/windex.php?oldid=290927658 *Contributors*: Alansohn, Andyphil, AngelOfSadness, Annabel, Banus, Batykefer, Bci2, BierHerr, Chris the speller, Closedmouth, D6, Davewild, Editore99, GeeJo, HYPN2457, Iridescent, JIP, Jim.henderson, Kkmurray, Mdd, Mkansiz, Natalie Erin, Skysmith, Ultraexactzz, Wilson003, 38 anonymous edits

Raman *Source*: http://en.wikipedia.org/windex.php?oldid=290238040 *Contributors*: Ahoerstemeier, Col tom, Dancarney, Defenestrating Monday, Fredericks, Iridescent, Jagged 85, Mshafqat, Pahari Sahib, Physicistjedi, Robert Skyhawk, Sam Vimes, Skumarla, Soccer2, Sonikku, Tejas81, Tide rolls, Ttennebkram, Xyzzyplugh, 15 anonymous edits

Fluorescence correlation spectroscopy *Source*: http://en.wikipedia.org/windex.php?oldid=291763472 *Contributors*: Bci2, BenFrantzDale, Berky, Danrs, Dkkim, Gogowitsch, Hbayat, Jcwf, John, Karol Langner, Lightmouse, Maartend8, ST47, Skier Dude, Tizeff, Wisdom89, 32 anonymous edits

Molecular models of DNA *Source*: http://en.wikipedia.org/windex.php?oldid=296455180 *Contributors*: Bci2, Chris the speller, CommonsDelinker, Oscarthecat, Until It Sleeps

Molecular graphics *Source*: http://en.wikipedia.org/windex.php?oldid=285442351 *Contributors*: ALoopingIcon, Agilemolecule, Altenmann, Arch dude, Chemistrannik, Chenmengen, CzarB, Dcrjsr, Dreftymac, Edguy99, Edward, EranHodis, Fvasconcellos, Harryboyles, Icep, JLSussman, Jweiss11, Karol Langner, Linforest, McVities, Mdd, Mobius, Mrug2, NapoliRoma, NicoV, Ohnoitsjamie, Outriggr, P99am, PBarak, Petermr, ProveIt, Rjwilmsi, Rogerb67, SchuminWeb, Shura58, Sjoerd de Vries, SkyWalker, Thumperward, Timrollpickering, Vriend, Walkerma, 16 anonymous edits

DNA structure *Source*: http://en.wikipedia.org/windex.php?oldid=293141623 *Contributors*: Andreww, Antandrus, Bci2, CDN99, Chodges, DVD R W, DabMachine, Dysmorodrepanis, Forluvoft, Gene Nygaard, Hannes Röst, Harold f, Joel7687, Josq, Luuva, Maikfr, Mr.Z-man, MrHaiku, Nasz, Patrick0Moran, Rajan.kartik, Reinyday, Rich Farmbrough, Thorwald, TimVickers, Tomgally, Wknight94, Yahel Guhan, Zephyris, 23 anonymous edits

Neutron scattering *Source*: http://en.wikipedia.org/windex.php?oldid=296496375 *Contributors*: Andyfaff, Calltl, Cardamon, Chipmonker, EBlackburn, Grj23, Hellbus, J bellingham, Jdrewitt, Joachim Wuttke, Karol Langner, Kdliss, Kiyabg, Msiebuhr, NSR, Nitrous x, Paula Pilcher, PhilBentley, PranksterTurtle, Qwerty Binary, Sam8, Sanders muc, Soarhead77, 12 anonymous edits

Paracrystalline lattices/Paracrystals *Source*: http://en.wikipedia.org/windex.php?oldid=291869326 *Contributors*: Bci2, CharlotteWebb, Furmanj, Giftlite, Sting au, Venny85, Warut, 1 anonymous edits

2D-FT NMRI and Spectroscopy *Source*: http://en.wikipedia.org/windex.php?oldid=292543320 *Contributors*: Bci2, Ched Davis, Drilnoth, H Padleckas, JaGa, Reedy, Rich Farmbrough, Rjwilmsi, 2 anonymous edits

FRET and FCS-Fluorescence correlation spectroscopy *Source*: http://en.wikipedia.org/windex.php?oldid=294258893 *Contributors*: Aciel, Aclapp, Alansohn, Alessandro Esposito, Aloening, Asger.kryger, Asgerk, Banderaazul, Bci2, Chodges, Cleggrobert, Clicketyclack, Cnickelfr, Cortonin, Cpichardo, DeadEyeArrow, Edgar181, Hankwang, Haukurth, Ian Pitchford, JOK, Jaganath, Jammedshut, Kawaiyas, Kungfuadam, Lantonov, Lifeisaserenade, Locos epraix, Looie, Mah159, Markus Poessel, Miguel Andrade, Mr d logan, Nono64, Oakwood, OldakQuill, PDH, Phi-Gastrein, RH, Rich Farmbrough, RockyRaccoon, Rushphoton, Sam Hocevar, Seans Potato Business, ShakingSpirit, Sintaku, SocratesJedi, TenOfAllTrades, Theron110, Tomgally, Trevva, V8rik, Wisdom89, Yiddy55, 101 anonymous edits

DNA Dynamics *Source*: http://en.wikipedia.org/windex.php?oldid=296104632 *Contributors*: Auntof6, Bci2, Cander0000, Chris the speller, CommonsDelinker, Ironholds, Potatoswatter

DNA nanotechnology *Source*: http://en.wikipedia.org/windex.php?oldid=294763628 *Contributors*: 0x38I9J*, Alnokta, Amaling, Anthonydelaware, Antony-22, Cyfal, Epbr123, Giftlite, Gioto, Pwkr, ShawnDouglas, Thorwald, Tolosthemagician, ZayZayEM, 30 anonymous edits

Imaging *Source*: http://en.wikipedia.org/windex.php?oldid=285115434 *Contributors*: Alai, Arcadian, Bact, Bme591wikiproject, Burt Harris, Carnildo, Chris the speller, David Shay, Dicklyon, Edcolins, Eleassar777, Kaeslin, Karol Langner, Kauczuk, Leonard G., Lights, Maikel, Nbarth, Oicumayberight, Patrick, Pde, Poweroid, Quantum2006, Quuxplusone, Qxz, Ringbang, Sander123, Seabhcan, Shawndkc, Srleffler, TBarregren, Tazmaniacs, Timtzeptel, Vladimir Drzik, Voicetalent, Wik, 18 anonymous edits

Atomic force microscope *Source*: http://en.wikipedia.org/windex.php?oldid=292261720 *Contributors*: .:Ajvol:., Admartch, Ahram, Ahram-kim, Alansohn, Allentchang, Alvestrand, Ambios, Ams627, Angela, Anthonydelaware, Antony-22, Arcfrk, Ase, Askewmind, Average Earthman, Bendzh, Bfollinprm, Bibble, Biophys, Bobblewik, Bochica, Bryan Derksen, Canjth, Cdnc, Chuckiesdad, Chych, Creepin475, Crm2kmsu, Crystallina, Cucumberslumber, Cyrus Grisham, Davidcastro, Dgrant, Doulos Christos, Edward, El C, Femto, Flipperinu, Fontissophy, Frosty0814snowman, Gaijinpl, Gene Nygaard, Gene93k, Geodesic42, Graphene, Grmf, HYPN2457, Halibutt, Jatosado, Jaxl, Jcwf, Jni, Joechao, Joeyfox10, John, John Dalton, Kamukwam, Kariteh, Keenan Pepper, KristianMolhave, LMB, Lauranrg, Leifisme, Maximus Rex, Mormegil, NanoMamaForReal, Nmnogueira, Oreo Priest, Physicistjedi, Pieter Kuiper, Quadell, Qxz, Raymondwinn, Rhandley123, RoB, Rob Hooft, Ronz, Rostislav Lapshin, Ruder, SJP, Satish.murthy, Sbyrnes321, SecretDisc, Seraphchoir, Shniken1, Sisyphos happy man, Skier Dude, Switchsonic, Tai89ch, Think outside the box, Tim Starling, Uglygizmo, Vfranceschi, Wiki alf, Wikiborg, XarBiogeek, Yapete, Yurko, Yyy, Zeamays, Zureks, 176 anonymous edits

Electron microscope *Source*: http://en.wikipedia.org/windex.php?oldid=296877389 *Contributors*: 007 n1, 5Q5, A. Carty, ABF, Aaronsharpe, Acroterion, Adam Mihalyi, Adambiswanger1, Adijr, AdjustShift, Aillema, Aitias, Alan012, Alansohn, Albany NY, Alex Klotz, Amaltheus, Andre Engels, Andrei Stroe, Antonio Lopez, Apparition11, ArchonMagnus, Aurelius173, Average Earthman, Backslash Forwardslash, Banus, Bencherlite, Bender235, Bensaccount, Blechnic, Bobo192, Bongwarrior, Borgx, Brianga, C0nanPayne, Calabraxthis, Camembert, Can't sleep, clown will eat me, CanisRufus, Capricorn42, Captain-tucker, Cbj77, Cetcher1159, Ceyockey, Cgarber, Chai, Chem-awb, Chris G, Chrislk02, Chych, Closenplay, Conversion script, Corpx, Csown, D, DVD R W, Daniel, DarkFalls, Darth Panda, Davewild, David R. Ingham, Davidbaca, Dcoetzee, Deglr6328, DeltaMicroscopyStudent, DerHexer, Dexarouskies, Dexter prog, Dgrant, Dicklyon, Dlohcierekim, Docu, DoubleBlue, Doyley, DrFO.Jr.Tn, DrMikeF, Dvratnam, Editor2020, El aprendelenguas, Elearning2000, Enchanter, Epbr123, Ephram Shizgal, EricV89, Esem0, Evan1991, EyeSerene, Fabricationary, Ferengi, Fieldday-sunday, Fireice, Frank, Frank A, Frankatca, Frankenpuppy, Fueled, Funnybunny, Gaius Cornelius, Gary King, Gene Nygaard, George Burgess, Gh5046, Giftlite, Gogo Dodo, Golfguy220-, GrahamColm, Grey Shadow, Ground, Hat'nCoat, Hedgemonkey, Heron, Horselover Frost, Hu, Hugo-cs, Hurricane Angel, Hydrogen Iodide, II MusLiM HyBRiD II, ILike2BeAnonymous, INkubusse, Ian Pitchford, IanOsgood, Imaninjapirate, Irfanhasmit, Isaac yagmoor, Itai, J.delanoy, JNighthawk, JRodeng, JTN, JaGa, Jaccardi, Jacopo Werther, Jeremiah, Jimp, Joelholdsworth, JohnOwens, JorgeGG, Joshua.morgan, Karnesky, Karol Langner, Keilana, Kesac, Kils, Kingpin13, Kissavos, KnowledgeOfSelf, Konsu, Kpjas, KristianMolhave, Kukini, Kuru, Kusunose, KyraVixen, Kzollman, LeilaniLad, Liferulez, Lindmere, Luna Santin, MER-C, Magnus Manske, MarcoTolo, Marek69, Mark.murphy, Maro91eg, Materialscientist, Mayapur, McSly, Mikaey, Mmxx, Monkeyknife, MoogleFan, Mschlindwein, Mwtoews, Myscrnnm, Nate1481, Nath87, Ncemer, Netkinetic, Neurolysis, Nickfor1, Nihiltres, Nikai, Nmnogueira, Novalis, Oceano30, Oysteinp, Paulhaiti, Pengo, Perfecto, Pharaoh of the Wizards, Piano non troppo, Pip2andahalf, Plantsurfer, Plasticup, Pliable, PrestonH, Quadell, R.rommel, RainbowOfLight, Rajah, Richard Arthur Norton (1958-), Riflemann, Risk one, Rjwilmsi, RobHarding, Rror, Rurik3, Rustavo, S0uj1r0, STHayden, Sceptre, Sciurinæ, Sean William, Selket, Shirulashem, Sikkema, Silsor, Simon Shek, Simonmn, Sludtke42, Snowmanradio, Snoyes, Sodium, Spbrandom, Spearhead, Speedyboy, Srdomingue, Srnec, Stahlkocher1, Steff, StephenBuxton, Steve Crossin, Stokerm, Sub-Angstrom, Svdmolen, Tacvek, Tahirulislam, Tapir Terrific, Terrace4, The Anome, Thedjatclubrock, Thermochap, Thingg, Tijadr, Til.Bartel, TimVickers, Tjmayerinsf, Tmopkisn, Travelbird, Twisted86, Ulfbastel, Utcursch, Vossman, WahreJakob, Willking1979, Wtmitchell, Xy7, Zephyris, Zzuuzz, Кодекс, ვიბა, 647 anonymous edits

X-ray microscope *Source*: http://en.wikipedia.org/windex.php?oldid=296734543 *Contributors*: AB, AndyBQ, Birge, Bouncingmolar, Can't sleep, clown will eat me, Chamal N, Deglr6328, Discospinster, Dratman, EbozMoore, Heron, Icairns, JTN, Marshman, NHSavage, Ptfptf, Rl, RoyBoy, Sommacal Alfonso, Stepp-Wulf, Stirling Newberry, The Anome, Томми Нёрд, 27 anonymous edits

Image Sources, Licenses and Contributors

File:ADN animation.gif *Source*: http://en.wikipedia.org/windex.php?title=File:ADN_animation.gif *License*: Public Domain *Contributors*: Aushulz, Bawolff, Brian0918, Kersti Nebelsiek, Magadan, Mattes, Origamiemensch, Stevenfruitsmaak, 3 anonymous edits

Image:DNA in water.jpg *Source*: http://en.wikipedia.org/windex.php?title=File:DNA_in_water.jpg *License*: unknown *Contributors*: User:Bbkkk

Image:DNA chemical structure.svg *Source*: http://en.wikipedia.org/windex.php?title=File:DNA_chemical_structure.svg *License*: unknown *Contributors*: Madprime, Wickey, 1 anonymous edits

File:DNA orbit animated static thumb.png *Source*: http://en.wikipedia.org/windex.php?title=File:DNA_orbit_animated_static_thumb.png *License*: GNU Free Documentation License *Contributors*: 84user adapting file originally uploaded by Richard Wheeler (Zephyris) at en.wikipedia

Image:GC DNA base pair.svg *Source*: http://en.wikipedia.org/windex.php?title=File:GC_DNA_base_pair.svg *License*: Public Domain *Contributors*: User:Isilanes

Image:AT DNA base pair.svg *Source*: http://en.wikipedia.org/windex.php?title=File:AT_DNA_base_pair.svg *License*: Public Domain *Contributors*: User:Isilanes

Image:A-DNA, B-DNA and Z-DNA.png *Source*: http://en.wikipedia.org/windex.php?title=File:A-DNA,_B-DNA_and_Z-DNA.png *License*: GNU Free Documentation License *Contributors*: Original uploader was Richard Wheeler (Zephyris) at en.wikipedia

Image:Parallel telomere quadruple.png *Source*: http://en.wikipedia.org/windex.php?title=File:Parallel_telomere_quadruple.png *License*: unknown *Contributors*: User:Splette

Image:Branch-dna.png *Source*: http://en.wikipedia.org/windex.php?title=File:Branch-dna.png *License*: unknown *Contributors*: Peter K.

Image:Multi-branch-dna.png *Source*: http://en.wikipedia.org/windex.php?title=File:Multi-branch-dna.png *License*: unknown *Contributors*: User:Peter K.

Image:Cytosine chemical structure.png *Source*: http://en.wikipedia.org/windex.php?title=File:Cytosine_chemical_structure.png *License*: GNU Free Documentation License *Contributors*: BorisTM, Bryan Derksen, Cacycle, Edgar181, Engineer gena

Image:5-methylcytosine.png *Source*: http://en.wikipedia.org/windex.php?title=File:5-methylcytosine.png *License*: unknown *Contributors*: EDUCA33E, Luigi Chiesa, Mysid

Image:Thymine chemical structure.png *Source*: http://en.wikipedia.org/windex.php?title=File:Thymine_chemical_structure.png *License*: GNU Free Documentation License *Contributors*: Arrowsmaster, BorisTM, Bryan Derksen, Cacycle, Edgar181, Leyo

Image:Benzopyrene DNA adduct 1JDG.png *Source*: http://en.wikipedia.org/windex.php?title=File:Benzopyrene_DNA_adduct_1JDG.png *License*: GNU Free Documentation License *Contributors*: Benjah-bmm27, Bstlee, 1 anonymous edits

Image:T7 RNA polymerase at work.png *Source*: http://en.wikipedia.org/windex.php?title=File:T7_RNA_polymerase_at_work.png *License*: unknown *Contributors*: User:Splette

Image:DNA replication.svg *Source*: http://en.wikipedia.org/windex.php?title=File:DNA_replication.svg *License*: unknown *Contributors*: Bibi Saint-Pol, Elborgo, En rouge, Helix84, Jnpet, LadyofHats, Leafnode, M.Komorniczak, MetalGearLiquid, Nikola Smolenski, Nl74, Sentausa, WarX, 2 anonymous edits

Image:Nucleosome 2.jpg *Source*: http://en.wikipedia.org/windex.php?title=File:Nucleosome_2.jpg *License*: Public Domain *Contributors*: Original uploader was TimVickers at en.wikipedia

Image:Nucleosome (opposites attracts).JPG *Source*: http://en.wikipedia.org/windex.php?title=File:Nucleosome_(opposites_attracts).JPG *License*: Public Domain *Contributors*: Illustration by David S. Goodsell of The Scripps Research Institute (see this site)

Image:Lambda repressor 1LMB.png *Source*: http://en.wikipedia.org/windex.php?title=File:Lambda_repressor_1LMB.png *License*: GNU Free Documentation License *Contributors*: Original uploader was Zephyris at en.wikipedia

Image:EcoRV 1RVA.png *Source*: http://en.wikipedia.org/windex.php?title=File:EcoRV_1RVA.png *License*: GNU Free Documentation License *Contributors*: Original uploader was Zephyris at en.wikipedia

Image:Holliday Junction cropped.png *Source*: http://en.wikipedia.org/windex.php?title=File:Holliday_Junction_cropped.png *License*: GNU Free Documentation License *Contributors*: Original uploader was TimVickers at en.wikipedia

Image:Holliday junction coloured.png *Source*: http://en.wikipedia.org/windex.php?title=File:Holliday_junction_coloured.png *License*: GNU Free Documentation License *Contributors*: Original uploader was Zephyris at en.wikipedia

Image:Chromosomal Recombination.svg *Source*: http://en.wikipedia.org/windex.php?title=File:Chromosomal_Recombination.svg *License*: Creative Commons Attribution 2.5 *Contributors*: User:Gringer

Image:DNA nanostructures.png *Source*: http://en.wikipedia.org/windex.php?title=File:DNA_nanostructures.png *License*: unknown *Contributors*: (Images were kindly provided by Thomas H. LaBean and Hao Yan.)

Image:JamesDWatson.jpg *Source*: http://en.wikipedia.org/windex.php?title=File:JamesDWatson.jpg *License*: Public Domain *Contributors*: Edward, RP88, Shizhao, Stellatomailing, Vonvon, 3 anonymous edits

Image:Francis Crick.png *Source*: http://en.wikipedia.org/windex.php?title=File:Francis_Crick.png *License*: unknown *Contributors*: Photo: Marc Lieberman

Image:FrancisHarryComptonCrick.jpg *Source*: http://en.wikipedia.org/windex.php?title=File:FrancisHarryComptonCrick.jpg *License*: unknown *Contributors*: Bunzil, Million Moments, PDH

Image:Rosalind Franklin.jpg *Source*: http://en.wikipedia.org/windex.php?title=File:Rosalind_Franklin.jpg *License*: Public Domain *Contributors*: unknown

Image:Raymond Gosling.jpg *Source*: http://en.wikipedia.org/windex.php?title=File:Raymond_Gosling.jpg *License*: GNU Free Documentation License *Contributors*: User:Davidruben

Image:maurice_wilkins.jpg *Source*: http://en.wikipedia.org/windex.php?title=File:Maurice_wilkins.jpg *License*: unknown *Contributors*: Anetode, PDH, Rvilbig

Image:Erwin Chargaff.jpg *Source*: http://en.wikipedia.org/windex.php?title=File:Erwin_Chargaff.jpg *License*: Public Domain *Contributors*: unknown

Image:Rosalindfranklinsjokecard.jpg *Source*: http://en.wikipedia.org/windex.php?title=File:Rosalindfranklinsjokecard.jpg *License*: unknown *Contributors*: Bci2, J.delanoy, Martyman, Nitramrekcap, Rjm at sleepers, 3 anonymous edits

Image:Sarfus.DNABiochip.jpg *Source*: http://en.wikipedia.org/windex.php?title=File:Sarfus.DNABiochip.jpg *License*: unknown *Contributors*: Nanolane

Image:Spinning DNA.gif *Source*: http://en.wikipedia.org/windex.php?title=File:Spinning_DNA.gif *License*: Public Domain *Contributors*: USDA

File:Methanol.pdb.png *Source*: http://en.wikipedia.org/windex.php?title=File:Methanol.pdb.png *License*: Creative Commons Attribution-Sharealike 2.5 *Contributors*: ALoopingIcon, Benjah-bmm27

File:DNA-fragment-3D-vdW.png *Source*: http://en.wikipedia.org/windex.php?title=File:DNA-fragment-3D-vdW.png *License*: Public Domain *Contributors*: Benjah-bmm27

File:Simple harmonic oscillator.gif *Source*: http://en.wikipedia.org/windex.php?title=File:Simple_harmonic_oscillator.gif *License*: Public Domain *Contributors*: User:Oleg Alexandrov

File:DNA chemical structure.svg *Source*: http://en.wikipedia.org/windex.php?title=File:DNA_chemical_structure.svg *License*: unknown *Contributors*: Madprime, Wickey, 1 anonymous edits

File:Parallel telomere quadruple.png *Source*: http://en.wikipedia.org/windex.php?title=File:Parallel_telomere_quadruple.png *License*: unknown *Contributors*: User:Splette

File:Four-way DNA junction.gif *Source*: http://en.wikipedia.org/windex.php?title=File:Four-way_DNA_junction.gif *License*: Public Domain *Contributors*: Aushulz, Molatwork, Origamiemensch, TimVickers, 1 anonymous edits

File:DNA replication.svg *Source*: http://en.wikipedia.org/windex.php?title=File:DNA_replication.svg *License*: unknown *Contributors*: Bibi Saint-Pol, Elborgo, En rouge, Helix84, Jnpet, LadyofHats, Leafnode, M.Komorniczak, MetalGearLiquid, Nikola Smolenski, Nl74, Sentausa, WarX, 2 anonymous edits

File:ABDNAxrgpj.jpg *Source*: http://en.wikipedia.org/windex.php?title=File:ABDNAxrgpj.jpg *License*: GNU Free Documentation License *Contributors*: I.C. Baianu et al.

File:Plos VHL.jpg *Source*: http://en.wikipedia.org/windex.php?title=File:Plos_VHL.jpg *License*: Creative Commons Attribution 2.5 *Contributors*: Akinom, Anniolek, Filip em, Thommiddleton

File:3D model hydrogen bonds in water.jpg *Source*: http://en.wikipedia.org/windex.php?title=File:3D_model_hydrogen_bonds_in_water.jpg *License*: GNU Free Documentation License *Contributors*: User:snek01

Image:Methanol.pdb.png *Source*: http://en.wikipedia.org/windex.php?title=File:Methanol.pdb.png *License*: Creative Commons Attribution-Sharealike 2.5 *Contributors*: ALoopingIcon, Benjah-bmm27

Image:DNA-(A)80-model.png *Source*: http://en.wikipedia.org/windex.php?title=File:DNA-(A)80-model.png *License*: unknown *Contributors*: User:P99am

File:Bragg diffraction.png *Source*: http://en.wikipedia.org/windex.php?title=File:Bragg_diffraction.png *License*: GNU General Public License *Contributors*: user:hadmack

File:DNA in water.jpg *Source*: http://en.wikipedia.org/windex.php?title=File:DNA_in_water.jpg *License*: unknown *Contributors*: User:Bbkkk

File:X ray diffraction.png *Source*: http://en.wikipedia.org/windex.php?title=File:X_ray_diffraction.png *License*: unknown *Contributors*: Thomas Splettstoesser

File:X Ray Diffractometer.JPG *Source*: http://en.wikipedia.org/windex.php?title=File:X_Ray_Diffractometer.JPG *License*: GNU Free Documentation License *Contributors*: Ff02::3, Pieter Kuiper

File:SLAC detector edit1.jpg *Source*: http://en.wikipedia.org/windex.php?title=File:SLAC_detector_edit1.jpg *License*: unknown *Contributors*: User:Mfield, User:Starwiz

File:ISIS exptal hall.jpg *Source*: http://en.wikipedia.org/windex.php?title=File:ISIS_exptal_hall.jpg *License*: unknown *Contributors*: wurzeller

File:Dna-SNP.svg *Source*: http://en.wikipedia.org/windex.php?title=File:Dna-SNP.svg *License*: unknown *Contributors*: User:Gringer

File:DNA Under electron microscope Image 3576B-PH.jpg *Source*: http://en.wikipedia.org/windex.php?title=File:DNA_Under_electron_microscope_Image_3576B-PH.jpg *License*: unknown *Contributors*: Original uploader was SeanMack at en.wikipedia

File:DNA Model Crick-Watson.jpg *Source*: http://en.wikipedia.org/windex.php?title=File:DNA_Model_Crick-Watson.jpg *License*: Public Domain *Contributors*: User:Alkivar

File:DNA labels.jpg *Source*: http://en.wikipedia.org/windex.php?title=File:DNA_labels.jpg *License*: GNU Free Documentation License *Contributors*: User:Raul654

File:AT DNA base pair pt.svg *Source*: http://en.wikipedia.org/windex.php?title=File:AT_DNA_base_pair_pt.svg *License*: Public Domain *Contributors*: User:Lijealso

File:A-B-Z-DNA Side View.png *Source*: http://en.wikipedia.org/windex.php?title=File:A-B-Z-DNA_Side_View.png *License*: Public Domain *Contributors*: Original uploader was Thorwald at en.wikipedia

File:Museo Príncipe Felipe. ADN.jpg *Source*: http://en.wikipedia.org/windex.php?title=File:Museo_Príncipe_Felipe._ADN.jpg *License*: Creative Commons Attribution-Sharealike 2.0 *Contributors*: Fernando

File:AGCT DNA mini.png *Source*: http://en.wikipedia.org/windex.php?title=File:AGCT_DNA_mini.png *License*: unknown *Contributors*: Iquo

File:BU Bio5.jpg *Source*: http://en.wikipedia.org/windex.php?title=File:BU_Bio5.jpg *License*: Creative Commons Attribution-Sharealike 2.0 *Contributors*: Original uploader was Elapied at fr.wikipedia

File:Circular DNA Supercoiling.png *Source*: http://en.wikipedia.org/windex.php?title=File:Circular_DNA_Supercoiling.png *License*: GNU Free Documentation License *Contributors*: Richard Wheeler (Zephyris)

File:Rosalindfranklinsjokecard.jpg *Source*: http://en.wikipedia.org/windex.php?title=File:Rosalindfranklinsjokecard.jpg *License*: unknown *Contributors*: Bci2, J.delanoy, Martyman, Nitramrekcap, Rjm at sleepers, 3 anonymous edits

File:Genomics GTL Pictorial Program.jpg *Source*: http://en.wikipedia.org/windex.php?title=File:Genomics_GTL_Pictorial_Program.jpg *License*: Public Domain *Contributors*: Mdd

File:RNA pol.jpg *Source*: http://en.wikipedia.org/windex.php?title=File:RNA_pol.jpg *License*: Public Domain *Contributors*: InfoCan

File:Primase 3B39.png *Source*: http://en.wikipedia.org/windex.php?title=File:Primase_3B39.png *License*: Public Domain *Contributors*: own work

File:DNA Repair.jpg *Source*: http://en.wikipedia.org/windex.php?title=File:DNA_Repair.jpg *License*: Public Domain *Contributors*: Courtesy of Tom Ellenberger, Washington University School of Medicine in St. Louis.

File:MGMT+DNA 1T38.png *Source*: http://en.wikipedia.org/windex.php?title=File:MGMT+DNA_1T38.png *License*: Public Domain *Contributors*: own work

File:DNA damaged by carcinogenic 2-aminofluorene AF .jpg *Source*: http://en.wikipedia.org/windex.php?title=File:DNA_damaged_by_carcinogenic_2-aminofluorene_AF_.jpg *License*: Public Domain *Contributors*: Brian E. Hingerty, Oak Ridge National Laboratory Suse Broyde, New York University Dinshaw J. Patel, Memorial Sloan Kettering Cancer Center

File:A-DNA orbit animated small.gif *Source*: http://en.wikipedia.org/windex.php?title=File:A-DNA_orbit_animated_small.gif *License*: GNU Free Documentation License *Contributors*: User:Bstlee, User:Zephyris

File:Plasmid emNL.jpg *Source*: http://en.wikipedia.org/windex.php?title=File:Plasmid_emNL.jpg *License*: GNU Free Documentation License *Contributors*: Denniss, Glenn, Rasbak

File:Chromatin chromosom.png *Source*: http://en.wikipedia.org/windex.php?title=File:Chromatin_chromosom.png *License*: Public Domain *Contributors*: User:Magnus Manske

File:Chromosome.svg *Source*: http://en.wikipedia.org/windex.php?title=File:Chromosome.svg *License*: unknown *Contributors*: User:Dietzel65, User:Magnus Manske, User:Tryphon

File:Chr2 orang human.jpg *Source*: http://en.wikipedia.org/windex.php?title=File:Chr2_orang_human.jpg *License*: Creative Commons Attribution-Sharealike 2.5 *Contributors*: Verena Schubel, Stefan Müller, Department Biologie der Ludwig-Maximilians-Universität München.

File:3D-SIM-3 Prophase 3 color.jpg *Source*: http://en.wikipedia.org/windex.php?title=File:3D-SIM-3_Prophase_3_color.jpg *License*: Creative Commons Attribution-Sharealike 3.0 *Contributors*: Lothar Schermelleh

File:Chromosome2 merge.png *Source*: http://en.wikipedia.org/windex.php?title=File:Chromosome2_merge.png *License*: Public Domain *Contributors*: Original uploader was Evercat at en.wikipedia

File:Transkription Translation 01.jpg *Source*: http://en.wikipedia.org/windex.php?title=File:Transkription_Translation_01.jpg *License*: Public Domain *Contributors*: User:Kuebi

File:RibosomaleTranskriptionsEinheit.jpg *Source*: http://en.wikipedia.org/windex.php?title=File:RibosomaleTranskriptionsEinheit.jpg *License*: GNU Free Documentation License *Contributors*: User:Merops

File:Chromosome Conformation Capture Technology.jpg *Source*: http://en.wikipedia.org/windex.php?title=File:Chromosome_Conformation_Capture_Technology.jpg *License*: Public Domain *Contributors*:

User:Kangyun1985

File:Mitochondrial DNA and diseases.png *Source*: http://en.wikipedia.org/windex.php?title=File:Mitochondrial_DNA_and_diseases.png *License*: unknown *Contributors*: User:XXXL1986

File:PCR.svg *Source*: http://en.wikipedia.org/windex.php?title=File:PCR.svg *License*: unknown *Contributors*: User:Madprime

File:Pcr gel.png *Source*: http://en.wikipedia.org/windex.php?title=File:Pcr_gel.png *License*: GNU Free Documentation License *Contributors*: Habj, Ies, PatríciaR, Retama, Saperaud

File:DNA nanostructures.png *Source*: http://en.wikipedia.org/windex.php?title=File:DNA_nanostructures.png *License*: unknown *Contributors*: (Images were kindly provided by Thomas H. LaBean and Hao Yan.)

File:SFP discovery principle.jpg *Source*: http://en.wikipedia.org/windex.php?title=File:SFP_discovery_principle.jpg *License*: unknown *Contributors*: User:Agbiotec

File:Cdnaarray.jpg *Source*: http://en.wikipedia.org/windex.php?title=File:Cdnaarray.jpg *License*: unknown *Contributors*: Mangapoco

File:Expression of Human Wild-Type and P239S Mutant Palladin.png *Source*: http://en.wikipedia.org/windex.php?title=File:Expression_of_Human_Wild-Type_and_P239S_Mutant_Palladin.png *License*: unknown *Contributors*: see above

File:Random genetic drift chart.png *Source*: http://en.wikipedia.org/windex.php?title=File:Random_genetic_drift_chart.png *License*: unknown *Contributors*: User:Professor marginalia

File:Co-dominance Rhododendron.jpg *Source*: http://en.wikipedia.org/windex.php?title=File:Co-dominance_Rhododendron.jpg *License*: Creative Commons Attribution 2.0 *Contributors*: Ayacop, Cillas, FlickrLickr, FlickreviewR, Horcha, Kanonkas, Kevmin, MPF, Para

File:DNA_nanostructures.png *Source*: http://en.wikipedia.org/windex.php?title=File:DNA_nanostructures.png *License*: unknown *Contributors*: (Images were kindly provided by Thomas H. LaBean and Hao Yan.)

File:Holliday junction coloured.png *Source*: http://en.wikipedia.org/windex.php?title=File:Holliday_junction_coloured.png *License*: GNU Free Documentation License *Contributors*: Original uploader was Zephyris at en.wikipedia

File:Holliday Junction cropped.png *Source*: http://en.wikipedia.org/windex.php?title=File:Holliday_Junction_cropped.png *License*: GNU Free Documentation License *Contributors*: Original uploader was TimVickers at en.wikipedia

File:Atomic force microscope by Zureks.jpg *Source*: http://en.wikipedia.org/windex.php?title=File:Atomic_force_microscope_by_Zureks.jpg *License*: unknown *Contributors*: User:Zureks

File:Atomic force microscope block diagram.png *Source*: http://en.wikipedia.org/windex.php?title=File:Atomic_force_microscope_block_diagram.png *License*: Public Domain *Contributors*: Original uploader was Askewmind at en.wikipedia

File:AFM view of sodium chloride.gif *Source*: http://en.wikipedia.org/windex.php?title=File:AFM_view_of_sodium_chloride.gif *License*: Public Domain *Contributors*: Courtesy of prof. Ernst Meyer, university of Basel

File:Single-Molecule-Under-Water-AFM-Tapping-Mode.jpg *Source*: http://en.wikipedia.org/windex.php?title=File:Single-Molecule-Under-Water-AFM-Tapping-Mode.jpg *License*: unknown *Contributors*: User:Yurko

File:AFMimageRoughGlass20x20.png *Source*: http://en.wikipedia.org/windex.php?title=File:AFMimageRoughGlass20x20.png *License*: Public Domain *Contributors*: Chych

File:Maldi informatics figure 6.JPG *Source*: http://en.wikipedia.org/windex.php?title=File:Maldi_informatics_figure_6.JPG *License*: Public Domain *Contributors*: Rbeavis

File:Stokes shift.png *Source*: http://en.wikipedia.org/windex.php?title=File:Stokes_shift.png *License*: unknown *Contributors*: User:Mykhal

File:CARS Scheme.svg *Source*: http://en.wikipedia.org/windex.php?title=File:CARS_Scheme.svg *License*: unknown *Contributors*: Onno Gabriel

File:HyperspectralCube.jpg *Source*: http://en.wikipedia.org/windex.php?title=File:HyperspectralCube.jpg *License*: Public Domain *Contributors*: Dr. Nicholas M. Short, Sr.

File:MultispectralComparedToHyperspectral.jpg *Source*: http://en.wikipedia.org/windex.php?title=File:MultispectralComparedToHyperspectral.jpg *License*: Public Domain *Contributors*: Dr. Nicholas M. Short, Sr.

File:Confocalprinciple.svg *Source*: http://en.wikipedia.org/windex.php?title=File:Confocalprinciple.svg *License*: GNU Free Documentation License *Contributors*: Danh

File:3D-SIM-1 NPC Confocal vs 3D-SIM detail.jpg *Source*: http://en.wikipedia.org/windex.php?title=File:3D-SIM-1_NPC_Confocal_vs_3D-SIM_detail.jpg *License*: Creative Commons Attribution-Sharealike 3.0 *Contributors*: Changes in layout by the uploader. Only the creator of the original (Lothar Schermelleh) should be credited.

File:Tirfm.svg *Source*: http://en.wikipedia.org/windex.php?title=File:Tirfm.svg *License*: Public Domain *Contributors*: Dawid Kulik

File:Inverted microscope.jpg *Source*: http://en.wikipedia.org/windex.php?title=File:Inverted_microscope.jpg *License*: unknown *Contributors*: Nuno Nogueira (Nmnogueira) Original uploader was Nmnogueira at en.wikipedia

File:Fluorescence microscop.jpg *Source*: http://en.wikipedia.org/windex.php?title=File:Fluorescence_microscop.jpg *License*: unknown *Contributors*: Masur

File:Microscope And Digital Camera.JPG *Source*: http://en.wikipedia.org/windex.php?title=File:Microscope_And_Digital_Camera.JPG *License*: GNU Free Documentation License *Contributors*: User:Zephyris

File:FluorescenceFilters 2008-09-28.svg *Source*: http://en.wikipedia.org/windex.php?title=File:FluorescenceFilters_2008-09-28.svg *License*: unknown *Contributors*: User:Mastermolch

File:FluorescentCells.jpg *Source*: http://en.wikipedia.org/windex.php?title=File:FluorescentCells.jpg *License*: Public Domain *Contributors*: DO11.10, Emijrp, NEON ja, Origamiemensch, Splette, Tolanor, 5 anonymous edits

File:Yeast membrane proteins.jpg *Source*: http://en.wikipedia.org/windex.php?title=File:Yeast_membrane_proteins.jpg *License*: unknown *Contributors*: User:Masur

File:S cerevisiae septins.jpg *Source*: http://en.wikipedia.org/windex.php?title=File:S_cerevisiae_septins.jpg *License*: Public Domain *Contributors*: Spitfire ch, Philippsen Lab, Biozentrum Basel

File:Dividing Cell Fluorescence.jpg *Source*: http://en.wikipedia.org/windex.php?title=File:Dividing_Cell_Fluorescence.jpg *License*: unknown *Contributors*: Will-moore-dundee

File:HeLa Hoechst 33258.jpg *Source*: http://en.wikipedia.org/windex.php?title=File:HeLa_Hoechst_33258.jpg *License*: Public Domain *Contributors*: TenOfAllTrades

File:FISH 13 21.jpg *Source*: http://en.wikipedia.org/windex.php?title=File:FISH_13_21.jpg *License*: Public Domain *Contributors*: Gregor1976

File:Bloodcell sun flares pathology.jpeg *Source*: http://en.wikipedia.org/windex.php?title=File:Bloodcell_sun_flares_pathology.jpeg *License*: Public Domain *Contributors*: Birindand, Karelj, NEON ja, 1 anonymous edits

File:Carboxysome 3 images.png *Source*: http://en.wikipedia.org/windex.php?title=File:Carboxysome_3_images.png *License*: Creative Commons Attribution 3.0 *Contributors*: Prof. Todd O. Yeates, UCLA Dept. of Chem. and Biochem.

Image:Microarray2.gif *Source*: http://en.wikipedia.org/windex.php?title=File:Microarray2.gif *License*: Public Domain *Contributors*: Original uploader was Paphrag at en.wikipedia

Image:Affymetrix-microarray.jpg *Source*: http://en.wikipedia.org/windex.php?title=File:Affymetrix-microarray.jpg *License*: unknown *Contributors*: Schutz

Image:Microarray-schema.jpg *Source*: http://en.wikipedia.org/windex.php?title=File:Microarray-schema.jpg *License*: Public Domain *Contributors*: Larssono, Million Moments

Image:Heatmap.png *Source*: http://en.wikipedia.org/windex.php?title=File:Heatmap.png *License*: Public Domain *Contributors*: Original uploader was Miguel Andrade at en.wikipedia

Image:Mutation Surveyor Trace.jpg *Source*: http://en.wikipedia.org/windex.php?title=File:Mutation_Surveyor_Trace.jpg *License*: Public Domain *Contributors*: Tammyz06

Image:Sequencing.jpg *Source*: http://en.wikipedia.org/windex.php?title=File:Sequencing.jpg *License*: GNU Free Documentation License *Contributors*: John Schmidt

Image:DNA Sequencin 3 labeling methods.jpg *Source*: http://en.wikipedia.org/windex.php?title=File:DNA_Sequencin_3_labeling_methods.jpg *License*: Public Domain *Contributors*: Abizar

Image:Radioactive Fluorescent Seq.jpg *Source*: http://en.wikipedia.org/windex.php?title=File:Radioactive_Fluorescent_Seq.jpg *License*: unknown *Contributors*: Original uploader was Abizar at en.wikipedia

Image:CE Basic.jpg *Source*: http://en.wikipedia.org/windex.php?title=File:CE_Basic.jpg *License*: Public Domain *Contributors*: Abizar

Image:Sanger sequencing read display.gif *Source*: http://en.wikipedia.org/windex.php?title=File:Sanger_sequencing_read_display.gif *License*: Public Domain *Contributors*: Loris

Image:DNA Sequencing gDNA libraries.jpg *Source*: http://en.wikipedia.org/windex.php?title=File:DNA_Sequencing_gDNA_libraries.jpg *License*: Public Domain *Contributors*: Abizar

Image:Zeolite-ZSM-5-3D-vdW.png *Source*: http://en.wikipedia.org/windex.php?title=File:Zeolite-ZSM-5-3D-vdW.png *License*: Public Domain *Contributors*: Benjah-bmm27

Image:Kepler conjecture 1.jpg *Source*: http://en.wikipedia.org/windex.php?title=File:Kepler_conjecture_1.jpg *License*: Public Domain *Contributors*: Ragesoss

Image:Snowflake8.png *Source*: http://en.wikipedia.org/windex.php?title=File:Snowflake8.png *License*: Public Domain *Contributors*: Nauticashades, Saperaud, WillowW

Image:3D model hydrogen bonds in water.jpg *Source*: http://en.wikipedia.org/windex.php?title=File:3D_model_hydrogen_bonds_in_water.jpg *License*: GNU Free Documentation License *Contributors*: User:snek01

Image:Bragg diffraction.png *Source*: http://en.wikipedia.org/windex.php?title=File:Bragg_diffraction.png *License*: GNU General Public License *Contributors*: user:hadmack

Image:Diamond and graphite.jpg *Source*: http://en.wikipedia.org/windex.php?title=File:Diamond_and_graphite.jpg *License*: GNU Free Documentation License *Contributors*: User:Itub

Image:penicillin.png *Source*: http://en.wikipedia.org/windex.php?title=File:Penicillin.png *License*: unknown *Contributors*: User:Bassophile

Image:Myoglobin.png *Source*: http://en.wikipedia.org/windex.php?title=File:Myoglobin.png *License*: Public Domain *Contributors*: User:AzaToth

Image:X ray diffraction.png *Source*: http://en.wikipedia.org/windex.php?title=File:X_ray_diffraction.png *License*: unknown *Contributors*: Thomas Splettstoesser

Image:Protein crystal.jpg *Source*: http://en.wikipedia.org/windex.php?title=File:Protein_crystal.jpg *License*: Public Domain *Contributors*: TimVickers

Image:X Ray Diffractometer.JPG *Source*: http://en.wikipedia.org/windex.php?title=File:X_Ray_Diffractometer.JPG *License*: GNU Free Documentation License *Contributors*: Ff02::3, Pieter Kuiper

Image:X-ray diffraction pattern 3clpro.jpg *Source*: http://en.wikipedia.org/windex.php?title=File:X-ray_diffraction_pattern_3clpro.jpg *License*: unknown *Contributors*: User:Jeff Dahl

Image:eden.png *Source*: http://en.wikipedia.org/windex.php?title=File:Eden.png *License*: unknown *Contributors*: User:Bassophile

File:Symmetrical stretching.gif *Source*: http://en.wikipedia.org/windex.php?title=File:Symmetrical_stretching.gif *License*: Public Domain *Contributors*: Tiago Becerra Paolini, 1 anonymous edits

File:Asymmetrical stretching.gif *Source*: http://en.wikipedia.org/windex.php?title=File:Asymmetrical_stretching.gif *License*: Public Domain *Contributors*: Tiago Becerra Paolini

File:Scissoring.gif *Source*: http://en.wikipedia.org/windex.php?title=File:Scissoring.gif *License*: Public Domain *Contributors*: Tiago Becerra Paolini

File:Twisting.gif *Source*: http://en.wikipedia.org/windex.php?title=File:Twisting.gif *License*: Public Domain *Contributors*: Tiago Becerra Paolini

File:Wagging.gif *Source*: http://en.wikipedia.org/windex.php?title=File:Wagging.gif *License*: Public Domain *Contributors*: Tiago Becerra Paolini

File:Agitation moléculaire en milieu aqueux.PNG *Source*: http://en.wikipedia.org/windex.php?title=File:Agitation_moléculaire_en_milieu_aqueux.PNG *License*: unknown *Contributors*: User:H'arnet

File:Amino-CORN.png *Source*: http://en.wikipedia.org/windex.php?title=File:Amino-CORN.png *License*: unknown *Contributors*: Original uploader was Password at en.wikipedia

File:GeneticCode21.svg *Source*: http://en.wikipedia.org/windex.php?title=File:GeneticCode21.svg *License*: unknown *Contributors*: Original uploader was Kosigrim at en.wikipedia

File:Monosodium-glutamate.png *Source*: http://en.wikipedia.org/windex.php?title=File:Monosodium-glutamate.png *License*: GNU Free Documentation License *Contributors*: Cacycle, Rob Hooft, Samulili

File:H-Gly-Ala-OH.jpg *Source*: http://en.wikipedia.org/windex.php?title=File:H-Gly-Ala-OH.jpg *License*: unknown *Contributors*: Csatazs

File:Zuiterrionball.svg *Source*: http://en.wikipedia.org/windex.php?title=File:Zuiterrionball.svg *License*: Public Domain *Contributors*: user:YassineMrabet

File:Peptidformationball.svg *Source*: http://en.wikipedia.org/windex.php?title=File:Peptidformationball.svg *License*: Public Domain *Contributors*: user:YassineMrabet

File:Aa structure function.svg *Source*: http://en.wikipedia.org/windex.php?title=File:Aa_structure_function.svg *License*: Public Domain *Contributors*: Jonathan

File:Protein Dynamics Cytochrome C 2NEW smaller.gif *Source*: http://en.wikipedia.org/windex.php?title=File:Protein_Dynamics_Cytochrome_C_2NEW_smaller.gif *License*: GNU Free Documentation License *Contributors*: Original uploader was Zephyris at en.wikipedia

File:Protein-primary-structure.png *Source*: http://en.wikipedia.org/windex.php?title=File:Protein-primary-structure.png *License*: Public Domain *Contributors*: National Human Genome Research Institute (NHGRI)

File:Lysozyme crystal1.JPG *Source*: http://en.wikipedia.org/windex.php?title=File:Lysozyme_crystal1.JPG *License*: unknown *Contributors*: Chrumps, Lode

File:1ezg Tenebrio molitor.png *Source*: http://en.wikipedia.org/windex.php?title=File:1ezg_Tenebrio_molitor.png *License*: GNU Free Documentation License *Contributors*: Original uploader was WillowW at en.wikipedia

File:Concanavalin A.png *Source*: http://en.wikipedia.org/windex.php?title=File:Concanavalin_A.png *License*: Public Domain *Contributors*: User:Lijealso

File:Porin.qutemol.ao.png *Source*: http://en.wikipedia.org/windex.php?title=File:Porin.qutemol.ao.png *License*: unknown *Contributors*: ALoopingIcon

File:Sucrose porin 1a0s.png *Source*: http://en.wikipedia.org/windex.php?title=File:Sucrose_porin_1a0s.png *License*: unknown *Contributors*: Opabinia regalis

File:Sucrose specific porin 1A0S.png *Source*: http://en.wikipedia.org/windex.php?title=File:Sucrose_specific_porin_1A0S.png *License*: GNU Free Documentation License *Contributors*: Snow64

File:StrictosidineSynthase.png *Source*: http://en.wikipedia.org/windex.php?title=File:StrictosidineSynthase.png *License*: unknown *Contributors*: User:Hannes Röst

File:Calmodulin 1CLL.png *Source*: http://en.wikipedia.org/windex.php?title=File:Calmodulin_1CLL.png *License*: Public Domain *Contributors*: Joolz, Lateiner, LeaMaimone, Lode, 1 anonymous edits

File:Haemoglobin-3D-ribbons.png *Source*: http://en.wikipedia.org/windex.php?title=File:Haemoglobin-3D-ribbons.png *License*: Public Domain *Contributors*: Benjah-bmm27

File:Hemoglobin t-r state ani.gif *Source*: http://en.wikipedia.org/windex.php?title=File:Hemoglobin_t-r_state_ani.gif *License*: GNU Free Documentation License *Contributors*: Conscious, Dbenbenn, Editor at Large, Habj, Lennert B, Noca2plus, Tomia, 2 anonymous edits

File:Clostridium perfringens Alpha Toxin Rotate.rsh.gif *Source*: http://en.wikipedia.org/windex.php?title=File:Clostridium_perfringens_Alpha_Toxin_Rotate.rsh.gif *License*: Public Domain *Contributors*: Ramin Herati

File:Bcl-2 Family.jpg *Source*: http://en.wikipedia.org/windex.php?title=File:Bcl-2_Family.jpg *License*: unknown *Contributors*: Hoffmeier

File:Bcl-2 3D.jpg *Source*: http://en.wikipedia.org/windex.php?title=File:Bcl-2_3D.jpg *License*: GNU Free Documentation License *Contributors*: CN3D

File:PBB Protein THPO image.jpg *Source*: http://en.wikipedia.org/windex.php?title=File:PBB_Protein_THPO_image.jpg *License*: unknown *Contributors*:

File:Bence Jones Protein MLE1.jpg *Source*: http://en.wikipedia.org/windex.php?title=File:Bence_Jones_Protein_MLE1.jpg *License*: Public Domain *Contributors*: Alex McPherson, University of California, Irvine

File:Duck Delta 1 Crystallin.jpg *Source*: http://en.wikipedia.org/windex.php?title=File:Duck_Delta_1_Crystallin.jpg *License*: Public Domain *Contributors*: Ragesoss

File:Michelson-morley.png *Source*: http://en.wikipedia.org/windex.php?title=File:Michelson-morley.png *License*: GNU Free Documentation License *Contributors*: user:bighead

File:Interferometer.JPG *Source*: http://en.wikipedia.org/windex.php?title=File:Interferometer.JPG *License*: unknown *Contributors*: User:Brews ohare

File:Michelson interferometer schematic.png *Source*: http://en.wikipedia.org/windex.php?title=File:Michelson_interferometer_schematic.png *License*: GNU Free Documentation License *Contributors*: Teebeutel

File:IR spectroscopy apparatus.jpg *Source*: http://en.wikipedia.org/windex.php?title=File:IR_spectroscopy_apparatus.jpg *License*: GNU Free Documentation License *Contributors*: Ewen

File:IR spectrometer.jpg *Source*: http://en.wikipedia.org/windex.php?title=File:IR_spectrometer.jpg *License*: Public Domain *Contributors*: S.Levchenkov

File:Michelson Interferometer.jpg *Source*: http://en.wikipedia.org/windex.php?title=File:Michelson_Interferometer.jpg *License*: unknown *Contributors*: Falcorian, Juiced lemon, Teebeutel

File:Ir hcl rot-vib mrtz.svg *Source*: http://en.wikipedia.org/windex.php?title=File:Ir_hcl_rot-vib_mrtz.svg *License*: unknown *Contributors*: mrtz

File:BandeIR.png *Source*: http://en.wikipedia.org/windex.php?title=File:BandeIR.png *License*: GNU Free Documentation License *Contributors*: User:Grimlock

File:Michelsoninterferometer.jpg *Source*: http://en.wikipedia.org/windex.php?title=File:Michelsoninterferometer.jpg *License*: Copyrighted free use *Contributors*: Juiced lemon, Skygazer, Tano4595, Teebeutel, Umherirrender, Xorx

File:Michelson couleur.jpg *Source*: http://en.wikipedia.org/windex.php?title=File:Michelson_couleur.jpg *License*: unknown *Contributors*: NicoB, Teebeutel

File:Bismuthine-2D-IR-MMW-dimensions.png *Source*: http://en.wikipedia.org/windex.php?title=File:Bismuthine-2D-IR-MMW-dimensions.png *License*: Public Domain *Contributors*: Ben Mills

File:Infrared spectrometer.jpg *Source*: http://en.wikipedia.org/windex.php?title=File:Infrared_spectrometer.jpg *License*: unknown *Contributors*: ishikawa

Image:HWB-NMRv900.jpg *Source*: http://en.wikipedia.org/windex.php?title=File:HWB-NMRv900.jpg *License*: Public Domain *Contributors*: MartinSaunders

Image:NMR sample.JPG *Source*: http://en.wikipedia.org/windex.php?title=File:NMR_sample.JPG *License*: Public Domain *Contributors*: User:Kjaergaard

Image:HyperspectralCube.jpg *Source*: http://en.wikipedia.org/windex.php?title=File:HyperspectralCube.jpg *License*: Public Domain *Contributors*: Dr. Nicholas M. Short, Sr.

Image:MultispectralComparedToHyperspectral.jpg *Source*: http://en.wikipedia.org/windex.php?title=File:MultispectralComparedToHyperspectral.jpg *License*: Public Domain *Contributors*: Dr. Nicholas M. Short, Sr.

Image:FIRST measurement of SF6 and NH3.jpg *Source*: http://en.wikipedia.org/windex.php?title=File:FIRST_measurement_of_SF6_and_NH3.jpg *License*: Creative Commons Attribution-Sharealike 3.0 *Contributors*: Andre Villemaire

Image:jmol1.png *Source*: http://en.wikipedia.org/windex.php?title=File:Jmol1.png *License*: unknown *Contributors*: Peter Murray-Rust

Image:Hemagglutinin molecule.png *Source*: http://en.wikipedia.org/windex.php?title=File:Hemagglutinin_molecule.png *License*: GNU Free Documentation License *Contributors*: U.S. National Institutes of Health.

Image:FormicAcid.pdb.png *Source*: http://en.wikipedia.org/windex.php?title=File:FormicAcid.pdb.png *License*: Public Domain *Contributors*: Csörföly D, Cwbm (commons)

Image:Isosurface on molecule.jpg *Source*: http://en.wikipedia.org/windex.php?title=File:Isosurface_on_molecule.jpg *License*: unknown *Contributors*: StoatBringer

Image:porin.qutemol.dl.png *Source*: http://en.wikipedia.org/windex.php?title=File:Porin.qutemol.dl.png *License*: unknown *Contributors*: ALoopingIcon

Image:porin.qutemol.ao.png *Source*: http://en.wikipedia.org/windex.php?title=File:Porin.qutemol.ao.png *License*: unknown *Contributors*: ALoopingIcon

Image:JmolStick.PNG *Source*: http://en.wikipedia.org/windex.php?title=File:JmolStick.PNG *License*: unknown *Contributors*: Peter Murray-Rust

Image:B&Z&A DNA formula.jpg *Source*: http://en.wikipedia.org/windex.php?title=File:B&Z&A_DNA_formula.jpg *License*: Public Domain *Contributors*: Original uploader was Lankenau at en.wikipedia

Image:Circular DNA Supercoiling.png *Source*: http://en.wikipedia.org/windex.php?title=File:Circular_DNA_Supercoiling.png *License*: GNU Free Documentation License *Contributors*: Richard Wheeler (Zephyris)

Image:Modern 3T MRI.JPG *Source*: http://en.wikipedia.org/windex.php?title=File:Modern_3T_MRI.JPG *License*: unknown *Contributors*: User:KasugaHuang

File:Macrophage ARF.png *Source*: http://en.wikipedia.org/windex.php?title=File:Macrophage_ARF.png *License*: unknown *Contributors*: See source

File:FRET.PNG *Source*: http://en.wikipedia.org/windex.php?title=File:FRET.PNG *License*: Public Domain *Contributors*: User:Gia.cossa

File:FRET application phosgene detection.png *Source*: http://en.wikipedia.org/windex.php?title=File:FRET_application_phosgene_detection.png *License*: GNU Free Documentation License *Contributors*: Qef, V8rik, 1 anonymous edits

File:Sarfus.DNABiochip.jpg *Source*: http://en.wikipedia.org/windex.php?title=File:Sarfus.DNABiochip.jpg *License*: unknown *Contributors*: Nanolane

File:Rothemund-DNA-SierpinskiGasket.jpg *Source*: http://en.wikipedia.org/windex.php?title=File:Rothemund-DNA-SierpinskiGasket.jpg *License*: Creative Commons Attribution 2.5 *Contributors*: Antony-22

File:Signal transduction v1.png *Source*: http://en.wikipedia.org/windex.php?title=File:Signal_transduction_v1.png *License*: GNU Free Documentation License *Contributors*: Original uploader was Roadnottaken at en.wikipedia

Image:Holliday Junction.png *Source*: http://en.wikipedia.org/windex.php?title=File:Holliday_Junction.png *License*: Public Domain *Contributors*: Ahruman, Crux, Infrogmation, TimVickers, Wickey

Image:Mao-DX-schematic.jpg *Source*: http://en.wikipedia.org/windex.php?title=File:Mao-DX-schematic.jpg *License*: Creative Commons Attribution 2.5 *Contributors*: Antony-22

Image:Mao-DXarray-schematic.gif *Source*: http://en.wikipedia.org/windex.php?title=File:Mao-DXarray-schematic.gif *License*: Creative Commons Attribution 2.5 *Contributors*: Antony-22

Image:SierpinskiTriangle.svg *Source*: http://en.wikipedia.org/windex.php?title=File:SierpinskiTriangle.svg *License*: Public Domain *Contributors*: User:PiAndWhippedCream

Image:Rothemund-DNA-SierpinskiGasket.jpg *Source*: http://en.wikipedia.org/windex.php?title=File:Rothemund-DNA-SierpinskiGasket.jpg *License*: Creative Commons Attribution 2.5 *Contributors*: Antony-22

Image:AFMimageRoughGlass20x20.png *Source*: http://en.wikipedia.org/windex.php?title=File:AFMimageRoughGlass20x20.png *License*: Public Domain *Contributors*: Chych

Image:Atomic force microscope by Zureks.jpg *Source*: http://en.wikipedia.org/windex.php?title=File:Atomic_force_microscope_by_Zureks.jpg *License*: unknown *Contributors*: User:Zureks

Image:Atomic force microscope block diagram.png *Source*: http://en.wikipedia.org/windex.php?title=File:Atomic_force_microscope_block_diagram.png *License*: Public Domain *Contributors*: Original uploader was Askewmind at en.wikipedia

Image:AFM (used) cantilever in Scanning Electron Microscope, magnification 1000x.GIF *Source*: http://en.wikipedia.org/windex.php?title=File:AFM_(used)_cantilever_in_Scanning_Electron_Microscope,_magnification_1000x.GIF *License*: unknown *Contributors*: User:SecretDisc

Image:AFM (used) cantilever in Scanning Electron Microscope, magnification 3000x.GIF *Source*: http://en.wikipedia.org/windex.php?title=File:AFM_(used)_cantilever_in_Scanning_Electron_Microscope,_magnification_3000x.GIF *License*: unknown *Contributors*: User:SecretDisc

Image:Single-Molecule-Under-Water-AFM-Tapping-Mode.jpg *Source*: http://en.wikipedia.org/windex.php?title=File:Single-Molecule-Under-Water-AFM-Tapping-Mode.jpg *License*: unknown *Contributors*: User:Yurko

Image:AFM noncontactmode.jpg *Source*: http://en.wikipedia.org/windex.php?title=File:AFM_noncontactmode.jpg *License*: unknown *Contributors*: User:Creepin475

Image:AFM beamdetection.jpg *Source*: http://en.wikipedia.org/windex.php?title=File:AFM_beamdetection.jpg *License*: unknown *Contributors*: User:Creepin475

Image:AFM view of sodium chloride.gif *Source*: http://en.wikipedia.org/windex.php?title=File:AFM_view_of_sodium_chloride.gif *License*: Public Domain *Contributors*: Courtesy of prof. Ernst Meyer, university of Basel

Image:Atomic Force Microscope Science Museum London.jpg *Source*: http://en.wikipedia.org/windex.php?title=File:Atomic_Force_Microscope_Science_Museum_London.jpg *License*: GNU Free Documentation License *Contributors*: John Dalton

Image:Piezoscanner.JPG *Source*: http://en.wikipedia.org/windex.php?title=File:Piezoscanner.JPG *License*: unknown *Contributors*: User:Creepin475

Image:Electron Microscope.png *Source*: http://en.wikipedia.org/windex.php?title=File:Electron_Microscope.png *License*: Public Domain *Contributors*: User:GrahamColm

Image:Ernst Ruska Electron Microscope - Deutsches Museum - Munich-edit.jpg *Source*: http://en.wikipedia.org/windex.php?title=File:Ernst_Ruska_Electron_Microscope_-_Deutsches_Museum_-_Munich-edit.jpg *License*: unknown *Contributors*: J Brew, uploaded on the English-speaking Wikipedia by .

Image:Ant SEM.jpg *Source*: http://en.wikipedia.org/windex.php?title=File:Ant_SEM.jpg *License*: unknown *Contributors*: Fanghong, Howcheng, Kersti Nebelsiek, Mattes, NEON ja, Neil916, Olei, Romary, Steff, 1 anonymous edits

Image:Golden insect 01 Pengo.jpg *Source*: http://en.wikipedia.org/windex.php?title=File:Golden_insect_01_Pengo.jpg *License*: unknown *Contributors*: Pengo

Image:Krillfilter2kils.jpg *Source*: http://en.wikipedia.org/windex.php?title=File:Krillfilter2kils.jpg *License*: GNU Free Documentation License *Contributors*: User:uwe kils

Image:Hohlraum irradiation on NOVA laser.jpg *Source*: http://en.wikipedia.org/windex.php?title=File:Hohlraum_irradiation_on_NOVA_laser.jpg *License*: Public Domain *Contributors*: Deglr6328, DynV, Gumby600

Image:Be foil square.jpg *Source*: http://en.wikipedia.org/windex.php?title=File:Be_foil_square.jpg *License*: GNU Free Documentation License *Contributors*: Deglr6328

License

GNU Free Documentation License
http://www.gnu.org/copyleft/fdl.html